frontiers | Research Topics

Nutrition, metabolism and infection

Edited by
Filippo Giorgio Di Girolamo, Nada Rotovnik Kozjek, Gianni Biolo, Nicola Fiotti and Filippo Mearelli

Published in
Frontiers in Nutrition
Frontiers in Immunology

ISSN 1664-8714
ISBN 978-2-8325-4527-0
DOI 10.3389/978-2-8325-4527-0

About Frontiers

Frontiers is more than just an open access publisher of scholarly articles: it is a pioneering approach to the world of academia, radically improving the way scholarly research is managed. The grand vision of Frontiers is a world where all people have an equal opportunity to seek, share and generate knowledge. Frontiers provides immediate and permanent online open access to all its publications, but this alone is not enough to realize our grand goals.

Frontiers journal series

The Frontiers journal series is a multi-tier and interdisciplinary set of open-access, online journals, promising a paradigm shift from the current review, selection and dissemination processes in academic publishing. All Frontiers journals are driven by researchers for researchers; therefore, they constitute a service to the scholarly community. At the same time, the *Frontiers journal series* operates on a revolutionary invention, the tiered publishing system, initially addressing specific communities of scholars, and gradually climbing up to broader public understanding, thus serving the interests of the lay society, too.

Dedication to quality

Each Frontiers article is a landmark of the highest quality, thanks to genuinely collaborative interactions between authors and review editors, who include some of the world's best academicians. Research must be certified by peers before entering a stream of knowledge that may eventually reach the public - and shape society; therefore, Frontiers only applies the most rigorous and unbiased reviews. Frontiers revolutionizes research publishing by freely delivering the most outstanding research, evaluated with no bias from both the academic and social point of view. By applying the most advanced information technologies, Frontiers is catapulting scholarly publishing into a new generation.

What are Frontiers Research Topics?

Frontiers Research Topics are very popular trademarks of the *Frontiers journals series*: they are collections of at least ten articles, all centered on a particular subject. With their unique mix of varied contributions from Original Research to Review Articles, Frontiers Research Topics unify the most influential researchers, the latest key findings and historical advances in a hot research area.

Find out more on how to host your own Frontiers Research Topic or contribute to one as an author by contacting the Frontiers editorial office: frontiersin.org/about/contact

Nutrition, metabolism and infection

Topic editors

Filippo Giorgio Di Girolamo — University of Trieste, Italy
Nada Rotovnik Kozjek — Institute of Oncology Ljubljana, Slovenia
Gianni Biolo — University of Trieste, Italy
Nicola Fiotti — University of Trieste, Italy
Filippo Mearelli — University of Trieste, Italy

Citation

Di Girolamo, F. G., Kozjek, N. R., Biolo, G., Fiotti, N., Mearelli, F., eds. (2024). *Nutrition, metabolism and infection*. Lausanne: Frontiers Media SA.
doi: 10.3389/978-2-8325-4527-0

Table of contents

frontiers | Frontiers in Nutrition

TYPE Systematic Review
PUBLISHED 28 July 2022
DOI 10.3389/fnut.2022.964484

OPEN ACCESS

EDITED BY
Filippo Giorgio Di Girolamo,
University of Trieste, Italy

REVIEWED BY
Guosheng Wu,
Second Military Medical University, China
Zahra Vahdat Shariatpanahi,
Shahid Beheshti University of Medical Sciences, Iran

*CORRESPONDENCE
Qiaoping Ye
1114703971@qq.com

SPECIALTY SECTION
This article was submitted to Clinical Nutrition, a section of the journal Frontiers in Nutrition

RECEIVED 08 June 2022
ACCEPTED 06 July 2022
PUBLISHED 28 July 2022

CITATION
Zhu H, Xu X, Zhang K and Ye Q (2022) The effect of intravenous vitamin C on clinical outcomes in patients with sepsis or septic shock: A meta-analysis of randomized controlled trials. *Front. Nutr.* 9:964484. doi: 10.3389/fnut.2022.964484

The effect of intravenous vitamin C on clinical outcomes in patients with sepsis or septic shock: A meta-analysis of randomized controlled trials

Huiyan Zhu[1], Xiaoya Xu[1], Kai Zhang[2] and Qiaoping Ye[1]*

[1]Department of General Surgery, Lishui People's Hospital, Lishui, China, [2]Department of Critical Care Medicine, Second Affiliated Hospital, Zhejiang University School of Medicine, Hangzhou, China

Objectives: Vitamin C deficiency is common among patients with sepsis and has been associated with poor clinical outcomes. Nevertheless, the effect of intravenous (IV) vitamin C for the treatment of sepsis remains controversial. The purpose of this meta-analysis was to evaluate the effect of IV vitamin C in patients with sepsis or septic shock.

Methods: Electronic databases (PubMed, Embase, Scopus, and Cochrane Library) were searched from inception through May 25, 2022 for randomized controlled trials evaluating the effect of IV vitamin C treatment in patients with sepsis. The primary outcome was short-term mortality, and secondary outcomes including the duration of vasopressor, length of intensive care unit (ICU) stay, and Sequential Organ Failure Assessment (SOFA) score after vitamin C treatment. Subgroup analyses were performed based on the type of disease, dose and duration of IV vitamin C.

Results: A total of 10 studies were included, with a total sample of 755 septic patients. The IV vitamin C was associated with a significant reduction in the short-term mortality (OR 0.51, 95% CI 0.37–0.69, I^2 = 0%) and duration of vasopressor (MD −27.88, 95% CI −49.84 to −5.92, I^2 = 95%). The length of ICU stay (MD −0.68, 95% CI −2.13 to 0.78, I^2 = 74%) and SOFA score (MD −0.05, 95% CI −1.69 to 1.58, I^2 = 86%) were not significantly different between two groups.

Conclusion: In patients with sepsis or septic shock, the IV vitamin C reduced the short-term mortality rate and duration of vasopressor, with no effect on the length of ICU stay and SOFA score. Further trials are required to explore the optimal dosage and duration of IV vitamin C.

Systematic Review Registration: https://inplasy.com/inplasy-2022-6-0013/, identifier INPLASY202260013.

KEYWORDS

vitamin C, ascorbic acid, sepsis, septic shock, meta-analysis

Introduction

Sepsis is a life-threatening syndrome associated with physiological, pathological, and biological abnormalities due to a dysregulated immune response to infections (1). Despite the advances in sepsis research improving the diagnosis and treatment (2), sepsis continues to be the most major cause of intensive care unit (ICU) admission and death (3, 4). Based on the Global Burden of Diseases 2017 estimates, there were 48.9 million incident sepsis cases worldwide, with nearly 11.0 million sepsis-related deaths, accounting for 19.7% of all global deaths (5). Even survivors are at high risk of developing functional limitations, cognitive impairment, and mental health problems, which significantly impair the quality of life (6).

It is well-established that patients with sepsis have decreased levels of vitamin C (also known as ascorbic acid), and this depletion has a dose-dependent association with increased organ dysfunction and mortality (7). The beneficial effects and associated mechanisms of vitamin C in sepsis including its anti-inflammatory and anti-oxidant properties (8, 9), acting as an enzymatic cofactor in the synthesis of vasopressin, cortisol, and catecholamine (10, 11), inhibiting the nitric oxide synthase and regulating the clearance of alveolar fluid (12, 13).

In recent years, multiple randomized controlled trials (RCTs) evaluating the effect of intravenous (IV) vitamin C with or without hydrocortisone and thiamine have been completed. Several recently published meta-analyses (14–20) assessed the combination of hydrocortisone, ascorbic acid, and thiamine (HAT) treatment in septic patients. The results indicated that the HAT treatment improved the Sequential Organ Failure Assessment (SOFA) score and reduced the duration of vasopressor, but was not associated with lower short-term mortality. However, the evidence-based medical evidence for using IV vitamin C as monotherapy in septic population are scarce. Therefore, this current study aimed to evaluate the effect of IV vitamin C alone on clinical outcomes among patients with sepsis or septic shock. Furthermore, we performed subgroup analyses to better understand the effectiveness of IV vitamin C in different populations and examined whether a dose-effect modified the treatment effect of vitamin C.

Methods

Data sources and study selection

We conducted our study on the basis of the updated PRISRMA statement (21) (checklist in **Supplementary Material**), and the study protocol was registered in International Platform of Registered Systematic Review and Meta-analysis Protocols (INPLASY 202260013). We systematically searched the PubMed, Embase, Scopus, and Cochrane Library for relevant studies in English from inception through May 25, 2022. The search used broad search terms containing "sepsis," "septic shock," "vitamin C," "ascorbic acid," and "randomized" (the comprehensive search strategies are listed in **Supplementary Data Sheet 2**).

Eligibility criteria

The inclusion criteria were as follows: 1. Population: adult patients (≥18 years of age) with sepsis or septic shock. Sepsis was defined as reported by the original authors, septic shock was defined as sepsis with the need for vasopressor support; 2. Intervention: IV vitamin C as monotherapy; 3. Comparison: placebo, or no intervention; 4. Outcomes: the primary outcome was short-term mortality, including hospital mortality, and 28/30-day mortality. Secondary outcomes including the duration of vasopressor, length of ICU stay, and SOFA score after vitamin C treatment; 5. Design: RCT.

Data extraction and quality assessment

Two authors (Huiyan Zhu, Qiaoping Ye) independently retrieved relevant studies, extracted characteristics of studies (first author, years of publication, population, intervention and control methods, vitamin C level) and predefined outcomes from included studies.

The Cochrane risk of bias tool (22) was utilized for assessing the methodological quality of including studies by two authors (Huiyan Zhu, Qiaoping Ye), any differences in opinion were resolved by a third adjudicator (Xiaoya Xu).

Statistical synthesis and analysis

We computed the pooled odds ratio (OR) with 95% confidence interval (CI) for dichotomous outcomes, and mean difference (MD) with 95% CI for continuous outcomes. The heterogeneity was assessed by the Higgins inconsistency (I^2) statistics (23). Substantial heterogeneity was identified when I^2 value $>$ 30% and a random-effects model was employed to perform the analysis, otherwise a fixed-effects model would be used. Publication bias was assessed by using the funnel plot and Egger's regression test (24).

A prespecified subgroup analysis stratified by the types of disease (sepsis vs. septic shock), dose [high dose was set to a daily dose of ≥100 mg/kg or 10000 mg/day, according to the review of Patel et al. (25)], and duration [<5 days vs. ≥5 days, according to the study by Jung et al. (26)] of IV vitamin C treatment. Finally, a sensitivity analysis was conducted to explore the effect of individual study by consecutive exclusion of each study at one time.

Results

Study characteristics

During the primary search, we identified 506 articles. Among them, 319 were duplicated articles, and 142 studies were excluded by screening the abstracts. During the evaluation of the full text, 35 studies were further removed with various reasons. Eventually, a total of ten RCTs (27–36) were included in our study (follow chart in **Figure 1**).

Table 1 presents the characteristics of included studies. A total of 755 patients were included in the analysis, whereof 384 patients received IV vitamin C and 371 patients received placebos or no intervention during the study period. The number of patients in each study ranged from a minimum of 20 up to 167. Seven trials (29–33, 35, 36) enrolled patients with sepsis or septic shock based on the Sepsis-3 criteria, three trials (27, 28, 34) diagnosed sepsis by the original investigators. According to whether the patients required vasopressor support, patients were categorized into sepsis (27–29, 35) and septic shock (30–34, 36) cohort. The dose and duration of IV vitamin C varied amongst included trials. Five trials administered low-dose vitamin C, four administered high-dose vitamin C, and one trial included one low-dose vitamin C cohort and one high-dose vitamin C cohort. In six trials (28, 29, 31–34), patients received IV vitamin C for 3–4 days, two trials (27, 35) administered vitamin C for 6–7 days, and the rest two trials (30, 36) administered vitamin C until ICU discharge. Four trials (28, 29, 31, 32) reported the pre-trial and post-trial plasma vitamin C level, the IV vitamin C treatment could increase the plasma vitamin C concentration. The serum level of vitamin C was significantly higher in intervention group compared with control group.

In addition, the duration of vasopressor, length of ICU stay, and SOFA score were expressed in the form of median and interquartile range in several trials. Thus, we used the methodology of Wan et al. (37) to convert these data into mean and standard deviation.

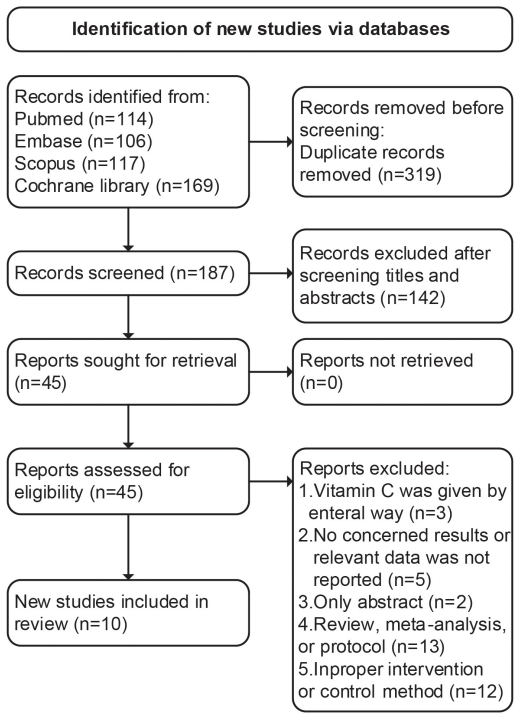

FIGURE 1
PRISMA 2020 flow diagram for the meta-analysis.

Quality assessment

The results of risk of bias assessment (**Figure 2**) showed that three studies were rated as high risk of bias: Habib et al. (36) used an open-label design, which carried the risk of bias; in the trial by Mahmoodpoor et al. (31), the SOFA score in intervention group was significantly higher than that in control group; Zhang et al. (35) enrolled critically ill patients with severe SARS-CoV-2-related pneumonia and SOFA score $\geq$ 2, which were different from other trials. Four trials (27, 30, 31, 36) did not provide the methods of random sequence generation or allocation concealment, four trials (27, 30, 32, 36) did not report the blinding method, which would either underestimate or overestimate the size of the effect. Moreover, six trials (27, 30, 32–34, 36) were rated as having an unclear risk of other bias since because the serum level of vitamin C of intervention and control groups were not provided.

In terms of publication bias, the funnel plot and Egger's test showed that there was no significant risk of publication bias (Egger's test, $P > 0.05$; **Supplementary Data Sheet 1**).

Primary outcome

All included trials reported the short-term mortality with different definitions. Three trials reported in-hospital mortality, five trials reported 28-day mortality, two trials reported multiple results and we chose in-hospital mortality in the analysis. The incidence of short-term mortality in vitamin C group was lower than that in control group, 26.6% (102/384) vs. 41.2% (153/371), respectively. The pooled result indicated that IV vitamin C treatment was associated with a significant lower short-term mortality (OR 0.51, 95% CI 0.37 to 0.69, $I^2 = 0\%$, **Figure 3**).

Secondary outcomes

Six trials reported the duration of vasopressor, seven reported the length of ICU stay, and five reported the SOFA

TABLE 1 Characteristics of studies included in the meta-analysis.

Study	Design	Sample size	Population	Interventions	Vitamin C status (μ mol/L)[a]	Outcomes
Rosengrave et al. (32)	Double-blind, randomized placebo-controlled trial	Total: 40 (Intervention: 20; Control: 20)	Adult patients with septic shock (Sepsis-3)	Intervention: vitamin C (100 mg/kg/day) for 4 days; Control: 5% dextrose	Baseline: Intervention: 10 (4, 13); Placebo: 8.2 (4.7, 11); 72 h: Intervention: 408 (227, 560); Placebo: 4.4 (3.1, 8.8)	Mortality (in-hospital, 30-day, 90-day), duration of vasopressor, ICU length of stay, SOFA score at 4-day
Wacker et al. (33)	Double-blind, randomized placebo-controlled trial	Total: 124 (Intervention: 60; Control: 64)	Adult patients within 24 h of onset of septic shock (Sepsis-3)	Intervention: vitamin C (6000 mg/day) for 4 days; Control: normal saline	NR	28-day mortality, duration of vasopressor, ICU length of stay
Mahmoodpoor et al. (31)	Double-blind, randomized placebo-controlled trial	Total: 80 (Intervention: 42; Control: 38)	Critically ill patients with severe pneumonia and SOFA $\geq$ 2 (Sepsis-3)	Intervention: vitamin C (60 mg/kg/day) for 4 days; Control: normal saline	Baseline: Intervention: 20.63 $\pm$ 12.74; Placebo: 22.77 $\pm$ 13.56; 72 h: Intervention: 79.20 $\pm$ 26.42; Placebo: 16.38 $\pm$ 10.33	In-hospital mortality, duration of vasopressor, SOFA score at 4-day, ICU length of stay
Zhang et al. (35)	Double-blind, randomized placebo-controlled trial	Total: 56 (Intervention: 27; Control: 29)	Critically ill patients with severe SARS-CoV-2-related pneumonia and SOFA $\geq$ 2 (Sepsis-3)	Intervention: vitamin C (24000 mg/day) for 7 days; Control: bacteriostatic water	NR	Mortality (28-day, in-hospital), SOFA score at 7-day, ICU length of stay, hospital length of stay
Lv et al. (30)	Randomized placebo-controlled trial	Total: 117 (Intervention: 61; Control: 56)	Adult ICU patients diagnosed with septic shock (Sepsis-3)	Intervention: vitamin C (3000 mg/day) until ICU discharge; Control: 5% dextrose	NR	28-day mortality, SOFA score at 3-day, ICU length of stay, duration of vasopressor
CITRIS-ALI trial (29)	Double-blind, randomized placebo-controlled trial	Total: 167 (Intervention: 84; Control: 83)	Adult patients diagnosed with sepsis (Sepsis-3) and developed ARDS	Intervention: vitamin C (200 mg/kg/day) for 4 days; Control: 5% dextrose	Baseline: Intervention: 22 (8, 39) Placebo: 22 (11, 37); 96 h: Intervention: 169 (87, 412); Placebo: 26 (9, 41)	28-day mortality, improvement in SOFA score, SOFA score at 4-day
Habib et al. (36)	Open-label, randomized controlled trial	Total: 100 (Intervention: 50; Control: 50)	Adult patients admitted to the critical care department with the diagnosis of septic shock (Sepsis-3)	Intervention: vitamin C (6000 mg/day) until ICU discharge; Control: conventional treatment	NR	In-hospital mortality, duration of vasopressor, ICU length of stay
Zabet et al. (34)	Double-blind, randomized placebo-controlled trial	Total: 28 (Intervention: 14; Control: 14)	Adult surgical critically ill patients with diagnosis of septic shock	Intervention: vitamin C (100 mg/kg/day) for 3 days; Control: 5% dextrose	NR	28-day mortality, duration of vasopressor, ICU length of stay
Fowler et al. (28)	Double-blind, randomized placebo-controlled trial	Total: 24 (Intervention: 16; Control: 8)	Adult patients with severe sepsis in the ICU	Intervention: vitamin C (50 mg/kg/day or 200 mg/kg/day) for 4 days; Control: 5% dextrose	Baseline: Low dose: 17 (14, 28) High dose: 17 (11, 50) Placebo: 20 (11, 45); 96 h: Low dose: 331 (110, 806) High dose: 3082 (1592, 5772) Placebo: 16 (7, 27)	28-day mortality
Ferrón-Celma et al. (27)	Double-blind, randomized placebo-controlled trial	Total: 20 (Intervention: 10; Control: 10)	Adult patients developed sepsis after abdominal surgery	Intervention: vitamin C (450 mg/day) for 6 days; Control: 5% dextrose	NR	In-hospital mortality

[a]The data represent median (IQR) or mean $\pm$ SD.

ICU, intensive care unit; mg, milligram; kg, kilogram; NR, not reported; SOFA, sequential organ failure assessment; ARDS, acute respiratory distress syndrome.

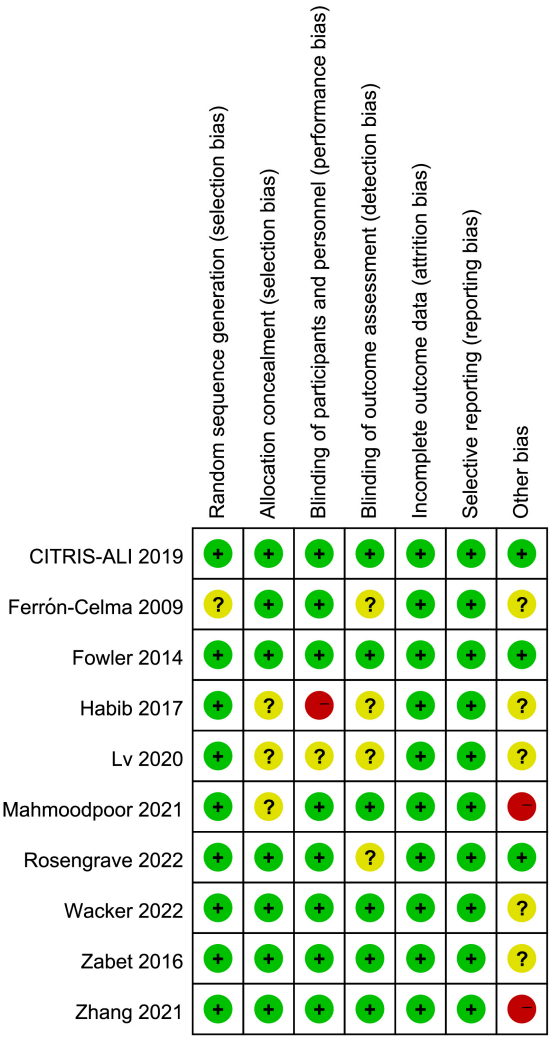

FIGURE 2
Assessment of quality by the Cochrane risk of bias tool.

score. The IV vitamin C treatment was associated with a reduction in the duration of vasopressor (MD −27.88, 95% CI −49.84 to −5.92, I^2 = 95%, Figure 4A) among patients with septic shock. However, there was no significant difference in length of ICU stay (MD −0.68, 95% CI −2.13 to 0.78, I^2 = 74%, Figure 4B) and SOFA score (MD −0.05, 95% CI −1.69 to 1.58, I^2 = 86%, Figure 4C) between two groups. Notably, the results were greatly weakened by significant heterogeneity.

Sensitivity and subgroup analysis

We assessed the effect of every single trial on the pooled result by omitting each study. Furthermore, the sensitivity analysis showed similar results to the overall analysis, indicating the good robustness (Supplementary Data Sheet 1).

We performed subgroup analyses to assess whether the types of disease, dose and duration of IV vitamin C treatment would affect the clinical outcomes. Four trials enrolled patients with sepsis (27–29, 35) and six enrolled patients with septic shock (30–34, 36). Five trials (27, 30, 31, 33, 36) administered low-dose vitamin C, four (29, 32, 34, 35) administered high-dose vitamin C, and one trial (28) included one low-dose vitamin C cohort and one high-dose vitamin C cohort. In six trials (28, 29, 31–34), patients received IV vitamin C for 3–4 days, two trials (27, 35) administered vitamin C for 6–7 days, and the rest two trials (30, 36) administered vitamin C until ICU discharge.

The IV vitamin C treatment was associated with a reduced mortality rate in both the patients with sepsis (OR 0.55, 95% CI 0.33–0.92, I^2 = 0%, Figure 5) and septic shock (OR 0.48, 95% CI 0.32–0.71, I^2 = 0%, Figure 5). Furthermore, the survival benefit was not associated with the dose or duration of IV vitamin C.

In terms of the duration of vasopressor, the high-does IV vitamin C was associated with reduction in the duration of vasopressor (MD −24.42, 95% CI −47.19 to −1.66, I^2 = 95%), whereas the low-does subgroup found no difference (MD −14.10, 95% CI −29.32 to 1.13, I^2 = 91%). Moreover, we did not observe significant difference in the duration of vasopressor between patients received IV vitamin C < 5 or ≥ 5 days.

In addition, the types of disease, dose and duration of IV vitamin C treatment did not have significant effects on the length of ICU and SOFA score (Supplementary Data Sheet 1). The results of subgroup analyses are shown in Table 2.

Discussion

In this meta-analysis, we included 10 RCTs with 755 patients to analyze the effect of IV vitamin C as monotherapy in patients with sepsis or septic shock. The preliminary analysis showed that the IV vitamin C treatment for patients with sepsis or septic shock was associated with a significant reduction in short-term mortality, but with no effect on the length of ICU stay and SOFA score. Meanwhile, the use of IV vitamin C treatment might reduce the duration of vasopressor for patients with septic shock. Furthermore, the dose and duration of vitamin C showed no significant effect on the clinical outcomes.

To our knowledge, this is the first comprehensive meta-analysis of RCTs to evaluate the effect of IV vitamin C as monotherapy in patients with sepsis or septic shock. Since recent meta-analyses (14–20) failed to find the association between HAT treatment and improved mortality among patients with sepsis, further research evaluating the HAT treatment in sepsis appears to be less necessary. In contrast, Patel et al. (25) performed the first meta-analysis to evaluate the role of IV vitamin C monotherapy in critically ill patients and revealed a significant treatment effect. On that basis, we hypothesized that IV vitamin C monotherapy still remain protective effect against sepsis, and further evaluated the

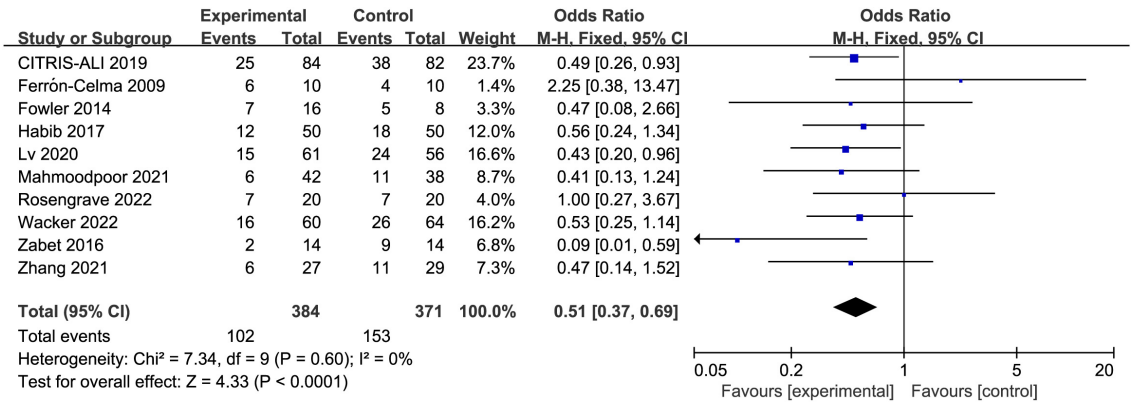

FIGURE 3
Forest plot showing the association between IV vitamin C and the risk of short-term mortality.

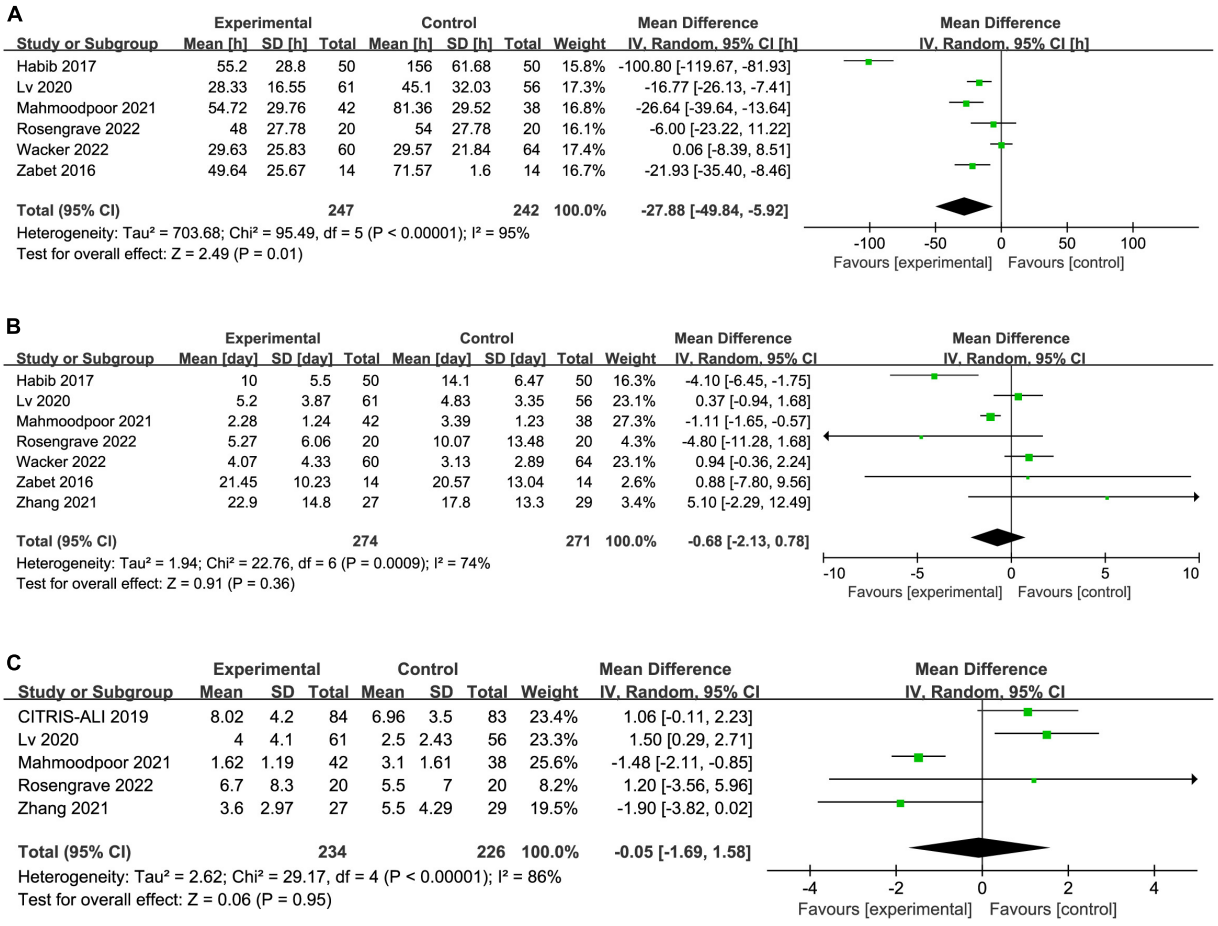

FIGURE 4
Forest plot showing the association between IV vitamin C and **(A)** duration of vasopressor, **(B)** length of ICU stay, **(C)** SOFA score.

effects of IV vitamin C in patients with sepsis or septic shock. The results of our meta-analysis are approximately consistent with the research by Patel et al. (25) that IV vitamin C treatment was associated with a significant lower short-term mortality, whereas with no difference in length of ICU stay and SOFA score.

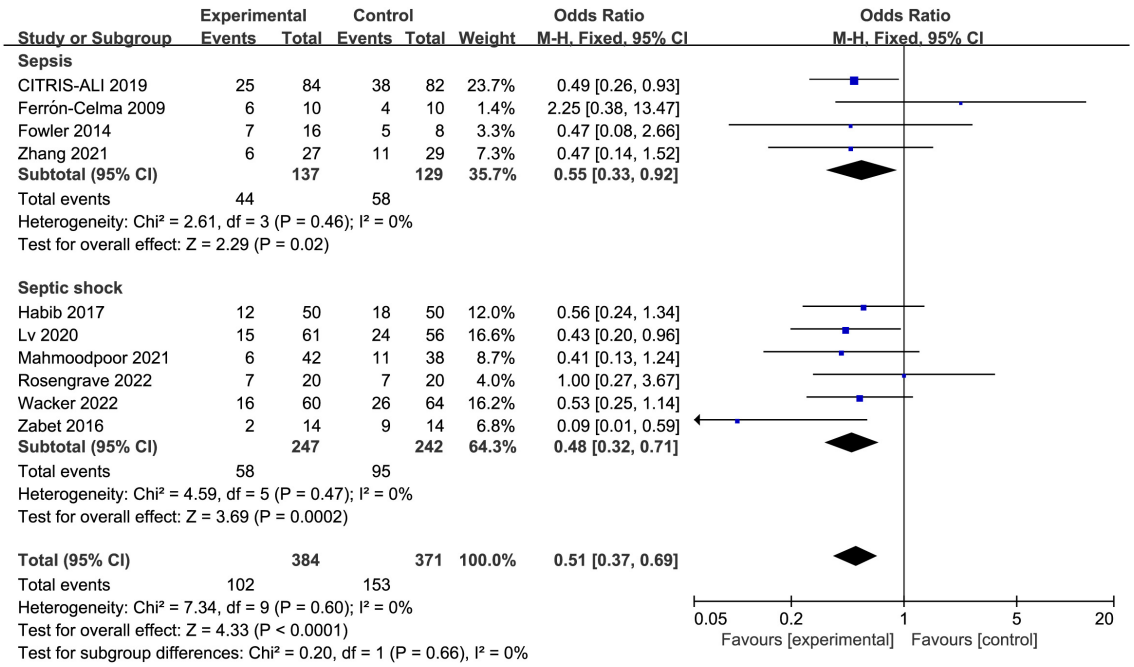

FIGURE 5
Forest plot showing the subgroup analysis of short-term mortality, patients with sepsis vs. patients with septic shock.

The possible mechanisms of the benefit of IV vitamin C treatment in patients with sepsis or septic shock can be explained in several ways. First of all, serum levels of vitamin C decline rapidly among septic patients, confirming their critical involvement in a worsening prognosis (38, 39). The IV vitamin C treatment could restore the plasma vitamin C concentration. All the trials analyzed in our meta-analysis reported an increased serum level of vitamin C in intervention group.

Secondly, some of the physiological effects of vitamin C are of great significance to improve the prognosis of septic patients. Vitamin C is an important antioxidant of the body (40), supports the synthesis of vasopressin, cortisol, and catecholamine (10, 11), increases lymphocytic and neutrophilic activity while attenuating neutrophil necrosis (41, 42). Furthermore, vitamin C also regulates gene expression of pro-inflammatory and coagulation (39, 43), nuclear cellular responses to stress and hypoxia (44), and orchestrates the immune system and circulating cytokine homeostasis in pleotropic ways (42). Therefore, the vital role of vitamin C and its depletion in septic states justifies the use of IV vitamin C in patients with sepsis or septic shock.

However, as suggested by the negative results of some secondary outcomes in our meta-analysis, the beneficial effect of reducing SOFA score or length of ICU stay does not happen. Previous research has demonstrated that some patients might experience hypovitaminosis C as early as 48 h after discontinuation of vitamin C infusion, regardless of the dosing regimen (45). Given that most included trials limited IV vitamin C use to a maximum of 4 days, sustained therapy may be needed to obtain the favorable effects of vitamin C over time. In the CITRIS-ALI trial (29), patients in the 4-day IV vitamin C treatment group had lower 28-day mortality rate, but the survival curve parallel to that of placebo after cessation of vitamin C infusion. The subgroup analysis showed that septic patients received high-dose vitamin C had lower mortality rate and shorter duration of vasopressor, indicating the improvements in clinical outcomes might be dose dependent. Considering the higher dose or longer medication time of IV vitamin C may have produced different results (46), the most effective dose of IV vitamin C and duration of treatment as well as its effects on clinical outcomes also remains to be seen.

However, our study has several limitations. First of all, this meta-analysis was limited by the small sample size of included RCTs, the sample size was relatively small (number of participants < 100 per arm), which may introduce small-study effects and get larger beneficial treatment effects conclusion (47).

Secondly, since sepsis is a clinically common syndrome with high heterogeneity, the studied population represents a heterogeneous population. For example, some were surgical patients after major operation, some had severe pneumonia or respiratory failure. Similarly, the clinical characteristics of included studies were heterogeneous. The baseline of vitamin C level, dose and duration of IV vitamin C, as well as the disease severity of enrolled patients are varied across all the studies. Thus, the pooled estimates should be interpreted with caution since the significant heterogeneity.

TABLE 2 Main findings and subgroup analysis.

Outcome	*N*	Result
Mortality	10	OR 0.51 (0.37, 0.69), I^2 = 0% (P = 0.60)
Type of disease		
Sepsis	7	OR 0.55 (0.33, 0.92), I^2 = 0% (P = 0.46)
Septic shock	3	OR 0.48 (0.32, 0.71), I^2 = 0% (P = 0.47)
		Test for subgroup difference: I^2 = 0%
Dose of vitamin C		
Low	6	OR 0.53 (0.35, 0.79), I^2 = 0% (P = 0.68)
High	5	OR 0.48 (0.30, 0.77), I^2 = 0% (P = 0.37)
		Test for subgroup difference: I^2 = 0%
Duration of vitamin C		
<5 days	6	OR 0.48 (0.32, 0.71), I^2 = 0% (P = 0.49)
≥5 days	4	OR 0.55 (0.34, 0.90), I^2 = 0% (P = 0.42)
		Test for subgroup difference: I^2 = 0%
Duration of vasopressor	6	MD −27.88, 95% CI −49.84 to −5.92, I^2 = 95% (P < 0.00001)
Dose of vitamin C		
Low	3	MD −14.10, 95% CI −29.32 to 1.13, I^2 = 91% (P < 0.00001)
High	5	MD −24.42, 95% CI −47.19 to −1.66, I^2 = 95% (P < 0.00001)
		Test for subgroup difference: I^2 = 0%
Duration of vitamin C		
<5 days	4	MD −13.37, 95% CI −27.42 to 0.68, I^2 = 80% (P = 0.002)
≥5 days	2	MD −58.37, 95% CI −140.71 to 23.97, I^2 = 98% (P < 0.00001)
		Test for subgroup difference: I^2 = 10%
Length of ICU stay	7	MD −0.68, 95% CI −2.13 to 0.78, I^2 = 74% (P = 0.0009)
Type of disease		
Sepsis	1	MD 5.10, 95% CI −2.29 to 12.49
Septic shock	6	MD −0.86, 95% CI −2.30 to 0.57, I^2 = 75% (P = 0.001)
		Test for subgroup difference: I^2 = 59%
Dose of vitamin C		
Low	3	MD −0.60, 95% CI −1.86 to 0.67, I^2 = 56% (P = 0.11)
High	6	MD −0.98, 95% CI −4.14 to 2.18, I^2 = 72% (P = 0.003)
		Test for subgroup difference: I^2 = 0%
Duration of vitamin C		
<5 days	4	MD −0.45, 95% CI −2.24 to 1.34, I^2 = 69% (P = 0.02)
≥5 days	3	MD −0.53, 95% CI −4.55 to 3.48, I^2 = 84% (P = 0.002)
		Test for subgroup difference: I^2 = 0%
SOFA score	5	MD −0.05, 95% CI −1.69 to 1.58, I^2 = 86% (P < 0.00001)
Type of disease		
Sepsis	2	MD −0.32, 95% CI −3.21 to 2.58, I^2 = 85% (P = 0.01)
Septic shock	3	MD 0.17, 95% CI −2.38 to 2.73, I^2 = 90% (P < 0.0001)
		Test for subgroup difference: I^2 = 0%
Dose of vitamin C		
Low	2	MD −0.04, 95% CI −2.96 to 2.88, I^2 = 95% (P < 0.0001)
High	3	MD −0.05, 95% CI −2.36 to 2.27, I^2 = 71% (P = 0.03)
		Test for subgroup difference: I^2 = 0%
Duration of vitamin C		
<5 days	3	MD −0.05, 95% CI −2.26 to 2.16, I^2 = 86% (P = 0.0006)
≥5 days	2	MD −0.11, 95% CI −3.44 to 3.21, I^2 = 88% (P = 0.003)
		Test for subgroup difference: I^2 = 0%

ICU, Intensive Care Unit; OR, Odds Ratio; MD, Mean Difference; CI, Confidence Interval; SOFA, Sequential Organ Failure Assessment.

Moreover, renal impairment is one of the important adverse effects when people receive high-dose IV vitamin C (48). Considering only a few articles reported the incidence of acute kidney injury as vitamin C related adverse event, there was not enough data to evaluate the incidence of acute kidney injury between vitamin C and control group.

Finally, the data for continuous variables were reported using the median, interquartile range, or range in several trials, which were calculated into mean and standard deviation. But there was a certain deviation from the real value that leading to bias into our results.

Conclusion

Among patients with sepsis or septic shock, the IV vitamin C treatment was associated with significant reduction in short-term mortality and duration of vasopressor. Although the statistical heterogeneity considerably weakens the conclusions, the observed favorable effect of IV vitamin C on reducing short-term mortality and duration of vasopressor should be considered. However, we cannot draw a definitive conclusion from this current meta-analysis regarding the optimal dosage or duration of IV vitamin C treatment. Further studies evaluating the effect of different dose or duration of IV vitamin C in septic population are warranted.

Data availability statement

The original contributions presented in this study are included in the article/**Supplementary material**, further inquiries can be directed to the corresponding author.

Author contributions

HZ and QY conceived the idea, performed the analysis, and drafted the initial writing of this manuscript. XX contributed to the collection and interpretation of data. KZ helped to frame the idea of the study and provided technical support. QY contributed to the revision of this manuscript and to the final approval of the version to be published. All authors contributed to the article and approved the submitted version.

Conflict of interest

The authors declare that the research was conducted in the absence of any commercial or financial relationships that could be construed as a potential conflict of interest.

Publisher's note

Supplementary material

The Supplementary Material for this article can be found online at: https://www.frontiersin.org/articles/10.3389/fnut.2022.964484/full#supplementary-material

References

1. Singer M, Deutschman CS, Seymour CW, Shankar-Hari M, Annane D, Bauer M, et al. The third international consensus definitions for sepsis and septic shock (Sepsis-3). *JAMA*. (2016) 315:801–10. doi: 10.1001/jama.2016.0287

2. Evans L, Rhodes A, Alhazzani W, Antonelli M, Coopersmith CM, French C, et al. Surviving sepsis campaign: international guidelines for management of sepsis and septic shock 2021. *Crit Care Med.* (2021) 49:e1063–143. doi: 10.1097/ccm.0000000000005337

3. Fleischmann C, Scherag A, Adhikari NK, Hartog CS, Tsaganos T, Schlattmann P, et al. Assessment of global incidence and mortality of hospital-treated sepsis. current estimates and limitations. *Am J Respir Crit Care Med.* (2016) 193:259–72. doi: 10.1164/rccm.201504-0781OC

4. Reinhart K, Daniels R, Kissoon N, Machado FR, Schachter RD, Finfer S. Recognizing sepsis as a global health priority - a who resolution. *N Engl J Med.* (2017) 377:414–7. doi: 10.1056/NEJMp1707170

5. Rudd KE, Johnson SC, Agesa KM, Shackelford KA, Tsoi D, Kievlan DR, et al. Global, regional, and national sepsis incidence and mortality, 1990–2017: analysis for the global burden of disease study. *Lancet.* (2020) 395:200–11. doi: 10.1016/s0140-6736(19)32989-7

6. Prescott HC, Angus DC. Enhancing recovery from sepsis: a review. *JAMA.* (2018) 319:62–75. doi: 10.1001/jama.2017.17687

7. Wald EL, Badke CM, Hintz LK, Spewak M, Sanchez-Pinto LN. Vitamin therapy in sepsis. *Pediatr Res.* (2022) 91:328–36. doi: 10.1038/s41390-021-01673-6

8. Carr AC, Maggini S. Vitamin c and immune function. *Nutrients.* (2017) 9:1211. doi: 10.3390/nu9111211

9. Spoelstra-de Man AME, Elbers PWG, Oudemans-van Straaten HM. Making sense of early high-dose intravenous vitamin C in ischemia/reperfusion injury. *Crit Care.* (2018) 22:70. doi: 10.1186/s13054-018-1996-y

10. Carr AC, Shaw GM, Fowler AA, Natarajan R. Ascorbate-dependent vasopressor synthesis: a rationale for vitamin C administration in severe sepsis and septic shock? *Crit Care.* (2015) 19:418. doi: 10.1186/s13054-015-1131-2

11. Wilson JX. Evaluation of vitamin C for adjuvant sepsis therapy. *Antioxid Redox Signal.* (2013) 19:2129–40. doi: 10.1089/ars.2013.5401

12. Fisher BJ, Kraskauskas D, Martin EJ, Farkas D, Wegelin JA, Brophy D, et al. Mechanisms of attenuation of abdominal sepsis induced acute lung injury by ascorbic acid. *Am J Physiol Lung Cell Mol Physiol.* (2012) 303:L20–32. doi: 10.1152/ajplung.00300.2011

13. Galley HF, Walker BE, Howdle PD, Webster NR. Regulation of nitric oxide synthase activity in cultured human endothelial cells: effect of antioxidants. *Free Radic Biol Med.* (1996) 21:97–101. doi: 10.1016/0891-5849(95)02216-3

14. Fujii T, Salanti G, Belletti A, Bellomo R, Carr A, Furukawa TA, et al. Effect of adjunctive vitamin C, glucocorticoids, and vitamin B1 on longer-term mortality in adults with sepsis or septic shock: a systematic review and a component network meta-analysis. *Intensive Care Med.* (2022) 48:16–24. doi: 10.1007/s00134-021-06558-0

15. Assouline B, Faivre A, Verissimo T, Sangla F, Berchtold L, Giraud R, et al. Thiamine, ascorbic acid, and hydrocortisone as a metabolic resuscitation cocktail in sepsis: a meta-analysis of randomized controlled trials with trial sequential analysis. *Crit Care Med.* (2021) 49:2112–20. doi: 10.1097/ccm.0000000000005262

16. Yao R, Zhu Y, Yu Y, Li Z, Wang L, Zheng L, et al. Combination therapy of thiamine, vitamin C and hydrocortisone in treating patients with sepsis and septic shock: a meta-analysis and trial sequential analysis. *Burns Trauma.* (2021) 9:tkab040. doi: 10.1093/burnst/tkab040

17. Zayed Y, Alzghoul BN, Banifadel M, Venigandla H, Hyde R, Sutchu S, et al. Vitamin C, thiamine, and hydrocortisone in the treatment of sepsis: a meta-analysis and trial sequential analysis of randomized controlled trials. *J Intensive Care Med.* (2022) 37:327–36. doi: 10.1177/0885066620987809

18. Na W, Shen H, Li Y, Qu D. Hydrocortisone, ascorbic acid, and thiamine (HAT) for sepsis and septic shock: a meta-analysis with sequential trial analysis. *J Intensive Care.* (2021) 9:75. doi: 10.1186/s40560-021-00589-x

19. Cai B, Lv X, Lin M, Feng C, Chen C. Clinical efficacy and safety of vitamin C in the treatment of septic shock patients: systematic review and meta-analysis. *Ann Palliat Med.* (2022) 11:1369–80. doi: 10.21037/apm-22-225

20. Li T, Zeng J, Li DH, Yang GY, Wang K, Deng HF, et al. Efficacy of intravenous vitamin C intervention for septic patients: a systematic review and meta-analysis based on randomized controlled trials. *Am J Emerg Med.* (2021) 50:242–50. doi: 10.1016/j.ajem.2021.08.012

21. Page MJ, McKenzie JE, Bossuyt PM, Boutron I, Hoffmann TC, Mulrow CD, et al. The PRISMA 2020 statement: an updated guideline for reporting systematic reviews. *BMJ.* (2021) 372:n71. doi: 10.1136/bmj.n71

22. Higgins JP, Altman DG, Gøtzsche PC, Jüni P, Moher D, Oxman AD, et al. The cochrane collaboration's tool for assessing risk of bias in randomised trials. *BMJ.* (2011) 343:d5928. doi: 10.1136/bmj.d5928

23. Higgins JP, Thompson SG, Deeks JJ, Altman DG. Measuring inconsistency in meta-analyses. *BMJ.*(2003) 327:557–60. doi: 10.1136/bmj.327.7414.557

24. Egger M, Davey Smith G, Schneider M, Minder C. Bias in meta-analysis detected by a simple, graphical test. *BMJ.* (1997) 315:629–34. doi: 10.1136/bmj.315.7109.629

25. Patel JJ, Ortiz-Reyes A, Dhaliwal R, Clarke J, Hill A, Stoppe C, et al. IV Vitamin C in critically ill patients: a systematic review and meta-analysis. *Crit Care Med.* (2022) 50:e304–12. doi: 10.1097/ccm.0000000000005320

26. Jung SY, Lee MT, Baek MS, Kim WY. Vitamin C for $\geq$ 5 days is associated with decreased hospital mortality in sepsis subgroups: a nationwide cohort study. *Crit Care.* (2022) 26:3. doi: 10.1186/s13054-021-03872-3

27. Ferrón-Celma I, Mansilla A, Hassan L, Garcia-Navarro A, Comino AM, Bueno P, et al. Effect of vitamin C administration on neutrophil apoptosis in septic patients after abdominal surgery. *J Surg Res.* (2009) 153:224–30. doi: 10.1016/j.jss.2008.04.024

28. Fowler AA, Syed AA, Knowlson S, Sculthorpe R, Farthing D, DeWilde C, et al. Phase I safety trial of intravenous ascorbic acid in patients with severe sepsis. *J Transl Med.* (2014) 12:32. doi: 10.1186/1479-5876-12-32

29. Fowler AA III, Truwit JD, Hite RD, Morris PE, DeWilde C, Priday A, et al. effect of vitamin c infusion on organ failure and biomarkers of inflammation and vascular injury in patients with sepsis and severe acute respiratory failure: the citris-ali randomized clinical trial. *JAMA.* (2019) 322:1261–70. doi: 10.1001/jama.2019.11825

30. Lv SJ, Zhang GH, Xia JM, Yu H, Zhao F. Early use of high-dose vitamin C is beneficial in treatment of sepsis. *Ir J Med Sci.* (2021) 190:1183–8. doi: 10.1007/s11845-020-02394-1

31. Mahmoodpoor A, Shadvar K, Sanaie S, Hadipoor MR, Pourmoghaddam MA, Saghaleini SH. Effect of Vitamin C on mortality of critically ill patients with severe pneumonia in intensive care unit: a preliminary study. *BMC Infect Dis.* (2021) 21:616. doi: 10.1186/s12879-021-06288-0

32. Rosengrave P, Spencer E, Williman J, Mehrtens J, Morgan S, Doyle T, et al. Intravenous vitamin C administration to patients with septic shock: a pilot randomised controlled trial. *Crit Care.* (2022) 26:26. doi: 10.1186/s13054-022-03900-w

33. Wacker DA, Burton SL, Berger JP, Hegg AJ, Heisdorffer J, Wang Q, et al. Evaluating Vitamin C in Septic Shock: a randomized controlled trial of Vitamin c monotherapy. *Crit Care Med.* (2022) 50:e458–67. doi: 10.1097/CCM.0000000000005427

34. Zabet MH, Mohammadi M, Ramezani M, Khalili H. Effect of high-dose ascorbic acid on vasopressor's requirement in septic shock. *J Res Pharm Pract.* (2016) 5:94–100. doi: 10.4103/2279-042X.179569

35. Zhang J, Rao X, Li Y, Zhu Y, Liu F, Guo G, et al. Pilot trial of high-dose vitamin C in critically ill COVID-19 patients. *Ann Intensive Care.* (2021) 11:5. doi: 10.1186/s13613-020-00792-3

36. Habib NT, Ahmed I. Early Adjuvant Intravenous Vitamin C Treatment in Septic Shock may Resolve the Vasopressor Dependence. *Int J Microbiol Adv Immunol.* (2017) 5:77–81. doi: 10.19070/2329-9967-1700015

37. Wan X, Wang W, Liu J, Tong T. Estimating the sample mean and standard deviation from the sample size, median, range and/or interquartile range. *BMC Med Res Methodol.* (2014) 14:135. doi: 10.1186/1471-2288-14-135

38. Carr AC, Rosengrave PC, Bayer S, Chambers S, Mehrtens J, Shaw GM. Hypovitaminosis C and vitamin C deficiency in critically ill patients despite recommended enteral and parenteral intakes. *Crit Care.* (2017) 21:300. doi: 10.1186/s13054-017-1891-y

39. Borrelli E, Roux-Lombard P, Grau GE, Girardin E, Ricou B, Dayer J, et al. Plasma concentrations of cytokines, their soluble receptors, and antioxidant vitamins can predict the development of multiple organ failure in patients at risk. *Crit. Care Med.* (1996) 24:392–7. doi: 10.1097/00003246-199603000-00006

40. Wilson JX. Mechanism of action of vitamin C in sepsis: ascorbate modulates redox signaling in endothelium. *Biofactors.* (2009) 35:5–13. doi: 10.1002/biof.7

41. Manning J, Mitchell B, Appadurai DA, Shakya A, Pierce LJ, Wang H, et al. Vitamin C promotes maturation of T-cells. *Antioxid Redox Signal.* (2013) 19:2054–67. doi: 10.1089/ars.2012.4988

42. Kashiouris MG, L'Heureux M, Cable CA, Fisher BJ, Leichtle SW, Fowler AA. The emerging role of vitamin c as a treatment for sepsis. *Nutrients.* (2020) 12:292. doi: 10.3390/nu12020292

43. Mikirova N, Riordan N, Casciari J. Modulation of cytokines in cancer patients by intravenous ascorbate therapy. *Med Sci Monit.* (2016) 22:14–25. doi: 10.12659/msm.895368

44. Oudemans-van Straaten HM, Spoelstra-de Man AM, de Waard MC. Vitamin C revisited. *Crit Care.* (2014) 18:460. doi: 10.1186/s13054-014-0460-x

45. de Grooth H-J, Manubulu-Choo W-P, Zandvliet AS, Spoelstra - de Man AME, Girbes AR, Swart EL, et al. Vitamin C pharmacokinetics in critically ill patients: a randomized trial of four iv regimens. *Chest.* (2018) 153:1368–77. doi: 10.1016/j.chest.2018.02.025

46. Fujii T, Deane AM, Nair P. Metabolic support in sepsis: corticosteroids and vitamins: the why, the when, the how. *Curr Opin Crit Care.* (2020) 26:363–8. doi: 10.1097/mcc.0000000000000736

47. Zhang Z, Xu X, Ni H. Small studies may overestimate the effect sizes in critical care meta-analyses: a meta-epidemiological study. *Crit Care.* (2013) 17:R2. doi: 10.1186/cc11919

48. Padayatty SJ, Sun AY, Chen Q, Espey MG, Drisko J, Levine M. Vitamin C: intravenous use by complementary and alternative medicine practitioners and adverse effects. *PLoS One.* (2010) 5:e11414. doi: 10.1371/journal.pone.0011414

frontiers | Frontiers in Nutrition

TYPE Original Research
PUBLISHED 29 July 2022
DOI 10.3389/fnut.2022.961697

OPEN ACCESS

EDITED BY
Nada Rotovnik Kozjek,
Institute of Oncology
Ljubljana, Slovenia

REVIEWED BY
Wei Hu,
Guilin People's Hospital, China
Haixin Huang,
Liuzhou Workers Hospital, China

*CORRESPONDENCE
Keng Po Lai
laikp_hospital@126.com

†These authors contributed equally to this work

SPECIALTY SECTION
This article was submitted to Clinical Nutrition, a section of the journal Frontiers in Nutrition

RECEIVED 05 June 2022
ACCEPTED 01 August 2022
PUBLISHED 29 July 2022

CITATION
Li J, Peng P and Lai KP (2022) Therapeutic targets and functions of curcumol against COVID-19 and colon adenocarcinoma. *Front. Nutr.* 9:961697. doi: 10.3389/fnut.2022.961697

Therapeutic targets and functions of curcumol against COVID-19 and colon adenocarcinoma

Jun Li[1†], Peng Peng[2†] and Keng Po Lai[3*]

[1]The Pharmaceutical Department, The Second Affiliated Hospital of Guangxi Medical University, Nanning, China, [2]Department of Gastroenterology, The Second Affiliated Hospital of Guangxi Medical University, Nanning, China, [3]Clinical Medicine Research Center, The Second Affiliated Hospital of Guangxi Medical University, Nanning, China

Since 2019, the coronavirus disease (COVID-19) has caused 6,319,395 deaths worldwide. Although the COVID-19 vaccine is currently available, the latest variant of the virus, Omicron, spreads more easily than earlier strains, and its mortality rate is still high in patients with chronic diseases, especially cancer patients. So, identifying a novel compound for COVID-19 treatment could help reduce the lethal rate of the viral infection in patients with cancer. This study applied network pharmacology and systematic bioinformatics analysis to determine the possible use of curcumol for treating colon adenocarcinoma (COAD) in patients infected with COVID-19. Our results showed that COVID-19 and COAD in patients shared a cluster of genes commonly deregulated by curcumol. The clinical pathological analyses demonstrated that the expression of gamma-aminobutyric acid receptor subunit delta (GABRD) was associated with the patients' hazard ratio. More importantly, the high expression of GABRD was associated with poor survival rates and the late stages of COAD in patients. The network pharmacology result identified seven-core targets, including solute carrier family 6 member 3, gamma-aminobutyric acid receptor subunit pi, butyrylcholinesterase, cytochrome P450 3A4, 17-beta-hydroxysteroid dehydrogenase type 2, progesterone receptor, and GABRD of curcumol for treating patients with COVID-19 and COAD. The bioinformatic analysis further highlighted their importance in the biological processes and molecular functions in gland development, inflammation, retinol, and steroid metabolism. The findings of this study suggest that curcumol could be an alternative compound for treating patients with COVID-19 and COAD.

KEYWORDS

colon adenocarcinoma, COVID-19, curcumol, bioinformatics, biological functions, pharmaceutics targets

Introduction

Since 2019, 537,591,764 confirmed coronavirus disease (COVID-19) cases, leading to 6,319,395 deaths worldwide, have been reported by WHO as of June 20, 2022 (https://covid19.who.int). Chronic health conditions were associated with the risk of COVID-19-related hospitalization and mortality (1). Patients with cancer are highly susceptible to

severe symptoms (2). A systematic review of 52 pooled studies showed that patients with cancer and infected with COVID-19 exhibited a higher death risk (3). Similarly, Ahmadi's group showed that COVID-19 brings unfavorable survival outcomes for patients with colon cancer *via* the alteration of the immune cell infiltration-linked process (4), and the COVID-19 pandemic led to widespread disruption of colorectal cancer services (5). So, there is a need to identify alternative therapeutic compounds to reduce the severity and mortality rate of COVID-19 in patients with cancer. Colon adenocarcinoma (COAD), the most frequently diagnosed histological subtype of colorectal cancer, is one of the most prevalent malignant tumors in the gastrointestinal system worldwide (6, 7). The 5-year survival rate of patients with advanced COAD is < 10% (8). Cumulating evidence has suggested the effectiveness of Traditional Chinese Medicines (TCMs) in cancer treatment (9, 10). One of the possible mechanisms is immune system regulation in patients with cancer (11). In addition, TCMs modulate the gut microbiota, which is considered a pathogenic factor of COAD (12). Besides the antitumor role, TCMs have also been reported to be effective in treating COVID-19 *via* their antiviral and anti-inflammatory activities (13, 14). Curcumol, a common TCM, is isolated from *Rhizoma curcumae*. The antitumor and antiviral effects of curcumol are well-documented (15, 16). Curcumol, in particular, has been shown to induce cell cycle arrest and increase the sensitivity of colon cancer to chemotherapy (17, 18). This study aimed to determine the pharmacological targets and the molecular mechanisms controlled by curcumol using network pharmacology and an *in vitro* COAD model. The results of this study will provide novel insight into the possible use of curcumol for treating patients with COAD and COVID-19.

Materials and methods

Identification of curcumol's targets against COAD and COVID-19

The transcriptome data from patients with COAD were obtained from The Cancer Genome Atlas (TCGA) database (https://portal.gdc.cancer.gov/) to identify COAD-associated genes. Using the DEseq2 package of R&Bioconductor, genes with a false discovery rate of <0.05 and a |logfold change| of >1 were considered differentially expressed genes (19). For the COVID-19-associated genes, keywords such as "coronavirus COVID-19," "coronavirus disease 2019," "severe acute respiratory syndrome coronavirus 2," and "COVID-19" were subjected to databases search, including the Genecards Database, Online Mendelian Inheritance in Man Database (https://omim.org/), Therapeutic Target Database (20), Comparative Toxicogenomics Database (21), and National Center for Biotechnology Information (https://www.ncbi.nlm.nih.gov/). The pharmacological targets of curcumol were determined using various online tools and databases, including Swiss Target Prediction and Bioinformatics Analysis Tool for Molecular Mechanisms of Traditional Chinese Medicine (Batman-TCM) (22, 23). The target genes were subjected to UniProt for human database correction (24). The COVID-19-, COAD-, and curcumol-associated genes were compared and overlapped to obtain the potential curcumol's targets for treating COVID-19 and COAD.

Clinicopathological analysis and functional characterization of curcumol's targets against COAD and COVID-19

To determine the pathological roles of the curcumol's targets in COAD, Cox proportional hazards models were applied in univariate survival analysis as a function of clinical variables and gene expression. The interaction of the identified curcumol's targets was analyzed using the STRING database (version 11.0) and Cytoscape (version 3.6.1) (25, 26). The functions and signaling pathways of curcumol's targets against COAD and COVID-19 were determined using Gene Ontology (GO) and Kyoto Encyclopedia of Genes and Genomes (KEGG) pathway enrichment analyses.

Cell culture study

The human lung adenocarcinoma cell line, A549, was incubated with high glucose Dulbecco's Modified Eagle Medium (DMEM, Solarbio, Beijing), 0.5% penicillin-streptomycin (Solarbio, Beijing), and 5% fetal bovine serum (Solarbio, Beijing) in 5% CO_2 at 37°C.

Cell proliferation analysis

The cells were cultured in a 96-well plate at a cell density of 2×10^4 cells/well and treated with different doses of curcumol (5, 25, and 75 μM) for 48 h. Following the co-incubation, cell proliferation was calculated using the cell-counting-kit-8 method (Beyotime Biotechnology, China), as reported previously (27).

Abbreviations: COAD, colon adenocarcinoma; COVID-19, coronavirus disease 2019; TCGA, The Cancer Genome Atlas; GO, gene ontology; KEGG, Kyoto Encyclopedia of Genes and Genomes; TCMSP, Traditional Chinese Medicine Systems Pharmacology Database and Analysis Platform; OS, overall survival; TCMs, Traditional Chinese Medicines; SLC6A3, solute carrier family 6 member 3; GABRP, gamma-aminobutyric acid receptor subunit pi; BCHE, butyrylcholinesterase; CYP3A4, cytochrome P450 3A4; HSD17B2, 17-beta-hydroxysteroid dehydrogenase type 2; PGR, progesterone receptor; GABRD, gamma-aminobutyric acid receptor subunit delta.

Immunostaining procedures

After the curcumol treatment, A549 cells were fixed with a freshly prepared paraformaldehyde solution (4%, v/v) for 30 min at room temperature, followed by blocking with bovine serum albumin solution (5%, v/v) for 1 h at room temperature. The cells were then incubated at 4°C overnight with primary antibodies against BCHE or CYP3A4 (1:200, Bioss, Beijing, China). The secondary antibody with a fluorescent dye (Beyotime Biotechnology, China) was applied to bind the antigen–antibody complex. The cell nuclei were stained using 4', 6-diamidino-2-phenylindole dihydrochloride dye (Abcam, United States). The fluorescence-labeled positive cells were counted under the fluorescence microscropy system.

Statistical analysis

The statistical data were expressed as the mean ± standard deviation. Comparisons between control and treatment groups were determined using the Statistical Product and Service Solutions (SPSS, 19.0 version) software (Chicago, IL, United States), followed by a one-way analysis of variance (ANOVA) using Tukey's *post-hoc* test. The statistical significance was identified as $p < 0.05$.

Results

Identification of pharmacological targets of curcumol for treating COVID-19 and COAD

We searched the available online databases and identified 8,339 genes associated with COVID-19 (Figure 1A). To identify COAD-associated genes, we analyzed the transcriptome data of patients with COAD and obtained 6,456 differentially expressed genes (Figure 1A). When the COVID-19- and COAD-associated genes were compared, 803 shared genes were found (Figure 1B), of which 414 downregulated and 389 upregulated genes were identified in patients with COAD (Figure 1B). In addition, we identified 151 curcumol-associated genes from different databases (Figure 1A). Then, we compared the curcumol-associated genes with COVID-19/COAD-associated genes to determine the pharmacological targets of curcumol in COVID-19 and COAD. We found 18 target genes shared by curcumol, COVID-19, and COAD (Figure 1A). The molecular network analysis using Cytoscape further highlighted the protein–protein interaction of the 7 core targets, including solute carrier family 6 member 3 (SLC6A3), gamma-aminobutyric acid receptor subunit pi (GABRP), butyrylcholinesterase (BCHE), cytochrome P450 3A4 (CYP3A4), 17-beta-hydroxysteroid dehydrogenase type 2 (HSD17B2), progesterone receptor (PGR), and gamma-aminobutyric acid receptor subunit delta (GABRD) of curcumol against COVID-19 and COAD (Figure 1C; Supplementary Table 1).

Clinicopathological analysis of curcumol's target genes for treating COVID-19 and COAD

Cox proportional hazards models were applied in univariate analysis of overall survival (OS) as a function of clinical variables and gene expression of the 7 core targets. Our results showed that the expression of GABRD was significantly associated with the hazard ratio of COAD (Supplementary Table 2). Survival analysis using the Kaplan–Meier estimator further highlighted that the COAD patients with higher expression of GABRD had a poorer OS rate (Figure 2A). In addition, the higher expression of GABRD was correlated with the later stage (Figure 2B), metastatic tumor (Figure 2C), and a higher number of tumors spread to the lymph nodes (Figure 2D) in COAD.

Functional characterization of curcumol for treating COVID-19 and COAD

The core targets of curcumol were subjected to GO and KEGG enrichment analyses to determine their functional role in treating COVID-19 and COAD. In the GO analysis, our results highlighted the biological processes related to metabolism and biosynthesis, especially fat metabolism and biosynthesis, such as long-chain fatty acid biosynthetic and metabolic processes and fat-soluble vitamin metabolic processes (Figure 3A). In addition, steroid hormone biosynthesis and steroid hormone-mediated signaling pathways were found to be controlled by curcumol's targets (Figure 3A). More importantly, we found curcumol's targets' contributions to the biological processes related to growth and development, especially gland development (Figure 3B). In terms of molecular function, our results highlighted the steroid binding and activities such as steroid hormone receptor, steroid dehydrogenase, and steroid hydroxylase activities (Figure 3C).

Moreover, many molecular functions related to ion channels, such as ion channel, anion transmembrane transporter, sodium symporter, chloride symporter, and extracellular ligand-gated ion channel activities, were observed (Figure 3C). The observed biological processes and molecular functions occurred in the chloride channel complex, nuclear envelope lumen, ion channel complex, transmembrane transporter complex, transporter complex, organelle envelope lumen, and plasma membrane raft (Figure 3D). Finally, the KEGG pathway enrichment further highlighted the involvement of curcumol's targets in steroid hormone biosynthesis, retrograde endocannabinoid signaling, chemical

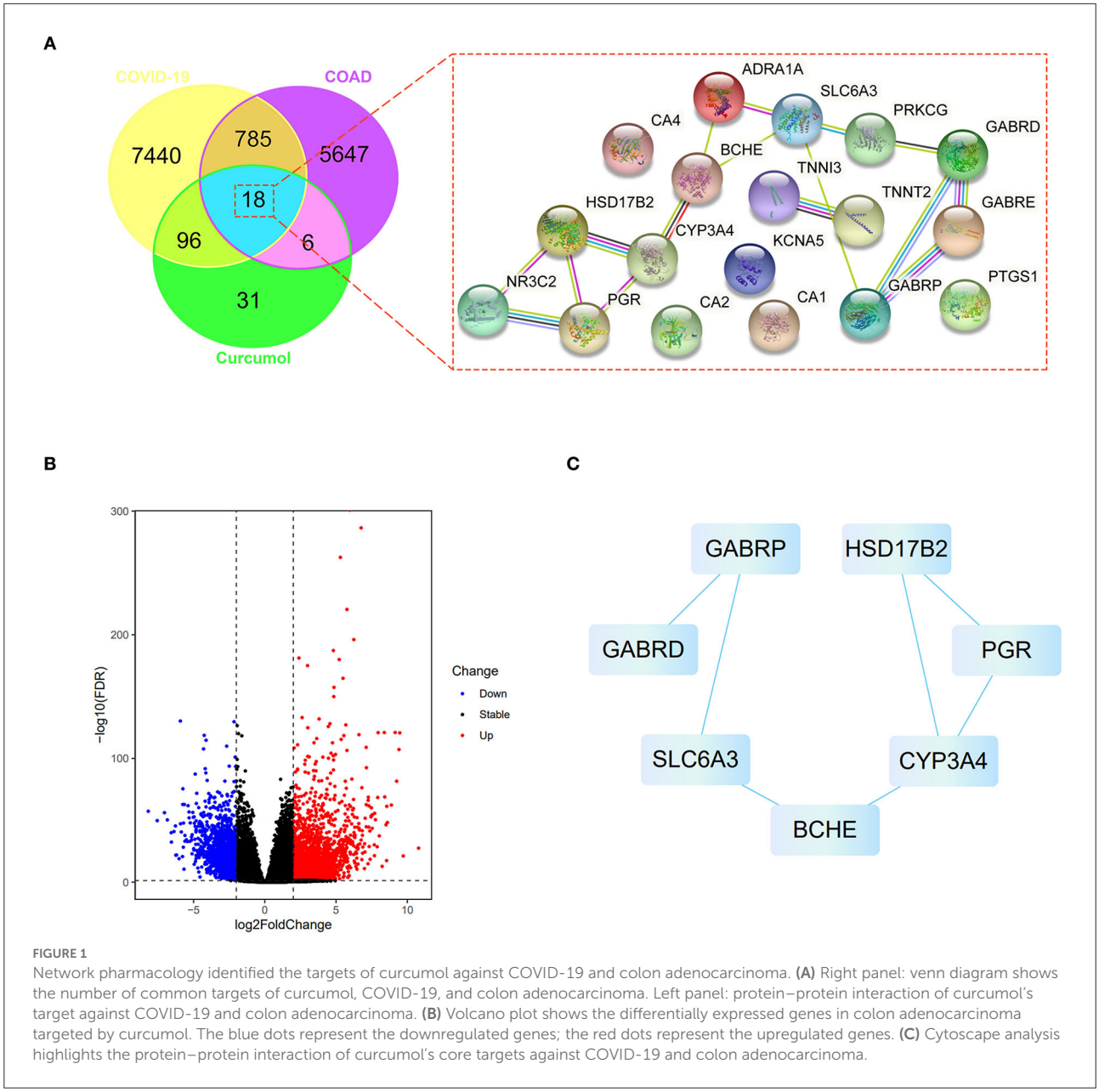

FIGURE 1
Network pharmacology identified the targets of curcumol against COVID-19 and colon adenocarcinoma. **(A)** Right panel: venn diagram shows the number of common targets of curcumol, COVID-19, and colon adenocarcinoma. Left panel: protein–protein interaction of curcumol's target against COVID-19 and colon adenocarcinoma. **(B)** Volcano plot shows the differentially expressed genes in colon adenocarcinoma targeted by curcumol. The blue dots represent the downregulated genes; the red dots represent the upregulated genes. **(C)** Cytoscape analysis highlights the protein–protein interaction of curcumol's core targets against COVID-19 and colon adenocarcinoma.

carcinogenesis through receptor activation, and DNA adducts linoleic acid and retinol metabolism (Figure 3E).

Curcumol treatment suppressed cell proliferation and altered the expression of BCHE and CYP3A4 in the COAD cell line

Cell proliferation was determined using the MTT assay to assess the pharmacological action of curcumol on lung cancer cells, A549. Our data indicated that the treatments with curcumol caused a significant dose-dependent inhibition of cell proliferation in lung adenocarcinoma cells (Figure 4A). In addition, immunofluorescence staining analysis showed that curcumol treatment resulted in increased expression of BCHE and reduced expression of CYP3A4 in A549 cells, as compared to the control group (Figure 4B).

Discussion

This study aimed to investigate the possible use of curcumol therapy for COVID-19 and COAD comorbidity. Using network pharmacology, we identified 7 core targets of

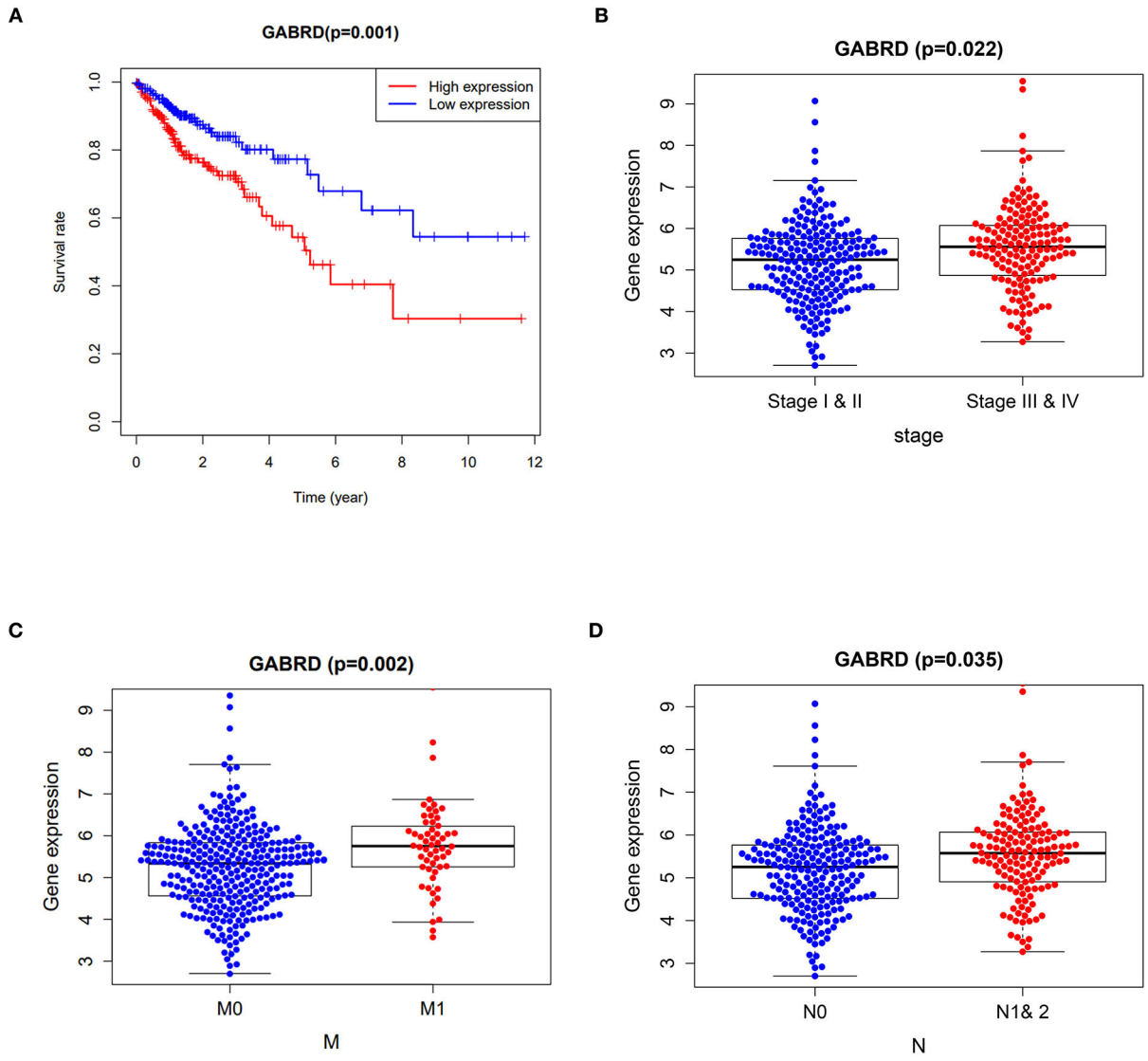

FIGURE 2
Clinicopathological analysis of curcumol's targets against COVID-19 and colon adenocarcinoma. **(A)** Survival analysis using the Kaplan–Meier estimator showed that the colon adenocarcinoma patients with higher expression of GABRD had poorer overall survival rates. Higher expressions of GABRD in colon adenocarcinoma patients are associated with **(B)** advanced stages, **(C)** metastatic tumors, and **(D)** a higher number of tumors spread to the lymph nodes. M0 means cancer has not spread to distant organs. M1 means cancer has spread to distant organs. N represents the number of lymph nodes containing the tumor.

curcumol against COVID-19 and COAD, including GABRD, GABRP, BCHE, CYP3A4, PGR, HSD17B2, and SLC6A3. Our clinicopathological analysis further suggested the prognostic value of GABRD in patients with COAD. GABRD, a subunit of GABAA receptor subtypes, has been reported to be associated with the development of many cancers (28). A clinical study suggested that GABRD promoted progression and predicted poor prognosis in colorectal cancer (29). In addition, gene set enrichment analysis further showed that the enhanced expression of GABRD predicted poor prognosis in patients with COAD (30). In our results, another GABA subunit, GABRP, was also found to be targeted by curcumol. It was reported that GABRP regulated macrophage recruitment and tumor progression in pancreatic cancer (31). In breast cancer, GABRP was found to control the stemness of triple-negative breast cancer cells through epidermal growth factor receptor signaling (32).

A study of the bronchial asthma mice model showed that the inhibition of GABRP could reduce the differentiation of airway epithelial progenitor cells into goblet cells, leading to reduced inflammation (33). So, the GABAA receptor subtypes GABRD and GABRP might be the promising targets of

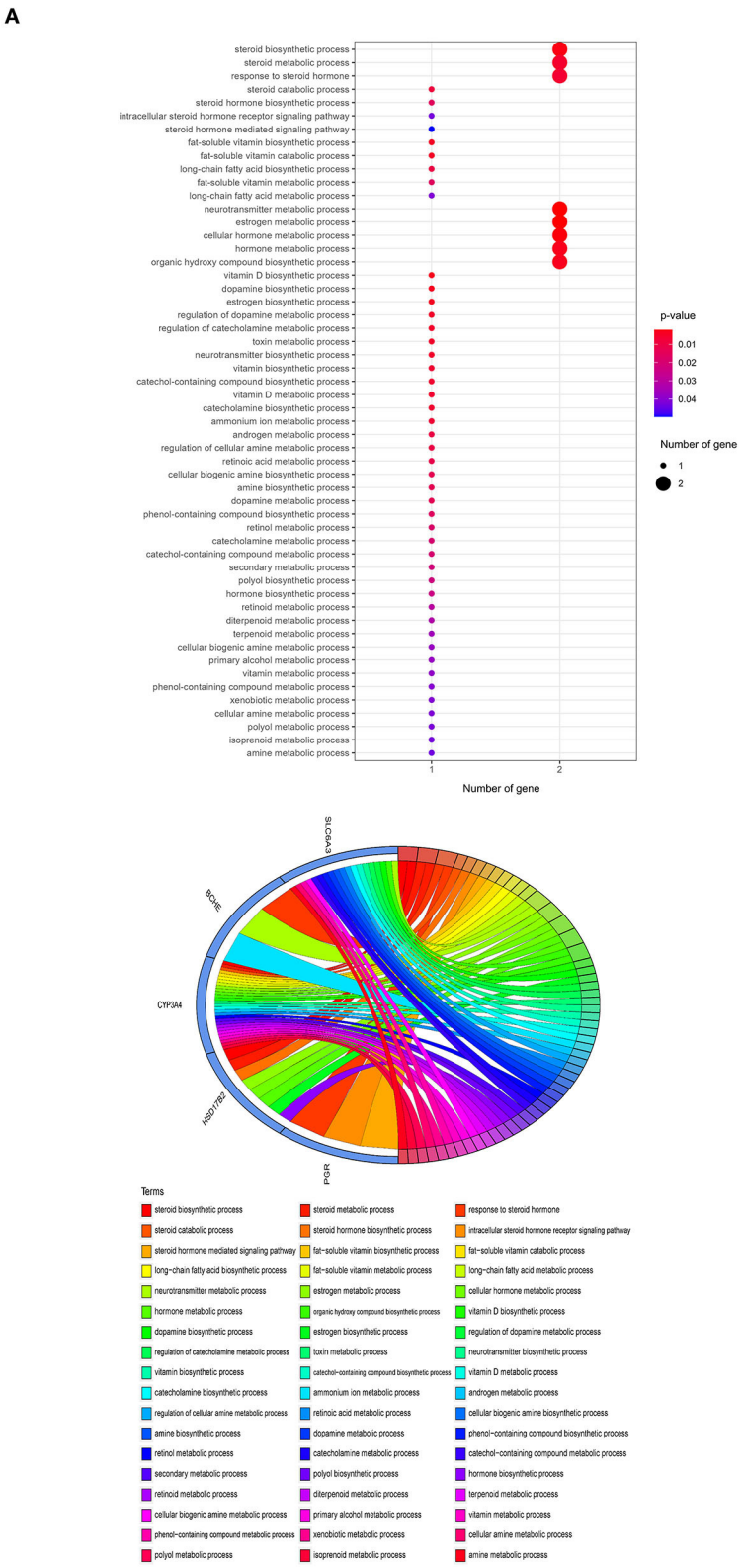

FIGURE 3
(Continued)

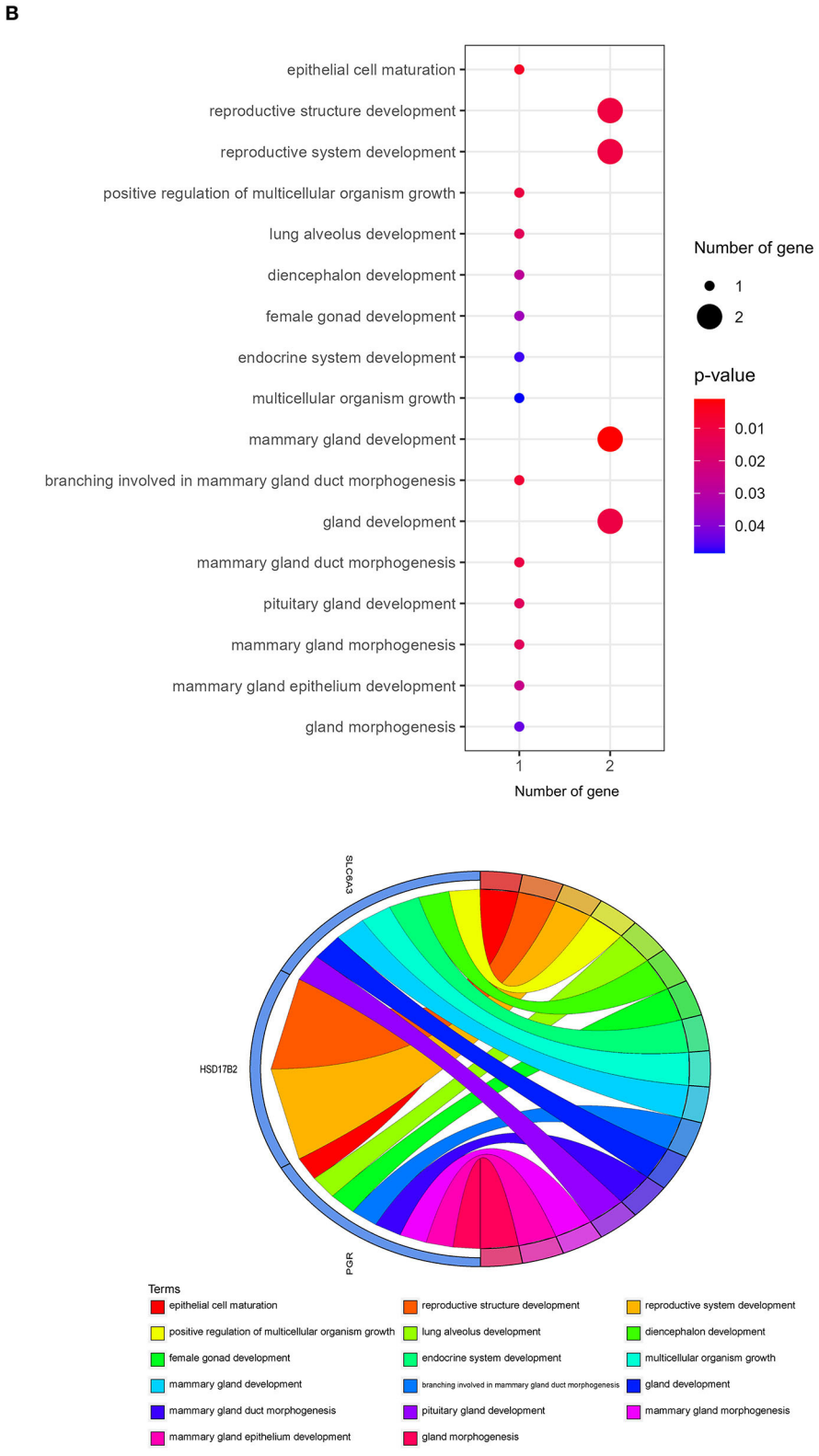

FIGURE 3
(Continued)

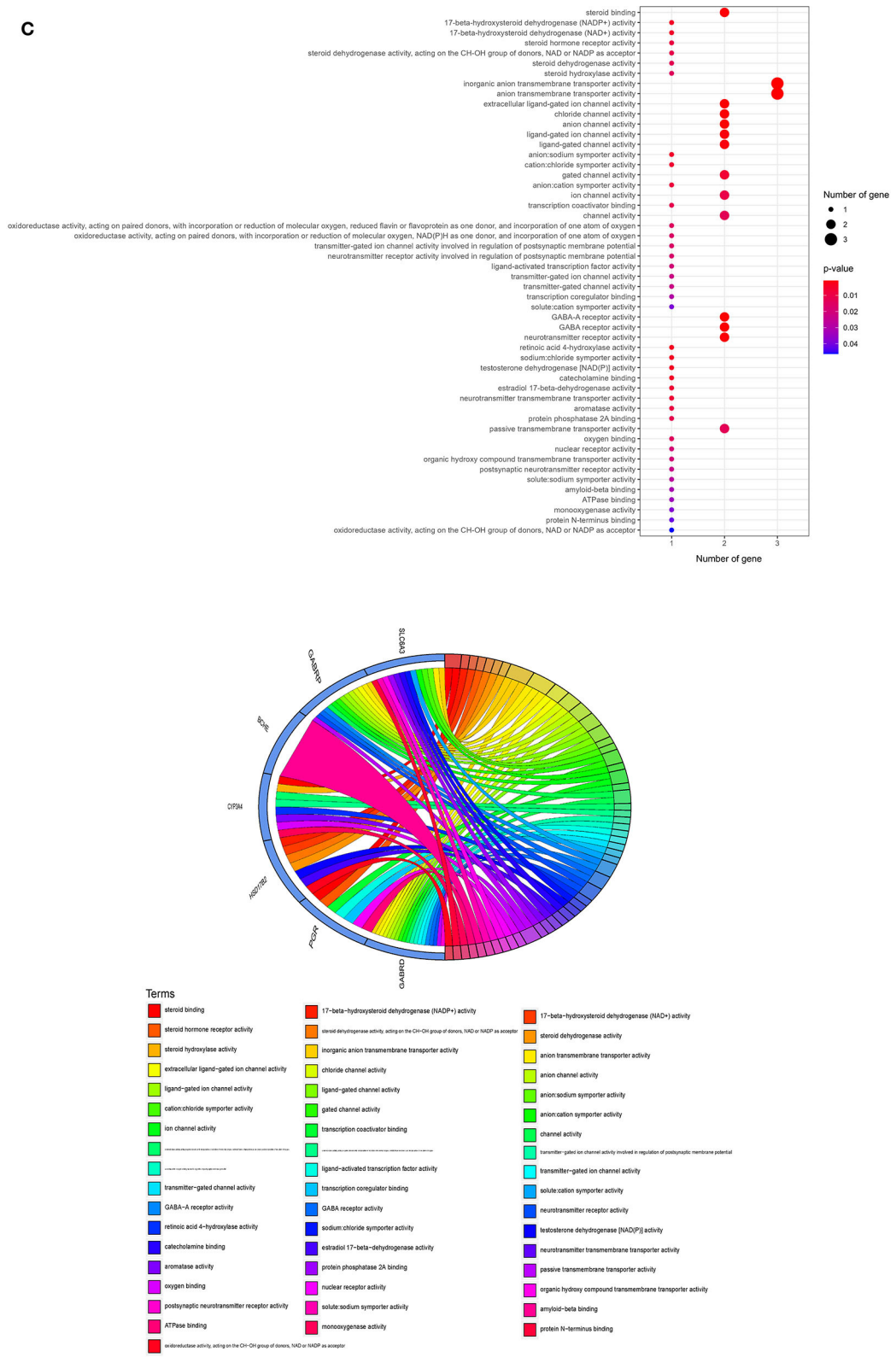

FIGURE 3
(Continued)

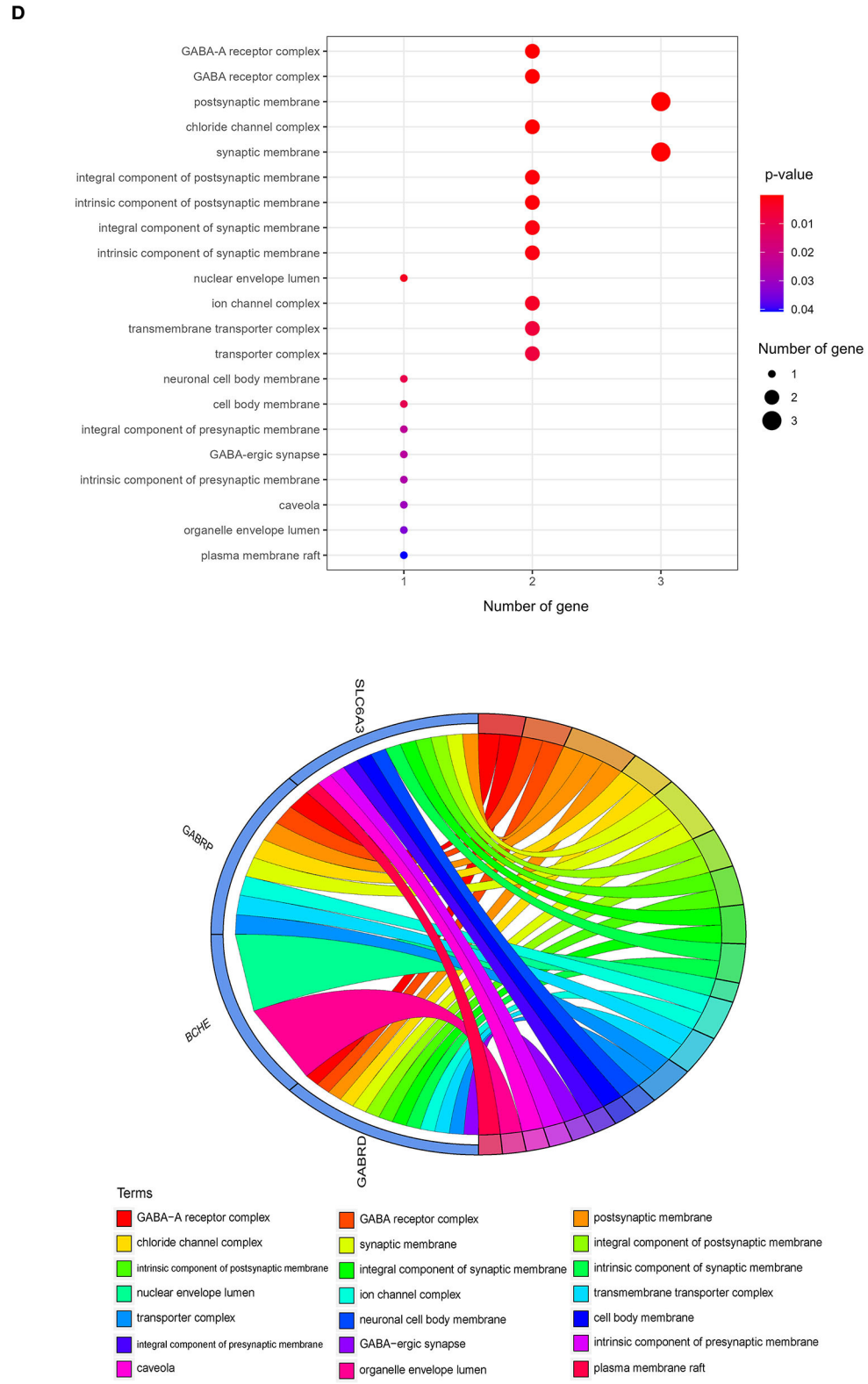

FIGURE 3
(Continued)

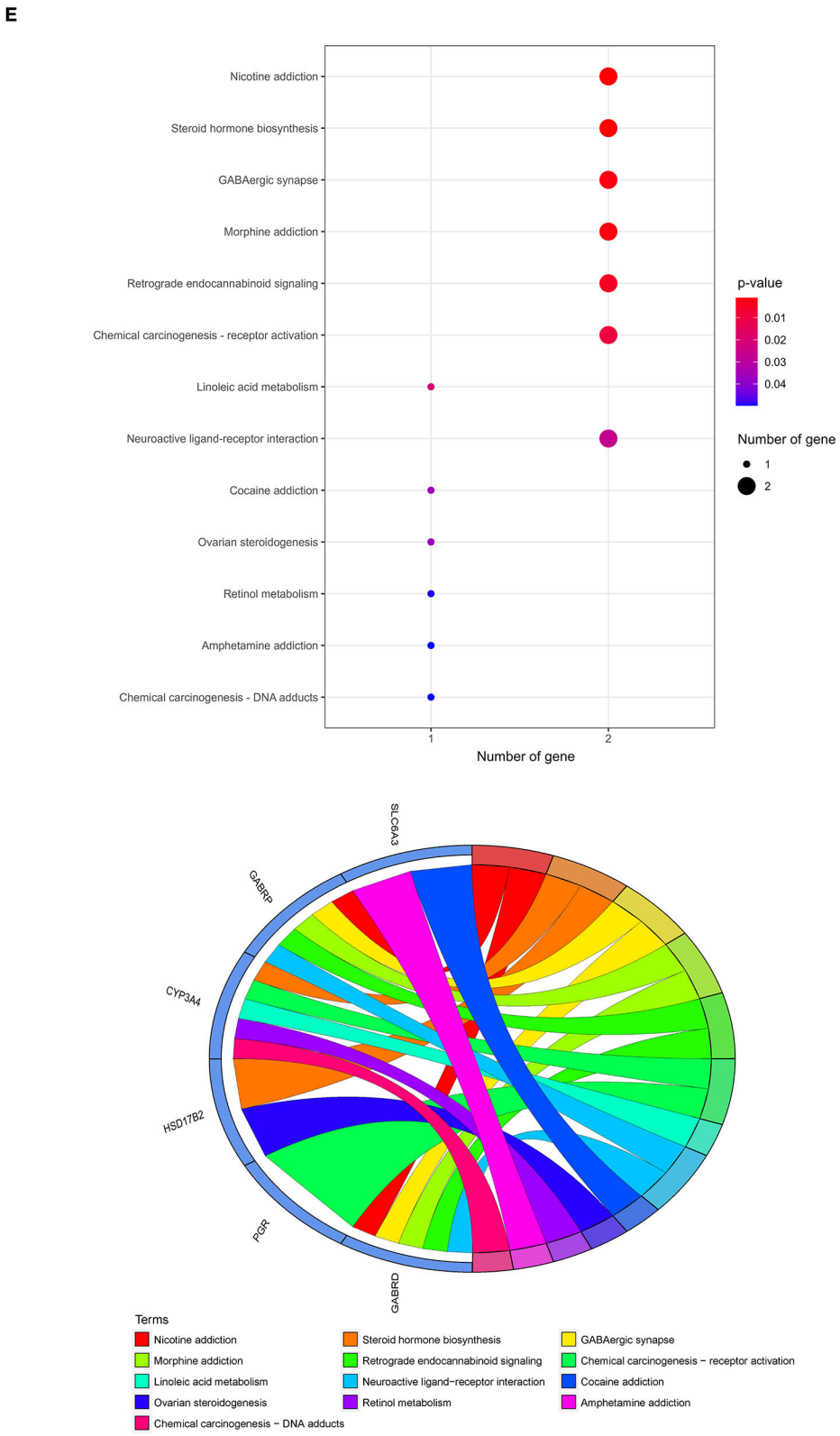

FIGURE 3
Functional characterization of curcumol's targets against COVID-19 and colon adenocarcinoma. The bubble plot highlights the involvement of curcumol's targets in biological processes related to **(A)** fat and steroid hormone biosynthesis, **(B)** gland development, and **(C)** steroid binding and ion channel activity. **(D)** Gene ontology showed the occurred cell components. **(E)** KEGG enrichment analysis showed the contribution of curcumol's targets in cell signaling pathways of carcinogenesis. The size of the bubble represents the number of genes. The color of the bubble represents the significance of the terms.

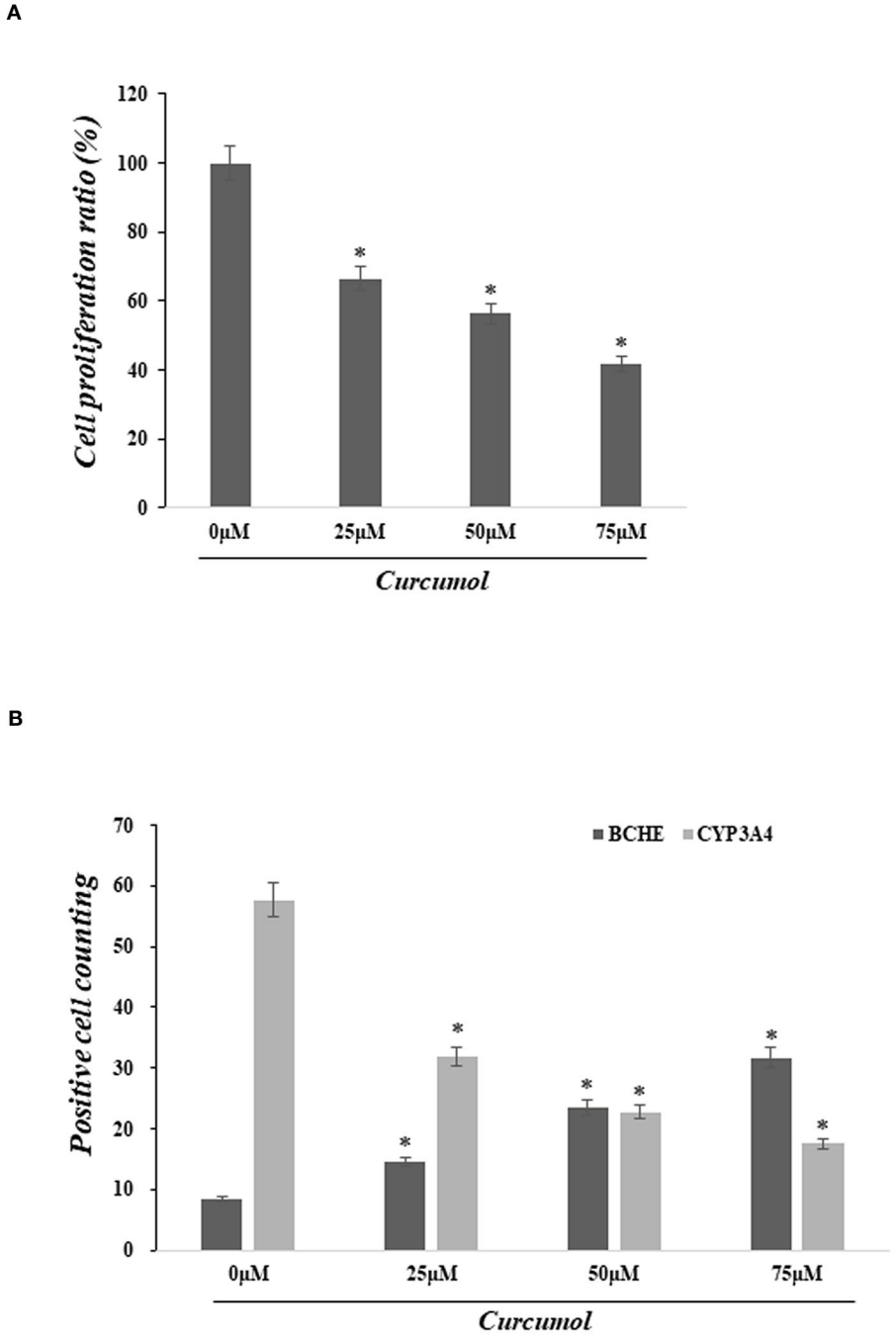

FIGURE 4
Curcumol treatment inhibited cell proliferation of colon adenocarcinoma and altered the expression of BCHE and CYP3A4. **(A)** MTT assay showed significant dose-dependent inhibition of cell proliferation in lung adenocarcinoma cell A594 caused by curcumol treatments (0–75 μM). **(B)** Immunofluorescence staining showed that the treatment of curcumol induced the expression of BCHE and reduced the expression of CYP3A4 in COAD cell, as compared to the control group. *$p < 0.05$.

curcumol for treating COAD and COVID-19. BCHE, an α-glycoprotein synthesized in the liver, is abundant in the intestine and lung (34). The serum level of BCHE was reported to be decreased in many clinical conditions such as inflammation and infections (35). BCHE's low expression level has been documented in colorectal cancer (36), and its activities were found to be decreased in COAD patients (37). In addition, inhibition of BCHE is considered to reduce immunity through the cholinergic anti-inflammatory pathway, although its role in lung inflammation is still unknown (38). A rat study of sepsis

suggested that BCHE can function as an inflammatory marker in sepsis (39), further supporting its role in inflammation. The other target of curcumol, CYP3A4, is a member of the cytochrome P450 superfamily of enzymes. Many clinical trials suggested the importance of the cytochrome P450 system in the drug discovery of COVID-19 (40–42) because CYP3A metabolism is altered in patients with COVID-19 having increased cytokine release. In addition, an *in vitro* study of colon cancer stem cells demonstrated the contribution of CYP3A4 in the chemoresistance of colon cancer and its negative impact on disease-free survival in the patients (43). So, targeting these genes with curcumol might provide an alternative approach for treating COVID-19 and COAD.

In the second part of our study, we focused on the functional roles of the curcumol targets. Our results highlighted the regulation of fat metabolism and biosynthesis by curcumol. Fat metabolism and excess visceral fat were reported to be closely associated with the severity of clinical outcomes in patients with COVID-19 (44, 45). It was further supported by an observational study and Mendelian randomization analysis that central fat distribution and metabolic consequences of excess weight are strongly associated with the severe COVID-19 outcomes (46). Furthermore, dietary fat and metabolism were reported to affect colonic tumorigenesis (47). A mice study showed that obesity is linked to altered metabolism in colon carcinogenesis through the JNK/STAT3-signaling pathway (48). Alex's group demonstrated that short-chain fatty acids stimulate tumor promoter angiopoietin-like 4 synthesis in human COAD cells (49).

Conclusion

This study predicts the pharmacological targets of curcumol for treating COVID-19 and COAD. Additionally, the predicted targets involved in the biological and molecular functions related to fat metabolism and gland development are reported to be associated with the pathogenesis and severity of COVID-19 and COAD, suggesting the possible use of curcumol as a therapeutic compound for these diseases. The findings of this study need further validation by additional animal and preclinical studies before clinical use.

Data availability statement

The original contributions presented in the study are included in the article/Supplementary material, further inquiries can be directed to the corresponding author.

Author contributions

KL contributed to the conception, design of the manuscript, drafted this manuscript, and revised this manuscript. JL and PP contributed to the acquisition, analysis, and interpretation of data in this manuscript. All authors contributed to the article and approved the submitted version.

Conflict of interest

The authors declare that the research was conducted in the absence of any commercial or financial relationships that could be construed as a potential conflict of interest.

Publisher's note

Supplementary material

The Supplementary Material for this article can be found online at: https://www.frontiersin.org/articles/10.3389/fnut.2022.961697/full#supplementary-material

References

1. Semenzato L, Botton J, Drouin J, Cuenot F, Dray-Spira R, Weill A, et al. Chronic diseases, health conditions and risk of COVID-19-related hospitalization and in-hospital mortality during the first wave of the epidemic in France: a cohort study of 66 million people. *Lancet Reg Health Eur.* (2021) 8:100158. doi: 10.1016/j.lanepe.2021.100158

2. Sinha S, Kundu CN. Cancer and COVID-19: why are cancer patients more susceptible to COVID-19? *Med Oncol.* (2021) 38:101. doi: 10.1007/s12032-021-01553-3

3. Saini KS, Tagliamento M, Lambertini M, McNally R, Romano M, Leone M, et al. Mortality in patients with cancer and coronavirus disease 2019: a systematic review and pooled analysis of 52 studies. *Eur J Cancer.* (2020) 139:43–50. doi: 10.1016/j.ejca.2020.08.011

4. Ahmadi M, Pashangzadeh S, Mousavi P, Saffarzadeh N, Amin Habibi M, Hajiesmaeili F, et al. ACE2 correlates with immune infiltrates in colon adenocarcinoma: implication for COVID-19. *Int Immunopharmacol.* (2021) 95:107568. doi: 10.1016/j.intimp.2021.107568

5. Shinkwin M, Silva L, Vogel I, Reeves N, Cornish J, Horwood J, et al. COVID-19 and the emergency presentation of colorectal cancer. *Colorectal Dis.* (2021) 23:2014–9. doi: 10.1111/codi.15662

6. Miao Y, Wang J, Ma X, Yang Y, Mi D. Identification prognosis-associated immune genes in colon adenocarcinoma. *Biosci Rep*. (2020) 40:BSR20201734. doi: 10.1042/BSR20201734

7. Siegel RL, Miller KD, Goding Sauer A, Fedewa SA, Butterly LF, Anderson JC. Colorectal cancer statistics, 2020. *CA Cancer J Clin.* (2020) 70:145–64. doi: 10.3322/caac.21601

8. Ting WC, Chen LM, Pao JB, Yang YP, You BJ, Chang TY, et al. Common genetic variants in Wnt signaling pathway genes as potential prognostic biomarkers for colorectal cancer. *PLoS ONE.* (2013) 8:e56196. doi: 10.1371/journal.pone.0056196

9. Xiang Y, Guo Z, Zhu P, Chen J, Huang Y. Traditional Chinese medicine as a cancer treatment: modern perspectives of ancient but advanced science. *Cancer Med.* (2019) 8:1958–75. doi: 10.1002/cam4.2108

10. So TH, Chan SK, Lee VH, Chen BZ, Kong FM, Lao LX. Chinese medicine in cancer treatment - how is it practised in the East and the West? *Clin Oncol (R Coll Radiol).* (2019) 31:578–88. doi: 10.1016/j.clon.2019.05.016

11. Wang S, Long S, Deng Z, Wu W. Positive role of Chinese herbal medicine in cancer immune regulation. *Am J Chin Med.* (2020) 48:1577–92. doi: 10.1142/S0192415X20500780

12. Zhao H, He M, Zhang M, Sun Q, Zeng S, Chen L, et al. Colorectal cancer, gut microbiota and traditional Chinese medicine: a systematic review. *Am J Chin Med.* (2021) 49:805–28. doi: 10.1142/S0192415X21500385

13. Guan W, Lan W, Zhang J, Zhao S, Ou J, Wu X, et al. COVID-19: antiviral agents, antibody development and traditional Chinese medicine. *Virol Sin.* (2020) 35:685–98. doi: 10.1007/s12250-020-00297-0

14. Lyu M, Fan G, Xiao G, Wang T, Xu D, Gao J, et al. Traditional Chinese medicine in COVID-19. *Acta Pharm Sin B.* (2021) 11:3337–63. doi: 10.1016/j.apsb.2021.09.008

15. Jennings MR, Parks RJ. Curcumin as an antiviral agent. *Viruses.* (2020) 12:1242. doi: 10.3390/v12111242

16. Liu F, Gao S, Yang Y, Zhao X, Fan Y, Ma W, et al. Antitumor activity of curcumin by modulation of apoptosis and autophagy in human lung cancer A549 cells through inhibiting PI3K/Akt/mTOR pathway. *Oncol Rep.* (2018) 39:1523–31. doi: 10.3892/or.2018.6188

17. Gao J, Hou D, Hu P, Mao G. Curcumol increases the sensitivity of colon cancer to 5-FU by regulating Wnt/β-catenin signaling. *Transl Cancer Res.* (2021) 10:2437–50. doi: 10.21037/tcr-21-689

18. Wang J, Li XM, Bai Z, Chi BX, Wei Y, Chen X. Curcumol induces cell cycle arrest in colon cancer cells via reactive oxygen species and Akt/ GSK3β/cyclin D1 pathway. *J Ethnopharmacol.* (2018) 210:1–9. doi: 10.1016/j.jep.2017.06.037

19. Ritchie ME, Phipson B, Wu D, Hu Y, Law CW, Shi W, et al. Limma powers differential expression analyses for RNA-sequencing and microarray studies. *Nucleic Acids Res.* (2015) 43:e47. doi: 10.1093/nar/gkv007

20. Wang Y, Zhang S, Li F, Zhou Y, Zhang Y, Wang Z, et al. Therapeutic target database 2020: enriched resource for facilitating research and early development of targeted therapeutics. *Nucleic Acids Res.* (2020) 48:1031–41. doi: 10.1093/nar/gkz981

21. Davis AP, Grondin CJ, Johnson RJ, Sciaky D, McMorran R, Wiegers J, et al. The Comparative toxicogenomics database: update 2019. *Nucleic Acids Res.* (2019) 47:948–54. doi: 10.1093/nar/gky868

22. Gfeller D, Grosdidier A, Wirth M, Daina A, Michielin O, Zoete V. SwissTargetPrediction: a web server for target prediction of bioactive small molecules. *Nucleic Acids Res.* (2014) 42:W32–8. doi: 10.1093/nar/gku293

23. Liu Z, Guo F, Wang Y, Li C, Zhang X, Li H, et al. BATMAN-TCM: a bioinformatics analysis tool for molecular mechANism of traditional Chinese medicine. *Sci Rep.* (2016) 6:21146. doi: 10.1038/srep21146

24. UniProt Consortium. UniProt: the universal protein knowledgebase in 2021. *Nucleic Acids Res.* (2021) 49:D480–9.

25. Szklarczyk D, Gable AL, Nastou KC, et al. The STRING database in 2021: customizable protein–protein networks, and functional characterization of user-uploaded gene/measurement sets. *Nucleic Acids Res.* (2021) 49:D605–12. doi: 10.1093/nar/gkaa1074

26. Shannon P, Markiel A, Ozier O, Baliga NS, Wang JT, Ramage D, et al. Cytoscape: a software environment for integrated models of biomolecular interaction networks. *Genome Res.* (2003) 13:2498–504. doi: 10.1101/gr.1239303

27. Yang L, Xiong H, Li X, Li Y, Zhou H, Lin X, et al. Network pharmacology and comparative transcriptome reveals biotargets and mechanisms of curcumol treating lung adenocarcinoma patients with COVID-19. *Front Nutr.* (2022) 9:870370. doi: 10.3389/fnut.2022.870370

28. Gross AM, Kreisberg JF, Ideker T. Analysis of matched tumor and normal profiles reveals common transcriptional and epigenetic signals shared across cancer types. *PLoS ONE.* (2015) 10:e0142618. doi: 10.1371/journal.pone.0142618

29. Niu G, Deng L, Zhang X, Hu Z, Han S, Xu K, et al. GABRD promotes progression and predicts poor prognosis in colorectal cancer. *Open Med (Wars).* (2020) 15:1172–83. doi: 10.1515/med-2020-0128

30. Wu M, Kim KY, Park WC Ryu HS, Choi SC, Kim MS, et al. Enhanced expression of GABRD predicts poor prognosis in patients with colon adenocarcinoma. *Transl Oncol.* (2020) 13:100861. doi: 10.1016/j.tranon.2020.100861

31. Jiang SH, Zhu LL, Zhang M, Li RK, Yang Q, Yan JY, et al. GABRP regulates chemokine signalling, macrophage recruitment and tumour progression in pancreatic cancer through tuning KCNN4-mediated Ca^{2+} signalling in a GABA-independent manner. *Gut.* (2019) 68:1994–2006. doi: 10.1136/gutjnl-2018-317479

32. Li X, Wang H, Yang X, Wang X, Zhao L, Zou L, et al. GABRP sustains the stemness of triple-negative breast cancer cells through EGFR signaling. *Cancer Lett.* (2021) 514:90–102. doi: 10.1016/j.canlet.2021.04.028

33. Wang A, Zhang Q, Wang Y, Li X, Li K, Li Y, et al. Inhibition of Gabrp reduces the differentiation of airway epithelial progenitor cells into goblet cells. *Exp Ther Med.* (2021) 22:720. doi: 10.3892/etm.2021.10152

34. Dave KR, Syal AR, Katyare SS. Tissue cholinesterases. A comparative study of their kinetic properties. ***Z Naturforsch C J Biosci***. (2000) 55:100–8. doi: 10.1515/znc-2000-1-219

35. Santarpia L, Grandone I, Contaldo F, Pasanisi F. Butyrylcholinesterase as a prognostic marker: a review of the literature. *J Cachexia Sarcopenia Muscle.* (2013) 4:31–9. doi: 10.1007/s13539-012-0083-5

36. Montenegro MF, Ruiz-Espejo F, Campoy FJ, Muñoz-Delgado E. de la Cadena MP, Rodríguez-Berrocal FJ, et al. Cholinesterases are down-expressed in human colorectal carcinoma. *Cell Mol Life Sci.* (2006) 63:2175–82. doi: 10.1007/s00018-006-6231-3

37. Montenegro MF, Ruiz-Espejo F, Campoy FJ, Muñoz-Delgado E. de la Cadena MP, Cabezas-Herrera J, et al. Acetyl- and butyrylcholinesterase activities decrease in human colon adenocarcinoma. *J Mol Neurosci.* (2006) 30:51–4. doi: 10.1385/JMN:30:1:51

38. Pohanka M. Inhibitors of acetylcholinesterase and butyrylcholinesterase meet immunity. *Int J Mol Sci.* (2014) 15:9809–25. doi: 10.3390/ijms15069809

39. Bitzinger DI, Gruber M, Tümmler S, Malsy M, Seyfried T, Weber F, et al. In vivo effects of neostigmine and physostigmine on neutrophil functions and evaluation of acetylcholinesterase and butyrylcholinesterase as inflammatory markers during experimental sepsis in rats. *Mediators Inflamm.* (2019) 2019:8274903. doi: 10.1155/2019/8274903

40. Biswas M, Roy DN. Potential clinically significant drug-drug interactions of hydroxychloroquine used in the treatment of COVID-19. *Int J Clin Pract.* (2021) 75:e14710. doi: 10.1111/ijcp.14710

41. Lenoir C, Terrier J, Gloor Y, Curtin F, Rollason V, Desmeules JA, et al. Impact of SARS-CoV-2 infection (COVID-19) on cytochromes P450 activity assessed by the Geneva cocktail. *Clin Pharmacol Ther.* (2021) 110:1358–67. doi: 10.1002/cpt.2412

42. Stader F, Battegay M, Sendi P, Marzolini C. Physiologically based pharmacokinetic modelling to investigate the impact of the Cytokine storm on CYP3A drug pharmacokinetics in COVID-19 patients. *Clin Pharmacol Ther.* (2022) 111:579–84. doi: 10.1002/cpt.2402

43. Olszewski U, Liedauer R, Ausch C, Thalhammer T, Hamilton G. Overexpression of CYP3A4 in a COLO 205 colon cancer stem cell model in vitro. *Cancers (Basel).* (2011) 3:1467–79. doi: 10.3390/cancers3011467

44. Cinti S, Graciotti L, Giordano A, Valerio A, Nisoli E. COVID-19 and fat embolism: a hypothesis to explain the severe clinical outcome in people with obesity. *Int J Obes (Lond).* (2020) 44:1800–2. doi: 10.1038/s41366-020-0624-5

45. Favre G, Legueult K, Pradier C, Raffaelli C, Ichai C, Iannelli A, et al. Visceral fat is associated to the severity of COVID-19. *Metabolism.* (2021) 115:154440. doi: 10.1016/j.metabol.2020.154440

46. Gao M, Wang Q, Piernas C, Astbury NM, Jebb SA, Holmes MV, et al. Associations between body composition, fat distribution and metabolic consequences of excess adiposity with severe COVID-19 outcomes: observational study and Mendelian randomisation analysis. *Int J Obes (Lond).* (2022) 14:1–8. doi: 10.1038/s41366-021-01054-3

47. Ocvirk S, O'Keefe SJD. Dietary fat, bile acid metabolism and colorectal cancer. *Semin Cancer Biol.* (2021) 73:347–55. doi: 10.1016/j.semcancer.2020.10.003

48. Nimri L, Saadi J, Peri I, Yehuda-Shnaidman E, Schwartz B. Mechanisms linking obesity to altered metabolism in mice colon carcinogenesis. *Oncotarget.* (2015) 6:38195–209. doi: 10.18632/oncotarget.5561

49. Alex S, Lange K, Amolo T, Grinstead JS, Haakonsson AK, Szalowska E, et al. Short-chain fatty acids stimulate angiopoietin-like 4 synthesis in human colon adenocarcinoma cells by activating peroxisome proliferator-activated receptor γ. *Mol Cell Biol.* (2013) 33:1303–16. doi: 10.1128/MCB.00858-12

frontiers | Frontiers in Nutrition

TYPE Original Research
PUBLISHED 31 August 2022
DOI 10.3389/fnut.2022.980188

OPEN ACCESS

EDITED BY
Filippo Giorgio Di Girolamo,
University of Trieste, Italy

REVIEWED BY
Seyed Pezhman Hosseini Shekarabi,
Islamic Azad University, Iran
Shuyan Chi,
Guangdong Ocean University, China

*CORRESPONDENCE
Juan Tian
tianjuan@yfi.ac.cn

†These authors share first authorship

SPECIALTY SECTION
This article was submitted to Nutrition and Metabolism, a section of the journal Frontiers in Nutrition

RECEIVED 28 June 2022
ACCEPTED 11 August 2022
PUBLISHED 31 August 2022

CITATION
Li M, Wen H, Huang F, Wu M, Yu L, Jiang M, Lu X and Tian J (2022) Role of arginine supplementation on muscular metabolism and flesh quality of Pacific white shrimp (*Litopenaeus vannamei*) reared in freshwater. *Front. Nutr.* 9:980188. doi: 10.3389/fnut.2022.980188

Role of arginine supplementation on muscular metabolism and flesh quality of Pacific white shrimp (*Litopenaeus vannamei*) reared in freshwater

Meifeng Li[1,2†], Hua Wen[1†], Feng Huang[2], Meili Wu[1,2], Lijuan Yu[1], Ming Jiang[1], Xing Lu[1] and Juan Tian[1*]

[1]Key Laboratory of Freshwater Biodiversity Conservation, The Ministry of Agriculture and Rural Affairs, Yangtze River Fisheries Research Institute, Chinese Academy of Fishery Sciences, Wuhan, China, [2]Key Laboratory for Animal Nutrition and Feed Science of Hubei Province, Wuhan Polytechnic University, Wuhan, China

It is no doubt that the improvement of flesh quality of Pacific white shrimp (*Litopenaeus vannamei*) reared in freshwater contributes to its development potential in aquaculture. In this study, we aimed to explore the effect of arginine supplementation on the flesh quality of *L. vannamei* reared in freshwater and its mechanism. *L. vannamei* were randomly fed with three diets for 56 days, of which arginine level was 10.15 g kg^{-1} (arginine-deficient diet), 21.82 g kg^{-1} (arginine-optimal diet), and 32.46 g kg^{-1} (arginine-excessive diet), respectively. Each diet was randomly assigned to triplicate tanks, and each tank was stocked with 35 shrimps (initial weight: 1.70 ± 0.02 g). Results showed the arginine-optimal diet increased the weight gain, flesh percentage, crude protein and flavor amino acid contents in muscle, and improved the flesh hardness by conversing fast myofibers to slow myofibers, increasing myofiber density and myofibrillar length, and promoting ornithine and collagen synthesis. The arginine-optimal diet influenced the purine metabolic pathway by reducing hypoxanthine, xanthine, and inosine contents. Ornithine, citrulline, and glutamate were identified as the key metabolites affecting flesh quality traits after arginine treatments. Only increasing the levels of dietary arginine did not result in an increase in endogenous creatine synthesis in muscle and hepatopancreas. Overall, the arginine-optimal diet improved the flesh quality traits of *L. vannamei* reared in freshwater due to the enhanced muscular hardness, protein deposition, and flavor, which may be contributing to the transformation of muscle fiber type and increase in protein synthesis by the metabolites of arginine (ornithine, citrulline, and glutamate).

KEYWORDS

arginine metabolites, hardness, myofiber, nutritional value, shrimp

Introduction

Pacific white shrimp (*Litopenaeus vannamei*) has been recognized as one of the excellent farming species in the world due to its advantages of high-temperature resistance, low-salt resistance, fast growth, strong disease resistance, and high survival rate out of water. It has been cultured in seawater, salt-fresh water, and freshwater for its ability to tolerate the wide salinity from 1 to 40‰ (1). Compared with freshwater-cultured shrimps, marine-cultured shrimps with higher nutritional value have a better flavor and a lighter earthy-musty taste, explaining why their price is higher than freshwater-cultured shrimps (2). However, freshwater aquaculture contributes 77% of the world's farmed aquatic products (excluding aquatic plants) as measured by edible aquaculture production, providing consumers with cost-effective, accessible, and stable supplies of aquatic products (3). It is no doubt that the improvement of the flesh quality of *L. vannamei* reared in freshwater promotes the development of its aquaculture.

Arginine is an essential amino acid since it plays a crucial physiological role in the growth performance of shrimps (4). Arginine is a precursor for creatine, as it is the only amino acid that can provide the amidino group for creatine synthesis. Our previous study on *L. vannamei* showed that diets supplemented with 8.28 g kg^{-1} creatine enhanced the hardness and chewiness of muscle by improving the diameter and density of myofibers and increasing collagen content (5). Arginine also plays a vital role in producing nitric oxide, polyamine synthesis, inflammation, and innate immune responses (6). Moreover, arginine is the central reserve of high-energy phosphate for the regeneration of ATP in the muscle. Diet is the primary source of arginine for farmed shrimp. The optimal arginine level was 19.60 g kg^{-1} for *L. vannamei* reared in freshwater by two slope broken-line model based on a specific growth rate (SGR) (7). Meanwhile, the optimal arginine in a diet has a positive effect on muscle quality in grass carp (8), finishing pigs (9), and broiler (10). To the best of our knowledge, the relationship between dietary arginine and flesh quality in *L. vannamei* remains largely unresolved.

Consequently, in the current study, three diets containing different arginine levels (deficient, optimal, and excessive) were formulated and hand-fed to juvenile *L. vannamei* for 56 days. To investigate the effect of dietary arginine on growth performance and flesh quality of *L. vannamei* cultured in freshwater and its mechanism, we assessed growth performance, proximate composition, flesh texture, hydroxyproline content, myofiber characteristics, muscular amino acid content, as well as untargeted and targeted metabolomics analyses of muscle in *L. vannamei*. Present study's findings will provide a deeper understanding of dietary arginine on the flesh quality and arginine metabolism of shrimp and thus eventually provide a novel technology to produce high-quality aquatic products.

Materials and methods

Experimental diets and design

Arginine (99.9% in purity) was obtained from Shanghai Macklin Biotechnology Co., Ltd. (Shanghai, China). We selected wheat gluten meal and fishmeal as the primary protein source and chose fish oil and soybean oil as the primary lipid source in the current study. We designed a basal diet including 420 g kg^{-1} protein and 50 g kg^{-1} lipid to fulfill the nutritional requirements of *L. vannamei* (4). We added arginine of 0, 10, and 20 g kg^{-1} to the basal diet, and arginine contents in three diets were analyzed to be 10.15 g kg^{-1} (arginine-deficient diet, LA), 21.82 g kg^{-1} (arginine-optimal diet, MA), and 32.64 g kg^{-1} (arginine-excessive diet, HA). All ingredients were ground into a powder-like condition, sifted, and mixed with oil and arginine. The dough was extruded through a 2-mm diameter template, and then the noodle-like diets were gelatinized at 90°C for 10 min and then dried in a 60°C oven. The feeds were broken into small pellets and stored at −20°C until used. The diets' raw ingredients, proximate composition, and amino acid profiles are shown in **Supplementary Tables 1**, **2**.

Feeding management

The feeding trial was conducted at Tongwei Special Aquatic Research Institute (Zhuhai, China). The juvenile *L. vannamei* were purchased from a commercial hatchery (Zhuhai, China). Before the formal feeding trial, the shrimps were stocked in 12 indoor circular tanks (0.70 m in diameter, 0.85 m in height; water volume: 320 L) and fed with the control diet for 2 weeks to acclimate to the experimental conditions. Subsequently, the healthy juvenile shrimps (initial body weight: 1.70 ± 0.02 g) were randomly transferred into nine circular tanks (0.70 m in diameter, 0.85 m in height; water volume: 320 L). Each tank was allocated 35 shrimps. Each experimental diet was randomly assigned to triplicate tanks. The experimental shrimps were hand-fed to apparent satiation four times every day at 7:00, 12:00, 17:00, and 22:00. Uneaten feed and feces were collected after feeding for 2 h. During the feeding period, the water quality was monitored daily, and the results were as follows: dissolved oxygen was >6 mg L^{-1}, salinity was 2–3‰, ammonia nitrogen was <0.5 mg L^{-1}, and water temperature and pH were maintained at 28.00 ± 2.00 and 7.60–7.8, respectively. The growth trial lasted 56 days.

Sample collection

After a 56-day feeding, shrimps were deprived of feeds for 24 h. The total number and weight of shrimps in each

tank were recorded to calculate survival rate (SR), weight gain rate (WGR), specific growth rate (SGR), and feed conversion ratio (FCR). Next, the body weight of six shrimps per tank was measured, and blood samples were collected using a 1-mL syringe from the pericardial cavity and then centrifuged at 5, 200 g for 15 min at 4°C. Serum samples were separated, transferred into centrifuge tubes of 1.5 mL, and stored at −80°C until analysis. Muscle and hepatopancreas tissues from these six shrimps were collected and weighed to calculate hepatosomatic index (HSI) and flesh percentage (FP). The muscle was cut of similar size and stored at −40°C for texture analysis. Another three shrimps from each tank were sampled to evaluate myofiber ultrastructure and microstructure structure: Approximately 8-mm^3 muscle from each shrimp was collected in a 10 mL centrifuge tube containing fixative fluid and stored at 4°C for transmission electron microscopy (TEM) analysis. Muscle with size (0.5 cm × 0.5 cm × 0.5 cm) per shrimp was suspended in 4% paraformaldehyde with phosphate buffered saline (PBS) for 24 h and stocked in 70% ethanol for histology. The muscle samples for histology and TEM were taken from the same region from different shrimp across treatment. Muscle and hepatopancreas tissues from another six shrimps per tank were stored at −80°C for gene expression analysis and metabolic profiling. The muscles of the remaining shrimp were collected and stored at −20°C until the determination of collagen contents, amino acid profile, and proximate composition.

Proximate composition analysis

The proximate composition of muscle and diets were detected by the standard methods (11). The moisture content was dried using a vacuum freeze dryer (Christ Beta 2–4 LD plus LT, Marin Christ Corporation, Osterode, Germany) for 48 h. Crude protein content was determined by an automatic Kjeldahl nitrogen analyzer (Haineng k9840, Shandong Haineng Scientific Instrument Co., Ltd., Dezhou, China) after acid digestion. Crude lipid content was determined by the petroleum-ether extraction method. Ash content was detected at 550°C for 24 h.

Determination of collagen content

The collagen concentration is calculated by hydroxyproline (Hyp) content. The muscular alkaline-soluble Hyp and alkaline-insoluble Hyp were separated according to the method described by Li et al. (12). In brief, after muscle samples were homogenizing, alkaline-soluble Hyp and alkaline-insoluble Hyp were extracted with sodium hydroxide (0.2 M) and 8 M hydrochloric acid (HCl) under an ice bath, respectively. The determination of Hyp was performed using the method described by Zhang et al. (13). Hydrolytic Hyp content was analyzed by a standard curve.

Muscular texture properties analysis

Prepared shrimp samples were cooked in boiling water for 1 min, and muscles from the same area were shaped into small cubes (1.0 cm × 1.0 cm × 1.0 cm). Texture parameters, including hardness, springiness, chewiness, cohesiveness, and resilience, were examined using a texture analyzer (model TVT-300XP, Beijing, China) and a cylindrical aluminum probe with a diameter of 50 mm. The measurement parameters were as follows: pre-test tested and post-test speed was set as 2 and 5 mm s^{-1}, respectively, and the deformation was 50% of muscle thickness. Each sample was pressed twice, 30 s per. The texture indices were analyzed using a texture analyzer program (version 3.42, Perten Instruments Inc., Hägersten, Sweden).

Histological properties and ultrastructure analysis

Muscle samples were dehydrated in graded ethanol and then cleared by xylene. Embedded in paraffin, cross-sections and longitudinal sections were sliced (5 μm) and stained with hematoxylin and eosin (H&E) to assess the morphology. The microstructure of muscle was observed using a light microscope (Olympus BX53, Tokyo, Japan). The myofiber characteristics, including myofiber diameter, density, length of the sarcomere, and I-band and A-band, were measured using Image-J Launcher software. Myofiber size is divided into three classes: Classes I, II, and III were categorized according to $d \leq 20$, $20 < d \leq 50$, and $d > 50$, respectively. Class I myofibers were classified as hyperplasia fibers. Class III fibers were categorized as hypertrophic fibers according to the method of Almeida et al. (14). Myofiber density (N/mm^2) was indicated as a rate of the total number of fibers in the whole area. The myofibrillar structure was conducted with TEM (Hitachi, Ltd., Tokyo, Japan, HT7800) at 80 kV in Wuhan Goodbio Technology Co., Ltd. (Wuhan, Hubei).

Analyses of hydrolyzed amino acids and free amino acids content

The HAAs were detected by an automatic Amino Acid Analyzer (HITACHI L-8900, Tokyo, Japan). The pretreatment of samples to be tested was as follows: Dried feed and flesh (conducted in vacuum freeze dryer) were transferred into sealed glass tubes and hydrolyzed with 6 M HCl at 110°C for 24 h. Subsequently, the hydrolysate was filtered and diluted to 100 mL with distilled water. The filtrate (2 mL) was taken out and evaporated to dryness at 60°C to remove the HCl in a vacuum dryer for 24 h. Distilled water (2 mL) was added and evaporated to dryness for 24 h again. Then, the sedimentation was dissolved

in 8 mL of 0.1 M HCl, which was filtered by a 0.22 μm Millipore membrane, and the supernatant of 1 mL was used for the analysis of HAAs.

The FAAs were measured by an automatic Amino Acid Analyzer (HITACHI L-8900, Tokyo, Japan). The preparation of muscle samples was as follows: the fresh muscle samples were mixed with 10% sulfosalicylic acid and homogenized for 1 min. The homogenate was centrifuged (14, 400 g, 15 min, 4°C) and kept at room temperature for 5 min. After filtering through a 0.22 μm Millipore membrane, the supernatant of 1 mL was used for the FAAs analysis.

Metabolic profiling

A comprehensive untargeted metabolomics profiling of shrimp muscles was conducted by liquid chromatography and mass spectrometry (LC-MS). Metabolite extraction was conducted as follows: muscle samples of 50 mg were mixed with 800 μL methanol (80%) and then ground for 90 s. After being vortexed (65 Hz, 30 min, 4°C), the samples were centrifuged for 15 min at 4°C with 14, 400 g. Again, the supernatant was collected and centrifuged (4°C, 14, 400 g, 15 min). Dichlorophenylalanine (5 μL) served as the internal standard was added to the supernatant (200 μL) and transferred to an injection vial for LC-MS analysis.

LC-MS analysis and data preprocessing: LC- MS (Waters, UPLC; Thermo, Q Exactive) was performed with an ACQUITY UPLC HSS T3 column (2.1 × 100 mm, 1.8 μm) that was used for the separation of metabolites. Chromatographic separation conditions were as follows: the column temperature was 40°C, and the flow rate was 0.30 mL min^{-1}. The mobile phase consisted of A: water +0.05% formic acid and B: acetonitrile. The prepared sample was placed in an automatic sampler at 4°C with an injection volume of 1 μL during the whole analysis process.

Metabolites were detected by electrospray ionization (ESI) positive and negative ion patterns. Detecting parameters for ESI+ mode were as follows: Heater temperature 300°C; sheath gas flow rate, 45 arb; aux gas flow rate, 15 arb; sweep gas flow rate, 1 arb; spray voltage, 3.0 kV; capillary temperature, 350°C; S-lens RF level, 30%. For ESI- model: Heater temperature 300°C, Sheath Gas Flow rate, 45 arb; Aux Gas Flow Rate, 15 arb; Sweep Gas Flow Rate, 1 arb; spray voltage, 3.2 kV; Capillary temperature, 350°C; S-Lens RF Level, 60%.

The raw data were extracted and preprocessed using Compound Discoverer software (Thermo). The data were normalized and post-edited in Excel 2010 software and finally edited into a two-dimensional data matrix. After the data is preprocessed, orthogonal partial least squares discriminant analysis (OPLS-DA) is performed. The variable importance in the projection (VIP) scores from OPLS-DA are calculated for each component. Differential metabolites (DFMs) between two groups were selected according to the following screening conditions: VIP > 1 and Student's *T*-test with *P*-value < 0.05. Then, the disturbed metabolic pathways of differential metabolites were analyzed by searching the online Kyoto Encyclopedia of Genes and Genomes (KEGG) database.

Metabolites analysis of arginine

There are nine representative metabolites of arginine in muscle and hepatopancreas, including citrulline, adenosine, adenine, inosine, glycocyamine, creatine, creatinine, and ornithine fumaric acid which were selected for quantitative analysis using an ultrahigh-performance LC/MS with a triple quadrupole mass spectrometry (UPLC-QQQ-MS) approach. Above samples of 50 mg were weighed and premixed with 600 μL acetonitrile (80%). After putting under vortex movement for 2 min, the samples were ground for 90 s at 60 Hz, and then conducted an ultrasound for 30 min at 4°C. The extracts were centrifuged at 14, 000 g for 15 min at 4°C. Finally, the supernatant of 500 μL was transferred to vials for determining the contents of the target components through the LC-MS/MS system.

Analyses of interest were separated from prepared samples using Waters Acquity UPLC (Ultra performance liquid chromatography) equipped with an Acquity UPLC HSS T3 column (1.8 μm, 2.1 mm × 100 mm) and its temperature was 40°C at a flow rate of 0.25 mL min^{-1}. Mobile phase A consisted of 0.10% aqueous formic acid, and mobile phase B was composed of methanol. The separated compounds were identified using AB SCIEX 5500 QQQ–MS (mass spectrometry). MS parameters were set as follow: (Curtain Gas): 35 arb; (Collision GAS): 7 arb; (IonSpray voltage): 4.5 kV; (IonSpray voltage): 4.5 kV; (Temperature): 450°C; (IonSource Gas1): 55 arb; (IonSource Gas2): 55 arb. Eventually, a prepared standard solution was added to the vial, and quantification was performed under multiple reaction monitoring (MRM) mode. MultiQuant software for integration and standard curve for content calculation. The standard solution was diluted with acetonitrile (80%) to prepare a series of appropriate concentrations for establishing the calibration curve. The calibration curve was plotted according to the peak areas of the standards at different concentrations and corresponding concentrations.

Gene expressions analysis in muscle

Total RNA was isolated from muscle using TRIzol reagent (Life Technologies, Carlsbad, CA, United States), and the cDNA was generated following the instructions of the PrimeScript® RT reagent kit (Takara Biotech, Dalian, China). SYBR® Premix Ex Taq™ (Takara Biotech, Dalian, China) was utilized to quantify the expressions of MyHCs gene (*sMyHC1*, *sMyHC2*, *sMyHC5*, *sMyHC6a,* and *sMyHC15*), and elongation factor 1-alpha1 (*EF-1α1*) acted as a reference gene. Real-time polymerase chain

reaction (Real-time PCR) was conducted on a quantitative thermal cycler (Light Cycler 480II, Roche) and was performed as in the previous study (5). Primer sequences were presented in **Supplementary Table 3** and were synthesized by Sangon Biotech Co., Ltd. (Shanghai, China). Relative quantification of transcript expression was calculated using the $2^{-\Delta\Delta CT}$ method, and the relative mRNA expressions of the LA group was set as standard.

Serum urea nitrogen analysis

Each serum sample (200 μL) was transferred into a sample cup, and the concentrations of urea nitrogen in the serum were quantified by urease/GLDH method using an automatic biochemistry analyzer (CHEMIX-800, Sysmex Corporation, Kobe, Japan). All kits were purchased from Sysmex Corporation.

Calculation and statistical analysis

All data were presented as mean ± S.D. (standard deviation). The homogeneity of variances and normality of the data was evaluated prior to statistical analysis, which included proximate composition, flesh texture, hydroxyproline content, myofiber characteristics, muscular amino acid content, metabolites of arginine contents. All data were analyzed by one-way analysis of variance (ANOVA) and Tukey's multiple comparison tests using the SPSS 22.0 (SPSS, United States) for Windows. The significant difference was set at $P < 0.05$.

Results

Growth performance

The growth performance of *L. vannamei* is provided in **Table 1**. Shrimps fed with the MA diet had the highest final body weight (FBW), SGR, WGR, flesh percentage (FP) and survival rate (SR), which were significantly higher than those with the LA and HA diets ($P < 0.05$). The highest hepatopancreas indexes (HSI) value occurred in the HA group. Feed conversion ratio (FCR) in the MA group was significantly lower than that in the LA and HA groups ($P < 0.05$).

Muscular texture analysis

As shown in **Table 2**, the LA group had the lowest hardness and chewiness of muscle than other groups ($P < 0.05$). No significant difference occurred in parameters including springiness, resilience, and cohesiveness among all groups ($P > 0.05$).

Proximate composition and collagen content in the flesh

As displayed in **Table 2**, there were no significant differences in the contents of moisture, crude lipid, and ash in muscle among all treatments ($P > 0.05$). The crude protein content and the protein-moisture ratio of muscle in the MA group were significantly higher than those in the LA group ($P < 0.05$). The LA group had the lowest alkaline-soluble Hyp, alkaline-insoluble Hyp, and total Hyp content.

Muscular hydrolyzed amino acids profiles

The muscular amino acid composition is presented in **Table 3**. The contents of aspartate, lysine, and arginine in the LA group were significantly lower than those in the MA and HA groups ($P < 0.05$). As compared to the LA group, the contents of valine, methionine, isoleucine, total amino acids (TAAs), and total essential amino acids (EAAs) were significantly higher in the MA group ($P < 0.05$).

Muscular free amino acids profiles

The FAAs contents of the flesh are displayed in **Table 3**. Significant higher threonine, phenylalanine, leucine, histidine, aspartate, glutamate, and proline contents were found in the

TABLE 1 The growth performance of *Litopenaeus vannamei* after dietary arginine treatment for 56 days.

Indexes	Diets[9]		
	LA	MA	HA
IBW[1] (g)	1.76 ± 0.10	1.71 ± 0.02	1.79 ± 0.06
FBW[2] (g)	10.65 ± 0.10^{b}	10.68 ± 0.21^{b}	10.18 ± 0.15^{a}
WGR[3] (%)	508.20 ± 15.13^{ab}	524.53 ± 8.48^{b}	469.81 ± 23.71^{a}
SGR[4] (% d^{-1})	3.22 ± 0.03^{b}	3.27 ± 0.02^{b}	3.10 ± 0.01^{a}
FCR[5]	1.15 ± 0.03^{b}	1.06 ± 0.02^{a}	1.17 ± 0.01^{b}
HSI[6] (%)	3.16 ± 0.29^{a}	3.23 ± 0.25^{ab}	3.47 ± 0.21^{b}
FP[7] (%)	47.40 ± 2.81^{ab}	49.61 ± 1.89^{b}	45.42 ± 43.32^{a}
SR[8] (%)	93.42 ± 1.51^{b}	96.22 ± 1.13^{b}	74.28 ± 0.62^{a}

[1]IBW, initial body weight.
[2]FBW, final body weight.
[3]WGR (weight gain rate, %) = 100 × [(final body weight)–(initial body weight)]/initial body weight.
[4]SGR (specific growth rate, % d^{-1}) = 100 × ln (final body weight/initial body weight)/days.
[5]FCR (feed conversion ratio) = dry feed consumed/(final biomass – initial biomass + dead fish).
[6]HSI (hepatosomatic index, %) = 100 × (hepatopancreas weight/the whole body weight).
[7]FP (flesh percentage, %) = 100 × (muscle weight/whole body weight).
[8]SR (survival rate,%) = 100 × (final number of shrimp/initial number of shrimp).
[9]LA, the arginine-deficient diet; MA, the arginine-optimal diet; HA, the arginine-excessive diet.
[10]Different letters are significantly different ($P < 0.05$).

TABLE 2 The muscular textural properties, proximate composition, and collagen contents of *L. vannamei* after dietary arginine treatment for 56 days.

Indexes	Diets[3]		
	LA	MA	HA
Texture properties			
Hardness (gf)	1280.29 ± 36.14[a]	1386.43 ± 40.17[b]	1506.43 ± 65.02[c]
Springiness	0.58 ± 0.04	0.59 ± 0.03	0.58 ± 0.04
Chewiness (gf)	407.62 ± 17.70[a]	461.81 ± 20.53[b]	487.37 ± 19.10[b]
Resilience	0.29 ± 0.02	0.28 ± 0.03	0.26 ± 0.02
Cohesiveness	0.57 ± 0.04	0.56 ± 0.04	0.55 ± 0.05
Proximate composition (g kg^{-1})			
Moisture	784.82 ± 4.55	781.73 ± 3.58	784.44 ± 2.36
Crude protein	188.35 ± 3.94[a]	197.43 ± 3.06[b]	193.53 ± 2.74[ab]
Crude lipid	5.14 ± 0.17	5.53 ± 0.31	5.18 ± 0.18
Ash	13.22 ± 0.22	13.65 ± 0.29	13.41 ± 0.24
Protein/moisture[1]	0.240 ± 0.006[a]	0.253 ± 0.003[b]	0.247 ± 0.003[ab]
Hyp (g kg^{-1})			
Alkaline-soluble Hyp[2]	0.25 ± 0.03[a]	0.40 ± 0.04[b]	0.40 ± 0.04[b]
Alkaline-insoluble Hyp	0.39 ± 0.04[a]	0.54 ± 0.04[b]	0.76 ± 0.03[c]
Total Hyp	0.65 ± 0.04[a]	0.94 ± 0.07[b]	1.16 ± 0.05[c]

[1] Protein/moisture, protein content/moisture content.
[2] Hyp, hydroxyproline.
[3] LA, the arginine-deficient diet; MA, the arginine-optimal diet; HA, the arginine-excessive diet.

HA group ($P < 0.05$). The MA group had the highest contents of isoleucine, arginine, alanine, Total EAAs, and total FAAs ($P < 0.05$). TAAs in the LA group were significantly lower than that in other groups. The contents of muscular serine and tryptophan in the LA group were significantly lower than that in the MA and HA groups ($P < 0.05$).

Histological properties and ultrastructure analysis

The effect of arginine on the muscle morphology of *L. vannamei* is shown in Figure 1A. The shape of myofiber exhibited irregular polygons, and the abundant connective tissue separates myofibers. The ultrastructure of myofiber is revealed in Figure 1B. Myofiber diameters and myofiber density are shown in Figure 1C. The muscle density of the MA group was significantly higher than that in the LA group ($P < 0.05$) but had no significant difference compared to the HA group ($P > 0.05$). The percentage of small-sized fiber (<20 μm) in the MA and HA groups was significantly higher than that in the LA group ($P < 0.05$). The highest percentage of fibers of 20–50 μm and the lowest percentage of large diameter fibers (>50 μm) have occurred in the LA group. The lengths of dark areas (A band), light areas (I band), and sarcomere as shown in Figure 1C. The A band length and sarcomeres length (SL) in the LA group significantly decreased compared to that in the MA and HA groups ($P < 0.05$). The I band length in the MA group significantly increased than that in other groups ($P < 0.05$).

Gene expression

Shrimps fed diets containing different arginine showed different expressions of muscle-related genes (Figure 1D). The fast-type muscle relative gene expressions (*sMyHC1*, *sMyHC2*, and *sMyHC6a*) in the HA group were significantly higher than that in other groups. The expressions of slow-type muscle relative gene (*sMyHC5* and *sMyHC15*) in the LA group were significantly lower than that in the MA and HA groups ($P < 0.05$).

Metabolomics analysis of metabolites in muscle after graded arginine treatments

Untargeted metabolomic analysis of muscle based on OPLS-DA analysis indicated that metabolic patterns changed after *L. vannamei* were fed diets containing different arginine levels. The score plots of OPLS-DA between different groups are depicted in Figure 2A. The cluster separations are acceptable in different groups under positive and negative models.

Heat maps based on the judgment criteria (VIP values > 1, $P < 0.05$) showed the relationships and relative abundances of DFMs between different groups (Figure 2B). The DFMs were analyzed using the MetaboAnalyst platform. The essential metabolic pathways relating to the DFMs are presented in Figure 2C. The plot revealed that purine metabolism might be the main differential pathway among the treatments based on enrichment and metabolic pathway analyses. Analysis of the purine metabolic pathway revealed that there existed four differential metabolites: adenosine monophosphate (AMP), inosine monophosphate (IMP), hypoxanthine, and xanthine, were concentrated in the purine metabolism pathway (Figure 2D). Muscular AMP relative content reached the highest value in the HA group ($P < 0.05$). The IMP relative content in the muscles of the HA group was significantly lower than that of the LA group ($P < 0.05$). The lowest hypoxanthine relative content in the muscle occurred in the MA group ($P < 0.05$). The xanthine relative content in the muscle of the LA group was significantly higher than other groups ($P < 0.05$).

The contents of metabolites of arginine in muscle, hepatopancreas, and serum

The concentration of nine metabolites related to arginine metabolism (adenosine, adenine, inosine, citrulline, glycocyamine, creatine, creatinine, ornithine, and fumaric acid) in the muscle and hepatopancreas are listed in Table 4. In hepatopancreas, the concentrations of citrulline, adenine, inosine, glycocyamine, creatine, ornithine, and fumaric acid showed no significant difference among all treatments

TABLE 3 Free amino acid (mg kg^{-1}) and hydrolyzed amino acid (g kg^{-1}) contents in the muscle of *L. vannamei* after dietary arginine treatment for 56 days.

Amino acids	LA		MA		HA	
	FAA	HAA	FAA	HAA	FAA	HAA
Essential amino acids						
Arg	4957.78 ± 87.01^{a}	16.09 ± 0.81^{a}	5555.73 ± 98.88^{b}	18.09 ± 0.88^{b}	5039.00 ± 154.58^{a}	18.34 ± 0.68^{b}
His	112.57 ± 7.14^{a}	3.19 ± 0.23	151.32 ± 8.33^{b}	3.46 ± 0.18	201.43 ± 5.63^{c}	3.52 ± 0.17
Ile	34.10 ± 1.76^{a}	6.12 ± 0.54^{a}	61.57 ± 2.06^{c}	7.59 ± 0.25^{b}	51.43 ± 2.99^{b}	6.94 ± 0.66^{ab}
Leu	76.46 ± 2.09^{a}	11.21 ± 1.06	84.84 ± 2.42^{b}	13.00 ± 0.45	104.21 ± 4.52^{c}	12.41 ± 0.79
Lys	253.22 ± 15.70^{a}	11.86 ± 0.99^{a}	294.71 ± 22.29^{b}	13.74 ± 0.49^{b}	271.12 ± 8.65^{ab}	13.77 ± 0.47^{b}
Met	63.15 ± 3.11	5.02 ± 0.47^{a}	66.74 ± 1.27	6.25 ± 0.10^{b}	65.50 ± 4.70	5.36 ± 0.52^{ab}
Phe	50.73 ± 2.04^{a}	6.71 ± 0.59	54.93 ± 2.10^{a}	7.30 ± 0.23	78.71 ± 4.22^{b}	7.00 ± 0.40
Thr	30.16 ± 2.42^{a}	5.44 ± 0.39	30.38 ± 2.16^{a}	6.05 ± 0.25	46.84 ± 2.74^{b}	6.03 ± 0.22
Val	106.96 ± 4.44	6.48 ± 0.55^{a}	117.77 ± 3.01	7.68 ± 0.28^{b}	115.71 ± 6.92	7.32 ± 0.39^{ab}
Non-essential amino acids						
Ala	2292.52 ± 45.92^{b}	9.09 ± 0.88	2471.67 ± 63.24^{c}	11.62 ± 0.65	2038.96 ± 48.15^{a}	11.28 ± 0.08
Asp	248.52 ± 12.95^{a}	14.22 ± 1.08^{a}	337.83 ± 39.97^{b}	16.47 ± 0.87^{b}	450.32 ± 18.75^{c}	16.49 ± 0.39^{b}
Glu	669.79 ± 50.95^{a}	24.62 ± 1.63	825.89 ± 29.32^{b}	26.95 ± 0.88	1137.47 ± 12.79^{c}	26.98 ± 0.68
Gly	3746.6 ± 178.85^{b}	13.14 ± 1.27	3724.87 ± 96.87^{b}	14.44 ± 0.70	3080.90 ± 120.76^{a}	14.02 ± 0.54
Pro	2376.83 ± 212.75^{a}	9.12 ± 0.70	2507.26 ± 177.43^{a}	9.11 ± 0.33	3204.81 ± 169.27^{b}	9.12 ± 0.37
Ser	93.49 ± 7.10^{a}	5.94 ± 0.44	128.90 ± 5.96^{b}	6.14 ± 0.19	112.98 ± 6.20^{b}	6.14 ± 0.19
Tyr	80.30 ± 2.06^{a}	6.26 ± 0.29	133.34 ± 1.50^{b}	7.22 ± 0.19	133.35 ± 1.88^{b}	6.86 ± 0.53
ΣFAA	6957.44 ± 118.09^{a}	–	7360.26 ± 26.50^{b}	–	6707.66 ± 154.48^{a}	–
ΣEAA	5685.12 ± 100.77^{a}	72.13 ± 4.61^{a}	6417.99 ± 97.43^{b}	83.16 ± 2.00^{b}	5973.96 ± 162.20^{a}	80.69 ± 4.67^{ab}
ΣNEAA	9508.05 ± 270.53	82.39 ± 6.37	10129.77 ± 174.15	91.95 ± 3.47	10158.80 ± 318.17	90.88 ± 2.41
TAAs	15193.17 ± 335.37^{a}	154.52 ± 9.32^{a}	16547.76 ± 135.07^{b}	175.10 ± 5.33^{b}	16132.76 ± 354.27^{b}	171.57 ± 6.66^{ab}

FAA, free amino acid.
HAA, hydrolyzed amino acid.
ΣFAA, Flavor amino acids.
ΣEAA, total essential amino acids.
ΣNEAA, total non-essential amino acids.
TAAs, total amino acids.
LA, the arginine-deficient diet; MA, the arginine-optimal diet; HA, the arginine-excessive diet.

($P > 0.05$). The contents of adenosine and creatinine in the hepatopancreas in the LA group were lower than that in other groups ($P < 0.05$).

Muscular citrulline content reached the highest value in shrimps fed with the HA diet. The lowest contents of muscular inosine and fumaric acid were detected in the HA group. Muscular adenosine, creatinine, and ornithine contents in the HA group were significantly higher than in the LA and MA groups ($P < 0.05$). Adenine, glycocyamine, and creatine contents in the muscle showed no significant difference among all groups ($P > 0.05$). Serum urea nitrogen content increased with the increasing dietary arginine levels.

Discussion

The current study showed that *L. vannamei* reared in freshwater fed a diet containing optimum arginine level had a good growth performance, which agreed with other crustaceans, such as juvenile Kuruma shrimp (*Marsupenaeus japonicus*) (15), *Penaeus monodon* (16). Notably, the present study indicated that excessive arginine in the diet led to a decline in growth and survival rate, together with a higher FCR of *L. vannamei* cultured in freshwater. Maybe excessive arginine disturbed physiological metabolism and consequently induced toxic effects and stress in the shrimps, leading to extra-energy expenditure used for deamination and excretion (4, 17, 18).

It is the key of this research to reveal the relationship between arginine metabolites and flesh quality, which will provide new insight into the design of effective nutritional strategies for improving the flesh quality of *L. vannamei*. We measured the metabolites of arginine using untargeted and targeted metabolomics. The enrichment analysis and metabolic pathway analysis showed that the differential metabolic pathways were "purine metabolism" pathway, and dietary arginine levels led to changes in the relative levels of AMP, IMP, hypoxanthine, and xanthine, which are involved in purine metabolism. AMP is a precursor of IMP, and IMP degrades into xanthine and hypoxanthine (19, 20). AMP and IMP present an umami taste (21), and hypoxanthine and xanthine are the sources of bitterness (22). Citrulline is one of the primary metabolites of arginine, and AMP is the product of citrulline catabolism (23). Our results suggested that excessive arginine enhanced hypoxanthine synthesis and deficient arginine increased xanthine synthesis,

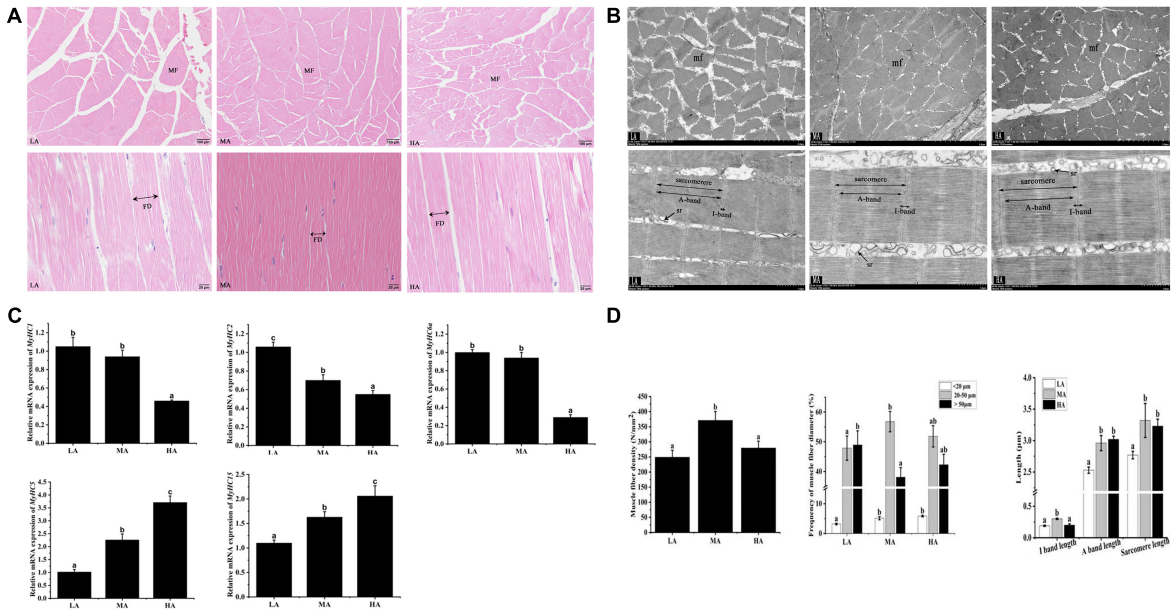

FIGURE 1
The morphology of myofiber of *Litopenaeus vannamei* after dietary arginine treatment for 56 days. **(A)** Myofiber microstructure of cross-section (Magnification 100×) and longitudinal section (Magnification 400×). **(B)** Transmission electron microscope of cross-section and longitudinal section at a magnification of 3,000× and 8,000×, respectively. **(C)** The density and the lengths of diameter, I band, A band, and sarcomere in myofiber of *L. vannamei*. **(D)** The relative mRNA expression of MyHCs in *L. vannamei*. MF, myofiber. mf, myofibril. FD, myofiber diameter. sr, sarcoplasmic reticulum. sMyHC1, sMyHC2, and sMyHC6a are mainly expressed in fast myofibers. sMyHC5 and sMyHC15 are mainly expressed in slow myofibers. LA, the arginine-deficient diet; MA, the arginine-optimal diet; HA, the arginine-excessive diet.

and changing trend of muscular AMP content was similar to muscular citrulline content. The adenosine content increased, whereas IMP synthesis decreased with the increasing dietary arginine levels. The above results may indicate that a diet with supplemented arginine led to the redirection of AMP deamination (24), which elevated citrulline content may cause. The non-targeted metabolic analysis indicated that dietary arginine levels affected the production of bitter substances. Inosine is the primary degradation product of IMP, which is related to bitter taste (25). Targeted metabolic analysis revealed that arginine deficiency enhanced muscular inosine content.

Subsequently, we further explored the effect of arginine levels on muscular FAAs related to flavor in crustaceans (26). Aspartate and glutamate are related to umami taste; alanine, glycine, and serine possess a sweet taste, while leucine and isoleucine take part in the Maillard reaction to synthesize aroma compounds (27). In the study, the contents of aspartate and glutamate increased with the increase of dietary arginine. Meanwhile, the MA group had the highest contents of alanine and serine and total flavor amino acids. These results suggest that an optimal arginine level improved the flavor of the flesh of *L. vannamei* farmed in freshwater. The flavor is one of the crucial factors for consumers in evaluating flesh quality (28). These results indicated that dietary arginine should be appropriate to reduce the production of bitter substances and increase the umami taste of *L. vannamei*.

Our previous study found that dietary supplementation creatine improved *L. vannamei* flesh quality cultured in freshwater (5). Creatine is an essential metabolite of arginine (29). However, our study found that the creatine content of hepatopancreas and muscle was not affected by adding dietary arginine. This result indicated that only increasing the concentration of exogenous arginine cannot bring an increasing endogenous creatine synthesis in muscle and hepatopancreas. Creatine synthesis is involved a complicated process. It requires not only arginine but also glycine and methionine and related enzymes, including L-arginine-glycine amidinotransferase (AGAT), methionine-adenosyltransferase (MAT), and guanidinoacetate-methyltransferase (GAMT) (24). The current study showed that dietary arginine did not affect free methionine content but decreased free glycine content, which may explain unaltered muscular creatine content. Creatine is forming in liver and then is mainly transported skeletal muscle. An important metabolite of creatine is creatinine (30). In our study, dietary arginine levels had no significant effect on muscular creatine content. Still, urea nitrogen content in serum and creatinine in hepatopancreas and muscle were increased with the increasing dietary arginine level and reached the highest values in the HA group. These results indicated that surplus arginine might lead to hepatopancreas disruption of *L. vannamei*. This result explained the decrease in survival of *L. vannamei* caused by excess arginine in this study.

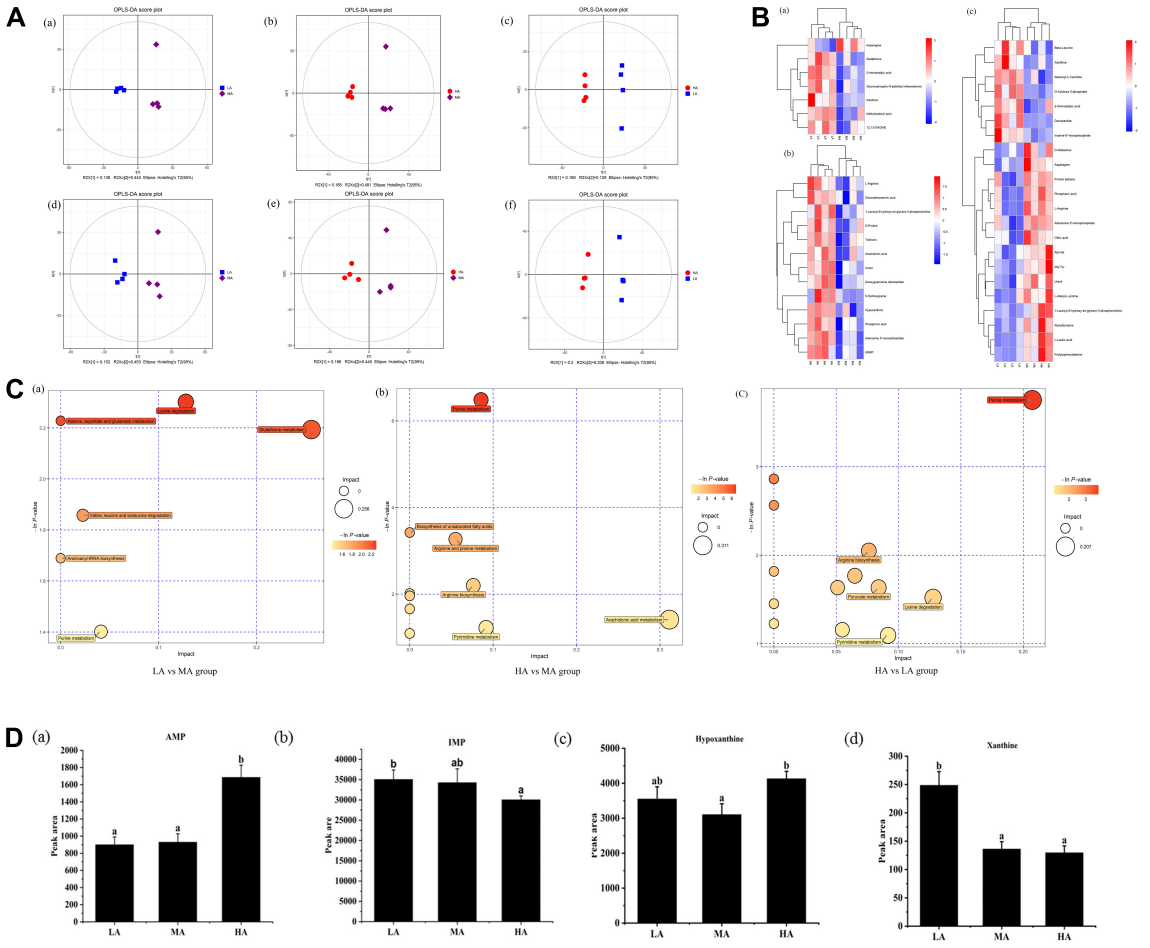

FIGURE 2
Untargeted metabolomics profiling of muscle in *L. vannamei* after dietary arginine treatment for 56 days. **(A)** OPLS-DA score plot of different comparison groups in ESI+ (a–c) and ESI− (d–f) model. **(B)** Heatmap of differential metabolites in different comparative groups. (a) Between LA and MA groups; (b) between HA and MA groups; (c) between LA and HA groups. **(C)** Metabolome view map of relevant metabolic pathways for change (a) between LA and MA groups; (b) between HA and MA groups; (c) between HA and LA groups. **(D)** Peak areas (× 106) of four flavoring substances involved in purine metabolism were detected based on muscle non-targeted metabolomics. (a) AMP; (b) IMP; (c) hypoxanthine; (d) xanthine. LA, the arginine-deficient diet; MA, the arginine-optimal diet; HA, the arginine-excessive diet.

Consumers prefer firmer aquatic products (31). The MA and HA diets improved textural properties in this study, including hardness and chewiness. Collagen content positively correlates with muscular hardness. Ornithine is an essential metabolite of arginine, and it is a precursor for collagen synthesis (32). In this study, muscular ornithine content increased with dietary arginine levels. Alkaline-soluble collagen includes the degraded collagen and the newly synthesized collagen molecules, and alkaline-insoluble collagen is related to the tensile strength of muscle, which contributes to the increase of muscular hardness (33). Our study found that arginine supplementation improved muscular hardness by increasing the content of alkaline-insoluble collagen. Similar results were found in grass carp (8). This result indicated that the increase in collagen content is due to an increase in ornithine content.

Meanwhile, glutamate is one of the primary metabolites of arginine metabolism. Dietary glutamate improved the muscle hardness of Atlantic salmon (34). In this study, shrimps fed the MA and HA diets had significantly higher hydrolyzed glutamate and free glutamate contents in muscle than those fed the LA diet, suggesting that increased muscular hardness may be partly linked to dietary arginine increased muscular glutamate content.

Previous studies indicated that muscular hardness positively correlates with fiber density (35, 36). In addition, smaller myofiber diameter and higher myofiber density reflected better flesh quality (37). In the present study, the myofiber density in the MA group was significantly higher than that in other treatments. On the other hand, the enhancement of flesh hardness in *L. vannamei* by arginine may link to the myofiber diameter. Myofiber diameter (<20 μm) suggests an active hyperplastic growth process during the developmental stage

TABLE 4 Relative metabolites of arginine contents in the hepatopancreas, muscle, and serum of *L. vannamei* after dietary arginine treatment.

Indexes	LA	MA	HA
Hepatopancreas (mg kg^{-1})			
Adenine	1.02 ± 0.07	1.11 ± 0.06	1.03 ± 0.04
Adenosine	2.55 ± 0.17^{a}	3.77 ± 0.58^{b}	3.85 ± 0.31^{b}
Citrulline	7.66 ± 0.21	8.04 ± 0.13	8.07 ± 0.42
Creatine	0.16 ± 0.01	0.17 ± 0.01	0.17 ± 0.01
Creatinine	1.72 ± 0.05^{a}	2.38 ± 0.36^{ab}	2.60 ± 0.44^{b}
Fumaric acid	3.60 ± 0.38	4.14 ± 0.20	4.14 ± 0.25
Glycocyamine	0.88 ± 0.08	0.92 ± 0.05	0.82 ± 0.05
Inosine	3638.66 ± 360.42	3643.60 ± 345.87	3669.17 ± 339.97
Ornithine	60.00 ± 2.44	63.33 ± 1.55	58.39 ± 2.26
Muscle (mg kg^{-1})			
Adenine	0.48 ± 0.02	0.50 ± 0.05	0.46 ± 0.02
Adenosine	3.10 ± 0.21^{a}	3.75 ± 0.56^{ab}	4.40 ± 0.43^{b}
Citrulline	10.45 ± 0.37^{a}	11.51 ± 0.45^{a}	13.96 ± 0.64^{b}
Creatine	1.15 ± 0.04	1.23 ± 0.08	1.29 ± 0.08
Creatinine	1.71 ± 0.10^{a}	2.18 ± 0.08^{b}	3.15 ± 0.20^{c}
Fumaric acid	44.92 ± 2.07^{c}	39.84 ± 2.56^{b}	26.62 ± 1.17^{a}
Glycocyamine	0.83 ± 0.05	0.81 ± 0.05	0.83 ± 0.02
Inosine	542.60 ± 32.50^{c}	369.61 ± 25.57^{b}	302.78 ± 18.94^{a}
Ornithine	43.34 ± 1.06^{a}	43.57 ± 1.03^{a}	69.40 ± 2.69^{b}
Serum (mmol L^{-1})			
Urea nitrogen	6.33 ± 0.25^{a}	6.93 ± 0.32^{ab}	7.13 ± 0.18^{b}

LA, the arginine-deficient diet; MA, the arginine-optimal diet; HA, the arginine-excessive diet.

(38). In the current study, the MA group showed a higher frequency of fibers diameter (<20 μm) and a lower frequency of fibers diameter (>50 μm) compared to the LA group, suggesting that optimum arginine level might improve the myofiber hyperplasia and skeletal muscle development (39). In this study, shrimps fed with MA diet and HA diets had longer sarcomere lengths. Sarcomeres consist of alternating light (I-band) and dark (A-band) bands, and longer sarcomeres decrease soluble protein loss and increase water holding capacity (40). This study indicated that arginine might prevent soluble protein loss and improve cooking flesh quality. In addition, sarcomere length is related to myofiber types (41). Myosin heavy chain gene family (MyHCs), a multi-gene family in vertebrate genomes, is closely related to the regulation of myofiber types (42). There are 13 muscle-type myosin genes found in *L. vannamei*, and five MyHCs were chosen to assess the relationship between arginine supplementation and myofiber type. For the first time, the current study showed that dietary arginine down-regulated the mRNA expressions of fast fiber *MyHCs* (*sMyHC1*, *sMyHC2*, and *sMyHC6a*) and up-regulated slow fiber MyHCs (*sMyHC5* and *sMyHC15*) in *L. vannamei*. Slow fibers have longer sarcomeres and shorter diameters than that fast fibers (41). These results are consistent with the trends in sarcomere length and myofiber diameter measured in this study.

Conclusion

Dietary optimal arginine (21.82 g kg^{-1}) improved muscle hardness by increasing the proportion of myofibers (<20 μm), myofiber density, sarcomere lengths, ornithine content and promoting fast myofibers conversion to slow myofibers. The dietary levels of arginine increased the contents of muscular umami amino acids (free aspartate and glutamate) and affected the purine metabolic pathway by reducing the content of hypoxanthine, xanthine, and inosine (bitter substance), thereby improving the flavor of the flesh. Additionally, the elevation of the protein-moisture ratio and hydrolyzed amino acids content, which improved the nutritional values of muscle. Finally, ornithine, citrulline, and glutamate were identified as critical metabolites in affecting flesh quality after arginine treatments. Whether these metabolites are more effective than arginine in improving shrimp flesh quality requires further study.

Data availability statement

The original contributions presented in this study are included in the article/**Supplementary material**, further inquiries can be directed to the corresponding author.

Ethics statement

The animal study was reviewed and approved by Pacific white shrimps (*Litopenaeus vannamei*) are widely cultivated in China and are not listed as endangered or protected species. All animal care and use procedures were approved by the Institutional Animal Care and Use Committee of Yangtze River Fisheries Research Institute (according to YFI 2018-40 of July 20, 2018). Pacific white shrimps were anesthetized with 30 mg eugenol L^{-1} water to minimum suffering before being assigned to cages and were anesthetized death with 60 mg eugenol L^{-1} water when sampling muscle and hepatopancreas in this experiment. Written informed consent was obtained from the owners for the participation of their animals in this study.

Author contributions

JT and HW designed the research. ML, MW, LY, MJ, and XL conducted the experiments and analyzed the data. ML, FH, and JT wrote the manuscript. All authors have read and approved the final manuscript.

Funding

This study was supported by the National Key Research and Development Program of China (No. 2018YFD0900400).

Acknowledgments

We thank Chuangju Li for providing essential facilities during the qRT–PCR analysis.

Conflict of interest

The authors declare that the research was conducted in the absence of any commercial or financial relationships that could be construed as a potential conflict of interest.

Publisher's note

Supplementary material

The Supplementary Material for this article can be found online at: https://www.frontiersin.org/articles/10.3389/fnut.2022.980188/full#supplementary-material

References

1. Li X, Wang Y, Li H, Jiang X, Ji L, Liu T, et al. Chemical and quality evaluation of Pacific white shrimp *Litopenaeus vannamei*: influence of strains on flesh nutrition. *Food Sci Nutr.* (2021) 9:5352–60. doi: 10.1002/fsn3.2457

2. Liang M, Wang S, Wang J, Chang Q, Mai K. Comparison of flavor components in shrimp *Litopenaeus vannamei* cultured in sea water and low salinity water. *Fisher Sci.* (2008) 74:1173–9. doi: 10.1111/j.1444-2906.2008.01637.x

3. Zhang W, Belton B, Edwards P, Henriksson PJG, Little DC, Newton R, et al. Aquaculture will continue to depend more on land than sea. *Nature.* (2022) 603:E2–4. doi: 10.1038/s41586-021-04331-3

4. Nrc. *Nutrient Requirements of Fish and Shrimp*. Washington, DC: National Academies Press (2011).

5. Cheng X, Li M, Leng X, Wen H, Wu F, Yu L, et al. Creatine improves the flesh quality of Pacific white shrimp (*Litopenaeus vannamei*) reared in freshwater. *Food Chem.* (2021) 354:129498. doi: 10.1016/j.foodchem.2021.129498

6. Hoseini SM, Khan MA, Yousefi M, Costas B. Roles of arginine in fish nutrition and health: insights for future researches. *Rev Aquacult.* (2020) 12:2091–108. doi: 10.1111/raq.12424

7. Zhou Q-C, Zeng W-P, Wang H-L, Wang T, Wang Y-L, Xie F-J. Dietary arginine requirement of juvenile Pacific white shrimp, *Litopenaeus vannamei*. *Aquaculture.* (2012) 364:252–8. doi: 10.1016/j.aquaculture.2012.08.020

8. Wang B, Liu Y, Feng L, Jiang W-D, Kuang S-Y, Jiang J, et al. Effects of dietary arginine supplementation on growth performance, flesh quality, muscle antioxidant capacity and antioxidant-related signalling molecule expression in young grass carp (*Ctenopharyngodon idella*). *Food Chem.* (2015) 167:91–9. doi: 10.1016/j.foodchem.2014.06.091

9. Ma X, Lin Y, Jiang Z, Zheng C, Zhou G, Yu D, et al. Dietary arginine supplementation enhances antioxidative capacity and improves meat quality of finishing pigs. *Amino Acids.* (2010) 38:95–102. doi: 10.1007/s00726-008-0213-8

10. Jiao P, Guo Y, Yang X, Long F. Effects of dietary arginine and methionine levels on broiler carcass traits and meat quality. *J Anim Vet Adv.* (2010) 9:1546–51. doi: 10.3923/javaa.2010.1546.1551

11. Aoac. *Official Method of Analysis*. 18th ed. Washington, DC: Association of Officiating Analytical Chemists (2005).

12. Li XJ, Bickerdike R, Lindsay E, Campbell P, Nickell D, Dingwall A, et al. Hydroxylysyl pyridinoline cross-link concentration affects the textural properties of fresh and smoked Atlantic salmon (*Salmo salar* L.) flesh. *J Agric Food Chem.* (2005) 53:6844–50. doi: 10.1021/jf050743+

13. Zhang K, Ai Q, Mai K, Xu W, Liufu Z, Zhang Y, et al. Effects of dietary hydroxyproline on growth performance, body composition, hydroxyproline and collagen concentrations in tissues in relation to prolyl 4-hydroxylase α (I) gene expression of juvenile turbot, *Scophthalmus maximus* L. fed high plant protein diets. *Aquaculture.* (2013) 404:77–84. doi: 10.1016/j.aquaculture.2013.04.025

14. Alves de Almeida FL, Carvalho RF, Pinhal D, Padovani CR, Martins C, Dal Pai-Silva M. Differential expression of myogenic regulatory factor MyoD in pacu skeletal muscle (*Piaractus mesopotamicus* Holmberg 1887: Serrasalminae, Characidae, Teleostei) during juvenile and adult growth phases. *Micron.* (2008) 39:1306–11. doi: 10.1016/j.micron.2008.02.011

15. Teshima S, Ishikawa M, Alam S, Koshio S, Michael FR. Supplemental effects and metabolic fate of crystalline arginine in juvenile shrimp *Marsupenaeus japonicus*. *Comp Biochem Physiol B Biochem Mol Biol.* (2004) 137:209–17. doi: 10.1016/j.cbpc.2003.11.005

16. Millamena OM, Bautista-Teruel M, Reyes O, Kanazawa A. Requirements of juvenile marine shrimp, *Penaeus monodon* (Fabricius) for lysine and arginine. *Aquaculture.* (1998) 164:95–104. doi: 10.1016/S0044-8486(98)00179-3

17. Ren M, Liao Y, Xie J, Liu B, Zhou Q, Ge X, et al. Dietary arginine requirement of juvenile blunt snout bream, *Megalobrama amblycephala*. *Aquaculture.* (2013) 414:229–34. doi: 10.1016/j.aquaculture.2013.08.021

18. Walton MJ, Cowey CB, Coloso RM, Adron JW. Dietary requirements of rainbow trout for tryptophan, lysine and arginine determined by growth and biochemical measurements. *Fish Physiol Biochem.* (1986) 2:161–9. doi: 10.1007/BF02264084

19. Du H, Lv H, Xu Z, Zhao S, Huang T, Manyande A, et al. The mechanism for improving the flesh quality of grass carp (*Ctenopharyngodon idella*) following the micro-flowing water treatment using a UPLC-QTOF/MS based metabolomics method. *Food Chem.* (2020) 327:126777. doi: 10.1016/j.foodchem.2020.126777

20. Wen D, Liu Y, Yu Q. Metabolomic approach to measuring quality of chilled chicken meat during storage. *Poult Sci.* (2020) 99:2543–54. doi: 10.1016/j.psj.2019.11.070

21. Zhang Y, Venkitasamy C, Pan Z, Wang W. Recent developments on umami ingredients of edible mushrooms – a review. *Trends Food Sci Technol.* (2013) 33:78–92. doi: 10.1016/j.tifs.2013.08.002

22. Bedini A, Zanolli V, Zanardi S, Bersellini U, Dalcanale E, Suman M. Rapid and simultaneous analysis of xanthines and polyphenols as bitter taste markers in bakery products by FT-NIR spectroscopy. *Food Anal Methods.* (2013) 6:17–27. doi: 10.1007/s12161-012-9405-7

23. Morris SM Jr. Arginine metabolism revisited. *J Nutr.* (2016) 146:2579–86. doi: 10.3945/jn.115.226621

24. Hristina K, Langerholc T, Trapecar M. Novel metabolic roles of l-arginine in body energy metabolism and possible clinical applications. *J Nutr Health Aging.* (2014) 18:213–8. doi: 10.1007/s12603-014-0015-5

25. Mateo J, Domínguez MC, Aguirrezábal MM, Zumalacárregui J. Taste compounds in chorizo and their changes during ripening. *Meat Sci.* (1996) 44:245–54. doi: 10.1016/S0309-1740(96)00098-8

26. Jiang W-D, Wu P, Tang R-J, Liu Y, Kuang S-Y, Jiang J, et al. Nutritive values, flavor amino acids, healthcare fatty acids and flesh quality improved by manganese referring to up-regulating the antioxidant capacity and signaling molecules TOR and Nrf2 in the muscle of fish. *Food Res Int.* (2016) 89:670–8. doi: 10.1016/j.foodres.2016.09.020Get

27. Tie H-M, Wu P, Jiang W-D, Liu Y, Kuang S-Y, Zeng Y-Y, et al. Dietary nucleotides supplementation affect the physicochemical properties, amino acid and fatty acid constituents, apoptosis and antioxidant mechanisms in grass carp (*Ctenopharyngodon idellus*) muscle. *Aquaculture.* (2019) 502:312–25. doi: 10.1016/j.aquaculture.2018.12.045

28. Huang X-H, Zheng X, Chen Z-H, Zhang Y-Y, Du M, Dong X-P, et al. Fresh and grilled eel volatile fingerprinting by e-Nose, GC-O, GC–MS and GC× GC-QTOF combined with purge and trap and solvent-assisted flavor evaporation. *Food Res Int.* (2019) 115:32–43. doi: 10.1016/j.foodres.2018.07.056

29. Wang Q, Xu Z, Ai Q. Arginine metabolism and its functions in growth, nutrient utilization, and immunonutrition of fish. *Anim Nutr.* (2021) 7:716–27. doi: 10.1016/j.aninu.2021.03.006

30. Mora L, Sentandreu MA, Toldra F. Contents of creatine, creatinine and carnosine in porcine muscles of different metabolic types. *Meat Sci.* (2008) 79:709–15. doi: 10.1016/j.meatsci.2007.11.002

31. Moreno HM, Montero MP, Gomez-Guillen MC, Fernandez-Martin F, Morkore T, Borderias J. Collagen characteristics of farmed Atlantic salmon with firm and soft fillet texture. *Food Chem.* (2012) 134:678–85. doi: 10.1016/j.foodchem.2012.02.160

32. Flynn NE, Meininger CJ, Haynes TE, Wu G. Dossier: free amino acids in human health and pathologies – The metabolic basis of arginine nutrition and pharmacotherapy. *Biomed Pharmacother.* (2002) 56:427–38. doi: 10.1016/s0753-3322(02)00273-1

33. Sun Y, Li B, Zhang X, Chen M, Tang H, Yu X. Dietary available phosphorus requirement of Crucian carp, *Carassius auratus*. *Aquacult Nutr.* (2018) 24:1494–501. doi: 10.1111/anu.12686

34. Larsson T, Koppang EO, Espe M, Terjesen BF, Krasnov A, Maria Moreno H, et al. Fillet quality and health of Atlantic salmon (*Salmo salar* L.) fed a diet supplemented with glutamate. *Aquaculture.* (2014) 426:288–95. doi: 10.1016/j.aquaculture.2014.01.034

35. Valente L, Cornet J, Donnay-Moreno C, Gouygou J-P, Bergé J-P, Bacelar M, et al. Quality differences of gilthead sea bream from distinct production systems in Southern Europe: intensive, integrated, semi-intensive or extensive systems. *Food Control.* (2011) 22:708–17. doi: 10.1016/j.foodcont.2010.11.001

36. Johnston IA, Alderson R, Sandham C, Dingwall A, Mitchell D, Selkirk C, et al. Muscle fibre density in relation to the colour and texture of smoked Atlantic salmon (*Salmo salar* L.). *Aquaculture.* (2000) 189:335–49. doi: 10.1016/S0044-8486(00)00373-2

37. Hurling R, Rodell J, Hunt H. Fiber diameter and fish texture. *J Texture Stud.* (1996) 27:679–85. doi: 10.1111/j.1745-4603.1996.tb01001.x

38. Wang C-C, Liu W-B, Huang Y-Y, Wang X, Li X-F, Zhang D-D, et al. Dietary DHA affects muscle fiber development by activating AMPK/Sirt1 pathway in blunt snout bream (*Megalobrama amblycephala*). *Aquaculture.* (2020) 518:734835. doi: 10.1016/j.aquaculture.2019.734835

39. Neu D, Boscolo W, Zaminhan M, Almeida F, Sary C, Furuya W. Growth performance, biochemical responses, and skeletal muscle development of juvenile Nile tilapia, *Oreochromis niloticus*, fed with increasing levels of arginine. *J World Aquacult Soc.* (2016) 47:248–59. doi: 10.1111/jwas.12262

40. Ertbjerg P, Puolanne EJMS. Muscle structure, sarcomere length and influences on meat quality: a review. *Meat Sci.* (2017) 132:139–52. doi: 10.1016/j.meatsci.2017.04.261

41. Wu M-P, Chang N-C, Chung C-L, Chiu W-C, Hsu C-C, Chen H-M, et al. Analysis of titin in red and white muscles: crucial role on muscle contractions using a fish model. *Biomed Res Int.* (2018) 2018:5816875. doi: 10.1155/2018/5816875

42. Berg JS, Powell BC, Cheney RE. A millennial myosin census. *Mol Biol Cell.* (2001) 12:780–94. doi: 10.1091/mbc.12.4.780

frontiers | Frontiers in Nutrition

TYPE Original Research
PUBLISHED 12 September 2022
DOI 10.3389/fnut.2022.962705

OPEN ACCESS

EDITED BY
Filippo Giorgio Di Girolamo,
University of Trieste, Italy

REVIEWED BY
Masoudreza Sohrabi,
Iran University of Medical Sciences, Iran
Emyr Reisha Isaura,
Airlangga University, Indonesia

*CORRESPONDENCE
Hongye Peng
20190931732@bucm.edu.cn
Wenliang Lv
lvwenliang@sohu.com

†These authors have contributed equally to this work and share first authorship

SPECIALTY SECTION
This article was submitted to Nutrition and Metabolism, a section of the journal Frontiers in Nutrition

RECEIVED 06 June 2022
ACCEPTED 22 August 2022
PUBLISHED 12 September 2022

CITATION
Peng H, Wang M, Pan L, Cao Z, Yao Z, Chen Q, Li Y, Wang Y and Lv W (2022) Associations of serum multivitamin levels with the risk of non-alcoholic fatty liver disease: A population-based cross-sectional study in U.S. adults. *Front. Nutr.* 9:962705. doi: 10.3389/fnut.2022.962705

Associations of serum multivitamin levels with the risk of non-alcoholic fatty liver disease: A population-based cross-sectional study in U.S. adults

Hongye Peng[1*†], Miyuan Wang[2†], Liang Pan[3†], Zhengmin Cao[1], Ziang Yao[1], Qiuye Chen[1], Yanbo Li[1], Yuhua Wang[3] and Wenliang Lv[1*]

[1]Department of Infection, Guang'anmen Hospital, China Academy of Chinese Medical Sciences, Beijing, China, [2]School of Public Health, Tongji Medical College, Huazhong University of Science and Technology, Wuhan, China, [3]Phase 1 Clinical Trial Center, Deyang People's Hospital, Deyang, China

Vitamins were closely associated with non-alcoholic fatty liver disease (NAFLD) development, but no study had explored the association of serum multivitamin levels with NAFLD risk. We assessed the association between serum levels of both single-vitamin and multivitamins (VA, VB6, VB9, VB12, VC, VD, and VE) and the risk of NAFLD, using the database of National Health and Nutrition Examination Survey (NHANES) (cycles 2003–2004 and 2005–2006). We employed multivariable logistic regression and weighted quantile sum (WQS) regression models to explore the association of serum multivitamin levels with NAFLD. Among all 2,294 participants, 969 participants with NAFLD were more likely to be male, older, less educated, or have hypertension/high cholesterol/diabetes. After adjustment of covariates, serum VC/VD/VB6/VB9 levels were negatively correlated with NAFLD risk, while serum VA/VE levels were positively correlated with NAFLD risk. In the WQS model, elevated serum VA/VE levels and lowered serum VC/VD/VB6 levels were linearly associated with increased NAFLD risk. There was a non-linear relationship between serum VB9/VB12 levels and NAFLD risk. There were evident associations between serum multivitamin levels and reduced NAFLD risk, which was mainly driven by VD/VB9/VC. In conclusion, our findings suggested that serum multivitamin levels were significantly associated with the risk of NAFLD.

KEYWORDS

multi-vitamins, NAFLD, weighted quantile sum, dose-response relationship, serum level

Introduction

Non-alcoholic fatty liver disease (NAFLD) is a syndrome characterized by excessive deposition of fat in hepatocytes other than factors from alcohol or other definite liver damage, encompassing a spectrum of non-alcoholic fatty liver, non-alcoholic steatohepatitis, related cirrhosis, liver cancer, and others. NAFLD has become the most common chronic liver disease worldwide and exerts influence on the health of 25.24% adults (1). With increasing living standards and obese population, the prevalence of NAFLD will rise continuously. In 2030, the prevalence of NAFLD is expected to reach 33.5% in population aged over 15 years and 28.4% in all ages, with 100.9 million newly increased cases (2). The increasing population with NAFLD imposes a growing societal and economic burden to the world. Presently, there is a lack of safe and effective drug for NAFLD, and the most effective way is lifestyle improvement (3). It is noteworthy that further research studies should focus on the prevention and relief of NAFLD development.

As a class of organic compounds necessary for maintaining the normal physiological function, vitamins play an important role in the growth, metabolism, and development of human body. More and more evidences suggest that vitamins are closely associated with the occurrence and development of NAFLD (4–7). However, some results are controversial. For example, individuals with elevated serum VB9 and VB12 levels have lower risk of NAFLD (8, 9), while those with elevated serum VA level possibly have higher risk of NAFLD (10). Most studies currently focus on the relationship between serum level of single-vitamin, instead of multivitamins, and the development of NAFLD. Previous studies demonstrate that some vitamins may affect the biological functions by interacting with other vitamins (11). So it is significant to explore the potential association between serum multivitamin levels and NAFLD risk.

The absorption of vitamins is affected by various factors, including gender, age, and BMI (12). And also there is vitamin loss during food storage, processing, and cooking. Therefore, the serum vitamin level is a more representative and persuasive indicator to evaluate vitamin circulation, comparing with vitamin intake from food.

Based on the data from 2003 to 2006 in the National Health and Nutrition Examination Survey (NHANES), this study aims to elaborate the relationship between the serum levels of 7 vitamins (VA, VB6, VB9, VB12, VC, VD, and VE) and the risk of NAFLD in American adults, as well as to explore the association between serum levels of both single-vitamin and multivitamins and the prevalence of NAFLD.

Materials and methods

Study design and participants

This study included all participants ≥ 20 years old from the 2003–2004 and 2005–2006 cycles of the NHANES in the United States. Profiles of the NHANES were introduced by other researchers (13). Employing a complex, multi-stage, and probability sampling design, the NHANES collected a representative sample from non-institutionalized American population. In those two cycles of NHANES, all baseline data were collected by household interviews, mobile physical examinations, and laboratory tests. **Figure 1** showed the flow chart of participant screening. Of all the 20,470 participants, we excluded those taking lipid-lowering drugs, antitubercular agents, glucocorticoids, or vitamin supplements within 30 days (n = 301), those < 20 years old (n = 10,195), those with positive serology for hepatitis B, C, and D (n = 275), those consuming alcohol > 20 g/day for female or > 30 g/day for male (n = 7,342), and those missing important data such as BMI, triglyceride, gamma-glutamyl transpeptidase (GGT), and waist circumference (n = 63) (**Figure 1**). At last, a total of 2,294 participants were included for the statistical analysis. The protocol of NHANES was reviewed and approved by the Research Ethics Review Board of the National Center for Health Statistics. All participants signed written informed consent before their participation.

Definition of non-alcoholic fatty liver disease

NAFLD was a condition of excessive fat accumulation in the liver, excluding fatty liver due to other causes by liver disease and/or excessive alcohol consumption. Fatty liver index (FLI) was considered a simple and accurate predicting index for hepatic steatosis in the general population and was widely used in NAFLD research, with an accuracy of 0.84 (95% CI: 0.81–0.87) (14). So we used FLI to predict the risk of NAFLD. FLI was calculated with the following Equation (15):

$$\begin{aligned}\mathrm{FLI} = (&e^{0.953\times \mathrm{LN\ (triglycerides)} + 0.139\times \mathrm{BMI} + 0.718\times \mathrm{LN\ (GGT)} \\ &+0.053\times \mathrm{waist\ circumference} - 15.745}) \div (1 + e^{0.953\times \mathrm{LN\ (triglycerides)} \\ &+0.139\times \mathrm{BMI} + 0.718\times \mathrm{LN(GGT)} + 0.053\times \mathrm{waist\ circumference} - 15.745}) \times 100,\end{aligned}$$

where triglycerides were in mg/dl, BMI in kg/m^2, GGT in mmol/L, and waist circumference in cm. This equation of FLI generated scores ranging from 0 to 100. An FLI < 30 suggested no presence of NAFLD, while an FLI ≥ 60 suggested the probable presence of fatty liver (15).

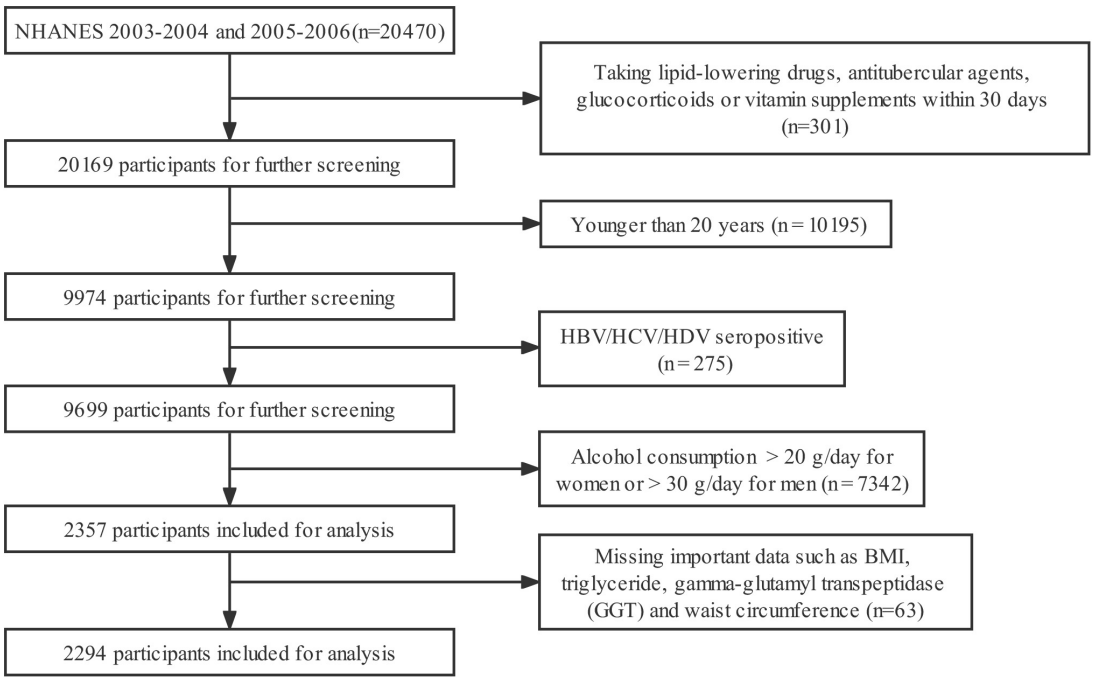

FIGURE 1
Flow chart for the selection of participants in the cohort study. HBV, hepatitis B virus; HCV, hepatitis C virus; HDV, hepatitis D virus.

Measurement of serum vitamin levels

All serum samples were processed and delivered to the Division of Environmental Health Laboratory Sciences, National Center for Environmental Health, and Centers for Disease Control and Prevention (CDC) for analysis. Serum levels of VA (retinol), VC (ascorbic acid), and VE (α-tocopherol) were measured with high-performance liquid chromatography (HPLC) and quantitatively determined with spectrophotometric methods. Serum 25-hydroxyvitamin D [25(OH)D] levels were first determined with the DiaSorin RIA kit. NHANES employed regression to convert equivalently all 25(OH)D measurements obtained from standardized liquid chromatography–tandem mass spectrometry (LC-MS/MS) methods, to integrate the laboratory test data from different cycles. Serum VB9 and VB12 levels were measured with the radio-assay kit from Bio-Rad Laboratories. Serum VB6 level was measured with reversed-phase HPLC methods. All the laboratory assay data were accessible to the public on the NHANES website.

Covariates

Demographic variables were extracted from the baseline household questionnaires as covariates, including age, gender, ethnicity (Mexican American, non-Hispanic white, non-Hispanic black, and others), family income—poverty ratio (FIPR), and education level (below high school, high school or equivalent, and college or above). Histories of hypertension, high cholesterol, and diabetes were also collected. More details of the above-mentioned covariates were accessible to the public on the NHANES website.

Statistical analysis

According to the analytic guidelines for the NHANES survey, we employed sampling weights in our analyses and estimated variances by considering clustering and stratification. Binary or categorical variables were presented with number (%), while continuous variables were presented with median (interquartile range, IQR). The differences of population characteristics within the survey cycle were analyzed with Rao–Scott Chi-square test and Wilcoxon rank-sum test for categorical and continuous variables, respectively.

Multivariate-adjusted logistic regression models were employed to explore the relationship between the serum level of single vitamin and NAFLD. Serum levels of vitamins were analyzed as both continuous and categorical variables (classified into four groups according to quartiles, with the first quartile as reference). We computed the odds ratio (OR) and corresponding 95% confidence intervals (95% CIs) in three models. Model 1 included only independent variables. Model 2 was additionally adjusted for gender, age, ethnicity, FIPR, and

education level. Model 3 was further adjusted for the disease history (hypertension, high cholesterol, and diabetes).

Weighted Quantile Sum (WQS) regression, a weighted quartile sum approach combined with logistic regression, was employed to examine the associations between both multivitamins/single-vitamin and the risk of NAFLD. The WQS regression integrated the serum levels of multivitamins into one index. The contribution of a single vitamin level was weighted according to its relevance to the overall association with the outcome. The weights are constrained to sum to 1, with higher numbers indicating a larger contribution (16, 17). The serum levels of vitamins were highly correlated, so there would be misleading results when employing linear regression models to examine the association of a single vitamin level with NAFLD while adjusting for other levels, due to the problem of collinearity. Therefore, we proposed WQS regression to examine the association of single serum vitamin level with NAFLD, while addressing the highly positive correlations among multivitamin levels.

All statistical analyses were completed with R 3.6.2, employing packages "lme4". $p < 0.05$ for a two-tailed test denoted statistical significance.

Results

Characteristics of the study participants

There were 969 individuals with NAFLD (42.24%) among the 2,294 participants (Table 1). The mean ± SD age was 51 (36, 67) years [54 (40, 67) in participants with NAFLD and 49 (34, 67) in those without]. The proportions of men and women were 56.8 and 43.2%, respectively. Except for ethnicity and FIPR, there were statistical differences between participants with and without NAFLD in the basic characteristics. Participants with NAFLD were more likely to be male, older, less educated, or have hypertension/high cholesterol/diabetes. Most serum vitamin levels were lower in participants with NAFLD than in those without, except for VA and VE (Table 1).

Pearson correlations (rs) of all studied vitamins are shown in Figure 2. Most of the vitamins were positively correlated with each other (rs = 0.1–0.4). The correlation coefficients between VB6 and VB9, VC and VB9, VE and VC, VE and VB9, and VA and VE were 0.4.

Serum level of single vitamin and the risk of non-alcoholic fatty liver disease

Table 2 showed the multi-variate adjusted OR and 95% CIs for the relationship between the risk of NAFLD and increment of serum level of seven studied vitamins. After adjusting for all covariates, negative associations with the risk of NAFLD were found for VC (OR = 0.985, 95% CI = 0.981–0.989), VD (OR = 0.981, 95% CI = 0.975–0.987), VB6 (OR = 0.995, 95% CI = 0.994–0.997), and VB9 (OR = 0.988, 95% CI = 0.979–0.997), while positive associations were found for VA (OR = 1.361, 95% CI = 1.045–1.772) and VE (OR = 1.020, 95% CI = 1.012–1.028). Moreover, we found that the risk of NAFLD increased by 36.1% (95% CI: 4.5%, 77.2%) with each unit increment of serum VA level in model 3.

We repeated the above-mentioned statistical analyses by using vitamins as categorical variables (quartiles) and acquired similar results (Table 3). In addition, the risk of NAFLD showed a stepwise decrease with the quartiles of VB9 (P for trend < 0.05) and was at the lowest point in the highest VB9 quartile group (Q4) (OR, 0.537; 95% CI, 0.364-0.793) after adjusting for all covariates. Similar trends were found for VC and VB6. After adjusting for all covariates in model 3, the risk of NAFLD was higher in Q4 group than that in the Q1 group for both serum VA (OR, 1.661 (1.093, 2.526)) and serum VE (OR, 1.976 (1.377, 2.836)).

Dose-response relationships between serum vitamin levels and non-alcoholic fatty liver disease

Dose–response curves for the relationships between all studied vitamins and the risk of NAFLD were presented in Figure 3, which showed similar directions to those curves in the single-vitamin logistic regression model.

Figure 3A showed the dose–response relationship between serum VA level and NAFLD. There was a positive linear correlation between NAFLD and VA (p overall = 0.007, p non-linear = 0.824). Lower serum VA level was uncorrelated with NAFLD risk. However, the risk of NAFLD increased linearly as serum VA levels elevated when the latter exceeded a certain threshold.

Figure 3B showed the dose–response relationship between serum VE level and NAFLD. There was a positive linear correlation between NAFLD and VE (p overall < 0.001, p non-linear = 0.519). Lower serum VE level could be protective against NAFLD (OR < 1), but its protective effect weakened with elevated levels. The risk of NAFLD increased as serum VE levels elevated when the latter exceeded a certain threshold (OR > 1).

Figure 3C showed the dose–response relationship between serum VC level and NAFLD. There was a negative linear correlation between NAFLD and VC (p overall < 0.001, p non-linear = 0.259). A lower serum VC level could be a risk factor for NAFLD (OR > 1), but its risk effect weakened with an elevated level. The risk of NAFLD decreased as serum VC levels elevated when the latter exceeded a certain threshold (OR < 1). However, serum VC was uncorrelated with NAFLD risk when it was above a limited level.

TABLE 1 Basic characteristics of participants by non-alcoholic fatty liver disease (NAFLD) in NHANES 2003–2006.

Variables	Non-NAFLD (*n* = 1325)	With NAFLD (*n* = 969)	Total (*n* = 2294)	*P*-value
Sex, ***n*** **(%)**				<0.001
Female	650 (49.1)	341 (35.2)	991 (43.2)	
Male	675 (50.9)	628 (64.8)	1303 (56.8)	
Age (years)	49 (34, 67)	54 (40, 67)	51 (36, 67)	<0.001
Race, ***n*** **(%)**				0.431
Mexican American	178 (13.4)	154 (15.9)	332 (14.5)	
Non-Hispanic black	225 (17)	158 (16.3)	383 (16.7)	
Non-Hispanic white	847 (63.9)	603 (62.2)	1450 (63.2)	
Other	75 (5.7)	54 (5.6)	129 (5.6)	
FIPR	3.3 (1.7, 5)	3 (1.6, 5)	3.2 (1.7, 5)	0.082
Missing	49 (3.7%)	37 (3.8%)	86 (3.7%)	
Education, ***n*** **(%)**				0.006
College or above	828 (62.5)	542 (55.9)	1370 (59.7)	
High school or equivalent	277 (20.9)	236 (24.4)	513 (22.4)	
Less than high school	219 (16.5)	191 (19.7)	410 (17.9)	
Missing	1 (0.1%)	0 (0%)	1 (0.0%)	
Hypertension, ***n*** **(%)**				<0.001
No	980 (74.2)	518 (53.8)	1498 (65.6)	
Yes	341 (25.8)	444 (46.2)	785 (34.4)	
Missing	4 (0.3%)	7 (0.7%)	11 (0.5%)	
High cholesterol, ***n*** **(%)**				<0.001
No	620 (62.2)	389 (48.9)	1009 (56.3)	
Yes	376 (37.8)	407 (51.1)	783 (43.7)	
Missing	329 (24.8%)	173 (17.9%)	502 (21.9%)	
Diabetes, ***n*** **(%)**				<0.001
No	1259 (95.8)	806 (85.3)	2065 (91.4)	
Yes	55 (4.2)	139 (14.7)	194 (8.6)	
Missing	11 (0.8%)	24 (2.5%)	35 (1.5%)	
VA (μmol/L)	2.0 (1.7, 2.4)	2.2 (1.8, 2.6)	2.1 (1.7, 2.5)	<0.001
Missing	11 (0.8%)	8 (0.8%)	19 (0.8%)	
VE (μmol/L)	27.9 (22.3, 35.8)	30.1 (24.1, 40.6)	28.7 (22.9, 37.8)	<0.001
Missing	11 (0.8%)	16 (1.7%)	27 (1.2%)	
VD (μmol/L)	62.4 (48.3, 75.3)	56.8 (42.2, 68.9)	59.2 (45.9, 72.9)	<0.001
Missing	3 (0.2%)	1 (0.1%)	4 (0.2%)	
VC (μmol/L)	63.0 (48.3, 77.2)	51.7 (34, 67.7)	59.1 (41.4, 73.8)	<0.001
Missing	7 (0.5%)	5 (0.5%)	12 (0.5%)	
VB6 (μmol/L)	53.3 (29.2, 93.1)	43.6 (26.9, 77)	49.5 (27.9, 85.7)	<0.001
Missing	41 (3.1%)	26 (2.7%)	67 (2.9%)	
VB12 (μmol/L)	366.0 (279.3, 493.0)	331.0 (250.2, 439.3)	352.0 (265.7, 467.3)	<0.001
Missing	17 (1.3%)	13 (1.3%)	30 (1.3%)	
VB9 (μmol/L)	30.8 (22, 41.7)	26.7 (19, 39.2)	29 (20.6, 40.6)	<0.001
Missing	8 (0.6%)	11 (1.1%)	19 (0.8%)	

FIPR, family income-poverty ratio; VA, vitamin A; VE, vitamin E; VC, vitamin C; VD, vitamin D; VB6, vitamin B6, VB12, vitamin B12; VB9, vitamin B9. *P*-values were calculated by Rao–Scott chi-square test and Wilcoxon rank-sum test for categorical and continuous variables, respectively.

Figure 3D showed the dose–response relationship between serum VD level and NAFLD. There was a negative linear correlation between NAFLD and VD (p overall < 0.001, p non-linear $= 0.353$). Lower serum VD level could be a risk factor for NAFLD (OR > 1), but its risk effect weakened with elevated levels. The risk of NAFLD decreased consistently as serum VD levels elevated when the latter exceeded a certain threshold (OR < 1).

Figure 3E showed the dose–response relationship between serum VB6 level and NAFLD. There was a

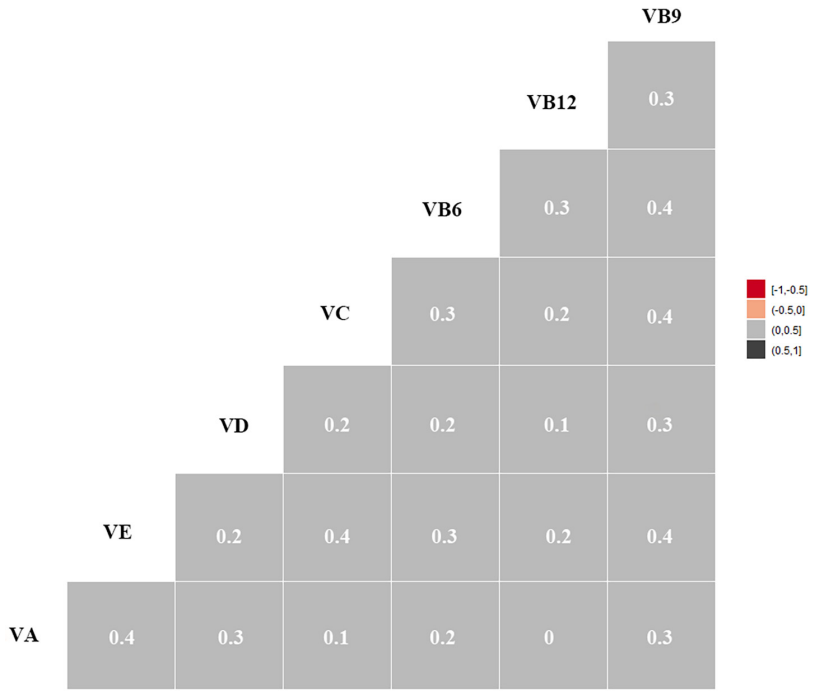

FIGURE 2
Heat Map for Spearman correlation between serum vitamins. Correlation intensity between two vitamins was indicated by square color. In the heat map, the black color shows a strong positive expression correlation, whereas the gray color depicts a weak expression correlation. VA, vitamin A; VE, vitamin E; VC, vitamin C; VD, vitamin D; VB6, vitamin B6, VB12, vitamin B12; VB9, vitamin B9.

negative linear correlation between NAFLD and VB6 (p overall < 0.001, p non-linear = 0.506). Its dose–response trend was similar to that of VD.

Figure 3F showed the dose–response relationship between serum VB12 level and NAFLD. There was a non-linear correlation between NAFLD and VB12 (p overall = 0.001, p non-linear = 0.043). Lower serum VB12 level could be a risk factor for NAFLD (OR > 1), but its risk effect weakened with elevated levels. However, serum VB12 was uncorrelated with NAFLD risk when it was above a limited level.

Figure 3G showed the dose–response relationship between serum VB9 level and NAFLD. There was a non-linear correlation between NAFLD and VB9 (p overall <0.001, p non-linear = 0.004). Its dose–response trend was similar to that of VB12.

Serum multivitamin levels and the risk of non-alcoholic fatty liver disease

Table 4 showed the results from rough and fully adjusted models with WQS regression. We found the indices in WQS were significantly associated with NAFLD. In the fully adjusted models, each increment of the index was associated with 41.5% lower odds of NAFLD (OR = 0.585, 95% CI: 0482–0.712). We also observed the highest weights in WQS model: 0.48 for VD, 0.28 for VB9, and 0.19 for VC in negative correlation. VE and VA were observed in positive correlation (Figure 4).

Discussion

To date, most population-based research studies focused on the relationship between single vitamin and the risk of NAFLD (9, 18, 19). A few research studies explored their

TABLE 2 Multi-variate adjusted odds ratio (95% CIs) for the relationship between the risk of NAFLD and increment of serum level of vitamins among participants in NHANES 2003–2006.

Variables	Model 1	Model 2	Model 3
VA	**1.768 (1.427, 2.189)**	**1.551 (1.226, 1.964)**	**1.361 (1.045, 1.772)**
VE	**1.017 (1.011, 1.024)**	**1.019 (1.011, 1.027)**	**1.020 (1.012, 1.028)**
VC	**0.981 (0.977, 0.985)**	**0.982 (0.978, 0.985)**	**0.985 (0.981, 0.989)**
VD	**0.985 (0.980, 0.990)**	**0.981 (0.976, 0.985)**	**0.981 (0.975, 0.987)**
VB6	**0.996 (0.994, 0.998)**	**0.995 (0.994, 0.997)**	**0.995 (0.994, 0.997)**
VB12	**0.999 (0.998, 1.000)**	**0.999 (0.998, 1.000)**	0.999 (0.998, 1.000)
VB9	**0.987 (0.979, 0.996)**	**0.985 (0.977, 0.994)**	**0.988 (0.979, 0.997)**

All estimates accounted for complex survey designs. Model 1 included only independent variables; model 2 was additionally adjusted for gender, age, ethnicity, FIPR and education level; and model 3 was further adjusted for the disease history (hypertension, high cholesterol and diabetes). Those results in bold had statistical significance.

TABLE 3 Multi-variate adjusted odds ratios (95% CIs) of risks of NAFLD in relation to serum vitamins levels among participants in NHANES 2003–2006.

Variables	The range of serum vitamin levels (μ mol/L)	Model 1	*P*-value	Model 2	*P*-value	Model 3	*P*-value
VA	0.34–4.78						
Q1	0.34–1.72	1		1		1	
Q2	1.72–2.07	**1.614 (1.239, 2.103)**	0.001	**1.441 (1.097, 1.892)**	0.017	1.35 (0.932, 1.955)	0.132
Q3	2.07–2.45	**1.619 (1.217, 2.155)**	0.003	1.248 (0.882, 1.766)	0.226	1.083 (0.715, 1.64)	0.712
Q4	2.45–4.78	**2.409 (1.761, 3.296)**	0.000	**1.934 (1.359, 2.752)**	0.002	**1.661 (1.093, 2.526)**	0.030
p for trend		<0.001		0.010			0.102
VE	2.04–89.12						
Q1	2.04–22.87	1		1		1	
Q2	22.89–28.68	1.185 (0.868, 1.619)	0.295	1.248 (0.893, 1.745)	0.210	1.393 (0.929, 2.09)	0.128
Q3	28.72–37.76	**1.397 (1.049, 1.861)**	0.030	**1.447 (1.043, 2.009)**	0.039	1.5 (1.014, 2.219)	0.059
Q4	37.83–89.12	**1.736 (1.303, 2.314)**	0.001	**1.905 (1.361, 2.666)**	0.001	**1.976 (1.377, 2.836)**	0.002
p for trend		<0.001		0.002		0.003	
VC	0.60–195.90						
Q1	0.60–41.40	1		1		1	
Q2	42.00–59.10	**0.585 (0.431, 0.795)**	0.002	**0.602 (0.437, 0.829)**	0.006	0.713 (0.498, 1.021)	0.083
Q3	59.60–73.80	**0.35 (0.262, 0.469)**	0.000	**0.374 (0.277, 0.505)**	0.000	**0.463 (0.338, 0.632)**	0.000
Q4	74.40–195.90	**0.301 (0.229, 0.396)**	0.000	**0.314 (0.246, 0.4)**	0.000	**0.377 (0.282, 0.503)**	0.000
p for trend		<0.001		<0.001		<0.001	
VD	9.10–166.00						
Q1	9.10–45.90	1		1		1	
Q2	47.10–59.20	0.951 (0.688, 1.314)	0.763	0.873 (0.603, 1.263)	0.479	0.987 (0.65, 1.499)	0.953
Q3	60.60–72.90	0.747 (0.562, 0.993)	0.055	**0.641 (0.475, 0.867)**	0.009	0.823 (0.552, 1.226)	0.352
Q4	73.80–166.00	**0.496 (0.372, 0.661)**	0.000	**0.411 (0.31, 0.546)**	0.000	**0.426 (0.286, 0.635)**	0.001
p for trend		<0.001		<0.001		<0.001	
VB6	3.80–400.00						
Q1	3.80–27.90	1		1		1	
Q2	28.00–49.50	1.136 (0.904, 1.427)	0.285	0.993 (0.786, 1.256)	0.955	0.871 (0.627, 1.211)	0.424
Q3	49.70–85.60	0.868 (0.672, 1.121)	0.288	0.741 (0.558, 0.985)	0.053	0.68 (0.472, 0.979)	0.055
Q4	85.80–400.00	**0.632 (0.486, 0.823)**	0.002	**0.528 (0.406, 0.688)**	0.000	**0.529 (0.383, 0.73)**	0.001
p for trend		0.001		<0.001		0.002	
VB12	25.09–2952.00						
Q1	25.09–265.68	1		1		1	
Q2	266.40–352.00	0.726 (0.511, 1.032)	0.086	0.714 (0.502, 1.017)	0.077	0.75 (0.472, 1.189)	0.239
Q3	352.80–467.10	**0.654 (0.49, 0.872)**	0.008	**0.656 (0.487, 0.885)**	0.012	0.738 (0.513, 1.062)	0.121
Q4	467.90–2952.00	**0.445 (0.324, 0.611)**	0.000	**0.456 (0.324, 0.64)**	0.000	**0.54 (0.36, 0.809)**	0.009
p for trend		<0.001		<0.001		0.005	
VB9	5.40–144.30						
Q1	5.40–20.60	1		1		1	
Q2	20.80–29.00	**0.683 (0.522, 0.894)**	0.010	**0.665 (0.503, 0.879)**	0.010	**0.668 (0.485, 0.92)**	0.025
Q3	29.20–40.50	**0.538 (0.395, 0.733)**	0.001	**0.535 (0.381, 0.753)**	0.002	**0.559 (0.357, 0.878)**	0.022
Q4	40.80–144.30	**0.52 (0.377, 0.716)**	0.000	**0.492 (0.359, 0.676)**	0.000	**0.537 (0.364, 0.793)**	0.006
p for trend		0.002		0.004		0.023	

All estimates accounted for complex survey designs. Model 1 contains only independent variables; model 2 was additionally adjusted for gender, age, ethnicity, FIPR and education level; and model 3 was further adjusted for the disease history (hypertension, high cholesterol and diabetes). Those results in bold had statistical significance. Q1, Q2, Q3, and Q4 indicated the 1st, 2nd, 3rd, and 4th quartiles across the lowest to the highest concentrations of circulating vitamins.

dose–response relationship. There was no reported evidence for the correlations between multivitamins and NAFLD risk. People normally encounter mixed exposures rather than a single exposure due to multivitamins contained in daily food. Unlike previous studies, in this cross-sectional study of a nationally representative sample, we explored for the first time

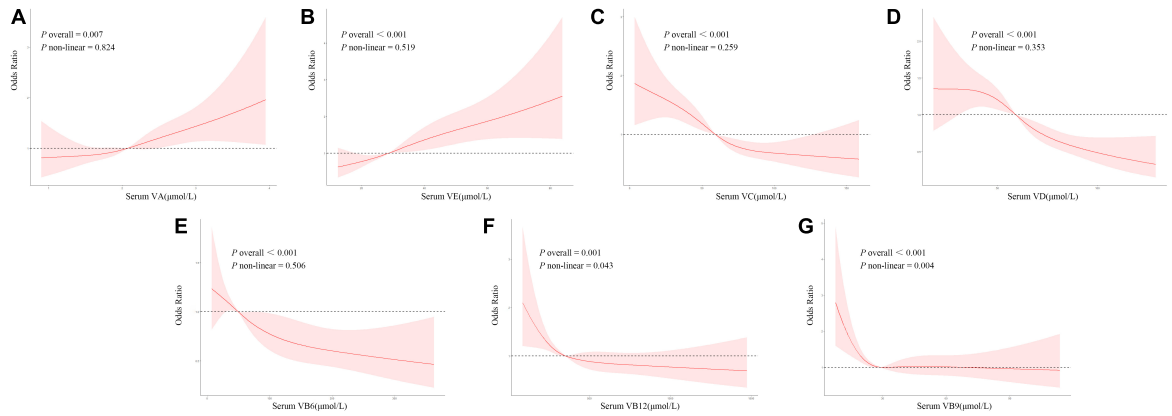

FIGURE 3
(A–G) Dose–response relationships between serum vitamin levels and the risk of NAFLD with restricted cubic spline model. The model was adjusted for gender, age, ethnicity, FIPR, education level, and disease history (hypertension, high cholesterol, and diabetes).

the associations between serum multivitamin levels and the risk of NAFLD as well as their dose–response relationships through comprehensive analyses with multiple novel statistical approaches. We found that serum levels of VC, VD, VB6, and VB9 were negatively correlated with the risk of NAFLD, while serum levels of VA and VE were positively correlated with the risk of NAFLD. We also observed linear correlations of those five vitamins with the risk of NAFLD from the dose–response curves. WQS regression suggested significant associations between serum multivitamin levels and reduced risk of NAFLD, with major contributors of VD, VB9, and VC. Our findings suggested that serum multivitamin levels were significantly associated with the risk of NAFLD.

Vitamin A and the risk of non-alcoholic fatty liver disease

As a lipid-soluble vitamin and an antioxidant, VA (retinol) existed abundantly in animals, especially in fish. Interestingly enough, VA intake might not guarantee any antioxidative and/or protective effects (20). Instead, long-term intake of VA would elevate the levels of alkaline phosphatase, triacylglycerol, and cholesterol (21), which were somehow associated with the risk of NAFLD. Based on the dose–response relationship curves, we suggested that there was a linear positive correlation between serum VA level and the risk of NAFLD. VA played an important role in both metabolic regulation and hepatic stellate cell activation, so it might be a critical factor during the exploration of NAFLD pathogenesis (22). Previous studies proposed some evidence for the association between VA and NAFLD. Similar to our findings, Bahcecioglu et al. suggested that patients with non-alcoholic steatohepatitis (NASH) or simple hepatic steatosis have elevated serum VA levels compared with healthy individuals (23). According to a prospective longitudinal study including 2,658 participants (24), higher serum VA level was associated with the progression of NAFLD, which was possibly attributed to increased triglycerides, insulin resistance, serum retinol-binding protein 4, and BMI. However, some studies proposed different conclusions. Botella-Carretero et al. suggested that serum VA level was negatively correlated with BMI for morbidly obese people as well as the level of serum transaminase for NAFLD patients (25). A study suggested that there was a significant association between low retinol levels and insulin resistance (26). Those discrepancies might be due to the differences in overall serum VA levels in the included population. According to the dose–response curves, a lower serum VA level was protective against NAFLD, while higher serum VA level became a risk factor for NAFLD. Therefore, we suggested that maintaining a proper serum VA level might be good for health.

Vitamin C and the risk of non-alcoholic fatty liver disease

We found that serum VC level was negatively correlated with the risk of NAFLD, as well as the most important

TABLE 4 Overall effects of the multivitamins estimates and 95% confidence interval.

Model	OR	*P*
Model 1	0.580 (0.508, 0.662)	<0.001
Model 2	0.527 (0.447, 0.622)	<0.001
Model 3	0.585 (0.482, 0.712)	<0.001

All estimates accounted for complex survey designs. Model 1 included only independent variables; model 2 was additionally adjusted for gender, age, ethnicity, FIPR, and education level; and model 3 was further adjusted for the disease history (hypertension, high cholesterol, and diabetes).

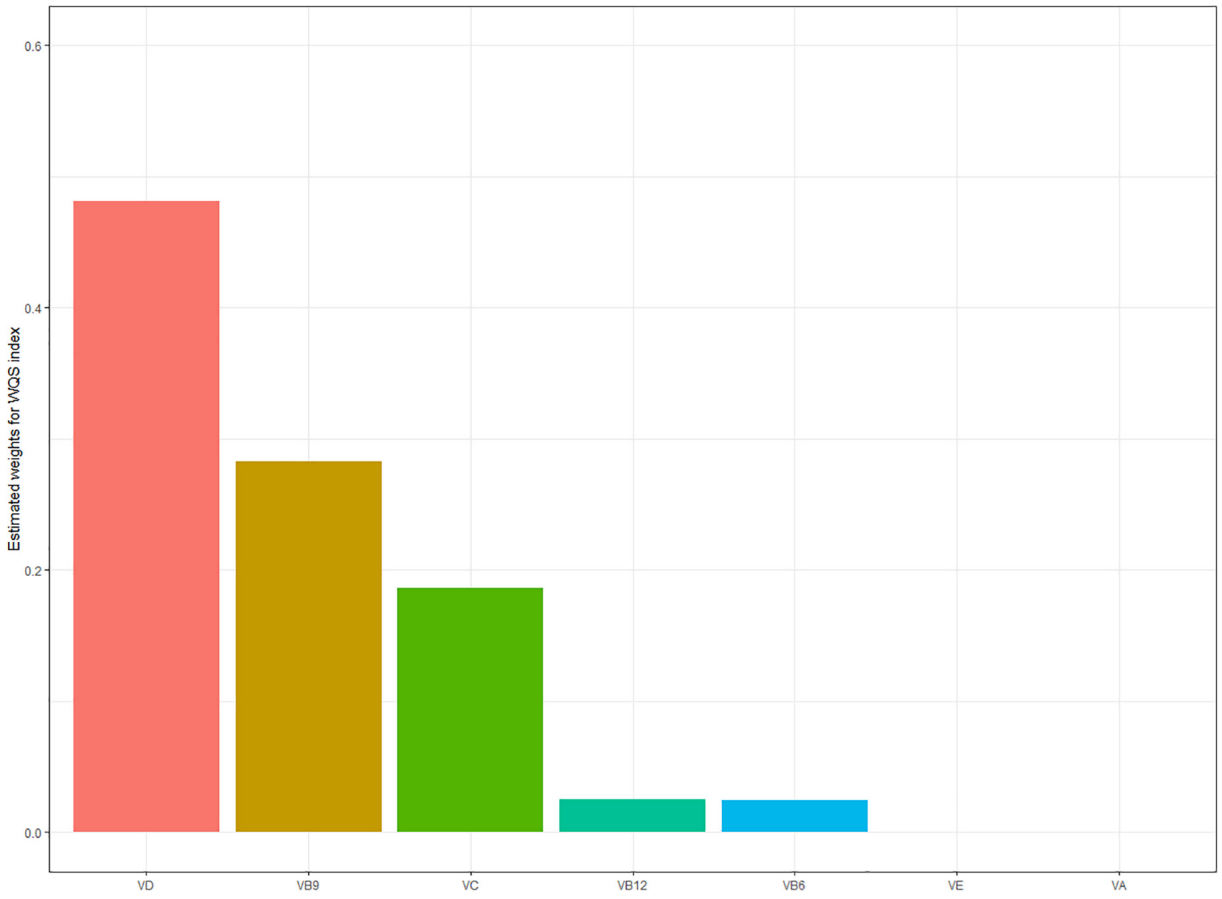

FIGURE 4
Estimated weights assigned to each vitamin level with the WQS regression model in a negative direction. Model adjusted for gender, age, ethnicity, FIPR, education level, and disease history (hypertension, high cholesterol, and diabetes).

contributor to the prevalence of NAFLD in U.S. adults. Vitamin C, also known as ascorbic acid, was a water-soluble vitamin and existed in a variety of vegetables and fruits. Wei et al. (27) found that the risk of NAFLD was decreased by 0.71 times in the highest quartile of dietary vitamin C intake compared with the lowest quartile, which was similar to our findings. More and more epidemiologic studies proposed that serum VC levels had a significant negative correlation with hepatic steatosis and hepatic fibrosis (28, 29). According to a prospective double-blinded randomized controlled trial, oral VC supplements could significantly improve liver function and glucose metabolism as well as guarantee intestinal microbial diversity and adiponectin concentration for patients with NAFLD (30). A suitable intake of VC could alleviate hepatic fibrosis for patients with NASH (31). And as an antioxidant, VC could scavenge free radicals, enhance the activity of manganese superoxide dismutase (SOD) and glutathione peroxidase (GPx), improve the secretion and expression of adiponectin, and lower the levels of low-density lipoprotein cholesterol (LDL-C) and triglycerides (TG) (32–35), which provided possible explanations for that VC could reduce the risk of NAFLD.

Vitamin D and the risk of non-alcoholic fatty liver disease

Vitamin D, a secosteroid, had an influence not only on calcium homeostasis but also on cell differentiation and proliferation, immune modulation, and inflammatory response. We found that there was a negative linear correlation between serum VD level and the risk of NAFLD. According to a cross-sectional study including 16,190 participants (36), serum VD level had a significant negative correlation with liver enzyme, insulin resistance, and the components of metabolic syndrome, which was similar to our findings. The elevated serum VD level might alleviate inflammation/steatosis of the liver and improve insulin sensitivity by activating liver macrophage vitamin D receptors (VDR) (37). However, some pieces of evidence for the association between VD deficiency (VDD)

and the risk of NAFLD were still controversial. Animal studies suggested that VDD would exacerbate NAFLD by activating Toll-like receptors (TLRs). Moreover, VDD would result in insulin resistance, up-regulation of hepatic inflammatory and oxidative stress genes, and higher hepatic resistin gene expression (38). On the contrary, a 16-week RCT study (39) reported that VD supplements in non-Western VDD immigrants with prediabetes failed to improve insulin sensitivity or β-cell function or change the incidence of metabolic syndrome. One possible explanation would be that the change in insulin sensitivity after the VD supplement was influenced by the single nucleotide polymorphisms (SNPs) of the VDR gene (40). Therefore, SNPs of the VDR gene should be considered when concluding that the VD supplement was beneficial to NAFLD.

Vitamin B6 and the risk of non-alcoholic fatty liver disease

VB6 was a key cofactor in the metabolism of amino acids, glucose, and fat. Similar to VC and VD, VB6 was also negatively correlated with the risk of NAFLD. Federico et al. found that patients with NASH had a less daily intake of VB6 than those in the control group (41). A prospective clinical study suggested that an oral VB6 supplement could significantly ameliorate liver fat accumulation in patients with NAFLD (42). Moreover, Lin et al. proposed that a borderline VB6 deficit was associated with the increased risk of dyslipidemia and coronary artery disease (43). The deficiency of VB6 resulted in homocysteine (Hcy) accumulation. Hcy would induce protein misfolding in the endoplasmic reticulum (ER), triggering a stress response in the ER. Then ER stress drives *de novo* lipogenesis by activating the transcription factor sterol response element-binding protein 1c (SREBP-1c), resulting in NAFLD development (44). VB6 could prevent insulin resistance, endothelial dysfunction, and liver fat accumulation (45), which were possible underlying mechanisms of VB6 to reduce the risk of NAFLD.

Vitamin B9 and the risk of non-alcoholic fatty liver disease

VB9, also known as folate, is a water-soluble vitamin widely distributed in green leafy vegetables such as spinach, beet, and kale. The dose–response curve showed that serum VB9 was non-linearly correlated with NAFLD risk and would increase the incidence of NAFLD when staying at a lower level. Similarly, Xia et al. (8) suggested that serum folate level was negatively correlated with the grade of hepatic steatosis and liver fat content, and low serum folate level was an independent risk factor for NAFLD. The liver was an essential organ for storage and metabolism of folate. More and more research studies confirmed that folate was closely associated with lipid metabolism. Folate deficiency might depress phospholipid *N*-methylation in the liver and reduce *de novo* phosphatidylcholine synthesis, resulting in TG accumulation in the liver (46), which was further verified in animal experiments by Pogribny et al. (47). Moreover, folate deficiency would accelerate the synthesis of hepatic lipid by inducing related genes, resulting in hepatic steatosis (48). It was noteworthy that excessive high serum folate levels might increase the risk of cognitive disorder and insulin resistance (49). Maintaining a proper serum folate level might be good for health.

Vitamin E and the risk of non-alcoholic fatty liver disease

In this study, serum VE level had a significant positive correlation with the risk of NAFLD. With each increment of the VE level, the risk of NAFLD elevated by approximately 1.9% (95% CI: 1.1–1.2%). Jeon et al. suggested that serum VE level was positively associated with the prevalence of NAFLD, which was similar to our findings (50). Alpha-tocopherol (VE) was identified as one of the predictors of MRI-determined liver fat (51). A cross-sectional study on Swedish adults proposed that serum VE level was positively associated with serum cholesterol and obesity (52). Waniek et al. (53) suggested that alpha-tocopherol level was positively associated with high triglycerides and low high-density lipoprotein cholesterol (HDL-C) levels. Moreover, serum VE levels played important roles in visceral adipose tissue and metabolic syndrome. Animal experiments indicated that mice with NAFLD had impaired liver metabolism and gene response of alpha-tocopherol (54). All these studies provided evidence that serum VE level was positively associated with the risk of NAFLD.

Multi-vitamins and the risk of non-alcoholic fatty liver disease

People were exposed to a variety of vitamins in daily life due to different dietary structures or nutritional components in food. It was necessary to explore the effect of multi-vitamins on health. In this study, we employed the WQS regression model to explore the association between serum levels of multivitamins and the risk of NAFLD. Results indicated that higher serum levels of multivitamins are associated with reduced NAFLD risk, despite different influences and weights of a single vitamin. There was no study exploring the relationship between multivitamins and NAFLD. It was incorrect to include all studied vitamins in a single generalized linear regression

model, which might distort the results due to the correlation that exists among vitamins (55). The WQS was a novel model to explore the influences of multivitamins on health, by considering highly correlated vitamins. Based on the weights empirically determined by bootstrap sampling, we used WQS to examine the whole-body burden with serum levels of multivitamins. The WQS enabled us to encompass the complex serum levels of multivitamins in the real world. In this study, VD, VB9, and VC were weighted highly. More prospective cohort and large-population studies are necessary to determine the contributions and mechanism of serum multivitamin levels to NAFLD.

Strengths and limitations

Strengths: We employed, in this study, for the first time both logistic regression and WQS regression models that enabled us to systematically assess the association between serum multivitamin levels and the risk of NAFLD, as well as to explore the dose–response relationship between single vitamin and the risk of NAFLD. Moreover, this study covered a wide range of participants with good sample representativeness. We also adjusted important covariates in our models, including demographic characteristics and disease history.

Limitations: First, serum levels of vitamins were tested only once at baseline, which might not represent a long-term status. Second, the diagnosis of NAFLD was based on the FLI model, instead of a gold standard in histology. Third, although we adjusted multiple covariates in our study, there might be other potential confounders such as dietary intakes, physical activities, and metabolic syndrome. And last, our work was based on a cross-sectional study and could not confirm the cause-and-effect relationships between the serum vitamin level and the risk of NAFLD. More large-scale and prospective cohort studies should be encouraged in the future.

Conclusion

This cross-sectional study explored the association between serum levels of 7 common vitamins and the risk of NAFLD. Among U.S. adults, high serum levels of VC, VD, VB6, and VB9 and low serum levels of VA/VE were associated with reduced risk of NAFLD. Among all the 7 kinds of vitamins, VD was weighted highest and the most important. Proper serum levels of multivitamins contributed to a lower risk of NAFLD. Our findings suggested a novel perspective to explore the association between multivitamins and NAFLD risk. Further studies are still required to reveal the underlying mechanisms of multivitamins to NAFLD.

Data availability statement

The original contributions presented in this study are included in the article/**Supplementary material**, further inquiries can be directed to the corresponding author/s.

Ethics statement

The protocol of NHANES was reviewed and approved by the Research Ethics Review Board of the National Center for Health Statistics. The patients/participants provided their written informed consent to participate in this study.

Author contributions

HP and WL conceived of the study. HP, MW, and LP conducted the data analysis and drafted the manuscript. ZC, ZY, and QC drafted the manuscript. YL and YW visualized the result. All authors edited the manuscript, read and approved the final manuscript.

Funding

This research was funded by the Scientific and Technological Innovation Project of China, Academy of Chinese Medical Sciences (CI2021A00801 and CI2021A00802).

Conflict of interest

The authors declare that the research was conducted in the absence of any commercial or financial relationships that could be construed as a potential conflict of interest.

Publisher's note

Supplementary material

The Supplementary Material for this article can be found online at: https://www.frontiersin.org/articles/10.3389/fnut.2022.962705/full#supplementary-material

References

1. Younossi ZM, Koenig AB, Abdelatif D, Fazel Y, Henry L, Wymer M. Global epidemiology of nonalcoholic fatty liver disease-meta-analytic assessment of prevalence, incidence, and outcomes. *Hepatology.* (2016) 64:73–84. doi: 10.1002/hep.28431

2. Estes C, Razavi H, Loomba R, Younossi Z, Sanyal AJ. Modeling the epidemic of nonalcoholic fatty liver disease demonstrates an exponential increase in burden of disease. *Hepatology.* (2018) 67:123–33. doi: 10.1002/hep.29466

3. Sheka AC, Adeyi O, Thompson J, Hameed B, Crawford PA, Ikramuddin S. Nonalcoholic steatohepatitis: a review. *JAMA.* (2020) 323:1175–83. doi: 10.1001/jama.2020.2298

4. Barchetta I, Cimini FA, Cavallo MG. Vitamin D and metabolic dysfunction-associated fatty liver disease (Mafld): an update. *Nutrients.* (2020) 12:3302. doi: 10.3390/nu12113302

5. Saeed A, Dullaart RPF, Schreuder T, Blokzijl H, Faber KN. Disturbed vitamin a metabolism in non-alcoholic fatty liver disease (NAFLD). *Nutrients.* (2017) 10:29. doi: 10.3390/nu10010029

6. Nagashimada M, Ota T. Role of vitamin E in nonalcoholic fatty liver disease. *IUBMB Life.* (2019) 71:516–22. doi: 10.1002/iub.1991

7. Fang H, Li Z, Graff EC, McCafferty KJ, Judd RL. Niacin increases diet-induced hepatic steatosis in B6129 mice. *Biochim Biophys Acta Mol Cell Biol Lipids.* (2020) 1865:158731. doi: 10.1016/j.bbalip.2020.158731

8. Xia MF, Bian H, Zhu XP, Yan HM, Chang XX, Zhang LS, et al. Serum Folic Acid Levels Are Associated with the Presence and Severity of Liver Steatosis in Chinese Adults. *Clin Nutr.* (2018) 37:1752–8. doi: 10.1016/j.clnu.2017.06.021

9. Li L, Huang Q, Yang L, Zhang R, Gao L, Han X, et al. The association between non-alcoholic fatty liver disease (Nafld) and advanced fibrosis with serological vitamin B12 markers: results from the Nhanes 1999-2004. *Nutrients.* (2022) 14:1224. doi: 10.3390/nu14061224

10. Saeed A, Bartuzi P, Heegsma J, Dekker D, Kloosterhuis N, de Bruin A, et al. Impaired hepatic vitamin a metabolism in Nafld mice leading to vitamin a accumulation in hepatocytes. *Cell Mol Gastroenterol Hepatol.* (2021) 11:309–325.e3. doi: 10.1016/j.jcmgh.2020.07.006

11. Renner S, Kuçi Z, d'Cruze H, Niethammer D, Bruchelt G. Isotachophoretic analysis of the dihydrofolate reductase reaction in the presence of methotrexate and ascorbic acid. *Electrophoresis.* (2000) 21:2828–33. doi: 10.1002/1522-2683(20000801)21:143.0.Co;2-r

12. Galan P, Viteri FE, Bertrais S, Czernichow S, Faure H, Arnaud J, et al. Serum concentrations of beta-carotene, vitamins C and E, zinc and selenium are influenced by sex, age, diet, smoking status, alcohol consumption and corpulence in a general french adult population. *Eur J Clin Nutr.* (2005) 59:1181–90. doi: 10.1038/sj.ejcn.1602230

13. Wolffenbuttel BHR, Heiner-Fokkema MR, Green R, Gans ROB. Relationship between serum B12 concentrations and mortality: experience in Nhanes. *BMC Med.* (2020) 18:307. doi: 10.1186/s12916-020-01771-y

14. Cueto-Galán R, Barón FJ, Valdivielso P, Pintó X, Corbella E, Gómez-Gracia E, et al. Changes in fatty liver index after consuming a mediterranean diet: 6-year follow-up of the predimed-malaga trial. *Med Clin.* (2017) 148:435–43. doi: 10.1016/j.medcli.2016.11.032

15. Bedogni G, Bellentani S, Miglioli L, Masutti F, Passalacqua M, Castiglione A, et al. The fatty liver index: a simple and accurate predictor of hepatic steatosis in the general population. *BMC Gastroenterol.* (2006) 6:33. doi: 10.1186/1471-230x-6-33

16. Carrico C, Gennings C, Wheeler DC, Factor-Litvak P. Characterization of weighted quantile sum regression for highly correlated data in a risk analysis setting. *J Agric Biol Environ Stat.* (2015) 20:100–20. doi: 10.1007/s13253-014-0180-3

17. Czarnota J, Gennings C, Colt JS, De Roos AJ, Cerhan JR, Severson RK, et al. Analysis of environmental chemical mixtures and non-hodgkin lymphoma risk in the nci-seer nhl study. *Environ Health Perspect.* (2015) 123:965–70. doi: 10.1289/ehp.1408630

18. Liu S, Liu Y, Wan B, Zhang H, Wu S, Zhu Z, et al. Association between vitamin D status and non-alcoholic fatty liver disease: a population-based study. *J Nutr Sci Vitaminol.* (2019) 65:303–8. doi: 10.3177/jnsv.65.303

19. Wan B, Gao Y, Zheng Y, Chen R. Association between serum 25-hydroxy vitamin D level and metabolic associated fatty liver disease (Mafld)-a population-based study. *Endocr J.* (2021) 68:631–7. doi: 10.1507/endocrj.EJ20-0758

20. Petiz LL, Girardi CS, Bortolin RC, Kunzler A, Gasparotto J, Rabelo TK, et al. Vitamin a oral supplementation induces oxidative stress and suppresses Il-10 and Hsp70 in skeletal muscle of trained rats. *Nutrients.* (2017) 9:353. doi: 10.3390/nu9040353

21. Cartmel B, Moon TE, Levine N. Effects of long-term intake of retinol on selected clinical and laboratory indexes. *Am J Clin Nutr.* (1999) 69:937–43. doi: 10.1093/ajcn/69.5.937

22. Blaner WS. Vitamin a signaling and homeostasis in obesity, diabetes, and metabolic disorders. *Pharmacol Ther.* (2019) 197:153–78. doi: 10.1016/j.pharmthera.2019.01.006

23. Bahcecioglu IH, Yalniz M, Ilhan N, Ataseven H, Ozercan IH. Levels of serum vitamin a, alpha-tocopherol and malondialdehyde in patients with non-alcoholic steatohepatitis: relationship with histopathologic severity. *Int J Clin Pract.* (2005) 59:318–23. doi: 10.1111/j.1742-1241.2004.00312.x

24. Xiao ML, Zhong HL, Lin HR, Liu CY, Yan Y, Ke YB, et al. Higher serum vitamin a is associated with a worsened progression of non-alcoholic fatty liver disease in adults: a prospective study. *Food Func.* (2022) 13:970–7. doi: 10.1039/d1fo03119h

25. Botella-Carretero JI, Balsa JA, Vázquez C, Peromingo R, Díaz-Enriquez M, Escobar-Morreale HF. Retinol and alpha-tocopherol in morbid obesity and nonalcoholic fatty liver disease. *Obes Surg.* (2010) 20:69–76. doi: 10.1007/s11695-008-9686-5

26. Villaça Chaves G, Pereira SE, Saboya CJ, Ramalho A. Non-alcoholic fatty liver disease and its relationship with the nutritional status of vitamin a in individuals with class iii obesity. *Obes Surg.* (2008) 18:378–85. doi: 10.1007/s11695-007-9361-2

27. Wei J, Lei GH, Fu L, Zeng C, Yang T, Peng SF. Association between dietary vitamin C intake and non-alcoholic fatty liver disease: a cross-sectional study among middle-aged and older adults. *PLoS One.* (2016) 11:e0147985. doi: 10.1371/journal.pone.0147985

28. Liu X, Shen H, Chen M, Shao J. Clinical relevance of vitamins and carotenoids with liver steatosis and fibrosis detected by transient elastography in adults. *Front Nutr.* (2021) 8:760985. doi: 10.3389/fnut.2021.760985

29. Xie ZQ, Li HX, Tan WL, Yang L, Ma XW, Li WX, et al. Association of serum vitamin C with Nafld and Mafld among adults in the United States. *Front Nutr.* (2021) 8:795391. doi: 10.3389/fnut.2021.795391

30. He Z, Li X, Yang H, Wu P, Wang S, Cao D, et al. Effects of oral vitamin C supplementation on liver health and associated parameters in patients with non-alcoholic fatty liver disease: a randomized clinical trial. *Front Nutr.* (2021) 8:745609. doi: 10.3389/fnut.2021.745609

31. Harrison SA, Torgerson S, Hayashi P, Ward J, Schenker S. Vitamin E and vitamin C treatment improves fibrosis in patients with nonalcoholic steatohepatitis. *Am J Gastroenterol.* (2003) 98:2485–90. doi: 10.1111/j.1572-0241.2003.08699.x

32. Buettner GR. The pecking order of free radicals and antioxidants: lipid peroxidation, alpha-tocopherol, and ascorbate. *Arch Biochem Biophys.* (1993) 300:535–43. doi: 10.1006/abbi.1993.1074

33. Rose FJ, Webster J, Barry JB, Phillips LK, Richards AA, Whitehead JP. Synergistic effects of ascorbic acid and thiazolidinedione on secretion of high molecular weight adiponectin from human adipocytes. *Diabetes Obes Metab.* (2010) 12:1084–9. doi: 10.1111/j.1463-1326.2010.01297.x

34. McRae MP. Vitamin C supplementation lowers serum low-density lipoprotein cholesterol and triglycerides: a meta-analysis of 13 randomized controlled trials. *J Chiropr. Med.* (2008) 7:48–58. doi: 10.1016/j.jcme.2008.01.002

35. Valdecantos MP, Pérez-Matute P, Quintero P, Martínez JA. Vitamin C, resveratrol and lipoic acid actions on isolated rat liver mitochondria: all antioxidants but different. *Redox Rep.* (2010) 15:207–16. doi: 10.1179/135100010x12826446921464

36. Hong HC, Lee JS, Choi HY, Yang SJ, Yoo HJ, Seo JA, et al. Liver enzymes and vitamin d levels in metabolically healthy but obese individuals: Korean national health and nutrition examination survey. *Metabolism.* (2013) 62:1305–12. doi: 10.1016/j.metabol.2013.04.002

37. Dong B, Zhou Y, Wang W, Scott J, Kim K, Sun Z, et al. Vitamin D receptor activation in liver macrophages ameliorates hepatic inflammation, steatosis, and insulin resistance in mice. *Hepatology.* (2020) 71:1559–74. doi: 10.1002/hep.30937

38. Roth CL, Elfers CT, Figlewicz DP, Melhorn SJ, Morton GJ, Hoofnagle A, et al. Vitamin D deficiency in obese rats exacerbates nonalcoholic fatty liver disease and increases hepatic resistin and toll-like receptor activation. *Hepatology.* (2012) 55:1103–11. doi: 10.1002/hep.24737

39. Oosterwerff MM, Eekhoff EM, Van Schoor NM, Boeke AJ, Nanayakkara P, Meijnen R, et al. Effect of moderate-dose vitamin d supplementation on insulin sensitivity in vitamin D-deficient non-western immigrants in the netherlands: a randomized placebo-controlled trial. *Am J Clin Nutr.* (2014) 100:152–60. doi: 10.3945/ajcn.113.069260

40. Jain R, von Hurst PR, Stonehouse W, Love DR, Higgins CM, Coad J. Association of vitamin D receptor gene polymorphisms with insulin resistance and response to vitamin D. *Metabolism.* (2012) 61:293–301. doi: 10.1016/j.metabol.2011.06.018

41. Federico A, Dallio M, Caprio GG, Gravina AG, Picascia D, Masarone M, et al. Qualitative and quantitative evaluation of dietary intake in patients with non-alcoholic steatohepatitis. *Nutrients.* (2017) 9:1074. doi: 10.3390/nu9101074

42. Kobayashi T, Kessoku T, Ozaki A, Iwaki M, Honda Y, Ogawa Y, et al. Vitamin B6 efficacy in the treatment of nonalcoholic fatty liver disease: an open-label, single-arm, single-center trial. *J Clin Biochem Nutr.* (2021) 68:181–6. doi: 10.3164/jcbn.20-142

43. Lin PT, Cheng CH, Liaw YP, Lee BJ, Lee TW, Huang YC. Low pyridoxal 5'-phosphate is associated with increased risk of coronary artery disease. *Nutrition.* (2006) 22:1146–51. doi: 10.1016/j.nut.2006.08.013

44. Ai Y, Sun Z, Peng C, Liu L, Xiao X, Li J. Homocysteine induces hepatic steatosis involving er stress response in high methionine diet-fed mice. *Nutrients.* (2017) 9:346. doi: 10.3390/nu9040346

45. Liu Z, Li P, Zhao ZH, Zhang Y, Ma ZM, Wang SX. Vitamin B6 prevents endothelial dysfunction, insulin resistance, and hepatic lipid accumulation in apoe (-/-) mice fed with high-fat diet. *J Diabetes Res.* (2016) 2016:1748065. doi: 10.1155/2016/1748065

46. Akesson B, Fehling C, Jägerstad M, Stenram U. Effect of experimental folate deficiency on lipid metabolism in liver and brain. *Br J Nutr.* (1982) 47:505–20. doi: 10.1079/bjn19820063

47. Pogribny IP, Kutanzi K, Melnyk S, de Conti A, Tryndyak V, Montgomery B, et al. Strain-dependent dysregulation of one-carbon metabolism in male mice is associated with choline- and folate-deficient diet-induced liver injury. *FASEB J.* (2013) 27:2233–43. doi: 10.1096/fj.12-227116

48. Champier J, Claustrat F, Nazaret N, Fèvre Montange M, Claustrat B. Folate depletion changes gene expression of fatty acid metabolism, dna synthesis, and circadian cycle in male mice. *Nutr Res.* (2012) 32:124–32. doi: 10.1016/j.nutres.2011.12.012

49. Smith AD, Kim YI, Refsum H. Is folic acid good for everyone? *Am J Clin Nutr.* (2008) 87:517–33. doi: 10.1093/ajcn/87.3.517

50. Jeon D, Son M, Shim J. Dynamics of serum retinol and alpha-tocopherol levels according to non-alcoholic fatty liver disease status. *Nutrients.* (2021) 13:1720. doi: 10.3390/nu13051720

51. Lim U, Turner SD, Franke AA, Cooney RV, Wilkens LR, Ernst T, et al. Predicting total, abdominal, visceral and hepatic adiposity with circulating biomarkers in caucasian and Japanese American women. *PLoS One.* (2012) 7:e43502. doi: 10.1371/journal.pone.0043502

52. Wallström P, Wirfält E, Lahmann PH, Gullberg B, Janzon L, Berglund G. Serum concentrations of beta-carotene and alpha-tocopherol are associated with diet, smoking, and general and central adiposity. *Am J Clin Nutr.* (2001) 73:777–85. doi: 10.1093/ajcn/73.4.777

53. Waniek S, di Giuseppe R, Plachta-Danielzik S, Ratjen I, Jacobs G, Koch M, et al. Association of vitamin E levels with metabolic syndrome, and mri-derived body fat volumes and liver fat content. *Nutrients.* (2017) 9:1143. doi: 10.3390/nu9101143

54. Bartolini D, Torquato P, Barola C, Russo A, Rychlicki C, Giusepponi D, et al. Nonalcoholic fatty liver disease impairs the cytochrome p-450-dependent metabolism of α-tocopherol (Vitamin E). *J Nutr Biochem.* (2017) 47:120–31. doi: 10.1016/j.jnutbio.2017.06.003

55. Marill KA. Advanced statistics: linear regression, part ii: multiple linear regression. *Acad Emerg Med.* (2004) 11:94–102. doi: 10.1197/j.aem.2003.09.006

frontiers | Frontiers in Nutrition

TYPE Original Research
PUBLISHED 14 September 2022
DOI 10.3389/fnut.2022.960409

OPEN ACCESS

EDITED BY
Nicola Fiotti,
University of Trieste, Italy

REVIEWED BY
Fred Ssempijja,
Kampala International University Western Campus, Uganda
Ronan Lordan,
University of Pennsylvania, United States

*CORRESPONDENCE
Elizabeth P. Ryan
e.p.ryan@colostate.edu

SPECIALTY SECTION
This article was submitted to Clinical Nutrition, a section of the journal Frontiers in Nutrition

RECEIVED 02 June 2022
ACCEPTED 09 August 2022
PUBLISHED 14 September 2022

CITATION
Stromberg S, Baxter BA, Dooley G, LaVergne SM, Gallichotte E, Dutt T, Tipton M, Berry K, Haberman J, Natter N, Webb TL, McFann K, Henao-Tamayo M, Ebel G, Rao S, Dunn J and Ryan EP (2022) Relationships between plasma fatty acids in adults with mild, moderate, or severe COVID-19 and the development of post-acute sequelae. *Front. Nutr.* 9:960409. doi: 10.3389/fnut.2022.960409

Relationships between plasma fatty acids in adults with mild, moderate, or severe COVID-19 and the development of post-acute sequelae

Sophia Stromberg[1], Bridget A. Baxter[2], Gregory Dooley[2], Stephanie M. LaVergne[2], Emily Gallichotte[3], Taru Dutt[3], Madison Tipton[2], Kailey Berry[2], Jared Haberman[2], Nicole Natter[2], Tracy L. Webb[4], Kim McFann[5], Marcela Henao-Tamayo[3], Greg Ebel[3], Sangeeta Rao[4], Julie Dunn[5] and Elizabeth P. Ryan[2]*

[1]Department of Food Science and Human Nutrition, Colorado State University, Fort Collins, CO, United States, [2]Department of Environmental and Radiological Health Sciences, Colorado State University, Fort Collins, CO, United States, [3]Department of Microbiology, Immunology and Pathology, Colorado State University, Fort Collins, CO, United States, [4]Department of Clinical Sciences, Colorado State University, Fort Collins, CO, United States, [5]University of Colorado Health, Medical Center of the Rockies, Loveland, CO, United States

Background: SARS-CoV-2 has infected millions across the globe. Many individuals are left with persistent symptoms, termed post-acute sequelae of COVID-19 (PASC), for months after infection. Hyperinflammation in the acute and convalescent stages has emerged as a risk factor for poor disease outcomes, and this may be exacerbated by dietary inadequacies. Specifically, fatty acids are powerful inflammatory mediators and may have a significant role in COVID-19 disease modulation.

Objective: The major objective of this project was to pilot an investigation of plasma fatty acid (PFA) levels in adults with COVID-19 and to evaluate associations with disease severity and PASC.

Methods and procedures: Plasma from adults with (N = 41) and without (N = 9) COVID-19 was analyzed by gas chromatography-mass spectrometry (GC-MS) to assess differences between the concentrations of 18 PFA during acute infection (≤14 days post-PCR + diagnosis) in adults with varying disease severity. Participants were grouped based on mild, moderate, and severe disease, alongside the presence of PASC, a condition identified in patients who were followed beyond acute-stage infection (N = 23).

Results: Significant differences in PFA profiles were observed between individuals who experienced moderate or severe disease compared to those with mild infection or no history of infection. Palmitic acid, a saturated fat, was elevated in adults with severe disease (p = 0.04), while behenic (p = 0.03)

and lignoceric acid (p = 0.009) were lower in adults with moderate disease. Lower levels of the unsaturated fatty acids, γ-linolenic acid (GLA) (p = 0.03), linoleic (p = 0.03), and eicosapentaenoic acid (EPA) (p = 0.007), were observed in adults with moderate disease. Oleic acid distinguished adults with moderate disease from severe disease (p = 0.04), and this difference was independent of BMI. Early recovery-stage depletion of GLA (p = 0.02) and EPA (p = 0.0003) was associated with the development of PASC.

Conclusion: Pilot findings from this study support the significance of PFA profile alterations during COVID-19 infection and are molecular targets for follow-up attention in larger cohorts. Fatty acids are practical, affordable nutritional targets and may be beneficial for modifying the course of disease after a COVID-19 diagnosis. Moreover, these findings can be particularly important for overweight and obese adults with altered PFA profiles and at higher risk for PASC.

Clinical trial registration: [ClinicalTrials.gov], identifier [NCT04603677].

KEYWORDS

COVID-19, plasma fatty acid profiles, persistent symptoms, disease severity, post-acute sequelae of COVID-19 (PASC), nutritional status, SARS-CoV-2

Introduction

SARS-CoV-2, the virus that causes COVID-19, has rapidly spread across the world, killing over 6 million people worldwide since its initial identification in December 2019 (1). Many have speculated that the high prevalence of metabolic dysfunction, obesity, and chronic disease in the United States (US) have contributed to morbidity and mortality surrounding COVID-19 (2, 3). Emerging evidence shows that obesity is an important risk factor for COVID-19 hospitalization and need for supplemental oxygen as well as poor disease outcomes and development of post-acute sequelae of COVID-19 (PASC) (4, 5).

The definition of PASC by the World Health Organization (WHO) describes symptoms that begin during acute COVID-19 infection (or shortly after) and last for at least two months following diagnosis without any alternative explanation (6). Common symptoms of PASC include fatigue, shortness of breath, and cognitive dysfunction, though there is notable breadth and diversity in the reporting of symptoms by those who experience and are diagnosed with this condition (4, 6). Females and individuals of more advanced age have been found to report a higher incidence of lasting symptoms, with the most common being extreme fatigue, headaches, dyspnea, and persistent anosmia (7). The percentage of individuals who experience PASC varies between countries and cohorts, though some have indicated over 50% of patients may experience lasting physical, emotional, or mental deficits (8–11).

Although the mechanisms causing severe COVID-19 are not definitively known, there has been some evidence to suggest that higher levels of inflammation may contribute to severe disease during acute infection and PASC (8, 9, 12, 13). Obesity is associated with higher levels of pro-inflammatory mediators, which may predispose individuals to a dysregulated immune response (14). Excess adipose tissue is a major source of the pro-inflammatory mediators observed in obesity, and this hyperinflammatory state can be further exacerbated by dietary inadequacies (15). Fatty acids are key modulators of inflammatory pathways within the body, and a high intake of saturated fatty acids with low intake of unsaturated fatty acids has been linked to a greater degree of systemic inflammation (16). Indeed, previous studies have found dyslipidemia and altered free fatty acid metabolism to be associated with COVID-19 infection (17–20). Additional studies have also shown that inflammatory downstream metabolites of certain fatty acids may contribute to increased pulmonary inflammation and vascular permeability, leading to a greater likelihood of developing acute respiratory distress syndrome (ARDS) during COVID-19 infection (21, 22). Thus, individuals with unfavorable fatty acid profiles may be at heightened risk for a more severe COVID-19 disease course.

This present study explores relationships between systemic fatty acid profiles and COVID-19 disease severity as well as in relation to the development of PASC.

Materials and methods

Participant identification

This study is part of the Northern Colorado Coronavirus Biobank (NoCO CoBIO): a biorepository for acute and convalescent patients. Colorado State University (CSU) and University of Colorado Health (UCHealth) networks were used to recruit COVID-19 survivors to participate in an observational, longitudinal cohort study, as previously described (5, 23). Inclusion criteria for this study were a positive SARS-CoV-2 polymerase chain reaction test (PCR). Individuals who received a COVID-19 diagnosis *via* home test kits or antigen tests were not included. Participants were also required to be at least 18 years of age. Exclusion criteria included pregnancy or incarceration at time of enrollment. Participants consented to undergo four study clinic visits: at enrollment and approximately 1, 4, and 6 months after enrollment with the choice for a one year follow-up. The complete account of all recruitment, enrollment, and data acquisition procedures and rationale was previously described (23). The subset of 50 participants included in this present study completed three study visits, deemed visit 1 (V1), visit 2 (V2), and visit 3 (V3). Study visit 1 was at time of enrollment, which was either during acute-stage infection (≤14 days post PCR+) or during the convalescent stage (≥14 days post PCR+). Study visit 2 was approximately 30 days after V1, and V3 was approximately 90 days after V1. The Northern Colorado Coronavirus Biobank has been approved by CSU's Institutional Review Board [IRB; protocol 2105 (20-10063H)] and UCHealth IRB (Colorado Multiple IRB 20-6043) and is registered at ClinicalTrials.gov (NCT04603677). All participants provided written informed consent. The biorepository was in accordance with the Helsinki Declaration and its 2013 amendments. A convenience sample of uninfected adults with no history of COVID-19 infection and with a negative SARS-CoV-2 PCR test were enrolled for the same study visit and specimen collections. 140 diagnosed and 18 uninfected adults completed their study visits between July 2020 and March 2021. Twenty-five-dollar cash compensation was given to all participants at each study visit.

Group stratification and clinical data acquisition

Participants were categorized as having mild, moderate, or severe disease based on the Yale Impact Scoring during their acute stage of infection, which is defined as the first 14 days of infection following a positive SARS-CoV-2 PCR test (24). Individuals who required greater than 5 L of supplemental oxygen were classified as having severe disease, while those who were hospitalized but required 1–5 L had moderate disease, and no oxygen requirement was classified as mild disease. Individuals who did not have a documented history of COVID-19 were also included in this study as uninfected. To assess for risk factors of disease severity, clinical data, including age, body mass index (BMI), comorbidities, and race/ethnicity, were collected on each participant either at clinic visits (N = 19) or obtained by hospital electronic medical records (N = 22). All demographic data from adults without COVID-19 infection was obtained at clinic visits (N = 9). This information was de-identified and stored in the password-protected Research Electronic Data Capture (REDCap) web platform. Participants provided written informed consent to a scheduled series of longitudinal visits following the PCR confirmed diagnosis, at which time a 70-symptom survey was administered. Results from this survey were used to identify new or persistent PASC. Participants were interviewed by clinic staff and asked to identify whether any previously reported symptoms were continuing. Participants were defined as having PASC according to the WHO guidelines, which defines this condition by the persistence of at least one of the following symptoms: fatigue, dyspnea, joint pain, chest pain, confusion, difficulty concentrating, forgetfulness or absent-mindedness for at least 60 days post acute infection (6). Dyspnea was defined as difficulty breathing or shortness of breath in participants.

Fatty acid profiling

The quantification of lauric, myristate, pentadecanoic, palmitic, palmitoleic, steric, oleic, linoleic, γ_linolenic, linolenic, arachidic, cis_11_Eicosenoic, arachidonic, cis_5_8_11_14_17_eicosapentaenoic, behenic, cis_13_16_docosadienoic, cis_4_7_10_13_16_19_Docosahexaenoic, and lignoceric acids were conducted on participant plasma samples according to standardized methods defined by the National Institute of Health (25). 100 μl of plasma, 10 μl of non-adecanoic acid (1 μg/ml) as an internal standard, and 1.5 ml of methanol were added to glass test tube, and the solution was vortexed. 0.1 ml of acetyl chloride was added while lightly vortexing the sample to mix. The capped samples were then derivatized at 90°C/min for 45 min. Following the incubation period, the samples were allowed to come to room temperature prior to adding 1.5 ml 6% sodium bicarbonate and 0.5 ml hexane. The samples were vortexed for approximately one minute and then placed in the centrifuge at 3,220 × g for 5 min. The upper hexane layer containing fatty acid methyl esters (FAME) was transferred in the autosampler vial for analysis by gas chromatography-mass spectrometry.

Samples were analyzed with an Agilent 6890 Gas Chromatograph and a Micromass Quattro Micro Mass Spectrometer. FAMEs were analyzed with a 1 μl sample injection and a 100:1 split ratio onto a Restek FAMEWAX column (30 m × 0.25 mm × 0.25 μm). The oven temperature profile was 50°C for 1 min to 200°C at 25°C/min, to 230°C

at 3°C/min, then held at 230°C for 33 min. The flow rate of helium was 1 ml/min, inlet temperature was 275°C, and the GC-mass spectrometer interface temperature was set at 280°C. The mass spectrometer was operated in selected ion monitoring (SIM) mode for the fragment ions of 55, 67, 69, 74, 79, 81, 87, 91, 95, and 99 m/z. The data collection and processing were performed by using Waters™ MassLynx software. Quantitation was performed with linear regression using 7-point calibration curves from 30 to 600 μg/ml.

Statistical analysis

The fatty acid data were continuous hence was evaluated for normality assumption prior to performing a linear mixed model. If the data were not normal, it was converted into log scale before performing the analysis. A linear mixed model was performed to compare the fatty acids between disease severity categories at baseline and between participants that developed PASC versus participants without PASC. Fatty acid profiles at 37.2 ± 33.2 days post-PCR + diagnosis were compared to those obtained 72.5 ± 34.8 and 134.0 ± 38.9 days post-PCR + diagnosis, with PASC vs No PASC, and interaction effects included as fixed effects in the mixed model. Tukey's method was used to adjust for multiple comparisons, and BMI was included as a covariate for analysis. A p-value of 0.05 was used as criteria to determine statistical significance. SAS v9.4 (SAS Institute Inc., Cary, NC, United States) was used to perform all statistical analyses. GraphPad Prism version 9 was used for all figures.

Results

Study cohort

Fifty participants were evaluated for fatty acid profiles (Table 1). Twenty participants diagnosed as having a mild acute infection (required no oxygen) had a mean age of 38 years and a mean BMI of 23.6. Seventy-five percent were women, and 15% were hospitalized. Twelve adults experienced a moderate infection (required 1–5 L oxygen) with a mean age of 57.1 years and a mean BMI of 35.5; fifty-eight percent were women, 42% received convalescent plasma, and 83% were hospitalized. Nine participants experienced a severe infection (>5L oxygen) with a mean age of 55.8 years and mean BMI of 39.7. Forty-five percent of the participants with severe disease were women, 89% received convalescent plasma, and 100% were hospitalized. Additionally, nine uninfected (no COVID-19 diagnosis) participants were enrolled with a mean age of 50 years and mean BMI of 23.2. 78% of the uninfected individuals were female.

Saturated fatty acids

Thirty-seven adults (9 mild, 10 moderate, 9 severe, and 9 uninfected) were analyzed for baseline fatty acids levels in plasma at V1. Table 2 shows seven saturated fatty acids from plasma were quantified and analyzed for significance in disease severity during acute infection (≤14 days post-PCR + diagnosis). Figure 1A, shows mean behenic acid (C22) was significantly lower in the adults with moderate disease when compared to the uninfected adults (1.8 vs 3.2 μg/ml, $p = 0.03$). There was no significant difference in behenic acid levels in adults with mild disease or severe disease compared to adults with no prior history of infection ($p = 0.36$ and $p = 0.22$, respectively). Palmitic acid (C16) was significantly higher in the infected adults with severe disease compared to the uninfected adults (755.1 vs 513.3 μg/ml, $p = 0.04$) (Table 2; Figure 1B). Those in the mild and moderate disease severity groups did not show significantly different levels in palmitic acid compared to the uninfected ($p = 0.79$ and $p = 0.99$, respectively). Levels of lignoceric acid (C23) were significantly lower in the moderate infected adults compared to the uninfected adults (1.6 vs 2.9 μg/ml, $p = 0.009$) (Table 2; Figure 1C). Lauric (C12), stearic (C18), pentadecanoic (C15), and arachidic acid (C20) levels were not significantly different between the different disease severity groups or compared to the uninfected adults (Table 2).

Monounsaturated fatty acids

A total of four monounsaturated fatty acids were quantified and analyzed for significant differences between the disease severity groups and the uninfected at baseline (Table 2). Figure 1D shows oleic acid (C18:1n9) was significantly different between the moderate infected adults (123.8 μg/ml) and severe infected adults (220.1 μg/ml), with those in the moderate disease group demonstrating a lower level of this fatty acid compared to the severe group ($p = 0.04$). The mean BMI of the moderate and severe disease groups was similar (35.5 vs 39.7 kg/m^2, respectively), thus indicating the significance of this finding was independent of BMI. There was no significant difference in oleic acid levels observed in those with mild disease when compared to the other disease severity groups or the uninfected ($p = 0.86$). Myristoleic (C14:1n5), eicosenoic (C20:1n9), and palmitoleic acids (C16:1n7) were not significantly different between the disease severity groups or compared to the uninfected adults (Table 2).

Polyunsaturated fatty acids

The levels of seven polyunsaturated fatty acids were quantified and analyzed for significant differences between the disease severity groups and uninfected individuals (Table 2).

TABLE 1 Baseline adult participant characteristics by COVID-19 disease severity (N = 50).

Characteristics	Uninfected (N = 9)	Mild (N = 20)	Moderate (N = 12)	Severe (N = 9)
Age, mean ± SD, year	50 + 9.3	38.1 + 18.2	56.8 ± 14.9	55.8 ± 13.1
Sex, no. (%)				
Female	7 (78)	15 (75)	7 (58)	4 (45)
Male	2 (22)	5 (25)	5 (42)	5 (56)
BMI, mean ± SD	23.2 + 3.1	23.6 + 5.8	35.5 + 10.8	39.7 + 11.7
Ethnicity, no. (%)				
Non-Hispanic/Latinx	9 (100)	19 (95)	10 (83)	6 (67)
Hispanic/Latinx	0 (0)	1 (5)	2 (17)	3 (33)
Hospitalized	–	3 (15)	10 (83)	9 (100)
Non-hospitalized	–	17 (85)	2 (17)	0 (0)
Convalescent Plasma	–	1 (5)	5 (42)	8 (89)
Pre-existing conditions no. (%)				
COPD	0 (0)	1 (5)	3 (25)	3 (33)
DM	0 (0)	2 (10)	5 (42)	6 (67)
HTN	0 (0)	1 (5)	5 (42)	8 (89)
CAD	0 (0)	1 (5)	1 (8)	1 (11)
Asthma	0 (0)	0 (0)	3 (25)	1 (11)
Liver disease (unspecified)	0 (0)	0 (0)	1 (8)	1 (11)

BMI denotes body mass index; Pre-existing conditions were self-reported for non-hospitalized participants and retrieved from electronic medical records and self-reported for hospitalized participants. COPD, chronic obstructive pulmonary disease; DM, diabetes mellitus; HTN, hypertension; CAD, coronary artery disease.

Figure 1E shows γ-linolenic acid (GLA) (C18:3n6) was significantly lower in the adults with moderate disease compared to the uninfected adults (9.1 vs 22.4 μg/ml, p = 0.03). Levels of this fatty acid were not significantly different in the mild and severe disease groups compared to other disease severities and the uninfected (p = 0.87 and p = 0.80, respectively). Additionally, linoleic acid (C18:2n9) was significantly higher in adults with mild disease (527.9 μg/ml) and uninfected adults (536.2 μg/ml) when compared to the adults with moderate disease (305.8 μg/ml) (p = 0.04 and p = 0.03, respectively) (Figure 1F). Eicosapentaenoic acid (C20:5n3) (EPA) levels were significantly lower in the mild group (11.4 μg/ml) and the moderate group (6.6 μg/ml) when compared to the uninfected adults (22.4 μg/ml) (p = 0.03 and p = 0.007, respectively) (Figure 1G). Docahexaenoic (C22:6n3), arachidonic (C20:4n6), and linolenic (C18:3n3) acid levels were detectable, though levels of these fatty acids were not significantly different between the disease severity groups or uninfected adults. Docosadienoic acid (C22:2n6) was not detected in any sample. Supplementary Table 1 shows all quantified PFA for the entire cohort.

Post-acute sequelae of COVID-19 associated fatty acid changes

Twenty-three participants completed two additional study visits several weeks after their initial infection (26–229 days post-PCR + diagnosis), for a total of three study visits. Twelve participants developed PASC (sampled at 55.8 ± 20.8 days post-PCR + diagnosis), while the remaining eleven participants did not report experiencing persisting symptoms when sampled at 121.2 ± 61.1 days post-PCR + diagnosis. Fatty acid levels were compared between study visits within the PASC vs No PASC groups to assess for fluctuations in fatty acids based on days post PCR +. There was variation in the study visits due to days post PCR +. Individuals who experienced PASC demonstrated significantly lower levels of GLA during the early recovery stage (16.8 ± 13.8 days post-PCR +) compared to samples taken during later recovery stages (55.8 ± 20.8 days post-PCR +) (20.4 vs 35.7 μg/ml) (p = 0.02). At 113.5 ± 23.4 days post-PCR +, mean levels of GLA were higher than levels observed at 16.8 ± 13.8 days post-PCR + (28.0 vs 20.4 μg/ml) but were lower than those observed at 55.8 ± 20.8 days post-PCR + (28.0 vs 35.7 μg/ml). This difference between 55.8 ± 20.8 days and 113.5 ± 23.4 days post-PCR + was not statistically significant, though it is interesting to note that GLA levels decreased several months into the recovery period for individuals who experience PASC. Levels of GLA between the acute and convalescent stages of recovery were not statistically different in those who did not develop PASC, and levels remained relatively stable during all periods of infection (Table 3). Similar to the findings observed for GLA, Table 3 illustrates that levels of EPA were significantly lower at 16.8 ± 13.8 days post-PCR + compared to 55.8 ± 20.8 days post-PCR + (11.1 vs 24.8 μg/ml, p = 0.0003) for those who developed PASC. Samples taken at 113.5 ± 23.4 days post-PCR + showed higher levels of EPA compared to 16.8 ± 13.8 days post-PCR + (14.2

TABLE 2 Baseline fatty acid profile in plasma for mild, moderate, and severe COVID-19 disease severity compared to uninfected adults.

	Uninfected ($N = 9$)	Mild ($N = 20$)	*p*-value			Moderate ($N = 12$)	*p*-value		Severe ($N = 9$)	*p*-value
			Mild moderate	Mild severe	Mild uninfected		Moderate severe	Moderate uninfected		Severe uninfected
Saturated fatty acids (μg/ml)										
Behenic (C22)	3.2 ± 0.7	2.7 ± 1.9	0.67	0.99	0.36	1.8 ± 0.9	0.84	**0.03**	2.2 ± 1.1	0.22
Palmitic (C16)	393.4 ± 109.5	513.4 ± 262.3	0.9	0.26	0.79	427.5 ± 224.7	0.07	0.99	755.1 ± 419.8	**0.04**
Lignoceric (C23)	2.9 ± 0.5	2.4 ± 1.4	0.27	0.71	0.43	1.6 ± 0.8	0.811	**0.009**	1.8 ± 0.9	0.06
Lauric (C12)	3.5 ± 3.3	3.2 ± 2.1	0.97	0.92	1	3.8 ± 2.6	0.99	0.96	7.0 ± 13.0	0.90
Stearic (C18)	178.0 ± 28.2	180.4 ± 73.5	0.39	0.99	0.99	129.9 ± 64.1	0.3	0.44	186.5 ± 94.6	0.99
Pentadecaoic (C15)	3.7 ± 1.9	3.9 ± 3.1	0.97	0.77	0.98	3.1 ± 2.8	0.49	0.83	5.0 ± 3.9	0.94
Arachidic (C20)	1.4 ± 0.3	1.4 ± 0.8	0.92	0.99	0.94	1.1 ± 0.5	0.76	0.61	1.4 ± 0.8	0.99
Monounsaturated fatty acids (μg/ml)										
Oleic (C18:1n9)	137.3 ± 57.2	158.8 ± 57.4	0.43	0.66	0.86	123.8 ± 69.9	**0.04**	0.85	220.1 ± 108.9	0.27
Myristoleic (C14:1n5)	0.7 ± 0.3	0.8 ± 0.4	1	0.99	0.97	0.8 ± 0.4	0.99	0.98	1.0 ± 1.3	0.91
Eicosenoic (C20:1n9)	1.9 ± 0.9	3 ± 1.7	0.69	0.7	0.46	2.2 ± 1.5	0.14	0.97	3.8 ± 1.9	0.07
Palmitoleic (C16:1n7)	24.3 ± 12.7	46.4 ± 34.3	0.99	0.56	0.63	41.0 ± 17.4	0.72	0.43	70.3 ± 59.2	0.08
Polyunsaturated fatty acids (μg/ml)										
γ-linolenic (C18:3n6)	22.4 ± 10.2	20.4 ± 15.9	0.18	0.99	0.87	9.1 ± 4.4	0.24	**0.03**	23.2 ± 20.4	0.8
Linoleic (C18:2n9)	536.2 ± 83.3	527.9 ± 222.9	**0.04**	0.8	0.99	305.8 ± 175.8	0.29	**0.03**	452.6 ± 196.2	0.75
Eicosapentaenoic (C20:5n3)	22.4 ± 12.8	11.4 ± 14.9	0.96	0.84	**0.03**	6.6 ± 3.2	0.53	**0.007**	12.6 ± 9.2	0.18
Docasahexaenoic (C22:6n3)	45.7 ± 18.6	39.7 ± 30.6	0.99	0.72	0.77	47.1 ± 26.8	0.83	0.87	50.3 ± 32.7	0.99
Arachidonic (C20:4n6)	205.2 ± 39.2	199.3 ± 104.2	1	0.84	0.91	189.3 ± 79.5	0.81	0.89	241.8 ± 147.2	0.99
Linolenic (C18:3n3)	18.6 ± 12.5	13.6 ± 8.3	0.99	0.31	0.8	18.3 ± 20.7	0.47	0.93	26.3 ± 16.9	0.83

Values presented as mean ± standard deviation. Linear mixed model was performed to compare the fatty acids between disease severity categories and the uninfected adults. SAS v9.4 (SAS Institute Inc., Cary, NC, United States) was used to perform all statistical analyses. $P < 0.05$ significant; bold = significant.

10.3389/fnut.2022.960409

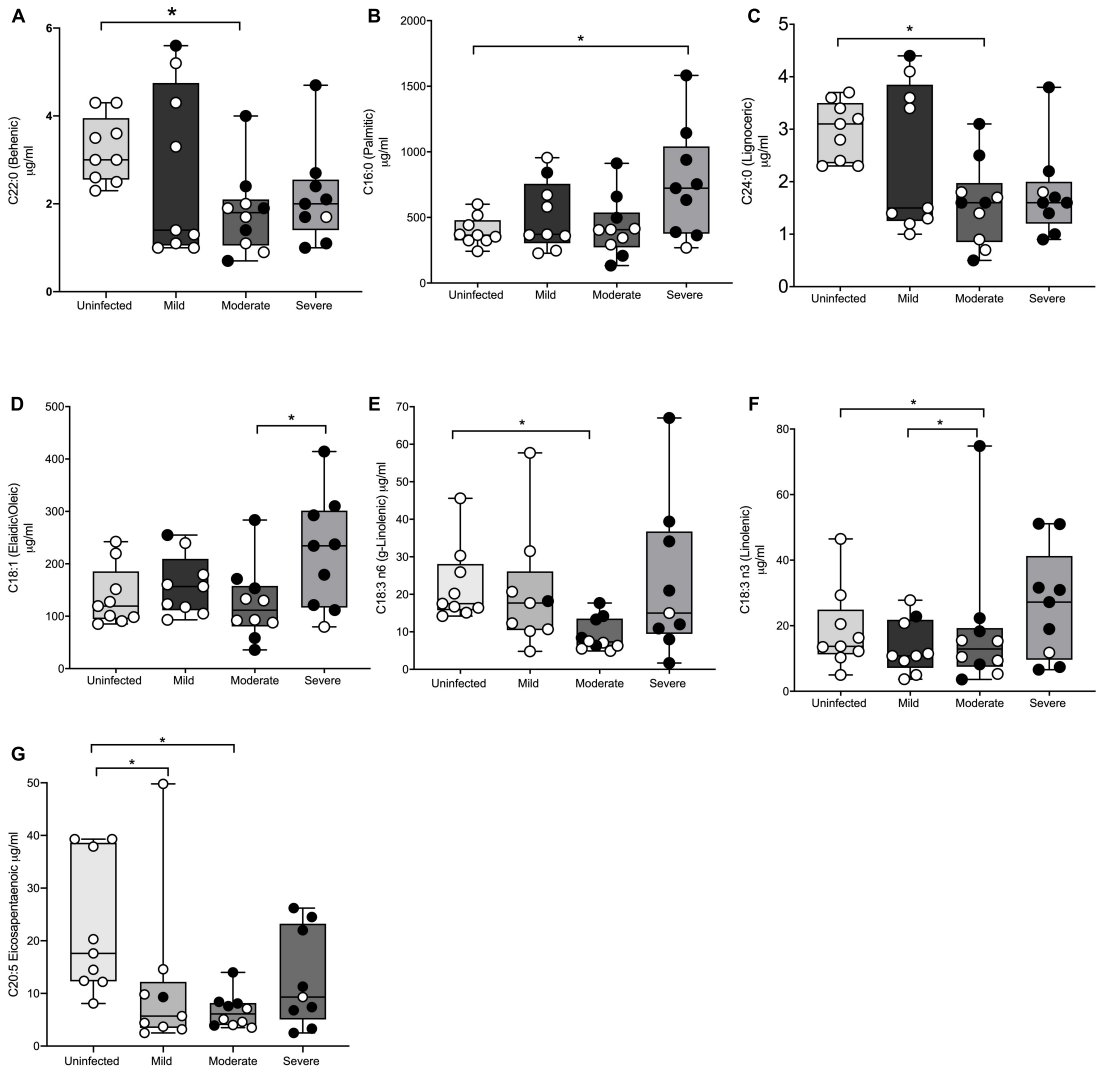

FIGURE 1
Significant differences in fatty acid profiles between disease severity groups and the uninfected adults. **(A)** Behenic acid lower in moderate adults compared to uninfected. **(B)** Palmitic acid elevated in adults with severe disease compared to uninfected. **(C,E)** Lignoceric acid and γ-linolenic acid lower in moderate disease compared to uninfected. **(D)** Oleic acid lower in moderate disease compared to severe disease. **(F)** Linolenic acid lower in moderate adults compared to mild disease and uninfected. **(G)** EPA lower in mild and moderate adults compared to uninfected. Shaded points represent adults who received convalescent plasma. * denotes statistical significance $p \leq 0.05$.

vs 11.1 µg/ml), though these levels were lower than those observed at 55.8 ± 20.8 days post-PCR + (14.2 vs 24.8 µg/ml). This difference between 113.5 ± 23.4 days post-PCR + and 16.8 ± 13.8 days post-PCR + was not statistically significant, though it is notable that similar fluctuations in EPA levels were not observed in the No PASC group (Table 3). BMI as a covariate was not significantly related to the fatty acid changes.

Discussion

In this pilot study of forty-one COVID-19 survivors and nine adults without history of infection, there were clear differences in the plasma fatty acid (PFA) profiles of those who experienced a moderate or severe disease course compared to the adults with mild disease and to the uninfected. Individuals who developed PASC also showed differences in PFA levels compared to the adults who did not develop PASC. Among the saturated fatty acid profiles, levels of palmitic acid were significantly higher in those who experienced a severe disease course relative to the uninfected adults. Previous analysis of fatty acid metabolism in COVID-19 has revealed that palmitic acid is likely to play a role in viral entry to host cells, as palmitic acid is known to lipidate the cysteine residues found on the SARS-CoV-2 spike and envelope proteins (26). Thus, individuals with higher levels of this fatty acid may

TABLE 3 Lower levels of anti-inflammatory fatty acids during early stages of recovery in adults with post-acute sequelae of COVID-19 (PASC).

	No PASC (N = 12)					PASC (N = 11)				
	Days post PCR +			p-value		Days post PCR +			p-value	
μg/ml	**66.2 ± 54.6 V1**	**121.2 ± 61.1 V2**	**187.8 ± 69.1 V3**	**V1/V2**	**V1/V3**	**16.8 ± 13.8 V1**	**55.8 ± 20.8 V2**	**113.5 ± 23.4 V3**	**V1/V2**	**V1/V3**
Saturated fatty acids (μg/ml)										
Behenic (C22)	2.7 ± 1.1	2.78 ± 1.4	3.33 ± 1.7	1.00	0.87	1.9 ± 0.73	2.8 ± 1.56	2.5 ± 2.2	0.24	0.95
Palmitic (C16)	424.5 ± 214.2	530.1 ± 440.0	487.1 ± 334.4	0.95	0.99	424.5 ± 214.2	787.3 ± 342.4	612.3 ± 291.9	0.38	0.96
Lignoceric (C23)	2.7 ± 1.1	2.7 ± 1.45	3.2 ± 1.6	0.99	0.95	1.8 ± 0.78	2.6 ± 1.5	2.3 ± 1.9	0.20	0.92
Lauric (C12)	3.3 ± 3.34	4.4 ± 5.40	3.31 ± 3.1	0.99	1.00	2.27 ± 1.1	5.86 ± 3.8	6.4 ± 5.8	0.21	0.26
Stearic (C18)	179.0 ± 67.2	201.0 ± 96.6	193.4 ± 86.8	0.99	0.99	163.0 ± 54.7	240.6 ± 109.2	192.9 ± 72.9	0.06	0.76
Pentadecaoic (C15)	4.2 ± 3.1	4.9 ± 4.8	4.7 ± 3.8	0.99	0.99	4.16 ± 2.4	6.71 ± 2.8	4.8 ± 1.9	0.10	0.87
Arachidic (C20)	1.8 ± 0.34	1.5 ± 0.80	1.8 ± 0.90	0.99	0.53	1.13 ± 0.44	1.82 ± 1.0	1.3 ± 0.7	0.06	0.87
Monounsaturated fatty acids (μg/ml)										
Oleic (C18:1n9)	127.3 ± 58.4	161.9 ± 143.0	146.9 ± 97.4	0.95	0.99	166.5 ± 50.1	224.8 ± 88.3	170.6 ± 60.9	0.38	1.00
Myristoleic (C14:1n5)	0.7 ± 0.26	1.02 ± 1.1	0.94 ± 1.0	0.98	0.99	1.0 ± 0.75	1.93 ± 1.7	0.7 ± 0.4	0.30	0.99
Eicosenoic (C20:1n9)	1.84 ± 1.1	2.27 ± 3.1	2.70 ± 2.4	0.97	0.92	2.9 ± 1.2	3.9 ± 2.24	2.5 ± 1.3	0.71	0.95
Palmitoleic (C16:1n7)	37.2 ± 29.8	46.5 ± 59.0	44.2 ± 45.0	1.00	0.99	45.8 ± 18.5	76.3 ± 41.5	57.9 ± 26.0	0.19	0.83
Polyunsaturated fatty acids (μg/ml)										
γ-linolenic (C18:3n6)	25.2 ± 13.1	26.3 + 17.1	29.8 ± 23.4	1.00	0.99	20.4 + 18.7	35.7 + 21.6	28.0 ± 14.2	**0.02**	0.08
Eicosapentaenoic (C20:5n3)	19.1 + 12.2	17.0 + 8.7	20.0 ± 9.5	0.99	0.99	11.1 + 8.0	24.8 + 13.4	14.2 ± 8.5	**0.0003**	0.42
Docosahexaenoic (C22:6n3)	46.8 ± 25.7	47.9 ± 19.3	49.9 ± 19.7	0.99	0.91	40.9 ± 11.7	52.5 ± 25.5	44.3 ± 20.9	0.63	1.00
Linoleic (C18:2n9)	508.0 ± 214.7	575.6 ± 205.9	539.7 ± 224.9	0.86	0.99	448.8 ± 179.9	617.3 ± 237.8	527.6 ± 271.3	0.09	0.80
Linolenic (C18:3n3)	15.9 ± 7.4	21.3 ± 21.9	19.5 ± 12.6	0.99	0.99	20.8 ± 13.6	32.4 ± 19.5	20.2 ± 10.4	0.26	1.00
Arachidonic (C20:4n6)	220.4 ± 83.3	234.8 ± 101.6	249.1 ± 100.7	0.99	0.72	189. ± 62.6	237. ± 80.1	225.0 ± 97.6	0.11	0.49

Values presented as mean ± standard deviation, apart from days post PCR, which are presented as mean ± average deviation. Abbreviations V1, V2, and V3 are study visits 1, 2, and 3, respectively. Linear mixed model was performed to compare the fatty acids quantification for no PASC and PASC groups at T2 and T3 compared to their T1. SAS v9.4 (SAS Institute Inc., Cary, NC) was used to perform all statistical analyses. $P < 0.05$ significant; bold = significant.

10.3389/fnut.2022.960409

have been more susceptible to viral invasion and subsequently developed a more severe disease course. Additionally, SARS-CoV-2 has also been hypothesized to promote activation of palmitic acid synthesis via upregulation of the genes responsible for signaling the transcription of fatty acid synthase (FASN), acetyl-CoA carboxylase (ACC), and stearoyl-CoA desaturase 1 (SCD1) (26). In doing so, the virus increases the lipid stock and further promotes its replication, increasing viral load within the body (26). Among the other saturated fatty acids included in this study, behenic and lignoceric acid levels were significantly different in adults with moderate disease compared to the uninfected individuals, with both showing depletion in the infected adults. Depletion of behenic acid in COVID-19 patients has been observed in one other study and is thought to be correlated with adverse disease outcomes, including intestinal inflammation and altered serum metabolites (27). Although levels of lignoceric acid in COVID-19 patients have not previously been explored, depletion in this fatty acid has been linked to unfavorable immune responses, particularly in cases of autoimmune diseases and response to cancer treatments (28, 29). Additional reports have also linked higher levels of lignoceric acid to decreased incidence of age-related diseases, thus further implicating its potential protective role within the body (30).

Analysis of unsaturated fatty acid profiles within this cohort of COVID-19 survivors revealed several significant findings. Oleic acid was significantly higher in those who experienced a severe disease course compared to the adults with moderate disease. Individuals within the moderate and severe disease groups were of similar BMI, thus indicating that this difference was independent of obesity level. Elevation of oleic acid in COVID-19 was previously described by Barberis et al., who showed that levels of oleic acid directly correlated with disease severity (31). Interestingly, unsaturated fatty acids, such as oleic, arachidonic, and linoleic acid, have been shown to mediate antiviral activity by disintegrating the envelope of certain animal viruses, including herpes and influenza (32). Oleic acid may not demonstrate this same capacity with the envelope of SARS-CoV-2 given its direct correlation with disease severity. However, depletion in linoleic acid was observed in the adults with moderate disease compared to the mild and uninfected adults, and this may be attributed to the capacity for linoleic acid to interfere with the envelope structure of SARS-CoV-2. In fact, linoleic acid has been shown to play a structural role in preventing entry of the SARS-CoV-2 virus into host cells by binding the spike protein on the viral envelope and locking it in a conformation that inhibits interaction with ACE2 (33). Additional studies have also implicated that linoleic acid, along with linolenic (n3) and EPA, interfere with the receptor binding domain sequence of the SARS-CoV-2 virus, further blocking interacting with host ACE2 receptors (34). While linolenic (n3) levels were not different between the disease severity groups in this study, GLA (n6) levels were significantly lower in the adults with moderate disease compared to the uninfected. Similar to the effect of linoleic acid previously described, omega-3 fatty acids, such as EPA and DHA, have been found to interfere with SARS-CoV-2 spike protein conformation to prevent interaction with host cells and indeed, EPA levels were significantly lower in the adults with moderate and mild disease compared to the uninfected (35). These findings support the postulations of Baral et al. and Mazidimoradi et al. in demonstrating that polyunsaturated fatty acids may act as important mediators in determining COVID-19 disease severity (36, 37).

In addition to analyzing the differences in fatty acid levels between individuals based on disease severity, this study compared the relative levels of individual fatty acids between three study visits to determine if depletion was associated with the development of PASC. To our knowledge, this is the first study to explore such a relationship. Currently, reference ranges for individual fatty acids are poorly defined and are typically represented as a percentage of total PFA composition, though a small number of population studies have defined the reference ranges of a limited suite of fatty acids in healthy adults (38, 39). EPA is typically found in the range of 12.0–68.6 μmol/L, while GLA concentrations are found in the range of 9.7–37.3 μmol/L (38). For the purposes of this study, depletion was measured based on significantly lower levels of fatty acid concentrations when measured during the early recovery period (16.8 ± 13.8 days post-PCR +) versus later recovery stages (55.8 ± 20.8 and 113.5 ± 23.4 days post-PCR +). Of the fatty acids measured, EPA levels were significantly lower at 16.8 ± 13.8 days post-PCR + compared to 55.8 ± 20.8 days post-PCR + in the individuals who developed PASC but were not different between the visits in the adults who did not experience persistent symptoms. This same relationship was observed for GLA, with levels in the PASC group being significantly lower at 16.8 ± 13.8 days post-PCR + compared to 55.8 ± 20.8 days post-PCR +. While the levels of EPA and GLA at 113.5 ± 23.4 days post-PCR + were not significantly different from those measured at 16.8 ± 13.8 days post-PCR + and 55.8 ± 20.8 days post-PCR +, the mean levels of these fatty acids did decrease at the 113.5 ± 23.4 day post-PCR + visit for those with PASC. These fluctuations in EPA and GLA levels were not observed in the individuals who did not develop PASC. It should be noted that the collection times (days post PCR +) differed between the PASC and No PASC groups, with sample collections occurring closer to initial PCR + in the PASC group (study V1 occurred at 16.8 ± 13.8 days post PCR + in the PASC group vs 66.2 ± 54.6 days post PCR + for No PASC). However, when comparing similar days post PCR + between groups (i.e., 55.8 ± 20.8 in PASC group vs 66.2 ± 54.6 in No PASC group and 113.5 ± 23.4 in PASC group vs 121.2 ± 61.1 in No PASC group), the symptoms reported by individuals experiencing PASC remained consistent. In other words, at all study visits, individuals with PASC

continued to experience persisting symptoms, while those in the No PASC group remained asymptomatic. Thus, despite the inconsistency in days post PCR + between the groups, it appears that the fluctuations in GLA and EPA did correlate to the persistence of symptoms. Additionally, it is notable that there was more fluctuation in EPA and GLA levels between each study visit in the PASC group, while levels of EPA and GLA remained fairly consistent in the No PASC group (see **Table 3**).

Although further research is warranted, these preliminary findings suggest that depletion in EPA and GLA may be a predictor for the development of persistent symptoms beyond the acute stage of infection. This correlation may be due to the anti-inflammatory properties of these fatty acids, as the development of PASC is increasingly linked to persistent elevations of inflammatory factors, such as C-reactive protein and interleukin-6 (IL-6) (40, 41). EPA has previously been shown to attenuate pro-inflammatory cytokines, and the benefits of supplementation to reduce COVID-19 severity has been suggested, with one small study indicating significantly improved survival rates after EPA supplementation in acutely ill patients (42–49). Although GLA is an omega 6 fatty acid, which are typically associated with pro-inflammatory effects, GLA has been found to demonstrate anti-inflammatory properties through its longer-chain derivative, 15-hydroxyeicosatraenoic acid, which acts to inhibit the formation of the pro-inflammatory leukotriene B4 (LTB4) (50, 51). The LTB4 pathway appears to be upregulated in individuals with severe COVID-19, thus inhibition by GLA may help prevent adverse disease outcomes (52). Additional studies have also shown that GLA acts to mediate endothelial cell tumor necrosis factor alpha (TNF-α) expression and reduce production of IL-6, thereby further quelling inflammation (53). Interestingly, levels of arachidonic acid, a pro-inflammatory fatty acid, were not significantly different between the disease severity groups in this cohort and were not associated with the development of PASC. However, additional studies analyzing the PFA profiles of COVID-19-infected individuals showed arachidonic acid levels were elevated during acute infection, and this elevation was associated with severe disease (31, 54).

Preliminary findings from this cohort demonstrate significant differences in fatty acid profiles in COVID-19-infected adults with more significant disease outcomes compared to those with mild infection or no infection, thus demonstrating the potential for fatty acids to act as key modifiers in the disease course. Although the results of this study are promising, further study is needed given the limited size of this pilot cohort. Due to sample size limitations and the pilot nature of this study, the demographics of the infected individuals were not mirrored in the individuals comprising the uninfected group. As shown in **Table 1**, the mean BMI of the uninfected group was similar to the mean BMI of the mild disease group but was much lower than that of the moderate and severe disease groups, thus presenting a limitation in the comparison of the moderate and severe disease groups to the uninfected. There was also more racial and ethnic diversity in the moderate and severe disease groups compared to the uninfected, which further limited comparison. Future studies should incorporate more demographic diversity in the uninfected group to yield more accurate comparisons. Additional difficulties in accurate comparison included sample collection dates, as there was notable difference in the days post initial PCR +, particularly in the comparison between individuals with PASC versus those without PASC. At the time of analysis, few participants in the NoCO CoBIO cohort had completed three study visits, thus presenting challenges in controlling for the amount of time that had passed between collection dates and initial PCR +. Future studies should control for this variable to better define the relationship between fatty acid profiles and PASC development. The use of convalescent plasma in many of the participants during early stages of the pandemic presented challenges in the analysis of fatty acid profiles obtained during the acute stage of infection, particularly among those with severe disease. This study did include patients that did not receive convalescent plasma and trends for differential profiles remained apparent. Finally, the precise role of diet to induce PFA changes is not definitive given *de novo* lipogenesis also accounts for the composition of PFA, particularly palmitic, stearic, palmitoleic, oleic, and myristoleic acid (55). However, the endogenous synthesis of polyunsaturated fatty acids, particularly EPA and DHA is limited, with some studies suggesting as little as 2–10% of *de novo* lipogenesis of these fatty acids occurs (56, 57). The findings of this study suggest that long-chain fatty acids are associated with lower incidence of PASC, thus making dietary intake of EPA and GLA a promising and safely administered applications for the convalescent stages of disease and for those at risk for PASC.

Further investigation into the role of PFA in determining COVID-19 disease severity and the development of PASC is warranted in larger cohorts based on findings of this pilot observational study indicating individuals with more severe COVID-19 infections have altered plasma fatty acid profiles. As potent inflammatory mediators and structural modifiers of SARS-CoV-2, dietary supplementation of behenic, lignoceric, linoleic, GLA, and EPA may be a cost effective and non-invasive method of preventing or controlling PASC, and particularly in overweight or obese individuals who are of heightened risk of severe disease outcomes.

Data availability statement

The original contributions presented in this study are included in the article/**Supplementary material**, further inquiries can be directed to the corresponding author.

Ethics statement

The studies involving human participants were reviewed and approved by Colorado State University Research Integrity and Compliance Review Office Institutional Review Board [IRB; protocol 2105 (20-10063H)] and University of Colorado Health Institutional Review Board (Colorado Multiple IRB 20-6043). The patients/participants provided their written informed consent to participate in this study.

Author contributions

ER and JD conceived, designed and conducted the research, and performed funding acquisition. SS and BB completed co-writing-original draft preparation. SS, BB, SL, EG, TW, TD, KM, MH-T, GE, and ER reviewed and edited the manuscript. SR performed the formal analysis. GD performed plasma fatty acid determinations. BB, SS, SL, KB, MT, JH, and NN administered symptom survey and data entry for analysis. All authors have read and agreed to the published version of the manuscript.

Funding

The Northern Colorado Coronavirus Biorepository project was created and designed with funding and translational research infrastructure in the Colorado State University Department of Environmental and Radiological Health Sciences and with pilot funds obtained from the CSU Vice President for Research Office to ER. Additional funding was supported by NIH/NCATS Colorado CTSA Grant Number UL1 TR002535. Contents are the authors' sole responsibility and do not necessarily represent official NIH views. This project was initiated in partnership with University of Colorado Health, Northern Colorado Trauma Research Department and funding support by JD.

Acknowledgments

We wish to thank Brian Cranmer for assistance in GC-MS fatty acid quantification, as well as Annika Weber for participant symptom surveillance and sample processing. Additional gratitude is given to Sangmi Pallickara and Shriram Gaddam for biobank database development and to Emma McGinnis and Sarah Mast from the CSU Human Performance Clinical Research Laboratory for phlebotomy assistance. Most importantly, we wish to thank our participants who willingly donated their blood and engaged in our questionnaires to further this research endeavor.

Conflict of interest

The authors declare that the research was conducted in the absence of any commercial or financial relationships that could be construed as a potential conflict of interest.

Publisher's note

All claims expressed in this article are solely those of the authors and do not necessarily represent those of their affiliated organizations, or those of the publisher, the editors and the reviewers. Any product that may be evaluated in this article, or claim that may be made by its manufacturer, is not guaranteed or endorsed by the publisher.

Supplementary material

The Supplementary Material for this article can be found online at: https://www.frontiersin.org/articles/10.3389/fnut.2022.960409/full#supplementary-material

References

1. BBC News. *Covid Map: Coronavirus Cases, Deaths, Vaccinations by Country*. London: BBC News (2022).

2. Ejaz H, Alsrhani A, Zafar A, Javed H, Junaid K, Abdalla AE, et al. COVID-19 and comorbidities: deleterious impact on infected patients. *J Infect Public Health.* (2020) 13:1833–9. doi: 10.1016/j.jiph.2020.07.014

3. Petrakis D, Margină D, Tsarouhas K, Tekos F, Stan M, Nikitovic D, et al. Obesity – a risk factor for increased COVID-19 prevalence, severity and lethality (review). *Mol Med Rep.* (2020) 22:9–19. doi: 10.3892/mmr.2020.11127

4. Rando HM, Bennett TD, Byrd JB, Bramante C, Callahan TJ, Chute CG, et al. Challenges in defining long COVID: striking differences across literature, electronic health records, and patient-reported information. *medRxiv.* (2021) [Preprint]. doi: 10.1101/2021.03.20.21253896

5. McFann K, Baxter BA, LaVergne SM, Stromberg S, Berry K, Tipton M, et al. quality of life (QoL) is reduced in those with severe COVID-19 disease, post-acute sequelae of COVID-19, and hospitalization in united states adults from Northern Colorado. *Int J Environ Res Public Health.* (2021) 18:11048. doi: 10.3390/ijerph182111048

6. World Health Organization. *A clinical Case Definition of Post COVID-19 Condition by a Delphi Consensus, 6 October 2021*. Geneva: World Health Organization (2021).

7. Sudre CH, Murray B, Varsavsky T, Graham MS, Penfold RS, Bowyer RC, et al. Attributes and predictors of Long-COVID: analysis of COVID cases and their symptoms collected by the covid symptoms study app. *medRxiv.* (2020). [Preprint]. doi: 10.1101/2020.10.19.20214494

8. Mandal S, Barnett J, Brill SE, Brown JS, Denneny EK, Hare SS, et al. "Long-COVID": a cross-sectional study of persisting symptoms, biomarker and imaging

abnormalities following hospitalisation for COVID-19. *Thorax.* (2021) 76:396–8. doi: 10.1136/thoraxjnl-2020-215818

9. Dani M, Dirksen A, Taraborrelli P, Torocastro M, Panagopoulos D, Sutton R, et al. Autonomic dysfunction in "long COVID": rationale, physiology and management strategies. *Clin Med Lond Engl.* (2021) 21:e63–7. doi: 10.7861/clinmed.2020-0896

10. Huang C, Huang L, Wang Y, Li X, Ren L, Gu X, et al. 6-month consequences of COVID-19 in patients discharged from hospital: a cohort study. *Lancet Lond Engl.* (2021) 397:220–32. doi: 10.1016/S0140-6736(20)32656-8

11. Carfì A, Bernabei R, Landi F, Gemelli Against Covid-19 Post-Acute Care Study Group. Persistent symptoms in patients after acute COVID-19. *JAMA.* (2020) 324:603–5. doi: 10.1001/jama.2020.12603

12. Chau AS, Weber AG, Maria NI, Narain S, Liu A, Hajizadeh N, et al. The longitudinal immune response to coronavirus disease 2019: chasing the cytokine storm. *Arthritis Rheumatol Hoboken NJ.* (2021) 73:23–35. doi: 10.1002/art.41526

13. Tan LY, Komarasamy TV, Rmt Balasubramaniam V. Hyperinflammatory immune response and COVID-19: a double Edged sword. *Front Immunol.* (2021) 12:742941. doi: 10.3389/fimmu.2021.742941

14. Ye Q, Wang B, Mao J. The pathogenesis and treatment of the 'cytokine storm' in COVID-19. *J Infect.* (2020) 80:607–13. doi: 10.1016/j.jinf.2020.03.037

15. Unamuno X, Gómez-Ambrosi J, Rodríguez A, Becerril S, Frühbeck G, Catalán V. Adipokine dysregulation and adipose tissue inflammation in human obesity. *Eur J Clin Invest.* (2018) 48:e12997. doi: 10.1111/eci.12997

16. Rogero MM, Calder PC. Obesity, inflammation, toll-like receptor 4 and fatty acids. *Nutrients.* (2018) 10:E432. doi: 10.3390/nu10040432

17. Wu D, Shu T, Yang X, Song JX, Zhang M, Yao C, et al. Plasma metabolomic and lipidomic alterations associated with COVID-19. *Natl Sci Rev.* (2020) 7:1157–68. doi: 10.1093/nsr/nwaa086

18. Thomas T, Stefanoni D, Reisz JA, Nemkov T, Bertolone L, Francis RO, et al. COVID-19 infection alters kynurenine and fatty acid metabolism, correlating with IL-6 levels and renal status. *JCI Insight.* (2020) 5:140327. doi: 10.1172/jci.insight.140327

19. Palmas F, Clarke J, Colas RA, Gomez EA, Keogh A, Boylan M, et al. Dysregulated plasma lipid mediator profiles in critically ill COVID-19 patients. *PLoS One.* (2021) 16:e0256226. doi: 10.1371/journal.pone.0256226

20. Sorokin AV, Karathanasis SK, Yang ZH, Freeman L, Kotani K, Remaley AT. COVID-19–Associated dyslipidemia: implications for mechanism of impaired resolution and novel therapeutic approaches. *FASEB J.* (2020) 34:9843–53. doi: 10.1096/fj.202001451

21. McReynolds CB, Cortes-Puch I, Ravindran R, Khan IH, Hammock BG, Shih P, et al. Plasma linoleate diols are potential biomarkers for severe COVID-19 infections. *Front Physiol.* (2021) 12:663869. doi: 10.3389/fphys.2021.663869

22. Zaid Y, Doré É, Dubuc I, Archambault AS, Flamand O, Laviolette M, et al. Chemokines and eicosanoids fuel the hyperinflammation within the lungs of patients with severe COVID-19. *J Allergy Clin Immunol.* (2021) 148:368.e–80.e. doi: 10.1016/j.jaci.2021.05.032

23. LaVergne SM, Stromberg S, Baxter BA, Webb TL, Dutt TS, Berry K, et al. A longitudinal SARS-CoV-2 biorepository for COVID-19 survivors with and without post-acute sequelae. *BMC Infect Dis.* (2021) 21:677. doi: 10.1186/s12879-021-06359-2

24. Lucas C, Wong P, Klein J, Castro TBR, Silva J, Sundaram M, et al. Longitudinal analyses reveal immunological misfiring in severe COVID-19. *Nature.* (2020) 584:463–9.

25. Masood A, Stark KD, Salem N. A simplified and efficient method for the analysis of fatty acid methyl esters suitable for large clinical studies. *J Lipid Res.* (2005) 46:2299–305. doi: 10.1194/jlr.D500022-JLR200

26. Tanner JE, Alfieri C. The fatty acid lipid metabolism nexus in COVID-19. *Viruses.* (2021) 13:90. doi: 10.3390/v13010090

27. Lv L, Jiang H, Chen Y, Gu S, Xia J, Zhang H, et al. The faecal metabolome in COVID-19 patients is altered and associated with clinical features and gut microbes. *Anal Chim Acta.* (2021) 1152:338267. doi: 10.1016/j.aca.2021.338267

28. Tsoukalas D, Fragoulakis V, Sarandi E, Docea AO, Papakonstaninou E, Tsilimidos G, et al. Targeted metabolomic analysis of serum fatty acids for the prediction of autoimmune diseases. *Front Mol Biosci.* (2019) 6:120. doi: 10.3389/fmolb.2019.00120

29. Karayama M, Inui N, Inoue Y, Yoshimura K, Mori K, Hozumi H, et al. Increased serum cholesterol and long-chain fatty acid levels are associated with the efficacy of nivolumab in patients with non-small cell lung cancer. *Cancer Immunol Immunother.* (2021) 71:203–17. doi: 10.1007/s00262-021-02979-4

30. Bockus LB, Biggs ML, Lai HTM, de Olivera Otto MC, Fretts AM, McKnight B, et al. Assessment of plasma phospholipid very-long-chain saturated fatty acid levels and healthy aging. *JAMA Netw Open.* (2021) 4:e2120616. doi: 10.1001/jamanetworkopen.2021.20616

31. Barberis E, Timo S, Amede E, Vanella VV, Puricelli C, Cappellano G, et al. Large-scale plasma analysis revealed new mechanisms and molecules associated with the host response to SARS-CoV-2. *Int J Mol Sci.* (2020) 21:8623. doi: 10.3390/ijms21228623

32. Kohn A, Gitelman J, Inbar M. Interaction of polyunsaturated fatty acids with animal cells and enveloped viruses. *Antimicrob Agents Chemother.* (1980) 18:962–8. doi: 10.1128/AAC.18.6.962

33. Toelzer C, Gupta K, Yadav SKN, Borucu U, Davidson AD, Kavanagh Williamson M, et al. Free fatty acid binding pocket in the locked structure of SARS-CoV-2 spike protein. *Science.* (2020) 370:725–30. doi: 10.1126/science.abd3255

34. Goc A, Niedzwiecki A, Rath M. Polyunsaturated ω-3 fatty acids inhibit ACE2-controlled SARS-CoV-2 binding and cellular entry. *Sci Rep.* (2021) 11:5207. doi: 10.1038/s41598-021-84850-1

35. Vivar-Sierra A, Araiza-Macías MJ, Hernández-Contreras JP, Vergara-Castañeda A, Ramírez-Vélez G, Pinto-Almazán R, et al. *In silico* study of polyunsaturated fatty acids as potential SARS-CoV-2 spike protein closed conformation stabilizers: epidemiological and computational approaches. *Molecules.* (2021) 26:711. doi: 10.3390/molecules26030711

36. Baral PK, Amin MT, Rashid MDMO, Hossain MS. Assessment of polyunsaturated fatty acids on COVID-19-associated risk reduction. *Rev Bras Farmacogn.* (2022) 32:50–64. doi: 10.1007/s43450-021-00213-x

37. Mazidimoradi A, Alemzadeh E, Alemzadeh E, Salehiniya H. The effect of polyunsaturated fatty acids on the severity and mortality of COVID patients: a systematic review. *Life Sci.* (2022) 299:120489. doi: 10.1016/j.lfs.2022.120489

38. Abdelmagid SA, Clarke SE, Nielsen DE, Badawi A, El-Sohemy A, Mutch DM, et al. Comprehensive profiling of plasma fatty acid concentrations in young healthy Canadian adults. *PLoS One.* (2015) 10:e0116195. doi: 10.1371/journal.pone.0116195

39. Sera RK, McBride JH, Higgins SA, Rodgerson DO. Evaluation of reference ranges for fatty acids in serum. *J Clin Lab Anal.* (1994) 8:81–5. doi: 10.1002/jcla.1860080205

40. Yong SJ. Long COVID or post-COVID-19 syndrome: putative pathophysiology, risk factors, and treatments. *Infect Dis.* (2021) 53:737–54. doi: 10.1080/23744235.2021.1924397

41. Pierce JD, Shen Q, Cintron SA, Hiebert JB. Post-COVID-19 syndrome. *Nurs Res.* (2021) 71:164–74. doi: 10.1097/NNR.0000000000000565

42. Rogero MM, Leão M, Santana TM, Pimentel MV, Carlini GCG, da Silveira TFF, et al. Potential benefits and risks of omega-3 fatty acids supplementation to patients with COVID-19. *Free Radic Biol Med.* (2020) 156:190–9. doi: 10.1016/j.freeradbiomed.2020.07.005

43. So J, Wu D, Lichtenstein AH, Tai AK, Matthan NR, Maddipati KR, et al. EPA and DHA differentially modulate monocyte inflammatory response in subjects with chronic inflammation in part via plasma specialized pro-resolving lipid mediators: a randomized, double-blind, crossover study. *Atherosclerosis.* (2021) 316:90–8. doi: 10.1016/j.atherosclerosis.2020.11.018

44. Torrinhas RS, Calder PC, Lemos GO, Waitzberg DL. Parenteral fish oil: an adjuvant pharmacotherapy for coronavirus disease 2019? *Nutr Burbank Los Angel Cty Calif.* (2021) 81:110900. doi: 10.1016/j.nut.2020.110900

45. Asher A, Tintle NL, Myers M, Lockshon L, Bacareza H, Harris WS. Blood omega-3 fatty acids and death from covid-19: a pilot study. *Prostaglandins Leukot Essent Fatty Acids.* (2021) 166:102250. doi: 10.1016/j.plefa.2021.102250

46. Weill P, Plissonneau C, Legrand P, Rioux V, Thibault R. May omega-3 fatty acid dietary supplementation help reduce severe complications in covid-19 patients? *Biochimie.* (2020) 179:275–80. doi: 10.1016/j.biochi.2020.09.003

47. Doaei S, Gholami S, Rastgoo S, Gholamalizadeh M, Bourbour F, Bagheri SE, et al. The effect of omega-3 fatty acid supplementation on clinical and biochemical parameters of critically ill patients with covid-19: a randomized clinical trial. *J Transl Med.* (2021) 19:128. doi: 10.1186/s12967-021-02795-5

48. Hathaway D, Pandav K, Patel M, Riva-Moscoso A, Singh BM, Patel A, et al. Omega 3 fatty acids and covid-19: a comprehensive review. *Infect Chemother.* (2020) 52:478–95. doi: 10.3947/ic.2020.52.4.478

49. Arnardottir H, Pawelzik SC, Öhlund Wistbacka U, Artiach G, Hofmann R, Reinholdsson I, et al. Stimulating the resolution of inflammation through omega-3 polyunsaturated fatty acids in covid-19: rationale for the covid-omega-F trial. *Front Physiol.* (2021) 11:624657. doi: 10.3389/fphys.2020.624657

50. Iversen L, Fogh K, Bojesen G, Kragballe K. Linoleic acid and dihomogammalinolenic acid inhibit leukotriene B4 formation and stimulate the formation of their 15-lipoxygenase products by human neutrophils *in vitro*. Evidence of formation of antiinflammatory compounds. *Agents Actions.* (1991) 33:286–91. doi: 10.1007/BF01986575

51. Iversen L, Fogh K, Kragballe K. Effect of dihomogammalinolenic acid and its 15-lipoxygenase metabolite on eicosanoid metabolism by human mononuclear leukocytes in vitro: selective inhibition of the 5-lipoxygenase pathway. *Arch Dermatol Res.* (1992) 284:222–6. doi: 10.1007/BF00375798

52. Bonyek-Silva I, Machado AFA, Cerqueira-Silva T, Nunes S, Silva Cruz MR, Silva J, et al. LTB4-driven inflammation and increased expression of ALOX5/ACE2 during severe COVID-19 in individuals with diabetes. *Diabetes.* (2021) 70:2120–30. doi: 10.2337/db20-1260

53. Baker EJ, Valenzuela CA, van Dooremalen WTM, Martínez-Fernández L, Yaqoob P, Miles EA, et al. gamma-linolenic and pinolenic acids exert anti-inflammatory effects in cultured human endothelial cells through their elongation products. *Mol Nutr Food Res.* (2020) 64:2000382. doi: 10.1002/mnfr.202000382

54. Nguyen M, Bourredjem A, Piroth L, Bouhemad B, Jalil A, Pallot G, et al. High plasma concentration of non-esterified polyunsaturated fatty acids is a specific feature of severe COVID-19 pneumonia. *Sci Rep.* (2021) 11:10824. doi: 10.1038/s41598-021-90362-9

55. Lee Y, Lai HTM, de Oliveira Otto MC, Lemaitre RN, McKnight B, King IB, et al. Serial biomarkers of de novo lipogenesis fatty acids and incident heart failure in older adults: the cardiovascular health study. *J Am Heart Assoc.* (2020) 9:e014119. doi: 10.1161/JAHA.119.014119

56. Goyens PLL, Spilker ME, Zock PL, Katan MB, Mensink RP. Compartmental modeling to quantify alpha-linolenic acid conversion after longer term intake of multiple tracer boluses. *J Lipid Res.* (2005) 46:1474–83. doi: 10.1194/jlr.M400514-JLR200

57. Swanson D, Block R, Mousa SA. Omega-3 fatty acids EPA and DHA: health benefits throughout life1. *Adv Nutr.* (2012) 3:1–7. doi: 10.3945/an.111.000893

frontiers | Frontiers in Nutrition

TYPE General Commentary
PUBLISHED 02 November 2022
DOI 10.3389/fnut.2022.1042324

OPEN ACCESS

EDITED BY
Nada Rotovnik Kozjek,
Institute of Oncology
Ljubljana, Slovenia

REVIEWED BY
William B. Grant,
Sunlight Nutrition and Health Research Center, United States

*CORRESPONDENCE
Tianjiao Zhang
tjzhang@nccl.org.cn
Chuanbao Zhang
cbzhang@nccl.org.cn

SPECIALTY SECTION
This article was submitted to Clinical Nutrition, a section of the journal Frontiers in Nutrition

RECEIVED 12 September 2022
ACCEPTED 20 October 2022
PUBLISHED 02 November 2022

CITATION
Zhang L, Zhang T and Zhang C (2022) Commentary: Adequate 25(OH)D moderates the relationship between dietary inflammatory potential and cardiovascular health risk during the second trimester of pregnancy. *Front. Nutr.* 9:1042324. doi: 10.3389/fnut.2022.1042324

Commentary: Adequate 25(OH)D moderates the relationship between dietary inflammatory potential and cardiovascular health risk during the second trimester of pregnancy

Li Zhang[1,2], Tianjiao Zhang[1]* and Chuanbao Zhang[1]*

[1]National Center for Clinical Laboratories, Institute of Geriatric Medicine, Beijing Hospital/National Center of Gerontology, Beijing Engineering Research Center of Laboratory Medicine, Chinese Academy of Medical Sciences, Beijing, China, [2]Department of Biochemistry, National Center for Clinical Laboratories, Peking Union Medical College, Chinese Academy of Medical Sciences, Beijing, China

KEYWORDS

25-hydroxyvitamin D, pregnancy, liquid chromatography tandem mass spectrometry, immunoassays, vitamin D binding protein

A Commentary on

Adequate 25(OH)D moderates the relationship between dietary inflammatory potential and cardiovascular health risk during the second trimester of pregnancy

by Yin, W. J., Yu, L. J., Wu, L., Zhang, L., Li, Q., Dai, F. C., et al. (2022). Front. Nutr. 9:952652.doi: 10.3389/fnut.2022.952652

Introduction

The commentary aims to provide a constructive critique on the chosen method for 25(OH)D measurement in the important and innovative study (1). As described, one of the objectives of this study is to investigate if vitamin D status modifies the association of pro-inflammatory diets with the cardiovascular risk among pregnant women. To assess vitamin D nutritional status for pregnant women at 16–23 gestational weeks, 25(OH)D concentrations in their blood samples were determined by commercial chemiluminescence immunoassay kits (DiaSorin Stillwater, MN, United States). The problem with the chosen 25(OH)D immunoassay is that, changes in sample matrix associated with pregnancy can have a significant impact on the accuracy of 25(OH)D immunoassays, including the DiaSorin assay used in this study (2–5). Inaccurate measurement results may have negative impact on the generation of study results.

Evidence and interpretation

Circulating 25(OH)D is measured commonly using liquid chromatography tandem mass spectrometry (LC-MS/MS) or immunoassays (2). As 25(OH)D is transported by vitamin D binding protein (VDBP) in bloodstream, it needs to be dissociated from VDBP before testing (2, 6). Unlike LC-MS/MS methods that use strong chemical solvents to extract 25(OH)D, immunoassays have been speculated to fail to release 25(OH)D completely when the concentrations of VDBP increase (5). During pregnancy, VDBP concentrations are increased by estrogen (2, 5). As a result, incomplete dissociation of 25(OH)D by immunoassays may occur, resulting in the under-recovery of 25(OH)D. As shown in Heijboer's (5) study, there was an inverse relationship between VDBP concentrations and deviations of 25(OH)D concentrations from LC-MS/MS results for immunoassays, including Diasorin assay. Cavalier et al. (4) showed that the DiaSorin assay underestimated 25(OH)D levels in pregnant women considerably. Specifically, the mean bias was $\sim -44\%$ for the DiaSorin assay, when serum samples from pregnant women were tested. The large negative bias means that a pregnant woman with 25(OH)D levels of 50 nmol/L may have a measured result of 28 nmol/L by the DiaSorin assay, and she will be misclassified to the group with 25(OH)D $<$ 50 nmol/L. Conceivably, a portion of pregnant women in the study by Yin et al. have been misclassified based on the test results by the Diasorin assay, so in fact, the 25(OH)D $<$ 50 nmol/L group also included pregnant women with 25(OH)D $\geq$ 50 nmol/L, and the unsuccessful stratification according to 25(OH)D concentrations may have negative impact on the final statistical results.

This study also found that the mean concentration for all pregnant women (16–23 gestational weeks) was about 38 nmol/L, and only 21.6% had adequate vitamin D levels, i.e., 25(OH)D concentrations $\geq$50 nmol/L (1). However, more than half of pregnant women in this study have a vitamin D supplementation frequency of $\geq$3 days/week. Since it has been demonstrated that supplementing VD $>$ 3 times/week reduces the risk of Vitamin D deficiency during pregnancy significantly (7), it seems unreasonable that the cohort in this study still have a high prevalence (78.4%) of vitamin D deficiency. Furthermore, the prevalence (78.4%) is much higher than that (33.56%) reported by Shen et al. for the second trimester pregnant women using LC-MS/MS. As both cohorts in studies by Shen et al. and Yin et al. were from southeastern China, we can speculate that it's the immunoassay-related underestimation of 25(OH)D that causes the apparent discrepancy in the prevalence of vitamin D deficiency in pregnancy.

Discussion

Researchers should pay more attention to the immunoassay-related underestimation of 25(OH)D in samples from pregnant women, as it will lead to unreliable study results and poor comparability of studies. At present, standardized LC-MS/MS method can avoid analytical problems observed in immunoassays and serve as the gold standard for 25(OH)D measurement. Therefore, when conducting studies involving 25(OH)D determination in pregnant women, standardized LC-MS/MS method should be considered as the first choice.

Author contributions

LZ wrote the manuscript. TZ and CZ were the guarantors of this work and revised the manuscript. All authors read and approved the final manuscript.

Conflict of interest

The authors declare that the research was conducted in the absence of any commercial or financial relationships that could be construed as a potential conflict of interest.

Publisher's note

References

1. Yin WJ Yu LJ, Wu L, Zhang L, Li Q, Dai FC, et al. Adequate 25(OH)D moderates the relationship between dietary inflammatory potential and cardiovascular health risk during the second trimester of pregnancy. *Front Nutr.* (2022) 9:952652. doi: 10.3389/fnut.2022.952652

2. Makris K, Bhattoa HP, Cavalier E, Phinney K, Sempos CT, Ulmer CZ, et al. Recommendations on the measurement and the clinical use of vitamin D metabolites and vitamin D binding protein—a position paper from the IFCC Committee on bone metabolism. *Clin Chim Acta.* (2021) 517:171–97. doi: 10.1016/j.cca.2021.03.002

3. Cavalier E, Lukas P, Bekaert AC, Peeters S, Le Goff C, Yayo E, et al. Analytical and clinical evaluation of the new Fujirebio Lumipulse®G non-competitive assay for 25(OH)-vitamin D and three immunoassays for 25(OH)D in healthy subjects, osteoporotic patients, third trimester pregnant women, healthy African subjects, hemodialyzed and intensive care patients. *Clin Chem Lab Med.* (2016) 54:1347–55. doi: 10.1515/cclm-2015-0923

4. Cavalier E, Lukas P, Crine Y, Peeters S, Carlisi A, Le Goff C, et al. Evaluation of automated immunoassays for 25(OH)-vitamin D determination in different critical populations before and after standardization of the assays. *Clin Chim Acta.* (2014) 431:60–5. doi: 10.1016/j.cca.2014.01.026

5. Heijboer AC, Blankenstein MA, Kema IP, Buijs MM. Accuracy of 6 routine 25-hydroxyvitamin D assays: influence of vitamin D binding protein concentration. *Clin Chem.* (2012) 58:543–8. doi: 10.1373/clinchem.2011.176545

6. Farrell CJ, Soldo J, McWhinney B, Bandodkar S, Herrmann M. Impact of assay design on test performance: lessons learned from 25-hydroxyvitamin D. *Clin Chem Lab Med.* (2014) 52:1579–87. doi: 10.1515/cclm-2014-0111

7. Shen Y, Pu L, Si S, Xin X, Mo M, Shao B, et al. Vitamin D nutrient status during pregnancy and its influencing factors. *Clin Nutr (Edinburgh, Scotland).* (2020) 39:1432–9. doi: 10.1016/j.clnu.2019.06.002

frontiers | Frontiers in Immunology

TYPE Review
PUBLISHED 18 November 2022
DOI 10.3389/fimmu.2022.968582

OPEN ACCESS

EDITED BY
Subash Babu,
International Centers for Excellence in Research (ICER), India

REVIEWED BY
Laura Rivino,
University of Bristol, United Kingdom
Carolyn Gould,
Centers for Disease Control and Prevention (CDC), United States

*CORRESPONDENCE
Muddassar Hameed
muddassarh@vt.edu
James Weger-Lucarelli
weger@vt.edu

SPECIALTY SECTION
This article was submitted to Viral Immunology, a section of the journal Frontiers in Immunology

RECEIVED 14 June 2022
ACCEPTED 04 November 2022
PUBLISHED 18 November 2022

CITATION
Hameed M, Geerling E, Pinto AK, Miraj I and Weger-Lucarelli J (2022) Immune response to arbovirus infection in obesity.
Front. Immunol. 13:968582.
doi: 10.3389/fimmu.2022.968582

Immune response to arbovirus infection in obesity

Muddassar Hameed[1*], Elizabeth Geerling[2], Amelia K. Pinto[2], Iqra Miraj[3] and James Weger-Lucarelli[1*]

[1]Department of Biomedical Sciences and Pathobiology, VA-MD Regional College of Veterinary Medicine, Virginia Tech, Blacksburg, VA, United States, [2]Department of Molecular Microbiology and Immunology, Saint Louis University, St. Louis, MO, United States, [3]College of Biosystems Engineering and Food Science, Zhejiang University, Hangzhou, China

Obesity is a global health problem that affects 650 million people worldwide and leads to diverse changes in host immunity. Individuals with obesity experience an increase in the size and the number of adipocytes, which function as an endocrine organ and release various adipocytokines such as leptin and adiponectin that exert wide ranging effects on other cells. In individuals with obesity, macrophages account for up to 40% of adipose tissue (AT) cells, three times more than in adipose tissue (10%) of healthy weight individuals and secrete several cytokines and chemokines such as interleukin (IL)-1β, chemokine C-C ligand (CCL)-2, IL-6, CCL5, and tumor necrosis factor (TNF)-α, leading to the development of inflammation. Overall, obesity-derived cytokines strongly affect immune responses and make patients with obesity more prone to severe symptoms than patients with a healthy weight. Several epidemiological studies reported a strong association between obesity and severe arthropod-borne virus (arbovirus) infections such as dengue virus (DENV), chikungunya virus (CHIKV), West Nile virus (WNV), and Sindbis virus (SINV). Recently, experimental investigations found that DENV, WNV, CHIKV and Mayaro virus (MAYV) infections cause worsened disease outcomes in infected diet induced obese (DIO) mice groups compared to infected healthy-weight animals. The mechanisms leading to higher susceptibility to severe infections in individuals with obesity remain unknown, though a better understanding of the causes will help scientists and clinicians develop host directed therapies to treat severe disease. In this review article, we summarize the effects of obesity on the host immune response in the context of arboviral infections. We have outlined that obesity makes the host more susceptible to infectious agents, likely by disrupting the functions of innate and adaptive immune cells. We have also discussed the immune response of DIO mouse models against some important arboviruses such as CHIKV, MAYV, DENV, and WNV. We can speculate that obesity-induced disruption of innate and adaptive immune cell function in arboviral infections ultimately affects the course of arboviral disease. Therefore, further studies are needed to explore

the cellular and molecular aspects of immunity that are compromised in obesity during arboviral infections or vaccination, which will be helpful in developing specific therapeutic/prophylactic interventions to prevent immunopathology and disease progression in individuals with obesity.

KEYWORDS

obesity, arboviruses, adipocytes, cytokines, interferons

Introduction

Obesity is defined as an excessive accumulation of body mass or an increased mass of adipose tissue beyond the body's requirement (1). According to a 2016 survey by WHO, 1.9 billion adults are overweight and the number of people with obesity has tripled since 1975 (2). Importantly, obesity is spreading rapidly worldwide due to numerous obesity-promoting factors such as physical inactivity, high caloric foods and drinks, and changing lifestyle habits due to internet use, smartphones, video games, etc. (3). This high prevalence increases the incidence of metabolic and cardiovascular diseases common in people with obesity such as type 2 diabetes mellitus, osteoarthritis, and hypertension (1, 4). It is thought that excessive adipose tissue contributes to increased incidence of associated diseases by promoting a chronic inflammatory state (5–7).

In addition to metabolic impacts, obesity has been identified as an independent risk factor for severe viral diseases such as influenza and coronavirus disease 2019 (COVID-19) (8–12). Epidemiologic data from the COVID-19 pandemic in the United States showed that individuals with higher body mass index (BMI ≥30-35 kg/m^2) were more likely to be admitted to the intensive care unit compared with individuals with a BMI of <30 (13, 14). Several studies from different part of world such as Singapore, France, England and China reports that the COVID-19 produces severe signs and symptoms in individuals with obesity compared to lean people and was also associated with a higher risk of COVID-19-associated death (15–18). A similar pattern was observed during the 2009 H1N1 influenza pandemic, in which obesity was first reported as an important comorbidity for increased disease severity and deaths (12, 19). Obese people with history of respiratory diseases becomes more susceptible to influenza and COVID-19, which is not same for arboviruses. The role of obesity in susceptibility to arbovirus diseases should take a note of caution.

There are very few data on the impact of obesity on arbovirus infections. Arboviruses cause significant disease each year; dengue virus, for example, is endemic in 129 countries and causes 390 million infections per year (20, 21), ZIKV caused more than 220,000 confirmed cases in 52 countries or territories in the America (22, 23), and CHIKV and WNV have spread to a number of countries, resulting in millions of cases (24–30). Several seroprevalence studies have found a strong association between obesity and previous arbovirus infections. In Madagascar, seroprevalence of antibodies to DENV, CHIKV, and Rift Valley fever virus (RVFV) was studied. This showed that CHIKV infection was significantly associated with higher body weight (31). Similar data were reported from La Réunion and India for CHIKV infections, where individuals who were overweight or obese had a higher risk of disease compared to the healthy population (32, 33). In addition, obesity has also been associated with higher seropositivity for DENV in Thailand (34), Sindbis virus (SINV) in Sweden (35), and Toscana virus (family *Phenuiviridae*) and Sicilian phlebovirus (family *Phenuiviridae*) in Italy (36). It is reported that obesity contributes to increase disease severity by promoting a chronic inflammatory state (5–7). It has also been reported that arboviral infection (DENV) is higher in obese people because Adenosine Monophosphate (AMP)-Activated Protein Kinase (AMPK) is down regulated in obesity which is a major regulator of cellular energy homeostasis (37, 38). Arboviruses downregulates AMPK activity to prevent lipid metabolism and increase lipid quantities available to form the lipid envelope during viral replication (38, 39). Obese individuals already have a low AMPK activity, which is further downregulated by viral infection in order boost ER cholesterol levels thus facilitating viral replication that could lead to more severe disease. In addition, the development of severe infections may be due to impaired CD8+T and natural killer (NK) cell activity in obese hosts (40–42). Efforts are continued for the development of host directed effective therapeutics such as the use of metformin in overweight and obese young dengue patients to monitor its effects on viral replication, endothelial dysfunction, and host immune responses (43). Recently, several laboratory studies report that DENV, WNV, and CHIKV (as well as other related alphaviruses) infections cause more severe symptoms in infected obese mice compared with infected healthy weight animals (44–46). In this review article, we describe the immunological impairment against arboviral infections in patients with obesity and discuss the implications on disease severity.

The effect of obesity on immunity

In obesity, more adipose tissue accumulates in the body. There are two main types of adipose tissue, white adipose tissue (WAT), which plays an important role in energy storage, and

brown adipose tissue (BAT), which has an important function in thermogenesis. Adipocytes are the major cell types of adipose tissue and are further subdivided based on their microscopic appearance (47, 48). In WAT, a unilocularly arranged lipid vacuole predominates, whereas in BAT, multilocular lipid vacuoles are present and intermediate cell forms are referred to as beige adipocytes (49). In addition to adipocytes and pre-adipocytes, fibroblasts, endothelial cells, leukocytes, and macrophages are also part of adipose tissue (50). The number of macrophages correlates positively with body mass, adipocyte size, and expression of pro-inflammatory cytokines (51, 52).

In people with obesity, an increase in adipose tissue is characterized by an increase in size (hypertrophy) and the number (hyperplasia) of adipocytes. Adipocyte hypertrophy is accompanied by inadequate vascularization, which creates hypoxic conditions in adipose tissue, induces apoptosis or necrosis, and increases secretion of inflammatory cytokines, chemokines, and adipokines, leading to severe infiltration of immune cells, as shown in Figure 1 (53–58). In parallel with this increase in size of adipocytes, adipose tissue undergoes a remodeling phase with overproduction of extracellular matrix (ECM) and increased infiltration of immune cells (59, 60). The interaction between adipocytes and macrophages and the metabolic inflammation triggered by macrophages play an important role in the remodeling process (61–64). Scientists have proposed that the most critical step in obesity-related infections is the initiation of macrophage migration into adipose tissue, which could be triggered by adipocyte death, hypoxic conditions, chemotactic regulation, and fatty acid flux, eventually leading to a state of low-grade chronic inflammation (59, 63, 65). Previous data also suggest the distinction between pathological and healthy adipose tissue development. In pathological expansion, the existing adipocytes increase rapidly, resulting in hypoxia due to decreased blood vessel formation, deposition of ECM, and increased infiltration of more pro-inflammatory M1 type macrophages, whereas, more anti-inflammatory M2 macrophages predominate in normal body weight AT and adequate oxygen supply and normal levels of immune cells and cytokines are maintained (66–68) (Figure 2).

Adipose tissue (AT) also has important endocrine functions and secretes different immune mediators that play a role in immune cell infiltration and disease following infection. These mediators include adipocytokines or adipokines such as leptin, adiponectin, resistin, visfatin and other important immunological factors such as tumor necrosis factor (TNFα), IL-1, IL-6, plasminogen activator inhibitor type I (PAI-I), CCL2, and different complement factors (50, 69–72). The increased level of adipokines such as leptin activates intracellular genes through different signaling pathways such as JAK-STAT, MAPK, PI3K, and AMPK, leading to the production of various intracellular inflammatory cytokines (73–76). In

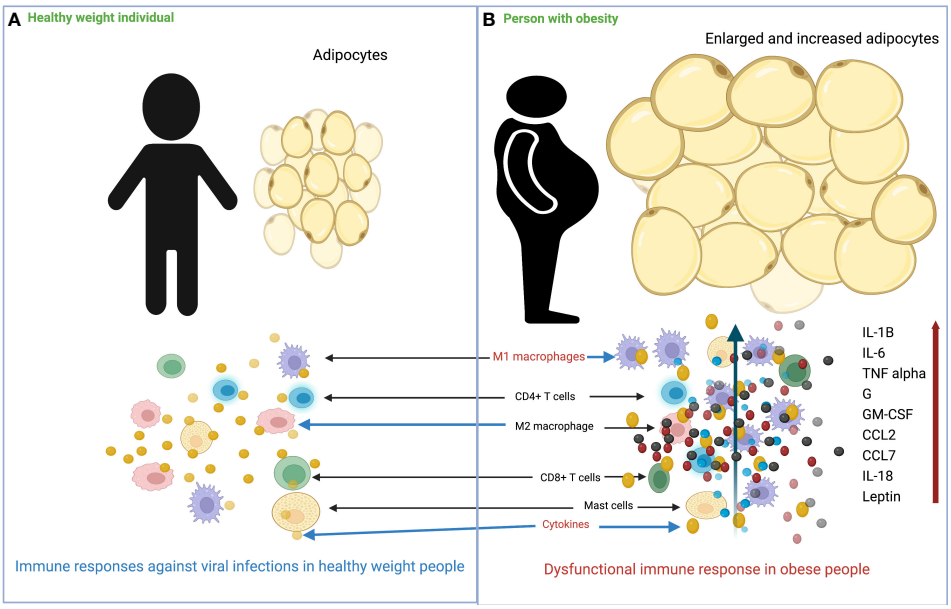

FIGURE 1
Overview of the differences in immune response to viral infection in healthy weight and obese individuals. **(A)** In healthy weight individuals, adipocytes are smaller and less numerous, and the immune system responds normally to viral infection. **(B)** In individuals with obesity, adipocytes increase in size and number, and there is massive infiltration of M1 macrophages into adipose tissue. Following viral infection, the immune system responds with impaired production of various cytokines/chemokines.

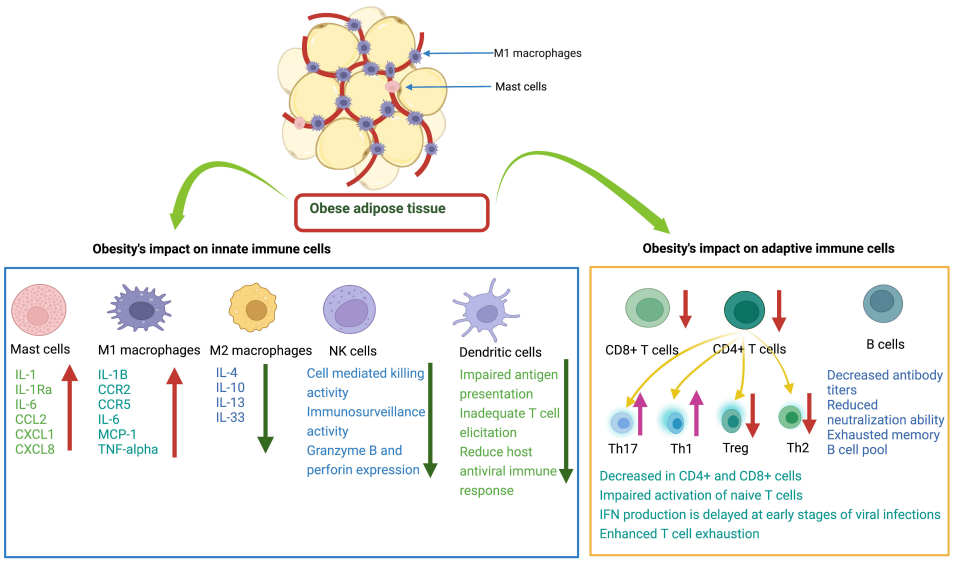

FIGURE 2
Effects of obesity on innate and adaptive immune cells. Mast cells (MCs) release various cytokines and chemokines that promote inflammation. M1 macrophages release proinflammatory mediators. M2 macrophages release anti-inflammatory cytokines. Natural killer cells decrease immune surveillance activity. Dendritic cells have impaired ability to present antigens to other immune cells. CD8+ T cells have decreased cytotoxic activity to kill infected cells. CD4+ T cells: there is a decrease in Treg and Th2 cells and an increase in Th17 and Th1 cells. B cells have decreased antibody production with reduced neutralizing ability.

people of a healthy weight, regulatory anti-inflammatory cells and cytokines such as Treg, Th2 cells and IL-4, IL-5, IL-10, IL-14, IL-33, are maintained to control excessive inflammation (77–79). However, in individuals with obesity, this regulatory, anti-inflammatory state of the immune system transforms into an inflammatory state by secreting various pro-inflammatory cytokines, including IL-1β, IL-6, IL-8, TNFα, and CCL2 (65, 77, 80, 81). These pro-inflammatory cytokines contributes to obesity-induced chronic low-grade inflammation.

Furthermore, obesity is also associated with the senescence of immune cells, which promote the release of pro-inflammatory cytokines (82, 83). Moreover, the role of microRNAs (miRNAs) in obesity has been explored and unmasked as an important biomarker for obesity (84, 85). MiRNAs affect the expression and regulation of many protein-coding genes involved in the regulation of inflammatory processes (86–88). MiRNA-146a, for example, interferes with the activation of nuclear factor kappa B (NF-κB) induced by TNFα and Toll-like receptor ligands (TLR), while miRNA-155 promotes the activation of LPS/TNF pathways (88–90). In conclusion, the excess adipose tissue in obesity activates intracellular signaling pathways, leading to the production of pro-inflammatory cytokines, and promotes the infiltration of more M1 phenotype pro-inflammatory macrophages. Overall, this section highlights the cellular and molecular differences in immune and inflammatory mediators between individuals with obesity or of healthy weight.

The influence of obesity on the generation of immune responses after viral infection

After viral infection, the host activates innate and adaptive immune cells to generate an antiviral immune response against the invading pathogen. In people with obesity, excessive fat deposition in immune tissues such as the spleen, thymus, lymph nodes, and bone marrow alters the cellular environment and disrupts the integrity of tissue, impairing proper development and maturation, diversity, phenotype, and activity of immune cells (91–93). This abnormal development of immune cells leads to impaired interferon and cytokine production, which impairs host antiviral immunity and increases the risk of severe viral disease in patients with obesity (91, 94).

Previously, O'Shea et al. investigated the characteristics of dendritic cells (DCs) in obesity and found that the number of circulating DCs decreased significantly in individuals with obesity and their abnormal function was characterized by decreased expression of CD83 after TLR stimulation compared to the control group (95). CD83 plays a critical role in triggering T cell responses, and its decreased expression leads to a weakened host antiviral immune response and increased severity of viral infections in patients with obesity (95–97). Experimental data show that DCs in DIO mice have a blunted ability to trigger the expansion of naïve T cells due to higher

levels of cytokines and chemokines such as IL-1α, IL-17, and TNFα (98, 99). During influenza virus infection, DCs from patients with obesity showed impaired antigen presentation and insufficient competence in directing antiviral orchestration of T cells (100, 101). This abnormal state was associated with increased pro-inflammatory cytokine levels in the lungs of DIO mice, particularly the IL-6 associated proinflammatory state that impairs the number and frequency of CD4+ and CD8+ T cells in the lungs. Furthermore, obesity has also been reported to impair the migration of DCs to the lymph nodes (102).

Studies have shown that humans or animals with obesity have functionally impaired NK cells, which increase the risk of cancer and viral infections (103–107). With the development of obesity, specific lipid uptake receptors expression is increased in NK cells which results in increase uptake of free fatty acids and activated NK cells fail to activate mTOR and glycolytic metabolism resulting in decrease IFN- γ production which is reviewed in detail previously (108). Veil and colleagues experiment data reveals the increased expression of activation markers such as CD69 on NK cells from obese patients which result in altered degranulation and reduced production of IFN- γ (107). Nave et al., observed that leptin treatment stimulated NK activity four times higher in lean than obese animals (41). The activation of post receptor signaling components (Janus kinase-2p, protein kinase B pT308, AMPalphapT172) was reduced after an *in vivo* leptin challenge in obese animals (41). Recently, it is reported that impaired NK cell function, and polymorphisms in NK cell cytolytic function genes are associated with hyperinflammation which enhances dengue severity (109). Collectively, these findings provide evidence obesity induced disturbance in NK cells function can lead to severe arboviruses diseases in obese patients which remains unknown.

There are currently limited data on the response of interferons/cytokines to arbovirus infection in obese humans/animals. It has been reported that humans with obesity do not elicit a robust type I IFN response in viral infections such as H1N1 influenza virus infection (110–112). Cabanillas et al. demonstrated that obese mice infected with H1N1 virus had significantly lower levels of IFN-α and IFN-β compared with the control group, and viral load and mortality were also higher (111). Obese H1N1 patients were also found to have decreased IFN-α production, which could be related to leptin levels, leading to dysregulated development of immune cells and their shift toward inflammatory phenotypes (42, 113). Leptin is chronically produced by AT in individuals with obesity and interferes with IFN signaling by increasing Suppressor of Cytokine Signaling 3 (SOCS3) (114). SOCS3 negatively regulates the JAK-STAT signaling pathway and limits IFN production by downregulating interferon stimulated gene (ISG) transcription in individuals with obesity (113, 115). Costanzo et al. reported that IFN-γ production was decreased in individuals with obesity infected with influenza A virus, which was due to dysfunctional γδT cells (116). In addition to the abnormal number of γδT cells during influenza virus infection in individuals with obesity, the surviving cells also become unresponsive to TLR ligands, further contributing to the IFN deficiency (116). This IFN deficiency could block the IFN signal transduction cascade. A comparative study of cytokine production after influenza virus infection revealed that the production of cytokines such as IL-6, TNF-α, IL-1β, and CCL-2 was delayed and decreased in the early stages of infection in obese subjects (103, 111, 117). This delayed immune response leads to low-grade chronic inflammation (112). However, in the later stages of infection, excessive cytokine secretion in obese subjects leads to cytokine storm (103, 117, 118). Thus, obesity-induced chronic inflammation and deregulated immune response lead to impaired clearance of viral particles in the early stage of infection.

The release of inflammatory mediators from adipose tissue is obesity such as leptin, adiponectin, resistin, visfatin and other important immunological factors such as tumor necrosis factor (TNFα), IL-1, IL-6, plasminogen activator inhibitor type I (PAI-I), CCL2, and different complement factors produce obesity-induced chronic inflammation (50, 69–72). This chronic inflammation leads to the T cells exhaustion through different ways. First, T cells from humans and animals with obesity exhibit decreased proliferative capacity and increased exhaustion, as evidenced by downregulated Ki67 and upregulated PD-1 (119). The higher leptin levels in obesity lead to the upregulation of phosphorylated STAT3, which induces PD-1 expression in T cells. This is also demonstrated by decreased IFN-γ and TNFα production in stimulated polyclonal T cells from individuals with obesity (119). Second, increase in glucose, FFAs, phospholipids, cholesterol, and other metabolites in individuals with obesity alters the metabolism of T cells, leading to impaired activation and decreased activity (118, 120, 121). Moreover, IFN production is delayed in the early stages of viral infections in obesity, and this delayed IFN production inhibits T cell proliferation, blocks their efflux from lymphoid organs, and leads to T cell exhaustion (122–124). The disruption of the antiviral immune response could increase cell apoptosis and impair normal T cell activation and proliferation during viral infections. Several studies have shown that patients with obesity infected with influenza or COVID-19 who become severely ill lack an effective antiviral T cell response (125–127).

The immune system of patients with obesity is also inherently weakened due to immune senescence (82, 83). The development of obesity induces oxidative stress and inflammation, which shortens telomere length and leads to cellular aging (128, 129). In adiposity, leptin levels increase in serum which also cause the telomere shortening (130, 131). Epigenetic studies reveal that obesity induces a widespread gene expression and methylation changes in multiple tissues of body including blood leukocyte DNA, which can cause immune dysfunction (132–134). It has been reported that senescent

cells expressing SA β-gal activity and p53 levels increase in obese animals (135, 136). It was seen that depletion of senescent cells from obese animals can ameliorate pathology (137, 138). In addition to the association between obesity and disease progression due to a reduction in T cells, obesity also promotes thymic degeneration and T cell senescence, which is seen in elderly individuals with obesity and even in children with obesity (139–141). There is epigenetic evidence of hypermethylation of T lymphocyte DNA in humans and animals that exhibit obesity-related T cell senescence (142, 143). Regulatory T cells are found to be important regulatory cells in AT that provide anti-inflammatory signals (99, 144). In an experimental study, Feuerer et al. found that when most Treg cells were removed from AT, pro-inflammatory transcripts were overexpressed compared to the experimental group, suggesting the key anti-inflammatory role of Treg cells (78). γδT cells also produce growth factors, induce maturation of DCs, recruit macrophages, and interact with Treg cells (145). In patients with obesity, the number of γδT cells is decreased, which could lead to an impaired antiviral response and worsening of disease pathology due to their sensitivity to inflammation (116). Impaired T-cell response in obesity caused by a combination of host and viral factors predisposes individuals with obesity to failure of viral control and development of severe disease (Figure 2).

B cells play a critical role in limiting viral replication and dissemination through antibody production. Non-neutralizing antibodies perform essential tasks, often through their constant (Fc) region, in ways like interacting with complement proteins to enhance opsonization or through Fc receptor interactions which mediate antibody-dependent cellular cytotoxicity. Similarly, neutralizing antibodies also serve essential functions in the immune response to pathogens by blocking viral entry into host cells. Previous experiments have shown that in individuals with obesity exposed to H1N1 influenza virus, the titer of virus specific antibodies is reduced, and antibodies primed in the obese state have a weakened neutralization capacity compared to those primed in healthy weight individuals (146, 147). This could be due to several factors, such as greater inflammation, DNA hypermethylation of B cells, and abnormal leptin levels that differentially regulate B cell development, maturation, and activity (142, 143, 148). It has been described that the peripheral B cell pool of individuals with obesity contains a higher proportion of pro-inflammatory late/exhausted memory B subsets and a lower proportion of anti-inflammatory transitional B cells (148, 149). Moreover, functional defects of B cells in individuals with obesity contribute to triggering an acute inflammatory state through the production of pro-inflammatory mediators. It is plausible that obesity leads to severe arbovirus infections by altering the number and function of B cells and the potential interaction with other lymphocytes (follicular T helper cells) by producing a hyperinflammation cascade and an imbalance of adipokines. Overall, the development of obesity may alter the function of innate and adaptive immune cells and weaken the host antiviral immune response to fight viral infections (see Figure 2).

The influence of obesity on the generation of protective immune responses after vaccination

To prevent severe viral diseases, it is best to develop vaccines against them, followed by comprehensive vaccination. Currently, several arbovirus vaccines are available, and some are under development (150–155). The use of vaccines has major implications for the control of these diseases in arbovirus-endemic areas. The live-attenuated vaccine against yellow fever, 17D, is one of the most effective vaccines ever produced. It was found that children with severe protein deficiency had a significantly lower seroconversion rate for 17D (12.5%) than healthy children (83.3%) (156). To date, no study has observed the effects of obesity on the development of protective immune response to arboviral vaccines. However, several investigations report that obesity can decrease the induction of immune response to various viruses and toxins, including influenza, SARS-CoV-2, tick-borne encephalitis virus, hepatitis B virus, and tetanus toxins (147, 157–164).

In the past, obesity has been found to interfere with the induction of an effective protective immune response to influenza virus vaccines (158, 159, 165). When individuals with obesity were vaccinated with an inactivated trivalent influenza vaccine, lower antibody titers were observed in participants with obesity 12 months post vaccination (159). Cellular and humoral immune responses were well maintained in healthy individuals after vaccination, whereas lower influenza virus antibody titers and decreases in CD8+ T-cell activation were observed in individuals with obesity 12 months after vaccination (159). Garner-Spitzer et al. studied the immune response to tick-borne encephalitis (TBE) virus vaccine in obese and healthy-weight and individuals with obesity (164). They observed that adults with obesity had a greater initial increase in TBE-specific antibody titers at day 7 to day 28, followed by a sharp decline 6 months post TBE vaccination that correlated with high BMI and leptin levels. Recently, a non-peer reviewed study from Italy analyzed antibody titer production in a cohort of 248 healthcare workers (158 women, 90 men) after vaccination with the second dose of an mRNA vaccine against COVID-19 (BNT162b2, Pfizer) (163). The results of this study show that the humoral immune response was significantly stronger in individuals without obesity compared to participants who were classified as being overweight or obese ($p<0.0001$) (163). In another investigation, Watanabe et al., investigated the variables associated with serological response following COVID-19 mRNA vaccines and found obesity as one of the most important factors associated with lower antibody

titers (166). These data highlight the impact of obesity on antibody titers, potentially impairing vaccine-conferred protective immune responses to viral vaccines. Based on these studies, individuals with obesity mount antigen-specific antibody responses equivalent to those of individuals of healthy weight at early time points post-vaccination, yet the antibody titers of individuals with obesity rapidly wane around a year post-vaccination. Thus, these insights suggest that altered vaccination schedules or higher vaccine formulation doses could benefit the durability of antibody responses primed in individuals with obesity. In addition, there is a possibility that people with obesity may be at higher risk for break through infections due to the impact of obesity on the priming of immune responses. Because of the continuous increase in arboviral infections worldwide and the rising obesity rates, future studies are needed to monitor the induction of the immune response after vaccination in people with obesity to determine the long-term protective role of arboviral vaccines. In addition, it is necessary to unravel the mechanism behind the poor immune response to vaccines and the development of severe disease in people with obesity to prevent severe cases and develop alternative strategies/therapies for people with obesity.

Arbovirus infection in people with obesity

Obesity has been found to affect the immune response to viral infections such as influenza, SARS-CoV-2, and coxsackievirus (19, 167–171). Several studies have also reported the association between obesity and disease severity in arboviral infections (172). Padmakumar et al. analyzed 1,111 patients with confirmed CHIKV infection and found that disease was more severe in individuals with obesity and was associated with severe inflammatory sequelae (33). Comparative data from clinical trials revealed that CHIKV was associated with more severe polyarthralgia and took longer to improve in diabetic vs. non-diabetic patients (173, 174). In addition, we have infected healthy weight, obese, and malnourished mice with arthritogenic arboviruses from the genus *Alphavirus* (CHIKV, Mayaro virus and Ross River virus) and observed increased morbidity such as footpad swelling and weight loss in obese mice under all conditions (46). Furthermore, higher levels of viremia and RNAemia were seen in obese mice compared to controls 1 day post MAYV infection. However, the group of obese mice had lower levels of both infectious virus and viral RNA 3 days after MAYV infection compared to lean controls. A similar pattern was observed 3 days post CHIKV infection, where the group of obese mice had significantly lower RNAemia compared to lean controls (46). Thus, consistent with the epidemiological data in humans, individuals with obesity have worse disease outcomes during arthritogenic alphavirus infection and may also have altered viral replication kinetics.

Recently, Geerling et al. used an obese mouse model to investigate the influence of obesity on the development WNV disease (45). They found that the group of obese mice had a higher mortality rate and increased virus titers in the central nervous system compared to animals in the control group. In addition, they observed that obesity also deregulated the host acute adaptive immune responses, as obese female mice exhibited significant disruption of neutralizing antibody function (45). Thus, obesity may promote altered viral pathogenesis and decreased neutralizing capacity of antibodies.

Several studies also reported that patients with obesity with DENV infections were more likely to develop severe symptoms compared with DENV patients without obesity (34, 175, 176). Chuong et al. investigated the influence of nutritional status on DENV replication, immune protection, transmission, and disease severity in obese mice (44). They observed that severe DENV disease in obese mice was associated with high levels of proinflammatory cytokines. The obese mice had increased circulating levels of B-cell activating factor (BAFF), CCL5, CCL17, Chitinase-3-like 1, CXCL5, and IFN-α after DENV infection compared to animals in the control group. These cytokine imbalances might contribute to increase disease severity in patients with obesity by inducing vascular leakage and reduced platelet levels (177–180). Overall, these studies provide evidence that obesity significantly alters host immunity to arboviral infections, which likely contributes to increased disease severity.

In Figure 3, we illustrate the general immune response of the host to arbovirus infection. When the mosquito inoculates the virus into the human body, DCs and mast cells (MCs) in the epidermis encounter the virus. MCs degranulate and release cytokines (IFN-α and TNFα), chemokines (CCL5, CXCL10 and CXCL12) and proteases that play a critical role in the recruitment of CD8+ T, CD4+ T, NK and NKT cells to the site of infection (181, 182). The DCs, macrophages or monocytes are targets of arbovirus infection and act as antigen-presenting cells and release other cytokines, which in turn activate other innate and adaptive immune cells (183). DCs activated by arboviruses present antigens to CD4+ T and CD8+ T cells by upregulating co-stimulatory molecules such as CD80 and CD86 (184). Activated CD4+ T cells release IFN-γ, IL-4, IL-5, IL-10 or IL-12, which activate CD8+ T cells and B cells to clonally expand to produce CD8+ effector/memory and B plasma/memory cells (185). B plasma cells produce virus-specific neutralizing antibodies to prevent virus entry into the cells. Cytotoxic CD8+ T, NK and NKT cells, on the other hand, kill virus-infected cells and promote viral clearance. The development of obesity may disrupt the normal function of innate and adaptive immune cells during arbovirus infection or vaccination. We can speculate that the disruption of innate and adaptive immune cell functions during arbovirus infection or vaccination will ultimately affect the course of arbovirus disease and the induction of protective immune responses following infection or vaccination, which requires further investigation. This highlights the need for

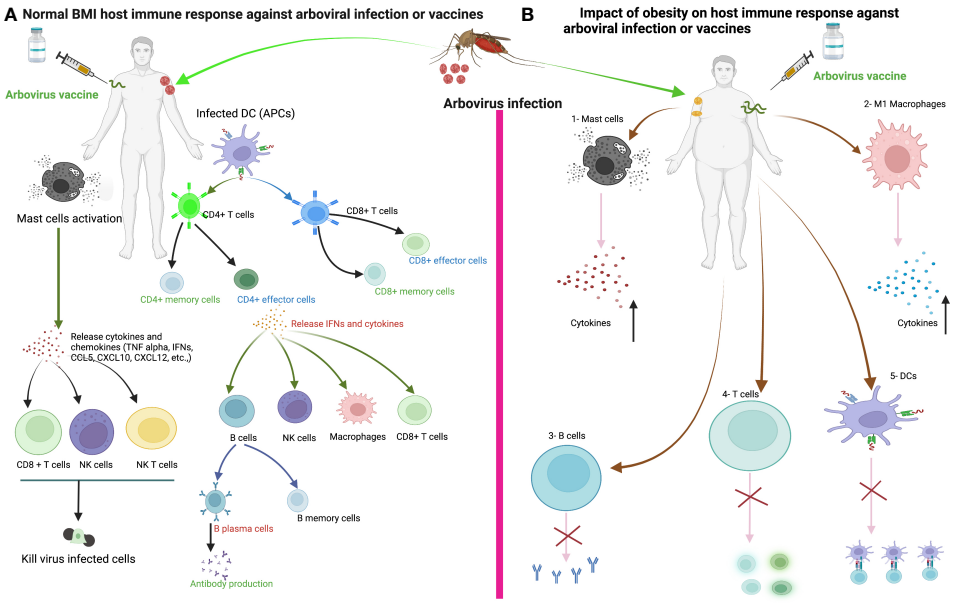

FIGURE 3
The immune response of healthy weight and obese individuals to arbovirus infection or vaccination. **(A)** The immune response of healthy individuals to arbovirus infection or vaccine. Sentinel cells of the immune system, such as dendritic cells, mast cells and macrophages, encounter the virus after infection from a mosquito bite or vaccine injection. Mast cells degranulate within minutes of recognizing the virus and release various cytokines/chemokines that activate other immune cells such as CD8+ T, natural killer (NK), NKT cells and macrophages against the viral infection to promote viral clearance. Dendritic cells or macrophages become infected and present viral antigens to CD4+ and CD8+ T cells to initiate an adaptive immune response. **(B)** We can speculate that the development of obesity disrupts the innate and adaptive immune cells during arboviral infection or vaccination, ultimately affecting the course of arboviral disease and the induction of the host immune response to the vaccine. 1-Increased production of proinflammatory cytokines from Mast cells in obesity. 2- Increase proinflammatory cytokines production from M1 macrophages in obesity. 3-Delayed antibody production. 4-Impaired activation of naïve T cells and Delayed CD4+ and CD8+ T cells response in obesity. 5-Impaired antigen presentation by DC in obesity.

vigilance in the preventive or clinical management of viral infections in patients with obesity.

Future perspectives

Obesity is a key public health problem. Nearly 13% of adults worldwide are obese and 40% are overweight. Obesity-induced chronic inflammation disrupts innate and adaptive immune cell functions, leading to impaired IFN and cytokine production, likely increasing the severity of viral disease. Recent epidemiological and experimental data strongly suggest that obesity is associated with increased disease severity in viral infections such as influenza virus, SARS-CoV-2, DENV, WNV, and CHIKV. The number of cases of arbovirus infections is steadily increasing worldwide. There are limited data on the host antiviral immune response and viral dynamics following arbovirus infection in individuals with obesity, highlighting the need for further studies to elucidate the cellular and molecular aspects of immunity that are compromised in obesity during arboviral infection and how these factors contribute to worsened disease outcomes. In addition, several studies have reported that individuals with obesity produce a poor protective immune response to vaccines or natural infections. Therefore, it is necessary to study the impact of obesity on antigen-specific immunity to ensure this population is protected following vaccination or natural infection. Obesity affects hundreds of millions of people around the world and a better understanding of the associated disorders will help scientists and physicians to develop specific therapeutic/prophylactic interventions to prevent immunopathology and disease progression in at-risk populations.

Author contributions

All authors contributed to the article and approved the submitted version.

Conflict of interest

The authors declare that the research was conducted in the absence of any commercial or financial relationships that could be construed as a potential conflict of interest.

Publisher's note

References

1. Haslam DW, James WP. Obesity. *Lancet (London England)* (2005) 366:1197–209. doi: 10.1016/S0140-6736(05)67483-1

2. Trends in adult body-mass index in 200 countries from 1975 to 2014: A pooled analysis of 1698 population-based measurement studies with 19·2 million participants. *Lancet* (2016) 387:1377–96. doi: 10.1016/S0140-6736(16)30054-X

3. Nicolaidis S. Environment and obesity. *Metabolism: Clin Exp* (2019) 100s:153942. doi: 10.1016/j.metabol.2019.07.006

4. Koenig SM. Pulmonary complications of obesity. *Am J Med Sci* (2001) 321:249–79. doi: 10.1097/00000441-200104000-00006

5. Luft VC, Schmidt MI, Pankow JS, Couper D, Ballantyne CM, Young JH, et al. Chronic inflammation role in the obesity-diabetes association: A case-cohort study. *Diabetol Metab syndrome* (2013) 5:1–8. doi: 10.1186/1758-5996-5-31

6. Divella R, De Luca R, Abbate I, Naglieri E, Daniele A. Obesity and cancer: The role of adipose tissue and adipo-cytokines-induced chronic inflammation. *J Cancer* (2016) 7:2346. doi: 10.7150/jca.16884

7. Monteiro R, Azevedo I. Chronic inflammation in obesity and the metabolic syndrome. *Mediators Inflammation* (2010) 2010:10. doi: 10.1155/2010/289645

8. Jackson-Morris AM, Nugent R, Ralston J, Barata Cavalcante O, Wilding J. Strengthening resistance to the COVID-19 pandemic and fostering future resilience requires concerted action on obesity. *Global Health Action* (2020) 13:1804700. doi: 10.1080/16549716.2020.1804700

9. Noor FM, Islam MM. Prevalence and associated risk factors of mortality among COVID-19 patients: A meta-analysis. *J Community Health* (2020) 45:1270–82. doi: 10.1007/s10900-020-00920-x

10. Honce R, Schultz-Cherry S. Impact of obesity on influenza a virus pathogenesis, immune response, and evolution. *Front Immunol* (2019) 10:1071. doi: 10.3389/fimmu.2019.01071

11. Díaz E, Rodríguez A, Martin-Loeches I, Lorente L, Del Mar Martín M, Pozo JC, et al. Impact of obesity in patients infected with 2009 influenza A(H1N1). *Chest* (2011) 139:382–6. doi: 10.1378/chest.10-1160

12. Moser JS, Galindo-Fraga A, Ortiz-Hernández AA, Gu W, Hunsberger S, Galán-Herrera JF, et al. Underweight, overweight, and obesity as independent risk factors for hospitalization in adults and children from influenza and other respiratory viruses. *Influenza other Respir viruses* (2019) 13:3–9. doi: 10.1111/irv.12618

13. Lighter J, Phillips M, Hochman S, Sterling S, Johnson D, Francois F, et al. Obesity in patients younger than 60 years is a risk factor for COVID-19 hospital admission. *Clin Infect Dis an Off Publ Infect Dis Soc America* (2020) 71:896–7. doi: 10.1093/cid/ciaa415

14. Petrilli CM, Jones SA, Yang J, Rajagopalan H, O'Donnell L, Chernyak Y, et al. Factors associated with hospital admission and critical illness among 5279 people with coronavirus disease 2019 in New York City: Prospective cohort study. *BMJ (Clinical Res ed.)* (2020) 369:m1966. doi: 10.1136/bmj.m1966

15. Ong SWX, Young BE, Leo Y-S, Lye DC. Association of higher body mass index with severe coronavirus disease 2019 (COVID-19) in younger patients. *Clin Infect Dis* (2020) 71:2300–2. doi: 10.1093/cid/ciaa548

16. Simonnet A, Chetboun M, Poissy J, Raverdy V, Noulette J, Duhamel A, et al. High prevalence of obesity in severe acute respiratory syndrome coronavirus-2 (SARS-CoV-2) requiring invasive mechanical ventilation. *Obes (Silver Spring Md.)* (2020) 28:1195–9. doi: 10.1002/oby.22831

17. Peng YD, Meng K, Guan HQ, Leng L, Zhu RR, Wang BY, et al. [Clinical characteristics and outcomes of 112 cardiovascular disease patients infected by 2019-nCoV]. *Zhonghua xin xue guan bing za zhi* (2020) 48:450–5. doi: 10.3760/cma.j.cn112148-20200220-00105

18. Williamson EJ, Walker AJ, Bhaskaran K, Bacon S, Bates C, Morton CE, et al. Factors associated with COVID-19-related death using OpenSAFELY. *Nature* (2020) 584:430–6. doi: 10.1038/s41586-020-2521-4

19. Sun Y, Wang Q, Yang G, Lin C, Zhang Y, Yang P. Weight and prognosis for influenza A(H1N1)pdm09 infection during the pandemic period between 2009 and 2011: A systematic review of observational studies with meta-analysis. *Infect Dis (London England)* (2016) 48:813–22. doi: 10.1080/23744235.2016.1201721

20. Wilder-Smith A, Ooi EE, Horstick O, Wills B. Dengue. *Lancet (London England)* (2019) 393:350–63. doi: 10.1016/S0140-6736(18)32560-1

21. Bhatt S, Gething PW, Brady OJ, Messina JP, Farlow AW, Moyes CL, et al. The global distribution and burden of dengue. *Nature* (2013) 496:504–7. doi: 10.1038/nature12060

22. Pierson TC, Diamond MS. The emergence of zika virus and its new clinical syndromes. *Nature* (2018) 560:573–81. doi: 10.1038/s41586-018-0446-y

23. Bhargavi BS, Moa A. Global outbreaks of zika infection by epidemic observatory (EpiWATCH), 2016-2019. *Global Biosecur* (2020) 2(1). doi: 10.31646/gbio.83

24. Vairo F, Haider N, Kock R, Ntoumi F, Ippolito G, Zumla A. Chikungunya: Epidemiology, pathogenesis, clinical features, management, and prevention. *Infect Dis Clinics North America* (2019) 33:1003–25. doi: 10.1016/j.idc.2019.08.006

25. Yactayo S, Staples JE, Millot V, Cibrelus L, Ramon-Pardo P. Epidemiology of chikungunya in the americas. *J Infect Dis* (2016) 214:S441–s445. doi: 10.1093/infdis/jiw390

26. Nsoesie EO, Kraemer MU, Golding N, Pigott DM, Brady OJ, Moyes CL, et al. Global distribution and environmental suitability for chikungunya virus, 1952 to 2015. *Euro surveillance Bull Europeen sur les maladies transmissibles = Eur communicable Dis Bull* (2016) 21(20):30234. doi: 10.2807/1560-7917.ES.2016.21.20.30234

27. Petersen LR, Carson PJ, Biggerstaff BJ, Custer B, Borchardt SM, Busch MP. Estimated cumulative incidence of West Nile virus infection in US adults, 1999-2010. *Epidemiol infection* (2013) 141:591–5. doi: 10.1017/S0950268812001070

28. Kramer LD, Ciota AT, Kilpatrick AM. Introduction, spread, and establishment of West Nile virus in the Americas. *J Med Entomology* (2019) 56:1448–55. doi: 10.1093/jme/tjz151

29. David S, Abraham AM. Epidemiological and clinical aspects on West Nile virus, a globally emerging pathogen. *Infect Dis* (2016) 48:571–86. doi: 10.3109/23744235.2016.1164890

30. Ronca SE, Ruff JC, Murray KO. A 20-year historical review of West Nile virus since its initial emergence in North America: Has West Nile virus become a neglected tropical disease? *PloS Negl Trop Dis* (2021) 15:e0009190. doi: 10.1371/journal.pntd.0009190

31. Schwarz NG, Girmann M, Randriamampionona N, Bialonski A, Maus D, Krefis AC, et al. Seroprevalence of antibodies against chikungunya, dengue, and rift valley fever viruses after febrile illness outbreak, Madagascar. *Emerging Infect Dis* (2012) 18:1780–6. doi: 10.3201/eid1811.111036

32. Gérardin P, Perrau J, Fianu A, Favier F. Determinants of chikungunya virus in the réunion island: Results of the serochik seroprevalence survey, august-October 2006. *Bull Epidemiol Hebd* (2008) 38:361–3. doi: 10.1186/1471-2334-8-99

33. Padmakumar B, Jayan JB, Menon R, Kottarathara AJ. Clinical profile of chikungunya sequelae, association with obesity and rest during acute phase. *Southeast Asian J Trop Med Public Health* (2010) 41:85–91.

34. Kalayanarooj S, Nimmannitya S. Is dengue severity related to nutritional status. *Southeast Asian J Trop Med Public Health* (2005) 36:378–84.

35. Ahlm C, Eliasson M, Vapalahti O, Evander M. Seroprevalence of sindbis virus and associated risk factors in northern Sweden. *Epidemiol Infection* (2014) 142:1559–65. doi: 10.1017/S0950268813002239

36. Calamusa G, Valenti RM, Vitale F, Mammina C, Romano N, Goedert JJ, et al. Seroprevalence of and risk factors for toscana and Sicilian virus infection in a sample population of Sicily (Italy). *J Infection* (2012) 64:212–7. doi: 10.1016/j.jinf.2011.11.012

37. Jeon SM. Regulation and function of AMPK in physiology and diseases. *Exp Mol Med* (2016) 48:e245. doi: 10.1038/emm.2016.81

38. Soto-Acosta R, Bautista-Carbajal P, Cervantes-Salazar M, Angel-Ambrocio AH, Del Angel RM. DENV up-regulates the HMG-CoA reductase activity through the impairment of AMPK phosphorylation: A potential antiviral target. *PloS Pathog* (2017) 13:e1006257. doi: 10.1371/journal.ppat.1006257

39. Jiménez de Oya N, Blázquez AB, Casas J, Saiz JC, Martín-Acebes MA. Direct activation of adenosine monophosphate-activated protein kinase (AMPK) by PF-

06409577 inhibits flavivirus infection through modification of host cell lipid metabolism. *Antimicrob Agents Chemother* (2018) 62(7):e00360–18. doi: 10.1128/AAC.00360-18

40. Gallagher P, Chan KR, Rivino L, Yacoub S. The association of obesity and severe dengue: Possible pathophysiological mechanisms. *J Infect* (2020) 81:10–6. doi: 10.1016/j.jinf.2020.04.039

41. Nave H, Mueller G, Siegmund B, Jacobs R, Stroh T, Schueler U, et al. Resistance of janus kinase-2 dependent leptin signaling in natural killer (NK) cells: A novel mechanism of NK cell dysfunction in diet-induced obesity. *Endocrinology* (2008) 149:3370–8. doi: 10.1210/en.2007-1516

42. Andersen CJ, Murphy KE, Fernandez ML. Impact of obesity and metabolic syndrome on immunity. *Adv Nutr (Bethesda Md.)* (2016) 7:66–75. doi: 10.3945/an.115.010207

43. Nguyen NM, Chanh HQ, Tam DTH, Vuong NL, Chau NTX, Chau NVV, et al. Metformin as adjunctive therapy for dengue in overweight and obese patients: A protocol for an open-label clinical trial (MeDO). *Wellcome Open Res* (2020) 5:160. doi: 10.12688/wellcomeopenres.16053.1

44. Chuong C, Bates TA, Akter S, Werre SR, LeRoith T, Weger-Lucarelli J. Nutritional status impacts dengue virus infection in mice. *BMC Biol* (2020) 18:106. doi: 10.1186/s12915-020-00828-x

45. Geerling E, Stone ET, Steffen TL, Hassert M, Brien JD, Pinto AK. Obesity enhances disease severity in female mice following West Nile virus infection. *Front Immunol* (2021) 12:739025. doi: 10.3389/fimmu.2021.739025

46. Weger-Lucarelli J, Carrau L, Levi LI, Rezelj V, Vallet T, Blanc H, et al. Host nutritional status affects alphavirus virulence, transmission, and evolution. *PloS Pathog* (2019) 15:e1008089. doi: 10.1371/journal.ppat.1008089

47. Fantuzzi G, tissue A. Adipokines, and inflammation. *J Allergy Clin Immunol* (2005) 115:911–9; quiz 920. doi: 10.1016/j.jaci.2005.02.023

48. Cinti S. White, brown, beige and pink: A rainbow in the adipose organ. *Curr Opin Endocrine Metab Res* (2019) 4:29–36. doi: 10.1016/j.coemr.2018.07.003

49. Boström P, Wu J, Jedrychowski MP, Korde A, Ye L, Lo JC, et al. A PGC1-α-dependent myokine that drives brown-fat-like development of white fat and thermogenesis. *Nature* (2012) 481:463–8. doi: 10.1038/nature10777

50. Tilg H, Moschen AR. Adipocytokines: mediators linking adipose tissue, inflammation and immunity. *Nat Rev Immunol* (2006) 6:772–83. doi: 10.1038/nri1937

51. Weisberg SP, McCann D, Desai M, Rosenbaum M, Leibel RL, Ferrante AWJr. Obesity is associated with macrophage accumulation in adipose tissue. *J Clin Invest* (2003) 112:1796–808. doi: 10.1172/JCI200319246

52. Suganami T, Ogawa Y. Adipose tissue macrophages: their role in adipose tissue remodeling. *J leukocyte Biol* (2010) 88:33–9. doi: 10.1189/jlb.0210072

53. Spencer M, Unal R, Zhu B, Rasouli N, McGehee REJr., Peterson CA, et al. Adipose tissue extracellular matrix and vascular abnormalities in obesity and insulin resistance. *J Clin Endocrinol Metab* (2011) 96:E1990–8. doi: 10.1210/jc.2011-1567

54. Gornicka A, Fettig J, Eguchi A, Berk MP, Thapaliya S, Dixon LJ, et al. Adipocyte hypertrophy is associated with lysosomal permeability both *in vivo* and *in vitro*: Role in adipose tissue inflammation. *Am J Physiology-Endocrinology Metab* (2012) 303:E597–606. doi: 10.1152/ajpendo.00022.2012

55. Revelo XS, Luck H, Winer S, Winer DA. Morphological and inflammatory changes in visceral adipose tissue during obesity. *Endocrine Pathol* (2014) 25:93–101. doi: 10.1007/s12022-013-9288-1

56. Hammarstedt A, Gogg S, Hedjazifar S, Nerstedt A, Smith U. Impaired adipogenesis and dysfunctional adipose tissue in human hypertrophic obesity. *Physiol Rev* (2018) 98:1911–41. doi: 10.1152/physrev.00034.2017

57. Pellegrinelli V, Rouault C, Rodriguez-Cuenca S, Albert V, Edom-Vovard F, Vidal-Puig A, et al. Human adipocytes induce inflammation and atrophy in muscle cells during obesity. *Diabetes* (2015) 64:3121–34. doi: 10.2337/db14-0796

58. Shin SK, Cho HW, Song SE, Im SS, Bae JH, Song DK. Oxidative stress resulting from the removal of endogenous catalase induces obesity by promoting hyperplasia and hypertrophy of white adipocytes. *Redox Biol* (2020) 37:101749. doi: 10.1016/j.redox.2020.101749

59. Sun K, Scherer PE. *Adipose tissue dysfunction: A multistep process, novel insights into adipose cell functions*. Berlin, Heidelberg: Springer (2010) p. 67–75.

60. Henegar C, Tordjman J, Achard V, Lacasa D, Cremer I, Guerre-Millo M, et al. Adipose tissue transcriptomic signature highlights the pathological relevance of extracellular matrix in human obesity. *Genome Biol* (2008) 9:R14. doi: 10.1186/gb-2008-9-1-r14

61. Sun K, Kusminski CM, Scherer PE. Adipose tissue remodeling and obesity. *J Clin Invest* (2011) 121:2094–101. doi: 10.1172/JCI45887

62. Engin AB. Adipocyte-macrophage cross-talk in obesity. *Adv Exp Med Biol* (2017) 960:327–43. doi: 10.1007/978-3-319-48382-5_14

63. Catrysse L, van Loo G. Adipose tissue macrophages and their polarization in health and obesity. *Cell Immunol* (2018) 330:114–9. doi: 10.1016/j.cellimm.2018.03.001

64. Goldstein N, Kezerle Y, Gepner Y, Haim Y, Pecht T, Gazit R, et al. Higher mast cell accumulation in human adipose tissues defines clinically favorable obesity sub-phenotypes. *Cells* (2020) 9:1508. doi: 10.3390/cells9061508

65. Guzik TJ, Skiba DS, Touyz RM, Harrison DG. The role of infiltrating immune cells in dysfunctional adipose tissue. *Cardiovasc Res* (2017) 113:1009–23. doi: 10.1093/cvr/cvx108

66. Lumeng CN, DelProposto JB, Westcott DJ, Saltiel AR. Phenotypic switching of adipose tissue macrophages with obesity is generated by spatiotemporal differences in macrophage subtypes. *Diabetes* (2008) 57:3239–46. doi: 10.2337/db08-0872

67. Liu Y, Lu X, Li X, Du P, Qin G. High-fat diet triggers obesity-related early infiltration of macrophages into adipose tissue and transient reduction of blood monocyte count. *Mol Immunol* (2020) 117:139–46. doi: 10.1016/j.molimm.2019.11.002

68. Zatterale F, Longo M, Naderi J, Raciti GA, Desiderio A, Miele C, et al. Chronic adipose tissue inflammation linking obesity to insulin resistance and type 2 diabetes. *Front Physiol* (2019) 10:1607. doi: 10.3389/fphys.2019.01607

69. Wellen KE, Hotamisligil GS. Inflammation, stress, and diabetes. *J Clin Invest* (2005) 115:1111–9. doi: 10.1172/JCI25102

70. Calle EE, Kaaks R. Overweight, obesity and cancer: Epidemiological evidence and proposed mechanisms. *Nat Rev Cancer* (2004) 4:579–91. doi: 10.1038/nrc1408

71. Wang T, He C. Pro-inflammatory cytokines: The link between obesity and osteoarthritis. *Cytokine Growth factor Rev* (2018) 44:38–50. doi: 10.1016/j.cytogfr.2018.10.002

72. Fain JN. Release of inflammatory mediators by human adipose tissue is enhanced in obesity and primarily by the nonfat cells: A review. *Mediators Inflammation* (2010) 2010:20. doi: 10.1155/2010/513948

73. Lam Q, Lu L. Role of leptin in immunity. *Cell Mol Immunol* (2007) 4:1–13.

74. Naylor C, Petri WAJr. Leptin regulation of immune responses. *Trends Mol Med* (2016) 22:88–98. doi: 10.1016/j.molmed.2015.12.001

75. Ornellas F, Souza-Mello V, Mandarim-de-Lacerda CA, Aguila MB. Combined parental obesity augments single-parent obesity effects on hypothalamus inflammation, leptin signaling (JAK/STAT), hyperphagia, and obesity in the adult mice offspring. *Physiol Behav* (2016) 153:47–55. doi: 10.1016/j.physbeh.2015.10.019

76. Yang R, Barouch LA. Leptin signaling and obesity: Cardiovascular consequences. *Circ Res* (2007) 101:545–59. doi: 10.1161/CIRCRESAHA.107.156596

77. Cătoi AF, Pârvu AE, Andreicuț AD, Mironiuc A, Crăciun A, Cătoi C, et al. Metabolically healthy versus unhealthy morbidly obese: Chronic inflammation, nitro-oxidative stress, and insulin resistance. *Nutrients* (2018) 10:1199. doi: 10.3390/nu10091199

78. Feuerer M, Herrero L, Cipolletta D, Naaz A, Wong J, Nayer A, et al. Lean, but not obese, fat is enriched for a unique population of regulatory T cells that affect metabolic parameters. *Nat Med* (2009) 15:930–9. doi: 10.1038/nm.2002

79. Lynch L, Nowak M, Varghese B, Clark J, Hogan AE, Toxavidis V, et al. Adipose tissue invariant NKT cells protect against diet-induced obesity and metabolic disorder through regulatory cytokine production. *Immunity* (2012) 37:574–87. doi: 10.1016/j.immuni.2012.06.016

80. Pereira S, Teixeira L, Aguilar E, Oliveira M, Savassi-Rocha A, Pelaez JN, et al. Modulation of adipose tissue inflammation by FOXP3+ treg cells, IL-10, and TGF-β in metabolically healthy class III obese individuals. *Nutr (Burbank Los Angeles County Calif.)* (2014) 30:784–90. doi: 10.1016/j.nut.2013.11.023

81. Travers RL, Motta AC, Betts JA, Bouloumié A, Thompson D. The impact of adiposity on adipose tissue-resident lymphocyte activation in humans. *Int J Obes* (2015) 39:762–9. doi: 10.1038/ijo.2014.195

82. Green WD, Beck MA. Obesity altered T cell metabolism and the response to infection. *Curr Opin Immunol* (2017) 46:1–7. doi: 10.1016/j.coi.2017.03.008

83. Pan XX, Yao KL, Yang YF, Ge Q, Zhang R, Gao PJ, et al. Senescent T cell induces brown adipose tissue "Whitening" *via* secreting IFN-γ. *Front Cell Dev Biol* (2021) 9:637424. doi: 10.3389/fcell.2021.637424

84. Landrier JF, Derghal A, Mounien L. MicroRNAs in obesity and related metabolic disorders. *Cells* (2019) 8:859. doi: 10.3390/cells8080859

85. Mori MA, Ludwig RG, Garcia-Martin R, Brandão BB, Kahn CR. Extracellular miRNAs: From biomarkers to mediators of physiology and disease. *Cell Metab* (2019) 30:656–73. doi: 10.1016/j.cmet.2019.07.011

86. Ge Q, Brichard S, Yi X, Li Q. microRNAs as a new mechanism regulating adipose tissue inflammation in obesity and as a novel therapeutic strategy in the metabolic syndrome. *J Immunol Res* (2014) 2014:987285. doi: 10.1155/2014/987285

87. Roos J, Enlund E, Funcke JB, Tews D, Holzmann K, Debatin KM, et al. miR-146a-mediated suppression of the inflammatory response in human adipocytes. *Sci Rep* (2016) 6:38339. doi: 10.1038/srep38339

88. Tili E, Michaille JJ, Cimino A, Costinean S, Dumitru CD, Adair B, et al. Modulation of miR-155 and miR-125b levels following lipopolysaccharide/TNF-alpha stimulation and their possible roles in regulating the response to endotoxin shock. *J Immunol (Baltimore Md.: 1950)* (2007) 179:5082–9. doi: 10.4049/jimmunol.179.8.5082

89. Sonkoly E, Ståhle M, Pivarcsi A. MicroRNAs and immunity: novel players in the regulation of normal immune function and inflammation. *Semin Cancer Biol* (2008) 18:131–40. doi: 10.1016/j.semcancer.2008.01.005

90. Baldeón RL, Weigelt K, de Wit H, Ozcan B, van Oudenaren A, Sempértegui F, et al. Decreased serum level of miR-146a as sign of chronic inflammation in type 2 diabetic patients. *PloS One* (2014) 9:e115209. doi: 10.1371/journal.pone.0115209

91. Kanneganti T-D, Dixit VD. Immunological complications of obesity. *Nat Immunol* (2012) 13:707–12. doi: 10.1038/ni.2343

92. Kinlen D, Cody D, O'Shea D. Complications of obesity. *QJM: Int J Med* (2018) 111:437–43. doi: 10.1093/qjmed/hcx152

93. Apostolopoulos V, De Courten MP, Stojanovska L, Blatch GL, Tangalakis K, De Courten B. The complex immunological and inflammatory network of adipose tissue in obesity. *Mol Nutr Food Res* (2016) 60:43–57. doi: 10.1002/mnfr.201500272

94. Blanco-Melo D, Nilsson-Payant BE, Liu WC, Uhl S, Hoagland D, Møller R, et al. Imbalanced host response to SARS-CoV-2 drives development of COVID-19. *Cell* (2020) 181:1036–1045.e9. doi: 10.1016/j.cell.2020.04.026

95. O'Shea D, Corrigan M, Dunne MR, Jackson R, Woods C, Gaoatswe G, et al. Changes in human dendritic cell number and function in severe obesity may contribute to increased susceptibility to viral infection. *Int J Obes* (2013) 2005) 37:1510–3. doi: 10.1038/ijo.2013.16

96. Lee B-C, Lee J. Cellular and molecular players in adipose tissue inflammation in the development of obesity-induced insulin resistance. *Biochim Biophys Acta (BBA)-Molecular Basis Dis* (2014) 1842:446–62. doi: 10.1016/j.bbadis.2013.05.017

97. Bertola A, Ciucci T, Rousseau D, Bourlier V, Duffaut C, Bonnafous S, et al. Identification of adipose tissue dendritic cells correlated with obesity-associated insulin-resistance and inducing Th17 responses in mice and patients. *Diabetes* (2012) 61:2238–47. doi: 10.2337/db11-1274

98. James BR, Tomanek-Chalkley A, Askeland EJ, Kucaba T, Griffith TS, Norian LA. Diet-induced obesity alters dendritic cell function in the presence and absence of tumor growth. *J Immunol (Baltimore Md. 1950)* (2012) 189:1311–21. doi: 10.4049/jimmunol.1100587

99. Yang H, Youm Y-H, Vandanmagsar B, Ravussin A, Gimble JM, Greenway F, et al. Obesity increases the production of proinflammatory mediators from adipose tissue T cells and compromises TCR repertoire diversity: Implications for systemic inflammation and insulin resistance. *J Immunol* (2010) 185:1836–45. doi: 10.4049/jimmunol.1000021

100. Macia L, Delacre M, Abboud G, Ouk TS, Delanoye A, Verwaerde C, et al. Impairment of dendritic cell functionality and steady-state number in obese mice. *J Immunol (Baltimore Md. 1950)* (2006) 177:5997–6006. doi: 10.4049/jimmunol.177.9.5997

101. Smith AG, Sheridan PA, Tseng RJ, Sheridan JF, Beck MA. Selective impairment in dendritic cell function and altered antigen-specific CD8+ T-cell responses in diet-induced obese mice infected with influenza virus. *Immunology* (2009) 126:268–79. doi: 10.1111/j.1365-2567.2008.02895.x

102. Weitman ES, Aschen SZ, Farias-Eisner G, Albano N, Cuzzone DA, Ghanta S, et al. Obesity impairs lymphatic fluid transport and dendritic cell migration to lymph nodes. *PloS One* (2013) 8:e70703. doi: 10.1371/journal.pone.0070703

103. Smith AG, Sheridan PA, Harp JB, Beck MA. Diet-induced obese mice have increased mortality and altered immune responses when infected with influenza virus. *J Nutr* (2007) 137:1236–43. doi: 10.1093/jn/137.5.1236

104. Michelet X, Dyck L, Hogan A, Loftus RM, Duquette D, Wei K, et al. Metabolic reprogramming of natural killer cells in obesity limits antitumor responses. *Nat Immunol* (2018) 19:1330–40. doi: 10.1038/s41590-018-0251-7

105. Jung YS, Park JH, Park DI, Sohn CI, Lee JM, Kim TI. Physical inactivity and unhealthy metabolic status are associated with decreased natural killer cell activity. *Yonsei Med J* (2018) 59:554–62. doi: 10.3349/ymj.2018.59.4.554

106. Tobin LM, Mavinkurve M, Carolan E, Kinlen D, O'Brien EC, Little MA, et al. NK cells in childhood obesity are activated, metabolically stressed, and functionally deficient. *JCI Insight* (2017) 2. doi: 10.1172/jci.insight.94939

107. Viel S, Besson L, Charrier E, Marçais A, Disse E, Bienvenu J, et al. Alteration of natural killer cell phenotype and function in obese individuals. *Clin Immunol* (2017) 177:12–7. doi: 10.1016/j.clim.2016.01.007

108. O'Shea D, Hogan AE. Dysregulation of natural killer cells in obesity. *Cancers (Basel)* (2019) 11:12–17. doi: 10.3390/cancers11040573

109. Vuong NL, Cheung K-W, Periaswamy B, Vi TT, Duyen HTL, Leong YS, et al. Hyperinflammatory syndrome, natural killer cell function, and genetic polymorphisms in the pathogenesis of severe dengue. *J Infect Dis* (2022) 226:1338–47. doi: 10.1093/infdis/jiac093

110. Namkoong H, Ishii M, Fujii H, Asami T, Yagi K, Suzuki S, et al. Obesity worsens the outcome of influenza virus infection associated with impaired type I interferon induction in mice. *Biochem Biophys Res Commun* (2019) 513:405–11. doi: 10.1016/j.bbrc.2019.03.211

111. Terán-Cabanillas E, Montalvo-Corral M, Silva-Campa E, Caire-Juvera G, Moya-Camarena SY, Hernández J. Production of interferon α and β, pro-inflammatory cytokines and the expression of suppressor of cytokine signaling (SOCS) in obese subjects infected with influenza A/H1N1. *Clin Nutr (Edinburgh Scotland)* (2014) 33:922–6. doi: 10.1016/j.clnu.2013.10.011

112. Green WD, Beck MA. Obesity impairs the adaptive immune response to influenza virus. *Ann Am Thorac Soc* (2017) 14:S406–s409. doi: 10.1513/AnnalsATS.201706-447AW

113. Terán-Cabanillas E, Hernández J. Role of leptin and SOCS3 in inhibiting the type I interferon response during obesity. *Inflammation* (2017) 40:58–67. doi: 10.1007/s10753-016-0452-x

114. Rebello CJ, Kirwan JP, Greenway FL. Obesity, the most common comorbidity in SARS-CoV-2: Is leptin the link? *Int J Obes* (2020) 44:1810–7. doi: 10.1038/s41366-020-0640-5

115. Almond MH, Edwards MR, Barclay WS, Johnston SL. Obesity and susceptibility to severe outcomes following respiratory viral infection. *Thorax* (2013) 68:684–6. doi: 10.1136/thoraxjnl-2012-203009

116. Costanzo AE, Taylor KR, Dutt S, Han PP, Fujioka K, Jameson JM. Obesity impairs γδ T cell homeostasis and antiviral function in humans. *PloS One* (2015) 10:e0120918. doi: 10.1371/journal.pone.0120918

117. Zhang AJ, To KK, Li C, Lau CC, Poon VK, Chan CC, et al. Leptin mediates the pathogenesis of severe 2009 pandemic influenza A(H1N1) infection associated with cytokine dysregulation in mice with diet-induced obesity. *J Infect Dis* (2013) 207:1270–80. doi: 10.1093/infdis/jit031

118. Milner JJ, Rebeles J, Dhungana S, Stewart DA, Sumner SC, Meyers MH, et al. Obesity increases mortality and modulates the lung metabolome during pandemic H1N1 influenza virus infection in mice. *J Immunol (Baltimore Md. 1950)* (2015) 194:4846–59. doi: 10.4049/jimmunol.1402295

119. Wang Z, Aguilar EG, Luna JI, Dunai C, Khuat LT, Le CT, et al. Paradoxical effects of obesity on T cell function during tumor progression and PD-1 checkpoint blockade. *Nat Med* (2019) 25:141–51. doi: 10.1038/s41591-018-0221-5

120. Mauro C, Smith J, Cucchi D, Coe D, Fu H, Bonacina F, et al. Obesity-induced metabolic stress leads to biased effector memory CD4(+) T cell differentiation *via* PI3K p110δ-Akt-Mediated signals. *Cell Metab* (2017) 25:593–609. doi: 10.1016/j.cmet.2017.01.008

121. Renner K, Geiselhöringer AL, Fante M, Bruss C, Färber S, Schönhammer G, et al. Metabolic plasticity of human T cells: Preserved cytokine production under glucose deprivation or mitochondrial restriction, but 2-deoxy-glucose affects effector functions. *Eur J Immunol* (2015) 45:2504–16. doi: 10.1002/eji.201545473

122. Acharya D, Liu G, Gack MU. Dysregulation of type I interferon responses in COVID-19. *Nat Rev Immunol* (2020) 20:397–8. doi: 10.1038/s41577-020-0346-x

123. Daryabor G, Kabelitz D, Kalantar K. An update on immune dysregulation in obesity-related insulin resistance. *Scandinavian J Immunol* (2019) 89:e12747. doi: 10.1111/sji.12747

124. Huh JY, Park YJ, Ham M, Kim JB. Crosstalk between adipocytes and immune cells in adipose tissue inflammation and metabolic dysregulation in obesity. *Molecules Cells* (2014) 37:365–71. doi: 10.14348/molcells.2014.0074

125. Snyder TM, Gittelman RM, Klinger M, May DH, Osborne EJ, Taniguchi R, et al. Magnitude and dynamics of the T-cell response to SARS-CoV-2 infection at both individual and population levels. *medRxiv Preprint Server Health Sci* (2020) 8 (Supplement_1):S77–S77. doi: 10.1101/2020.07.31.20165647

126. Rojas-Osornio SA, Cruz-Hernández TR, Drago-Serrano ME, Campos-Rodríguez R. Immunity to influenza: Impact of obesity. *Obes Res Clin Pract* (2019) 13:419–29. doi: 10.1016/j.orcp.2019.05.003

127. Su Y, Chen D, Yuan D, Lausted C, Choi J, Dai CL, et al. Multi-omics resolves a sharp disease-state shift between mild and moderate COVID-19. *Cell* (2020) 183:1479–1495.e20. doi: 10.1016/j.cell.2020.10.037

128. Kim S, Parks CG, DeRoo LA, Chen H, Taylor JA, Cawthon RM, et al. Obesity and weight gain in adulthood and telomere length. *Cancer Epidemiol Biomarkers Prev* (2009) 18:816–20. doi: 10.1158/1055-9965.EPI-08-0935

129. Mundstock E, Sarria EE, Zatti H, Mattos Louzada F, Kich Grun L, Herbert Jones M, et al. Effect of obesity on telomere length: systematic review and meta-analysis. *Obesity* (2015) 23:2165–74. doi: 10.1002/oby.21183

130. Lee M, Martin H, Firpo MA, Demerath EW. Inverse association between adiposity and telomere length: The fels longitudinal study. *Am J Hum Biol* (2011) 23:100–6. doi: 10.1002/ajhb.21109

131. Valdes AM, Andrew T, Gardner JP, Kimura M, Oelsner E, Cherkas LF, et al. Obesity, cigarette smoking, and telomere length in women. *Lancet* (2005) 366:662–4. doi: 10.1016/S0140-6736(05)66630-5

132. Kaushik P, Anderson JT. Obesity: Epigenetic aspects. *Biomol Concepts* (2016) 7:145–55. doi: 10.1515/bmc-2016-0010

133. Wang X, Zhu H, Snieder H, Su S, Munn D, Harshfield G, et al. Obesity related methylation changes in DNA of peripheral blood leukocytes. *BMC Med* (2010) 8:1–8. doi: 10.1186/1741-7015-8-87

134. Nevalainen T, Kananen L, Marttila S, Jylhävä J, Mononen N, Kähönen M, et al. Obesity accelerates epigenetic aging in middle-aged but not in elderly individuals. *Clin Epigenet* (2017) 9:1–9. doi: 10.1186/s13148-016-0301-7

135. Minamino T, Orimo M, Shimizu I, Kunieda T, Yokoyama M, Ito T, et al. A crucial role for adipose tissue p53 in the regulation of insulin resistance. *Nat Med* (2009) 15:1082–7. doi: 10.1038/nm.2014

136. Shirakawa K, Sano M. T Cell immunosenescence in aging, obesity, and cardiovascular disease. *Cells* (2021) 10(9):2435. doi: 10.3390/cells10092435

137. Palmer AK, Xu M, Zhu Y, Pirtskhalava T, Weivoda MM, Hachfeld CM, et al. Targeting senescent cells alleviates obesity-induced metabolic dysfunction. *Aging Cell* (2019) 18:e12950. doi: 10.1111/acel.12950

138. Kirkland JL, Tchkonia T. Cellular senescence: A translational perspective. *EBioMedicine* (2017) 21:21–8. doi: 10.1016/j.ebiom.2017.04.013

139. Linton PJ, Dorshkind K. Age-related changes in lymphocyte development and function. *Nat Immunol* (2004) 5:133–9. doi: 10.1038/ni1033

140. Spielmann G, Johnston CA, O'Connor DP, Foreyt JP, Simpson RJ. Excess body mass is associated with T cell differentiation indicative of immune ageing in children. *Clin Exp Immunol* (2014) 176:246–54. doi: 10.1111/cei.12267

141. Yang H, Youm YH, Vandanmagsar B, Rood J, Kumar KG, Butler AA, et al. Obesity accelerates thymic aging. *Blood* (2009) 114:3803–12. doi: 10.1182/blood-2009-03-213595

142. Simar D, Versteyhe S, Donkin I, Liu J, Hesson L, Nylander V, et al. DNA Methylation is altered in b and NK lymphocytes in obese and type 2 diabetic human. *Metabolism: Clin Exp* (2014) 63:1188–97. doi: 10.1016/j.metabol.2014.05.014

143. Jacobsen MJ, Mentzel CM, Olesen AS, Huby T, Jørgensen CB, Barrès R, et al. Altered methylation profile of lymphocytes is concordant with perturbation of lipids metabolism and inflammatory response in obesity. *J Diabetes Res* (2016) 2016:8539057. doi: 10.1155/2016/8539057

144. Wang Q, Wang Y, Xu D. The roles of T cells in obese adipose tissue inflammation. *Adipocyte* (2021) 10:435–45. doi: 10.1080/21623945.2021.1965314

145. Cheung KP, Taylor KR, Jameson JM. Immunomodulation at epithelial sites by obesity and metabolic disease. *Immunologic Res* (2012) 52:182–99. doi: 10.1007/s12026-011-8261-7

146. Milner JJ, Sheridan PA, Karlsson EA, Schultz-Cherry S, Shi Q, Beck MA. Diet-induced obese mice exhibit altered heterologous immunity during a secondary 2009 pandemic H1N1 infection. *J Immunol (Baltimore Md. 1950)* (2013) 191:2474–85. doi: 10.4049/jimmunol.1202429

147. Kim YH, Kim JK, Kim DJ, Nam JH, Shim SM, Choi YK, et al. Diet-induced obesity dramatically reduces the efficacy of a 2009 pandemic H1N1 vaccine in a mouse model. *J Infect Dis* (2012) 205:244–51. doi: 10.1093/infdis/jir731

148. Frasca D, Diaz A, Romero M, Vazquez T, Blomberg BB. Obesity induces pro-inflammatory b cells and impairs b cell function in old mice. *Mech Ageing Dev* (2017) 162:91–9. doi: 10.1016/j.mad.2017.01.004

149. Frasca D, Diaz A, Romero M, Blomberg BB. Ageing and obesity similarly impair antibody responses. *Clin Exp Immunol* (2017) 187:64–70. doi: 10.1111/cei.12824

150. Adams LE, Waterman S, Paz-Bailey G. Vaccination for dengue prevention. *Jama* (2022) 327:817–8. doi: 10.1001/jama.2021.23466

151. Paz-Bailey G, Adams L, Wong JM, Poehling KA, Chen WH, McNally V, et al. Dengue vaccine: Recommendations of the advisory committee on immunization practices, United States, 2021. *MMWR Recomm Rep* (2021) 70:1–16. doi: 10.15585/mmwr.rr7006a1

152. Dowd KA, Ko SY, Morabito KM, Yang ES, Pelc RS, DeMaso CR, et al. Rapid development of a DNA vaccine for zika virus. *Science* (2016) 354:237–40. doi: 10.1126/science.aai9137

153. Satchidanandam V. Japanese Encephalitis vaccines. *Curr Treat Options Infect Dis* (2020) 4:375–386. doi: 10.1007/s40506-020-00242-5

154. Frierson JG. The yellow fever vaccine: A history. *Yale J Biol Med* (2010) 83:77.

155. Ulbert S. West Nile Virus vaccines–current situation and future directions. *Hum Vaccines Immunotherapeutics* (2019) 15:2337–42. doi: 10.1080/21645515.2019.1621149

156. Brown RE, Katz M. Failure of antibody production to yellow fever vaccine in children with kwashiorkor. *Trop geographical Med* (1966) 18:125–8.

157. Karlsson EA, Beck MA. The burden of obesity on infectious disease. *Exp Biol Med* (2010) 235:1412–24. doi: 10.1258/ebm.2010.010227

158. Park H-L, Shim S-H, Lee E-Y, Cho W, Park S, Jeon H-J, et al. Obesity-induced chronic inflammation is associated with the reduced efficacy of influenza vaccine. *Hum Vaccines immunotherapeutics* (2014) 10:1181–6. doi: 10.4161/hv.28332

159. Sheridan PA, Paich HA, Handy J, Karlsson EA, Hudgens MG, Sammon AB, et al. Obesity is associated with impaired immune response to influenza vaccination in humans. *Int J Obes* (2012) 36:1072–7. doi: 10.1038/ijo.2011.208

160. Karlsson EA, Hertz T, Johnson C, Mehle A, Krammer F, Schultz-Cherry S. Obesity outweighs protection conferred by adjuvanted influenza vaccination. *mBio* (2016) 180(7):4476–86. doi: 10.1128/mBio.01144-16

161. Eliakim A, Schwindt C, Zaldivar F, Casali P, Cooper DM. Reduced tetanus antibody titers in overweight children. *Autoimmunity* (2006) 39:137–41. doi: 10.1080/08916930600597326

162. Weber DJ, Rutala WA, Samsa GP, Santimaw JE, Lemon SM. Obesity as a predictor of poor antibody response to hepatitis b plasma vaccine. *Jama* (1985) 254:3187–9. doi: 10.1001/jama.1985.03360220053027

163. Pellini R, Venuti A, Pimpinelli F, Abril E, Blandino G, Campo F, et al. Obesity may hamper SARS-CoV-2 vaccine immunogenicity. *medRxiv preprint server Health Sci* (2021). doi: 10.1101/2021.02.24.21251664

164. Garner-Spitzer E, Poellabauer EM, Wagner A, Guzek A, Zwazl I, Seidl-Friedrich C, et al. Obesity and sex affect the immune responses to tick-borne encephalitis booster vaccination. *Front Immunol* (2020) 11:860. doi: 10.3389/fimmu.2020.00860

165. Tagliabue C, Principi N, Giavoli C, Esposito S. Obesity: Impact of infections and response to vaccines. *Eur J Clin Microbiol Infect Dis* (2016) 35:325–31. doi: 10.1007/s10096-015-2558-8

166. Watanabe M, Balena A, Tuccinardi D, Tozzi R, Risi R, Masi D, et al. Central obesity, smoking habit, and hypertension are associated with lower antibody titres in response to COVID-19 mRNA vaccine. *Diabetes Metab Res Rev* (2022) 38:e3465. doi: 10.1002/dmrr.3465

167. Yan T, Xiao R, Wang N, Shang R, Lin G. Obesity and severe coronavirus disease 2019: Molecular mechanisms, paths forward, and therapeutic opportunities. *Theranostics* (2021) 11:8234–53. doi: 10.7150/thno.59293

168. Beck MA, Shi Q, Morris VC, Levander OA. Rapid genomic evolution of a non-virulent coxsackievirus B3 in selenium-deficient mice results in selection of identical virulent isolates. *Nat Med* (1995) 1:433–6. doi: 10.1038/nm0595-433

169. Malik P, Patel U, Patel K, Martin M, Shah C, Mehta D, et al. Obesity a predictor of outcomes of COVID-19 hospitalized patients-a systematic review and meta-analysis. *J Med Virol* (2021) 93:1188–93. doi: 10.1002/jmv.26555

170. Huang Y, Lu Y, Huang YM, Wang M, Ling W, Sui Y, et al. Obesity in patients with COVID-19: A systematic review and meta-analysis. *Metabolism: Clin Exp* (2020) 113:154378. doi: 10.1016/j.metabol.2020.154378

171. Yang J, Tian C, Chen Y, Zhu C, Chi H, Li J. Obesity aggravates COVID-19: An updated systematic review and meta-analysis. *J Med Virol* (2021) 93:2662–74. doi: 10.1002/jmv.26677

172. Weger-Lucarelli J, Auerswald H, Vignuzzi M, Dussart P, Karlsson EA. Taking a bite out of nutrition and arbovirus infection. *PloS Negl Trop Dis* (2018) 12:e0006247. doi: 10.1371/journal.pntd.0006247

173. Jean-Baptiste E, von Oettingen J, Larco P, Raphaël F, Larco NC, Cauvin MM, et al. Chikungunya virus infection and diabetes mellitus: A double negative impact. *Am J Trop Med hygiene* (2016) 95:1345–50. doi: 10.4269/ajtmh.16-0320

174. Borgherini G, Poubeau P, Staikowsky F, Lory M, Le Moullec N, Becquart JP, et al. Outbreak of chikungunya on reunion island: Early clinical and laboratory features in 157 adult patients. *Clin Infect Dis an Off Publ Infect Dis Soc America* (2007) 44:1401–7. doi: 10.1086/517537

175. Pichainarong N, Mongkalangoon N, Kalayanarooj S, Chaveepojnkamjorn W. Relationship between body size and severity of dengue hemorrhagic fever among children aged 0-14 years. *Southeast Asian J Trop Med Public Health* (2006) 37:283–8.

176. Tan VPK, Ngim CF, Lee EZ, Ramadas A, Pong LY, Ng JI, et al. The association between obesity and dengue virus (DENV) infection in hospitalised patients. *PloS One* (2018) 13:e0200698. doi: 10.1371/journal.pone.0200698

177. Rathakrishnan A, Wang SM, Hu Y, Khan AM, Ponnampalavanar S, Lum LC, et al. Cytokine expression profile of dengue patients at different phases of illness. *PloS One* (2012) 7:e52215. doi: 10.1371/journal.pone.0052215

178. Conroy AL, Gélvez M, Hawkes M, Rajwans N, Tran V, Liles WC, et al. Host biomarkers are associated with progression to dengue haemorrhagic fever: A nested case-control study. *Int J Infect Dis IJID Off Publ Int Soc Infect Dis* (2015) 40:45–53. doi: 10.1016/j.ijid.2015.07.027

179. Marques RE, Guabiraba R, Del Sarto JL, Rocha RF, Queiroz AL, Cisalpino D, et al. Dengue virus requires the CC-chemokine receptor CCR5 for replication and infection development. *Immunology* (2015) 145:583–96. doi: 10.1111/imm.12476

180. Soe HJ, Khan AM, Manikam R, Samudi Raju C, Vanhoutte P, Sekaran SD. High dengue virus load differentially modulates human microvascular endothelial

barrier function during early infection. *J Gen Virol* (2017) 98:2993–3007. doi: 10.1099/jgv.0.000981

181. St John AL, Rathore AP, Yap H, Ng ML, Metcalfe DD, Vasudevan SG, et al. Immune surveillance by mast cells during dengue infection promotes natural killer (NK) and NKT-cell recruitment and viral clearance. *Proc Natl Acad Sci USA* (2011) 108:9190–5. doi: 10.1073/pnas.1105079108

182. Rivino L, Kumaran EA, Thein TL, Too CT, Gan VC, Hanson BJ, et al. Virus-specific T lymphocytes home to the skin during natural dengue infection. *Sci Trans Med* (2015) 7:278ra35. doi: 10.1126/scitranslmed.aaa0526

183. Kyle JL, Beatty PR, Harris E. Dengue virus infects macrophages and dendritic cells in a mouse model of infection. *J Infect Dis* (2007) 195:1808–17. doi: 10.1086/518007

184. Cerny D, Haniffa M, Shin A, Bigliardi P, Tan BK, Lee B, et al. Selective susceptibility of human skin antigen presenting cells to productive dengue virus infection. *PloS Pathog* (2014) 10:e1004548. doi: 10.1371/journal.ppat.1004548

185. St John AL, Rathore APS. Adaptive immune responses to primary and secondary dengue virus infections. *Nat Rev Immunol* (2019) 19:218–30. doi: 10.1038/s41577-019-0123-x

frontiers | Frontiers in Nutrition

TYPE Original Research
PUBLISHED 24 November 2022
DOI 10.3389/fnut.2022.1024631

OPEN ACCESS

EDITED BY
Filippo Giorgio Di Girolamo,
University of Trieste, Italy

REVIEWED BY
Shuang Zhang,
Guangdong Ocean University, China
Yusheng Liang,
University of Michigan, United States
Xiaohui Dong,
Guangdong Ocean University, China

*CORRESPONDENCE
Qinghui Ai
qhai@ouc.edu.cn

SPECIALTY SECTION
This article was submitted to Nutrition and Metabolism, a section of the journal Frontiers in Nutrition

RECEIVED 22 August 2022
ACCEPTED 20 September 2022
PUBLISHED 24 November 2022

CITATION
Du J, Zhang J, Xiang X, Xu D, Cui K, Mai K and Ai Q (2022) Activation of farnesoid X receptor suppresses ER stress and inflammation *via* the YY1/NCK1/PERK pathway in large yellow croaker (*Larimichthys crocea*). *Front. Nutr.* 9:1024631. doi: 10.3389/fnut.2022.1024631

Activation of farnesoid X receptor suppresses ER stress and inflammation *via* the YY1/NCK1/PERK pathway in large yellow croaker (*Larimichthys crocea*)

Jianlong Du[1,2], Junzhi Zhang[1,2], Xiaojun Xiang[1,2], Dan Xu[1,2], Kun Cui[1,2], Kangsen Mai[1,2,3] and Qinghui Ai[1,2,3]*

[1]Key Laboratory of Aquaculture Nutrition and Feed (Ministry of Agriculture and Rural Affairs), The Key Laboratory of Mariculture (Ministry of Education), Ocean University of China, Qingdao, China, [2]Laboratory for Marine Fisheries Science and Food Production Processes, Qingdao National Laboratory for Marine Science and Technology, Qingdao, China, [3]Laboratory for Marine Fisheries Science and Food Production Processes, Qingdao National Laboratory for Marine Science and Technology, Qingdao, China

Unfolded protein responses from endoplasmic reticulum (ER) stress have been implicated in inflammatory signaling. The vicious cycle of ER stress and inflammation makes regulation even more difficult. This study examined effects of farnesoid X receptor (FXR) in ER-stress regulation in large yellow croakers. The soybean-oil-diet-induced expression of ER stress markers was decreased in fish with FXR activated. In croaker macrophages, FXR activation or overexpression significantly reduced inflammation and ER stress caused by tunicamycin (TM), which was exacerbated by FXR knockdown. Further investigation showed that the TM-induced phosphorylation of PERK and EIF2α was inhibited by the overexpression of croaker FXR, and it was increased by FXR knockdown. Croaker NCK1 was then confirmed to be a regulator of PERK, and its expression in macrophages is increased by FXR overexpression and decreased by FXR knockdown. The promoter activity of croaker NCK1 was inhibited by yin-yang 1 (YY1). Furthermore, the results show that croaker FXR overexpression could suppress the P65-induced promoter activity of YY1 in HEK293t cells and decrease the TM-induced expression of *yy1* in macrophages. These results indicate that FXR could suppress P65-induced *yy1* expression and then increase NCK1 expression, thereby inhibiting the PERK pathway. This study may benefit the understanding of ER stress regulation in fish, demonstrating that FXR can be used in large yellow croakers as an effective target for regulating ER stress and inflammation.

KEYWORDS

FXR, ER stress, inflammation, large yellow croaker, PERK

Introduction

Inflammation occurs when the body responds to harmful stimuli (1). Poor diets such as excessive fat, unbalanced nutrition and specific nutrient deficiency, are important factors that promote chronic inflammation that can last for months or years (2–5). The replacement of fish oil with vegetable oil (VO) has become increasingly common in aquaculture. However, the excessive use of vegetable oil has been shown to alter the metabolic balance and induce inflammation in fish, causing growth inhibition and health issues (6–9). Thus, there is an urgent need to develop strategies to regulate inflammation in fish. The endoplasmic reticulum (ER) is crucial for cell housekeeping (10). Under stress, the ER becomes stressed from the accumulation of misfolded and unfolded proteins, resulting in the unfolded protein response (UPR) (11). Mammals (12, 13) and fish (14, 15) have both been shown to develop inflammation when exposed to chronic and excessive ER stress. It has been shown that the UPR pathway plays an important role in inflammation (10–13), and some studies have shown that inflammatory stimuli induce ER stress (16, 17). In many diseases, inflammation and ER stress occur at the same time. The interplay between ER stress and inflammation could cause a vicious circle that may worsen the disease (18, 19). As a result, there is a need to explore targets that would regulate ER stress, which may be helpful to break the vicious cycle and alleviate inflammation in fish.

Farnesoid X receptor (NR1H4) is a transcription factor regulating a variety of genes that are involved in bile acid metabolism, lipid metabolism, glucose metabolism and inflammation (20). As a member of the nuclear receptors, FXR can be activated or suppressed by ligands, making it a potential target for exogenous regulation (20, 21). However, only a small amount of research on FXR in fish has been conducted. Our previous studies showed that the FXR is highly expressed in the liver, kidney and intestine of large yellow croakers (*Larimichthys crocea*) (8), and GW4064 and chenodeoxycholic acid (CDCA) could effectively activate it (22). Furthermore, in croakers, FXR is also implicated in lipid metabolism and inflammation (22, 23). Our previous study showed that FXR had anti-inflammatory properties in croakers by directly and indirectly suppressing the activity of NFκB-P65 activity. Previous studies in mammals found that FXR interacted with endoplasmic reticulum stress (24, 25). When ER stress was activated in aging mice, the expression of FXR in the liver decreased (25). Our previous study showed that ER stress also reduced FXR expression in fish fed a high-lipid diet (23). A study in mice showed that FXR activation could suppress the ER-stress-induced expression of NLRP3 *via* Non-catalytic region of tyrosine kinase adaptor protein 1 (NCK1) (24). However, the role of FXR and NCK1 in regulating ER stress and how FXR activation affects NCK1 expression in fish is unknown.

Large yellow croaker is widely cultured in China and is of high economic value. In previous studies, large yellow croakers showed frequent inflammation induced by VO diets (22, 26, 27). A macrophage cell line for large yellow croakers has been well established (28). Based on this research, large yellow croaker is an appropriate model for immunological studies (28–30). This study focused on understanding the role of FXR in regulating ER stress and inflammation and the underlying mechanisms which could pinpoint a potential target for breaking the cycle of ER stress and inflammation in fish.

Methods

Feeding experiment

As described previously, an animal feeding experiment was conducted (31). In brief, Fish oil (FO) and soybean oil (SO) diets, as well as soybean oil (SO) diets that contain CDCA (C9377, Sigma) at 300 mg or 900 mg/kg (SO-CDCA 300 or SO-CDCA 900) were developed (31) (Supplementary Table 1). Randomly, each diet was assigned to a cage (60 fish/cage, 10.03 ± 0.02 g) in triplicate. Fish were fed two times a day at 05:00 and 17:00 until satiation with under appropriate conditions for 10 weeks. After fasting for 24 hours, the fish were anesthetized with eugenol (1:10,000) at the end of the feeding trial. Then, six individuals in one cage were sampled for head kidney tissues and immediately frozen in liquid nitrogen.

Cell culture and treatment

Croaker macrophages were cultured as previously described (27°C and Dulbecco's Modified Eagle Medium: Nutrient Mixture F-12 with 15% fetal bovine serum) (28). HEK 293T cells were cultured as previously described (5% CO_2, 37°C, and Dulbecco's Modified Eagle Medium with 10% fetal bovine serum) (23). To explore the role of FXR in ER stress regulation, we established macrophages stably transfected for FXR overexpression or knockdown. Macrophages were stably transfected with a recombinant lentivirus encoding the croaker FXR (LvFXR) and a lentivirus-based shRNA vector targeting FXR (siFXR). Macrophages infected with a negative-control lentivirus were used as a control. The cells were treated with lentivirus for 48 h before they were screened with puromycin in gradient concentrations until they could continue to grow and pass on.

To investigate the effect of LA on ER stress, macrophages were treated with linoleic acid (LA, 100 μm) for 0, 0.5, 1, 2, 4, and 6 hours or treated with LA (0, 100, 200, and 400 μm) for 4 hours. To confirm the effect of activation of ER stress

on inflammation, macrophages were treated with an ER stress inducer tunicamycin (TM, 4 μm, MCE) for 0, 0.5, 1, 2, 4, and 6 hours. In order to determine whether the FXR regulates ER stress and inflammation, macrophages were pre-treated with FXR agonists CDCA (50μm, Sigma) and GW4064 (2μm, MCE) for 1 h and then stimulated with TM (4 μm) for 4 hours. To find out how FXR affected ER stress, the control cells, LvFXR cells, and siFXR cells were treated with 4 μM TM for 4 h. To confirm the effect of NCK1 on PERK of large yellow croaker, HKE 293T cells were co-transfected with croaker NCK1 and PERK-GFP plasmids and then stimulated with TM (4 μm) for 4 h.

QRT-PCR

Real-time quantitative PCR was used to determine gene mRNA expression as described by Du et al. (31). The mRNA level of activating transcription factor 4 (ATF4), ATF6, cyclooxygenase 2 (COX2), IL6, NCK1, interleukin 1 beta (IL1β), C/EBP homologous protein (CHOP), tumor necrosis factor alpha (TNFα), glucose-regulated protein 78 (GRP78), eukaryotic initiation factor 2α (EIF2α), yin-yang 1 (YY1) and X-box-binding protein 1s (XBP1s) was detected (Supplementary Table 2). Housekeeping genes were β-actin and GAPDH. A normalized gene expression level was calculated and normalized using the the $2^{-\Delta\Delta CT}$ method (32).

Western blotting

According to Tan et al., western blots were performed (26). In the present study, antibodies against FXR (Bioss, China), HA (CST, USA), GRP78 (CST, USA), GAPDH (ZSGB-Bio, China), p-PERK (Bioss, China), PERK (CST, USA), p-EIF2α (CST, USA), XBP1s (CST, USA), and ATF6 (Bioss, China) were used.

Luciferase reporter assay

Croaker NCK1 and YY1 promoters were cloned into a pGL3-basic reporter vector (Promega, USA). The plasmids expressing croaker FXR, small heterodimer partner (SHP), P65, PERK-GFP, NCK1, and YY1 were stored in our laboratory. To explore the effect of YY1 on NCK1 promoter of large yellow croaker, HKE 293T cells were co-transfected with reporter plasmids (NCK1 promoter), phRL-CMV plasmid, and expression plasmid (croaker YY1) for 24 h. To investigate the effect of FXR and SHP on the activity of YY1 promoter, HKE 293T cells were co-transfected with reporter plasmids (YY1 promoter), phRL-CMV plasmid, and expression plasmid (croaker P65, FXR or SHP) for 24 h. Following the previous description, cell transfection and fluorescence detection were performed (22, 23).

Statistical analysis

The data (means ± SEMs.) were analyzed with SPSS 20.0 (SPSS, USA), utilizing ANOVA and Duncan's multiple-range test for significance. The difference between the two groups was tested with Student's *t*-tests. Statistical significance was determined by $P < 0.05$.

Results

CDCA supplementation suppressed SO-diet-induced ER stress *in vivo*

Compared to the FO group, the SO diet significantly increased gene expression associated with ER stress, such as GRP78, EIF2α, CHOP, XBP1S, ATF4, and ATF6 ($P < 0.05$) (Figure 1A). CDCA supplementation significantly decreased the SO-diet-induced mRNA level of GRP78, EIF2α, CHOP, XBP1S, ATF4, and ATF6 ($P < 0.05$) (Figure 1A). As well, the SO-CDCA300 group had a lower level of GRP78 protein than the SO group ($P < 0.05$) (Figure 1B).

Effects of LA treatment on ER stress in croaker macrophages

To investigate the effect of LA on ER stress, macrophages were treated with LA. The mRNA level of GRP78, EIF2α, CHOP, XBP1S, ATF4, and ATF6 was significantly increased in macrophages after LA treatment ($P < 0.05$) (Figure 2A). Additionally, in croaker macrophages, increased protein levels of GRP78 were observed following LA treatment ($P < 0.05$) (Figure 2B).

TM treatment increased pro-inflammatory gene expression

To confirm the effect of activation of ER stress on inflammation, macrophages were treated with an ER stress inducer TM for 0.5, 1, 2, 4, and 6 hours. Following 0.5, 1 and 2 hours of TM treatment, TNFα expression was significantly increased ($P < 0.05$) (Figure 3). In addition, the mRNA level of IL1β, IL16, and COX2 was significantly induced after TM treatment for 4 and 6 hours ($P < 0.05$) (Figure 3).

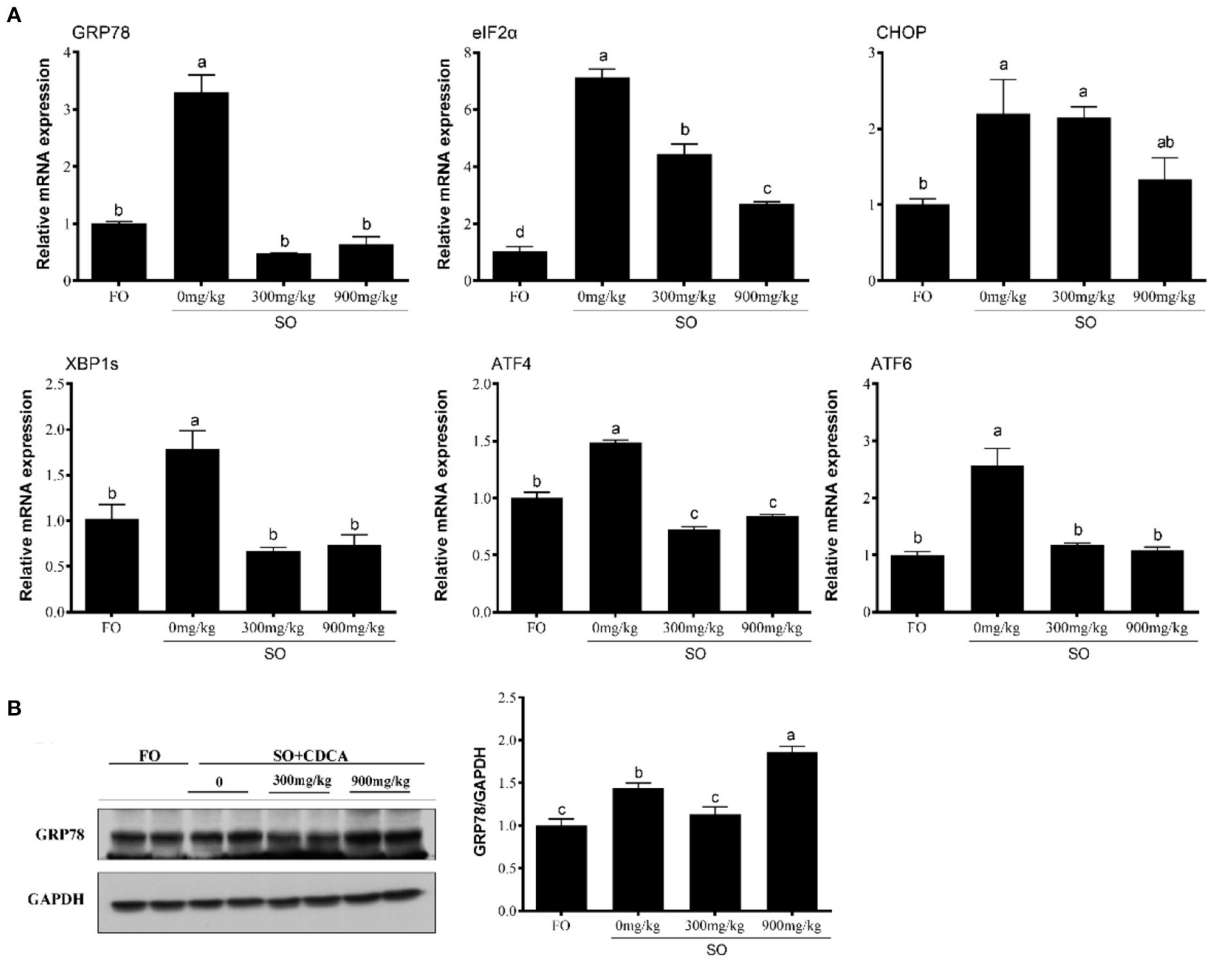

FIGURE 1
Expression of **(A)** ER stress-related genes and **(B)** GRP78 protein levels in the head kidney of fish after SO feeding and CDCA supplementation. The significance was analyzed by one-factor ANOVA and Duncan's Multiple Range Test (means ± SEMs; $n = 3$). Means without the same label were considered different, $P < 0.05$.

Activation of FXR suppressed TM-induced ER stress and pro-inflammatory genes expression

In order to investigate FXR's influence on ER-induced inflammation, macrophages were treated with TM and FXR agonists (GW4064 and CDCA). The mRNA levels of GRP78, EIF2α, CHOP, XBP1S, and ATF4 were significantly decreased with GW4064 and CDCA treatment in comparison to TM alone ($P < 0.05$) (Figure 4A). Compared with the control group, TM treatment significantly increased the protein level of GRP78. Compared with the cells treated with TM alone, the protein level of GRP78 was significantly lower in cells after GW4064 or CDCA treatment ($P < 0.05$) (Figure 4B). Treatment with GW4064 or CDCA also significantly inhibited the TM-induced gene expression of IL1β and IL6 ($P < 0.05$) (Figure 4C).

FXR overexpression suppressed TM-induced ER stress and pro-inflammatory genes expression

Croaker FXR was overexpressed in macrophages stably transfected with the FXR (LvFXR group) (Figure 5A). Compared with that in the control group, FXR overexpression had no significant impact on the gene expression of GRP78, EIF2α, CHOP, XBP1S ATF4, and ATF6 ($P > 0.05$) (Figure 5B). However, the overexpression of FXR significantly decreased the TM-induced gene expression of GRP78, EIF2α, XBP1S, ATF4,

10.3389/fnut.2022.1024631

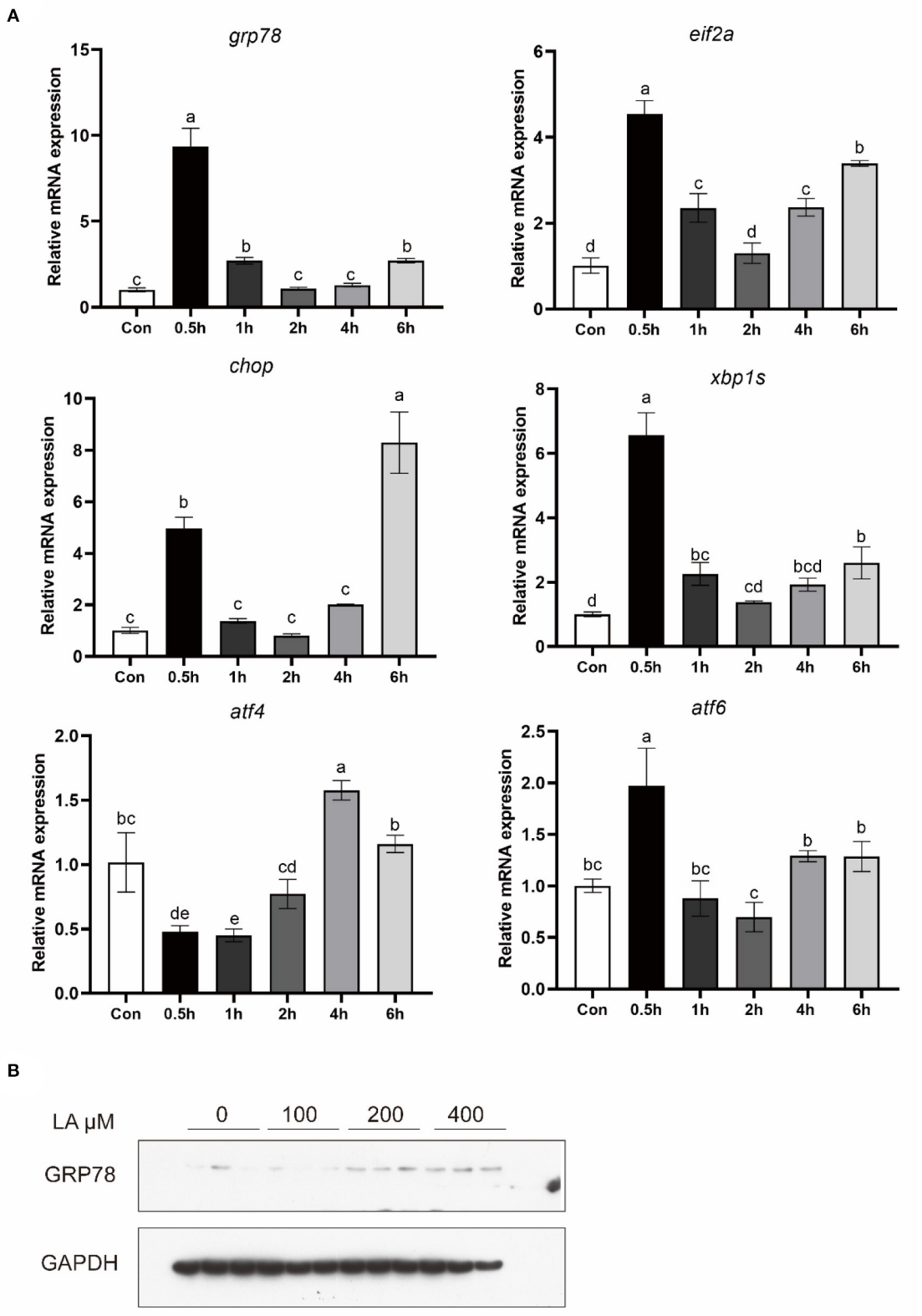

FIGURE 2
Expression of **(A)** ER stress-related genes and **(B)** GRP78 protein levels in croaker macrophages treated with LA. The significance was analyzed by one-factor ANOVA and Duncan's Multiple Range Test (means ± SEMs; $n = 3$). Means without the same label were considered different, $P < 0.05$.

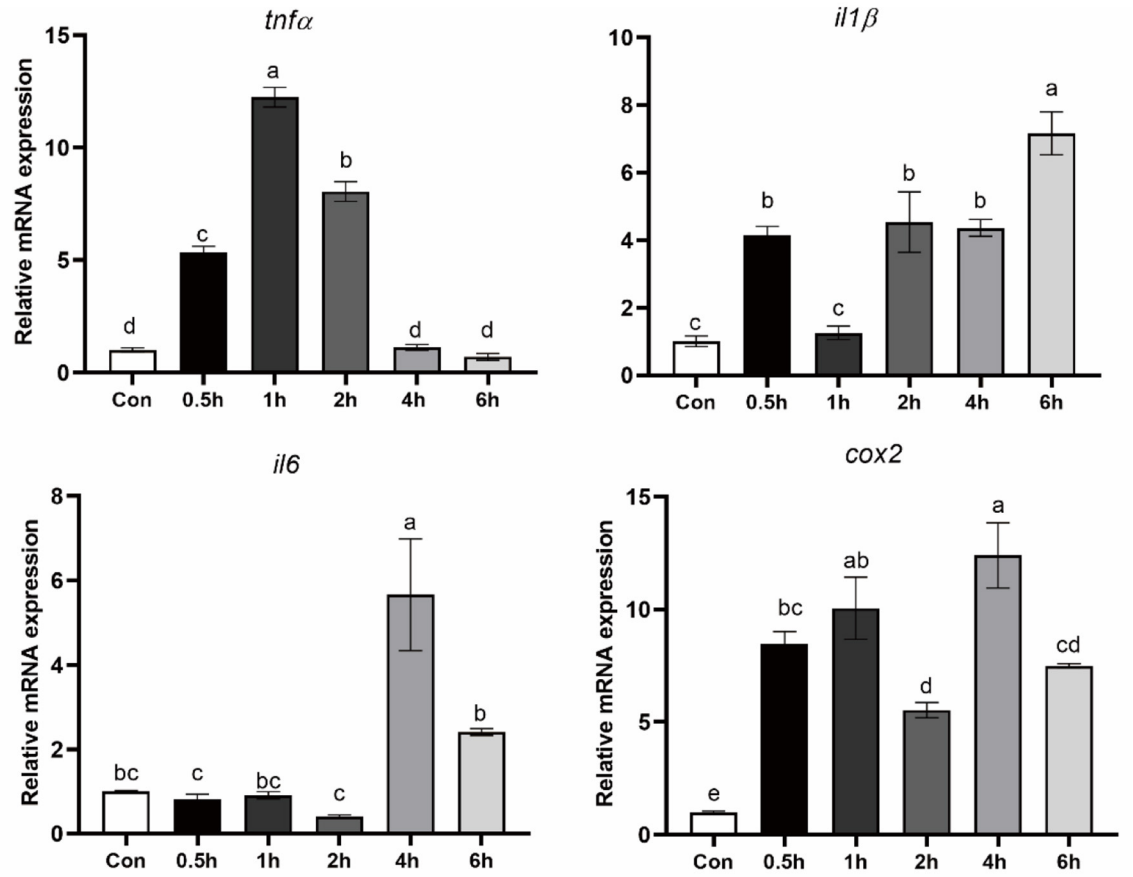

FIGURE 3
Expression of pro-inflammatory genes in croaker macrophages after treatment with TM. The significance was analyzed by one-factor ANOVA and Duncan's Multiple Range Test (means ± SEMs; $n = 3$). Means without the same label were considered different, $P < 0.05$.

and ATF6, and phosphorylation of PERK, phosphorylation of EIF2α, and protein levels of GRP78 and XBP1s ($P < 0.05$) (Figures 5B,C). In addition, the induction of the expression of IL1β and IL6 by TM was significantly inhibited by the overexpression of FXR ($P < 0.05$) (Figure 5D).

Knocking down FXR Promoted TM-induced ER stress and pro-inflammatory genes expression

The expression of FXR was knocked down in macrophages with stable interference for FXR (siFXR group) (Figure 6A). The siFXR group significantly showed higher levels of ATF4 mRNA, GRP78 protein, and phosphorylated EIF2α compared with the control group ($P < 0.05$) (Figure 6B). The knockdown of FXR significantly enhanced the mRNA levels (GRP78, CHOP, ATF4, AND ATF6) and protein levels (phosphorylated PERK, phosphorylated EIF2α, GRP78, and XBP1s) induced by TM in croaker macrophages ($P < 0.05$) (Figures 6B,C). Additionally, as a result of FXR knockdown, gene expression of IL16 and IL1β were significantly enhanced in macrophages induced by TM ($P < 0.05$) (Figure 6D).

NCK1 was involved in the regulation of PERK in the large yellow croaker

To investigate the effect of croaker NCK1 on PERK, HEK 293T cells were transfected with croaker NCK1 and PERK-GFP plasmids. When NCK1 and PERK-GFP plasmids were co-transfected into HEK 293T cells, PERK phosphorylation was significantly lower than in cells only transfected with PERK-GFP plasmid ($P < 0.05$) (Figure 7A). Further, NCK1 expression in macrophages was significantly reduced after TM and LA treatment ($P < 0.05$) (Figures 7B,C).

10.3389/fnut.2022.1024631

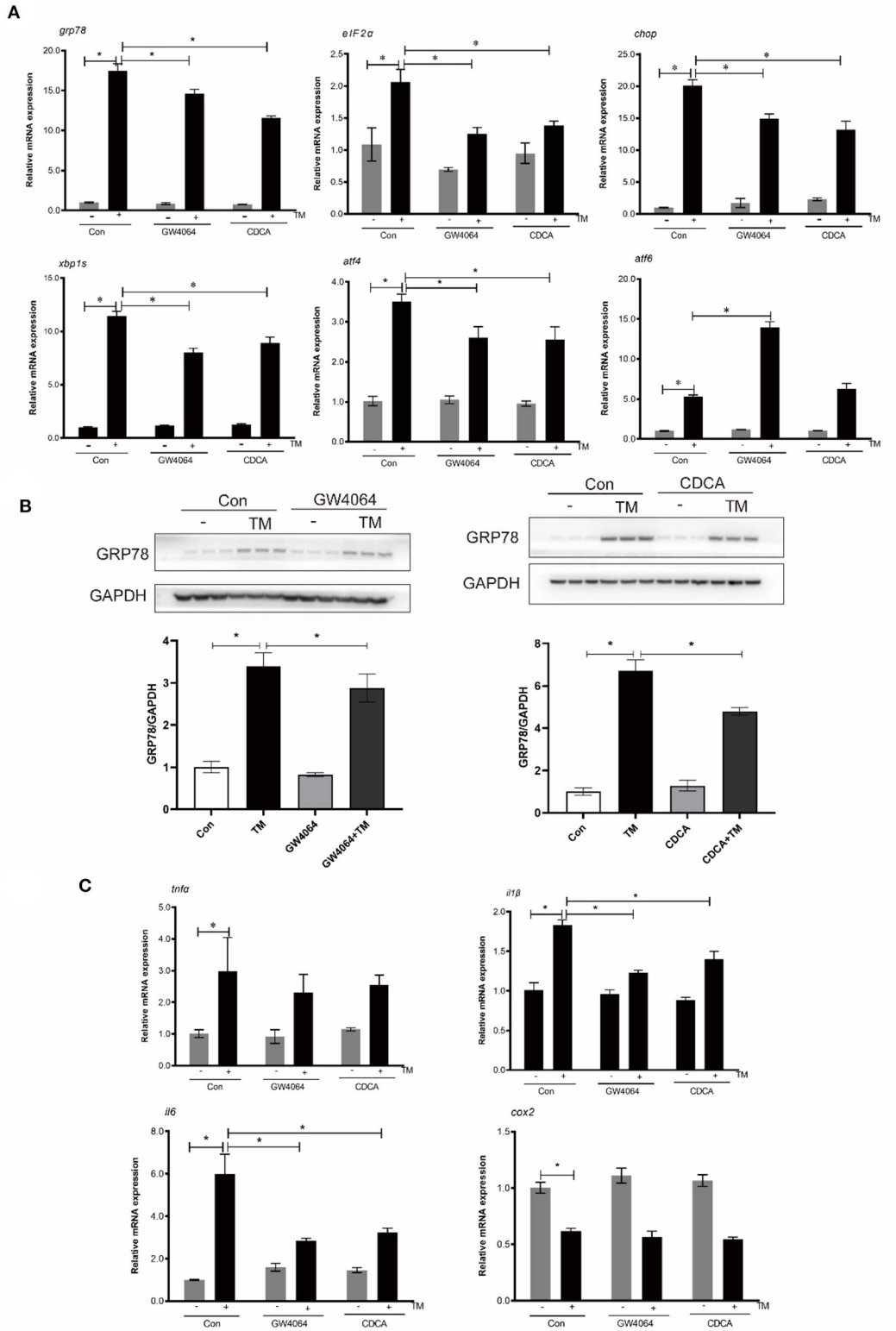

FIGURE 4
Effects of activation of FXR by ligands on TM-induced ER stress and inflammation in croaker macrophages. **(A)** Gene expression and **(B)** protein level of ER-stress markers in macrophages after TM stimulation alone or with FXR agonists (GW4064 and CDCA). **(C)** Gene expression of pro-inflammatory genes in in macrophages after TM stimulation alone or with FXR agonists. *Different between two groups; $P < 0.05$ (means ± SEMs; $n = 3$; Student's *t*-test).

10.3389/fnut.2022.1024631

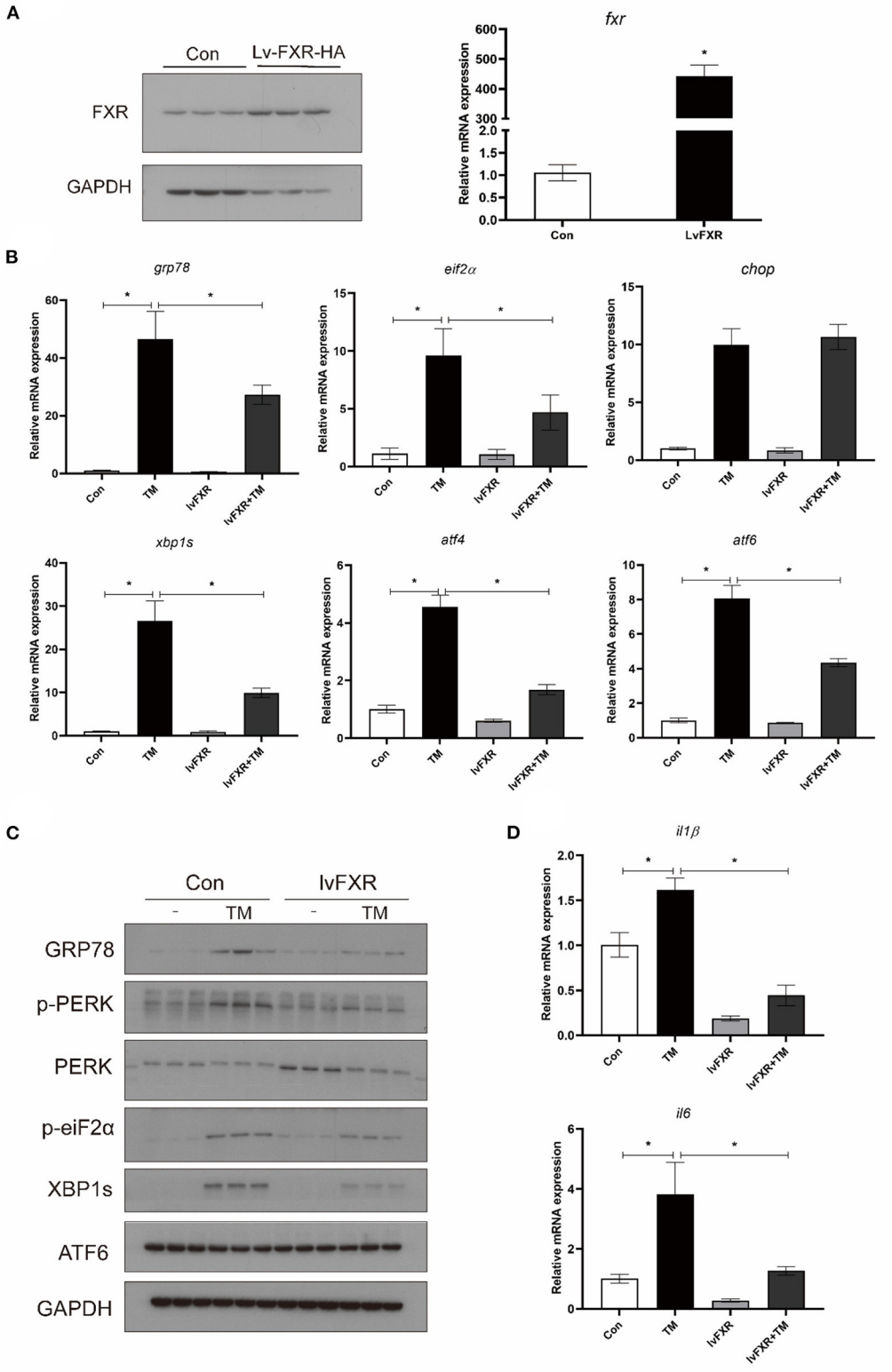

FIGURE 5
Effects of **(A)** FXR overexpression on TM-induced ER stress and inflammation in croaker macrophages. **(B)** Gene expression and **(C)** protein level of ER-stress markers in stably FXR-transfected macrophages after TM treatment. **(D)** Expression of IL1β and IL6 in stably FXR-transfected macrophages after TM treatment. *Different between two groups; $P < 0.05$ (means ± SEMs; $n = 3$; Student's t-test).

10.3389/fnut.2022.1024631

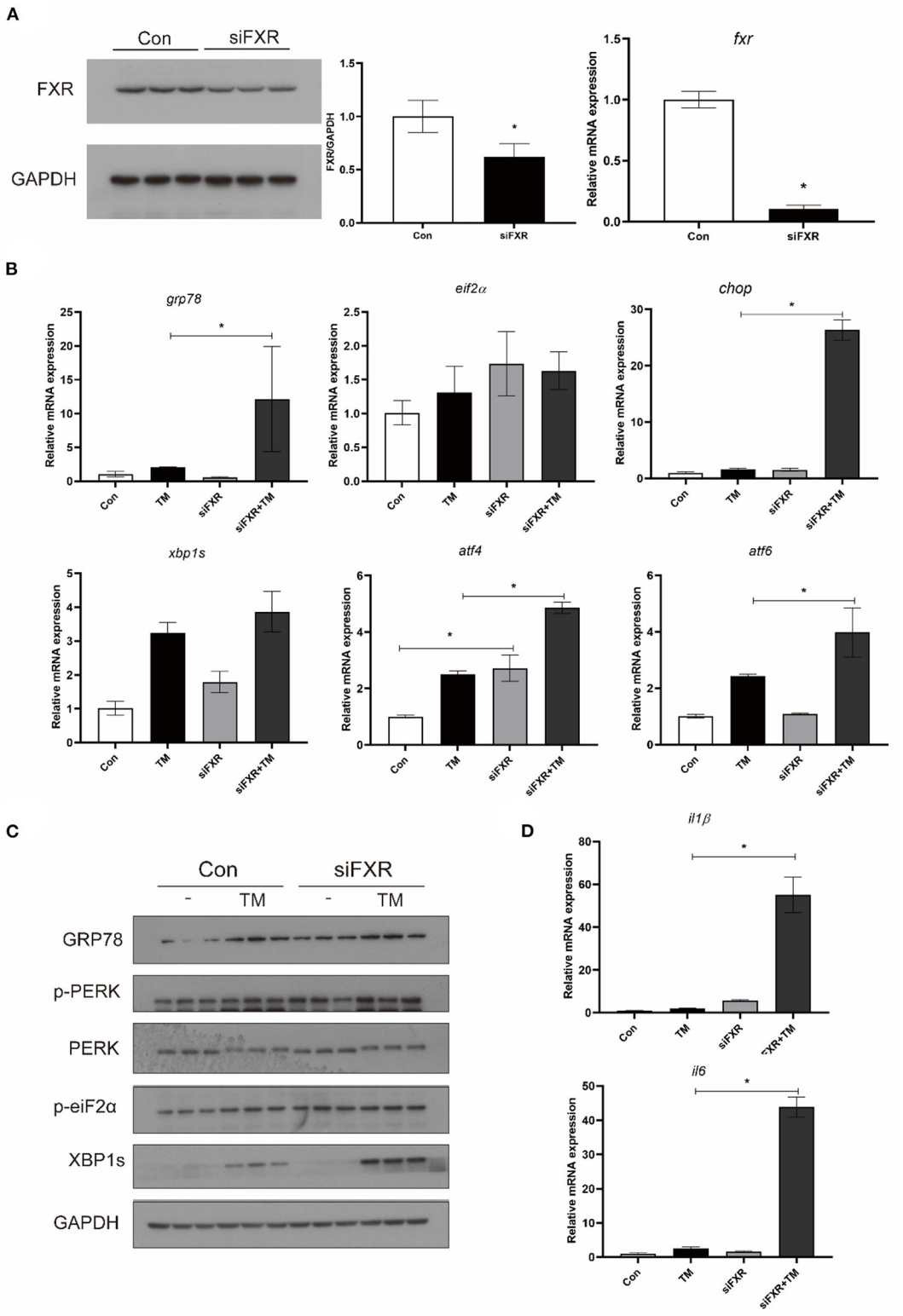

FIGURE 6
Effects of **(A)** FXR knockdown on TM-induced ER stress and inflammation in croaker macrophages. **(B)** Gene expression and **(C)** protein level of ER-stress markers in macrophages with stable interference for FXR after TM treatment. **(D)** Expression of IL1β and IL6 in macrophages with stable interference for FXR after TM treatment. *Different between two groups; $P < 0.05$ (means ± SEMs; $n = 3$; Student's t-test).

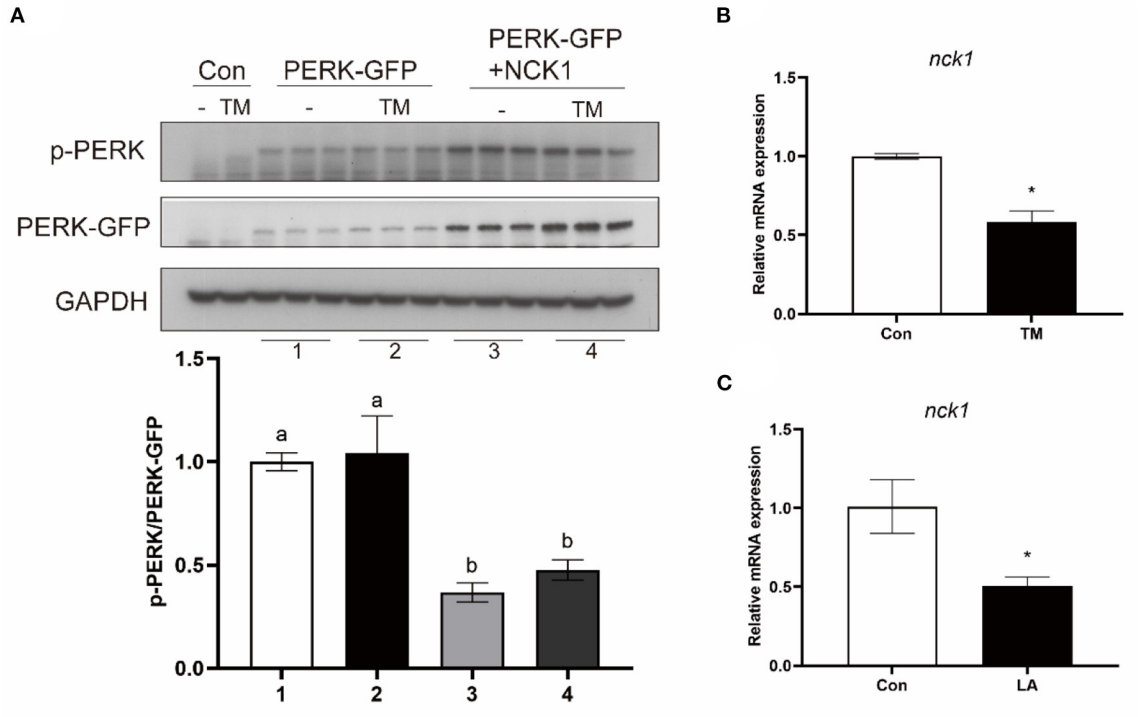

FIGURE 7
Effects of NCK1 on PERK in large yellow croakers. **(A)** Phosphorylated PERK immunoblot in HEK 293T cells after NCK1 overexpression. **(B,C)** NCK1 expression in macrophages after treatment with TM and LA. The significance was analyzed by one-factor ANOVA and Duncan's Multiple Range Test (means ± SEMs; $n = 3$). Means without the same label were considered different, $P < 0.05$. *Different between two groups (Student's *t*-test).

FXR increased NCK1 expression *via* YY1 and P65

The gene expression of NCK1 was significantly higher in the stably FXR-transfected macrophages than in the control group, and it was decreased by FXR knockdown ($P < 0.05$) (Figures 8A,B). In the luciferase reporter assay, croaker YY1 overexpression inhibited NCK1 promoter activity significantly ($P < 0.05$) (Figure 8C). Moreover, croaker FXR and SHP overexpression significantly inhibited the promoter activity of YY1 induced by P65 in HEK 293T cells ($P < 0.05$) (Figure 8D). Treatment with TM significantly increased YY1 expression in macrophages, which was suppressed by FXR overexpression and enhanced by knockdown of FXR ($P < 0.05$) (Figures 8E,F).

Discussion

Excessive and sustained inflammation and ER stress will damage the health of the body, which needs to be tightly regulated. The vicious circle that exists between ER stress and inflammation could aggravate the disease and increases the difficulty of regulation. Studies in mammals and fish showed that inflammation and ER stress could be induced by high dietary levels of vegetable oils (6, 7, 14, 33) and activation of ER stress could induce inflammation (12, 13, 15). Our previous study showed that high dietary levels of soybean oil which is rich in linoleic acid (LA) could cause inflammation in the liver, head kidney, intestine and spleen of large yellow croakers (8, 22). The present study found that high dietary levels of soybean oil and LA treatment induced ER-stress markers in head kidney of croakers and macrophages. These results suggested that high LA intake could lead to inflammation and ER stress in large yellow croakers. Based on these findings, we investigated whether ER stress regulates inflammation and how ER stress is regulated by FXR. Results showed that the ER stress inducer TM significantly increased expression of pro-inflammatory genes such as TNFα, IL1β, IL6 and COX2. Meanwhile, FXR agonist CDCA supplementation decreased SO-diet-induced ER stress *in vivo*, while croaker FXR activation by ligands reduced TM-induced ER stress and inflammation in macrophages. It appears that croaker FXR may regulate ER-stress response in fish.

In order to understand FXR's role in ER stress regulation, we established macrophages stably transfected for FXR overexpression or knockdown. By overexpressing croaker FXR, the results indicated that the TM-induced expression of ER

10.3389/fnut.2022.1024631

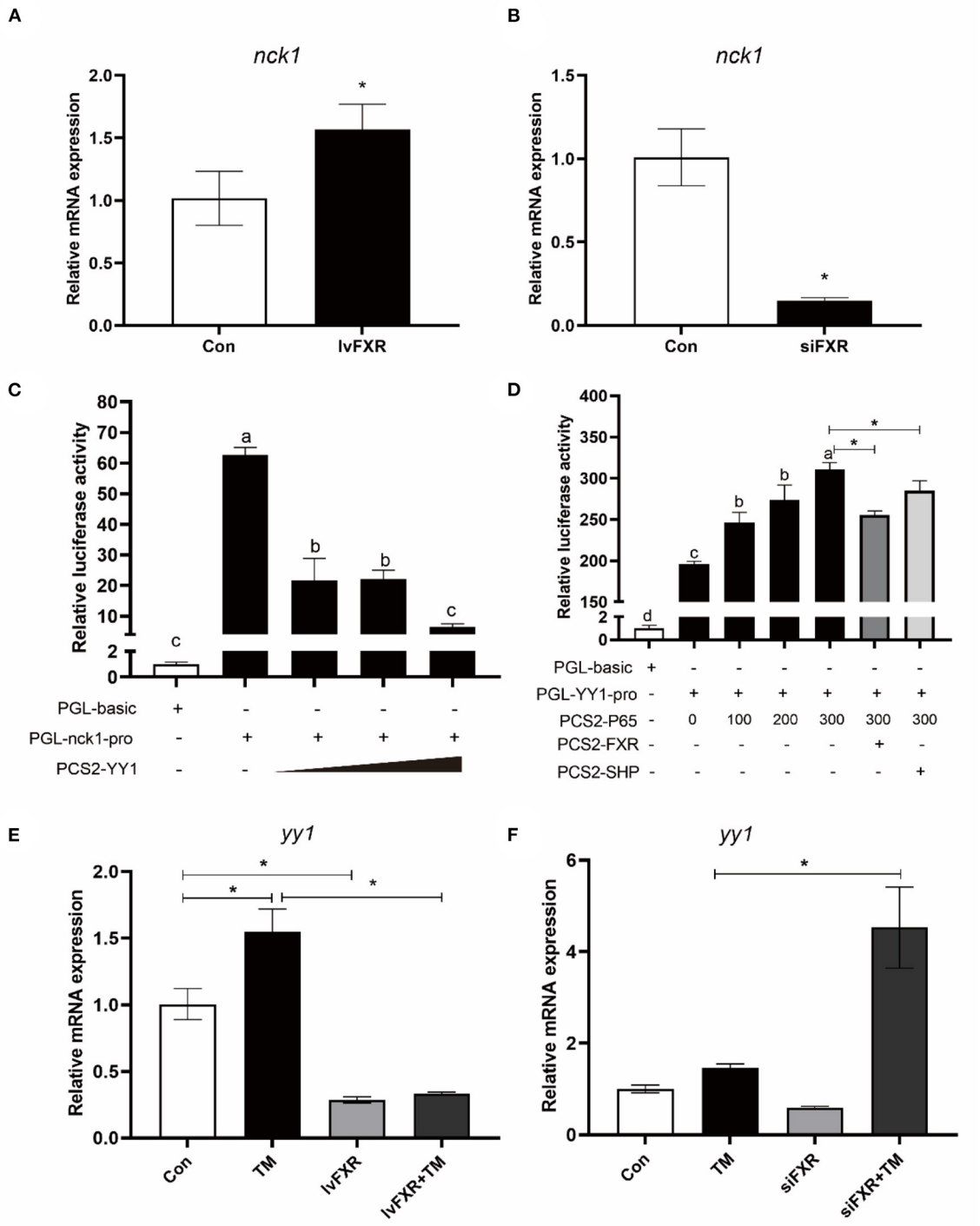

FIGURE 8
FXR regulated the expression of NCK1 *via* YY1. Effects of **(A)** FXR overexpression or **(B)** knockdown on NCK1 expression in croaker macrophages. **(C)** Relative luciferase activities of croaker NCK1 promoter in HEK 293T cells after overexpression of YY1. **(D)** Relative luciferase activities of croaker YY promoter in HEK 293T cells after overexpression of P65 and FXR. **(E,F)** Effects of FXR overexpression or knockdown on the TM-induced expression of YY1 in croaker macrophages. The significance was analyzed by one-factor ANOVA and Duncan's Multiple Range Test (means ± SEMs; $n = 3$). Means without the same label were considered different, $P < 0.05$. *Different between two groups (Student's *t*-test).

stress markers was decreased, and the IL1β and IL16 expression were inhibited. By contrast, the knockdown of FXR significantly increased mRNA and protein levels of ER-stress-related genes and the gene expression of IL1β and IL16. In mice, FXR had an inhibitory effect on ER stress, and treating mice with FXR ligands reduced the effects of ER stress on liver cells and hepatocyte death (24). According to these results, FXR might be a promising target for reducing ER stress and inflammation in fish.

Our study explored how FXR modulated ER stress and inflammation further. All three pathways (PERK, IRE1, and ATF6) triggered by ER stress have been confirmed to be involved in inflammatory signaling (10, 11). The results of our above experiment showed that FXR overexpression inhibited the TM-induced phosphorylation of PERK and EIF2α, while the knockdown of FXR enhanced the TM-induced phosphorylation of PERK and EIF2α. These results are consistent with previous findings in mice showing that FXR activation inhibited the ER-stress-activated PERK pathway (24). According to studies in mammals, autophosphorylation activates PERK, which then phosphorylates EIF2α and increases the expression of ATF4 and CHOP (10). Through activation of the PERK-EIF2α pathway, inflammation can be induced by activating the NF-κB pathway (34–36). Meanwhile, the direct binding of ATF4 to IL6 increases inflammation (37). Previous research in large yellow croakers found that ATF4 or CHOP overexpression could increase the promoter activity of TNFα, IL1β, or COX2 (15). In addition, the present results showed that FXR overexpression inhibited the TM-induced protein levels of XBP1s which was enhanced by the knockdown of FXR. The IRE1α-XBP1s pathway has been shown to participate in the regulation of inflammation (10, 38). According to these results, the activation of FXR may regulate inflammation and ER stress by affecting the PERK and IRE1α pathways in fish.

After elucidating the effect of croaker FXR on the PERK and IRE1α pathway, we investigated the underlying mechanism. Studies in mice showed that FXR could affect the expression of NCK1 which is a negative regulator of ER stress in mammals (24, 39, 40). NCK1 affects the activation of PERK and IRE1α through its interaction with them (39–41). However, a study in obese mice showed that deletion of NCK1 attenuates hepatic ER stress signaling (42). Then, we further confirmed the effect of croaker NCK1 on PERK pathway in the present study. The results showed that overexpression of croaker NCK1 in HEK 293T cells decreased the phosphorylation of croaker PERK. In croaker macrophages, the gene expression of NCK1 was decreased after TM and LA treatment or knock-down of FXR, while FXR overexpression increased the NCK1 expression. These results indicate that FXR may affect the PERK pathway by regulating the expression of NCK1. Then, we further explored how FXR affected NCK1 expression. FXR frequently functions as a transcription factor. However, an FXR binding site was not predicted in the croaker NCK1 promoter sequence. By contrast, several binding sites for YY1, which is recognized as a transcriptional repressor protein (43), were found in the croaker NCK1 promoter. In croakers, the activity of NCK1 promoter was decreased by overexpression of YY1. Previous studies in mammals have demonstrated that nuclear factor-kB P65 induced the expression of YY1 (44). Our previous research has shown that croaker FXR and its target gene SHP can inhibit P65 transcriptional activity *via* protein interaction (22). This study shows that overexpression of croaker FXR and SHP inhibited the activity of the YY1 promoter induced by P65. Moreover, FXR overexpression suppressed the TM-induced gene expression of YY1, while the knockdown of FXR enhanced Tm-induced YY1 expression. Therefore, croaker FXR may enhance NCK1 expression by suppressing P65-induced YY1 expression, which then inhibits the PERK pathway.

In conclusion, we found that FXR was a regulator of the ER-stress response in large yellow croakers. In response to FXR activation, YY1 expression is suppressed and NCK1 expression is increased, thereby inhibiting the PERK pathway. This study contributes to enriching the knowledge of FXR as a potential target for regulating ER stress and inflammation.

Data availability statement

The raw data supporting the conclusions of this article will be made available by the authors, without undue reservation.

Ethics statement

The animal study was reviewed and approved by Animal Ethics Committee of Ocean University of China.

Author contributions

JD, QA, and KM designed the research. The experiments were conducted by JD. With the help of JZ, XX, DX, and KC. Data analysis and article writing were done by JD and QA. Final approval of the manuscript was given by all authors.

Funding

Support for this study was provided by the National Natural Science Foundation of China (Grant No. 32002398), the Key Program of National Natural Science Foundation of China (Grant No. 31830103), and the Scientific and Technological Innovation of Blue Granary (Grant No. 2018YFD0900402).

Acknowledgments

The authors thank Wei Fang, Qiuchi Chen, and Jiamin Li for their participation in this study.

Conflict of interest

The authors declare that the research was conducted in the absence of any commercial or financial relationships that could be construed as a potential conflict of interest.

Publisher's note

All claims expressed in this article are solely those of the authors and do not necessarily represent those of their affiliated organizations, or those of the publisher, the editors and the reviewers. Any product that may be evaluated in this article, or claim that may be made by its manufacturer, is not guaranteed or endorsed by the publisher.

Supplementary material

The Supplementary Material for this article can be found online at: https://www.frontiersin.org/articles/10.3389/fnut.2022.1024631/full#supplementary-material

References

1. Kroemer G, Mariño G, Levine B. Autophagy and the integrated stress response. *Mol Cell.* (2010) 40:280–93. doi: 10.1016/j.molcel.2010.09.023

2. Massironi S, Rossi R, Cavalcoli F, Della Valle S, Fraquelli M, Conte D. Nutritional deficiencies in inflammatory bowel disease: therapeutic approaches. *Clin Nutr.* (2013) 32:904–10. doi: 10.1016/j.clnu.2013.03.020

3. Cigliano L, Spagnuolo M, Crescenzo R, Cancelliere R, Iannotta L, Mazzoli A, et al. Short-term fructose feeding induces inflammation and oxidative stress in the hippocampus of young and adult rats. *Mol Neurobiol.* (2018) 55:2869–83. doi: 10.1007/s12035-017-0518-2

4. Cani P, Bibiloni R, Knauf C, Waget A, Neyrinck A, Delzenne N, et al. Changes in gut microbiota control metabolic endotoxemia-induced inflammation in high-fat diet-induced obesity and diabetes in mice. *Diabetes.* (2008) 57:1470–81. doi: 10.2337/db07-1403

5. Pahwa R, Goyal A, Bansal P, Jialal I. *StatPearls: Chronic Inflammation*. Florida, USA: Treasure Island (2021).

6. Xu H, Zhang Y, Wang J, Zuo R, Mai K, Ai Q. Replacement of fish oil with linseed oil or soybean oil in feeds for Japanese seabass, *Lateolabrax japonicus* effects on growth performance, immune response, and tissue fatty acid composition. *J World Aquacult Soc.* (2015) 46:349–62. doi: 10.1111/jwas.12205

7. Montero D, Mathlouthi F, Tort L, Afonso J, Torrecillas S, Fernández-Vaquero A, et al. Replacement of dietary fish oil by vegetable oils affects humoral immunity and expression of pro-inflammatory cytokines genes in gilthead sea bream *Sparus aurata*. *Fish Shellfish Immunol.* (2010) 29:1073–81. doi: 10.1016/j.fsi.2010.08.024

8. Du J, Xiang X, Li Y, Ji R, Xu H, Mai K, et al. Molecular cloning and characterization of farnesoid X receptor from large yellow croaker (*Larimichthys crocea*) and the effect of dietary CDCA on the expression of inflammatory genes in intestine and spleen. *Comp Biochem Physiol B Biochem Mol Biol.* (2018) 216:10–7. doi: 10.1016/j.cbpb.2017.09.007

9. Montero D, Benitez-Dorta V, Caballero M, Ponce M, Torrecillas S, Izquierdo M, et al. Dietary vegetable oils: effects on the expression of immune-related genes in Senegalese sole (*Solea senegalensis*) intestine. *Fish Shellfish Immunol.* (2015) 44:100–8. doi: 10.1016/j.fsi.2015.01.020

10. Grootjans J, Kaser A, Kaufman R, Blumberg R. The unfolded protein response in immunity and inflammation. *Nat Rev Immunol.* (2016) 16:469–84. doi: 10.1038/nri.2016.62

11. Hetz C, Papa F. The Unfolded Protein Response and Cell Fate Control. *Mol Cell.* (2018) 69:169–81. doi: 10.1016/j.molcel.2017.06.017

12. Lebeaupin C, Proics E, Bieville C de, Rousseau D, Bonnafous S, Patouraux S, et al. ER stress induces NLRP3 inflammasome activation and hepatocyte death. *Cell Death Dis.* (2015) 6:e1879. doi: 10.1038/cddis.2015.248

13. Zhang K, Shen X, Wu J, Sakaki K, Saunders T, Rutkowski D, et al. Endoplasmic reticulum stress activates cleavage of CREBH to induce a systemic inflammatory response. *Cell.* (2006) 124:587–99. doi: 10.1016/j.cell.2005.11.040

14. Zhang J, Liu Q, Pang Y, Xu X, Cui K, Zhang Y, et al. Molecular cloning and the involvement of IRE1α-XBP1s signaling pathway in palmitic acid induced—Inflammation in primary hepatocytes from large yellow croaker (*Larimichthys crocea*). *Fish Shellfish Immunol.* (2020) 98:112–21. doi: 10.1016/j.fsi.2019.12.089

15. Fang W, Chen Q, Li J, Liu Y, Zhao Z, Shen Y, et al. Endoplasmic Reticulum Stress Disturbs Lipid Homeostasis and Augments Inflammation in the Intestine and Isolated Intestinal Cells of Large Yellow Croaker (*Larimichthys crocea*). *Front Immunol.* (2021) 12:738143. doi: 10.3389/fimmu.2021.738143

16. Kacheva S, Lenzen S, Gurgul-Convey E. Differential effects of proinflammatory cytokines on cell death and ER stress in insulin-secreting INS1E cells and the involvement of nitric oxide. *Cytokine.* (2011) 55:195–201. doi: 10.1016/j.cyto.2011.04.002

17. Hasnain S, Lourie R, Das I, Chen A, McGuckin M. The interplay between endoplasmic reticulum stress and inflammation. *Immunol Cell Biol.* (2012) 90:260–70. doi: 10.1038/icb.2011.112

18. Dara L, Ji C, Kaplowitz N. The contribution of endoplasmic reticulum stress to liver diseases. *Hepatology.* (2011) 53:1752–63. doi: 10.1002/hep.24279

19. Sukhorukov V, Khotina V, Bagheri Ekta M, Ivanova E, Sobenin I, Orekhov A. Endoplasmic reticulum stress in macrophages: the vicious circle of lipid accumulation and pro-inflammatory response. *Biomedicines.* (2020) 8:210. doi: 10.3390/biomedicines8070210

20. Jiao Y, Lu Y, Li X. Farnesoid X receptor: a master regulator of hepatic triglyceride and glucose homeostasis. *Acta Pharmacol Sin.* (2015) 36:44–50. doi: 10.1038/aps.2014.116

21. Wang Y, Chen W, Moore D, Huang W, FXR. a metabolic regulator and cell protector. *Cell Res.* (2008) 18:1087–95. doi: 10.1038/cr.2008.289

22. Du J, Chen Q, Li Y, Xiang X, Xu W, Mai K, et al. Activation of the Farnesoid X Receptor (FXR) suppresses linoleic acid-induced inflammation in the large yellow croaker (*Larimichthys crocea*). *J Nutr.* (2020) 150:2469–77. doi: 10.1093/jn/nxaa185

23. Du J, Xiang X, Xu D, Zhang J, Fang W, Xu W, et al. FXR, a key regulator of lipid metabolism, is inhibited by er stress-mediated activation of JNK and p38 MAPK in large yellow croakers (*Larimichthys crocea*) fed high fat diets. *Nutrients.* (2021) 13:4343. doi: 10.3390/nu13124343

24. Han C, Rho H, Kim A, Kim T, Jang K, Jun D, et al. FXR inhibits endoplasmic reticulum stress-induced NLRP3 inflammasome in hepatocytes and ameliorates liver injury. *Cell Rep.* (2018) 24:2985–99. doi: 10.1016/j.celrep.2018.07.068

25. Xiong X, Wang X, Lu Y, Wang E, Zhang Z, Yang J, et al. Hepatic steatosis exacerbated by endoplasmic reticulum stress-mediated downregulation of FXR in aging mice. *J Hepatol.* (2014) 60:847–54. doi: 10.1016/j.jhep.2013.12.003

26. Tan P, Dong X, Mai K, Xu W, Ai Q. Vegetable oil induced inflammatory response by altering TLR-NF-κB signalling, macrophages infiltration and polarization in adipose tissue of large yellow croaker (*Larimichthys crocea*). *Fish Shellfish Immunol.* (2016) 59:398–405. doi: 10.1016/j.fsi.2016.11.009

27. Li X, Ji R, Cui K, Chen Q, Chen Q, Fang W, et al. High percentage of dietary palm oil suppressed growth and antioxidant capacity and induced the inflammation by activation of TLR-NF-κB signaling pathway in large yellow croaker (*Larimichthys crocea*). *Fish Shellfish Immunol.* (2019) 87:600–8. doi: 10.1016/j.fsi.2019.01.055

28. Cui K, Li Q, Xu D, Zhang J, Gao S, Xu W, et al. Establishment and characterization of two head kidney macrophage cell lines from large yellow croaker (*Larimichthys crocea*). *Dev Comp Immunol.* (2020) 102:103477. doi: 10.1016/j.dci.2019.103477

29. Li Q, Cui K, Wu M, Xu D, Mai K, Ai Q. Polyunsaturated fatty acids influence LPS-induced inflammation of fish macrophages through differential modulation of pathogen recognition and p38 MAPK/NF-κB Signaling. *Front Immunol.* (2020) 11:559332. doi: 10.3389/fimmu.2020.559332

30. Wu M, Li Q, Mai K, Ai Q. Regulation of Free Fatty Acid Receptor 4 on Inflammatory Gene Induced by LPS in Large Yellow Croaker (*Larimichthys crocea*). *Front Immunol.* (2021) 12:703914. doi: 10.3389/fimmu.2021.703914

31. Du J, Xu H, Li S, Cai Z, Mai K, Ai Q. Effects of dietary chenodeoxycholic acid on growth performance, body composition and related gene expression in large yellow croaker (*Larimichthys crocea*) fed diets with high replacement of fish oil with soybean oil. *Aquaculture.* (2017) 479:584–90. doi: 10.1016/j.aquaculture.2017.06.023

32. Livak K, Schmittgen T. Analysis of relative gene expression data using real-time quantitative PCR and the 2(-Delta Delta C(T)) Method. *Methods.* (2001) 25:402–8. doi: 10.1006/meth.2001.1262

33. Nivala A, Reese L, Frye M, Gentile C, Pagliassotti M. Fatty acid-mediated endoplasmic reticulum stress in vivo: differential response to the infusion of Soybean and Lard Oil in rats. *Metabolism.* (2013) 62:753–60. doi: 10.1016/j.metabol.2012.12.001

34. Deng J, Lu P, Zhang Y, Scheuner D, Kaufman R, Sonenberg N, et al. Translational repression mediates activation of nuclear factor kappa B by phosphorylated translation initiation factor 2. *Mol Cell Biol.* (2004) 24:10161–8. doi: 10.1128/MCB.24.23.10161-10168.2004

35. Guthrie L, Abiraman K, Plyler E, Sprenkle N, Gibson S, McFarland B, et al. Attenuation of PKR-like ER Kinase (PERK) signaling selectively controls endoplasmic reticulum stress-induced inflammation without compromising immunological responses. *J Biol Chem.* (2016) 291:15830–40. doi: 10.1074/jbc.M116.738021

36. Jiang H-Y, Wek S, McGrath B, Scheuner D, Kaufman R, Cavener D, et al. Phosphorylation of the alpha subunit of eukaryotic initiation factor 2 is required for activation of NF-kappaB in response to diverse cellular stresses. *Mol Cell Biol.* (2003) 23:5651–63. doi: 10.1128/MCB.23.16.5651-5663.2003

37. Iwasaki Y, Suganami T, Hachiya R, Shirakawa I, Kim-Saijo M, Tanaka M, et al. Activating transcription factor 4 links metabolic stress to interleukin-6 expression in macrophages. *Diabetes.* (2014) 63:152–61. doi: 10.2337/db13-0757

38. Kaneko M, Niinuma Y, Nomura Y. Activation signal of nuclear factor-kappa B in response to endoplasmic reticulum stress is transduced via IRE1 and tumor necrosis factor receptor-associated factor 2. *Biol Pharm Bull.* (2003) 26:931–5. doi: 10.1248/bpb.26.931

39. Yamani L, Latreille M, Larose L. Interaction of Nck1 and PERK phosphorylated at $Y56^{1}$ negatively modulates PERK activity and PERK regulation of pancreatic β-cell proinsulin content. *Mol Biol Cell.* (2014) 25:702–11. doi: 10.1091/mbc.e13-09-0511

40. Kebache S, Cardin E, Nguyên D, Chevet E, Larose L. Nck-1 antagonizes the endoplasmic reticulum stress-induced inhibition of translation. *J Biol Chem.* (2004) 279:9662–71. doi: 10.1074/jbc.M310535200

41. Nguyên D, Kebache S, Fazel A, Wong H, Jenna S, Emadali A, et al. Nck-dependent activation of extracellular signal-regulated kinase-1 and regulation of cell survival during endoplasmic reticulum stress. *Mol Biol Cell.* (2004) 15:4248–60. doi: 10.1091/mbc.e03-11-0851

42. Yamani L, Li B, Larose L. Nck1 deficiency improves pancreatic β cell survival to diabetes-relevant stresses by modulating PERK activation and signaling. *Cell Signal.* (2015) 27:2555–67. doi: 10.1016/j.cellsig.2015.09.016

43. Verheul T, van Hijfte L, Perenthaler E, Barakat T. The Why of YY1: Mechanisms of Transcriptional Regulation by Yin Yang 1. *Front Cell Dev Biol.* (2020) 8:592164. doi: 10.3389/fcell.2020.592164

44. Wang H, Hertlein E, Bakkar N, Sun H, Acharyya S, Wang J, et al. NF-kappaB regulation of YY1 inhibits skeletal myogenesis through transcriptional silencing of myofibrillar genes. *Mol Cell Biol.* (2007) 27:4374–87. doi: 10.1128/MCB.02020-06

frontiers | Frontiers in Nutrition

TYPE Systematic Review
PUBLISHED 01 December 2022
DOI 10.3389/fnut.2022.1009666

OPEN ACCESS

EDITED BY
Nada Rotovnik Kozjek,
Institute of Oncology Ljubljana, Slovenia

REVIEWED BY
Mohanchandra Mandal,
Institute of Post Graduate Medical Education and Research, India
Samuele Ceruti,
Clinica Luganese Moncucco, Switzerland

*CORRESPONDENCE
Xinjuan Wu
wuxinjuan@sina.com

SPECIALTY SECTION
This article was submitted to Clinical Nutrition, a section of the journal Frontiers in Nutrition

RECEIVED 02 August 2022
ACCEPTED 18 November 2022
PUBLISHED 01 December 2022

CITATION
Li J, Sun X and Wu X (2022) Effects of implementation strategies aimed at improving high-value verification methods of nasogastric tube placement: A systematic review. *Front. Nutr.* 9:1009666. doi: 10.3389/fnut.2022.1009666

Effects of implementation strategies aimed at improving high-value verification methods of nasogastric tube placement: A systematic review

Jiamin Li, Xiangyu Sun and Xinjuan Wu*

Department of Nursing, Chinese Academy of Medical Sciences and Peking Union Medical College, Peking Union Medical College Hospital, Beijing, China

Background: X-ray and pH testing, which clinical practice guidelines have proven to be effective in determining nasogastric tube (NGT) placement, were named the high-value methods. Implementation strategies can help to integrate high-value methods into particular contexts. The aim of this systematic review was to summarize the evidence of implementation strategies aimed at improving high-value verification methods of NGT placement.

Methods: PubMed, ProQuest, and CINAHL were searched until June 2022. The Cochrane Effective Practice and Organization of Care (EPOC) taxonomy was used to categorize implementation strategies.

Results: The initial search identified 1,623 records. Of these, 64 full-text studies were reviewed. Finally, 12 studies were included and used for qualitative synthesis. Eleven studies used an education component as an implementation strategy. Only one study based their implementation strategy on a barriers and facilitators assessment. None of the studies reported enough detail of the implementation strategy used in their studies. Seven studies were eligible for inclusion in the meta-analysis. Three of these seven studies revealed a significant improvement of the high-value method after strategy implementation. As heterogeneity was present in the high level, the pooled effect estimated was not calculated.

Conclusion: Most studies used an implementation strategy with an educational component. Unfortunately, no conclusion can be drawn about which strategy is most effective for improving high-value verification methods of NGT placement due to a high level of heterogeneity and

a lack of studies. We recommend that future studies fully connect their implementation strategies to influencing factors and better report the details of implementation strategies.

Systematic review registration: [www.crd.york.ac.uk/PROSPERO/], identifier [CRD42022349997].

KEYWORDS

implementation strategies, high-value, verification methods, nasogastric tube placement, systematic review

Introduction

Nasogastric tubes (NGT) are widely used to deliver food to patients. Over 790,000 NGT are used in the National Health Service (NHS) each year (1). Most of the time, nurses at the beside insert these tubes blindly, while this is generally considered a reasonably harmless practice, it is not. During the insertion procedures, the NGT can easily misplace into the respiratory tract, often leading to serious consequences if the misplace is not recognized before feedings are provided. These problems tend to occur, especially in patients undergoing sedation and intubation, when the cough reflex has been abolished (2), with a high incidence of complications during NGT positioning (3). According to the NHS report (1), in an approximate 5-year period, there were 95 cases of feed being injected into the respiratory tract. The patient is mentioned as having died in 32 of these cases, although this is not always obvious if the death was directly connected, considering that several patients were critically ill before the NGT was inserted.

To avoid serious events of NGT being inadvertently positioned, it is necessary to determine NGT placement. Methods to identify NGT placement mainly include radiography, aspirate pH, auscultation and aspirate appearance. However, several guidelines (4–6) state that auscultation methods should be avoided completely because air introduced *via* the tube can be heard in a number of bodily regions. It is insufficient to distinct between NGT location in the stomach and respiratory tracts. Observing aspirate appearance as a sign of correct NGT placement is against by guidelines (1, 5, 6) because the appearance of aspirates from the stomach and respiratory tract appear to overlap. These methods, which have been shown to be ineffective, can potentially hurt patients and waste precious resources, were named low-value care (7). While a method in which evidence has proven to be effective and beneficial to patients is called high-value care (8). There is general consensus among all guidelines that an X-ray, when correctly taken and read, is the most precise method for differentiating between the placement of an NGT in the gastric and respiratory tract (9). Aspirate pH is a distinct difference between fasting gastric juice and respiratory tract aspirates. Compared to X-ray, pH testing of aspirates is cost-effective. Several guidelines (1, 6) suggest that aspirate pH can be used as the first-line test to identify NGT placement. Thus, X-ray and aspirate pH, which are suggested by evidence, are high-value verification methods of NGT placement.

However, high-value verification methods of NGT placement are not always used in practice. Recent surveys showed that only 11% of critical nurses use the pH method to identify NGT placement (10); only 26.9% of nurses chose X-ray as the gold standard (11). Implementation research can help to address the challenge between high-value care and clinical practice. Implementation strategies are central to implementation research, which is defined as "the study of strategies to integrate evidence-based interventions into particular contexts" (12). Including the particular means or methods for adopting and maintaining evidence-based intervention (13), e.g., education, reminders, audit, and feedback. These implementation strategies should be determined by an assessment of the barriers and facilitators that impact high-value care because it is considered to promote the compliance, acceptance, and effectiveness of these implementation strategies (14, 15). Descriptions of implementation strategies (e.g., actor, action, action goal, and dosage) must be specific and clear enough to support repeatability in both research and practice, similar to all intervention studies (16). To improve the high-value verification methods of NGT placement, many implementation strategies have been performed in some studies (17, 18). However, an understanding of implementation strategies aimed at improving high-value verification methods of NGT placement and the effectiveness of these different strategies is lacking. Therefore, the purpose of this systematic review is to summarize the evidence of implementation strategies that have been used to improve high-value verification methods of NGT placement.

Methods

This systematic review was conducted according to the Preferred Reporting Items for Systematic Reviews and Meta-analyses (PRISMA) statement. This systematic review protocol was registered in PROSPERO (number: CRD42022349997). The

PICO (population, intervention, comparison, and outcome) used to guide this review was as follows. P: the medical worker who determined NGT placement; I: implementation strategy aimed to improve high-value verification methods of NGT placement; C: without an implementation strategy; and O: effect on the volume of the high-value verification method of NGT placement.

Search strategies

To find all relevant studies that focus on implementation strategies aiming to improve high-value verification methods of NGT placement, a systematic literature search was performed in the PubMed, ProQuest, and CINAHL electronic databases. The search strategies were tailored to the characteristics of each database using the following medical subject headings (MeSH) or keywords as search terms: "enteral nutrition," "nasogastric," "tube," "intubate," "pH," "X-ray," "radiograph," "evidence-based practice," "quality improvement," and "implement." The search was restricted to the studies released until June 2022. Other search filter restrictions were not implemented. An expert health librarian guided the search. An example PubMed search is as follows: (("enteral nutrition"[Mesh]) OR ("enteral nutrition"[TI/AB]) OR ("nasogastric"[TI/AB])) AND (("tube*"[TI/AB]) OR ("intubat*"[TI/AB])) AND (("pH"[TI/AB]) OR ("X-ray*"[TI/AB]) OR ("radiograph"[TI/AB])) AND (("evidence-based practice"[Mesh]) OR ("evidence-based practice"[TI/AB]) OR ("implement*"[TI/AB]) OR ("quality improvement"[Mesh]) OR ("quality improvement" [TI/AB])).

Selection of studies

All search results were imported into Endnote (version X9). Two authors (A and B) independently screened the titles and abstracts after eliminating duplicates. For relevant records, full-text versions of manuscripts were acquired and screened. In these processes, disparities that could not be resolved by discussion between the two reviewers were resolved with the help of the third author (C). The high-value verification method of NGT placement was defined as a method that has been proven effective and benefits the patient by evidence. In this review, high-value verification methods of NGT placement refer to pH testing and X-ray. The following criteria were used to determine study eligibility in this systematic review.

a) Study type: Any study that includes a control group, such as randomized controlled trial (RCT), cluster RCT, quasi-RCT, non-RCT, before-after study.
b) Setting: Hospitals, community settings, long-term care facilities, and nursing homes.
c) Outcome: The study had to report on the effect of the implementation strategy on the volume of the high-value verification method of NGT placement.
d) Language: English language articles.

Animal studies, letters, case studies, and editorials were not included. The meta-analysis included studies with available data.

Quality evaluation

The quality of the studies was assessed using "the Joanna Briggs Institute Meta-Analysis of Statistics Assessment and Review Instrument standardized critical appraisal instrument (JBI MAStARI) for quasi-experimental studies" (19) by two independent authors (A and B). This instrument is made up of nine items: cause effect clear, participants similar, similar care other than intervention, control group, multiple measurements, follow-up, standardized measurement, reliable measurement, and statistical analysis. Those items can be rated yes, no, unclear, or not applicable. A point is given if the item is selected as "yes." Disparities in the scores were addressed by consensus between two reviewers or by discussion with a third researcher (C).

Data extraction

Data from the included studies were extracted by one researcher (A) using a self-designed standardized data extraction tool. A second researcher (B) verified the extracted data independently. Any disagreements were settled by discussion among the researchers until agreement was obtained. If this was not attainable, a third researcher (C) made a decision based on the information provided. Information about country, design, type of high-value method, implementation strategy, barriers and facilitators assessment, target population, and outcome was collected from all included studies. The outcome refers to the change in volume of the high-value verification method of NGT placement (e.g., use rate, score).

The implementation strategies were categorized using the "Cochrane Effective Practice and Organization of Care (EPOC)" taxonomy. The EPOC taxonomy includes implementation strategies, governance arrangements, financial arrangements, and delivery arrangements 4 main domains and more than 100 subcategories, such as education, reminders, organizational culture, audit and feedback.

Statistical analysis

The information from all included studies was extracted and summarized to present a descriptive and narrative synthesis of the overall evidence of implementation strategies

aimed at improving the high-value verification method of NGT placement.

The results are shown in forest plots created with Review Manager 5.4 to help evaluate the efficacy of implementation strategies. Mantel-Haenszel's random effects model was used to pool the data, and relative risk (RR) and 95% confidence intervals were computed. To assess the degree of heterogeneity among the included studies, the I^2 statistics of Higgins were utilized. We could see the results as indicating a moderate to high level of heterogeneity when the I^2 was 50% or above. Subgroup analyses were carried out in cases of heterogeneity. Subgroup analyses were conducted based on the type of implementation strategy (type of strategy according to EPOC taxonomy and single vs. multifaceted) and type of high-value verification method of NGT placement (X or pH). We conducted subgroup analysis for the type of implementation strategy to determine which strategy was more advanced. We conducted subgroup analysis for the type of high-value verification method of NGT placement since the factors (e.g., supporting evidence, credibility, and feasibility) of the implemented high-value method might influence the effectiveness of the implementation strategy. A subgroup analysis was only carried out when at least two studies with, respectively, the same implementation strategy or same high-value method could be included in each subgroup. When $I^2 > 50\%$ after subgroup analysis, the pooled effect estimate was not performed. When very few studies for a similar result were found, funnel plot analysis, which helps to explore the problem of publication bias, would not be carried out.

Results

Search and screening results

Electronic databases yielded 1,623 records, and 291 duplicates were then deleted. Sixty-four full-text studies were obtained and screened after the titles and abstracts were screened, and 52 were excluded. Finally, 12 articles (17, 18, 20–29) were included and used for qualitative synthesis in this review (**Figure 1**). The excluded articles were due to (1) studies that did not have a reference group ($n = 23$), (2) studies that did not include implementation strategies to improve high-value verification methods of NGT placement ($n = 16$), and (3) other (e.g., full text was not available, no outcomes showed on the volume of the high-value method, combined results of pH/X and other methods) ($n = 13$).

Quality of the included studies

Table 1 shows the risk of bias of the 12 included studies evaluated by the JBI MAStARI tool. Generally, the included studies were moderate quality. All studies obtained a score ranging from 5 to 8 (in a whole range of 0–9). Three studies obtained a score of 5 (23, 25, 28). Two studies obtained a score of 6 (20, 27). Five studies obtained a score of 7 (17, 21, 22, 24, 29). Two studies obtained a score of 8 (18, 26). Most studies did not obtain a high score, which was primarily the result of a low score on the "establishment control group" and "outcome measured in a reliable way" items.

Characteristics of the included studies

In this review, the 12 included studies were published between 2006 and 2019 (**Table 2**). All included studies used a quasi-experimental design. Of these, eleven studies used a before-after design. Most studies were performed in the United States (USA) ($n = 4$) (17, 22, 25, 28) and the United Kingdom (UK) ($n = 4$) (20, 23, 24, 27). Of the 12 included studies, three focused their implementation strategy on improving pH testing (17, 26, 29), three on improving X-ray (23–25), and six on improving these two methods (18, 20–22, 27, 28). Of the 9 studies (17, 18, 20–22, 26–29) that used pH testing, four used a pH level of 5.5 as the cutoff point (20, 26, 27, 29), three used a pH level of 5 as the cutoff point (17, 18, 22), one used a pH value of 4 as the cutoff point (28), and one used a pH value of 6 as the cutoff point (21). The implementation strategy used was directed at nurses ($n = 7$) (17, 18, 21, 22, 25, 26, 28), doctors ($n = 2$) (23, 27), radiographers ($n = 1$) (24), and multidisciplinary staff ($n = 2$) (20, 29).

Strategies to improve high-value methods

Ten of 12 included studies had multifaceted implementation strategies (17, 20–23, 25–29) (**Table 2**). The other two studies had a single implementation strategy (18, 24), which indicates that there was only one strategy component found in the implementation strategies. A total of 18 kinds of implementation strategies were used by the included studies. Education (materials, meetings, and games) is the most commonly used strategy. Eleven of the 12 included studies used an education component as an implementation strategy (17, 18, 20, 21, 23–29). Half of the studies used audit and feedback as an implementation strategy (17, 21–23, 26, 28). Health information systems, reminders, and packages of care strategies were used separately by one-third of the included studies. Local consensus processes and organizational culture were used separately by three and two studies. The other 11 kinds of implementation strategies were used by only one study. However, only one of 12 included studies based their implementation strategy on barriers and facilitators assessment (29). Additionally, none of the included studies

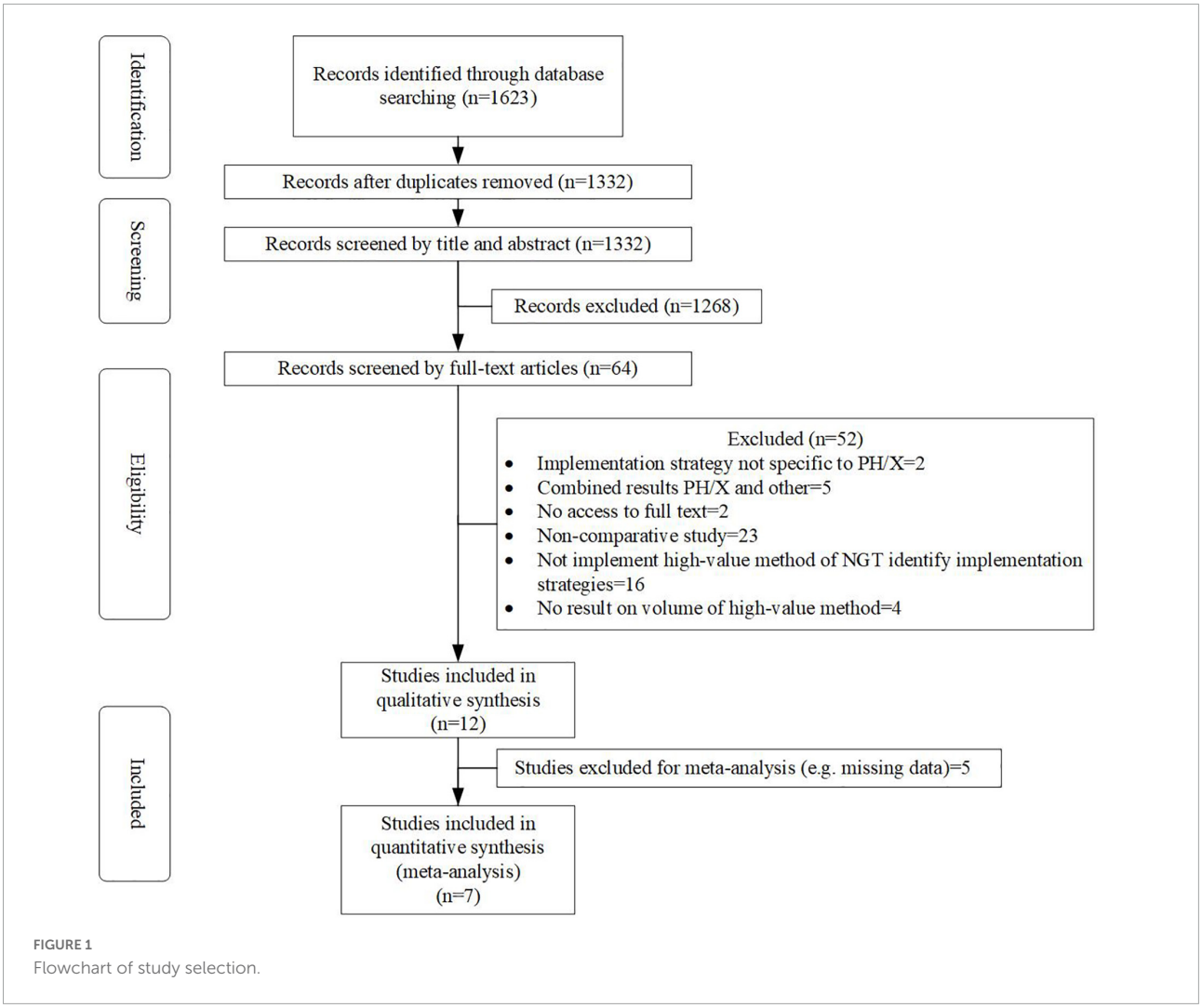

FIGURE 1
Flowchart of study selection.

TABLE 1 Results of critical appraisal (n = 12).

References	Q1	Q2	Q3	Q4	Q5	Q6	Q7	Q8	Q9	Score
Kisting et al. (17)	Yes	Yes	Yes	No	Yes	Yes	Yes	Unclear	Yes	7
Roe et al. (24)	Yes	Yes	Yes	No	Yes	Yes	Yes	Unclear	Yes	7
Guerrero et al. (18)	Yes	Yes	Yes	No	Yes	Yes	Yes	Yes	Yes	8
Cole (20)	Yes	Unclear	Yes	Yes	No	Yes	Yes	Unclear	Yes	6
Law et al. (23)	Yes	Yes	Yes	No	No	Not applicable	Yes	Unclear	Yes	5
Tho et al. (21)	Yes	Yes	Yes	No	Yes	Yes	Yes	Unclear	Yes	7
Richardson et al. (22)	No	Yes	Yes	Yes	No	Yes	Yes	Yes	Yes	7
Taylor et al. (29)	Yes	Yes	Yes	No	Yes	Yes	Yes	Unclear	Yes	7
Lee et al. (27)	Yes	Yes	Yes	No	Yes	Not applicable	Yes	Unclear	Yes	6
Farrington et al. (28)	Yes	Yes	Yes	No	No	Unclear	Yes	Unclear	Yes	5
Kenny and Goodman (25)	Yes	Unclear	Yes	No	Yes	Not applicable	Yes	Unclear	Yes	5
Yang et al. (26)	Yes	Yes	Unclear	Yes	Yes	Yes	Yes	Yes	Yes	8

reported enough detail of each implementation strategy used in the studies. Relatively, details of education (meetings, materials, games, and outreach visits) strategy get the clearest reported than other strategies. There are three studies (18, 21, 24) have clearly described the period of the education strategy. It differed from 30 to 90 min. Other details (e.g.,

TABLE 2 Characteristics of the included studies (n = 12).

References	Country	Design	Type of high-value method	Implementation strategy (sorted by EPOC taxonomy)	Barriers and facilitators identified (Yes/No)	Target group	Outcome	Before	After	Difference	Statistical analyses (Yes/No)	$P \leq 0.05$ (Yes/No)
Kisting et al. (17)	USA	Before-after	pH	Education; audit and feedback; local opinion leaders; health information system	No	Nurses	The use rate of pH	8/71 (11.3%)	59/64 (92.2%)	80.9%	No	–
Roe et al. (24)	UK	Before-after	X	Education	No	Radiographers	The rate of confidence in image interpretation	58/98 (59.2%)	96/98 (98.0%)	38.8%	Yes	Yes
Guerrero et al. (18)	Spain	Before-after	pH; X	Education	No	Nurses	The use rate of pH	42/553 (7.6%)	133/245 (54.3%)	46.7%	Yes	Yes
Cole (20)	UK	Before-after	pH or X	Education; reminders; health information system; packages of care	No	Nurses, doctors	The use rate of pH /X	4/13 (31%)	9/12 (75%)	44.0%	No	–
Law et al. (23)	UK	Before-after	X	Education; organizational culture; audit and feedback; health information system; packages of care	No	Doctors	The accuracy of image interpretation	185/192 (96%)	199/200 (99.5%)	3.5%	No	–
Tho et al. (21)	Singapore	Before-after	pH; X	Education; local consensus processes; clinical practice guidelines; audit and feedback; packages of care	No	Nurses	The use rate of pH (X for special cases)	22/26 (84.6%)	40/46 (87%)	2.4%	No	–
Richardson et al. (22)	USA	Before-after	pH; X	Audit and feedback; continuous quality improvement; interprofessional education; local consensus processes; managerial supervision; stakeholder involvement in policy decisions	No	Nurses	The use rate of pH (X for special cases)	12/15 (80%)	20/20 (100%)	20%	No	–

(Continued)

10.3389/fnut.2022.1009666

TABLE 2 (Continued)

References	Country	Design	Type of high-value method	Implementation strategy (sorted by EPOC taxonomy)	Barriers and facilitators identified (Yes/No)	Target group	Outcome	Before	After	Difference	Statistical analyses (Yes/No)	$P \leq 0.05$ (Yes/No)
Taylor et al. (29)*	Australia	Before-after	pH	Education; organizational culture; reminders; tailored intervention; staffing models; community mobilization; packages of care	Yes	Nurses, doctors, dieticians	The use rate of pH as first-line (Median)	11%	60%	49%	No	–
Lee et al. (27)*	UK	Before-after	pH; X	Education; reminders	No	Doctors	The accuracy of knowledge	3%	33%	30%	No	–
Farrington et al. (28)*	USA	Before-after	pH; X	Education; audit and feedback; health information system; local opinion leaders; reminders; communities of practice; monitoring the performance of the delivery of healthcare	No	Nurses	The use rate of pH	18%	52.8%	34.8%	No	–
Kenny and Goodman (25)*	USA	Before-after	X	Education; reminders	No	Nurses	Knowledge score (Mean, standard deviation)	0.62 (0.48)	0.71 (0.46)	0.09	Yes	No
Yang et al. (26)*	China	Non-RCT	pH	Education, audit and feedback; reminders; local consensus processes	No	Nurses	Knowledge score (Mean)	4.1	5.2	1.1	No	–

*Result not used for meta-analysis.

10.3389/fnut.2022.1009666

actor, action, justification) of the education strategy were not described.

Different outcome measurements of implementation strategy were used by the included studies (**Table 2**), which included the use rate of pH/X (n = 7) (17, 18, 20–22, 28, 29), the accuracy of knowledge (n = 1) (27), the accuracy of image interpretation (n = 1) (23), the rate of confidence in image interpretation (n = 1) (24) and knowledge score (n = 2) (25, 26). Outcome measurements about contextual factors (e.g., cost, appropriateness) were not found in these studies. The improvement in volume of the high-value method ranged from 2.4 (21) to 80.9% (17) (n = 10) and from a score of 0.09 (25) to 1.1 (26) (n = 2). Three studies (18, 24, 25) performed statistical analysis; of these, two studies (18, 24) had a positive significant effect on the volume of the high-value method. These two positive significant studies (18, 24) had a single implementation strategy.

Effectiveness of implementation strategies (meta-analysis)

Seven (17, 18, 20–24) of the 12 included studies were eligible for inclusion in the meta-analysis (**Figure 1**). Four studies (26–29) were excluded because of missing data, and one study (25) was excluded because outcomes could not be calculated with other studies (**Table 2**).

Seven studies (17, 18, 20–24) included for meta-analysis used the rate of the high-value method as outcome measurements. A forest plot is used to display the data and computed RR (**Figure 2**). Considerable heterogeneity was present in the high level among the seven studies. Subgroup analyses were performed for the type of implementation strategy and type of high-value verification method of NGT placement. As heterogeneity was still large after subgroup analyses, we did not calculate a pooled effect estimated. Of seven studies (17, 18, 20–24), three studies (17, 18, 24) revealed a significant improvement in the high-value method after strategy implementation. The RR for these three studies was 8.18 [95% CI 4.24, 15.78] (17), 7.15 [95% CI 5.23, 9.77] (18), and 1.66 [95% CI 1.40, 1.96] (24), respectively. The other four studies showed a nonsignificant small (20) or no improvement (21–23) of the high-value NGT placement verification method.

Discussion

To the best of our knowledge, the current study is the first systematic review on implementation strategies for high-value verification methods of NGT placement. This review identifies X-ray and pH as high-value verification methods of NGT placement based on current evidence (1, 6, 9). As research progresses, a future device capable of combining the presence of two separate methods (such as CO_2 and pH) could have higher diagnostic accuracy in identifying the correct positioning of NGT (30). This "combined" method may substitute for pH testing and become a high-value confirmation method of NGT placement in the future.

The majority of the included studies were conducted in the USA and the UK. The reason may be that the problem of NGT misplacement has prompted high concern by these two countries. For example, NGT misplacement has been classified as a warning incident by the Joint Commission of Healthcare Organizations in the USA (31). Similarly, NGT misplacement was identified as one of the original eight "never events" by the National Patient Safety Agency (NASP) in the UK (32).

The design of almost all studies was quasi-experimental. The goal of implementation science is to increase the adoption, application, and sustainability of effective healthcare practices by physicians, hospitals, and systems (33). Politicians or managers may be unwilling in certain implementation science settings to have a portion of engaged patients or locations randomized to a controlled group, particularly for high-profile or high-urgency clinical situations. In these circumstances, quasi-experimental designs enable implementation scientists to perform robust analyses, although the type of study design has intrinsic limitations (33). To give academics increasingly reliable and practical methods for responding to important implementation science questions, design innovations are still needed.

The included studies used different pH values as the cutoff point to determine NGT placement. Several studies have been published in the literature investigating the diagnostic accuracy of different pH cutoff points to distinguish between gastric and other placement (30, 34). However, there is still much indecision regarding the best cutoff point for pH at the present time (9). Moreover, the pH method has some limitations; for example, gastric acid inhibiting medications (such as proton pump inhibitors) elevate gastric pH and make it more difficult to determine NGT placement on the basis of pH testing (9). Therefore, even though the pH method has several advantages, such as reducing the need for costly X-ray, and being easy to apply, the use of this method should be cautious about identifying the pH cutoff level in clinical practice.

The educational component (materials, meetings, and games) is the most common implementation strategy among almost all studies. This is similar to other systematic reviews of implementation studies (35). However, given that both studies with a significant beneficial effect and studies without an effect contained an educational component, there can be no direct correlation between the incorporation of education components and successful implementation. Multifaceted implementation strategies were not more

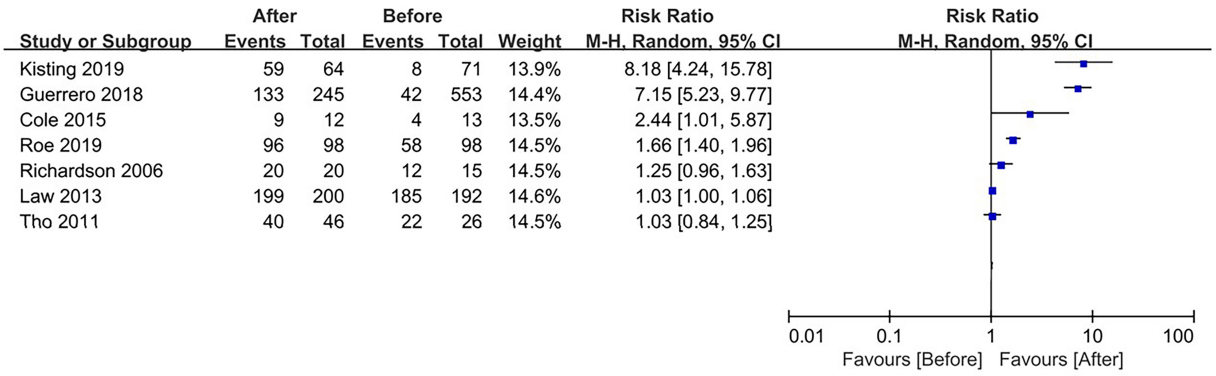

FIGURE 2
Forest plot for the effect of the implementation strategy.

effective than a single implementation strategy in this review. Two studies (18, 24) had a single implementation strategy among three studies (17, 18, 24), which revealed a significant improvement in the high-value method after strategy implementation. This may be because multiple strategies can be mutually exclusive. More research focusing on optimal combinations and interactions of implementation strategies is needed.

Using an implementation strategy based on barriers and facilitators assessment was recommended to boost the efficacy of implementation strategies (14, 15). However, the results show that only one study (29) included in this review assessed the barriers and facilitators prior to creating the implementation strategy, and the study (29) showed a 50% improvement of the high-value identification method (no statistical testing). Ineffective implementation strategies in this review may have been caused by a lack of assessment of barriers and facilitators impacting the implementation of the high-value verification methods of NGT placement. Future implementation studies should consider the determinants when determining an implementation strategy.

Additionally, none of the studies included sufficient details on implementation strategy. Specification limitations raise important issues that hinder repeatability in both practice and research. Similar to all intervention research, the implementation strategies must be thoroughly and accurately stated, such as action target, dose and temporality (16). There are some relevant guidelines that might help authors (16, 36, 37) describe and report implementation strategies.

The interstudy heterogeneity hindered the meta-analysis in our review, which is consistent with other systematic reviews addressing the effectiveness of implementation strategies to change healthcare (38). The included studies varied mainly in terms of implementation strategies, target populations, outcome indicators and countries. More studies that explore the effect of implementation strategies aimed at improving high-value verification methods of NGT placement are needed. Implementation also necessitates consideration of a variety of critical contextual issues, such as service system and provider attitudes. Implementation outcomes also need to include provider attitudes (acceptability) and contextual factors (penetration, appropriateness, cost) (39). Therefore, to assist in explaining the mechanisms and causal links within implementation processes and advance an evidence base around successful implementation, future research should also concentrate on analyzing additional outcomes in addition to the efficacy of implementation strategies (39).

Strengths and limitations

The search strategies in the current review were designed with the help of an experienced librarian. This ensured that the search strategies were professional, comprehensive, and effective. However, some relevant articles were likely to have been overlooked because of language or publication restrictions. In addition, due to missing data, not all studies could be included in the meta-analysis.

Conclusion

Most studies used the educational component as an implementation strategy. However, no conclusion can be drawn on the most effective implementation strategy for improving high-value verification methods of NGT placement because of a lack of studies and the high level of heterogeneity. Future research is required to determine whether implementation strategies are more successful for implementation if they completely link their strategy to the barriers and facilitators. To

enable reproducibility in both practice and research, the details of implementation strategies need to be reported.

Data availability statement

The original contributions presented in this study are included in the article/supplementary material, further inquiries can be directed to the corresponding author.

Author contributions

XW: conception, study design, execution, acquisition of data, analysis and interpretation, and substantially revised or critically reviewed the article. JL: conception, study design, execution, acquisition of data, analysis and interpretation, and drafted or written. XS: study design, execution, acquisition of data, and analysis and interpretation. All authors contributed to data analysis, drafting or revising the article, agreed on the journal to which the article will be submitted, gave final approval of the version to be published, and agreed to be accountable for all aspects of the work.

Conflict of interest

The authors declare that the research was conducted in the absence of any commercial or financial relationships that could be construed as a potential conflict of interest.

Publisher's note

All claims expressed in this article are solely those of the authors and do not necessarily represent those of their affiliated organizations, or those of the publisher, the editors and the reviewers. Any product that may be evaluated in this article, or claim that may be made by its manufacturer, is not guaranteed or endorsed by the publisher.

References

1. National Health Service [NHS]. *Resource set: initial placement checks fornasogastric and orogastric tubes.* (2016). Available online at: https://improvement.nhs.uk/documents/193/Resource_set__Initial_placement_checks_for_NG_tubes_1.pdf. (accessed June 20, 2022).

2. Sanaie S, Mahmoodpoor A, Najafi M. Nasogastric tube insertion in anaesthetized patients: a comprehensive review. *Anaesthe Int Ther.* (2017) 49:57–65.

3. Harris MR, Huseby JS. Pulmonary complications from nasoenteral feeding tube insertion in an intensive care unit: incidence and prevention. *Crit Care Med.* (1989) 17:917–9. doi: 10.1097/00003246-198909000-00016

4. Metheny N. Initial and ongoing verification of feeding tube placement in adults (applies to blind insertions and placements with an electromagnetic device). *Crit Care Nurse.* (2016) 36:e8–13. doi: 10.4037/ccn2016141

5. New South Wales (NSW) Government Health. *Infants and children insertion and confirmation of placement of nasogastric and orogastric tubes; GL2016_006.* (2016). Available online at: https://www1.health.nsw.gov.au/pds/ActivePDSDocuments/GL2016_006.pdf. (accessed March 20, 2022).

6. Irving SY, Rempel G, Lyman B, Sevilla WMA, Northington L, Guenter P, et al. Pediatric nasogastric tube placement and verification: best practice recommendations from the NOVEL project. *Nutr Clin Pract.* (2018) 33:921–7. doi: 10.1002/ncp.10189

7. Blumenthal-Barby JS. "Choosing wisely" to reduce low-value care: a conceptual and ethical analysis. *J Med Philos.* (2013) 38:559–80. doi: 10.1093/jmp/jht042

8. Elshaug AG, Rosenthal MB, Lavis JN, Brownlee S, Schmidt H, Nagpal S, et al. Levers for addressing medical underuse and overuse: achieving high-value health care. *Lancet.* (2017) 390:191–202. doi: 10.1016/S0140-6736(16)32586-7

9. Metheny NA, Krieger MM, Healey F, Meert KL. A review of guidelines to distinguish between gastric and pulmonary placement of nasogastric tubes. *Heart Lung.* (2019) 48:226–35. doi: 10.1016/j.hrtlng.2019.01.003

10. Bourgault AM, Powers J, Aguirre L, Hines RB, Sebastian AT, Upvall MJ. National survey of feeding tube verification practices: an urgent call for auscultation deimplementation. *Dimens Crit Care Nurs.* (2020) 39:329–38. doi: 10.1097/DCC.0000000000000440

11. Xu LC, Huang XJ, Lin BX, Zheng JY, Zhu HH. Clinical nurses' nasogastric feeding practices in adults: a multicenter cross-sectional survey in China. *J Int Med Res.* (2020) 48:300060520920051. doi: 10.1177/0300060520920051

12. National Cancer Institute National Institutes of Health. *Implementation science: about IS.* (2015). Available online at: https://cancercontrol.cancer.gov/is. (accessed June 6, 2022).

13. Lomas J. Diffusion, dissemination, and implementation: who should do what? *Ann NY Acad Sci.* (1993) 703:226–35; discussion 235–7.

14. Michie S, Johnston M, Francis JJ, Hardeman W, Eccles M. From theory to intervention: mapping theoretically derived behavioural determinants to behaviour change techniques. *Appl Psychol.* (2008) 57:660–80. doi: 10.1111/j.1464-0597.2008.00341.x

15. van Bodegom-Vos L, Davidoff F, Marang-van de Mheen PJ. Implementation and de-implementation: two sides of the same coin? *BMJ Qual Saf.* (2017) 26:495–501. doi: 10.1136/bmjqs-2016-005473

16. Proctor EK, Powell BJ, McMillen JC. Implementation strategies: recommendations for specifying and reporting. *Implement Sci.* (2013) 8:139.

17. Kisting MA, Korcal L, Schutte DL. Lose the whoosh: an evidence-based project to improve NG tube placement verification in infants and children in the hospital setting. *J Pediatr Nurs.* (2019) 46:1–5. doi: 10.1016/j.pedn.2019.01.011

18. Guerrero Márquez G, Martínez Serrano A, Gutiérrez Juárez M, García Lozano A, Mayordomo Casado B, Torrijos Rodríguez MI, et al. Effectiveness of an educational intervention to improve nurses' knowledge on pediatric nasogastric intubation. *Arch Argent Pediatr.* (2018) 116:402–8. doi: 10.5546/aap.2018.eng.402

19. The Joanna Briggs Institute. *Joanna briggs institute reviewers' manual.* Australia: The Joanna Briggs Institute (2016).

20. Cole E. Improving the documentation of nasogastric tube insertion and adherence to local enteral nutrition guidelines. *BMJ Qual Improv Rep.* (2015) 4:u203207w1513. doi: 10.1136/bmjquality.u203207.w1513

21. Tho PC, Mordiffi S, Ang E, Chen H. Implementation of the evidence review on best practice for confirming the correct placement of nasogastric tube in patients in an acute care hospital. *Int J Evid Based Healthc.* (2011) 9:51–60. doi: 10.1111/j.1744-1609.2010.00200.x

22. Richardson DS, Branowicki PA, Zeidman-Rogers L, Mahoney J, MacPhee M. An evidence-based approach to nasogastric tube management: special considerations. *J Pediatr Nurs.* (2006) 21:388–93.

23. Law RL, Pullyblank AM, Eveleigh M, Slack N. Avoiding never events: improving nasogastric intubation practice and standards. *Clin Radiol.* (2013) 68:239–44.

24. Roe G, Lambie H, Hood A, Tolan D. Acceptability of a new practice development for radiographers focussed on reducing 'never events' related to nasogastric feeding tubes in adult patients. *Radiography*. (2019) 25:235–40. doi: 10.1016/j.radi.2019.02.002

25. Kenny DJ, Goodman P. Care of the patient with enteral tube feeding: an evidence-based practice protocol. *Nurs Res.* (2010) 59:S22–31.

26. Yang FH, Lin FY, Hwu YJ. The feasibility study of a revised standard care procedure on the capacity of nasogastric tube placement verification among critical care nurses. *J Nurs Res.* (2019) 27:e31. doi: 10.1097/jnr.0000000000000302

27. Lee S, Mason E. Competence in confirming correct placement of nasogastric feeding tubes amongst FY1 doctors. *BMJ Qual Improv Rep.* (2013) 2:u201014. doi: 10.1136/bmjquality.u201014.w1198

28. Farrington M, Lang S, Cullen L, Stewart S. Nasogastric tube placement verification in pediatric and neonatal patients. *Pediatr Nurs.* (2009) 35:17–24.

29. Taylor N, Lawton R, Slater B, Foy R. The demonstration of a theory-based approach to the design of localized patient safety interventions. *Implement Sci.* (2013) 8:123. doi: 10.1186/1748-5908-8-123

30. Ceruti S, Dell'Era S, Ruggiero F, Bona G, Glotta A, Biggiogero M, et al. Nasogastric tube in mechanical ventilated patients: ETCO2 and pH measuring to confirm correct placement. A pilot study. *PLoS One.* (2022) 17:e0269024. doi: 10.1371/journal.pone.0269024

31. Operative and postoperative complications: lessons for the future. *Joint commission on accreditation of healthcare organizations*. (2000). Available online at: http://www.jointcommission.org/SentinelEvents/ SentinelEventAlert/sea_12.htm. (accessed August 12, 2021).

32. Department of Health. *Department of health public policy and guidance.the "never events"*. (2011). Available online at: www.dh.gov.uk.(accessed February 12, 2022).

33. Miller CJ, Smith SN, Pugatch M. Experimental and quasi-experimental designs in implementation research. *Psychiatry Res.* (2020) 283:112452.

34. Boeykens K, Steeman E, Duysburgh I. Reliability of pH measurement and the auscultatory method to confirm the position of a nasogastric tube. *Int J Nurs Stud.* (2014) 51:1427–33. doi: 10.1016/j.ijnurstu.2014.03.004

35. Rietbergen T, Spoon D, Brunsveld-Reinders AH, Schoones JW, Huis A, Heinen M, et al. Effects of de-implementation strategies aimed at reducing low-value nursing procedures: a systematic review and meta-analysis. *Implement Sci.* (2020) 15:38. doi: 10.1186/s13012-020-00995-z

36. Pinnock H, Barwick M, Carpenter CR, Eldridge S, Grandes G, Griffiths CJ, et al. Standards for reporting implementation studies (StaRI): explanation and elaboration document. *BMJ Open.* (2017) 7:e013318. doi: 10.1136/bmjopen-2016-013318

37. Goodman D, Ogrinc G, Davies L, Baker GR, Barnsteiner J, Foster TC, et al. Explanation and elaboration of the SQUIRE (standards for quality improvement reporting excellence) guidelines, V.2.0: examples of SQUIRE elements in the healthcare improvement literature. *BMJ Qual Saf.* (2016) 25:e7. doi: 10.1136/bmjqs-2015-004480

38. Orelio CC, Heus P, Kroese-van Dieren JJ, Spijker R, van Munster BC, Hooft L, et al. Reducing inappropriate proton pump inhibitors use for stress ulcer prophylaxis in hospitalized patients: systematic review of de-implementation studies. *J Gen Intern Med.* (2021) 36:2065–73. doi: 10.1007/s11606-020-06425-6

39. Proctor E, Silmere H, Raghavan R, Hovmand P, Aarons G, Bunger A, et al. Outcomes for implementation research: conceptual distinctions, measurement challenges, and research agenda. *Adm Policy Ment Health.* (2011) 38:65–76. doi: 10.1007/s10488-010-0319-7

frontiers | Frontiers in Nutrition

TYPE Original Research
PUBLISHED 06 December 2022
DOI 10.3389/fnut.2022.1037861

OPEN ACCESS

EDITED BY
Nicola Fiotti,
University of Trieste, Italy

REVIEWED BY
Israr Ahmad,
University of Alabama at Birmingham, United States
Jyoti Mehta,
Shoolini University of Biotechnology and Management Sciences, India

*CORRESPONDENCE
Ali Tarighat-Esfanjani
tarighata@tbzmed.ac.ir

SPECIALTY SECTION
This article was submitted to Clinical Nutrition, a section of the journal Frontiers in Nutrition

RECEIVED 06 September 2022
ACCEPTED 21 November 2022
PUBLISHED 06 December 2022

CITATION
Karimi A, Pourreza S, Vajdi M, Mahmoodpoor A, Sanaie S, Karimi M and Tarighat-Esfanjani A (2022) Evaluating the effects of curcumin nanomicelles on clinical outcome and cellular immune responses in critically ill sepsis patients: A randomized, double-blind, and placebo-controlled trial. *Front. Nutr.* 9:1037861. doi: 10.3389/fnut.2022.1037861

Evaluating the effects of curcumin nanomicelles on clinical outcome and cellular immune responses in critically ill sepsis patients: A randomized, double-blind, and placebo-controlled trial

Arash Karimi[1,2], Sanaz Pourreza[3], Mahdi Vajdi[4], Ata Mahmoodpoor[5], Sarvin Sanaie[6], Mozhde Karimi[7] and Ali Tarighat-Esfanjani[1,2]*

[1]Department of Clinical Nutrition, Faculty of Nutrition and Food Sciences, Tabriz University of Medical Sciences, Tabriz, Iran, [2]Nutrition Research Center, Faculty of Nutrition and Food Sciences, Tabriz University of Medical Sciences, Tabriz, Iran, [3]Department of Community Nutrition, School of Nutritional Sciences and Dietetics, Tehran University of Medical Sciences, Tehran, Iran, [4]Student Research Committee, Department of Clinical Nutrition, School of Nutrition and Food Sciences, Isfahan University of Medical Sciences, Isfahan, Iran, [5]Department of Anesthesiology and Intensive Care, Faculty of Medicine, Tabriz University of Medical Sciences, Tabriz, Iran, [6]Research Center for Integrative Medicine in Aging, Aging Research Institute, Tabriz University of Medical Sciences, Tabriz, Iran, [7]Department of Immunology, School of Medicine, Tarbiat Modares University, Tehran, Iran

Introduction: In sepsis, the immune system is overreacting to infection, leading to organ dysfunction and death. The purpose of this study was to investigate the impacts of curcumin nanomicelles on clinical outcomes and cellular immune responses in critically ill sepsis patients.

Method: For 10 days, 40 patients in the intensive care units (ICU) were randomized between the nano curcumin (NC) and placebo groups in a randomized study. We evaluated serum levels of biochemical factors, inflammatory biomarkers, the mRNA expression levels of FOXP3, NLRP-3, IFN-γ, and NF-κp genes in the PBMCs, and clinical outcomes before the beginning of the supplementation and on days 5 and 10.

Results: NLR family pyrin domain containing 3 (NLRP3), interferon gamma (IFN-γ), and nuclear factor kappa-light-chain-enhancer of activated B cells (NF-κB) mRNA expression levels significantly $P = 0.014$, $P = 0.014$, and $P = 0.019$, respectively) decreased, but forkhead box P3 (FOXP3) mRNA expression levels increased significantly ($P = 0.008$) in the NC group compared to the placebo group after 10 days. NC supplementation decreased serum levels of IL-22, IL-17, and high mobility group box 1 (HMGB1) ($P < 0.05$). Nevertheless, biochemical factors and nutritional status did not differ significantly ($P > 0.05$). NC supplementation resulted in decreased sequential

organ failure assessment and multiple organ dysfunction syndromes scores, while it did not have significant impacts on length of stay in the ICU, systolic blood pressure, diastolic blood pressure, a saturation of oxygen (%), and respiratory rate (breaths/min) PaO2/FiO2 ($p > 0.05$).

Conclusion: For critically ill patients with sepsis, NC supplementation may be an effective therapeutic strategy. More randomized clinical trials involving longer follow-up periods and different doses are needed to achieve the best results.

KEYWORDS

curcumin, immune response, clinical outcome, sepsis, inflammation

Introduction

Sepsis is a complex and severe disorder that is caused by a strong response of the body's immune system to an infection. The disease is by far the most serious medical problem related to acute organ dysfunction and the high hazard of death in the intensive care unit (ICU) (1). The immune system's excessive response leads to an enhancement in inflammatory oxidative stress and an increase in organ failure (2, 3). In the world, disease continues to be the leading cause of death (2, 3). Globally, sepsis affects an estimated 30 million people worldwide, and this number has increased annually by nine to 13 percent. According to global statistics, sepsis affected 48.9 million people worldwide in 2017 and caused 11.0 million deaths (4).

There are two parts to the human immune system: innate and adaptive (5). The innate immune system responds non-specifically to infections (6). Adaptive immunity is slower than innate immunity but may recognize unique antigens and establish immunity after multiple exposures. Innate system cells include basophils, mast cells, eosinophils, natural killer (NK) cells, dendritic cells, macrophages, and neutrophils (7). B and T cells comprise the adaptive immune system responding to pathogens (8). B cells generate antibodies and plasma cells for long-term immunity, whereas T cells, namely gamma delta (γδ), CD8+, CD4+, and regulatory T cells (Tregs), create plasma cells and antibodies for long-term immunity (9). In addition to activating immune responses, the entry of pathogens into the body leads to the activation of various inflammatory pathways, namely NLRs, HMGB-1, and NF-κB (10). The NLRs play a significant role in recognizing invading bacteria and initiating the innate immune response. Inflammasomes can be activated during sepsis to augment inflammatory responses (11). As a result of NLRP3 inflammasome activation, caspase-1 is activated, producing pro-inflammatory cytokines, IL-18, and IL-1β (12).

On the other hand, the activation of NLRP3 leads to up-regulated NF-κB pathway, which can cause the production of various swelling factors. The nuclear protein HMGB1 regulates innate immune responses both intracellularly and extracellularly and is found ubiquitously in almost all cells (13). HMGB1 also functions as an acute-phase cytokine during infection. Serum and tissue HMGB1 levels rise during infection, particularly in sepsis, and play a crucial role in systemic inflammation (14). On the other hand, the enhancement in the serum level of inflammatory cytokines causes a decrease in the level of albumin, urea, and BUN bilirubin, LDH, in sepsis patients (15). Impaired nutritional variables (energy intake and serum albumin) are expected to exacerbate clinical outcomes, namely sequential organ failure assessment (SOFA) and multiple organ dysfunction syndromes (MODS) score, PaO2/FiO2, duration of mechanical ventilation, and duration of ICU stay (16). In addition, sepsis is associated with an excessive reduction of forkhead box P3 (FOXP3) (12). FOXP3 regulates the development and activity of $CD25^+$ $CD4^+$ Treg cells, which play an important role in the immune response (12).

Notwithstanding the complexity of sepsis in people admitted to the ICU, a variety of treatments, such as corticosteroids and broad-spectrum antibiotics, are used today, but efforts to find effective treatment with minimal side effects are still ongoing (17). Accordingly, various studies indicate that natural immunomodulatory agents might ameliorate bacterial and virus diseases when combined with routine treatment (18). Rolta et al. (19), Rolta et al. (20) showed that herbal compounds can be used as an adjunctive treatment in corona. In other studies Rolta et al. (21) phytocompounds indicated (emodin, rhein13c6, chrysophenol dimethyl ether and resveratrol) have antibacterial and antifungal properties.

A hydrophobic polyphenol and an active component in turmeric is curcumin, derived from Curcuma longa rhizomes. Curcuminoids are comprised of three components, including bisdemethoxycurcumin (10 to 15%), demethoxycurcumin (20 to 27%), and curcumin (60 to 70%) (22). Numerous pieces of evidence show that curcumin has many pharmacological and therapeutic activities, including antimicrobial, antioxidant,

and antiviral effects, anti-cancer, and anti-inflammatory (23). Curcumin works by targeting multiple biochemical pathways, such as reducing lipid peroxidation, increasing the expression of antioxidant-producing genes, attenuating NF-κB and NRLP3 signaling pathways, and, most importantly, modulating the immune system response (24). Although curcumin has many medicinal benefits, it is unfortunately absorbed in very small amounts due to its low bioavailability and rapid metabolism, which is exacerbated in patients admitted to the ICU (23). However, today, through effective methods such as the use of liposomes, the use of nanoparticles, including non-polar sandwich technology, nano micelles, complexing with phospholipids or piperine and solid lipid particle formulations leads to a substantial rise in the absorption of hydrophobic substances such as curcumin (25). Also, due to the proven advantageous impacts of curcumin in cell lines and on models of septic rats, as well as some human studies on sepsis (24), this randomized clinical trial (RCT) aims to the effects of NC on immune system responses and clinical outcomes in critically ill patients with sepsis.

Materials and methods

Study design

We conducted this study on the 40 hospitalized patients in the ICUs at Imam Reza and Shohada Hospitals (Tabriz University of Medical Sciences, Tabriz, Iran). Criteria for inclusion included critically ill patients feeding enteral nutrition and patients who had been in the ICU for at least 10 days. Furthermore, An exclusion criteria included participants with the following conditions: patients with intestinal ischemia, pancreatitis, intolerance to enteral feeding, short bowel syndrome, pregnant and lactating women, intestinal obstruction, and use of non-steroidal anti-inflammatory drugs (NSAIDs). Researchers registered the study at the Iranian Registry of Clinical Trials (IRCT) website (IRCT20110123005670N7). A nosocomial infection is defined by the most recent guidelines of the CDC (26).

Randomization and intervention

Patients in blocks arranged according to gender and age score were randomly divided into placebo or NC groups in a 1:1 ratio using RAS software. Both patients and researchers were blind to the allocation of the study. Patients in the supplementation group received routine therapy, namely antibiotics (Meropenem, Imipenem, Ciprofloxacin) with two 80 mg NC capsules, while the placebo group received routine therapy with a placebo for 10 days. Enteral feedings were administered through the nasogastric tube to all patients from their first 24 h of admission (Karen Company, Tehran, Iran; **Table 1**). Depending on each patient's metabolic status and weight, the amount of energy required was calculated at 25 to 30 kcal/kg. Starting with 25 ml/h of enteral feeding, the rate was enhanced by 25 ml/h every 4 h until the aim rate was reached. In cases where the gastric residual volume exceeded 150 ml, prokinetic agents were administered. Exir-Nano-Sina company produced a placebo and NC capsules (batch

TABLE 1 Contents of patients enteral formulas.

Nutrient	Amount per 11.3 g	%DV	Amount per 1000 ml solution	Nutrient	Amount per 11.3 g	%DV	Amount per 1000 ml solution
Calories (Kcal)	50		1000	Biotin (mcg)	8.2	3	163.7
Protein (g)	1.8	3.6	36	Calcium (mg)	28.15	3	563
Total carbohydrate (g)	6.76	2.2	135	Chromium (mcg)	1	0.8	19.2
Dietary Fiber (g)	0.23	0.9	4.4	Copper (mcg)	42	2	851
Total Fat (g)	1.8	3	36	Fluoride (mg)	0.1	–	2.2
Vitamin A (IU)	108	2	2160	Iodine (mcg)	4.9	3.3	98.2
Vitamin D (IU)	9.8	2.5	196.4	Iron (mg)	0.48	2.7	9.5
Vitamin E (IU)	1.3	4	25.6	Magnesium (mg)	12.2	3	243.7
Vitamin K (mcg)	3.3	4	65.3	Manganese (mg)	0.08	4	1.6
Vitamin C (mg)	4.9	8	98.2	Molybdenum (mcg)	1.5	2	29.5
Vitamin B1 (mg)	0.08	5	1.6	Phosphorus (mg)	27	2.7	530
Vitamin B2 (mg)	0.09	5	1.7	Zinc (mg)	0.48	3	9.7
Niacin (mg)	0.65	3	13	Selenium (mcg)	1.8	2.6	3.6
Vitamin B6 (mg)	0.07	3	1.35	Sodium (mg)	50.7	2	1013.4
Folic acid (mcg)	13.1	3	261.9	Potassium (mg)	73.2	2	1435.4
Vitamin B12 (mcg)	0.26	4	5.1	Chloride (mg)	42.8	1.2	855.7
Pantothenic Acid (mg)	0.3	3	6.5	L- Carnitine (mg)	4.5	–	90.1

number: 17003). In NC supplements, curcumin accounted for bis-desmethoxycurcumin for 3%, for 25%, and 72%, emethoxycurcumin. The NC formulation included polysorbate 80 as a component of the placebo capsules. A specialist evaluated patients according to inclusion criteria before enrolling them in the study. Nurses without knowing which is the placebo and the NC, every 12 h (9:00 a.m. and 9:00 p.m.), an hour later than enteral feeding (to prevent interaction with the contents of the formula received), NC capsules and placebo (in terms of form and size) were given to patients as a solution through a nasogastric tube.

Since the vast majority of patients with sepsis have a low Glasgow Coma Score, in this study, we obtained informed consent from first-degree (but legal) relatives such as mothers, fathers, sons, or daughters of patients before entering the study.

Laboratory evaluates

Before the intervention, 5th, and 10th, every day between 12:00 and 3:00 p.m., venous blood samples were taken from each patient. The biochemical factors, namely blood urea nitrogen (BUN), albumin, fasting blood sugar (FBS), hemoglobin, indirect bilirubin, direct bilirubin, lactate dehydrogenase (LDH) and total plasma protein, were specified using Abbott ALCYON-350 auto-analyzer kits. The blood samples of patients were centrifuged for 10 min at a speed of 2500 rpm (Beckman Avanti J-25 - Beckman Coulter, Brea, CA). The serum was stored at 70°C before biochemical assessments. According to dual biotin antibody sandwich technology, inflammatory markers (IL-17 and IL-22) were assessed using the enzyme-linked immunoassay (ELISA) method. In the present study, Human IL-17 and IL-22 ELISA kits made by the Assessment Technology Laboratory (Crystal Day Biotech Co., Ltd., Shanghai, China) and HMGB1 were used.

Peripheral blood mononuclear cells and RNA isolation

Whole blood samples were directly examined for isolation of peripheral blood mononuclear cells (PBMCs). Separating PBMCs by density gradient centrifugation was accomplished using Ficoll-Histopaque solution gradient centrifugation. To isolate total RNA from the blood, TRIzol was used (Sigma Aldrich, Germany). Quantitative and qualitative characteristics of extracted RNA were determined using a NanoDrop spectrophotometer (Nano-Drop One/Once, Thermo Scientific). Then, we performed reverse transcription with random hexamer primers and oligo (dT) to transform the total RNA into complementary DNA (cDNA) based on the producer's instructions (BioFact, RTase, South Korea). Gel electrophoresis on 1% agarose gel was used to determine the RNA integration.

Real-time polymerase chain reaction for genes

Measuring the levels of mRNA expression levels of FOXP3, NLRP3, IFN-γ, and NF-kβ was done using real-time polymerase chain reaction (RT-PCR) (Sigma Aldrich, Germany). The manufacturer's instructions were followed for the reverse transcription of 25 ng of total RNA and for constructing complementary DNA using reverse transcription reagent kits (Thermo Scientific, EU). With the Light-Cycler 480 instrument (Roche, Germany), qRT-PCR was performed in a volume of 10 μl using SYBR Green PCR Master Mix (Sigma-Aldrich, Germany). A three-phase thermal cycling procedure was conducted: phase one (primary denaturation: 95°C for two min), phase two (30 s at 63°C, and 30 s at 74°C, 34 to 42 cycles of 30 s at 96°C), and last phase to form the melt curve (5 min at 74°C). A Primer Bank sequence was used to design the primers. The characteristic primers for the human of FOXP3, NLRP-3, IFN-γ NF-kβ, and β-actin genes are resumed in Table 2. Using the $2^{-\Delta\Delta CT}$ method as the comparison of placebo/post-intervention, the relative expression levels for each gene were calculated for each reaction in triplicate.

Statistical analysis

In this study, sampling based on the standard equation (Pukak) and based on mean and standard deviation with a significance level test of 5% ($\alpha = 0.05$) with considering 80% ($\beta = 0.2$) power and distance 95% confidence was performed. According to the method for calculating the sample size for clinical trials, each group's sample size was 17 individuals (27). In addition, 20% of dropouts were taken into account, increasing this to 20 people. The data was analyzed using SPSS software version 24 (Chicago, IL, USA). For the assessment of the normal distribution of continuous variables, the Kolmogorov-Smirnov test was used. Quantitative data are presented as frequency (%). For normally distributed data, the means and standard

TABLE 2 Sequence of gene primers for qRT-PCR.

Genes	Forward and reverse	Sequences
FOXP3	F	5′-TTCAGCCAGCCCAGCACATC-3′
	R	5′-CGTAGCCGAAGAAACCTCATTGTC-3′
NLRP-3	F	5′-ATGTGTGTGGAGAGCGTCAACC-3′
	R	5′-TGAGCAGAGTCTTCAGAGACAGCC-3′
IFN-γ	F	5′-CCTTTTCTACTTTGCCAGCAAAC-3′
	R	5′-GAGGCCGTCCCAACCAC-3′
NF-kβ	F	5′-TCCCTGAACCCTATGAAC-3′
	R	5′-CTAAACCAGCCAGACCTT-3′
β-Actin	F	5′-GAGCTACGAGCTGCCTGACG-3′
	R	5′-GTAGTTTCGTGGATGCCACAG-3′

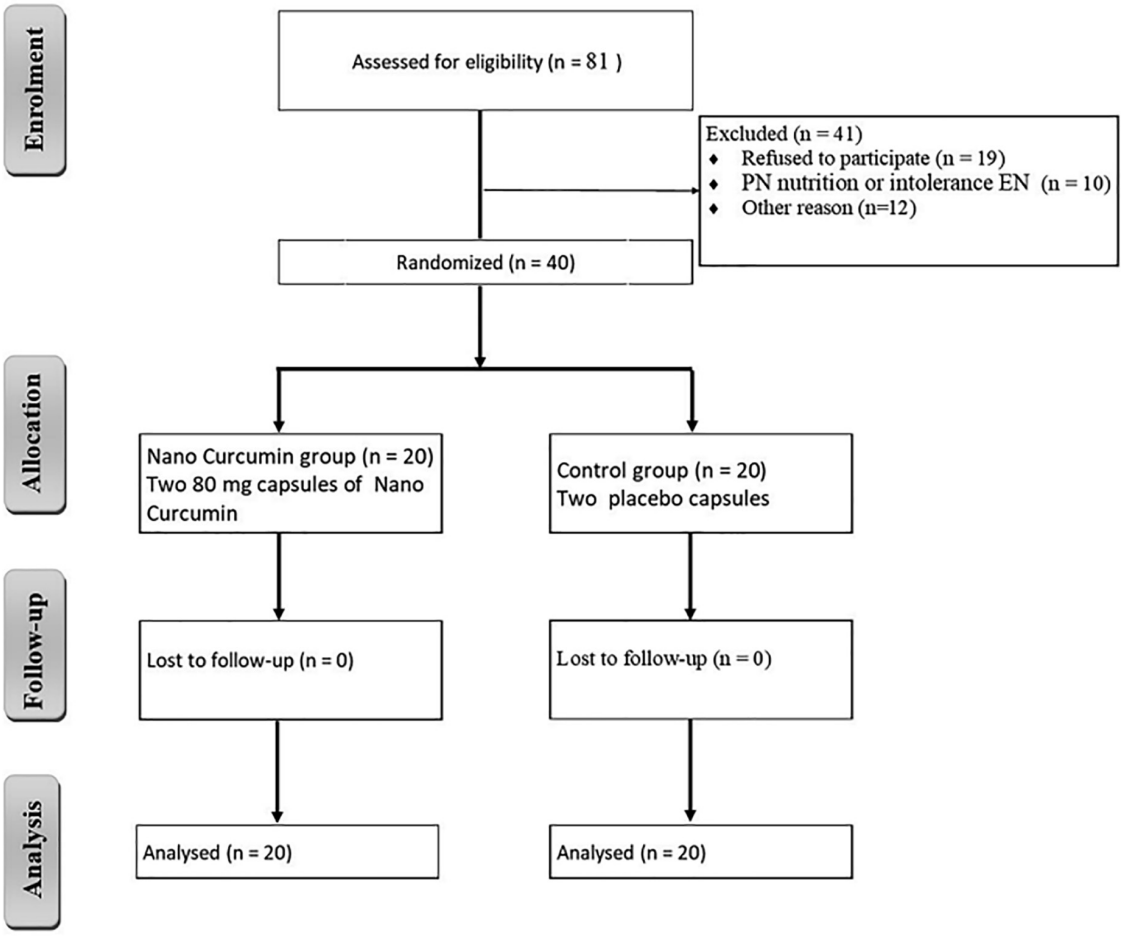

FIGURE 1
Study flow diagram.

deviations (SDs) are shown as a mean ± standard deviation; for non-normally distributed data, the Q1 and Q3. We used Mann–Whitney U, independent *t*-tests, and chi-square tests to compare group changes (endpoint minus baseline). A paired *t*-test was used to determine if there were significant differences between baseline and after the intervention. Analyzing covariance (ANCOVA) was used to eliminate confounding variables and examine differences between post-intervention groups.

Results

Characteristics of patients participating

In this clinical study, 81 patients were included in the study. Also, 41 patients were excluded from the study due to discharge, refusal to participate, and intolerance to enteral nutrition. A total of 20 patients in the NC group and 20 patients in the placebo group participated in the current study, as shown in Figure 1. Table 3 summarizes the demographic data of participants. The baseline characteristics of the participants did not significantly differ between the two groups.

Effect of nano curcumin on nutritional status

Between the NC group and placebo group, there were no considerable alterations in energy intake during the study period, as shown in Table 4.

Effect of nano curcumin on biochemical factors

In Table 5 the effect of curcumin on biochemical factors during the study stages is shown. Albeit serum levels of BUN, FBS, albumin, hemoglobin, total bilirubin, direct bilirubin,

TABLE 3 Summary of baseline characteristics of the patients.

Variables	Nano-curcumin group (n = 20)	Placebo group (n = 20)	Pv
Age, yrs	48.75 ± 7.19	49.10 ± 5.01	0.057¥
Sex, n (%)			
Males	11(55)	13(65)	0.257†
Females	9 (45)	7(35)	
Body Temperature (°C)	38.52 ± 0.87	38.39 ± 0.61	0.874¥
Heart rate (beats/min)	99.64 ± 22.74	97.51 ± 23.14	0.613¥
Respiratory rate (breaths/min)	18 (15–23)	18 (16–23)	0.911§
WBC (10^9/L)	14.30 ± 2.15	13.02 ± 2.59	0.828¥
Lactate (mmol/L)	6.89 ± 4.6	6.16 ± 3.9	0.716¥
Na^+ (mmol/L)	146.16 ± 4.87	148.66 ± 5.01	0.531¥
K^+ (mmol/L)	4.51 ± 0.88	4.49 ± 0.76	0.767¥
APACH II score	17 (13–21)	16.60 (13–19)	0.231§
SOFA score	8.10 (5–11)	7.50 (6–11)	0.538§
Reason for ICU admission, n(%)			
Medical	4 (20)	5(25)	0.487†
Surgical, Trauma	12 (80)	14 (75)	
Energy requirements (Kcal/day)	2059.51 ± 153.27	1979.23 ± 133.98	0.614¥
Energy intake (Kcal/day)	1445.74 ± 149.90	1462.45 ± 132.24	0.231¥
Source of sepsis			
Pulmonary infection (n,%)	7 (35)	6 (30)	0.698†
Abdominal infection (n,%)	6 (30)	5 (25)	
Urinary tract infection (n,%)	3 (15)	3 (15)	
Bacteriemia (n,%)	4 (20)	6 (30)	

APACHE, acute physiology and chronic health evaluation; SOFA, sequential organ failure assessment, ICU, intensive care unit; WBC, white blood cell.
Data are presented as mean ± SD or number (%).
¥ Based on independent sample t-test.
† Based on Pearson's chi-squared test.
§ Based on Mann–Whitney U Test.

lactate, and total plasma protein decreased significantly in the NC group, the intergroup changes were not statistically significant.

Effect of nano curcumin on inflammatory factors

In Table 6, the effect of nano curcumin supplementation on inflammatory factors during the study stages is shown. There were no considerable alterations between the study groups in the baseline serum levels of HMGB-1, IL-17, and IL-22, however, compared to the placebo group, HMGB-1, IL-17, and IL-22 serum concentrations were significantly lower in the NC group after 10 days.

TABLE 4 Changes nutritional status during the study.

Variables		Nano-curcumin group (n = 20)	Placebo group (n = 20)	Pv
Energy requirements (kcal/day)	Day 0	2059.51 ± 153.27	1979.23 ± 133.98	0.614¥
	Day 10	2487.05 ± 169.1	2296.87 ± 115.30	0.736$
	P†	**0.002**	**0.034**	
Mean caloric intake (kcal/day)	Day 0	1445.74 ± 149.90	1462.45 ± 132.24	0.718
	Day 10	1721.65 ± 146.82	1691.97 ± 146.71	0.232$
	P†	<**0.0001**	<**0.0001**	

Data are presented as means ± SD; Numbers in bold are statistically significant p-value < 0.05.
† Based on paired t-test.
¥ Based on independent sample t-test.
$ Based on analysis of covariance (ANCOVA); adjusted for sex, BMI, age, standard treatment, type of disease and baseline values.
α Based on Mann–Whitney U Test.

Effect of nano curcumin on forkhead box P3, NLR family pyrin domain containing 3, interferon gamma, and nuclear factor kappa B genes expression

Forkhead box P3 (FOXP3), NLR family pyrin domain containing 3 (NLRP-3), interferon gamma (IFN-γ), and nuclear factor kappa B (NF-kβ) levels did not change substantially after 5 days of supplementation with NC, as shown in Figure 2. In the NC group, FOXP3 expression considerably increased compared to the placebo group, after 10 days (fold change: 2.69 ± 0.99 vs. 3.24 ± 0.74 (P = 0.022) (Figure 2A). At the end of the study, NC supplementation significantly reduced mRNA expression of IFN-γ (fold change: 0.39 ± 0.11) compared to placebo (fold change: 1.26 ± 0.07). (P = 0.006) (Figure 2B). Also, on the 10th day, the NC group's NF-kβ expression level (fold change: 1.13 ± 0.11) was higher than the placebo group's fold change: 1.51 ± 0.07) (P = 0.014) (Figure 2C). Moreover, NC supplementation led to a significant decrease in NLRP-3 mRNA expression (fold change: 2.07 ± 0.79) than placebo (fold change: 2.99 ± 0.46), (P = 0.039) (Figure 2D).

Effect of nano curcumin on Clinical outcomes

In Table 7, effect of curcumin on clinical outcomes are presented for the participants. At the end of the study, the NC group's MODS and SOFA scores decreased significantly compared to the placebo group (P < 0.05). Furthermore, there was no remarkable alteration between the two groups in the length of stay in the ICU, systolic blood pressure, dystopic blood pressure saturation (%), respiratory rate (breaths/min) PaO2/FiO2.

TABLE 5 Effect of curcumin on biochemical factors during the study stages.

Variables		Nano-curcumin group (n = 20)	Placebo group (n = 20)	Pv
BUN (mg/dL)	Day 0	71.6 ± 20.8	67.32 ± 18.36	0.453¥
	Day 5	62.6 ± 18.92	59.56 ± 17.15	0.323¥
	Day 10	50.6 ± 17.26	49.06 ± 15.74	0.501£
	P‡	**0.012**	**0.026**	
Albumin (g/dL)	Day 0	3.16 ± 0.62	3.12 ± 0.58	0.699¥
	Day 5	3.34 ± 0.52	3.36 ± 0.14	0.739 £
	Day 10	3.86 ± 0.70	3.59 ± 0.61	0.314£
	P‡	0.011	0.039	
FBS (mmol/L)	Day 0	130.53 ± 51.33	132.91 ± 39.17	0.721¥
	Day 5	126.76 ± 40.16	129.85 ± 26.64	0.564 £
	Day 10	121.27 ± 29.33	125.12 ± 51.33	0.237£
	P‡	**0.063**	0.116	
Hemoglobin, (g/dL)	Day 0	15.23 ± 2.89	14.83 ± 3.03	0.465¥
	Day 5	14.15 ± 2.43	13.75 ± 2.72	0.369 £
	Day 10	12.89 ± 1.98	12.36 ± 2.10	0.212£
	P‡	**0.035**	0.063	
Indirect bilirubin, (mg/dL)	Day 0	1.01 ± 0.25	1.23 ± 0.31	0.704¥
	Day 5	09.34 ± 0.14	09.75 ± 0.21	0.520£
	Day 10	07.86 ± 0.23	08.26 ± 0.38	0.281£
	P‡	**0.036**	**0.075**	
Direct bilirubin, (mg/dL)	Day 0	06.21 ± 0.07	07.01 ± 0.07	0.408¥
	Day 5	05.11 ± 0.04	05.81 ± 0.04	0.616 £
	Day 10	03.41 ± 0.03	04.01 ± 0.08	0.225£
	P‡	**0.041**	0.069	
LDH (mg/dL)	Day 0	20.61 ± 4.6	19.84 ± 3.9	0.510¥
	Day 5	18.24 ± 3.26	17.63 ± 3.06	0.411 £
	Day 10	15.89 ± 2.79	16.03 ± 2.53	0.140£
	P‡			
Total plasma protein, (mg/dL)	Day 0	101.63 ± 9.07	114.08 ± 10.24	0.617¥
	Day 5	98.71 ± 3.01	100.98 ± 3.01	0.821 £
	Day 10	84.12 ± 2.58	90.42 ± 2.58	0.459£
	P‡	**0.011**	**0.045**	

FBS, fasting blood sugar; LDH: lactate dehydrogenase; BUN: blood urea nitrogen.
Data are presented as means ± SD; Numbers in bold are statistically significant p-value < 0.05.
¥ Based on independent sample t-test.
£ Based on analysis of covariance (ANCOVA); adjusted for sex, BMI, age, standard treatment, type of disease and baseline values.
‡ Based on repeated-measure analysis of variance.

TABLE 6 Effect of nano curcumin supplementation on inflammatory factors.

Variables		Nano curcumin group (n = 20)	Placebo group (n = 20)	Pv
HMGB-1	Day 0	13.32 ± 2.02	15.48 ± 2.82	0.515¥
	Day 5	11.05 ± 1.73	13.56 ± 1.94	0.754 £
	Day 10	7.86 ± 1.34	11.59 ± 1.53	0.006£
	P‡	0.016	0.384	
IL-17	Day 0	36.30 ± 3.62	41.03 ± 4.49	0.329¥
	Day 5	29.95 ± 3.14	38.09 ± 3.67	0.156£
	Day 10	19.37 ± 2.73	32.78 ± 3.03	0.018£
	P‡	**0.001**	0.211	
IL-22	Day 0	186.30 ± 22.15	201.03 ± 20.52	0.403¥
	Day 5	164.75 ± 14.88	190.09 ± 16.03	0.211£
	Day 10	109.37 ± 10.03	177.78 ± 15.68	0.004£
	P‡	< **0.0001**	0.409	

Data are presented as means ± SD; Numbers in bold are statistically significant p-value < 0.05.
HMGB: High mobility group box 1; IL: interleukin.
¥ Based on independent sample t-test.
£ Based on analysis of covariance (ANCOVA); adjusted for sex, age, type of disease and baseline values.
‡ Based on Repeated-measure analysis of variance.

Discussion

The present RCT evaluated the impacts of NC supplementation on immune response in septic patients admitted to ICU. The current study revealed that 10 days of NC supplementation could significantly reduce IL-17, IL-22, SOFA, and MODS scores serum levels. It also decreased the mRNA expression of NLRP-3, NF-êB, HMGB-1, and IFN-γ genes and increased the mRNA expression of FOXP3. As far as we are aware, this is the first study to evaluate NC's effect on immune response in patients with sepsis. Sepsis, which is defined as the excessive activity of the immune system in dealing with pathogenic factors, leads to systemic inflammatory response, coagulation disorders, endothelial function, and immune response (28), and it is a major cause of death in ICUs (29). We found that NC supplementation significantly decreased serum concentrations of IL-17 and IL-22 in septic patients after 10 days of intervention. Various studies have assessed the effect of curcumin on pro-inflammatory cytokines. A study conducted by Silva et al. (30) showed that treatment of septic rats with 100 mg/kg of curcumin remarkably lessened the pro-inflammatory cytokines, namely IL-1β and IL-6. In another study, Djalali et al. (31) reported that 2 months of NC supplementation declined the serum concentration of IL-17 and its mRNA expression in patients with episodic migraine. There is growing evidence that high concentrations of IL-17 are correlated to a higher peril of sepsis, which could provide a biomarker for the prognosis of sepsis (32). IL-17 interacts with various mediators, namely IL-1β, TNF-α, and IL-22 to exert its pro-inflammatory impact (33). Also, IL-22 plays a pivotal role in chronic inflammatory diseases and polymicrobial sepsis (34). In a trial conducted by Antiga et al. (27), curcumin (2g/day) supplementation considerably decreased the serum levels of IL-22 in participants with mild-to-moderate psoriasis Vulgaris. However, unlike the results of our study, curcumin did not significantly affect the serum level of IL-17 (27). This contrary finding might be due to the different underlying diseases of the participants and the distinct forms of curcumin used in the trials.

The inflammatory responses during sepsis might lead to the dysfunction of vital organs, including the lung, kidneys, heart, and liver, and thus, cause MODS (28). The number of organs engaged in MODS is positively correlated to the mortality of sepsis (35). Scores such as SOFA and MODS are used to properly identify septic patients at higher risk of mortality (29). In the present study, although NC supplementation did not affect the respiratory rate, PaO2/FiO2, and blood pressure, it significantly

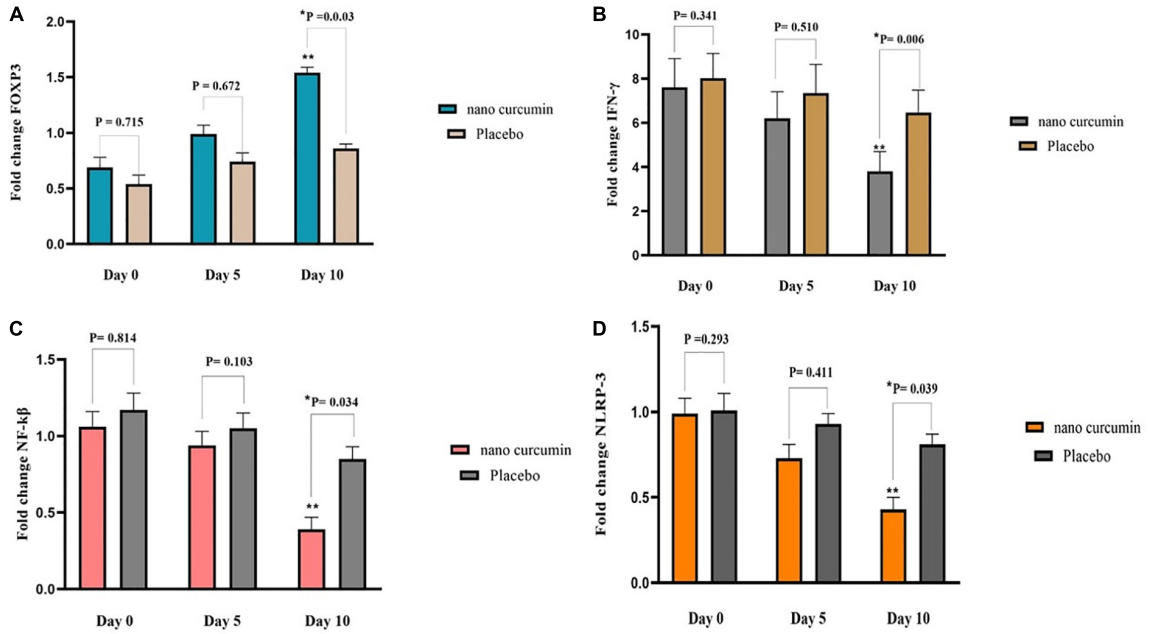

FIGURE 2
The effects of the intervention on FOXP3, NLRP3, IFN-γ, and NF-kβ expression in two study groups. **(A)** Fold change of FOXP3 **(B)** fold change of NLRP3 **(C)** fold change of IFN-γ **(D)** fold change of NF-kβ. Values are mean of fold change ± SEM. Data analysis was done using the ANCOVA test (adjusted for sex, age, type of disease, and baseline values; *$p < 0.05$ vs. placebo) and Repeated measures ANOVA (**$p < 0.05$ vs. baseline). $P < 0.05$, statistically significant. FOXP3, forkhead box P3; NF-κB, nuclear factor kappa B; NLRP3, NLR family pyrin domain containing 3; IFN-γ, interferon gamma.

decreased the SOFA and MODS scores after 10 days. This finding is in line with the results of several animal studies (36, 37). Chen et al. (36) presented that supplementation with curcumin diminished tissue injury and improved survival rates in septic mice. Moreover, the results of another experimental study indicated that curcumin could prevent dysfunction of the kidneys, liver, and small bowel in rats with experimentally formed sepsis (37).

Additionally, the present study showed that septic patients who received NC for 10 days had significantly lower levels of NLRP-3. This finding was in agreement with an animal study that reported the suppression of NLRP-3 inflammasome activation in mice treated with a curcumin analog (38). Moreover, Gong et al. (39) indicated that curcumin could decrease the level of IL-1β by inhibiting the activation of NLRP-3 in an *in vivo* study. On the contrary, 12 weeks of curcumin supplementation among hemodialysis patients did not substantially influence NLRP-3 mRNA expression (40). This might be explained by different study sample sizes, carriers of the curcumin, as well as different participants of the studies. NLRP3 is a major component of the innate immune system that is prompted by pathogens and releases pro-inflammatory cytokines (41, 42).

Additionally, NC significantly reduced NF-kB expression in septic patients. In an animal study (43), both treatment and pretreatment with curcumin lessened NF-êB activation in renal tissues of septic rats. Xie et al. (44) also revealed that curcumin exerts its protective effects on lipopolysaccharide (LPS)/D-galactosamine (D-GalN)-induced acute liver injury in rats by up-regulating nuclear Nrf-2 and downregulate NF-êB. The activated NF-êB is a chief regulator of inflammatory gene expression, including NLRP-3 (Figure 3) (45).

Several mechanisms have been suggested for the effects of curcumin administration on the components of the immune response mentioned above. Curcumin can down-regulate the Th1 and Th17 cell pathways and help modulate T-helper immune responses (27). It is speculated that curcumin adjusts the Treg/Th17 rebalance by inhibiting the IL-23/Th17 pathway (46). Another hypothesis is that curcumin down-regulates the expression of IL-22 and IL-17 indirectly by repressing IL-1β and IL-6 due to their synergistic activities with IL-17 (47). In addition, curcumin blocks the phosphorylation and degradation of IêB, the inhibitor protein of NF-êB, and averts the nuclear translocation of NF-êB (30). By inhibiting the activation of NF-êB, the transcription of genes engaged in the expression of pro-inflammatory cytokines is suppressed (48). Additionally, curcumin increases the expression of peroxisome proliferator—activated receptor gamma (PPARγ), which contributes to the suppression of NF-êB and lowers the release of pro-inflammatory cytokines (49).

The inhibition of the NF-êB pathway can alleviate the severity of MODS (50). Also, myeloperoxidase which represents

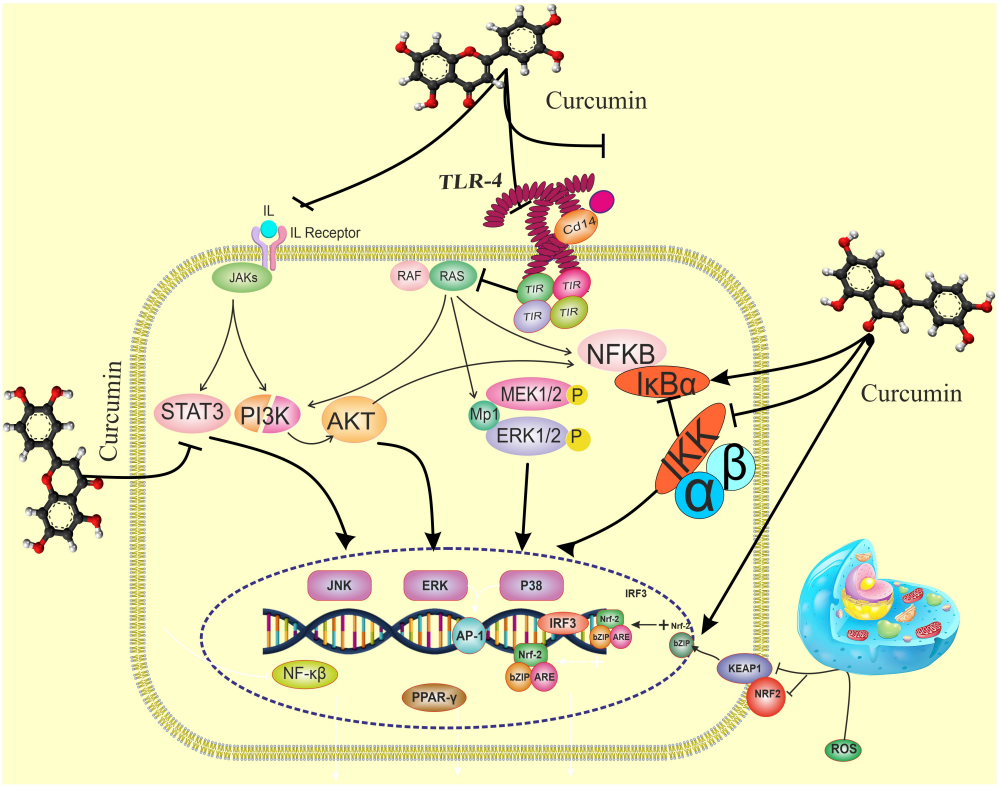

FIGURE 3
The effects of curcumin on the immune response pathway. Curcumin can bind directly to MD2 (protein appears to connect with toll-like receptor 4 on the cell surface). Curcumin also inhibits LPS-induced activation of MyD88- and TRIF-dependent TLR4 pathways, resulting in suppression of both IRF3 and NF-B. Curcumin promotes the expression of the Nrf-2 gene by boosting the antioxidant capacity and synthesis of antioxidant enzymes such as SOD, GPX CAT, and CAT. TANK-binding kinase 1; TRAF, TNF receptor-associated factor; TRAM, TRIF-related adaptor molecule; TRIF, TIR-domain- containing adapter-inducing interferon-β, Nrf-2, nuclear factor erythroid 2-related factor 2; p-IκBα, phosphorylated-IκBα; s; ROS, reactive oxygen species, STAT1, signal transducer and activator of transcription 1; TGF-1β, transforming growth factor-β1; TIRAP, toll-interleukin 1 receptor domain-containing adaptor protein; TLR4, toll-like receptor 4; TNF-α, tumor necrosis factor-α.

polymorphonucleocytes infiltration, is a major indicator of tissue damage (50). By blocking myeloperoxidase activity, curcumin decreases tissue injury (37, 50). Curcumin's anti-inflammatory and antioxidant properties generally reduce organ dysfunction during sepsis (36, 37, 50).

The important role of NF-κB activation is the regulation of NLRP3, ASC, and caspase-1 gene expression as well as the production of pro-inflammatory cytokines (51, 52). Thus, curcumin inhibits NF-êB signaling and suppresses NLRP-3 activation (53). Besides, curcumin attaches to peroxiredoxin 1 (PRDX1), which interacts with pro-caspase-1 and suppresses the link between pro-caspase-1 and ASC; therefore, the assembly of NLRP-3 inflammasome discontinues (38).

The mRNA expression level of HMGB1 was considerably reduced after 10 days of NC supplementation in patients with sepsis. During sepsis, high concentrations of HMGB-1 stimulate the production of pro-inflammatory cytokines, which are associated with MOD and mortality (54, 55). In accordance with our study, Ahn et al. (56) reported inhibiting the production of HMGB1 in endotoxemia mice with curcumin longa extract-loaded nanoemulsion. In addition, in a study by Kim et al. (57), curcumin inhibited the LPS-mediated release of HMGB-1 by endothelial cells and down-regulated the expression of HMGB-1 receptors. The proposed mechanism for the effect of curcumin on HMGB-1 is the blocking of nitric oxide due to the suppression of c-Jun N-terminal kinase, which leads to the inhibited release of HMGB-1 by macrophages (56).

Another finding of the current study was that mRNA expression of IFN-γ was considerably reduced after 10 days of NC supplementation. An experimental study by Gao et al. (58) indicated that curcumin treatment markedly suppressed the IFN-γ gene expression by splenic T lymphocytes. In addition, Kang et al. (59) demonstrated that in macrophages stimulated with LPS or heat-killed *Listeria monocytogenes*, pretreatment with curcumin decreased the production of IFN-γ. When concentrations of IFN-γ exceed a particular level in sepsis, resistance to infections is impaired, leading to an increased lethality rate (60, 61). Therefore, suppressing IFN-γ to normal levels is beneficial to the host due to preventing bacterial outflow

TABLE 7 Effect of curcumin on clinical outcomes are presented for the participants.

Variables		Nano-curcumin group ($n = 20$)	Placebo group ($n = 20$)	*Pv*
Length of hospital stay (day)		27.40 ± 6.18	32.10 ± 9.17	0.083¥
SOFA score	Day 0	8.10 (5–11)	7.50 (6–11)	0.538†
	Day 5	7.55 (5–9)	6.95 (6–10)	0.207£
	Day 10	6.1 (7–4)	6.7 (5–8)	**0.027** £
	P ∓	**0.0001**	0.120	
MODS score	Day 0	9.14 (6–15)	10.06 (8–15)	0.715†
	Day 5	7.54 (6–12)	8.95 (7–13)	0.346£
	Day 10	5.04 (5–8)	7.01 (5–9)	**0.025** £
	P ∓	**0.0015**	0.060	
DBP (mmHg)	Day 0	9.98 (8–11)	9.71 (8–11)	0.641†
	Day 5	9.21 (8–10)	9.15 (8–10)	0.417£
	Day 10	8.16 (7–9)	8.2 (7–9)	0.136 £
	P ∓	**0.036**	0.054	
SBP (mmHg)	Day 0	15.21 (14–18)	16.06 (14–19)	0.541†
	Day 5	13.80 (13–17)	14.89 (13–17)	0.892£
	Day 10	11.63 (12–14)	12.94 (12–14)	0.125 £
	P ∓	**0.0032**	**0.0045**	
PaO2/FiO2 (mmHg)	Day 0	176.50 ± 21.32	183.42 ± 23.01	0.439¥
	Day 5	155.83 ± 17.40	166.77 ± 16.49	0.241 £
	Day 10	123.10 ± 20.74	137.62 ± 18.28	0.077£
	P‡	**0.003**	**0.031**	
Respiratory rate (breaths/min)	Day 0	18.21 ± 2.84	19.12 ± 2.20	0.518¥
	Day 5	16.98 ± 2.76	17.16 ± 2.59	0.414 £
	Day 10	14.85 ± 2.32	15.21 ± 2.73	0.097£
	P‡	0.061	0.114	

ICU, intensive care unit; SOFA, Sequential Organ Failure Assessment, MODS: Multiple Organ Dysfunction Score; SBP: systolic blood pressure DBP: diastolic blood pressure; partial pressure (PaO2 in mmHg) to fractional inspired oxygen (FiO2).

Data are presented as means ± SD; Numbers in bold are statistically significant p-value < 0.05.

£Based on analysis of covariance (ANCOVA) after logarithmically converting; adjusted for sex, BMI, age, type of disease and baseline values.

¥ Based on independent sample t-test.

† Based on Mann–Whitney U Test.

(62). The mechanism by which curcumin reduces IFN-γ is that curcumin decreases $CD4^+$ and IFN-γ^+ and thereby inhibits the Th1 response (63). In addition, curcumin inhibits the Th1 cytokine profile by inhibiting IL-12 production (59).

The other immune response factor that we assessed in the current study was FOXP3. The results showed that NC supplementation considerably increased the mRNA expression of FOXP3. In line with our finding, Chen et al. (36) reported that curcumin administration elevates the expression of FOXP3 in septic mice compared to mice treated with corn oil. FOXP3, a key regulator of T regulatory (Treg) cell development and function, is expressed on $CD4^+$ $CD25^+$ Treg cells (64, 65). In a study by Chai et al. (66), curcumin attenuated the acute lung injury of cecal ligation and puncture-induced mouse model by boosting the differentiation of naïve $CD4^+$ T cells to $CD4^+$ $CD25^+$ $FOXP3^+$ Tregs. Regarding the mechanism underlying the effect of curcumin on FOXP-3, it is suggested that curcumin increases the $CD4^+$, $CD25^+$, and $FOXP3^+$ Treg cells (36), which in turn increases the expression of anti-inflammatory cytokine IL-10 and decreases the proliferation activity of $CD4^+$, $CD25^-$, and T cells (36, 67).

So far as we are aware, no previous research has assessed the effect of NC on immune response among septic patients in ICU. In addition, randomizing the participants minimized the possibility of confounding factors. However, this study is not without limitations. First, the results cannot be generalized since we did not include refractory septic shock patients. Second, a longer supplementation duration and higher NC doses might lead to greater efficacy.

In conclusion, our results indicated that NC supplementation for 10 days in ICU patients with sepsis significantly decreased pro-inflammatory cytokines, MODS, and SOFA scores, the mRNA expression of NF-êB, NLRP-3, IFN-γ, and increased the expression of FOXP3. Further trials with a longer intervention period and larger sample size are warranted to confirm these findings.

Data availability statement

The original contributions presented in this study are included in the article/supplementary material, further inquiries can be directed to the corresponding author.

Ethics statement

The studies involving human participants were reviewed and approved by Tabriz University of Medical Sciences (IR.TBZMED.REC.1396.762). The patients/participants provided their written informed consent to participate in this study.

Author contributions

AK, SP, MV, AM, SS, and MK designed the first hypothesis of the work and searched the data. AK and MV read and extracted the data. AK and AT-E wrote the draft of the manuscript. All authors have read and approved the final manuscript.

Funding

We thank the Tabriz University of Medical Sciences, Tabriz, Iran, for provided the study grant to conduct this research.

Conflict of interest

The authors declare that the research was conducted in the absence of any commercial or financial relationships that could be construed as a potential conflict of interest.

Publisher's note

References

1. Dolin H, Papadimos T, Chen X, Pan Z. Characterization of pathogenic sepsis etiologies and patient profiles: a novel approach to triage and treatment. *Microbiol Insights.* (2019) 12:1178636118825081. doi: 10.1177/1178636118825081

2. Chen X, Yin Y, Zhang J. Sepsis and immune response. *World J Emerg Med.* (2011) 2:88.

3. Karimi A, Naeini F, Azar V, Hasanzadeh M, Niazkar H, Tutunchi H. A comprehensive systematic review of the therapeutic effects and mechanisms of action of quercetin in sepsis. *Phytomedicine.* (2021) 86:153567. doi: 10.1016/j.phymed.2021.153567

4. Rudd K, Johnson S, Agesa K, Shackelford K, Tsoi D, Kievlan D, et al. Global, regional, and national sepsis incidence and mortality, 1990-2017: analysis for the global burden of disease study. *Lancet.* (2020) 395:200–11.

5. Gloria Y, Fuchs K, Chang T, Engels P, Rusch E, Gouttefangeas C, et al. Chitin oligomers directly promote lymphoid innate and adaptive immune cell activation. *bioRxiv.* (2022) [Preprint]. doi: 10.1101/2022.04.06.487356

6. Wu C, Xu Y, Zhao Y. Two kinds of macrophage memory: innate and adaptive immune-like macrophage memory. *Cell Mol Immunol.* (2022) 19:852–4. doi: 10.1038/s41423-022-00885-y

7. Nalos M, Santner-Nanan B, Parnell G, Tang B, McLean AS, Nanan R. Immune effects of interferon gamma in persistent staphylococcal sepsis. *Am J Respir Crit Care Med.* (2012) 185:110–2. doi: 10.1164/ajrccm.185.1.110

8. Vos Q, Lees A, Wu Z, Snapper C, Mond J. B-cell activation by T-cell-independent type 2 antigens as an integral part of the humoral immune response to pathogenic microorganisms. *Immunol Rev.* (2000) 176:154–70. doi: 10.1034/j.1600-065x.2000.00607.x

9. Pati S, Chowdhury A, Mukherjee S, Guin A, Mukherjee S, Sa G. Regulatory lymphocytes: the dice that resolve the tumor endgame. *Appl Cancer Res.* (2020) 40:1–9.

10. Castellheim A, Brekke O, Espevik T, Harboe M, Mollnes T. Innate immune responses to danger signals in systemic inflammatory response syndrome and sepsis. *Scand J Immunol.* (2009) 69:479–91.

11. Wiersinga W, Leopold S, Cranendonk D, van Der Poll T. Host innate immune responses to sepsis. *Virulence.* (2014) 5:36–44.

12. Karimi A, Ghodsi R, Kooshki F, Karimi M, Asghariazar V, Tarighat-Esfanjani A. Therapeutic effects of curcumin on sepsis and mechanisms of action: a systematic review of preclinical studies. *Phytother Res.* (2019) 33:2798–820. doi: 10.1002/ptr.6467

13. Karimi A, Naeini F, Asghari Azar V, Hasanzadeh M, Ostadrahimi A, Niazkar H, et al. A comprehensive systematic review of the therapeutic effects and mechanisms of action of quercetin in sepsis. *Phytomedicine.* (2021) 86:153567.

14. Yang H, Wang H, Andersson U. Targeting inflammation driven by HMGB1. *Front Immunol.* (2020) 11:484. doi: 10.3389/fimmu.2020.00484

15. Gustot T, Durand F, Lebrec D, Vincent J, Moreau R. Severe sepsis in cirrhosis. *Hepatology.* (2009) 50:2022–33.

16. Sharath C. *Use of SOFA (Sequential Organ Failure Assessment) Scoring in Assessing the Incidence and Severity of Organ Dysfunction and Predicting the Outcome in Patients with Sepsis in Surgical Unit*. Coimbatore: Coimbatore Medical College (2016).

17. Warunek J, Jin R, Blair S, Garis M, Marzullo B, Wohlfert E. Tbet expression by regulatory T cells is needed to protect against Th1-mediated immunopathology during toxoplasma infection in mice. *Immunohorizons.* (2021) 5:931–43. doi: 10.4049/immunohorizons.2100080

18. Liew K, Hafiz M, Chong Y, Harith H, Israf D, Tham C. A review of Malaysian herbal plants and their active constituents with potential therapeutic applications in sepsis. *Evid Based Complement Alternat Med.* (2020) 2020:8257817. doi: 10.1155/2020/8257817

19. Rolta R, Salaria D, Sharma P, Sharma B, Kumar V, Rathi B, et al. Phytocompounds of *Rheum emodi*, *Thymus serpyllum*, and *Artemisia annua* inhibit spike protein of SARS-CoV-2 binding to ACE2 receptor: in silico approach. *Curr Pharmacol Rep.* (2021) 7:135–49. doi: 10.1007/s40495-021-00259-4

20. Rolta R, Yadav R, Salaria D, Trivedi S, Imran M, Sourirajan A, et al. In silico screening of hundred phytocompounds of ten medicinal plants as potential inhibitors of nucleocapsid phosphoprotein of COVID-19: an approach to prevent virus assembly. *J Biomol Struct Dyn.* (2021) 39:7017–34. doi: 10.1080/07391102.2020.1804457

21. Rolta R, Kumar V, Sourirajan A, Upadhyay N, Dev K. Bioassay guided fractionation of rhizome extract of *Rheum emodi* wall as bio-availability enhancer of antibiotics against bacterial and fungal pathogens. *J Ethnopharmacol.* (2020) 257:112867. doi: 10.1016/j.jep.2020.112867

22. Karimi A, Mahmoodpoor A, Kooshki F, Niazkar H, Shoorei H, Tarighat-Esfanjani A. Effects of nanocurcumin on inflammatory factors and clinical outcomes in critically ill patients with sepsis: a pilot randomized clinical trial. *Eur J Integr Med.* (2020) 36:101122.

23. Naeini F, Tutunchi H, Razmi H, Mahmoodpoor A, Vajdi M, Sefidmooye Azar P, et al. Does nano-curcumin supplementation improve hematological indices in critically ill patients with sepsis? a randomized controlled clinical trial. *J Food Biochem.* (2022) 46:e14093. doi: 10.1111/jfbc.14093

24. Karimi A, Naeini F, Niazkar H, Tutunchi H, Musazadeh V, Mahmoodpoor A, et al. Nano-curcumin supplementation in critically ill patients with sepsis: a randomized clinical trial investigating the inflammatory biomarkers, oxidative stress indices, endothelial function, clinical outcomes and nutritional status. *Food Funct.* (2022) 13:6596–612. doi: 10.1039/d1fo03746c

25. Ferguson J, Abbott K, Garg M. Anti-inflammatory effects of oral supplementation with curcumin: a systematic review and meta-analysis of randomized controlled trials. *Nutr Rev.* (2021) 79:1043–66.

26. Mayhall C. *Hospital Epidemiology and Infection Control*. Philadelphia, PA: Lippincott Williams & Wilkins (2012).

27. Antiga E, Bonciolini V, Volpi W, Del Bianco E, Caproni M. Oral curcumin (Meriva) Is effective as an adjuvant treatment and is able to reduce IL-22 serum levels in patients with psoriasis vulgaris. *Biomed Res Int.* (2015) 2015:283634. doi: 10.1155/2015/283634

28. Chen F, Jiang Y, Liu S, Zou L, Cao Y, Zhu Y. The expression changes and correlation analysis of high mobility group box-1 and tissue factor in the serum of rats with sepsis. *Eur Rev Med Pharmacol Sci.* (2019) 23:1634–40. doi: 10.26355/eurrev_201902_17123

29. Cai J, Lin Z. Correlation of blood high mobility group box-1 protein with mortality of patients with sepsis: a meta-analysis. *Heart Lung.* (2021) 50:885–92. doi: 10.1016/j.hrtlng.2021.07.010

30. Silva L, Catalão C, Felippotti T, Oliveira-Pelegrin G, Petenusci S, de Freitas L, et al. Curcumin suppresses inflammatory cytokines and heat shock protein 70 release and improves metabolic parameters during experimental sepsis. *Pharm Biol.* (2017) 55:269–76. doi: 10.1080/13880209.2016.1260598

31. Djalali M, Abdolahi M, Hosseini R, Miraghajani M, Mohammadi H, Djalali M. The effects of nano-curcumin supplementation on Th1/Th17 balance in migraine patients: a randomized controlled clinical trial. *Complement Therap Clin Pract.* (2020) 41:101256. doi: 10.1016/j.ctcp.2020.101256

32. Ge Y, Huang M, Yao Y. Biology of Interleukin-17 and its pathophysiological significance in sepsis. *Front Immunol.* (2020) 11:1558. doi: 10.3389/fimmu.2020.01558

33. Cua D, Tato C. Innate IL-17-producing cells: the sentinels of the immune system. *Nat Rev Immunol.* (2010) 10:479–89.

34. Weber G, Schlautkötter S, Kaiser-Moore S, Altmayr F, Holzmann B, Weighardt H. Inhibition of interleukin-22 attenuates bacterial load and organ failure during acute polymicrobial sepsis. *Infect Immun.* (2007) 75:1690–7. doi: 10.1128/IAI.01564-06

35. Vachharajani V, Wang S, Mishra N, El Gazzar M, Yoza B, McCall C. Curcumin modulates leukocyte and platelet adhesion in murine sepsis. *Microcirculation.* (2010) 17:407–16. doi: 10.1111/j.1549-8719.2010.00039.x

36. Chen L, Lu Y, Zhao L, Hu L, Qiu Q, Zhang Z, et al. Curcumin attenuates sepsis-induced acute organ dysfunction by preventing inflammation and enhancing the suppressive function of Tregs. *Int Immunopharmacol.* (2018) 61:1–7. doi: 10.1016/j.intimp.2018.04.041

37. Memis D, Hekimoglu S, Sezer A, Altaner S, Sut N, Usta U. Curcumin attenuates the organ dysfunction caused by endotoxemia in the rat. *Nutrition.* (2008) 24:1133–8. doi: 10.1016/j.nut.2008.06.008

38. Liu W, Guo W, Zhu Y, Peng S, Zheng W, Zhang C, et al. Targeting peroxiredoxin 1 by a curcumin analogue, AI-44, Inhibits NLRP3 inflammasome activation and attenuates lipopolysaccharide-induced sepsis in mice. *J Immunol.* (2018) 201:2403–13. doi: 10.4049/jimmunol.1700796

39. Gong Z, Zhou J, Li H, Gao Y, Xu C, Zhao S, et al. Curcumin suppresses NLRP3 inflammasome activation and protects against LPS-induced septic shock. *Mol Nutr Food Res.* (2015) 59:2132–42. doi: 10.1002/mnfr.201500316

40. Alvarenga L, Salarolli R, Cardozo L, Santos R, de Brito J, Kemp J, et al. Impact of curcumin supplementation on expression of inflammatory transcription factors in hemodialysis patients: a pilot randomized, double-blind, controlled study. *Clin Nutr.* (2020) 39:3594–600.

41. Danielski L, Giustina A, Bonfante S, Barichello T, Petronilho F. The NLRP3 inflammasome and its role in sepsis development. *Inflammation.* (2020) 43:24–31.

42. Chen B, Li H, Ou G, Ren L, Yang X, Zeng M. Curcumin attenuates MSU crystal-induced inflammation by inhibiting the degradation of IκBα and blocking mitochondrial damage. *Arthritis Res Ther.* (2019) 21:193. doi: 10.1186/s13075-019-1974-z

43. Abd-Elrazek A, Mahmoud S, Abd ElMoneim A. The comparison between curcumin and propolis against sepsis-induced oxidative stress, inflammation, and apoptosis in kidney of adult male rat. *Future J Pharm Sci.* (2020) 6:1–13.

44. Xie Y, Chu J, Jian X, Dong J, Wang L, Li G, et al. Curcumin attenuates lipopolysaccharide/d-galactosamine-induced acute liver injury by activating Nrf2 nuclear translocation and inhibiting NF-kB activation. *Biomed Pharmacother.* (2017) 91:70–7. doi: 10.1016/j.biopha.2017.04.070

45. Selvaraj V, Nepal N, Rogers S, Manne N, Arvapalli R, Rice K, et al. Inhibition of MAP kinase/NF-kB mediated signaling and attenuation of lipopolysaccharide induced severe sepsis by cerium oxide nanoparticles. *Biomaterials.* (2015) 59:160–71. doi: 10.1016/j.biomaterials.2015.04.025

46. Wei C, Wang J, Xiong F, Wu B, Luo M, Yu Z, et al. Curcumin ameliorates DSS-induced colitis in mice by regulating the Treg/Th17 signaling pathway. *Mol Med Rep.* (2021) 23:34. doi: 10.3892/mmr.2020.11672

47. Sun J, Zhao Y, Hu J. Curcumin inhibits imiquimod-induced psoriasis-like inflammation by inhibiting IL-1beta and IL-6 production in mice. *PLoS One.* (2013) 8:e67078. doi: 10.1371/journal.pone.0067078

48. Wang Q, Ye C, Sun S, Li R, Shi X, Wang S, et al. Curcumin attenuates collagen-induced rat arthritis via anti-inflammatory and apoptotic effects. *Int Immunopharmacol.* (2019) 72:292–300. doi: 10.1016/j.intimp.2019.04.027

49. Siddiqui A, Cui X, Wu R, Dong W, Zhou M, Hu M, et al. The anti-inflammatory effect of curcumin in an experimental model of sepsis is mediated by up-regulation of peroxisome proliferator-activated receptor-gamma. *Crit Care Med.* (2006) 34:1874–82. doi: 10.1097/01.CCM.0000221921.71300.BF

50. Liu S, Zhang J, Pang Q, Song S, Miao R, Chen W, et al. The protective role of curcumin in Zymosan-induced multiple organ dysfunction syndrome in mice. *Shock.* (2016) 45:209–19. doi: 10.1097/SHK.0000000000000502

51. Chen S, Tang C, Ding H, Wang Z, Liu X, Chai Y, et al. Maf1 ameliorates sepsis-associated encephalopathy by suppressing the NF-kB/NLRP3 inflammasome signaling pathway. *Front Immunol.* (2020) 11:594071. doi: 10.3389/fimmu.2020.594071

52. Luo M, Yan D, Sun Q, Tao J, Xu L, Sun H, et al. Ginsenoside Rg1 attenuates cardiomyocyte apoptosis and inflammation via the TLR4/NF-kB/NLRP3 pathway. *J Cell Biochem.* (2020) 121:2994–3004. doi: 10.1002/jcb.29556

53. Ran Y, Su W, Gao F, Ding Z, Yang S, Ye L, et al. Curcumin ameliorates white matter injury after ischemic stroke by inhibiting microglia/macrophage pyroptosis through NF-κB suppression and NLRP3 inflammasome inhibition. *Oxid Med Cell Longev.* (2021) 2021:1552127. doi: 10.1155/2021/1552127

54. Yang H, Ochani M, Li J, Qiang X, Tanovic M, Harris H, et al. Reversing established sepsis with antagonists of endogenous high-mobility group box 1. *Proc Natl Acad Sci USA.* (2004) 101:296–301. doi: 10.1073/pnas.2434651100

55. Yoo H, Im Y, Ko R, Lee J, Park J, Jeon K. Association of plasma level of high-mobility group box-1 with necroptosis and sepsis outcomes. *Sci Rep.* (2021) 11:9512. doi: 10.1038/s41598-021-88970-6

56. Ahn M, Hwang J, Lee S, Ham S, Hur J, Kim J, et al. Curcumin longa extract-loaded nanoemulsion improves the survival of endotoxemic mice by inhibiting nitric oxide-dependent HMGB1 release. *PeerJ.* (2017) 5:e3808. doi: 10.7717/peerj.3808

57. Kim D, Lee W, Bae J. Vascular anti-inflammatory effects of curcumin on HMGB1-mediated responses in vitro. *Inflamm Res.* (2011) 60:1161–8. doi: 10.1007/s00011-011-0381-y

58. Gao X, Kuo J, Jiang H, Deeb D, Liu Y, Divine G, et al. Immunomodulatory activity of curcumin: suppression of lymphocyte proliferation, development of cell-mediated cytotoxicity, and cytokine production in vitro. *Biochem Pharmacol.* (2004) 68:51–61. doi: 10.1016/j.bcp.2004.03.015

59. Kang B, Song Y, Kim K, Choe Y, Hwang S, Kim T. Curcumin inhibits Th1 cytokine profile in CD4+ T cells by suppressing interleukin-12 production in macrophages. *Br J Pharmacol.* (1999) 128:380–4. doi: 10.1038/sj.bjp.0702803

60. Souza-Fonseca-Guimaraes F, Parlato M, Philippart F, Misset B, Cavaillon J, Adib-Conquy M. Toll-like receptors expression and interferon-γ production by NK cells in human sepsis. *Crit Care.* (2012) 16:R206. doi: 10.1186/cc11838

61. Schütze S, Kaufmann A, Bunkowski S, Ribes S, Nau R. Interferon-gamma impairs phagocytosis of *Escherichia coli* by primary murine peritoneal macrophages stimulated with LPS and differentially modulates proinflammatory cytokine release. *Cytokine.* (2021) 3:100057. doi: 10.1016/j.cytox.2021.100057

62. Wang D, Zhong X, Huang D, Chen R, Bai G, Li Q, et al. Functional polymorphisms of interferon-gamma affect pneumonia-induced sepsis. *PLoS One.* (2014) 9:e87049. doi: 10.1371/journal.pone.0087049

63. Kanakasabai S, Casalini E, Walline C, Mo C, Chearwae W, Bright J. Differential regulation of CD4(+) T helper cell responses by curcumin in experimental autoimmune encephalomyelitis. *J Nutr Biochem.* (2012) 23:1498–507. doi: 10.1016/j.jnutbio.2011.10.002

64. Bao R, Hou J, Li Y, Bian J, Deng X, Zhu X, et al. Adenosine promotes Foxp3 expression in Treg cells in sepsis model by activating JNK/AP-1 pathway. *Am J Transl Res.* (2016) 8:2284–92.

65. Forward N, Conrad D, Power Coombs M, Doucette C, Furlong S, Lin T, et al. Curcumin blocks interleukin (IL)-2 signaling in T-lymphocytes by inhibiting IL-2 synthesis, CD25 expression, and IL-2 receptor signaling. *Biochem Biophys Res Commun.* (2011) 407:801–6. doi: 10.1016/j.bbrc.2011.03.103

66. Chai Y, Chen Y, Lin S, Xie K, Wang C, Yang Y, et al. Curcumin regulates the differentiation of naïve CD4+T cells and activates IL-10 immune modulation against acute lung injury in mice. *Biomed Pharmacother.* (2020) 125:109946. doi: 10.1016/j.biopha.2020.109946

67. Toden S, Theiss A, Wang X, Goel A. Essential turmeric oils enhance anti-inflammatory efficacy of curcumin in dextran sulfate sodium-induced colitis. *Sci Rep.* (2017) 7:814. doi: 10.1038/s41598-017-00812-6

frontiers | Frontiers in Nutrition

TYPE Original Research
PUBLISHED 08 December 2022
DOI 10.3389/fnut.2022.1062667

OPEN ACCESS

EDITED BY
Filippo Giorgio Di Girolamo,
University of Trieste, Italy

REVIEWED BY
Jiabin Tu,
Fujian Medical University, China
Mahsa Malekahmadi,
Tehran University of Medical Sciences, Iran

*CORRESPONDENCE
Sheng-Der Hsu
f1233j@gmail.com

SPECIALTY SECTION
This article was submitted to Clinical Nutrition, a section of the journal Frontiers in Nutrition

RECEIVED 06 October 2022
ACCEPTED 25 November 2022
PUBLISHED 08 December 2022

CITATION
Chiu Y-C, Liang C-M, Chung C-H, Hong Z-J, Chien W-C and Hsu S-D (2022) The influence of early selenium supplementation on trauma patients: A propensity-matched analysis. *Front. Nutr.* 9:1062667. doi: 10.3389/fnut.2022.1062667

The influence of early selenium supplementation on trauma patients: A propensity-matched analysis

Yu-Cheng Chiu[1], Chia-Ming Liang[2], Chi-Hsiang Chung[3], Zhi-Jie Hong[4], Wu-Chien Chien[5] and Sheng-Der Hsu[2]*

[1]Division of General Surgery, Tri-Service General Hospital, National Defense Medical Center, Taipei, Taiwan, [2]Division of Trauma Surgery and Critical Care Medicine, Tri-Service General Hospital, National Defense Medical Center, Taipei, Taiwan, [3]Department of Medical Research, Tri-Service General Hospital, National Defense Medical Center, Taipei, Taiwan, [4]Division of Trauma Surgery, Tri-Service General Hospital, National Defense Medical Center, Taipei, Taiwan, [5]School of Public Health, National Defense Medical Center, Taipei, Taiwan

Introduction: Oxidative stress is involved in numerous inflammatory diseases, including trauma. Micronutrients, such as selenium (Se), which contribute to antioxidant defense, exhibit low plasma levels during critical illness. This study aimed to investigate the impact of early Se supplementation on trauma patients.

Materials and methods: A total of 6,891 trauma patients were registered at a single medical center from January 2018 to December 2021. Twenty trauma patients with Se supplemented according to the protocol were included in the study group. Subsequently, 1:5 propensity score matching (PSM) analysis was introduced. These patients received 100 mcg three times a day for 5 days. The primary outcome was overall survival (OS); the secondary outcomes were hospital/intensive care unit (ICU) length of stay (LOS), serologic change, ventilator dependence days, and ventilation profile.

Results: The hospital LOS (20.0 ± 10.0 vs. 37.4 ± 42.0 days, $p = 0.026$) and ICU LOS (6.8 ± 3.6 vs. 13.1 ± 12.6 days, $p < 0.006$) were significantly shorter in the study group. In terms of serology, improvement in neutrophil, liver function, and C-reactive protein (CRP) level change percentile indicated better outcomes in the study group as well as a better OS rate (100 vs. 83.7%, $p = 0.042$). Longer ventilator dependence was found to be an independent risk factor for mortality and pulmonary complications in 6,891 trauma patients [odds ratio (OR) = 1.262, 95% confidence interval (CI) = 1.039–1.532, $p < 0.019$ and OR = 1.178, 95% CI = 1.033–1.344, $p = 0.015$, respectively].

Conclusion: Early Se supplementation after trauma confers positive results in terms of decreasing overall ICU LOS/hospital LOS and mortality. Organ injury, particularly hepatic insults, and inflammatory status, also recovered better.

KEYWORDS

selenium supplement, selenoproteins, trauma, pulmonary complication, length of stay

Introduction

Critical diseases, such as trauma, major burn, and sepsis, trigger oxidative stress by increasing the production of reactive oxygen species and reactive nitrogen species, which significantly contributes to systemic inflammatory response syndrome (SIRS), thereby causing vessel/pulmonary endothelial damage, acute respiratory distress syndrome, and multiple organ failure (1, 2). Recent studies have reported that both SIRS and counter-inflammatory response syndrome simultaneously develop in the initial phase following an injury. Depletion of several endogenous micronutrients, such as selenium (Se), ascorbic acid, zinc, glutamine, and tocopherols, is associated with poor prognosis (3–6). These inflammatory processes also impair normal cells and make them evolve toward degradation in numerous clinical conditions, including cardiovascular diseases, cancers, autoimmune disorders, pancreatitis, neurodegenerative disorders, burns, and traumas. Moreover, Kaushal et al. (7) have comprehensively discussed mechanisms focusing on the anti-inflammatory role of Se and their correlations. Several studies have demonstrated that Se plays a key role in regulating immunity and inflammation responses as an essential micronutrient, which is required for more than 25 proteins in the body (8).

Trauma accounts for 1 of the 10 leading causes of death (9). Initial mortality depends on injury severity (10). However, late deaths that developed from days to weeks following an initial injury are associated with inflammatory processes after a traumatic injury (11). Sepsis, acute respiratory distress syndrome, and multiorgan failure are substitutes for the cause of death. Serum concentration of Se and its transport protein "selenoproteins" (mainly as selenocysteine) are extremely low within the first hour of trauma (mean Se: 33.6 μg/L; SELENOP: 1.4 mg/L, trauma patients vs. mean Se: 80.1 μg/L; SELENOP: 4.1 mg/L, healthy general population, Braunstein et al.); a subsequently increased selenoprotein biosynthesis that dominates serum Se concentration occurs at 6–12 h after an injury (mean Se: 48.6 μg/L; SELENOP: 1.9 mg/L) (12). This drastic Se-decline phenomenon may offer an explanation about the benefits of Se supplementation in critical diseases (13) and that supplemental Se may efficiently support selenoprotein biosynthesis during the first hours. A previous study has generally indicated that Se supplementation confers positive effects with less mortality rates and lower infection and multiorgan failure rates (14–16). Recent nutritional therapy guidelines [American Society for Parenteral and Enteral Nutrition (ASPEN)] (17) have suggested that patients should receive trace elements or special nutrients. In in a meta-analysis by Huang et al. (18), they reported a decrease in the length of intensive care unit (ICU) stay and mortality without specific adverse effects. However, ensuring treatment benefits and lung protection were reported as major challenges owing to the small sample size and moderate heterogeneity ($I2$ = 45.496%, $p < 0.001$).

This study aimed to retrospectively review the effectiveness of Se supplementation on mortality, length of ICU/ventilator dependence, and serological changes in major trauma patients.

Materials and methods

Study participants and design

A total of 6,891 patients were registered in Tri-Service General Hospital Medical Center Trauma Databank from January 2018 to December 2021. Information on these trauma patients was collected following the selection protocol presented in **Figure 1**. At the time of resuscitation in the emergency room, written informed consent was obtained from the patients or their closest relatives if they agreed to the Se supplement. Regardless of hemodynamic stability, enteral nutrition establishment, and surgical intervention, intravenous sodium selenite 100 mcg Q8H was administered for 5 consecutive days since the day of ICU admission. The exclusion criteria for the study were as follows: (I) patients who died in the emergency room or upon admission; (II) patients who were transferred to another hospital; (III) patients aged below 18 years; (IV) patients who were lost to follow-up or had incomplete data. A total of 6,535 patients were eligible, and 20 trauma patients who were admitted to the ICU of Tri-Service General Hospital and were receiving Se supplementation were entered in the study group. Patients included in this study were categorized into the following two groups: Se treatment group and non-Se treatment group,

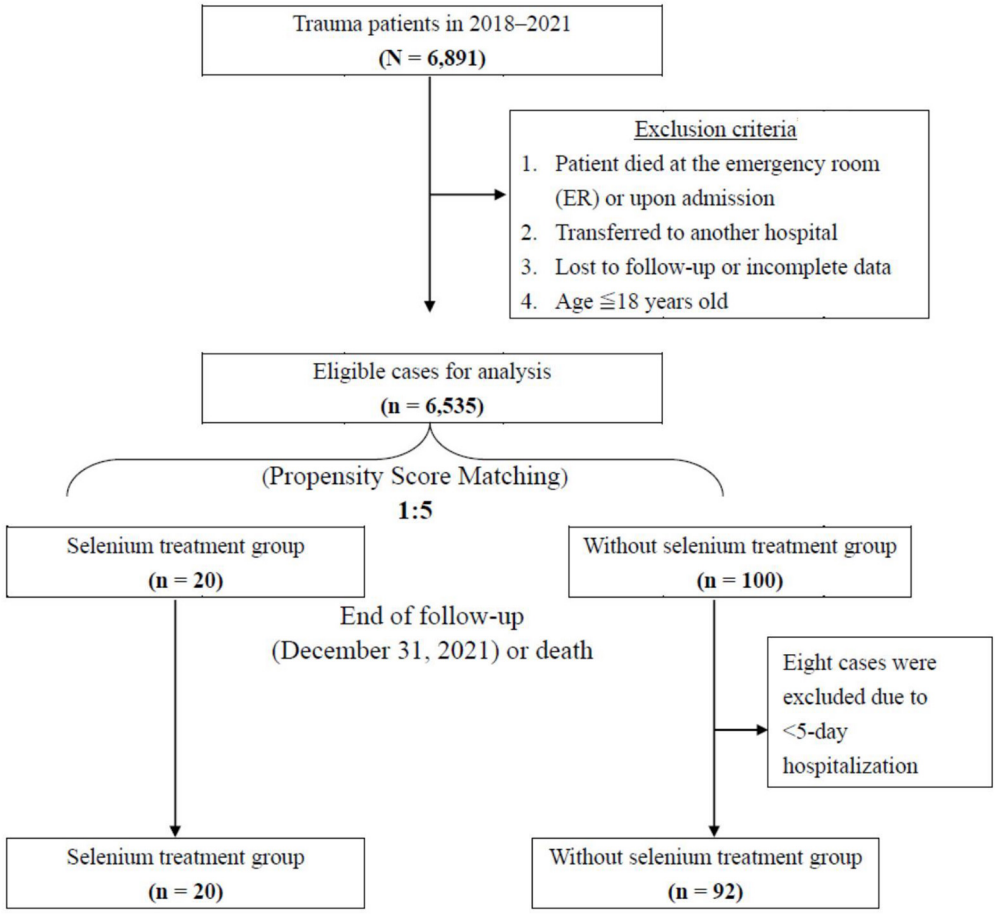

FIGURE 1
Flowchart of study sample selection from registration in the Tri-Service General Hospital Trauma Data Bank.

based on whether Se supplementation was started in the first consecutive 5 days or not. Subsequently, 1:5 propensity score matching (PSM) analysis was introduced following the exclusion of patients with <5-day hospitalization. Finally, the Se and non-Se treatment groups included 20 and 92 patients, respectively. All covariate imbalances were alleviated. The primary outcome was OS; the secondary outcomes were hospital/ICU length of stay (LOS), serologic change, ventilator dependence days, and ventilation profile.

This retrospective cohort study utilized a single-center trauma databank for data collection. The study was approved by the ethics committee of Tri-Service General Hospital and conducted in accordance with the Declaration of Helsinki.

Data collection

Data were collected from Tri-Service General Hospital Trauma Data Bank. All data collectors were blinded to the study aims at the time of data abstraction. All medical records were reviewed by three independent physicians. Inconsistent clinical scores were recalculated until consensus was achieved.

Demographic information and nominal variables, including age, sex, alcoholic ingestion, extracorporeal membrane oxygenation (ECMO) use, and comorbidity, were collected. Continuous variable evaluation and clinical scores were also investigated. Trauma and injury severity score (TRISS), revised trauma score (RTS), new injury severity score (NISS), and injury severity score (ISS) (19) were collected to assess the severity of trauma. Glasgow Coma Scale and vital signs, including blood pressure, respiratory rate, and heart rate, were recorded. Moreover, serum albumin, liver function [glutamic oxaloacetic transaminase (GOT) and glutamic pyruvic transaminase (GPT)], neutrophil percentage, C-reactive protein (CRP) level, and Ratio of arterial oxygen partial pressure to fractional inspired oxygen (PaO2/FiO2) ratio at days 1 and 5 were measured for inflammatory response and lung injury severity. ICU LOS, days of weaning of ventilators, and outcomes were surveyed for therapeutic indicators.

Propensity score matching analysis and statistical analysis

Propensity score matching analysis was performed using the matching package in R software (version 4.0.2 for Windows, Bell Laboratories, Murray Hill, NJ, USA). Logistic regression was used for the estimation algorithm of PSM, and the matching algorithm used was the nearest neighbor matching. The option for nearest neighbor was set as random matching order, non-replacement, no caliper, tolerance was set at 0.15, and 1:5 matching according to age, sex, and ISS. The standardized differences of the matching score were set at 0.20.

Continuous variables were presented as means (±standard deviations). Fisher's exact test determined the association between categorical variables, as appropriate. The Mann–Whitney *U*-test was used for continuous data, as appropriate. Condition logistic regression analysis of risk factors for mortality and pulmonary complication among propensity-matched trauma patients were also investigated, as appropriate. Statistical analysis was performed using SPSS version 26.0 for Windows (SPSS Inc., Chicago, IL, USA). $P < 0.05$ was considered statistically significant.

Results

Baseline characteristics

Baseline characteristics of patients allocated to the Se and without Se treatment groups are described in Table 1. The alcohol exposure percentage (95.0 vs. 71.4%, $p = 0.019$) and thoracic area injury [Abbreviated Injury Scale (AIS): 3.6 ± 0.6 vs. 2.3 ± 1.7, $p = 0.002$] were higher in the Se treatment group than those in the non-Se treatment group. In the non-Se treatment group, the incidence of head and neck area injury (AIS: 3.6 ± 1.3 vs. 2.8 ± 1.0, $p = 0.003$) was higher than that in the Se treatment group; however, no statistical difference in the ISS score was noted (28.8 ± 7.5 vs. 29.3 ± 7.2, $p = 0.711$). Furthermore, no significant differences in age, sex, vital signs on admission, Glasgow Coma Scale, comorbidities, trauma scores (RTS, NISS, TRISS, and ISS), and ECMO support between the two groups were noted. Baseline clinicopathological characteristics and injury severity were generally balanced.

Comparison of clinical outcomes between the two groups

In the matched cohort, the clinical outcomes of the two groups are shown in the lower part of Table 1. The hospital LOS (20.0 ± 10.0 vs. 37.4 ± 42.0 days, $p = 0.026$) and ICU LOS (6.8 ± 3.6 vs. 13.1 ± 12.6 days, $p < 0.006$) revealed significantly fewer number of days in the Se treatment group

TABLE 1 Comparison of variables between patients with or without selenium treatment after 1:5 propensity score matching (PSM).

Variable	Selenium treatment ($n = 20$)	Without selenium treatment ($n = 92$)	*P*-value
Age, y	43.2 ± 18.0	49.8 ± 20.1	0.180
Sex, male	15 (75.0%)	69 (75.0%)	0.623
Vital signs on admission			
Systolic blood pressure (mmHg)	123.3 ± 35.5	132.4 ± 29.9	0.461
Respiratory rate	25.9 ± 24.6	20.3 ± 3.4	0.351
Heart rate (bpm)	96.3 ± 25.2	91.1 ± 17.7	0.169
Glasgow Coma Scale	10.6 ± 3.6	10.8 ± 4.2	0.797
With comorbidities	7 (35.0%)	41 (44.6%)	0.467
Comorbidity category			
Central nervous system	1 (5.0%)	12 (13.0%)	0.457
Cardiovascular system	4 (20.0%)	24 (26.1%)	0.777
Respiratory system	0 (0%)	3 (3.3%)	0.413
Digestive system	0 (0%)	2 (2.2%)	0.506
Genitourinary system	0 (0%)	1 (1.1%)	0.640
Endocrine system	3 (15.0%)	18 (19.6%)	0.761
Cancer	1 (5.0%)	0 (0%)	0.179
With alcohol exposure	19 (95.0%)	65 (71.4%)	0.019*
RTS	6.67 ± 0.76	6.70 ± 1.33	0.391
NISS	33.7 ± 8.4	32.2 ± 7.9	0.359
TRISS	0.82 ± 0.14	0.76 ± 0.24	0.690
ISS	28.8 ± 7.5	29.3 ± 7.2	0.711
AIS body region			
Head and neck	2.8 ± 1.0	3.6 ± 1.3	0.003*
Face	0.2 ± 0.6	0.6 ± 0.9	0.090
Thorax	3.6 ± 0.6	2.3 ± 1.7	0.002*
Abdomen	1.2 ± 1.6	0.8 ± 1.4	0.289
Extremities	1.9 ± 0.9	1.6 ± 1.2	0.383
External	0.3 ± 0.5	0.5 ± 0.7	0.245
Hospital LOS, days	20.0 ± 10.0	37.4 ± 42.0	0.026*
ICU LOS, days	6.8 ± 3.6	13.1 ± 12.6	0.006*
Ventilator dependence, days	6.0 ± 8.4	13.9 ± 17.7	0.259
With ECMO support	1 (5.0%)	1 (1.1%)	0.327
Serum albumin change (%)	−11.55 ± 7.69	−2.89 ± 23.26	0.011*

(Continued)

10.3389/fnut.2022.1062667

TABLE 1 (Continued)

Variable	Selenium treatment (n = 20)	Without selenium treatment (n = 92)	P-value
Neutrophil percentage change (%)	−26.36 ± 9.79	29.65 ± 47.06	<0.001*
Liver function change (%)			
GOT	−62.63 ± 27.53	12.04 ± 161.03	<0.001*
GPT	−59.38 ± 28.37	67.39 ± 223.45	<0.001*
CRP change (%)	−71.94 ± 16.57	121.21 ± 264.01	<0.001*
Gas exchange			
PaO2/FiO2 ratio, day 1	277.74 ± 119.17	329.32 ± 161.90	0.012*
PaO2/FiO2 ratio, day 5	488.57 ± 139.73	412.86 ± 152.40	0.053
Outcome, survival	20 (100%)	77 (83.7%)	0.042*

RTS, revised trauma score; NISS, new injury severity score; ISS, injury severity score; AIS, abbreviated injury scale; LOS, length of stay; ICU, intensive care unit; ECMO, extracorporeal membrane oxygenation; GOT, glutamic oxaloacetic transaminase; GPT, glutamic pyruvic transaminase; CRP, C-reactive protein; PaO2/FiO2, Ratio of arterial oxygen partial pressure to fractional inspired oxygen.
*Significant difference.

than those in the non-Se treatment group (Figure 2A). Although ventilator dependence days were less in the Se treatment group (6.0 ± 8.4 vs. 13.9 ± 17.7 days), this did not reach statistical significance (p = 0.259) (Figure 2B). Regarding serology, improvement of neutrophil left shift percentage (−26.36 ± 9.79 vs. 29.65 ± 47.06%, $p < 0.001$), liver function (GOT: −62.63 ± 27.53 vs. 12.04 ± 161.03%, $p < 0.001$; GPT: −59.38 ± 28.37 vs. 67.39 ± 223.45%, $p < 0.001$), and CRP level change percentile (−71.94 ± 16.57 vs. 121.21 ± 264.01%, $p < 0.001$) all indicated better outcomes in the Se treatment group (Figures 3A–C); however, serum albumin decline was more prominent in the Se treatment group (−11.55 ± 7.69 vs. −2.89 ± 23.26%, p = 0.011). The proportion of gas exchange was lower on day 1 admission (277.74 ± 119.17 vs. 329.32 ± 161.90, $p < 0.012$); however, it became better on day 5 of hospitalization in the Se treatment group (488.57 ± 139.73 vs. 412.86 ± 152.40, p = 0.053). In summary, the overall survival (OS) rate in the Se treatment group showed superior results than that in the Se treatment group (100 vs. 83.7%, p = 0.042).

Risk stratifications of mortality and pulmonary complications

We thereafter performed univariate and multivariate logistic regression analyses for risk stratifications of mortality and pulmonary complications (Tables 2, 3). Regression analysis revealed a value of 0.000 in the Se treatment group because there were no mortality cases. Multivariable logistic regression analysis revealed that longer ventilator dependence was positively correlated with higher risk of mortality and pulmonary complications [odds ratio (OR) = 1.262, 95% confidence interval (CI) = 1.039–1.532, $P < 0.019$ and OR = 1.178, 95% CI = 1.033–1.344, P = 0.015, respectively]. Furthermore, hospital LOSs were negatively associated with pulmonary complications and mortality in both univariate and multivariate analyses (OR for mortality: 0.712, 95% CI = 0.551–0.920, $P < 0.010$; OR for pulmonary complications: 0.793, 95% CI = 0.873–0.933, $P < 0.005$). Overall, no correlations between demographic factors and either pulmonary complications or mortality, including age, sex, comorbidity, ventilation, ISS score, and ICU LOS, were noted.

Discussion

This retrospective study disclosed that trauma patients can benefit from early phase utilization of Se supplement. Mortality rate, ICU LOS, hospital LOS, systemic inflammation (CRP and neutrophil downgrade), and acute hepatitis were significantly reduced. Although data on ventilator dependence and post-treatment ventilation (day 5 gas exchange) did not achieve statistical significance, they displayed pulmonary protective tendency in the Se supplement group.

Consistent with our results, the results of several previous studies have also presented positive correlations between low initial Se levels and adverse outcomes in critically ill patients (20–23). Moreover, in a recently published meta-analysis by Jen-Fu Huang (24), it has been reported that Se supplementation after trauma confers positive effects in decreasing mortality and ICU and hospital LOSs. Six randomized controlled trials or retrospective studies were included in this systematic review, and doses of Se were 200–500 mcg per day. It appeared safe, and major side effects were not observed.

Compared with other systemic inflammatory diseases, a study in Berlin in 2019 (12) revealed dramatic changes in serum Se and selenoprotein concentrations in trauma patients; however, this was in contrast to the low Se status observed in patients with sepsis, wherein a slow and gradual decline in serum biomarkers was observed. Therefore, this may offer an explanation for the observed beneficial effects of supplemental Se in critical illness (13), where some additional Se may efficiently help selenoprotein biosynthesis during the first hours after the traumatic injury.

Substantial Se-based micronutrient supplementation is currently being widely used for patients with critical illness, cancer, or neurodegenerative disorders. However, various cytotoxicity and adverse effects have been reported. A study by Wenyi Zheng (25) proposed extracellular albumin binding as a predominant factor in determining the cytotoxicity of selenocompounds (SeCs). The available

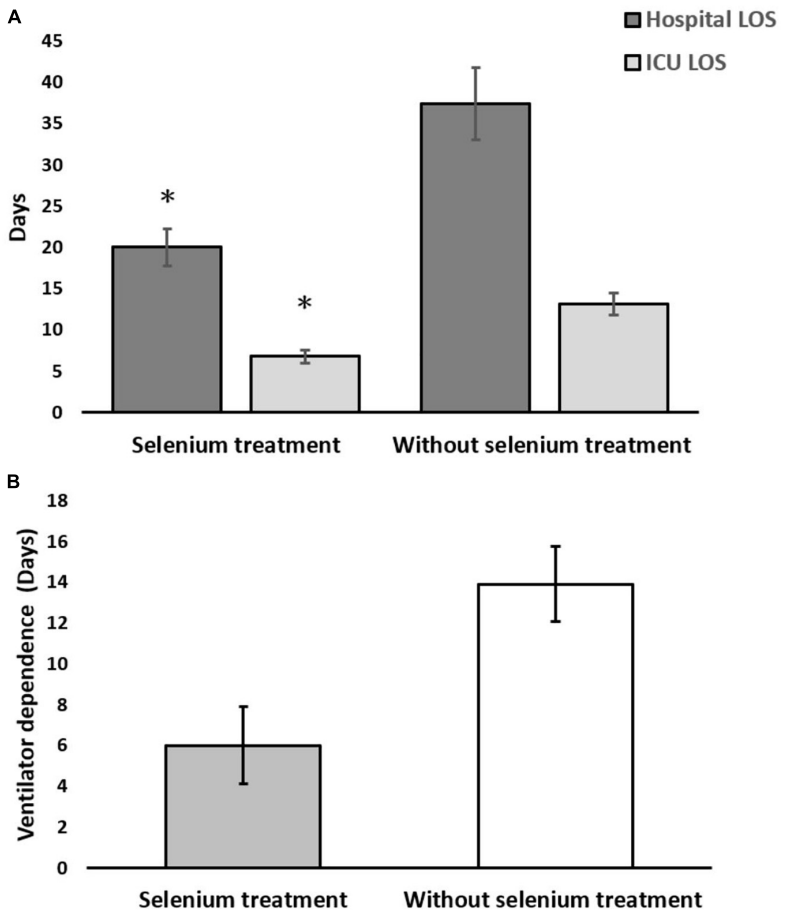

FIGURE 2
(A) Hospital and intensive care unit (ICU) length of stay (LOS); **(B)** ventilator-dependent days in the selenium treatment and non-selenium treatment group. *$p < 0.05$.

evidence of SeC cytotoxicity is limited to intracellular factors. In comparison, scattered information suggests that SeCs show strong albumin binding; therefore, cellular uptake and downstream cytotoxicity, which are orchestrated by extracellular albumin, are hypothesized. Based on this study, we could explain that a remarkable decrease in albumin levels in the Se supplementation group may contribute to extracellular albumin binding for additional SeCs on their cellular uptake and cytotoxicity.

Selenium deficiency may cause reduced glutathione peroxidase activity that indirectly regulates the expression of cyclooxygenases and lipoxygenases *via* the mitogen-activated protein kinase pathway and cyclooxygenases-2, by controlling the nuclear factor kappa-light-chain-enhancer of activated B-cells. These enzymes are involved in the production of lipid mediators, such as prostaglandins, thromboxanes, prostacyclins, leukotrienes, and oxidized fatty acids, which are well-known inflammatory biomarkers from tissues and immune cells in response to stress, free radicals, and infections. Moreover, these molecules are key factors in the modulation of pivotal metabolic signaling pathways and convert pro-inflammatory macrophages (M1) to anti-inflammatory macrophages (M2). Increasing Se concentrations in patients with critical illness, for example, is reported to be associated with the decrease in pro-inflammatory cytokines [interleukin (IL)-6, IL-8, and IL-17] and the increase in the Se concentration in protein metabolites, which are expressed as antioxidant selenoproteins [e.g., glutathione peroxidases and selenoprotein thioredoxin reductase (TXNRD1)]. Selenium is essential for selenoenzyme biosynthesis and functional activity. Previously identified TXNRD1, which is mainly expressed by airway epithelia, is a promising therapeutic target for pulmonary injury prevention, most likely *via* nuclear factor E2-related factor 2 (Nrf2)-dependent mechanisms. A recent study (25) showed that Se levels positively correlated with Nrf2 and selenoprotein activation following TXNRD1 inhibition. These data indicate that Se levels significantly influence physiologic responses to TXNRD1 inhibitors. In summary, clinical Se deficiency must be corrected for the optimal therapeutic effectiveness of TXNRD1 inhibitors in the prevention of lung disease.

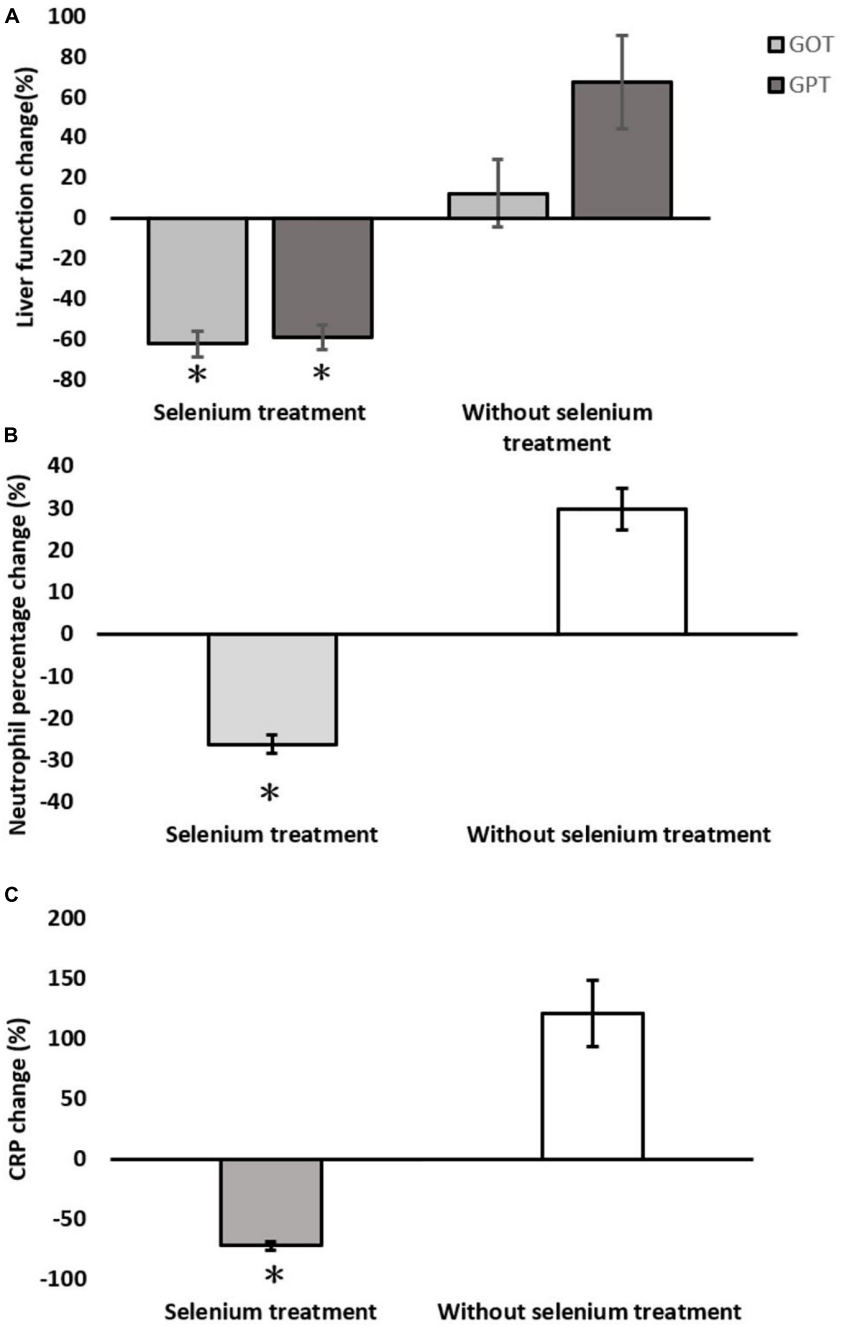

FIGURE 3
Serological changes between the selenium treatment and non-selenium group. **(A)** Liver function change; **(B)** neutrophil percentage change; **(C)** C-reactive protein (CRP) change. *$p < 0.05$.

A guideline published by the ASPEN in collaboration with the Society of Critical Care Medicine concludes that a recommendation regarding Se supplementation in sepsis cannot be made because of conflicting studies (26). In contrast, the Cochrane Collaboration (27) and Landucci et al. (28) both conducted systematic reviews of Se supplementation in ICU patients and concluded that parenteral supplementation with high-dose Se would be effective in reducing mortality in critically ill patients. However, these reviews were conducted using different designs, and heterogenicity is high. Thus, high-quality prospective randomized control trials to evaluate traumatic critical illness patients are warranted.

This retrospective review revealed that early Se supplementation after trauma confers positive results in

TABLE 2 Demographic and risk factors for mortality in trauma patients.

Variable	Crude OR (95% CI)	*P*-value	Multivariable OR (95% CI)	*P*-value
Group (Selenium treatment)	0.000		0.000	
Age	1.027 (0.996–1.058)	0.084	1.063 (0.986–1.145)	0.111
Sex, male	5.400 (0.677–43.085)	0.111	0.075 (0.001–3.800)	0.196
Comorbidity				
Central nervous system	2.175 (0.523–9.038)	0.285	13.628 (0.564–329.497)	0.108
Cardiovascular system	1.609 (0.499–5.189)	0.426	9.938 (0.304–325.065)	0.197
Respiratory system	3.393 (0.288–39.918)	0.331	17.906 (0.014–39.192)	0.854
Digestive system	6.857 (0.405–115.960)	0.182	5.249 (0.701–188.452)	0.971
Genitourinary system	No mortality	0.999	No mortality	0.999
Endocrine system	0.632 (0.131–3.038)	0.566	0.026 (0.001–4.911)	0.172
Cancer	No mortality	0.999	No mortality	0.999
PaO2/FiO2 ratio, day 1	0.998 (0.995–1.002)	0.366	0.997 (0.982–1.013)	0.719
PaO2/FiO2 ratio, day 5	0.998 (0.994–1.001)	0.210	1.010 (0.992–1.027)	0.275
ISS	1.065 (0.993–1.143)	0.077	1.084 (0.909–1.294)	0.370
ICU LOS, days	0.996 (0.947–1.047)	0.876	1.238 (0.878–1.746)	0.224
Hospital LOS, days	0.947 (0.902–0.994)	0.026*	0.712 (0.551–0.920)	0.010*
Ventilator dependence, days	1.007 (0.977–1.038)	0.641	1.262 (1.039–1.532)	0.019*

OR, odds ratio; CI, confidence interval; RTS, revised trauma score; ISS, injury severity score; LOS, length of stay; ICU, intensive care unit; PaO2/FiO2, Ratio of arterial oxygen partial pressure to fractional inspired oxygen.
*Significant difference.

TABLE 3 Demographic risk of pulmonary complications in trauma patients.

Variables	Crude OR (95% CI)	*P*-value	Multivariable OR (95% CI)	*P*-value
Group (Selenium treatment)	0.000		0.000	
Age	1.027 (0.996–1.058)	0.084	1.036 (0.986–1.088)	0.157
Sex, male	5.400 (0.677–43.085)	0.111	0.200 (0.016–2.435)	0.207
Respiratory comorbidity	3.393 (0.288–39.918)	0.331	11.979 (0.038–425.032)	0.703
PaO2/FiO2 ratio, day 1	0.998 (0.995–1.002)	0.366	1.000 (0.988–1.011)	0.973
PaO2/FiO2 ratio, day 5	0.998 (0.994–1.001)	0.210	1.003 (0.992–1.027)	0.763
ISS	1.065 (0.993–1.143)	0.077	1.026 (0.913–1.153)	0.667
ICU LOS, days	0.996 (0.947–1.047)	0.876	1.121 (0.939–1.338)	0.208
Hospital LOS, days	0.947 (0.902–0.994)	0.026*	0.793 (0.873–0.933)	0.005*
Ventilator dependence, days	1.007 (0.977–1.038)	0.641	1.178 (1.033–1.344)	0.015*

OR, odds ratio; CI, confidence interval; RTS, revised trauma score; ISS, injury severity score; LOS, length of stay; ICU, intensive care unit; PaO2/FiO2, Ratio of arterial oxygen partial pressure to fractional inspired oxygen.
*Significant difference.

decreasing the overall lengths of ICU and hospital stays and mortality. In addition, it seemed to have lung-protective tendencies. Organ injury, particularly hepatic insults and inflammatory status, also recovered better than the control group under balanced severity of illness, comorbidity, and baseline characteristics. Additional randomized control studies and subgroup studies to elucidate the concentration effect are needed, especially on the pulmonary protection effect.

Limitations

This study has some limitations. The major limitation of this study is its retrospective nature, which is associated with information and selection bias. To achieve an ideal random effect, we selected patients as study groups based on their willingness to take Se supplements rather than physician consideration. Selection bias from unknown confounders was inevitable given the difficulty of the trauma scenario. In addition, the serum level of Se was not measured before, during, or after treatment. In Taiwan, the average serum Se concentrations of males and females are 112.9 ± 20.5 and 109.4 ± 19.8 μg/L, respectively (29), indicating optimal serum levels (>100 μg/L). In contrast, we have observed a strong deficit of Se and selenoproteins (12) at the early stage of trauma. We used 1:5 PSM analysis to minimize bias in the abovementioned factors, including baseline demographics, intervention, medication, and nutrition status. The criteria for Se supplementation could be made for a specific type or group of injury for subgroup and secondary analysis.

Additionally, consecutive serum concentrations could be collected for data and clinical implications correlation. However, the results enhance the generalizability of this study as it reflects the current real-world practice. The large sample size generated from this single-center study also allowed robust statistical analysis, which is important when we are studying a particular treatment where the expected difference is uncertain. To more precisely determine the role of early Se supplementation in trauma patients, a large prospective study is needed.

Data availability statement

The original contributions presented in this study are included in the article/supplementary material, further inquiries can be directed to the corresponding author.

Ethics statement

The studies involving human participants were reviewed and approved by Ethics Committee of Tri-Service General Hospital. Written informed consent for participation was not required for this study in accordance with the national legislation and the institutional requirements.

Author contributions

Y-CC, C-ML, Z-JH, and S-DH conceptualized and wrote the manuscript. C-HC and W-CC were responsible for data curation and formal analysis. All authors read and agreed to the published version of the manuscript.

Conflict of interest

The authors declare that the research was conducted in the absence of any commercial or financial relationships that could be construed as a potential conflict of interest.

Publisher's note

All claims expressed in this article are solely those of the authors and do not necessarily represent those of their affiliated organizations, or those of the publisher, the editors and the reviewers. Any product that may be evaluated in this article, or claim that may be made by its manufacturer, is not guaranteed or endorsed by the publisher.

References

1. Huber-Wagner S, Mand C, Ruchholtz S, Kühne C, Holzapfel K, Kanz K, et al. Effect of the localisation of the CT scanner during trauma resuscitation on survival – a retrospective, multicentre study. *Injury.* (2014) 45(Suppl. 3):S76–82. doi: 10.1016/j.injury.2014.08.022

2. Guisasola M, Alonso B, Bravo B, Vaquero J, Chana F. An overview of cytokines and heat shock response in polytraumatized patients. *Cell Stress Chaperones.* (2018) 23:483–9. doi: 10.1007/s12192-017-0859-9

3. Goodyear-Bruch C, Pierce J. Oxidative stress in critically ill patients. *Am J Crit Care.* (2002) 11:543–51;quiz52–3. doi: 10.4037/ajcc2002.11.6.543

4. Lovat R, Preiser J. Antioxidant therapy in intensive care. *Curr Opin Crit Care.* (2003) 9:266–70. doi: 10.1097/00075198-200308000-00003

5. Bulger E, Helton W. Nutrient antioxidants in gastrointestinal diseases. *Gastroenterol Clin North Am.* (1998) 27:403–19. doi: 10.1016/S0889-8553(05)70010-8

6. Nathens A, Neff M, Jurkovich G, Klotz P, Farver K, Ruzinski J, et al. Randomized, prospective trial of antioxidant supplementation in critically ill surgical patients. *Ann Surg.* (2002) 236:814–22. doi: 10.1097/00000658-200212000-00014

7. Maehira F, Luyo G, Miyagi I, Oshiro M, Yamane N, Kuba M, et al. Alterations of serum selenium concentrations in the acute phase of pathological conditions. *Clin Chim Acta.* (2002) 316:137–46. doi: 10.1016/S0009-8981(01)00744-6

8. Burk R, Hill K. Regulation of selenium metabolism and transport. *Annu Rev Nutr.* (2015) 35:109–34. doi: 10.1146/annurev-nutr-071714-034250

9. Demetriades D, Kimbrell B, Salim A, Velmahos G, Rhee P, Preston C, et al. Trauma deaths in a mature urban trauma system: is "trimodal" distribution a valid concept? *J Am Coll Surg.* (2005) 201:343–8. doi: 10.1016/j.jamcollsurg.2005.05.003

10. Sobrino J, Shafi S. Timing and causes of death after injuries. *Proc (Bayl Univ Med Cent).* (2013) 26:120–3. doi: 10.1080/08998280.2013.11928934

11. Gunst M, Ghaemmaghami V, Gruszecki A, Urban J, Frankel H, Shafi S. Changing epidemiology of trauma deaths leads to a bimodal distribution. *Proc (Bayl Univ Med Cent).* (2010) 23:349–54. doi: 10.1080/08998280.2010.11928649

12. Braunstein M, Kusmenkov T, Zuck C, Angstwurm M, Becker N, Böcker W, et al. Selenium and selenoprotein P deficiency correlates with complications and adverse outcome after major trauma. *Shock.* (2020) 53:63–70. doi: 10.1097/SHK.0000000000001344

13. Angstwurm M, Engelmann L, Zimmermann T, Lehmann C, Spes C, Abel P, et al. Selenium in intensive care (SIC): results of a prospective randomized, placebo-controlled, multiple-center study in patients with severe systemic inflammatory response syndrome, sepsis, and septic shock. *Crit Care Med.* (2007) 35:118–26. doi: 10.1097/01.CCM.0000251124.83436.0E

14. Berger M, Soguel L, Shenkin A, Revelly J, Pinget C, Baines M, et al. Influence of early antioxidant supplements on clinical evolution and organ function in critically ill cardiac surgery, major trauma, and subarachnoid hemorrhage patients. *Crit Care.* (2008) 12:R101. doi: 10.1186/cc6981

15. Jang J, Shim H, Lee S, Lee J. Serum selenium and zinc levels in critically ill surgical patients. *J Crit Care.* (2014) 29:317.e5–8. doi: 10.1016/j.jcrc.2013.12.003

16. Berger M, Baines M, Raffoul W, Benathan M, Chiolero R, Reeves C, et al. Trace element supplementation after major burns modulates antioxidant status and clinical course by way of increased tissue trace element concentrations. *Am J Clin Nutr.* (2007) 85:1293–300. doi: 10.1093/ajcn/85.5.1293

17. Lee J, Kang J, Park S, Jin H, Jang S, Kim S, et al. Nutrition and clinical outcomes of nutrition support in multidisciplinary team for critically ill patients. *Nutr Clin Pract.* (2018) 33:633–9. doi: 10.1002/ncp.10093

18. Huang J, Hsu C, Ouyang C, Cheng C, Wang C, Liao C, et al. The impact of selenium supplementation on trauma patients-systematic review and meta-analysis. *Nutrients.* (2022) 14:342. doi: 10.3390/nu14020342

19. Singh J, Gupta G, Garg R, Gupta A. Evaluation of trauma and prediction of outcome using TRISS method. *J Emerg Trauma Shock.* (2011) 4:446–9.

20. Cirino Ruocco M, Pacheco Cechinatti E, Barbosa F Jr., Navarro A. Zinc and selenium status in critically ill patients according to severity stratification. *Nutrition.* (2018) 45:85–9. doi: 10.1016/j.nut.2017.07.009

21. Broman M, Lindfors M, Norberg Å, Hebert C, Rooyackers O, Wernerman J, et al. Low serum selenium is associated with the severity of organ failure in critically ill children. *Clin Nutr.* (2018) 37:1399–405. doi: 10.1016/j.clnu.2017.06.014

22. Rusolo F, Pucci B, Colonna G, Capone F, Guerriero E, Milone M, et al. Evaluation of selenite effects on selenoproteins and cytokinome in human hepatoma cell lines. *Molecules.* (2013) 18:2549–62. doi: 10.3390/molecules18032549

23. Nogueira C, Rocha J. Toxicology and pharmacology of selenium: emphasis on synthetic organoselenium compounds. *Arch Toxicol.* (2011) 85:1313–59. doi: 10.1007/s00204-011-0720-3

24. Zheng W, Boada R, He R, Xiao T, Ye F, Simonelli L, et al. Extracellular albumin covalently sequesters selenocompounds and determines cytotoxicity. *Int J Mol Sci.* (2019) 20:4734. doi: 10.3390/ijms20194734

25. Tindell R, Wall S, Li Q, Li R, Dunigan K, Wood R, et al. Selenium supplementation of lung epithelial cells enhances nuclear factor E2-related factor 2 (Nrf2) activation following thioredoxin reductase inhibition. *Redox Biol.* (2018) 19:331–8. doi: 10.1016/j.redox.2018.07.020

26. Koekkoek W, van Zanten A. Antioxidant vitamins and trace elements in critical illness. *Nutr Clin Pract.* (2016) 31:457–74. doi: 10.1177/0884533616653832

27. Allingstrup M, Afshari A. Selenium supplementation for critically ill adults. *Cochrane Database Syst Rev.* (2015) 2015:Cd003703. doi: 10.1002/14651858.CD003703.pub3

28. Landucci F, Mancinelli P, De Gaudio A, Virgili G. Selenium supplementation in critically ill patients: a systematic review and meta-analysis. *J Crit Care.* (2014) 29:150–6. doi: 10.1016/j.jcrc.2013.08.017

29. Chen C, Lai J, Wu C, Lin T. Serum selenium in adult Taiwanese. *Sci Total Environ.* (2006) 367:448–50. doi: 10.1016/j.scitotenv.2006.03.004

frontiers | Frontiers in Nutrition

TYPE Original Research
PUBLISHED 19 December 2022
DOI 10.3389/fnut.2022.1014502

OPEN ACCESS

EDITED BY
Nicola Fiotti,
University of Trieste, Italy

REVIEWED BY
Ishtiyaq Ahmad,
University of Kashmir, India
Vincenzo Parrino,
The University of Messina, Italy

*CORRESPONDENCE
Beiping Tan
bptan@126.com

†These authors have contributed equally to this work

SPECIALTY SECTION
This article was submitted to Nutrition and Metabolism, a section of the journal Frontiers in Nutrition

RECEIVED 08 August 2022
ACCEPTED 18 November 2022
PUBLISHED 19 December 2022

CITATION
Zhang W, Pang A, Tan B, Xin Y, Liu Y, Xie R, Zhang H, Yang Q, Deng J and Chi S (2022) Tryptophan metabolism and gut flora profile in different soybean protein induced enteritis of pearl gentian groupers. *Front. Nutr.* 9:1014502. doi: 10.3389/fnut.2022.1014502

Tryptophan metabolism and gut flora profile in different soybean protein induced enteritis of pearl gentian groupers

Wei Zhang[1,2,3†], Aobo Pang[1,2,3†], Beiping Tan[1,2,3*], Yu Xin[1,2,3], Yu Liu[1,2,3], Ruitao Xie[3], Haitao Zhang[3], Qihui Yang[1,2,3], Junming Deng[1,2,3] and Shuyan Chi[1,2,3]

[1]Laboratory of Aquatic Animal Nutrition and Feed, College of Fisheries, Guangdong Ocean University, Zhanjiang, Guangdong, China, [2]Aquatic Animals Precision Nutrition and High Efficiency Feed Engineering Research Center of Guangdong Province, Zhanjiang, Guangdong, China, [3]Key Laboratory of Aquatic, Livestock and Poultry Feed Science and Technology in South China, Ministry of Agriculture, Zhanjiang, Guangdong, China

The substitution of high-level soy meals for fish meal (FM) generally leads to fish enteritis, accompanied by significant variations in gut flora. Relevant studies have pointed out a close relationship between tryptophan metabolism mediated by gut flora and vertebrate inflammatory bowel disease. Present study examines the role of tryptophan metabolism and gut flora profile in fish enteritis caused by different soybean meals. The 960 groupers were randomly assigned into 4 groups (n = 4), which including: (1) FM (the control group, fed with 50% FM feed), (2) SBM40 (replacing 40% FM with soybean meal), (3) SPC40 (replacing 40% FM with soybean protein concentrate), and (4) FSBM40 (replacing 40% FM with fermented soybean meal). Under average temperature and natural light, the groupers were cultivated with feeds of iso-nitrogen and iso-lipid for 10 weeks. The results showed that soybean meal feeds at all experimental levels had negative effects on fish gut physiology and growth performance. Typical enteritis features and fluctuations of immune system occur, which can be observed in the enzyme activities of total superoxide dismutase and lysozyme and in the contents of immunoglobulin M, complement 3 and complement 4. 16SrDNA high-throughput sequencing indicated that it greatly influenced the gut flora with the abundance of maleficent bacteria, like Vibrio, amplified with increasing dietary soybean meals. According to the "3 + 2" full-length transcriptome sequencing, soy meals at the three experimental levels inhibited the key gene expressions of tryptophan metabolic pathway in fish gut, however, there are some differences in the types of key genes that are inhibited. The canonical correlation analysis showed that the changes in key gene expressions in tryptophan metabolic pathway had a positive correlation with the expressions of pro-inflammatory genes ($P < 0.05$) and negatively correlated with the expression of anti-inflammatory genes ($P < 0.05$). It is speculated from this study that tryptophan metabolism is closely related to fish soy meal-related enteritis, and the abnormal tryptophan metabolism caused by intestinal flora

imbalance may play an important role. In the future research, we can further study the tolerance of fish to soy meals feed from two aspects of tryptophan metabolism and intestinal flora changes.

KEYWORDS

Epinephelus fuscoguttatus♀ × *E. lanceolatus*♂, soy meal, gut flora, tryptophan metabolism, enteritis

Introduction

In recent years, the total amount of aquaculture has continued to increase, but the fish meal (FM) output almost remained unchanged. Since FM presents to be a key source of protein for aquaculture, aquaculture farmers urgently need new and sustainable alternatives for it (1). Thus, attention has been paid to plant materials during the procedure. Among them, soy products are considered one of the most promising FM substitutes because of their high yield and relatively balanced amino acid composition (2). However, soy products with high substitution levels, especially soybean meal (SBM), are easy to cause gut mucosal damage and enteritis in fish, which seriously endangers the gut health of fish, and limits its extensive application in aquaculture industry.

According to former research, the influence of SBM on fish enteritis varies with its anti-nutritional factors (ANFs), including phytates, protease inhibitors, saponins, lectins, phytosterols, and oligosaccharides (3). The histological characteristics of SBM induced enteritis (SBMIE) in fish include infiltration of different inflammatory cells, the swelling submucosa and lamina propria, the shortening of mucosal fold, and a decrease in absorption vacuoles of gut epithelial cell (4). It has been found that high-level SBM has negative impact on the gut health of a variety of fish, such as zebrafish, carp, rainbow trout, and Atlantic salmon (5–7). Fish SBMIE mainly occurs in the hindgut, a crucial part of protein absorption by endocytosis and is more susceptible to food stimulation, causing intestinal diseases (8). In order to reduce the antigen content, the SBM is often processed into different product types.

In aquatic feed, soy products used mainly include SBM, soybean protein concentrate (SPC), as well as fermented soybean meal (FSBM). SBM, a by-product of soybean oil extraction, contained various ANFs mentioned above. SPC is a product made from soy by extracting oil and low molecular weight soluble protein components by alcohol. Compared with SBM, SPC removed most ANFs and is a good plant protein source in the fish and shrimp diet (9). However, the solubility of SPC extracted by the alcohol method is decreased, and the nitrogen solubility index is reduced to about 10%, which limits its application (10). FSBM refers to a protein material prepared by fermentation of SBM by microorganisms. Fermentation of microorganism significantly purifies the content of ANFs in SBM, and decomposes soybean protein into small molecular proteins, small peptides, and amino acids, thus improving the digestion and absorption abilities (11). However, at present, due to the different fermentation technology, there are also many problems in FSBM, such as the lack of strict standards and specifications, and its product quality is still uneven (12).

Previous studies on fish SBMIE mostly focused on the influence of ANFs in SBM on gut health. But researchers found that the role of ANFs is complex, such as fish enteritis induced by soy saponins may be related to the basal protein source (13); or dose-dependent and independent of the basal protein source (14); or it is a secondary effect on the interference characteristics of cell membrane, and the SBMIE is mainly induced by external antigens (15). According to existing research, no clear results about the pathogenic mechanism of fish SBMIE have been made, but researchers generally believe that the gut flora play an important role during this process (16–18).

Tryptophan is an essential amino acid. In recent years, lysine and methionine have been widely used in formula diets, making tryptophan the main limiting amino acid in diet (19). In aquaculture, researchers found that tryptophan can promote the growth and gut development of carp and shrimp, regulate the gut microecological balance, and improve the survival rate (SR) of groupers (20–22). The related studies have shown the benefits of tryptophan on the gut health of aquaculture objects, but there are few reports on the fish SBMIE. However, in mammals, the relationship between tryptophan metabolism and human inflammatory bowel disease has become a research hotspot in recent years (23, 24). In present study, we also found that different soy meal substitution for FM at high levels, resulting in abnormal tryptophan metabolism in the gut tract of pearl gentian grouper.

Pearl gentian grouper is a typical marine carnivorous fish and is the important cultivated varieties in China and many places in the world. Its meat is tender, grows fast, has strong disease resistance, obvious hybridization advantages, and good market price. It can also be used as an ornamental fish, and has a broad market prospect. This study analysed the effects of different soy meals with high substitution levels on the growth physiology and gut tryptophan metabolism pathway of pearl gentian grouper, and preliminary analysed the gut flora profile

variations. Present research offers a theoretical basis for the study of gut health problems caused by the substitution for FM with high level of plant proteins.

Materials and methods

Experimental diets

The experimental diets and their chemical compositions are shown in **Table 1**. The red FM, produced by Corporación Pesquera Inca S.A.C. at Bayovar Plant in Peru, contains 72.53% crude protein. The SBM (48.92% crude protein) and SPC (70.72% crude protein) were purchased from Zhanjiang Haibao Feed (Zhanjiang, China). The FSBM, containing 60.75% crude protein, was purchased from Xijie Foshan Co. Ltd. (Foshan, China). Four experimental diets of iso-lipid (about 10% total lipid) and iso-nitrogen (about 50% crude protein) were used by SBM, SPC, and FSBM to substitute 40% of FM protein; these diets were designated as FM (the control group), SBM40, SPC40, and FSBM40, respectively. To achieve amino acid balance, the experimental feeds were mixed with methionine and lysine (25). The specific preparation and storage methods of the four kinds of feeds were explained as below: first, the researchers ground the raw materials into powder, then screened it with 60-mesh sieves and weighed the following formula, before using the sequential expansion method to mix the micro constituents evenly. Second, the researchers added lipids and deionised water into it and then stirred it to get a fine mixture. Afterward, the feeds were air-dried to 10% humidity using pelletisers with diameters of 2.0 and 3.0 mm, respectively. The experimental diets were then conserved in sealed plastic bags at −20°C (26).

Feeding experiment design

The healthy juvenile groupers, which weighed about 9 g, were bought from a commercial hatchery in Zhanjiang City, Guangdong, China. Before the experiment, 960 groupers were given 1 week to adapt to the experimental conditions, after which they were offered nothing to eat for a day. The researchers then anaesthetised the groupers with eugenol and divided them into four groups. According to size, fishes were randomly placed in 1,000 L cylindrical glass tanks. Every tank contained 60 fish. The experimental feeds were offered from 8:00 a.m. to 4:00 p.m. every day for 10 weeks, with four replicates. The uneaten feeds were siphoned to calculate the weight of the intake feeds, and the feed consumption ratio was determined (27). The feeding experiment was conducted within inner cultural systems belonging to the Marine Biological Research Base of Zhanjiang City (Guangdong, China). To ensure saturated oxygen concentration, air stones were used to continuously inflate air into containers. The experimental environment in containers involved a natural light cycle and a temperature of 29 ± 1°C. The concentrations of ammonia and nitrate were both lower than 0.03 mg L^{-1}, and the dissolved oxygen involved in this study was ≥7 mg L^{-1}. Within the first 14 days, 60% of the water in each container was exchanged every day, and after that, nearly 100% of the water was exchanged every day.

Sample collection

The study was supported by the Expert Committee of the Fisheries College of Guangdong Ocean University. The research methods followed all applicable regulations and guidelines. Before sampling, the studied groupers were starved for 24 h. Then, they were anaesthetised with eugenol (1:10,000). After counting and weighing all fish in each tank, their specific growth rate (SGR), weight gain rate (WGR), hepatosomatic index (HSI), SR, and feed conversion ratio (FCR) were determined. To determine the enzyme activity, the researchers randomly

TABLE 1 Formulation and proximate composition of the experimental diets (%, dry matter).

Ingredients (%)	Diets			
	FM	SBM40	SPC40	FSBM40
Red fish meal	50.00	30.00	30.00	30.00
Soybean meal	0.00	29.65	21.74	23.89
Vital wheat gluten	5.00	5.00	5.00	5.00
Wheat flour	18.00	18.00	18.00	18.00
Casein	4.60	4.60	4.60	4.60
Gelatin	1.00	1.00	1.00	1.00
Fish oil	3.02	4.48	4.41	4.49
Soybean oil	2.00	2.00	2.00	2.00
Soybean lecithin	2.00	2.00	2.00	2.00
Microcrystalline cellulose	11.48	0.00	8.14	5.84
Calcium monophosphate	1.50	1.50	1.50	1.50
Ascorbic acid	0.05	0.05	0.05	0.05
Choline chloride	0.50	0.50	0.50	0.50
Vitamin premix[a]	0.30	0.30	0.30	0.30
Mineral premix[b]	0.50	0.50	0.50	0.50
Ethoxyquin	0.05	0.05	0.05	0.05
Lysine[c]	0.00	0.24	0.05	0.13
Methionine[c]	0.00	0.13	0.16	0.15
Proximate composition (%, dry matter)				
Crude protein	50.97	50.85	50.63	50.45
Crude lipid	10.15	10.44	10.71	10.54

[a]Vitamin premix consisted of (g/kg premix): VB_1 17.00 g, VB_2 16.67 g, VB_6 33.33 g, VB_{12} 0.07 g, VK 3.33 g, VE 66.00 g, retinyl acetate 6.67 g, VD 33.33 g, nicotinic acid 67.33 g, D-calcium pantothenate 40.67 g, biotin 16.67 g, folic acid 4.17 g, inositol 102.04 g, and cellulose 592.72 g.

[b]Mineral premix consisted of (g/kg premix): $FeSO_4 \cdot H_2O$ 18.785 g, $ZnSO_4 \cdot H_2O$ 32.0991 g, $MgSO_4 \cdot H_2O$ 65.1927 g, $CuSO_5 \cdot 5H_2O$ 11.0721 g, $CoCl_2 \cdot 6H_2O$ (10%) 5.5555 g, KIO_3 0.0213 g, KCl 22.7411 g, Na_2SeO_3 (10%) 0.5555 g, and zeolite powder 843.9777 g.

[c]Lysine and methionine were added to balance amino acid with FM control group.

selected six groupers from each water tank, drew blood from their tail veins, and stored it at 4°C for a night, before using a centrifuge at 3,500 rpm for 10 min to obtain serum. The blood was then stored at −80°C, preparing for analysing the enzyme activity. The hindgut tissues were excised, and any mesenteric and adipose tissues were removed. Hindgut samples were cut into small pieces and put in test tubes filled with RNAlater at 4°C for a night before being stored at −80°C for gene expression analysis.

For gut flora and transcriptome sequencing, the researchers randomly chose eight groupers. The hindgut tissue samples were obtained as mentioned above and placed in cryopreservation tubes, then directly put into liquid nitrogen, half of which was employed for 16S high-throughput sequencing, while the rest for transcriptome sequencing.

$$\text{Weight gain rate (WGR, \%)} = \frac{100 \times (\text{final body weight} - \text{initial body weight})}{\text{initial body weight}}$$

$$\text{Specific growth rate (SGR, \%/d)} = \frac{100 \times [\text{Ln (final body weight)} - \text{Ln (initial body weight)}]}{\text{days}}$$

$$\text{Feed conversion ratio (FCR)} = \frac{\text{feed intake}}{\text{(final body weight io (FCR) n (initi}}$$

$$\text{Hepatosomatic index (HSI, \%)} = 100 \times \left(\frac{\text{hepatic weight}}{\text{body weight}}\right)$$

$$\text{Survival rate (SR, \%)} = 100 \times \left(\frac{\text{final fish number}}{\text{initial fish number}}\right).$$

Histological observation of enteritis

After the diet experiment, three fish were randomly chosen from every container. The DI sample was stored in 4% paraformaldehyde universal tissue fixative, which belongs to the Servicebio Technology Company of Wuhan, from China, for 24 h before being H&E stained. The stained sections were observed and photographed under 10 × 10 times microscopically (Olympus CKX41 microscope, Tokyo, Japan).

Analysis of physiological indexes

In the present study, the researchers employed the BCA method to analyse the gut and serum samples (Beyotime Biotechnology Co., Ltd., Shanghai, China).

The enzyme activities of lysozyme (LYS) in serum and total superoxide dismutase (T-SOD) in hindgut were measured by fish ELISA kits, which were then employed to determine immunoglobulin M (IgM) content, complement 3 (C3) content, and complement 4 (C4) content in hindgut tissues. The testing kits were products of Shanghai Jianglai Biotechnology Co., Ltd. (Shanghai, China). The methods were performed according to the operating instructions in detail.

Immune-related gene expressions

TRIzol kits (Invitrogen, Carlsbad, CA, USA) were applied to test the total RNA of the hindgut tissues. An Evo M-MLV reverse transcription kit (Takara, Japan) was employed to prepare qualified RNA samples to cDNA. They were then stored at −20°C for use. The primers were designed by Shenggong Bioengineering Co., Ltd. (Shanghai, China). The researchers obtained the template sequences of these primers from the sequencing of the "3 + 2" full-length transcriptome of the hindgut tissues of the studied groupers within the lab. The original data were recorded in the NCBI Sequential Read Archive (SRA) with accession numbers PRJNA664623 and PRJNA66441. Primers carried out by Primer Premier 5.0 software for pro-inflammatory genes were interleukin (*IL*)*1*β, *IL12*, *IL17*, *IL32*, and tumour necrosis factor (*TNF*)α, and anti-inflammatory genes were *IL4*, *IL5*, *IL10*, and transforming growth factor (*TGF*)β*1* (**Table 2**). The β-actin is presented to be the internal reference gene. The gene expressions were examined with RT-qPCR (Mastercycler ep realplex, Eppendorf, Germany). The PCR reaction environment were 95°C for 2 min with 1 cycle, 95°C for 15 s, 60°C for 10 s and 72°C for 20 s with 40 cycles, respectively. The target gene expressions were calculated using the $2^{-\Delta\Delta Ct}$ method.

16S high-throughput analysis of intestinal flora

According to the operation instructions, E.Z.N.A.^{TM} Kit (Omega Bio-Tek, Norcross, GA, USA) was applied to extract the total RNA from the DI flora. Gene Denovo Co., Ltd. (Guangzhou, China) assisted in sequence detection and data analysis. The original data were recorded in the NCBI SRA, with the accession number PRJNA666309. The **Supplementary File** included specified analysis procedures.

Transcriptome sequencing and KEGG annotation

Through the PacBio Sequel and Illumina HiSeq^{TM} 4000 platforms, the "3 + 2" full-length transcriptome sequencing was carried out. Gene Denovo Co., Ltd. (Guangzhou, China) completed the sequencing process. The original data of the

TABLE 2 PCR primers for gut immune-related genes of grouper.

Gene	Forward 5′-3′	Revise 3′-5′	Annealing temperature (°C)	Primer efficiency (%)	Size (bp)
IL1β	AAGGTGGACGCCAACAGACA	GTTCACTGCAGGCTCAGGGA	56	95	153
IL17	GAGAGGACGGTGTCTGTGTGG	CATGCACAGTTGAGGGTGTGG	58	98	101
p65	TCAACCCAGTCCAAGCAGCA	GATGCTGCCAGCTGAACGTC	63	96	107
IκBα	ATGCAAAGGAGCAGCGTAACG	GAGGTTGGGGTCTGCTCCT	62	99	107
TNFα	AACTGTGTGTCCCCACTGCC	CCACAGATGGCCCAGGTCAT	58	95	81
IL5	GGCCAACAGTCAAGATGTCTGCC	GAATGACCAGGAGCAGTTCAGTGT	59	98	160
IL10	ACACAGCGCTGCTAGACGAG	TAGACTTGTGCCACGACGGG	66	94	142
TGFβ1	CTTCTCCTCCTCCTCGCTGC	GATGTTGCTGAGGGCTTCGC	62	99	195
β-actin	GGCTACTCCTTCACCACCACA	TCTCCAAGGCAACGGGTCT	65	99	188

IL, interleukin; *TNF*, tumour necrosis factor; *p65*, NF-κB-p65; *IκBα*, I-kappa-B-alpha; *TGF*, transforming growth factor.

sequencing are stored as mentioned above. The gene expressions of $|\log2FC| > 1$ and $P < 0.05$ were classified as differential genes (DEGs). The researchers put the DEGs gene into the KEGG database and carried out an in-depth analysis of the significantly activated signal pathways, which were relevant to signal transduction, infectious diseases and immune diseases/systems ($P < 0.05$).

Validation of the tryptophan metabolism-related genes by RT-qPCR

To validate the accuracy of the "3 + 2" full-length transcriptome data, 10 DEGs from the tryptophan metabolism pathway were chosen for RT-qPCR: *AO*, *DDC*, *IDO2*, *AOX1*, *ALDH*, *DAO1*, *KYN*, *KAT1*, *CYP1A1*, and *LAAO*. The primer templates were the same as those mentioned above, and the primers are presented in Table 3.

The β-actin is presented to be the internal control gene. QRT-PCR (Mastercycler ep realplex in Eppendorf, Germany) helped in detecting gene expression. The reaction environment of PCR and analysing approaches were identical, as mentioned above.

Correlation analysis

To explore the correlation between downstream inflammatory genes and tryptophan metabolism, the crucial DEGs in the signal pathway of tryptophan metabolism were studied using canonical correlation analysis (CCA) with the inflammatory genes in internal tissue in the SBM40, SPC40, and FSBM40 groups, respectively. The key DEGs selected in the tryptophan metabolism signalling pathway include *AO, DDC, IDO2, AOX1, ALDH, DAO1, KYN, KAT1, CYP1A1*, and *LAAO*; the inflammatory genes include pro-inflammatory genes (*IL1β*, *TNFα*, and *IκBα*) and anti-inflammatory- related genes (*IL10* and *TGFβ1*) in the hindgut tissues.

Statistics

With the help of free online omicshare tools, the CCA method was carried out to process the original data[1]. After homogeneity variance tests by SPSS 22.0 (SPSS Inc., Chicago, IL, USA), the results were studied with one-way ANOVA and are shown as the mean ± SD, with $P < 0.05$ indicating a statistically significant difference.

Results

Growth performance

As indicated in Table 4, the WGR and SGR of the experimental groups were lower than that of the FM, which served as the control group ($P < 0.05$). Among the experimental groups, there was little difference in WGR and SGR ($P > 0.05$). On the contrary, FCR increased significantly in each experimental group ($P < 0.05$). Among the experimental groups, there was little difference in FCR ($P > 0.05$). In addition, there was little difference in HSI and SR among the groups ($P > 0.05$).

Histological observations

The H&E staining and semi-quantitative analysis showed that the experimental levels of SBM, SPC and FSBM all caused enteritis, and they presented significant distinctions compared to the control group ($P < 0.05$), among which the SBM40 and FSBM40 groups were more serious, and enteritis induced by SPC40 was significantly lighter than the SBM40 and FSBM40 groups ($P < 0.05$) (Figure 1 and Table 5).

1 https://www.omicshare.com/tools

TABLE 3 PCR primers for gut tryptophan metabolism pathway-related genes of grouper.

Gene	Forward 5′-3′	Revise 3′-5′	Annealing temperature (°C)	Primer efficiency (%)	Size (bp)
AO	TGGACGAGATGGGCAAGG	AAGCAGCGAAGCGGTGT	59	96	134
DDC	CGAGAACCAGGAGTCAG	CCAAACAGAAGGCAAAC	65	98	100
IDO2	GCTAACTGGAGGAAGAGG	AAGTCAGAAGATACCGTAA	58	95	294
AOX1	TGACGGAAGGATTGTTG	GTGAAGCTGTTACGGATG	57	94	112
ALDH	GAGGCTCTTTGCTGTCC	AGTTGTCCTCGGTCATAC	62	96	196
DAO1	GTCCCACAAAGTCAAGAT	ATTGACGAGACTGGCGA	64	98	176
KYN	ATCCGCCATTATTACAGC	ATCTTTGGGACCCTCGC	59	94	255
KAT1	AGTTCTTCGGTAGGATTG	GATAGTCGGTTACCACT	55	96	165
CYP1A1	CATCAACGAAGGCAAGA	GACAGCGATTACACTAGAC	54	99	255
LAAO	AGAAGCCAGTAACCGTATT	GACGAAAGGAAACGGAG	59	93	123
β-*actin*	GGCTACTCCTTCACCACCACA	TCTCCAAGGCAACGGGTCT	65	99	188

AO, amine oxidase; *DDC*, aromatic-L-amino-acid decarboxylase; *IDO2*, indoleamine 2,3-dioxygenase 2; *AOX1*, aldehyde oxidase 1; *ALDH*, aldehyde dehydrogenase; *DAO1*, amiloride-sensitive amine oxidase; *KYN*, kynureninase; *KAT1*, kynurenine–oxoglutarate transaminase 1; *CYP1A1*, cytochrome P450 family 1 subfamily A polypeptide 1; *LAAO*, L-amino-acid oxidase.

TABLE 4 Effect of different soy meals at 40% substitution level for fish meal on the growth of grouper (n = 4).

Parameters	FM	SBM40	SPC40	FSBM40	*P*-value
IBW (g)	12.55 ± 0.00	12.55 ± 0.04	12.55 ± 0.02	12.55 ± 0.04	0.04
WGR (%)	485.14 ± 7.08^{a}	426.50 ± 9.59^{b}	431.73 ± 12.00^{b}	427.22 ± 7.28^{b}	0.03
SGR (%/day)	2.60 ± 0.02^{a}	2.44 ± 0.03^{b}	2.46 ± 0.03^{b}	2.44 ± 0.02^{b}	0.04
FCR	0.84 ± 0.01^{a}	0.95 ± 0.02^{b}	0.94 ± 0.03^{b}	0.95 ± 0.02^{b}	0.04
HSI (%)	2.43 ± 0.45	2.18 ± 0.25	2.36 ± 0.39	2.19 ± 0.19	0.02
SR (%)	99.17 ± 0.96	99.17 ± 0.96	99.58 ± 0.84	99.58 ± 0.84	0.03

IBW, initial body weight; FBD, final body weight; WGR, weight gain rate; SGR, specific growth rate; FCR, feed conversion ratio; HSI, hepatosomatic index; SR, survival rate.
^{a,b}Values in the same row with different superscripts indicate significant differences ($P < 0.05$).

Physiological indexes determination

As exhibited in Table 6, IgM content, C3 content, and C4 content were all significantly reduced in hindgut tissues of all soy meal substitution groups ($P < 0.05$), while the T-SOD and LYS enzyme activities increased substantially in all soy meal substitution groups ($P < 0.05$).

Immune-related gene expressions

As presented in Table 7, except for the gene expressions of p65, which significantly decreased ($P < 0.05$) and there was a little difference in *IκBα* ($P > 0.05$) in the SPC40 group, the pro-inflammatory gene expressions of *IL1β*, *IL8*, *TNFα*, *p65*, and *IκBα* significantly increased in all soy meal substitution groups ($P < 0.05$). The anti-inflammatory-related gene expressions of *IL5*, *IL10*, and *TGFβ1* were reduced considerably in all substitution groups ($P < 0.05$).

Sample diversity analysis of 16S sequencing

From the 12 samples, there were 983,965 original reads. The average amount of original reads of the FM, SBM40, SPC40, and FSBM40 groups were 79,339.67 ± 4,821.81, 86,036.67 ± 790.22, 81,344.00 ± 4,753.11 and 81,268.00 ± 4,575.00, respectively. After clustering into identical operational taxonomic units (OTUs) by sequences with similarity ≥97%, the researchers gained 899 OTUs. The average number of OTUs in the FM, SBM40, SPC40, and FSBM40 groups were 175.00 ± 32.79, 608.67 ± 56.84, 368.00 ± 42.58, and 717.33 ± 156.62, respectively. Except for a small significant difference between SBM40 and FSBM40 ($P > 0.05$), there were significant differences among the FM and SPC40 groups ($P < 0.05$). A Venn plot showed that 133 OTUs were among the groups (Figure 2A). The PCoA analysis revealed that different experimental groups could be clustered well, indicating that our samples were reasonably processed (Figure 2B).

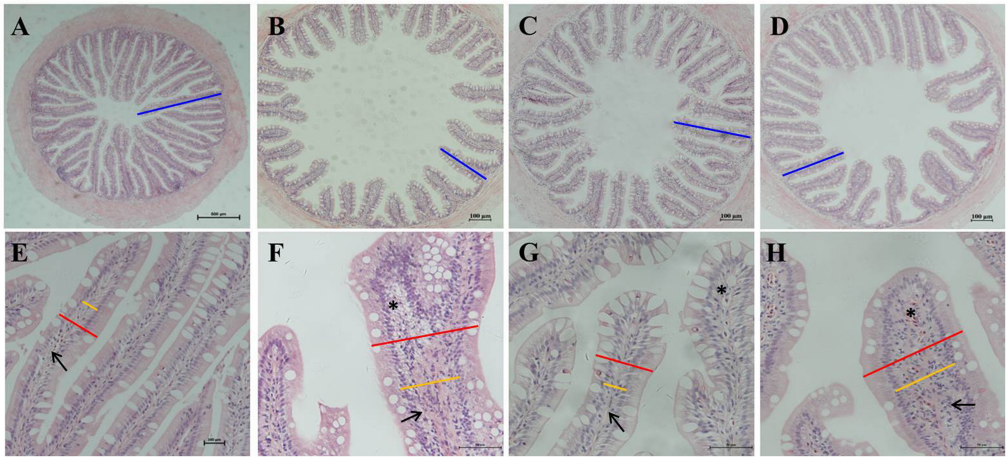

FIGURE 1
Hematoxylin-eosin staining in the hindgut of pearl gentian grouper. **(A–D)** Reduction and fusion of mucosal folds in SBM40, SPC40, and FSBM40 groups. **(E–H)** Increased width of lamina propria and inflammatory cell infiltration SBM40, SPC40, and FSBM40 groups. **(A,E)** Fish meal control group; **(B,F)** 40% SBM substitution for fish meal group; **(C,G)** 40% SPC substitution for fish meal group; **(D,H)** 40% FSBM substitution for fish meal group. Blue bar, the height of plica; red bar, the width of plica; yellow bar, the width of lamina propria; arrow, lamina propria; asterisk, inflammatory infiltration.

TABLE 5 Semi-quantitative histological evaluation of gut sections (n = 10).

Parameters	FM	SBM40	SPC40	FSBM40	*P*-value
Mucosal folds	1.27 ± 0.12^{a}	4.87 ± 0.15^{b}	3.83 ± 0.35^{c}	4.17 ± 0.55^{d}	0.03
Lamina propria	1.47 ± 0.35^{a}	4.77 ± 0.25^{b}	3.97 ± 0.15^{c}	4.50 ± 0.10^{b}	0.01
Supranuclear vacuoles	1.77 ± 0.21^{a}	4.80 ± 0.10^{b}	3.77 ± 0.35^{c}	4.13 ± 0.35^{d}	0.03
Connective tissue	1.47 ± 0.25^{a}	4.83 ± 0.21^{b}	3.20 ± 0.36^{c}	4.30 ± 0.46^{b}	0.04

$^{a-d}$Values in the same row with different superscripts indicate significant differences ($P < 0.05$).

TABLE 6 Effect of different soy meals at 40% substitution levels for fish meal on the enzyme activities of pearl gentian grouper (n = 3).

Parameters	FM	SBM40	SPC40	FSBM40	*P*-value
T-SOD (U/mg)	78.23 ± 9.95^{a}	115.50 ± 12.07^{b}	154.04 ± 13.35^{c}	135.55 ± 14.25^{c}	0.02
IgM (μg/mg)	94.33 ± 4.22^{a}	64.70 ± 3.63^{b}	37.77 ± 3.15^{c}	50.84 ± 5.60^{b}	0.03
C3 (μg/mg)	85.58 ± 5.31^{a}	61.70 ± 8.21^{b}	39.97 ± 7.49^{c}	51.34 ± 7.73^{b}	0.03
C4 (μg/mg)	128.83 ± 10.17^{a}	92.88 ± 5.62^{b}	60.32 ± 5.23^{c}	76.83 ± 8.28^{d}	0.01
LYS (U/g)	5.45 ± 0.47^{a}	7.95 ± 0.64^{b}	7.64 ± 0.64^{b}	4.13 ± 0.86^{c}	0.02

T-SOD, total superoxide dismutase; IgM, immunoglobulin M; C3, complement 3; C4, complement 4; LYS, lysozyme. $^{a-d}$Values in the same row with different superscripts indicate significant differences ($P < 0.05$).

Comparison of gut flora composition and abundance

The relatively abundant top six species at the phylum level are ranked as follows: (1) Proteobacteria, (2) Firmicutes, (3) Bacteroidetes, (4) Acidobacteria, (5) Actinobacteria, and (6) Cyanobacteria. The abundance of Proteobacteria significantly decreased in all soy meal substitution groups ($P < 0.05$), while the abundances of Firmicutes, Bacteroidetes, and Actinobacteria had a significant increase in all soy meal substitution groups ($P < 0.05$). There was little difference in acidobacteria abundance between the SBM40 group and the SPC40 groups, but it significantly increased in the FSBM40 group (Figures 3A,B).

The relatively abundant top six species at the genus level are ranked as follows: (1) *Photobacterium*, (2) *Stenotrophomonas*, (3) *Vibrio*, (4) *Phyllobacterium*, (5) *Neisseria*, and (6) *Bacteroides*. The abundance of *Photobacterium* experienced a significant decrease in all soy meal substitution groups ($P < 0.05$). The abundances of *Phyllobacterium* and *Neisseria* had little difference in the SPC40 group ($P > 0.05$), and the abundance of unidentified_*Rikenellaceae* had little difference

TABLE 7 Effect of different soy meals at 40% substitution levels for fish meal on the inflammatory-related gene expressions in hindgut of pearl gentian grouper (n = 3).

Gene	FM	SBM40	SPC40	FSBM40	*P*-value
IL1β	1.16 ± 0.16^{a}	1.85 ± 0.12^{b}	1.58 ± 0.09^{c}	1.74 ± 0.23^{c}	0.04
IL8	1.00 ± 0.08^{a}	2.35 ± 0.17^{b}	1.86 ± 0.16^{c}	1.62 ± 0.04^{c}	0.03
TNFα	1.01 ± 0.15^{a}	1.52 ± 0.23^{b}	1.33 ± 0.03^{b}	4.09 ± 0.61^{c}	0.01
p65	1.00 ± 0.10	1.59 ± 0.10^{b}	0.42 ± 0.14^{c}	1.63 ± 0.15^{b}	0.02
iκBα	1.01 ± 0.14	2.20 ± 0.50^{b}	0.95 ± 0.18^{a}	2.49 ± 0.09^{b}	0.02
IL5	1.00 ± 0.05^{a}	0.71 ± 0.03^{b}	0.55 ± 0.10^{c}	0.40 ± 0.05^{d}	0.03
IL10	1.03 ± 0.06^{a}	0.36 ± 0.09^{b}	0.56 ± 0.04^{c}	0.56 ± 0.03^{c}	0.04
TGFβ1	1.00 ± 0.08^{a}	0.46 ± 0.16^{b}	0.18 ± 0.05^{c}	0.13 ± 0.01^{c}	0.03

IL, interleukin; TNF, tumour necrosis factor; p65, NF-κB-p65; IκBa, I-kappa-B-alpha; TGF, transforming growth factor. $^{a-d}$Values in the same row with different superscripts indicate significant differences ($P < 0.05$).

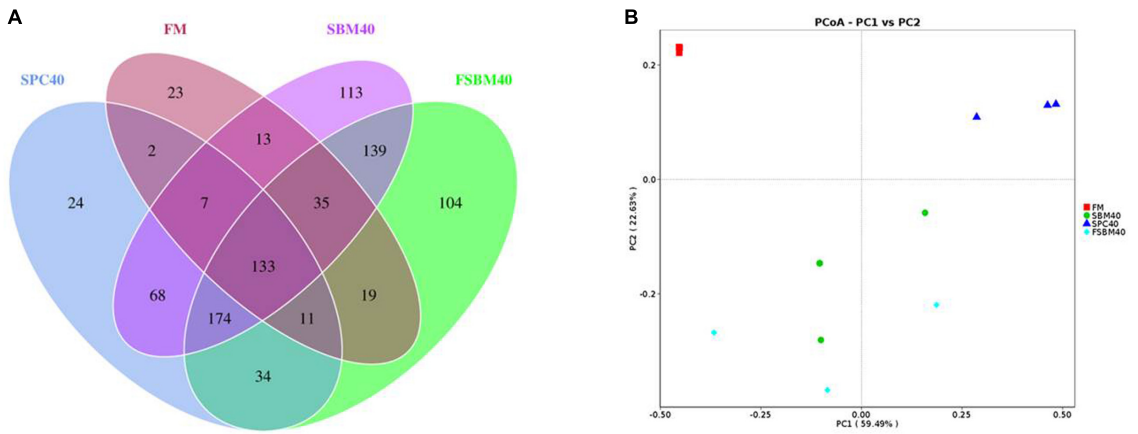

FIGURE 2
Venn plot **(A)** and PCoA **(B)** analysis of OTU by high-throughput sequencing after replacing fish meal with different soy meals in pearl gentian grouper (n = 3).

between the SPC40 and FSBM40 groups ($P > 0.05$). The abundances of the left species significantly increased in all soy meal substitution groups ($P < 0.05$; Figures 3C,D).

Statistics and KEGG enrichment of differential genes

Compared to the FM group, there were 554 co-contained DEGs in the SBM40, SPC40, and FSBM40 groups, named profile A. The numbers of unique DEGs were 1,003, 2,254, and 1,656, named profile B, profile C, and profile D, respectively (Figure 4).

In profile A, the enrichment result showed that there were 238 pathways, of which 30 pathways indicated significant enrichment ($P < 0.05$). Among these pathways, there were 60 pathways relevant to nutrition metabolism, of which 12 pathways indicated significant enrichment ($P < 0.05$). Thus, within all the significant enrichment pathways, 40% (12/30) significant enrichment pathways were related to nutrition metabolism (Figure 4A). In profile B, the enrichment result showed that there were 297 pathways, of which 51 were significantly enriched ($P < 0.05$). Among these pathways, 81 pathways were relevant to nutrition metabolism, of which 17 pathways indicated significant enrichment ($P < 0.05$). In other words, within all the significant enrichment pathways, 33.33% (17/51) pathways were related to nutrition metabolism (Figure 4B). In profile C, the enrichment result showed 320 pathways, of which 35 were significantly enriched ($P < 0.05$). Among them, 98 pathways were relevant to nutrition metabolism, of which 26 indicated a significant enrichment ($P < 0.05$). Hence, within all the significant enrichment pathways, 74.3% (26/35) significant enrichment pathways were related to nutrition metabolism (Figure 4C). In profile D, the enrichment result showed that 305 pathways, of which 38 were significantly enriched ($P < 0.05$). Among them, 75 pathways were related to nutrition metabolism, of which six pathways indicated significant enrichment ($P < 0.05$). Thus, within all the significant enrichment pathways, 13.2% (5/38) were related to nutrition metabolism (Figure 4D). The tryptophan metabolism

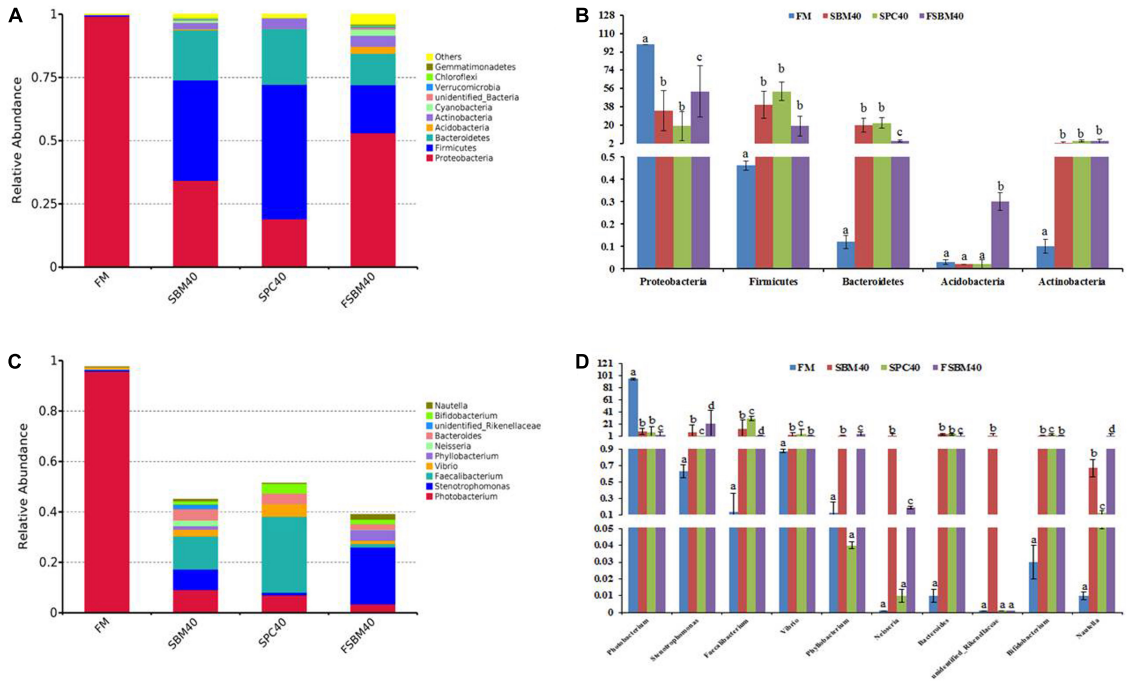

FIGURE 3
The gut flora composition and abundance of different soy meals substitution for fish meal in pearl gentian grouper [**(A,B)** phylum level and **(C,D)** genus level]. **(A)** Rarefaction curve; **(B)** rank abundance; **(C)** species accumulation boxplot. Different letters distributed on the column represented significant variances between the groups at $P < 0.05$ ($n = 3$).

pathway was significantly affected in the experiments of all three soy meal substitutions for FM ($P < 0.05$).

Validation of the tryptophan metabolism pathway by RT-qPCR

In general, the results of RT-qPCR corresponded to the results of transcriptome sequencing data, which confirmed the accuracy of RNA-seq (Figure 5). Therefore, RNA-seq in this study can provide a relatively valuable reference for further analysis. The results of the RT-qPCR showed that the key genes selected from the tryptophan metabolism pathway in different soy meal substitution groups were generally significantly inhibited ($P < 0.05$). However, there were some differences in the types of key genes of the tryptophan metabolism pathway affected in different treatment groups (Figure 6).

Correlation analysis

Figure 7 shows the correlations between the significant genes in the inflammatory genes and tryptophan metabolism pathways using the Envfit test. The results show that with increases in SBM, the key genes inhibited in tryptophan metabolism pathways were generally significantly correlated with the enteritis-related inflammatory genes ($P < 0.05$, Supplementary Tables 1–3). Thus, it had a negative correlation with the anti-inflammatory gene and a positive correlation with the pro-inflammatory gene.

Discussion

The present study exhibited that different soy meals (SBM, SPC, and FSBM) substitution for FM at the experimental level obviously lowered the growth performance, gut physiology and immune state, and gut flora composition. Studies on *Epinephelus coioides* (initial weight of 84 ± 2.5 g) found that 20% SBM substitution for FM (60% basal FM) presented optimal growth performance (10). Studies on the brown-marbled grouper (initial weight of 6.1 ± 0.7 g) showed that using 20–50% SBM to substitute for FM (50% basal FM) was unlikely to lower growth performance, but it significantly decreased at a 60% substitution level (12). SPC with substitution levels lower than 40% presented a significant reduction in the WGR, SGR, and FCR of turbot and Japanese flounder (28, 29). The optimal amount of FSBM in the hybrid tilapia diet substitution for FM is 34.2% (30), and FSBM in channel catfish diet can substitute 100% FM, but 25% is best (31). The present study found that WGR and SGR at a high level of substitution (40%) were significantly lower than in the FM control group. A previous study indicated that the

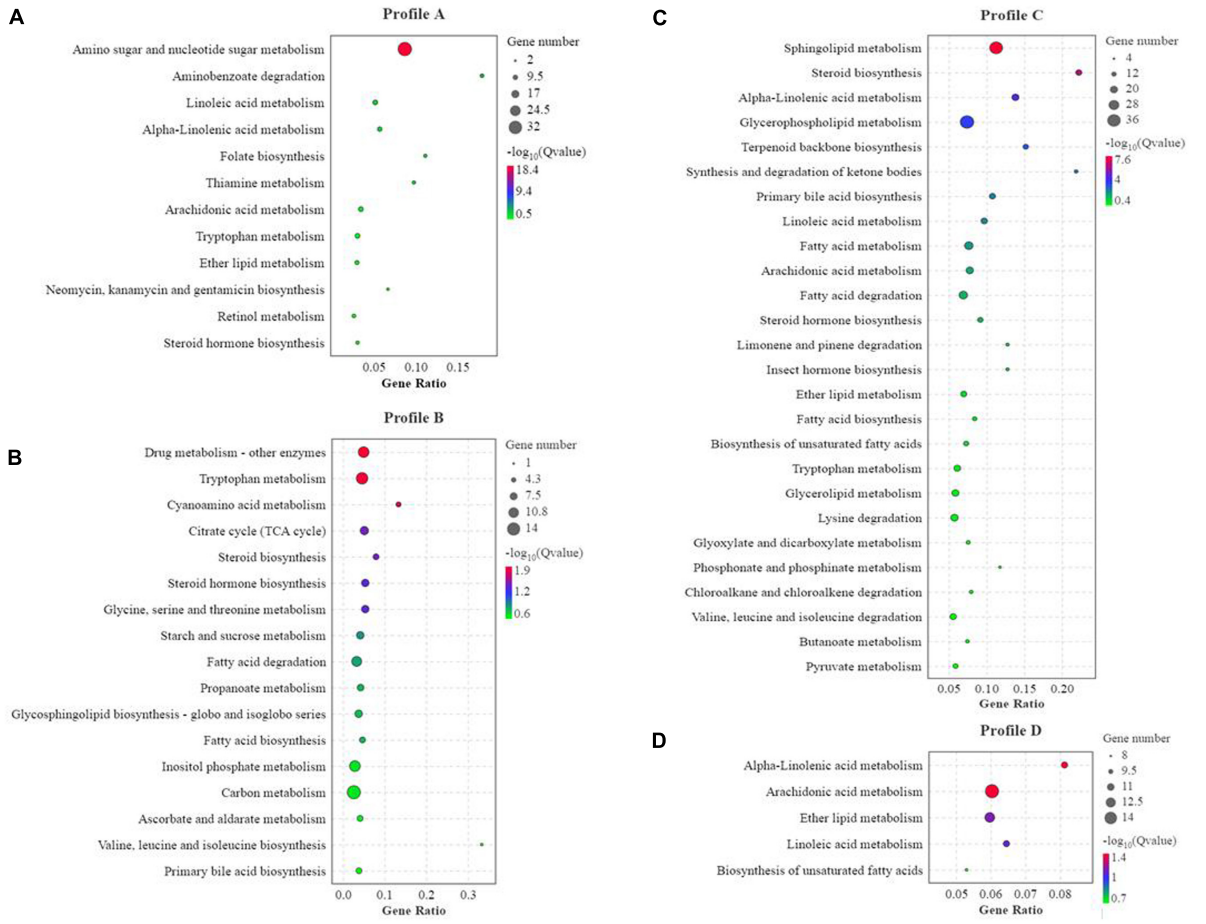

FIGURE 4
KEGG enrichment analysis of differential genes of different soy meals substitute for fish meal in hindgut of pearl gentian grouper (n = 4). **(A)** KEGG enrichment of co-contained DEGs in SBM40, SPC40, and FSBM40 group related to nutrition metabolism; **(B)** KEGG enrichment of unique DEGs in SBM40 group related to nutrition metabolism; **(C)** KEGG enrichment of unique DEGs in SPC40 group related to nutrition metabolism; **(D)** KEGG enrichment of unique DEGs in FSBM40 group related to nutrition metabolism (n = 4).

soy protein replacing FM in fish growth physiology may be related to the ANFs it contains (3). SBM, SPC, and FSBM, as three soy protein sources with different processing forms, have different content and types of ANFs. The unpublished feed test results in the present research showed that alcohol-soluble ANFs in SPC were basically completely removed, such as soybean isoflavones and (7S and 11S) and conglycinin. Although FSBM was fermented, compared with the SBM diet, the content of soybean isoflavones and (7S and 11S) conglycinin and other ANFs showed little change. However, compared with SBM and FSBM, the pearl gentian grouper fed with SPC feed did not show obvious advantages. It is speculated that ANFs may not be the only main influencing factor, but they may also be the influence of other unknown antigens or non-alcohol-soluble ANFs (such as phytic acid). FSBM did not improve the growth performance of pearl gentian groper, which may be due to its high content of ANFs or palatability problems (32). Previous studies on *E. coicoiaes* found that adding more than 14% FSBM to the diet would significantly reduce WGR and SGR, and the most suitable amount of FSBM to replace white FM (52% of basal FM) was 10% (10).

The present research also indicated that for pearl gentian groupers, the experimental level of soy proteins also had a significant impact on their gut enzyme activity. The LYS plays an important role in non-specific immunity in fish and IgM for specific immunity. Both C3 and C4 are crucial for activating their complement systems (33). In the research, all the soy protein sources with a 40% substitution level reduced the contents of C3, C4, and IgM, in which the addition of soy proteins may lead to the impaired gut immune system of pearl gentian groupers. This is also reflected in immune-related genes, such as inflammatory-related genes. In addition, previous research confirmed that the occurrence of enteritis in fish always goes with down-regulation of anti-inflammatory genes and up-regulation of pro-inflammatory genes (34). The present experiment found similar results.

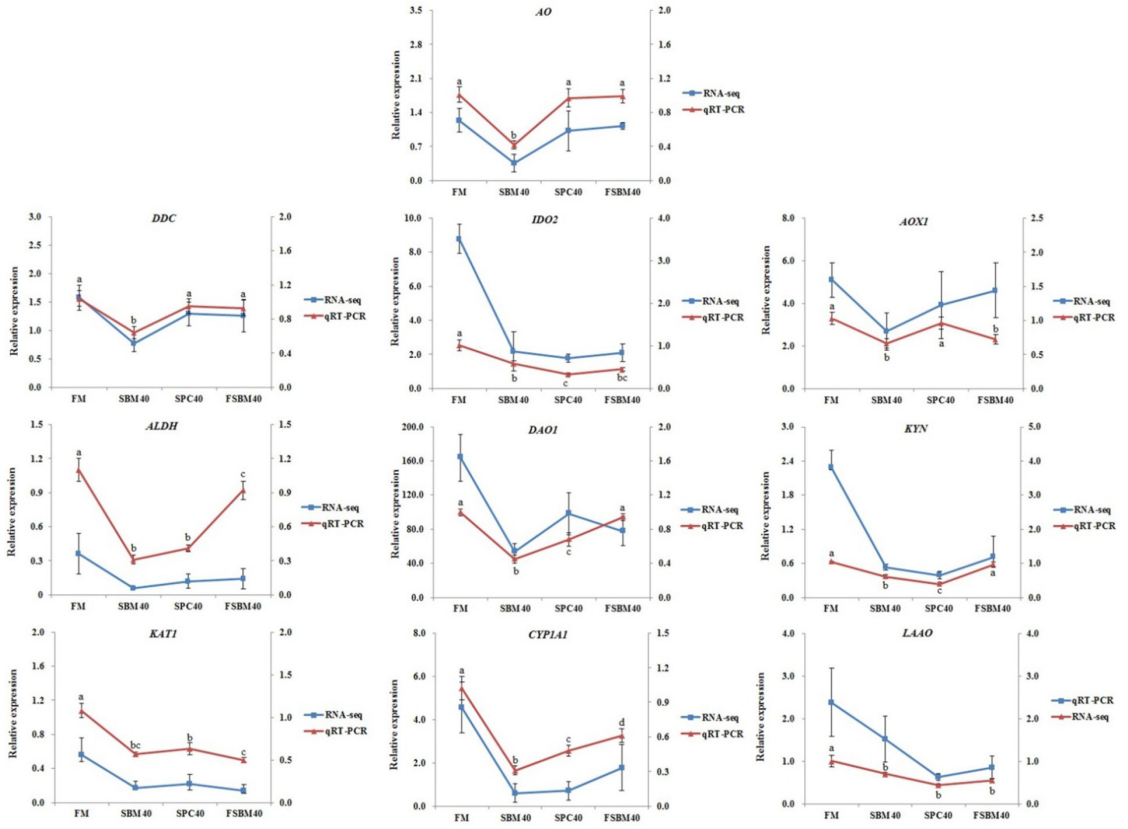

FIGURE 5
The contrast of RNA-seq and RT-qPCR results and the expressions of the key genes in tryptophan metabolism pathway in hindgut were chosen to confirm the precision of "3 + 2" transcriptome sequencing. The relative expression degree in RNA-seq analysis was counted by FPKM value. Different letters distributed on the broken line represented significant variances between the groups at $P < 0.05$ ($n = 4$).

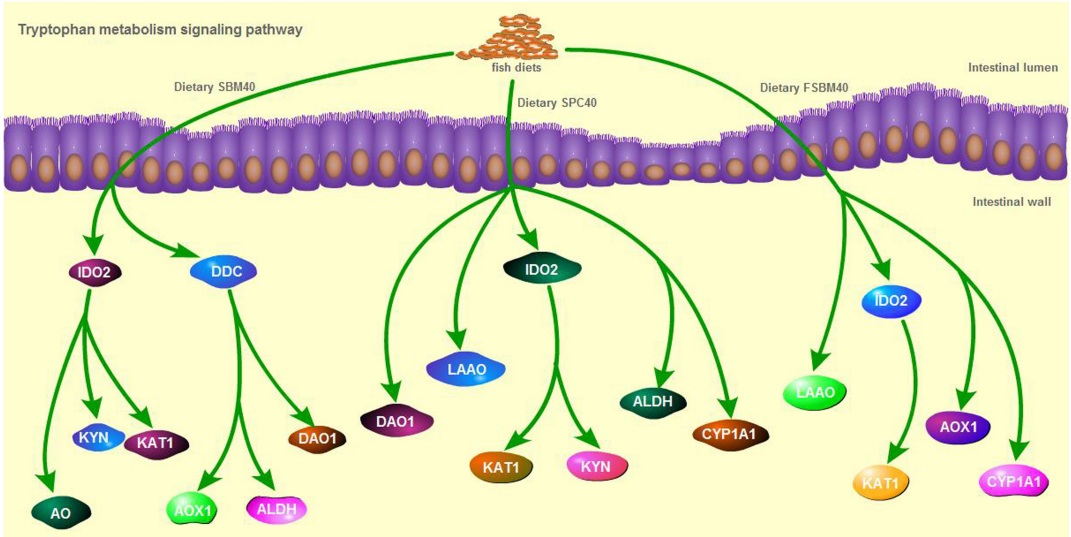

FIGURE 6
The key genes inhibited in tryptophan metabolism pathway of different soy meals induced enteritis in pearl gentian grouper.

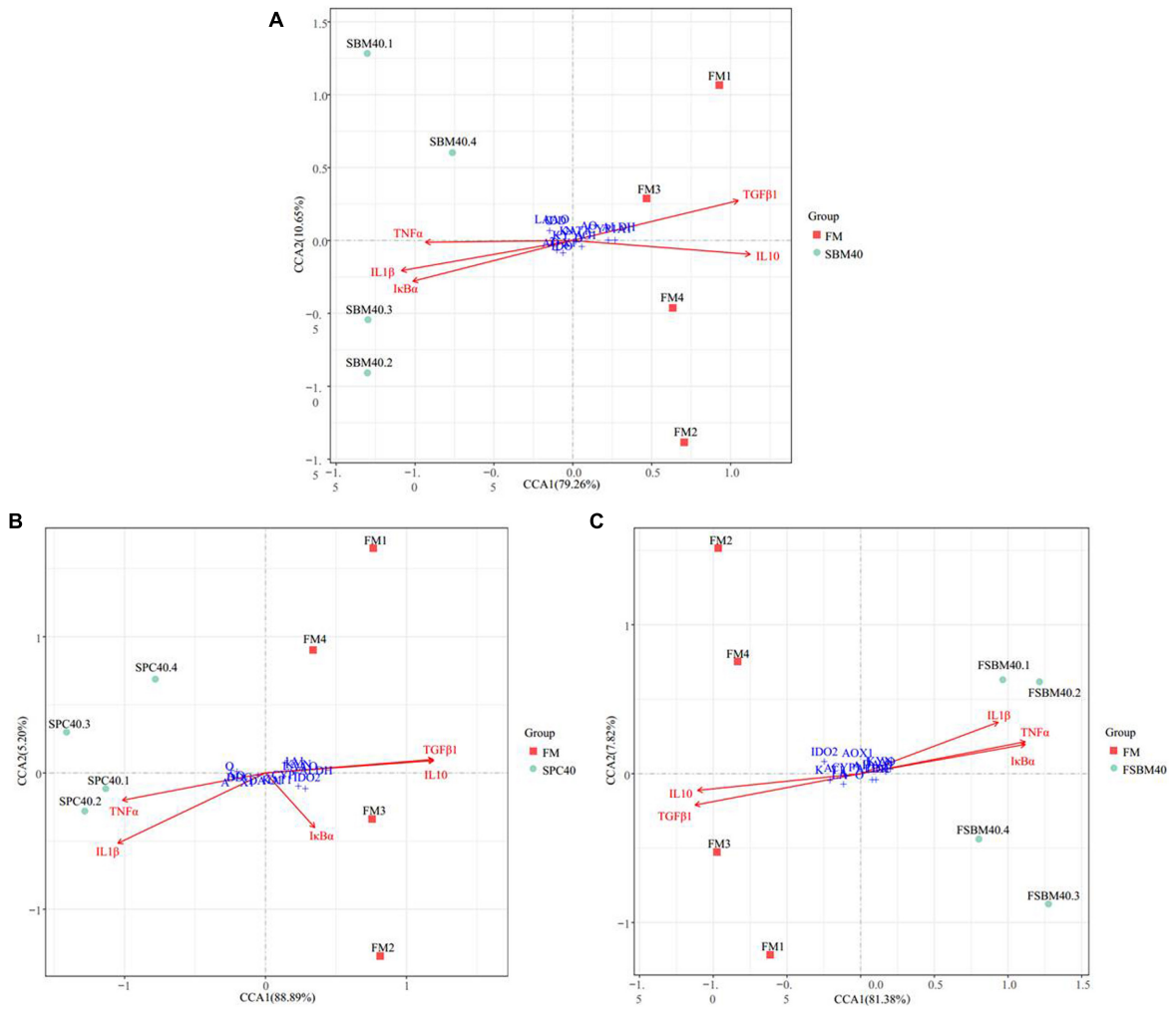

FIGURE 7
The canonical correlation analysis (CCA) between the key genes inhibited in tryptophan metabolism pathway and the inflammatory genes of different soy meals induced enteritis in groupers (n = 4). In CCA plot, the arrows represent explanatory variables and the points represent response variables. The lengths of the arrows represent the strength of the influence of the explanatory variable on the response variable; the longer lengths indicate greater influences. The angles between the arrows and coordinate axis represent the correlation between the explanatory variable and coordinate axis; smaller angles indicate stronger correlation. A sample point located in the same direction as the arrow indicates that the changes in explanatory and response variables are positively correlated, while in the opposite direction which indicates a negative correlation. The value in the coordinate axis label in the plot represents the interpretation proportion of the explanatory variables combination and the response variable variation. FM, fish meal control group; SBM40, 40% SBM substitution for FM; SPC40, 40% SPC substitution for FM; FSBM40, 40% FSBM substitution for FM.

Our previous analysis of the gut immune system of SBMIE pearl gentian groupers found that among the signal pathways significantly activated in the gut, 55.17% were related to intestinal immunity, contagious disease, and signal transduction; in the signal pathways greatly inhibited in the gut, nutrient metabolism-related pathways accounted for 67.44% (35). The results showed that for pearl gentian groupers, the production of SBMIE is likely to be the result of the combined action of immune and nutritional imbalance. Combined with this study, we found different gut responses of SBMIE pearl gentian groupers that ate SPC and FSBM. After eating SPC, grouper mainly showed that the pathways relevant to intestinal nutrient metabolism were restrained in general (74.3%, 26/35), while after eating FSBM, the pathways related to immunity, contagious disease, and signal transduction were generally inhibited (60.5%, 23/38). Among them, the tryptophan metabolism pathway is significantly inhibited in the SBMIE pearl gentian groupers caused by the studied soy protein sources in the present study. According to existing research, tryptophan, as a communication medium between gut flora and the host, generates many tryptophan metabolites under the action of a series of endogenous enzymes or biological metabolisms, and its metabolites regulate various physiological processes of the host to varying degrees. Tryptophan deficiency directly leads

to the reduction of metabolites, which is closely related to gut imbalance, and even induced IBD (36).

Tryptophan is the only amino acid in animals that combines with serum protein through covalent bonds. It is widely involved in the synthesis of proteins and nucleic acids, and it can enter the liver through the hepatic portal vein and regulate protein deposition and metabolism. Insufficient tryptophan content will reduce the absorption and utilisation rate of protein and immune function of livestock and poultry and increase the susceptibility of livestock and poultry to disease (37, 38). There are three main pathways of tryptophan catabolism: the kynurenine pathway, 5-hydroxytryptamine (5-HT) pathway and the gut flora pathway. The kynurenine pathway is the most important metabolic pathway through which about 95% of tryptophan is metabolised (39, 40). This pathway occurs in three parts of the body, which, in order of degree, are the liver, brain, and small intestine. The rate-limiting enzymes are TDO and –2,3–dioxygenase IDO, respectively (41). Tryptophan is catalysed by a series of enzymes, such as TDO/IDO to produce a variety of metabolites, such as N-formyl kynurenine, kynurenine, 3-hydroxykynurenine, kynurenic acid, and picolinic acid, which are finally decomposed into CO_2 and ATP (42). After being absorbed by the body, these metabolites can regulate intestinal barrier immunity in a variety of ways. Second, 1–2% of tryptophan intake is converted through the 5-HT pathway, mainly in the gastrointestinal tract, of which 90% occurs in enterochromaffin cells and 10% in gut neurons, and the rate-limiting enzymes are tryptophan hydroxylase (43). 5-HT not only regulates the immune activity of the body, but it also plays a key role as a neurotransmitter in the brain-gut axis, which is a bidirectional system that connects the gastrointestinal tract with the central nervous system (44). In addition, 4–6% of tryptophan can be directly metabolised by intestinal flora into ligands of aromatic hydrocarbon receptor (AhR), including indole and indole derivatives (45, 46). In terrestrial animal studies, it is pointed out that AhR can bind to its ligand through TLR-NF-κB signalling pathway, and then it regulates the expression of downstream target genes. For example, studies in mammals have found that a tryptophan-rich diet can activate the expression of the AhR gene and subsequently increase the expression of the IL22 gene in the colon (47). AhR is a negative regulator of IL17-mediated signal transduction and plays an important role in resisting pathogens of immune diseases (48). IL10 is an effective anti-inflammatory cytokine that can inhibit the production of pro-inflammatory mediators. IL10 signals through IL10 receptors, which act on various cell types, such as intestinal epithelial cells, where IL10 receptors are associated with the development and maintenance of barrier function (49). In fish SBMIE, NF-κB signalling pathway presents to be quite conservative, and similar results were obtained in our previous analysis of pearl gentian groupers enteritis induced by SBM and FSBM (35). In this experiment, through CCA analysis, we found that there was a significant correlation between the key genes of the tryptophan metabolism pathway and enteritis induced by three soy protein sources of pearl gentian grouper, which also suggested that abnormal tryptophan metabolism in fish soy enteritis deserves special attention.

Some studies have pointed out that the gut flora variation will lead to a change in tryptophan metabolism and then affect the intestinal physiological function (50). Similarly, tryptophan deficiency in feed can also change the composition of gut flora and damage intestinal immune function (51). Previous research has pointed out that the tryptophan content in SBM is generally equivalent to that in FM (∼0.65%), while the tryptophan content in SPC and FSBM is higher than that in FM (52). However, the three kinds of soy protein feeds in this research have led to the inhibition of tryptophan metabolism, which is likely to be closely related to gut flora variation. The three soy protein sources at this experimental level significantly influenced the intestinal flora of pearl gentian groupers. In mammalian studies, it was found that the abundance changes in Bacteroides, Bacteroides, Bifidobacterium, Fusobacterium, Lactobacillus, and Faecalibacterium (53–55) were significantly correlated with the degree of IBD. Similarly, the abundance changes in some species at the level of gut flora were also found in the SBMIE pearl gentian grouper, but the change trend was opposite. Previous research pointed out that under pathological state, the OTU abundance variations of mammalian gut flora at the level of the phylum or genus run contrary to those of fish sometimes (56–58). At present, the analysis of intestinal flora in this experiment is only at the genus level, and it should be further studied at the species level in the future.

Conclusion

This study found that the tryptophan metabolic pathway has an important impact on the enteritis of pearl gentian groupers induced by soy protein, during which gut flora may play a crucial role. However, a more in-depth analysis should be further improved in future work. Technically, targeted metabonomics can be used to analyse the changes of tryptophan metabolites, such as indoles and indole derivatives produced by gut flora metabolism; using metagenomics to analyse the species of tryptophan metabolising flora in the gut at the species level, as a potential probiotic additive for repairing fish soy-induced enteritis. The research offers a theoretical reference for the development of new feed additives to prevent soy-induced enteritis in fish and has important economic and ecological benefits.

Data availability statement

The datasets presented in this study can be found in online repositories. The names of the repository/repositories

and accession number(s) can be found in the article/**Supplementary material**.

Ethics statement

All experimental methods were approved by the Ethics Review Board of Guangdong Ocean University. All of the procedures were performed in accordance with the relevant guidelines and regulations.

Author contributions

WZ and AP were engaged in the whole experiment and formulated the draft of this manuscript. BT designed the experiment and composed and amended the draft critically. YX and YL took part in the tests. RX amended the first draft. HZ and QY completed the data analysis. JD and SC approved the final version. All authors contributed to the article and approved the submitted version.

Funding

This research was supported by the National Key R&D Program of China (2019YFD0900200), the National Natural Science Foundation of China (NSFC 31772864), and the China Agriculture Research System of MOF and MARA (CARS-47).

Acknowledgments

We are grateful to the Key Laboratory of Aquatic, Livestock and Poultry Feed Science and Technology in South China, Ministry of Agriculture, for providing technical assistances.

Conflict of interest

The authors declare that the research was conducted in the absence of any commercial or financial relationships that could be construed as a potential conflict of interest.

Publisher's note

All claims expressed in this article are solely those of the authors and do not necessarily represent those of their affiliated organizations, or those of the publisher, the editors and the reviewers. Any product that may be evaluated in this article, or claim that may be made by its manufacturer, is not guaranteed or endorsed by the publisher.

Supplementary material

The Supplementary Material for this article can be found online at: https://www.frontiersin.org/articles/10.3389/fnut.2022.1014502/full#supplementary-material

References

1. Mohan K, Rajan D, Muralisankar T, Ganesan A, Sathishkumar P, Revathi N. Use of black soldier fly (*Hermetia illucens L.*) larvae meal in aquafeeds for a sustainable aquaculture industry: a review of past and future needs. *Aquaculture.* (2022) 553:738095. doi: 10.1016/j.aquaculture.2022.738095

2. Watson A, Casu F, Bearden D, Yost J, Denson M, Gaylord T, et al. Investigation of graded levels of soybean meal diets for red drum, *Sciaenops ocellatus*, using quantitative PCR derived biomarkers. *Comp Biochem Physiol Part D Genomics Proteomics.* (2019) 29:274–85. doi: 10.1016/j.cbd.2019.01.002

3. Krogdahl Å, Penn M, Thorsen J, Refstie S, Bakkle A. Important antinutrients in plant feedstuffs for aquaculture: an update on recent findings regarding responses in salmonids. *Aquac Res.* (2010) 41:333–44. doi: 10.1111/j.1365-2109.2009.02426.x

4. Sahlmann C, Sutherland B, Kortner T, Koop B, Krogdahl Å, Bakkle A. Early response of gene expression in the distal intestine of Atlantic salmon (*Salmo salar L.*) during the development of soybean meal induced enteritis. *Fish Shellfish Immunol.* (2013) 34:599–609. doi: 10.1016/j.fsi.2012.11.031

5. Yamamoto T, Goto T, Kine Y, Endo Y, Kitaoka Y, Sugita T, et al. Effect of an alcohol extract from a defatted soybean meal supplemented with a casein-based semi-purified diet on the biliary bile status and intestinal conditions in rainbow trout *Oncorhynchus mykiss* (Walbaum). *Aquac Res.* (2008) 39:986–94. doi: 10.1111/j.1365-2109.2008.01969.x

6. Urán P, Gonçalves A, Taverne-Thiele J, Schrama J, Rombout J. Soybean meal induces intestinal inflammation in common carp (*Cyprinus carpio L.*). *Fish Shellfish Immunol.* (2008) 25:751–60. doi: 10.1016/j.fsi.2008.02.013

7. Fuentes-Appelgren P, Opazo R, Barros L, Feijoó C, Romero J. Effect of the dietary inclusion of soybean components on the innate immune system in zebrafish. *Zebrafish.* (2014) 11:41–9. doi: 10.1089/zeb.2013.0934

8. Bakke-Mckellep A, Press C, Baeverfjord G, Krogdahl Å, Landsverk T. Changes in immune and enzyme histochemical phenotypes of cells in the intestinal mucosa of Atlantic salmon, *Salmo salar L.* with soybean meal-induced enteritis. *J Fish Dis.* (2000) 23:115–27. doi: 10.1046/j.1365-2761.2000.00218.x

9. Ai Q, Xie X. The nutrition of *Silurus meridionalis*: effects of different levels of dietary soybean protein on growth. *Acta Hydrobiol Sin.* (2002) 26:57–65.

10. An M, Fan Z, Wang Q, Sun J, Xu D, Guo Y, et al. Effects of substituting fish meal with soybean meal on growth, digestion and antioxidant capacity of *Epinephelus coicoiaes*. *Jiangsu Agric Sci.* (2018) 46:128–32. doi: 10.15889/j.issn.1002-1302.2018.16.032

11. Zhou W, Yan Y, Yang H, Sun Y. Effects of soybean meal partially replacing fish meal on growth, digestive enzyme activity and immune function of *Epinephelus coioides*. *Feed Res.* (2014) 19:61–4. doi: 10.13557/j.cnki.issn1002-2813.2014.19.041

12. Faudzi N, Yong A, Shapawi R, Senoo S, Biswas A, Takii K. Soy protein concentrate as an alternative in replacement of fish meal in the feeds of hybrid grouper, brown-marbled grouper (*Epinephelus fuscoguttatus*) × giant grouper (*E. lanceolatus*) juvenile. *Aquac Res.* (2017) 49:431–41. doi: 10.1111/are.13474

13. Krogdahl Å, Bakke A. Antinutrients. In: Lee C editor. *Dietary Nutrients, Additives and Fish Health*. Hoboken, NJ: Wiley Blackwell (2015). p. 211–35.

14. Kortner T, Skugor S, Penn M, Mydland L, Djordjevic B, Hillestad M, et al. Dietary soyasaponin supplementation to pea protein concentrate reveals

nutrigenomic interactions underlying enteropathy in Atlantic salmon (*Salmo salar*). *BMC Vet Res.* (2012) 8:101. doi: 10.1186/1746-6148-8-101

15. Knudsen D, Jutfelt F, Sundh H, Sundell K, Koppe W, Frøkiaer H. Dietary soya saponins increase gut permeability and play a key role in the onset of soya bean-induced enteritis in Atlantic salmon (*Salmo salar L.*). *Br J Nutr.* (2008) 100:120–9. doi: 10.1017/S0007114507886338

16. Gu M, Bai N, Xu B, Xu X, Jia Q, Zhang Z. Protective effect of glutamine and arginine against soybean mealinduced enteritis in the juvenile turbot (*Scophthalmus maximus*). *Fish Shellfish Immunol.* (2017) 70:95–105. doi: 10.1016/j.fsi.2017.08.048

17. Hu Y, Zhang J, Xue J, Chu W, Hu Y. Effects of dietary soy isoflavone and soy saponin on growth performance, intestinal structure, intestinal immunity and gut microbiota community on rice field eel (*Monopterus albus*). *Aquaculture.* (2021) 537:736506. doi: 10.1016/j.aquaculture.2021.736506

18. Gu M, Pan S, Li Q, Qi Z, Bai N. Protective effects of glutamine against soy saponins-induced enteritis, tight junction disruption, oxidative damage and autophagy in the intestine of *Scophthalmus maximus* L. *Fish Shellfish Immunol.* (2021) 114:49–57. doi: 10.1016/j.fsi.2021.04.013

19. Sun M, Ma N, He T, Johnston L, Ma X. Tryptophan (Trp) modulates gut homeostasis via aryl hydrocarbon receptor (AhR). *Crit Rev Food Sci.* (2020) 60:1760–8. doi: 10.1080/10408398.2019.1598334

20. Tang L. *The Study of the Effects Tryptophan on Digestive and Absorbtive Capacity, Disease Resistant, and the TOR Expression in Organs and Tissue in Jian carp (Cyprinus carpio var. Jian)*. Yaan: Sichuan Agriculture University (2010).

21. Ma Y. *Effects of Tryptophan in Two Protein Levels Diets on Feed Intake, Growth Performance, and Immunity of Litopenaeus vannamei*. Hubei: Huazhong Agricultural University (2016).

22. Hseu J, Lu F, Su H, Wang L, Tsai C, Hwang P. Effect of exogenous tryptophan on cannibalism, survival and growth in juvenile grouper, *Epinephelus coioides*. *Aquaculture.* (2003) 218:251–63. doi: 10.1016/S0044-8486(02)00503-3

23. Agus A, Planchais J, Soko H. Gut microbiota regulation of tryptophan metabolism in health and disease. *Cell Host Microbe.* (2018) 23:716.

24. Fan Y, Pedersen O. Gut microbiota in human metabolic health and disease. *Nat Rev Microbiol.* (2020) 19:55–71. doi: 10.1038/s41579-020-0433-9

25. Miao S, Zhao C, Zhu J, Hu J, Dong X, Sun L. Dietary soybean meal affects intestinal homoeostasis by altering the microbiota, morphology and inflammatory cytokine gene expression in northern snakehead. *Sci Rep.* (2018) 8:113–23. doi: 10.1038/s41598-017-18430-7

26. Zhang W, Tan B, Ye G, Wang J, Dong X, Yang Q, et al. Identification of potential biomarkers for soybean meal-induced enteritis in juvenile pearl gentian grouper, *Epinephelus fuscoguttatus*♀×*Epinephelus lanceolatus*♂. *Aquaculture.* (2019) 512:734337. doi: 10.1016/j.aquaculture.2019.734337

27. Zhang W, Tan B, Deng J, Yang Q, Chi S, Pang A, et al. PRR-mediated immune response and intestinal flora profile in soybean meal induced enteritis of pearl gentian groupers, *Epinephelus fuscoguttatus* ♀ × *Epinephelus lanceolatus* ♂. *Front Immunol.* (2022) 13:814479. doi: 10.3389/fimmu.2022.814479

28. Liu X, Ai Q, Mai K, Liu F, Xu W. Effects of replacing fish meal with soy protein concentrate on feed intake and growth of turbot (*Scophthalmus maximus*). *J Fish China.* (2014) 38:91–8. doi: 10.3724/SP.J.1231.2014.48852

29. Deng J, Mai K, Ai Q, Zhang W, Wang X, Xu W, et al. Effects of replacing fish meal with soy protein concentrate on feed intake and growth of juvenile Japanese flounder, *Paralichthys olivaceus*. *Aquaculture.* (2006) 258:503–13. doi: 10.1016/j.aquaculture.2006.04.004

30. Cheng C, Liu Y. Study on fermented soybean meal instead of fish meal in hybrid tilapia feed. *Guangdong Feed.* (2004) 13:26–7.

31. Li H, Huang F, Hu B, Zhou Y, Zhang L. Effects of replacement of fish meal with fermented soybean in the diet channel catfish (*Ictalurus punctutus*) on growth performance and apparent digestibility of feed. *Freshw Fish.* (2007) 37:41–4.

32. Shen W, Matsui T. Intestinal absorption of small peptides: a review. *Int J Food Sci Tech.* (2019) 54:1942–8. doi: 10.1111/ijfs.14048

33. Uribe C, Folch H, Enriquez R, Moran G. Innate and adaptive immunity in teleost fish: a review. *Vet Med Czech.* (2011) 56:486–503. doi: 10.17221/3294-VETMED

34. Lepage P, Seksik P, Sutren M, Cochetière M, Jian R, Marteau P, et al. Biodiversity of the mucosa-associated microbiota is stable along the distal digestive tract in healthy individuals and patients with IBD. *Inflamm Bowel Dis.* (2005) 11:473–80. doi: 10.1097/01.mib.0000159662.62651.06

35. Zhang W. *Study on the Differential Mechanism of Intestinal Mucosal Barrier Damage in Epinephelus fuscoguttatus*♀×*E. lanceolatus*♂ *Caused by Three Kinds of Soybean Protein*. Zhanjiang: Guangdong Ocean University (2020).

36. Cui C, Li Y, Yang H, Jin W, Wu J, Han C, et al. Research progress of tryptophan metabolism and inflammatory bowel disease. *Med Recapitulate.* (2021) 27:2726–30.

37. Floc'h N, Otten W, Merlot E. Tryptophan metabolism, from nutrition to potential therapeutic applications. *Amino Acids.* (2011) 41:1195–205. doi: 10.1007/s00726-010-0752-7

38. Wu G. Amino acids: metabolism, functions, and nutrition. *Amino Acids.* (2009) 37:1–17. doi: 10.1007/s00726-009-0269-0

39. Kaszaki J, Érces D, Gabriella V, Szabó A, Vécsei L, Boros M. Kynurenines and intestinal neurotransmission: the role of N-methyl-D-aspartate receptors. *J Neural Transm.* (2012) 119:211–23. doi: 10.1007/s00702-011-0658-x

40. Agus A, Planchais J, Sokol H. Gut microbiota regulation of tryptophan metabolism in health and disease. *Cell Host Microbe.* (2018) 23:716–24. doi: 10.1016/j.chom.2018.05.003

41. Ebrahimi A, Kardar G, Toolabi L, Ghanbari H, Sadroddiny E. Inducible expression of indoleamine 2,3-dioxygenase attenuates acute rejection of tissue-engineered lung allografts in rats. *Gene.* (2016) 576:412–20. doi: 10.1016/j.gene.2015.10.054

42. Platten M, Nollen E, Röhrig U, Fallarino F, Opitz C. Tryptophan metabolism as a common therapeutic target in cancer, neurodegeneration and beyond. *Nat Rev Drug Discov.* (2019) 18:379–401. doi: 10.1038/s41573-019-0016-5

43. Qin H, Wong H, Zang K, Li X, Bian Z. Enterochromaffin cell hyperplasia in the gut: factors, mechanism and therapeutic clues. *Life Sci.* (2019) 239:116886. doi: 10.1016/j.lfs.2019.116886

44. O'Mahony S, Clarke G, Borre Y, Dinan T, Cryan J. Serotonin, tryptophan metabolism and the brain-gut-microbiome axis. *Behav Brain Res.* (2015) 277:32–48. doi: 10.1016/j.bbr.2014.07.027

45. Wang G, Huang S, Wang Y, Cai S, Yu H, Liu H, et al. Bridging intestinal immunity and gut microbiota by metabolites. *Cell Mol Life Sci.* (2019) 76:3917–37. doi: 10.1007/s00018-019-03190-6

46. Huć T, Nowinski A, Drapala A, Konopelski P, Ufnal M. Indole and indoxyl sulfate, gut bacteria metabolites of tryptophan, change arterial blood pressure via peripheral and central mechanisms in rats. *Pharmacol Res.* (2018) 130:172–9. doi: 10.1016/j.phrs.2017.12.025

47. Comai S, Bertazzo A, Brughera M, Crotti S. Tryptophan in health and disease. *Adv Clin Chem.* (2020) 95:165–218. doi: 10.1016/bs.acc.2019.08.005

48. Vyhlídalová B, Krasulová K, Pečinková P, Marcalíková A, Vrzal R, Zemánková L, et al. Gut microbial catabolites of tryptophan are ligands and agonists of the aryl hydrocarbon receptor: a detailed characterization. *Int J Mol Sci.* (2020) 21:2614. doi: 10.3390/ijms21072614

49. Perez L, Kempski J, Mcgee M, Pelzcar P, Agalioto T, Giannou A, et al. TGF-βsignaling in Th17 cells promotes IL-22 production and colitis-associated colon cancer. *Nat Commun.* (2020) 11:2608. doi: 10.1038/s41467-020-16363-w

50. Golubeva A, Joyce S, Moloney G, Burokas A, Sherwin E, Arboleya S, et al. Microbiota-related changes in bile acid&tryptophan metabolism are associated with gastrointestinal dysfunction in a mouse model of autism. *Ebiomedicine.* (2017) 24:166–78. doi: 10.1016/j.ebiom.2017.09.020

51. Hashimoto T, Perlot T, Rehman A, Trichereau J, Ishiguro H, Paolino M, et al. ACE2 links amino acid malnutrition to microbial ecology andintestinal inflammation. *Nature.* (2012) 487:477–81. doi: 10.1038/nature11228

52. National Research Council [NRC]. *Nutrient Requirements of Fish and Shrimp*. Washington, DC: The National Academic Press (2011). p. 401.

53. Frank D, Amand A, Feldman R, Boedeker E, Harpaz N, Pace N. Molecular-phylogenetic characterization of microbial community imbalances in human inflammatory bowel diseases. *Proc Natl Acad Sci USA.* (2007) 104:13780–5. doi: 10.1073/pnas.0706625104

54. Nemoto H, Kataoka K, Ishikawa H, Ikata K, Arimochi H, Iwasaki T, et al. Reduced diversity and imbalance of fecal microbiota in patients with ulcerative colitis. *Dig Dis Sci.* (2012) 57:2955–64. doi: 10.1007/s10620-012-2236-y

55. Kostic A, Xavier R, Gevers D. The microbiome in inflammatory bowel disease: current status and the future ahead. *Gastroenterology.* (2014) 146:1489–99. doi: 10.1053/j.gastro.2014.02.009

56. Jing G, Kang X, Liu H, Gang L, Bai M, Li T, et al. Impact of the gut microbiota on intestinal immunity mediated by tryptophan metabolism. *Front Cell Infect Microbiol.* (2018) 8:13. doi: 10.3389/fcimb.2018.00013

57. Lin L, Zhang J. Role of intestinal microbiota and metabolites on gut homeostasis and human diseases. *BMC Immunol.* (2017) 18:2. doi: 10.1186/s12865-016-0187-3

58. Sanders D, Inniss S, Sebepos-Rogers G, Rahman F. The role of the microbiome in gastrointestinal inflammation. *Biosci Rep.* (2021) 41:BSR20203850. doi: 10.1042/BSR20203850

frontiers | Frontiers in Nutrition

TYPE Original Research
PUBLISHED 22 December 2022
DOI 10.3389/fnut.2022.965356

OPEN ACCESS

EDITED BY
Filippo Giorgio Di Girolamo,
University of Trieste, Italy

REVIEWED BY
Asima Karim,
University of Sharjah,
United Arab Emirates
Ana Sofia Sousa,
Fernando Pessoa University, Portugal

*CORRESPONDENCE
Pamela Acosta-Méndez
ipam12@hotmail.com

SPECIALTY SECTION
This article was submitted to Clinical Nutrition, a section of the journal Frontiers in Nutrition

RECEIVED 09 June 2022
ACCEPTED 25 November 2022
PUBLISHED 22 December 2022

CITATION
Rosas-Carrasco O, Núñez-Fritsche G, López-Teros MT, Acosta-Méndez P, Cruz-Oñate JC, Navarrete-Cendejas AY and Delgado-Moreno G (2022) Low muscle strength and low phase angle predicts greater risk to mortality than severity scales (APACHE, SOFA, and CURB-65) in adults hospitalized for SARS-CoV-2 pneumonia. *Front. Nutr.* 9:965356. doi: 10.3389/fnut.2022.965356

Low muscle strength and low phase angle predicts greater risk to mortality than severity scales (APACHE, SOFA, and CURB-65) in adults hospitalized for SARS-CoV-2 pneumonia

Oscar Rosas-Carrasco [1], Gisela Núñez-Fritsche[1], Miriam Teresa López-Teros[1], Pamela Acosta-Méndez[2]*, Juan Carlos Cruz-Oñate[2], Ada Yuseli Navarrete-Cendejas[2] and Gerardo Delgado-Moreno[2]

[1]Department of Health, Universidad Iberoamericana, Mexico City, Mexico, [2]General Hospital Penjamo, Guanajuato, Mexico

Introduction: The acute physiology and chronic health evaluation (APACHE), sepsis-related organ failure assessment (SOFA), score for pneumonia severity (CURB-65) scales, a low phase angle (PA) and low muscle strength (MS) have demonstrated their prognostic risk for mortality in hospitalized adults. However, no study has compared the prognostic risk between these scales and changes in body composition in a single study in adults with SARS-CoV-2 pneumonia. The great inflammation and complications that this disease presents promotes immobility and altered nutritional status, therefore a low PA and low MS could have a higher prognostic risk for mortality than the scales. The aim of the present study was to evaluate the prognostic risk for mortality of PA, MS, APACHE, SOFA, and CURB-65 in adults hospitalized with SARS-CoV-2 pneumonia.

Methodology: This was a longitudinal study that included n = 104 SARS-CoV-2-positive adults hospitalized at General Hospital Penjamo, Guanajuato, Mexico, the PA was assessed using bioelectrical impedance and MS was measured with manual dynamometry. The following disease severity scales were applied as well: CURB-65, APACHE, and SOFA. Other variables analyzed were: sex, age, CO-RADS index, fat mass index, body mass index (BMI), and appendicular muscle mass index. A descriptive analysis of the study variables and a comparison between the group that did not survive and survived were performed, as well as a Cox regression to assess the predictive risk to mortality.

Results: Mean age was 62.79 ± 15.02 years (31–96). Comparative results showed a mean PA of 5.43 ± 1.53 in the group that survived vs. 4.81 ± 1.72 in the group that died, p = 0.030. The mean MS was 16.61 ± 10.39 kg vs. 9.33 ± 9.82 in the group that died, p = 0.001. The cut-off points for low

PA was determined at 3.66° and ≤ 5.0 kg/force for low grip strength. In the Cox multiple regression, a low PA [heart rate (HR) = 2.571 0.726, 95% CI = 1.217–5.430] and a low MS (HR = 4.519, 95% CI = 1.992–10.252) were associated with mortality.

Conclusion: Phase angle and MS were higher risk predictors of mortality than APACHE, SOFA, and CURB-65 in patients hospitalized for COVID-19. It is important to include the assessment of these indicators in patients positive for SARS-CoV-2 and to be able to implement interventions to improve them.

KEYWORDS

phase angle, sepsis-related organ failure assessment (SOFA), score for pneumonia severity (CURB-65), APACHE II, dynapenia, low grip strength, sarcopenia

Introduction

In December 2019 in the city of Wuhan China, an outbreak of pneumonia was recorded, caused by the SARS-CoV-2 virus, also known as Coronavirus-19, associated with high morbidity and mortality (1). The SARS-CoV-2 infection produces an inflammatory process characterized by an increase in inflammatory cytokines such as tumor necrosis factor-alpha (TNF-α), interleukins 1 and 6 (lL-1 and IL-6), and C-reactive protein (CRP), among others. This inflammation, together with the immobility and inadequate nutrition seen in patients hospitalized for pneumonia, contributes to the loss of muscle mass and strength (2, 3).

Due to the high mortality rates resulting from SARS-CoV-2 infection in people with risk factors and unvaccinated, early markers are needed to help the clinical team identify patients at high risk of death in order to implement timely interventions to reduce this risk. So far, different disease severity and mortality risk scales have been applied in hospitalized critically ill patients: the acute physiology and chronic health evaluation II (APACHE II), the sepsis-related organ failure assessment (SOFA), and the score for pneumonia severity (CURB-65) (4, 5). These scales have proven useful for predicting mortality in SARS-CoV-2-infected patients (6).

On the other hand, other predictors of mortality in hospitalized patients with SARS-CoV-2 infection have been proposed, such as the phase angle (PA), obtained from bioelectrical impedance analysis (BIA) (7–9). PA is an effective marker to detect health conditions and take preventive action, as well as a predictor of mortality, morbidity, length of hospital in patients with COVID-19 (9–11). Muscle strength (MS) is another predictive marker to mortality and longer hospital stay in patients hospitalized for COVID-19 (11, 12). These recently published studies show the importance of continuing to study markers with better predictive capacity to mortality in hospitalized patients with SARS-CoV-2. At present, these severity scales as low PA and MS, have been shown to be predictive of mortality, but individually, no study has shown which represents a greater risk of mortality in the same group of patients. The great inflammation, support ventilation, use the tubes and catheters and others; promotes immobility, loss of appetite, increased caloric expenditure and others factors together impact nutritional status (including the body composition and MS), therefore a low PA and low MS could have a higher prognostic risk for mortality than the severity scales.

Therefore, the aim of this study is to determine if low MS and PA predicts greater risk to mortality than severity scales (APACHE, SOFA, and CURB-65) in a group of adults hospitalized for SARS-CoV-2 pneumonia.

Materials and methods

Study design and population

This is a longitudinal, prognostic, cohort study that included 104 SARS-CoV-2-positive adults hospitalized at General Hospital Penjamo, in the state of Guanajuato, Mexico during the COVID-19 pandemic, from August to December, 2020. All patients admitted with a diagnosis of SARS-CoV-2-positive pneumonia of any degree of severity were included. The diagnosis of pneumonia was made by the medical team in charge of the hospitalization and supported by plain computed axial tomography (CAT) and/or chest tele radiography. Participants with pacemaker or defibrillator, pleural, peritoneal, legs oedema, renal replacement therapy (hemodialysis or peritoneal dialysis, current intake of diuretics, presence of fever, and diarrhea were excluded from the study, resulting from the use of BIA).

Measurements

Mortality: the number of deaths that occurred during the follow-up period was recorded.

Phase angle: it was assessed using the BIA Quantum V device, by RJL Systems. The crude data were obtained for resistance (R), reactance (Xc), and PA at a frequency of 50 Hz. All the participants were evaluated within the first 24 h of admission, lying down, with the bed tilted at 45°, electrodes were placed on the both sides of the body on the dorsal surface of the metacarpophalangeal and metatarsophalangeal joints, medially between the distal prominences of the radius and ulna and between the medial and lateral malleoli at the ankle. The cut-off point for low PA ($\leq$ 3.66°), considering the fifth percentile (−SD 1.65) as the lower limit of normality based on previous studies and considering that this study included adults aged from 31 to 96 years, men and women hospitalized with pneumonia due to COVID-19 (9).

Muscle strength: it was evaluated by the Takei 5001 Hand Grip Analog Dynamometer, all participants were evaluated within the first 24 h of admission, lying down with your bed tilted at 90°; with the elbow flexed at 90°, the test was carried out three times from each arm and the highest score was considered for the analysis. The cut-off point for low grip strength $\leq$ 5.0 kg/force was determined by the 20th percentile of the total data of the sample included in this study and considering that this study included adults aged from 31 to 96 years, men and women hospitalized with pneumonia due to COVID-19 (13).

Body composition and anthropometric variables: fat mass index (FMI) and appendicular muscle mass index (AMMI) were assessed using the aforementioned BIA (Quantum V, RJL Systems, MI, USA), specific equations were used in the study population to assess FMI and AMMI (14). Body weight (kg), height (meters) and body mass index (BMI), i.e., weight/height^2, were also assessed.

Disease severity scales: CURB-65 (5) is a severity index of community-acquired pneumonias, and is composed of the following dimensions: confusion (defined by a mental test score $\leq$ 8, new disorientation in person, place or time); blood urea nitrogen (BUN) $>$ 20 mg/dL; respiratory rate $\geq$ 30 breaths/min, blood pressure (systolic $<$ 90 mm Hg or diastolic $\leq$ 60 mm Hg), and age $\geq$ 65 years. Classification is as follows: 0–1: probably suitable for home treatment, low risk of death; 2: consider hospital-supervised treatment, and $\geq$ 3: manage at the hospital as severe pneumonia; high risk of death.

Sepsis-related organ failure assessment (4) is a system for assessing the onset and progression of multiorgan failure in intensive care unit (ICU) patients. It uses constants for six organs systems and for some treatment regimens (vasoactive agents): breathing (PaO_2/FiO_2), coagulation (platelets $\times$ $10^3/mm^3$), liver (bilirubin), cardiovascular (hypotension), nervous system (Glasgow Coma Scale), renal (creatinine mg/dl). Each of the organs is assigned a score from 0 to 4. The score is the sum of all the individual organ assessments. A score different from 0 to $<$ 3 is evaluated as organ dysfunction, while higher scores indicate organ failure. The total score was considered for the purposes of this study.

The acute physiology and chronic health evaluation II (4) is a prognostic classification system that stratifies patients using a score based on the baseline values of 12 physiological measurements [heart rate (HR), rectal temperature, arterial pH, Glasgow Coma Scale, oxygenation (FiO_2), bicarbonate (HCO_3), creatinine, leukocytes/mm^3, serum Na, serum K, age, and previous health status] to provide an overall measure of disease severity. The higher the score (range 0–71) the greater the severity. For the purposes of this study the total score was considered.

CO-RADS scale: a categorical CT assessment scheme for patients with suspected COVID-19, this scale should be used in patients with moderate to severe symptoms. Set seven categories: (1) CO-RADS 0 (not interpretable, the technique was insufficient to assigning a score), (2) CO-RADS 1 (very low, normal, or non-infectious), CO-RADS 2 (low, typical findings for another infection, but not COVID-19), (3) CO-RADS 3 (equivocal/unsure, characteristics compatible with COVID-19 but also with other diseases), (4) CO-RADS 4 (high suspicion of COVID-19), (5) CO-RADS 5 (very high, typical for COVID-19), and (6) CO-RADS 6 [proven, real time polymerase chain reaction (RT-PCR) for SARS-CoV-2] (15).

Other health conditions: comorbidity was determined using the Charlson comorbidity index and the total score was divided in to groups: high comorbidity $\geq$ 3 and low comorbidity $\leq$ 2 points (16, 17). Sociodemographic variables included sex, age in years, years of education, employment status, and occupation.

Statistical analysis

In the descriptive analysis, means $\pm$ SD were used for continuous variables, as well as frequencies and percentages for categorical variables. For the comparison of variables between groups (those who died and those who did not), *t*-tests were used for continuous variables and Chi^2 for categorical variables. A multivariate analysis was performed including raw values adjusted with Cox regression to see the association of PA and MS with mortality adjusting for other variables. The graphic representation of survival was performed using Kaplan–Meier curves. These analyses were carried out using the STATA software, version 16. Sample size was calculated considering our hypothesis that PA will be associated with mortality. We use the findings of Cornejo-Pareja et al. (7) they reported an OR of 2.48 between PA and mortality, with a mortality rate of 32.4% in the low PA group versus the normal PA group (6.5%). Considering an alpha error of 0.05, a power of 80% and a loss rate of 10%, requiring a minimum of 78 patients, we recruited n = 104 patient.

Ethics statements

This study was reviewed and approved by the Bioethics Committee of General Hospital Penjamo, Guanajuato, Mexico. The patients/participants provided their written informed consent to participate in this study.

Results

The mean age of the patients was 62.7 ± 15.0 (31–96), 48.1% were females (n = 51). A total of 59.6% had less than 10 years of education and 36.5% did not have a job. The most common pre-existing diseases were diabetes without complications (32.08%), chronic obstructive pulmonary disease (COPD) (10.3%), diabetes with complications (6.6%), and kidney failure (2.8%). As regards the baseline body composition and anthropometric data, the following averages were obtained: FMI was 12.71 ± 5.5 kg/m^2, AMMI was 7.4 ± 1.5 kg/m^2, PA was 5.1° ± 1.6°, weight was 81.3 ± 18.4 kg, and BMI was 30.2 ± 6.7 kg/m^2. The mean of grip strength was 14.1 ± 10.7 kg. At the time of admission, the scores in the prognostic scales used-SOFA, APACHE II, and CURB-65-were, respectively, as follows: 4 ± 1.6, 8.9 ± 4.7, and 2.3 ± 1.03 (Table 1).

In the comparison between the group of patients who died and those who did not, the following variables were significant: age was higher in those who died, 66.8 ± 14.7, vs. those who survived, 59.9 ± 14.3, p = 0.0216. The group that died also had a higher comorbidity index (Charlson index ≥ 3 in the total score) of 59.6% vs. the group that survived, whose index was 37.5%, p = 0.030. The significant body composition variables were: AMMI, which showed that the group that died had lower values, 6.03 ± 1.2, vs. 7.2 ± 0.9 in the group that survived, p = 0.0148. PA values were also lower in the group that died, 4.8 ± 1.7, vs. 5.43 ± 1.5 in the group that survived, p = 0.0309. MS was also lower in the group that died vs. the group that survived (9.3 ± 9.8 vs. 16.6 ± 10.3, p = 0.0010). In the prognostic scales, the scores were higher in the group that died: SOFA (4.6 ± 2.1 vs. 3.56 ± 1.06, p = 0.0008); APACHE II (11.6 ± 5.1 vs. 7.1 ± 3.4, p = 0.0000) and CURB-65 (2.7 ± 1.09 vs. 2.1 ± 0.94, p = 0.0009) (Table 1). CO-RADS scale (4.8 ± 0.6 vs. 4.4 ± 0.09, p = 0.009).

Table 2 shows the results of the Cox regression model, which indicate that the variables that were significantly associated with mortality were: a low PA (HR = 2.2, 95% CI = 1.2–5.1), a low MS (HR = 3.6, 95% CI = 1.6–8.0), and the APACHE II score (HR = 1.1, 95% CI = 1.0–1.2). All of them remained associated with mortality, regardless of sex, age, comorbidity, other prognostic scales (CURB-65 and SOFA) and AMMI (Table 2).

Figures 1, 2 show the Kaplan–Meier curves that depict a positive relationship of PA and MS with survival.

Discussion

The main results of this study demonstrate that a low PA (≤ 3.66°), HR = 2.5, (95% CI: 1.2–5.4), and that a low MS (≤ 5.0 kg/force), HR = 4.5, (95% CI: 1.9–10.2) represents a higher risk of mortality in hospitalized SARS-CoV-2 patients than the prognostic and severity scales prognostics; APACHE, HR = 1.1 (95% CI: 1.0–1.2), CURB-65 and SOFA were not significant. To our knowledge, no study has compared the three main predictive scales for mortality in critically ill patients (APACHE; CURB-65 and SOFA) against low MS, low PA, and other body composition assessments (FMI, AMMI, and BMI). Several reasons could be explain the lower risk shown by the prognostic scales in this study; all the evaluations were made at the admission of the patients, scales such as APACHE, SOFA, and CURB-65 include physical and biochemical parameters that can change constantly. As an example, SOFA which was designed and includes parameters of organ failure (liver, kidney, central nervous system, lung), which could occur in a severe phase of the COVID-19 disease (few days before death) (18).

The acute physiology and chronic health evaluation is a very complete scale that includes different parameters, physical, vital signs, biochemical, and complete blood count; however, hematocrit or a blood low pH are not good predictors of mortality in COVID-19 early stage or at admission. Moreover, leukocytosis is related to bacterial pneumonia (6). About the age, it is included into CURB-65 and APACHE, in our sample we included people aged 40 years and older, which might affect the risk predictive to mortality. Further studies including trajectories analysis are needed to confirm the mechanisms underlying these findings (18).

About the association between a low PA and mortality are consistent with previous studies (8, 9). Our results agree with previous studies that low MS is a good predictor of mortality (13, 18). Therefore, low MS plays a key role in recovery from critical illness, especially from SARS-CoV-2 infection, as strength, which is an indicator of muscle function, is key during the disease process and recovery (19). In case of pre-existing or early MS impairment prior to the onset of acute illness, hospitalization may make it worse and lead to the patient not recovering normal muscle function and being at increased the risk of developing cachexia during the inflammatory process and sarcopenia at a later stage (once the acute inflammation subsides) (18, 19). Our study not found association with low muscle mass measured by AMMI, similar to the findings of Osuna-Padilla et al. (9) who did not find an association with mortality. The difference between muscle quantity and quality has been attributed to the fact that the low MS is a combination of neural and muscular factors, such as deficiencies in neural activation, the need for voluntary capability to activate the required muscular system, and the fact that low MS may occur earlier than of mass muscle loss, which makes it more sensitive

TABLE 1 Baseline characteristics: sociodemographic, clinical, anthropometry, and body composition and disease severity scales.

Baseline characteristics	Total $n = 104$ Mean ± SD or n, %	Participants who died $n = 42$ (40.4%) Mean ± SD or n, %	Participants who survived $n = 62$ (59.6%) Mean ± SD or n, %	p-value
Age (years)	62.79 ± 15.02	66.81 ± 14.78	59.9 ± 14.83	0.0216
Gender				
Females	51 (48.11%)	16 (38.10)	34 (54, 84)	0.094
Education				
1–10 years	62 (59.62%)	24 (57.14)	38 (61, 29)	
> 10 years	9 (8.65%)	3 (7.14)	6 (9.68)	0.737
Occupation				
Not employed	38 (36.54%)	19 (45.24)	19 (30.65)	0.129
Charlson index ≥ 3	8 (7.55)	5 (59.62)	3 (37.50)	0.030
Anthropometry and body composition				
BMI, kg/m^2	30.23 ± 6.73	30.60 ± 6.35	29.98 ± 7.02	0.6513
Fat mass index kg/m^2	12.71 ± 5.59	11.80 ± 6.32	13.34 ± 5.02	0.2829
Appendicular muscle mass index kg/m^2	7.44 ± 1.51	6.03 ± 1.29	7.25 ± 0.92	0.0148
Phase angle°	5.10 ± 1.60	4.81 ± 1.72	5.43 ± 1.53	0.0309
Phase angle ≤ 3.66°	27 (25.96)	17 (40.48)	10 (16.13)	0.0055
Grip strength, kg/force	14.18 ± 10.72	9.33 ± 9.82	16.61 ± 10.39	0.0000
Grip strength, ≤ 5.0 kg/force	55 (56.12)	21 (51.22)	34 (59.65)	0.4068
Disease severity instruments				
CO-RADS (total score)	4.61 ± 0.71	4.83 ± 0.65	4.46 ± 0.09	0.0098
SOFA (total score)	4 ± 1.64	4.64 ± 2.10	3.56 ± 1.06	0.0008
APACHE II (total score)	8.96 ± 4.76	11.66 ± 5.18	7.10 ± 3.42	0.0000
CURB-65 (total score)	2.38 ± 1.03	2.78 ± 1.09	2.11 ± 0.94	0.0009

APACHE II, the acute physiology and chronic health evaluation II; SOFA, sepsis-related organ failure assessment; CURB-65, score for pneumonia severity; CO-RAD, a categorical CT assessment scheme for patients with suspected COVID-19; BMI, body mass index; AMMI, appendicular muscle mass index; PA, phase angle, MS, muscle strength.

TABLE 2 Association between low phase angle, low muscle strength, and severity scales with mortality.

Variables	Unadjusted HR	95% CI	p	Adjusted HR	95% CI	p
Sex (male)	1.504	0.799–2.833	0.206	1.458	0.6637–3.204	0.348
Age (years)	1.026	1.002–1.051	0.029	1.005	0.9722–1.039	0.761
APACHE II (total score)	1.113	1.054–1.174	0.000	1.162	1.063–1.270	0.001
CURB-65 (total score)	1.433	1.036–1.981	0.029	0.943	0.593–1.498	0.805
SOFA (total score)	1.125	0.982–1.287	0.087	0.876	0.6768–1.134	0.317
CO-RADS (total score)	1.705	1.004–2.896	0.048	1.969	1.095–3.541	0.024
Charlson index (score ≥ 3)	1.659	0.506–5.433	0.403	0.690	0.191–2.488	0.573
Low phase angle ≤ 3.66°	2.957	1.517–5.765	0.001	2.571	1.217–5.430	0.013
Appendicular muscular mass index (kg)	0.950	0.781–1.15	0.611	0.9292	0.728–1.1847	0.554
Muscle strength ≤ 5.0 kg/force	3.390	1.742–6.599	0.000	4.519	1.992–10.252	0.000

APACHE II, the acute physiology and chronic health evaluation II; SOFA, sepsis-related organ failure assessment; CURB-65, score for pneumonia severity; CO-RAD, a categorical CT assessment scheme for patients with suspected COVID-19; BMI, body mass index; AMMI, appendicular muscle mass index; PA, phase angle, MS, muscle strength.

to change and may explain its association with mortality in patients with COVID-19 pneumonia (20–22).

Regarding the low PA, it is a mixed indicator composed of resistance, reactance and capacitance, these parameters are directly related to the conduction of the electrical current through the intercellular, interstitial and intracellular spaces; the great inflammatory state that characterizes COVID-19 pneumonia promotes a greater resistance to the passage of the electrical current through different tissues, including muscle tissue in the early stages of the disease, this could explain why the PA is remained associated as a risk predictor for mortality in this study and similar studies (7, 8).

The association between the FMI and the BMI with mortality was not demonstrated. This lack of association

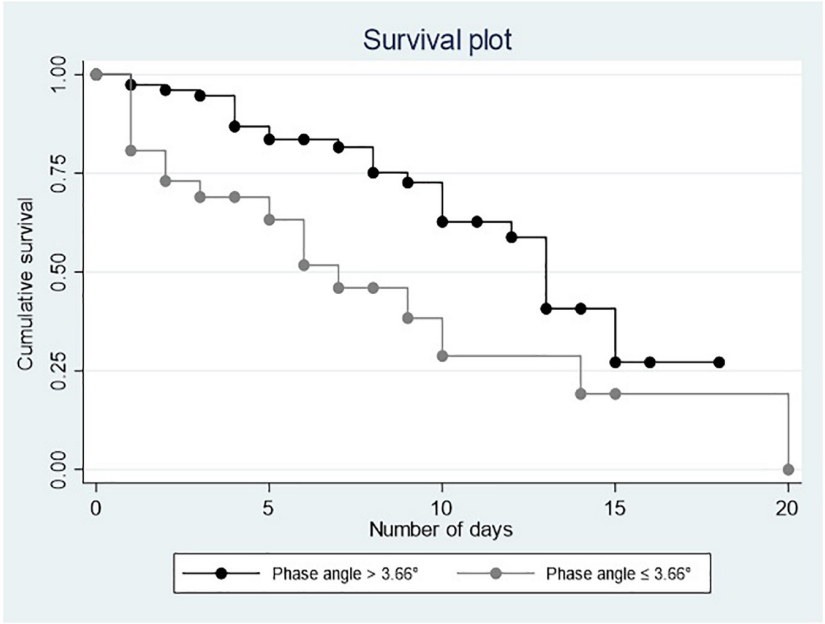

FIGURE 1
Survival plots for phase angle.

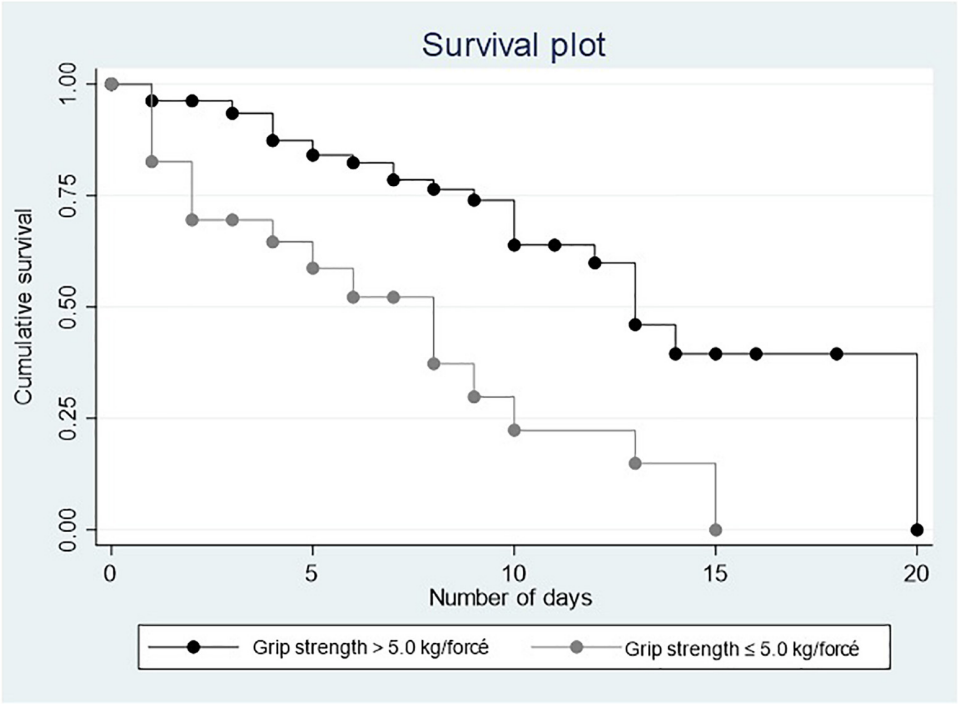

FIGURE 2
Survival plots for muscle strength.

is consistent with the results in several studies included in an interesting systematic review, (23) in which it is shown that there is an association between the high fat mass with hospital admission, severity of the disease, orotracheal intubation, among others, but with a contradictory association with mortality.

The limitations of this study should be borne in mind. The first one is that mortality was the only negative outcome studied; future studies derived from this cohort or other cohorts should consider whether a low PA and a low MS have a higher risk to predict a longer hospital stay and need for intubation versus APACHE, CURB-65, and SOFA. Another limitation is that the cut-off points for PA and low MS were similar to others studies above mentioned but are only representative of people with the following characteristics: Mexican adults hospitalized with the diagnosis of SARS-CoV-2 pneumonia, adults aged from 31 to 96 years, males and females. However, the main strength of this study is one of the first to demonstrate that a low PA and a low MS upon admission are higher risk predictors of mortality than prognostic scales such as SOFA, APACHE II, and CURB-65. Further studies with trajectories analysis for MS and PA, are needed to demonstrate whether changes in body composition remain as predictors beyond hospital admission.

Conclusion

Study results suggest that low MS and low PA are greater risk predictors for mortality than APACHE, SOFA, and CURB-65 indexes, at hospital admission. It is recommended to include them as part of the initial evaluation in all patients admitted with pneumonia due to COVID-19, it will help to implement interventions aimed at improving strength and PA to reduce the risk of mortality.

Data availability statement

The raw data supporting the conclusions of this article will be made available by the authors, without undue reservation.

Ethics statement

The studies involving human participants were reviewed and approved by the Bioethics Committee of General Hospital Penjamo, Guanajuato, Mexico. The patients/participants provided their written informed consent to participate in this study.

Author contributions

OR-C: conceptualization and supervision. OR-C and ML-T: methodology. ML-T and GN-F: formal analysis. PA-M, OR-C, JC-O, AN-C, and GD-M: investigation. ML-T, OR-C, GN-F, and PA-M: writing—original draft. All authors contributed to the writing, review, and editing.

Conflict of interest

The authors declare that the research was conducted in the absence of any commercial or financial relationships that could be construed as a potential conflict of interest.

Publisher's note

All claims expressed in this article are solely those of the authors and do not necessarily represent those of their affiliated organizations, or those of the publisher, the editors and the reviewers. Any product that may be evaluated in this article, or claim that may be made by its manufacturer, is not guaranteed or endorsed by the publisher.

References

1. Secretaria de Salud. *Información Internacional y Nacional Sobre Nuevo Coronavirus (COVID-2019)*. (2022). Available online at: https://www.gob.mx/salud/documentos/informe-tecnicodiario-covid19-2022 (accessed April 15, 2022).

2. Bello-Chavolla OY, Bahena-López JP, Antonio-Villa NE, Vargas-Vázquez A, González-Díaz A, Márquez-Salinas A, et al. Predicting mortality due to SARS-CoV-2: a mechanistic score relating obesity and diabetes to COVID-19 outcomes in Mexico. *J Clin Endocrinol Metab.* (2020) 105:dgaa346. doi: 10.1210/clinem/dgaa346

3. Morley JE, Kalantar-Zadeh K, Anker SD. COVID-19: a major cause of cachexia and sarcopenia? *J Cachexia Sarcopenia Muscle.* (2020) 11:863–5. doi: 10.1002/jcsm.12589

4. Beigmohammadi MT, Amoozadeh L, Rezaei Motlagh F, Rahimi M, Maghsoudloo M, Jafarnejad B, et al. Mortality predictive value of APACHE II and SOFA scores in COVID-19 patients in the intensive care unit. *Can Respir J.* (2022) 2022:5129314. doi: 10.1155/2022/5129314

5. Nguyen Y, Corre F, Honsel V, Curac S, Zarrouk V, Fantin B, et al. Applicability of the CURB-65 pneumonia severity score for outpatient treatment of COVID-19. *J Infect.* (2020) 81:e96–8. doi: 10.1016/j.jinf.2020.05.049

6. Chalmers JD, Singanayagam A, Akram AR, Mandal P, Short PM, Choudhury G, et al. Severity assessment tools for predicting mortality in hospitalised patients with community-acquired pneumonia. Systematic review and meta-analysis. *Thorax.* (2010) 65:878–83. doi: 10.1136/thx.2009.133280

7. Cornejo-Pareja I, Vegas-Aguilar IM, García-Almeida JM, Bellido-Guerrero D, Talluri A, Lukaski H, et al. Phase angle and standardized phase angle from bioelectrical impedance measurements as a prognostic factor for mortality at 90 days in patients with COVID-19: a longitudinal cohort study. *Clin Nutr.* (2021):S0261–5614(21)00091–1. [Epub ahead of print]. doi: 10.1016/j.clnu.2021.02.017

8. Moonen HP, Bos AE, Hermans AJ, Stikkelman E, van Zanten FJ, van Zanten AR. Bioelectric impedance body composition and phase angle in relation to 90-day adverse outcome in hospitalized COVID-19 ward and ICU patients: the prospective BIAC-19 study. *Clin Nutr ESPEN.* (2021) 46:185–92. doi: 10.1016/j.clnesp.2021.10.010

9. Osuna-Padilla IA, Rodríguez-Moguel NC, Rodríguez-Llamazares S, Aguilar-Vargas A, Casas-Aparicio GA, Ríos-Ayala MA, et al. Low phase angle is associated with 60-day mortality in critically ill patients with COVID-19. *J Parenter Enteral Nutr.* (2021) 46:828–35. doi: 10.1002/jpen.2236

10. Wilhelm-Leen ER, Hall YN, Horwitz RI, Chertow GM. Phase angle, frailty and mortality in older adults. *J Gen Intern Med.* (2014) 29:147–54. doi: 10.1007/s11606-013-2585-z

11. Gil S, Jacob Filho W, Shinjo SK, Ferriolli E, Busse AL, Avelino-Silva TJ, et al. Muscle strength and muscle mass as predictors of hospital length of stay in patients with moderate to severe COVID-19: a prospective observational study. *J Cachexia Sarcopenia Muscle.* (2021) 12:1871–8. doi: 10.1002/jcsm.12789

12. Cheval B, Sieber S, Maltagliati S, Millet GP, Formánek T, Chalabaev A, et al. Muscle strength is associated with COVID-19 hospitalization in adults 50 years of age or older. *J Cachexia Sarcopenia Muscle.* (2021) 12:1136–43. doi: 10.1002/jcsm.12738

13. Cruz-Jentoft AJ, Baeyens JP, Bauer JM, Boirie Y, Cederholm T, Landi F, et al. Sarcopenia: European consensus on definition and diagnosis: report of the European working group on sarcopenia in older people. *Age Ageing.* (2010) 39:412–23. doi: 10.1093/ageing/afq034

14. Rangel-Peniche DG, Raya-Giorguli G, Alemán-Mateo H. Accuracy of a predictive bioelectrical impedance analysis equation for estimating appendicular skeletal muscle mass in a non-Caucasian sample of older people. *Arch Gerontol Geriatr.* (2015) 61:39–43. doi: 10.1016/j.archger.2015.03.007

15. Prokop M, van Everdingen W, van Rees Vellinga T, Quarles van Ufford H, Stöger L, Beenen L, et al. CO-RADS: a categorical CT assessment scheme for patients suspected of having COVID-19-definition and evaluation. *Radiology.* (2020) 296:E97–104. doi: 10.1148/radiol.2020201473

16. Charlson ME, Pompei P, Ales KL, MacKenzie CR. A new method of classifying prognostic comorbidity in longitudinal studies: development and validation. *J Chron Dise.* (1987) 40:373–83. doi: 10.1016/0021-9681(87)90171-8

17. Rosas-Carrasco O, Gonzalez-Flores E, Brito-Carrera AM, Vazquez-Valdez OE, Peschard-Saenz E, Gutierrez-Robledo LM, et al. Assessment of comorbidity in elderly [Evaluación de la comorbilidad en el adulto mayor [Assessment of comorbidity in elderly]. *Rev Med Insti Mexic Seguro Soc.* (2011) 49:153–62.

18. Zou X, Li S, Fang M, Hu M, Bian Y, Ling J, et al. Acute physiology and chronic health evaluation II score as a predictor of hospital mortality in patients of coronavirus disease 2019. *Crit Care Med.* (2020) 48:e657–65. doi: 10.1097/CCM.0000000000004411

19. Scheerman K, Meskers CGM, Verlaan S, Maier AB. Sarcopenia, low handgrip strength, and low absolute muscle mass predict long-term mortality in older hospitalized patients: an observational inception cohort study. *J Am Med Dir Assoc.* (2021) 22:816–20.e2. doi: 10.1016/j.jamda.2020.12.016

20. Wolfe RR. The underappreciated role of muscle in health and disease. *Am J Clin Nutr.* (2006) 84:475–82.

21. Neves T, Ferriolli E, Lopes MBM, Souza MGC, Fett CA, Fett WCR. Prevalence and factors associated with sarcopenia and dynapenia in elderly people. *J Frailty Sarcopenia Falls.* (2018) 3:194–202. doi: 10.22540/JFSF-03-194

22. Clark BC, Manini TM. What is dynapenia? *Nutrition.* (2012) 28:495–503. doi: 10.1016/j.nut.2011.12.002

23. Vulturar DM, Crivii CB, Orăsan OH, Palade E, Buzoianu AD, Zehan IG, et al. Obesity impact on SARS-CoV-2 infection: pros and cons "Obesity Paradox"-a systematic review. *J Clin Med.* (2022) 11:3844. doi: 10.3390/jcm11133844

frontiers | Frontiers in Nutrition

TYPE Brief Research Report
PUBLISHED 06 January 2023
DOI 10.3389/fnut.2022.964797

OPEN ACCESS

EDITED BY
Filippo Giorgio Di Girolamo,
University of Trieste, Italy

REVIEWED BY
Ajibola Abioye,
Avicenna Research and Insights Center, Nigeria
Meghit Boumediene Khaled,
University of Sidi-Bel-Abbès, Algeria

*CORRESPONDENCE
Alvina Widhani
✉ alvina.widhani@gmail.com

SPECIALTY SECTION
This article was submitted to Clinical Nutrition, a section of the journal Frontiers in Nutrition

RECEIVED 09 June 2022
ACCEPTED 16 December 2022
PUBLISHED 06 January 2023

CITATION
Widhani A, Yunihastuti E, Setiati S, Witjaksono F and Karjadi TH (2023) Ramadan fasting reduces high-sensitivity C-reactive protein among HIV-infected patients receiving antiretroviral therapy. *Front. Nutr.* 9:964797. doi: 10.3389/fnut.2022.964797

Ramadan fasting reduces high-sensitivity C-reactive protein among HIV-infected patients receiving antiretroviral therapy

Alvina Widhani[1,2]*, Evy Yunihastuti[1,2], Siti Setiati[3,4], Fiastuti Witjaksono[5] and Teguh H. Karjadi[1,2]

[1]Allergy and Clinical Immunology Division, Department of Internal Medicine, Faculty of Medicine, Dr. Cipto Mangunkusumo General Hospital, Universitas Indonesia, Central Jakarta, Jakarta, Indonesia, [2]HIV Integrated Clinic, Dr. Cipto Mangunkusumo General Hospital, Central Jakarta, Jakarta, Indonesia, [3]Geriatric Division, Department of Internal Medicine, Faculty of Medicine, Dr. Cipto Mangunkusumo General Hospital, Universitas Indonesia, Central Jakarta, Jakarta, Indonesia, [4]Center for Clinical Epidemiology and Evidence Based Medicine, Faculty of Medicine, Dr. Cipto Mangunkusumo General Hospital, Universitas Indonesia, Central Jakarta, Jakarta, Indonesia, [5]Department of Clinical Nutrition, Faculty of Medicine, Dr. Cipto Mangunkusumo General Hospital, Universitas Indonesia, Central Jakarta, Jakarta, Indonesia

Background: Inflammatory conditions and oxidative stress increase in HIV infection, and inflammation increases the risk of cardiovascular disease. Ramadan fasting is known to reduce inflammation and oxidative stress in diabetic patients. This study examined the effects of Ramadan fasting on high-sensitivity C-reactive protein (hs-CRP) levels and total antioxidant status (TAOS) in HIV patients on antiretroviral therapy (ART).

Methods: This was a prospective cohort study comparing HIV-infected patients on stable ART who fasted throughout Ramadan to HIV-infected patients who did not fast during Ramadan. Inclusion criteria were men aged 20–40 years, taking first-line ART for at least 6 months, Muslims intent to fast for Ramadan, no current hospitalization because of acute conditions and not being treated for opportunistic infections.

Results: After 2 weeks, hs-CRP had decreased significantly in the fasting group (−0.41 mg/L [IQR = −1; 0.10]) compared to the non-fasting group (0.20 mg/L [IQR = −0.30; 1.50]) (p = 0.004). The linear regression analysis has shown that Ramadan fasting contributed to 10.10% of the variance in hs-CRP value (R^2 = 0.101) and decreased its value by 0.317 points (B = −0.317). Changes in TAOS did not significantly different (p = 0.405) between the fasting group (0.05 mmol/L [IQR = −0.03; 0.12]) and the non-fasting group (0.04 mmol/L [IQR = −0.13; 0.36]). In the fasting group, there were

significant changes in polyunsaturated fatty acid consumption (p = 0.029), body weight (p = 0.001), cigarette smoking (p = 0.001), and sleeping duration (p = 0.001).

Conclusion: Ramadan fasting reduces hs-CRP concentrations among HIV patients on ART.

KEYWORDS

Ramadan, fasting, C-reactive protein, inflammation, HIV

1. Introduction

Human immunodeficiency virus (HIV) infection causes chronic immune activation and increases inflammatory cytokine release. Antiretroviral therapy (ART) can limit but not completely normalize these inflammatory conditions. Inflammation increases the risk of cardiovascular disease, metabolic complications, and malignancies (1). ART and HIV infection alone can also increase oxidative stress (2). Total antioxidant status (TAOS) has been shown to decline in HIV patients receiving ART (3).

Ramadan fasting, a type of intermittent fasting in which Muslims abstain from food and drink from dawn until sunset during the holy month of Ramadan, may reduce inflammation. Ramadan fasting has been shown to reduce high-sensitivity C-reactive protein (hs-CRP) levels significantly in patients with metabolic syndrome (4) and to improve oxidative stress. After fasting, malondialdehyde levels significantly decrease and glutathione levels increase in both normal people and diabetic patients (5). During the second trimester in pregnant women, TAOS increases significantly after 10 days of Ramadan fasting (6).

We hypothesized that Ramadan fasting may limit inflammation and oxidative stress among HIV patients receiving ART. To our knowledge, no studies have explored this effect of fasting, so in this study, we investigated the effects of Ramadan fasting on hs-CRP concentration and TAOS in HIV patients on ART.

2. Materials and methods

2.1. Study design and population

A prospective cohort study design was used to examine the effects of Ramadan fasting on high-sensitivity C-reactive protein (hs-CRP) levels and total antioxidant status (TAOS) in HIV patients on antiretroviral therapy (ART). The data collected from HIV patients on ART who fasted during Ramadan for 14 consecutive days were compared with a group of non-fasting HIV patients also on ART. The participants were recruited at the HIV Integrated Clinic of Dr. Cipto Mangunkusumo Hospital, Jakarta, Indonesia, and were followed up for 14 days. The inclusion criteria for the fasting group were HIV patients receiving first-line ART for at least 6 months, men aged 20–40 years, Muslims intent to fast for Ramadan, no current hospitalization because of acute conditions, and not being in the initial phase of treatment for an opportunistic infection (e.g., tuberculosis, cytomegalovirus, toxoplasmosis, or *Pneumocystis carinii* pneumonia). Patients who consumed steroids or other immunosuppressants and those with poor ART adherence (less than 95%) were excluded from the study. Those who fasted for less than the two consecutive weeks were classified as drop-outs from the study. HIV patients who were not planning to do Ramadan fasting and did not fulfill any of the exclusion criteria were recruited as participants in the non-fasting group. Participants in fasting and non-fasting groups were matched by age, ART regimen, and duration of ART treatment.

2.2. Study procedures

Participants were selected by consecutive sampling. Demographic data and other information (e.g., route of HIV transmission, history of cigarette smoking, hepatitis B or hepatitis C coinfection, ART combination, duration of ART treatment, antioxidant supplement intake, CD4 cell counts, and HIV RNA level) were collected at the start of the study.

Some data were collected both before and after the 2 weeks of follow-up. These data included ART adherence, food intake, physical activity, body weight, waist circumference, anxiety and depression assessment, and sleep quality assessment. Dietary assessment was performed at enrollment and after 2 weeks of follow up using a 3-day food record, 24-h food recall, and semi-quantitative food frequency questionnaire to record food intake. The dietary data were analyzed by the Indonesian food composition database and the nutrisurvey software. Anxiety and depression were evaluated using the Hospital Anxiety and Depression Scale (HADS) questionnaire. The HADS questionnaire comprises 7 items related to anxiety and 7 items related to depression, which are scored 0–3 for each item. The score range for either anxiety or depression was,

therefore, 0–21. Sleep quality was assessed using the Pittsburgh Sleep Quality Index (PSQI), which is a self-report questionnaire of sleep quality within 1 month. The PSQI measures several aspects of sleep, including subjective sleep quality, sleep latency, sleep duration, habitual sleep efficiency, sleep disturbances, use of sleep medication, and daytime dysfunction. Each item has a 0–3 interval scale. The global PSQI score is calculated by the summation of 7 component scores, resulting in an overall score in the ranged of 0–21 where a higher score reflects poorer sleep quality.

High-sensitivity C-reactive protein concentration and TAOS were assessed before and after the 2-week follow-up. Blood was collected at 9.00–11.00 a.m. local time. Serum hs-CRP concentration was measured using CRP (latex) high-sensitivity immunoturbidimetric assay on a Cobas Integra instrument (Roche diagnostics, Indianapolis, IN, US). The normal range for hs-CRP is ≤10 mg/L. TAOS was measured using a colorimetric assay on an ADVIA 1800 instrument (Siemens Healthcare GmbH, Erlangen, Germany). The normal range for TAOS is 1.30–1.77 mmol/L.

2.3. Statistical analysis

Statistical analyses were performed using IBM SPSS statistics (version 20.0.0; IBM Corp., Armonk, NY, USA). Data were expressed as mean and standard deviation (for normally distributed data) and median (interquartile range for data with skewed distributions). If the data were distributed normally, comparisons of the results before and after fasting in each group and between the two groups were analyzed using paired or independent *t*-tests. Otherwise, the comparisons were analyzed using the non-parametric Wilcoxon rank-sum test and the Mann–Whitney *U* test, *p*-values < 0.05 were considered statistically significant. Linear regression analysis was used to determine the percentage of change of the main outcome variables (hs-CRP and TAOS).

2.4. Ethics statement

All participants gave written informed consent before study enrollment. Ethical approval was granted by the Research Ethics Board of the Faculty of Medicine, University of Indonesia (487/UN2.F1/ETIK/2015) and the Research Ethics Board of Dr. Cipto Mangunkusumo Hospital, Jakarta, Indonesia.

3. Results

3.1. Baseline characteristics

At the beginning of the study, the fasting group included 30 HIV patients, all were Muslims. On the other hand, the control group consisted of Muslims not willing to do Ramadan fasting and non-Muslims. After 2 weeks of follow-up, 1 patient in the fasting group was dropped out from the study because he had fasted for less than 14 days. Data were analyzed for 29 participants in the fasting group and 29 in the control group. The median age was 35 years old (IQR = 33; 37.25), and the median CD4 cell count was 398 cells/mm^3 (IQR = 307; 512.50).

At the baseline, age, route of HIV transmission, ART combination, duration of ART, hepatitis B or hepatitis C status, HADS score, antioxidant supplement consumption, CD4 cell count, HIV-RNA, and hs-CRP concentration did not differ significantly between the fasting and control groups (Table 1). At the baseline, the fasting group smoked more cigarettes per day. Body mass index, waist circumference, and baseline TAOS were lower in the fasting group. No participant was receiving treatment for an opportunistic infection.

3.2. Changes during the follow up period

During the 2-week follow-up, ART adherence did not change in either group. Caloric intake decreased in the fasting group during the 2 weeks of fasting, but this decrease was not significantly different from the non-fasting group (Table 2). Changes in the intake of carbohydrate, protein, lipid, cholesterol, vitamin A, vitamin E, vitamin C, and carotene also did not differ significantly between the fasting and control group after the 2 weeks. Intake of polyunsaturated fatty acid (PUFA) decreased significantly in the fasting group compared to the control group ($p = 0.012$).

Changes in physical activity, Anxiety-HADS score, and Depression-HADS score did not differ between groups after 2 weeks (Table 3). The number of cigarettes smoked per day and body weight did decrease significantly in the fasting group after 2 weeks of fasting compared to the control group ($p < 0.001$). The total sleep hours per day decreased significantly in the fasting group compared to the control group ($p = 0.024$).

3.3. Serum hs-CRP concentration and TAOS after the 2-week follow-up

The participants were followed for at least 2 weeks. Final assessment was done in the third or fourth week of Ramadan. Because hs-CRP and TAOS data were not normally distributed, analysis was done using non-parametric test. After the 2-week follow-up (Table 4), hs-CRP concentration decreased significantly ($p = 0.011$) in the fasting group (–0.41 mg/L [IQR = –1 to 0.10]) compared to the control group (0.20 mg/L [IQR = –0.30; 1.50]).

TABLE 1 Baseline characteristics of the fasting and control groups.

Characteristics	Fasting (n = 29)	Control (n = 29)	P-value
Age, years (IQR)	35 (33.5; 38)	35 (32; 37)	0.702
Route of HIV transmission, n (%)			
History of IDU (+)	5 (1.20)	11 (37.90)	0.080
History of IDU (−)	24 (82.80)	18 (62.10)	
ART combination, n (%)			
AZT + 3TC + NVP	12 (41.40)	12 (41.40)	1.000
AZT + 3TC + EFV	9 (31)	9 (31)	
TDF + 3TC + NVP	4 (13.80)	4 (13.80)	
TDF + 3TC/FTC + EFV	4 (13.80)	4 (13.80)	
Duration of ART, n (%)			
<2 years	8 (27.60)	8 (27.60)	1.000
≥2 years	21 (72.40)	21 (72.40)	
Hepatitis B, n (%)	2 (6.90)	4 (13.80)	0.670
Hepatitis C, n (%)	16 (55.20)	17 (58.60)	0.790
Antioxidant supplement consumption, n (%)	7 (24.10)	12 (41.40)	0.160
Number of cigarettes smoked per day	6 (1; 12)	1 (0; 6)	0.041
Body mass index, kg/m^2 (SD)	21.3 (2.48)	23.43 (3.80)	0.014
Waist circumference, cm (SD)	79.64 (8.39)	85.55 (9.21)	0.013
A-HADS (IQR)	2 (2; 4)	3 (2; 5)	0.135
D-HADS (IQR)	1 (1; 3)	2 (1; 2.50)	0.726
CD4 cell count, cells/μL (IQR)	379 (280.50; 481)	423 (321.5; 519)	0.370
HIV-RNA ≤ 400 copies/ml, n (%)	28 (96.55)	28 (96.55)	1.000
Baseline hs-CRP, mg/L (SD)	0.15 (0.52)	0.12 (0.46)	0.800
Baseline total antioxidant status, mmol/L (IQR)	1.47 (1.34; 1.58)	1.63 (1.48; 1.83)	0.005

Data are given as median [interquartile range (IQR)] or mean [standard deviation (SD)] values. IDU, injecting drug user; ART, antiretroviral therapy; AZT, zidovudine; 3TC, lamivudine; NVP, nevirapine; EFV, efavirenz; TDF, tenofovir; A-HADS, anxiety-hospital anxiety and depression scale; D-HADS, depression-hospital anxiety and depression scale; CD, cluster of differentiation; HIV-RNA, human immunodeficiency virus-ribonucleic acid; hs-CRP, high sensitivity-C reactive protein.

TAOS increased in both groups even though the changes were not significant (0.05 mmol/L [IQR = –0.03; 0.12] vs. 0.04 mmol/L [IQR = –0.13; 0.36], fasting vs. non-fasting, p = 0.408). The post-Ramadan fasting hs-CRP variable was then log-transformed to be entered in a linear regression model predicting the change of hs-CRP after Ramadan fasting. Ramadan fasting did explain a significant amount of the variance in hs-CRP [$F_{(1,56)}$ = 6.26, p = 0.015, R^2 = 0.101]. The regression coefficient (B = −0.317, 95% CI −0.636; −0.07) indicated that Ramadan fasting decrease hs-CRP value by 0.317 points.

4. Discussion

To our knowledge, this is the first study on the effects of Ramadan fasting on hs-CRP levels and TAOS in HIV patients on ART. In our study, Ramadan fasting reduced some indicators of inflammation in HIV patients on ART. At the baseline, hs-CRP concentration did not differ between the fasting and control groups, but it did decrease significantly in the fasting group after the 2 weeks of Ramadan fasting.

Our data are consistent with the results of other studies on hs-CRP levels and fasting, such as those by Shariatpanahi et al. (4) on patients with metabolic syndrome and by Askari et al. (7) on asthmatic patients. By contrast, our results differ from those of Fawzi et al. (8), who reported increased hs-CRP levels during Ramadan fasting in schizophrenic patients. This difference may be explained by the increases in caloric intake and body weight observed during Ramadan fasting in their study. Their study was also limited by the absence of a control group and physical activity record.

HIV infection is associated with chronic immune activation and pro-inflammatory conditions (9). Studies have shown that

TABLE 2 Changes in calorie, macronutrient, and antioxidant intake after 2 weeks.

	Fasting (n = 29)					Non-fasting (n = 29)					P	95% CI
	Pre	Post	P	95% CI	Change post-pre	Pre	Post	P	95% CI	Change post-pre		
Energy (kcal/day)	1357.28 ± 279.93	1248.97 ± 335.76	0.112	−26.70; 243.31	−108.31 ± 354.94	1220.43 ± 241.88	1249.39 ± 282.44	0.603	−141.55; 83.65	28.95 ± 296.03	0.115	−309.18; 34.67
Carbohydrate (%)	59.50 ± 5.42	62 ± 6.05	0.111	−5.80; 0.62	2.59 ± 8.45	58.13 ± 8.16	59.14 ± 5.66	0.601	−4.93; 2.91	1.01 ± 10.31	0.527	−3.38; 6.53
Protein (%)	14 ± 2.10	13.13 ± 1.96	0.051	−0.006; 1.86	−0.93 ± 2.46	14.79 ± 3.61	15 ± 2.67	0.714	−1.39; 0.96	0.21 ± 3.10	0.125	−2.61; 0.32
Lipid (%)	26.43 ± 5.31	24.06 ± 4.86	0.11	−0.57; 5.30	−2.37 ± 7.73	26.45 ± 7.04	25.75 ± 5.19	0.675	−2.70; 4.10	−0.71 ± 8.98	0.453	−6.06; 2.74
Cholesterol (mg)	262.92 ± 138.86	174.49 ± 102.91	0.001	37.88; 138.98	−88.44 ± 132.89	247.60 ± 149.49	207.72 ± 141.02	0.183	−20.01; 99.78	−39.88 ± 157.46	0.21	−125.19; 28.09
PUFA (g)	11.23 ± 5.52	7.83 ± 3.64	0.012	0.79; 6	−3.40 ± 6.85	9.10 ± 4.15	9.46 ± 4.95	0.743	−2.60; 1.87	0.36 ± 5.89	0.029	−7.12; −0.40
Vitamin A (μg)	483.50 (269; 986.51)	601.90 (262.83; 1180.93)	0.954	0.948; 0.959	−49.63 (−305.37; 377.05)	530.60 (245.65; 667)	461.83 (295.21; 805.68)	0.918	0.911; 0.925	84.84 (−374.71; −332.06)	0.913	0.906; 0.92
Carotene (mg)	0.001 (0.001; 0.40)	0.13 (0.001; 0.53)	0.487	0.474; 0.50	0 (−0.20; 0.40)	0.001 (0.001; 0.166)	0.001 (0.001; 0.166)	0.644	0.631; 0.656	0 (−0.08; 0.17)	0.595	0.582; 0.607
Vitamin E (mg)	4.10 (2.63; 5.15)	2.96 (2.43; 4.08)	0.067	0.06; 0.073	−0.77 (−2.05; 0.57)	3.56 (2.40; 4.43)	3.36 (1.96; 4.61)	0.848	0.839; 0.857	−0.10 (−0.63; 1.42)	0.172	0.162; 0.181
Vitamin C (mg)	29.80 (14.20; 87.23)	40.06 (23.23; 95.70)	0.019	0.016; 0.023	11.83 (−6.95; 32.95)	49.60 (26.98; 153.45)	60.83 (19.51; 204.45)	0.869	0.86; 0.877	8.47 (−30.29; 31.55)	0.222	0.211; 0.233

Data are presented as the mean ± standard deviation or median (interquartile range). PUFA, polyunsaturated fatty acid.

10.3389/fnut.2022.964797

10.3389/fnut.2022.964797

TABLE 3 Changes in physical activity, smoking habits, anxiety, depression, and sleep quality after 2 weeks.

	Fasting (n = 29)					Non-fasting (n = 29)					P	95% CI
	Pre	Post	P	95% CI	Change post-pre	Pre	Post	P	95% CI	Change post-pre		
Physical activity, METS/day	1.46 (1.40; 1.65)	1.48 (1.36; 1.56)	0.171	0.168; 0.187	0 (−0.12; 0.01)	1.47 (1.38; 1.58)	1.45(1.38; 1.55)	0.271	0.260; 0.283	0 (0; 0.005)	0.093	0.086; 0.101
Number of cigarettes smoked per day	6 (1–12)	3 (0–4)	<0.001	0; 0	−1 (−6; 0)	1 (0; 6)	1 (0; 6)	1	1; 1	0 (0; 0)	<0.001	0; 0
A-HADS	2 (2; 4)	3 (2; 4)	0.383	0.370; 0.395	0 (−1; 1)	3 (2; 5)	3 (2; 4)	0.386	0.374; 0.399	0 (−1; 1)	0.294	0.282; 0.306
D-HADS	1 (1; 3)	1 (1; 3)	0.751	0.739; 0.762	0 (−1; 1)	2 (1; 2.5)	2 (1; 3)	0.884	0.876; 0.892	0 (−1; 0.5)	0.622	0.610; 0.635
PSQI score	3 (2; 5)	4 (3; 6)	0.103	0.950; 0.111	1 (−0.5; 2)	5 (4; 7)	5 (3; 7)	0.661	0.648; 0.673	0 (−1; 0)	0.025	0.021; 0.029
Sleep hours per day	7 (6; 8)	5 (4; 6)	<0.001	0; 0	−2 (−3; −0.5)	6 (5–8)	6 (5–8)	0.491	0.478; 0.504	0 (0; 0)	<0.001	0; 0
Body weight (kg)	61.62 ± 8.19	59.64 ± 8.28	<0.001	1.44; 2.52	−2 (−2.75; −1)	68.42 ± 9.57	68.27 ± 9.96	0.745	−0.77; 1.07	0 (−1.25; 0.65)	0.001	−2.88; −0.78

Data are presented as the mean ± standard deviation or median (interquartile range). METS, metabolic equivalents; A-HADS, anxiety-hospital anxiety and depression scale; D-HADS, depression-hospital anxiety and depression scale; PSQI, Pittsburgh sleep quality index.

inflammatory parameters in HIV patients are higher than in the general population. Antiretroviral therapy does not entirely improve this pro-inflammatory condition (1, 10). Inflammation is associated with endothelial dysfunction in HIV patients who received ART and patients who have not (11).

People living with HIV also have higher levels of monocyte activation and altered coagulation than people who do not have HIV. Many of these biomarkers are linked to atherogenesis, an inflammatory process that leads to atherosclerotic cardiovascular disease (12, 13).

Studies have found that people living with HIV have a higher risk of cardiovascular disease than people who do not have HIV. HIV-specific risk factors and classic and non-traditional cardiovascular disease risk factors are among the mechanisms driving this risk (13). Among the established risks are elevated hs-CRP values. Elevated hs-CRP in HIV patients is associated with non-AIDS events [cardiovascular disease, non-AIDS-related malignancies, diabetes, and lung disease (11, 14)]. The significant correlation between hsCRP and cardiovascular disease is likely due to its strong correlation with other established risk factors such as smoking, diabetes, visceral obesity, and inflammation markers (15). Moreover, high hs-CRP is independently associated with atherosclerotic cardiovascular disease including in patients with good atherogenic lipid level (16). Therefore, high inflammation markers should be one of the concerns in the HIV care continuum. The decrease in hs-CRP levels due to the influence of Ramadan fasting is expected to reduce the risk of non-AIDS events, especially cardiovascular disease in HIV patients.

The significant reduction of hs-CRP concentration in the fasting group observed in our study was not related to total caloric intake, macronutrient intake, micronutrient intake (i.e., vitamin A, vitamin E, vitamin C, and carotene intake), physical activity, or anxiety or depression level during Ramadan fasting because no significant changes in these parameters were observed during fasting. Although caloric intake and physical activity did not change in the fasting group, body weight decreased after the 2 weeks of Ramadan fasting.

Ramadan fasting is a unique intermittent fast. During Ramadan fasting, people are prohibited from eating, drinking, and smoking from dawn until sunset. Although the total caloric intake per day may not change, the frequency of large meal portions decreases from 3 times to twice daily and the timing of meals also changes. These changes can affect metabolism and the circadian system and can attenuate inflammation, as shown by previous studies (17, 18). A study by Kahleova et al. (17) of people with type 2 diabetes mellitus showed that a diet of 2 large-portion meals resulted in greater reduction in body weight and improvement in insulin sensitivity than 6 small-portion meals did. Intermittent fasting can modify brain neurochemistry and neural activity to optimize brain function and peripheral energy metabolism.

10.3389/fnut.2022.964797

TABLE 4 Changes in main outcomes (hs-CRP and total antioxidant status) after 2 weeks.

	Fasting (n = 29)					Non-fasting (n = 29)					P	95% CI	R^2	B (95% CI)
	Pre	Post	P	95% CI	Change post-pre	Pre	Post	P	95% CI	Change post-pre				
hs-CRP (mg/L)	1.30 (0.60; 2.65)	0.80 (0.30; 1.60)	0.011*	0.008; 0.014	−0.41 (−1; 0.10)	1.20 (0.6; 3.5)	1.90 (0.6; 4.8)	0.097	0.910; 0.106	0.20 (−0.30; 1.50)	0.004*	0.002; 0.006	0.101	−0.317 (−0.636; −0.070)*
Total antioxidant status (mmol/L)	1.47 (1.34; 1.58)	1.50 (1.40; 1.59)	0.089	0.081; 0.096	0.05 (−0.03; 0.12)	1.63 (1.47; 1.83)	1.80 (1.62; 1.89)	0.21	0.209; 0.23	0.04 (−0.13; 0.36)	0.408	0.396; 0.421	–	–

*$p < 0.05$. Data are presented as the mean ± standard deviation or median (interquartile range). hs-CRP, high sensitivity-C reactive protein.

Another study showed that intermittent fasting increased leptin and insulin sensitivity, reduced leptin and insulin levels, reduced insulin-like growth factor 1, and increased adiponectin and ghrelin, which are factors that can attenuate inflammation (18).

In our study, PUFA intake decreased significantly during fasting. PUFA intake included omega-3 PUFA (α-linolenic acid) and omega-6 PUFA (linoleic acid). An increased ratio of omega-6 to omega-3 is related to increased cardiovascular risk (19). A previous study by Hanafiah et al. (20) showed that the ratio of omega-6 to omega-3 consumption is high in Indonesians: 46.1 ± 6.1 in coronary heart disease populations and 31.2 ± 2.1 in the healthy population. Decreased PUFA intake in the fasting group in our study may reflect a decrease in omega-6 intake. The lower intake of omega-6, which is proinflammatory, may have contributed to the observed decrease in hs-CRP concentration.

The significant decrease in the number of cigarettes smoked per day may also have contributed to the reduction in hs-CRP concentration in the fasting group. A study by Jamal et al. (21) showed that serum hs-CRP levels are higher in smokers than in non-smokers.

In our study, the number of total sleep hours per day decreased in the fasting group. A previous study by Meier-Ewert et al. (22) showed that shorter total sleep duration is related to higher hs-CRP levels. The contrasting finding in our study might reflect the influence of other factors on hs-CRP levels.

Although TAOS increased more in the fasting group than in the control group, the difference between groups was not significant. Future studies with longer observation periods and larger samples are needed to confirm the changes in TAOS.

Our study has several strengths, such as including a control group whose members did not fast and recording caloric intake, physical activity, and smoking habits. However, our study does have some limitations. The improvement in inflammatory markers in the fasting group may be attributed to changes in the frequency and timing of large-portion meals, PUFA intake, total cigarette smoking per day, or body weight. We could not determine which of the observed changes led to the decreased hs-CRP concentration because of the small sample size.

Additionally, blood sampling is only done before fasting and during Ramadan fasting. It is advisable to take a third sample after Ramadan fasting to see if the hs-CRP level increases or the TAOS level decreases again outside Ramadan. Another limitation of our study was that it did not exclude patients taking antioxidant supplements and still smoking. This is a factor that can affect the TAOS results obtained.

In conclusion, we found that hs-CRP concentration was lower after 2 weeks of Ramadan fasting in HIV patients on ART. This result suggests that Ramadan fasting may reduce inflammation caused by chronic immune response activation in HIV patients on ART.

Data availability statement

The raw data supporting the conclusions of this article will be made available by the authors, without undue reservation.

Ethics statement

The studies involving human participants were reviewed and approved by Research Ethics Board of the Faculty of Medicine, University of Indonesia and the Research Ethics Board of Dr. Cipto Mangunkusumo Hospital, Jakarta, Indonesia. The patients/participants provided their written informed consent to participate in this study.

Author contributions

AW, EY, SS, and FW: research design, manuscript drafting, data analysis, and interpretation. AW and TK: data collection. All authors manuscript revision, read, and approved the final version of the manuscript.

Acknowledgments

The authors thank Ghina Shabrina Awanis and Utami Susilowati for the statistical analysis and Ade Rosanti for dietary assessment.

Conflict of interest

The authors declare that the research was conducted in the absence of any commercial or financial relationships that could be construed as a potential conflict of interest.

Publisher's note

References

1. Nixon D, Landay A. Biomarkers of immune dysfunction in HIV. *Curr Opin HIV AIDS.* (2010) 5:498–503. doi: 10.1097/COH.0b013e32833ed6f4

2. Mandas A, Iorio E, Congiu M, Balestrieri C, Mereu A, Cau D, et al. Oxidative imbalance in HIV-1 infected patients treated with antiretroviral therapy. *J Biomed Biotechnol.* (2009) 2009:749575. doi: 10.1155/2009/749575

3. Suresh D, Annam V, Pratibha K, Prasad B. Total antioxidant capacity – a novel early bio-chemical marker of oxidative stress in HIV infected individuals. *J Biomed Sci.* (2009) 16:61. doi: 10.1186/1423-0127-16-61

4. Shariatpanahi M, Shariatpanahi Z, Shahbazi S, Moshtaqi M. Effect of fasting with two meals on BMI and inflammatory markers of metabolic syndrome. *Pak J Biol Sci.* (2012) 15:255–8. doi: 10.3923/pjbs.2012.255.258

5. Al-Shafei A. Ramadan fasting ameliorates oxidative stress and improves glycemic control and lipid profile in diabetic patients. *Eur J Nutr.* (2014) 53:1475–81. doi: 10.1007/s00394-014-0650-y

6. Ozturk E, Balat O, Ugur M, Yazıcıoglu C, Pence S, Erel Ö, et al. Effect of ramadan fasting on maternal oxidative stress during the second trimester: a preliminary study. *J Obstet Gynaecol Res.* (2011) 37:729–33. doi: 10.1111/j.1447-0756.2010.01419.x

7. Askari V, Alavinezhad A, Boskabady M. The impact of "ramadan fasting period" on total and differential white blood cells, haematological indices, inflammatory biomarker, respiratory symptoms and pulmonary function tests of healthy and asthmatic patients. *Allergol Immunopathol.* (2016) 44:359–67. doi: 10.1016/j.aller.2015.10.002

8. Fawzi M, Fawzi M, Said N, Fawzi M, Fouad A, Abdel-Moety H. Effect of ramadan fasting on anthropometric, metabolic, inflammatory and psychopathology status of egyptian male patients with schizophrenia. *Psychiatry Res.* (2015) 225:501–8. doi: 10.1016/j.psychres.2014.11.057

9. Guimarães M, Greco D, Figueiredo S, Fóscolo R, Oliveira A, Machado L. High-sensitivity C-reactive protein levels in HIV-infected patients treated or not with antiretroviral drugs and their correlation with factors related to cardiovascular risk and HIV infection. *Atherosclerosis.* (2008) 201:434–9. doi: 10.1016/j.atherosclerosis.2008.02.003

10. Lv T, Cao W, Li THIV-. Related immune activation and inflammation: current understanding and strategies. *J Immunol Res.* (2021) 2021:7316456.

11. Cerrato E, Calcagno A, D'Ascenzo F, Biondi-Zoccai G, Mancone M, Grosso Marra W, et al. Cardiovascular disease in HIV patients: from bench to bedside and backwards. *Open Heart.* (2015) 2:e000174. doi: 10.1136/openhrt-2014-000174

12. Abelman R, Mugo B, Zanni M. Conceptualizing the risks of coronary heart disease and heart failure among people aging with HIV: sex-specific considerations. *Curr Treat Options Cardiovasc Med.* (2019) 21:41. doi: 10.1007/s11936-019-0744-1

13. So-Armah K, Benjamin L, Bloomfield G, Feinstein M, Hsue P, Njuguna B, et al. HIV and cardiovascular disease. *Lancet HIV.* (2020) 7:e279–93. doi: 10.1016/S2352-3018(20)30036-9

14. McComsey G, Kitch D, Sax P, Tierney C, Jahed N, Melbourne K, et al. Associations of inflammatory markers with AIDS and non-AIDS clinical events after initiation of antiretroviral therapy: AIDS clinical trials group A5224s, a substudy of ACTG A5202. *J Acquir Immune Defic Syndr.* (2014) 65:167–74. doi: 10.1097/01.qai.0000437171.00504.41

15. Yousuf O, Mohanty B, Martin S, Joshi P, Blaha M, Nasir K, et al. High-sensitivity c-reactive protein and cardiovascular disease: a resolute belief or an elusive link? *J Am Coll Cardiol.* (2013) 62:397–408. doi: 10.1016/j.jacc.2013.05.016

16. Quispe R, Michos ED, Martin S, Puri R, Toth P, Al Suwaidi J, et al. High-sensitivity c-reactive protein discordance with atherogenic lipid measures and incidence of atherosclerotic cardiovascular disease in primary prevention: the ARIC study. *J Am Heart Assoc.* (2020) 9:e013600. doi: 10.1161/JAHA.119.013600

17. Kahleova H, Belinova L, Malinska H, Oliyarnyk O, Trnovska J, Skop V, et al. Eating two larger meals a day (breakfast and lunch) is more effective than six smaller meals in a reduced-energy regimen for patients with type 2 diabetes: a randomised crossover study. *Diabetologia.* (2014) 57:1552–60. doi: 10.1007/s00125-014-3253-5

18. Longo V, Mattson M. Fasting: molecular mechanisms and clinical applications. *Cell Metab.* (2014) 19:181–92. doi: 10.1016/j.cmet.2013.12.008

19. Simopoulos A. The importance of the omega-6/omega-3 fatty acid ratio in cardiovascular disease and other chronic diseases. *Exp Biol Med.* (2008) 233:674–88. doi: 10.3181/0711-MR-311

20. Hanafiah A, Karyadi D, Lukito W, Supari F. Desirable intakes of polyunsaturated fatty acids in indonesian adults. *Asia Pac J Clin Nutr.* (2007) 16:632–40.

21. Jamal O, Aneni E, Shaharyar S, Ali S, Parris D, McEvoy J, et al. Cigarette smoking worsens systemic inflammation in persons with metabolic syndrome. *Diabetol Metab Syndr.* (2014) 6:79. doi: 10.1186/1758-5996-6-79

22. Meier-Ewert H, Ridker P, Rifai N, Regan M, Price N, Dinges D, et al. Effect of sleep loss on C-reactive protein, an inflammatory marker of cardiovascular risk. *J Am Coll Cardiol.* (2004) 43:678–83. doi: 10.1016/j.jacc.2003.07.050

frontiers | Frontiers in Nutrition

TYPE Original Research
PUBLISHED 20 January 2023
DOI 10.3389/fnut.2023.1082250

OPEN ACCESS

EDITED BY
Nada Rotovnik Kozjek,
Institute of Oncology Ljubljana, Slovenia

REVIEWED BY
Xi Liang,
Qingdao University, China
Minhao Xie,
Nanjing University of Finance and Economics, China

*CORRESPONDENCE
Zhonghua Liu
✉ larkin-liu@hotmail.com
Lixin Wen
✉ sfwlx8015@sina.com
Ji Wang
✉ wangjics@163.com

†These authors have contributed equally to this work

SPECIALTY SECTION
This article was submitted to Nutrition and Metabolism, a section of the journal Frontiers in Nutrition

RECEIVED 28 October 2022
ACCEPTED 02 January 2023
PUBLISHED 20 January 2023

CITATION
Qu J, Ye M, Wen C, Cheng X, Zou L, Li M, Liu X, Liu Z, Wen L and Wang J (2023) Compound dark tea ameliorates obesity and hepatic steatosis and modulates the gut microbiota in mice. *Front. Nutr.* 10:1082250. doi: 10.3389/fnut.2023.1082250

Compound dark tea ameliorates obesity and hepatic steatosis and modulates the gut microbiota in mice

Jianyu Qu[1†], Mengke Ye[1†], Chi Wen[2], Xianyu Cheng[1], Lirui Zou[1], Mengyao Li[1], Xiangyan Liu[1], Zhonghua Liu[3*], Lixin Wen[1*] and Ji Wang[1,4,5*]

[1]Hunan Engineering Research Center of Livestock and Poultry Health Care, Colleges of Veterinary Medicine, Hunan Agricultural University, Changsha, China, [2]Hunan Chu Ming Tea Industry Co., Ltd., Changsha, China, [3]Key Laboratory of Tea Science of Ministry of Education, National Research Center of Engineering Technology for Utilization of Functional Ingredients from Botanicals, College of Horticulture, Hunan Agricultural University, Changsha, China, [4]Animal Nutritional Genome and Germplasm Innovation Research Center, College of Animal Science and Technology, Hunan Agricultural University, Changsha, China, [5]Changsha Lvye Biotechnology Co., Ltd., Changsha, China

Dark tea is a fermented tea that plays a role in regulating the homeostasis of intestinal microorganisms. Previous studies have found that dark tea can improve obesity and has a lipid-lowering effect. In this study, green tea, *Ilex latifolia Thunb* (kuding tea) and *Momordica grosvenori* (Luo Han Guo) were added to a new compound dark tea (CDT), to improve the taste and health of this beverage. High-fat diet-fed C57BL/6J mice were treated with low- (6 mg/mL) or high- (12 mg/mL) concentrations of CDT for 18 weeks to assess their effect on lipid metabolism. Our results suggest that low- and high-concentrations of CDT could reduce body weight by 15 and 16% and by 44 and 38% of body fat, respectively, by attenuating body weight gain and fat accumulation, improving glucose tolerance, alleviating metabolic endotoxemia, and regulating the mRNA expression levels of lipid metabolism-related genes. In addition, low concentrations of CDT were able to reduce the abundance of *Desulfovibrio*, which is positively associated with obesity, and increase the abundance of *Ruminococcus*, which are negatively associated with obesity. This study demonstrates the effect of CDT on ameliorating lipid metabolism and provides new insights into the research and development of functional tea beverages.

KEYWORDS

compound dark tea, gut microbiota, obesity, lipid metabolism, hepatic steatosis

1. Introduction

Obesity, which causes glucose and lipid metabolism disorder by excessive accumulation of adipose tissue in the body, further leads to the occurrence of chronic metabolic diseases such as atherosclerosis, diabetes, and non-alcoholic fatty liver (1). Currently, there are approximately one billion people with obesity worldwide (2). A 25% prevalence of non-alcoholic fatty liver disease (NAFLD) has been reported worldwide (3). The estimated prevalence of NAFLD in children and adolescents with obesity is 36.1% (4). The prevalence of NAFLD in children and adolescents is expected to increase along with the global obesity epidemic. Therefore, improving and preventing obesity is a major challenge for us. In recent years, an increasing number of studies have found that gut microbiota plays an important role in human health. Intestinal flora disorders are closely linked to diseases, such as diabetes, non-alcoholic fatty liver disease and obesity (5). In addition, intestinal flora disorders can alter the production of

gastrointestinal peptides associated with satiety, leading to increased food intake (6). Studies have shown that dietary foods and their functional components can alter the structure and composition of the gut microbiota. For example, probiotics containing prebiotic components reduce body mass index (BMI) and body fat levels through the gut microbiota (7). Similarly, fecal transplantation experiments have shown that the gut microbiota of mice fed with resveratrol can reduce obesity in high-fat diet (HFD)-fed mice (8). Thus, gut microbes have been established as possible therapeutic targets for preventing or treating overweight, obesity, and diseases linked to these conditions.

Tea, one of the most popular beverages in the world, contains a variety of bioactive ingredients that is beneficial to human health, such as polysaccharides, polyphenols, and catechins (9). As a dietary structure, tea exhibits antioxidative, anti-inflammatory, antimicrobial, anticarcinogenic, antihypertensive, neuroprotective, cholesterol-lowering, lipid-lowering, blood glucose-lowering, and thermogenic properties (10, 11). According to the different treatment method, tea is mainly divided into unfermented, semifermented, and fully fermented teas. As an unfermented tea, green tea can change the serum and liver metabolomic profiles of mice with high-fat diet-induced obesity (12). It has been reported that caffeine and catechins in green tea increase thermogenesis and fatty oxidation substrates by affecting the sympathetic nervous system (13). As a fully fermented tea, *Ilex latifolia Thunb* (Kuding tea) is a traditional bitter-tasting herbal tea that has been widely recognized over the past decade for its antihypertensive, lipid-lowering, blood-glucose-lowering, and antiobesity properties by the major bioactive components of triterpene saponins and polyphenols (14). Dark tea, including Pu'er, Liupao, and Fu brick teas, is also a fully fermented tea and has been gradually favored by consumers in recent years. It has been reported that Pu'er tea exerts lipid-lowering effects. Moreover, genetic and microbiology studies have discovered that some biomarkers of diabetes and obesity have improved following Pu'er tea intervention (15). Liupao tea, a dark tea, can alleviate symptoms associated with obesity by regulating lipid metabolism and oxidative stress, including lipid metabolism disorders, liver damage, and chronic inflammation (16). Fu brick tea is fermented by the solid-state fermentation of tea leaves with the probiotic *Eurotium cristatum* (golden flora) as the only dominant fungus (17). As the main active components of Fu brick tea, polyphenols are converted to new products by *Eurotium cristatum* (golden flora) during solid-state fermentation, including A-ring and B-ring fission derivatives of flavan-3-ols such as fuzhuanins A–F, teadenol A, teadenol B, xanthocerin, and planchol A (18–21). Fu brick tea can effectively reduce obesity in HFD rats and improve intestinal flora disorders, inflammation, and oxidative stress (22). In addition, drinking dark tea can attenuate systemic metabolic endotoxemia (23). Tea has been extensively studied in recent decades for its beneficial health effects in preventing obesity, metabolic syndrome, diabetes, and other diseases (24). Although these beneficial effects have been demonstrated in most laboratory studies, they are difficult to apply in real life. For example, green tea, *Ilex latifolia Thunb* (kuding tea), and dark tea drinks can have good weight loss results (22, 25–27), but we ignore the high concentration of tea that has bitter and astringent tastes to reduce its palatability (28).

Therefore, we developed a novel functional compound dark tea, to solve this problem. To increase the palatability of functional compound dark tea (CDT), including Fu brick tea, green tea, and *Ilex latifolia Thunb* (kuding tea), we added the *Momordica grosvenori* (Luo Han Guo). As a natural sweetener, *Momordica grosvenori* (Luo Han Guo) has been used as a sugar substitute for those with obesity and those with diabetes (29). *Momordica grosvenori* (Luo Han Guo) has also been used to prepare hot drinks to treat sore throat and as an expectorant for thousands of years in China (30). Our study would improve the taste and antiobesity effects of dark tea, we developed a compound dark tea (CDT) based on Fu brick tea, adding green tea, *Ilex latifolia Thunb* (kuding tea) and *Momordica grosvenori* (Luo Han Guo) to explore the effect and mechanism of CDT on lipid metabolism and gut microbiota in mice.

2. Materials and methods

2.1. Preparation and characterization of CDT

The main ingredients of CDT include Fu brick tea (50%), green tea (25%), *Ilex latifolia Thunb* (kuding tea) (10%) and *Momordica grosvenori* (Luo Han Guo) (15%), which were purchased from Hunan Chu Ming Tea Industry Co., Ltd. (Hunan, China). The preparation of CDT aqueous extracts was as follows: low concentration CDT (6 mg/mL, CDT_L group), 1.8 g CDT was soaked in 300 mL boiling water for 25 min, then filtered out the tea residue and allowed the mixture to cool; high concentration CDT (12 mg/mL, CDT_H group), 3.6 g CDT was soaked in 300 mL boiling water for 25 min, then filtered out the tea residue and allowed the mixture to cool.

2.2. Diet, animals, and treatment

Mouse diet preparation was performed by Trophic Animal Feed High-tech Co., Ltd. (Jiangsu, China). Diet composition and calorie levels in mice are shown in Supplementary Tables S1, S2. In addition, 36 male C57BL/6J mice (6 weeks old) were purchased from Hunan Slake Jingda Experimental Animals Co., Ltd. (Hunan, China). All mice were maintained at a controlled temperature of 22 ± 2 °C, humidity of 65 ± 5%, and a 12-h light/dark cycle. All the mice had *ad libitum* access to food and water. After 1 week of adaptive feeding, 6-week-old male C57BL/6J mice were randomly divided into four groups: the Con (including the common diet group, $n = 9$), HFD (HFD group, $n = 9$), CDT_L (HFD + low-concentration CDT group, $n = 9$), and CDT_H (HDF + high-concentration CDT group, $n = 9$) groups. Mice in the CDT_L and CDT_H groups all received drinking CDT in sterile plastic bottles, which were replaced every 2 days with freshly made low- and high-concentration CDT, with the surplus being collected and measured. Food consumption and body weight were recorded once a week for 18 weeks. At the end of the experiment, the mice were anesthetized with tribromoethanol after 8 h of fasting. The cecum contents, liver, serum, perirenal, epididymal, subcutaneous, and brown adipose tissues were collected for follow-up experiments, immediately frozen in liquid nitrogen, and stored at −80 °C. The experimental procedures were performed following the Animal Care and Use Guidelines of China and were approved by the Animal Care Committee of Hunan Agricultural University and the Use Committee at HUNAU (No. 43322108).

2.3. Oral glucose tolerance test

After 18 weeks, an oral glucose tolerance test (OGTT) was performed as previously described (31). Briefly, the mice were fasted for 6 h, followed by oral administration of glucose (2.0 g/kg body weight). Then, the blood glucose concentrations were analyzed at 0, 30, 60, 90, and 120 min after the oral administration of glucose, and a glucose concentration-time plot was prepared to offer the integrated areas under each curve (AUC) for OGTT. The glucose levels were measured using an ACCU-CHEK glucose meter (Roche, Shanghai, China). The data were recorded and analyzed.

2.4. Biochemical assessment

The serum levels of triglyceride (TG), total cholesterol (TC), low-density lipoprotein cholesterol (LDL-C), high-density lipoprotein cholesterol (HDL-C), alkaline phosphatase (ALP), and aspartate aminotransferase (AST) were determined using a model BS-240 automatic biochemical analyzer (Shenzhen Mindray Bio-Medical Electronics, Shenzhen, Guangdong, China). Liver TG, TC, and FFA levels were assessed using commercial kits (Beijing Box Shenggong Technology Co., Ltd., Beijing, China). The serum levels of insulin, resistin, leptin, and glucagon-like peptide 1 (GLP-1) were assessed using commercial kits (Supplementary Table S3). Additionally, fasting blood glucose content was measured using an Accu-Chek Performa glucose meter (Roche, Shanghai, China). The fasting blood glucose and fasting insulin values were used to calculate the homeostasis model assessment of insulin resistance (HOMA-IR) index as follows: HOMA-IR = (fasting glucose × fasting insulin)/22.5 (32).

2.5. Histological analysis

Subcutaneous adipose, brown adipose, and liver samples were cut into small pieces, dehydrated, cleared, embedded in paraffin wax, and sectioned after fixation in 10% neutral-buffered paraformaldehyde. Sections (5 mm) of each sample were prepared using hematoxylin and eosin (H&E) staining methods. To validate the vacuolization analysis and quantify lipid droplets, frozen liver samples were sectioned, stained with 0.2% oil red O in 60% isopropanol, and washed three times with phosphate-buffered saline (PBS). Images of stained liver tissues were collected using an orthographic light microscope (Nikon).

2.6. Quantification of brown adipose with immunohistochemistry

Brown adipose tissue was fixed in 4% paraformaldehyde and embedded in paraffin. Each sample was sliced into five sections discontinuously and then used for evaluation of relative brown adipose tissue by immunohistochemistry. After antigen repair and blockage of the endogenous peroxidase, sections were washed in PBS three times for 10 min and then incubated overnight at 4 °C with a rabbit antibody specific for GLP-1 (1:200, AiFang biological, AF11181). Tissue sections were washed three times in PBS for 10 min and incubated for 2 h at room temperature with the secondary antibody (HRP-Polymer anti-mouse/rabbit universal IHC kit, AiFang biological, AFIHC001, Changsha, China). After washing in PBS three times, tissue sections were stained with the chromogenic substrate 3,3′-diaminobenzidine (DAB), and the positive cell number was observed under the microscope. The number of positive cells was recorded at every high magnification, and the average of each sample was calculated. Sections from five animals from different treatment groups were analyzed (33).

2.7. Quantitative real-time polymerase chain reaction

Total RNA was isolated using TRIzol reagent (Accurate Biology, Hunan, China). RNA was then converted into complementary DNA (cDNA) using the Evo M-MLV Reverse Transcription Kit (Accurate Biology). Reverse transcription-quantitative polymerase chain reaction (RT-qPCR) assays were performed using the SYBR Green Premix Pro Taq HS qPCR Kit (AG11701; Accurate Biology, Hunan, China) and on a high-throughput PCR instrument (WaferGen Biosystems, Fremont, CA, USA). Thermal cycling conditions were as follows: one cycle at 95 °C for 10 min, 95 °C for 30 s, and 60 °C for 30 s. Expression levels of genes were normalized to β-actin expression. The quantitative changes in gene expression were calculated using the $2-\Delta\Delta Ct$ method, where Ct = Ct (target gene) – Ct (β-actin). The primer sequences are listed in Supplementary Table S4.

2.8. Gut microbiota analysis

The intestinal microbiota diversity detection experiment was commissioned by Majorbio Bio-Pharm Technology Co., Ltd. (Shanghai, China) based on the Illumina MiSeq PE300 platform. The specific operation was the same as that in previous research methods (34). Bacterial genomic DNAs in feces ($n = 7$ per group) were sequenced by Majorbio Bio-Pharm Technology Co., Ltd. (Shanghai, China). Alpha diversity, including the Shannon and Sobs indexes, was calculated using Mothur (version 1.30.2). Comparative analysis of samples between groups was performed using partial least squares discriminant analysis (PLS-DA). Spearman's correlation analysis was conducted to explore the correlation between bacterial flora and physiological factors.

2.9. Statistical analysis

The results were presented as the mean ± standard error of the mean (SEM). Statistical Package for the Social Sciences (SPSS) (version 25.0; IBM SPSS, Chicago, IL, USA) and GraphPad Prism (version 9.0; GraphPad Software, San Diego, CA, USA) were used for the statistical analyses. Data were tested for normality using the Shapiro–Wilk test. Normally distributed data were analyzed using a one-way analysis of variance (ANOVA). Non-normally distributed data were

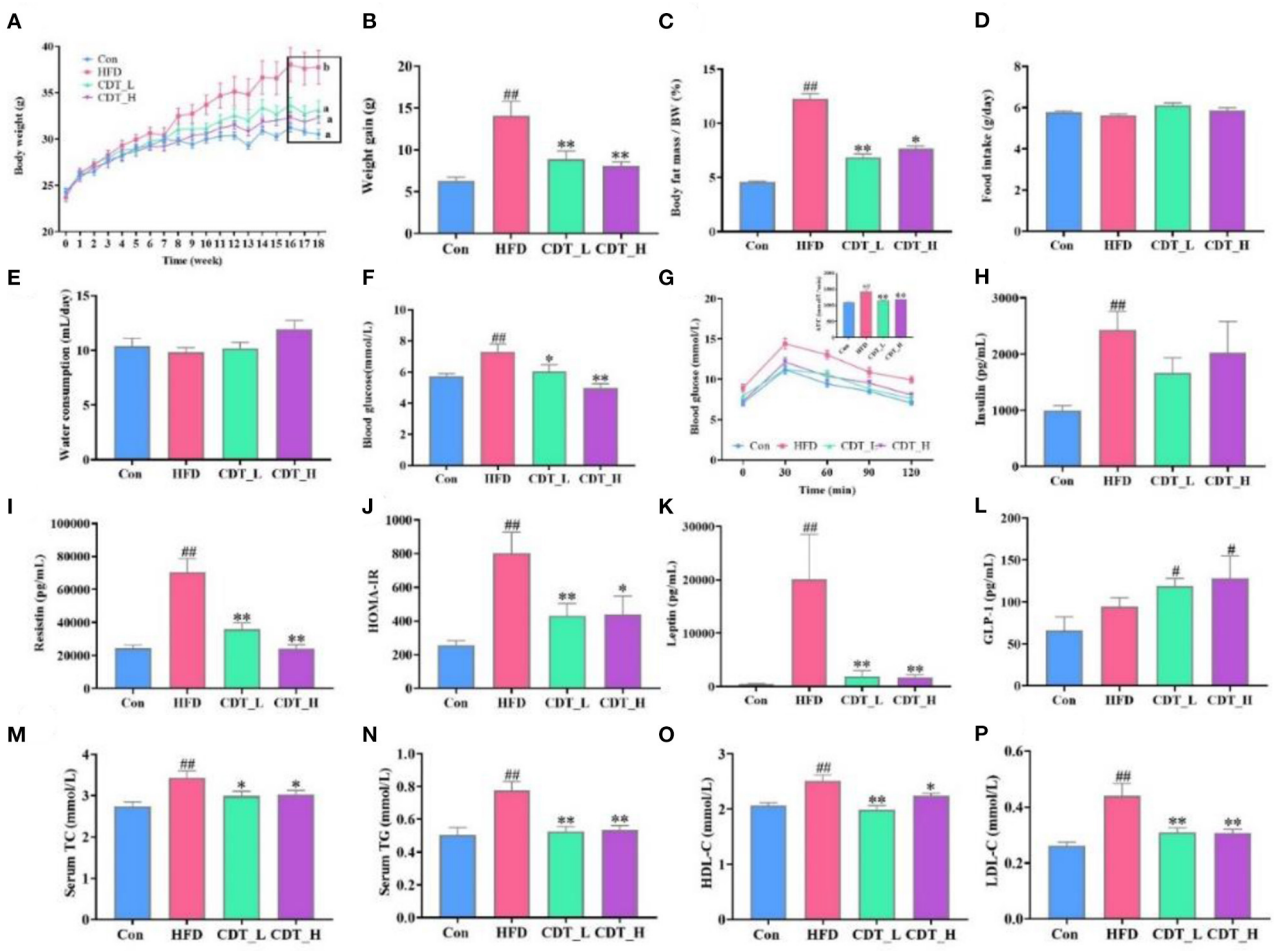

FIGURE 1
CDT improves glucose-lipid metabolism disorders in HFD-fed mice. **(A)** Body weight. **(B)** Body weight gain. **(C)** Body fat percentage. **(D)** Food intake. **(E)** Water consumption. **(F)** Blood glucose. **(G)** Oral glucose tolerance test (OGTT) curve and the area under the curve (AUC). **(H)** Insulin. **(I)** Resistin. **(J)** Homeostatic model assessment of insulin resistance (HOMA-IR). **(K)** Leptin. **(L)** Glucagon-like peptide-1 (GLP-1) **(M)** total cholesterol (TC). **(N)** Serum triglyceride (TG). **(O)** High-density lipoprotein-cholesterol (HDL-C). **(P)** Low-density lipoprotein-cholesterol (LDL-C). $N = 9$. All data are shown as mean ± SEM. $^{*}P < 0.05$, $^{**}P < 0.01$ by one-way ANOVA $^{*}P < 0.05$, $^{**}P < 0.01$ compared with that of the HFD group. $^{\#}P < 0.05$, $^{\#\#}P < 0.01$ compared with that of the Con group by one-way ANOVA.

analyzed using the Kruskal–Wallis rank-sum test. Statistical significance was set at $P < 0.05$, while $P < 0.01$ was considered highly significant.

3. Results

3.1. Effect of CDT on glucose-lipid metabolism in HFD-fed mice

C57BL/6 mice were supplemented with CDT under continuous HFD feeding for 18 weeks to investigate the anti-obesity effects of CDT in HFD-fed mice. As shown in Figures 1A, B, the CDT_L and CDT_H groups had significantly lower body weights than that of the HFD group ($P < 0.01$), which decreased by 15 and 16%, respectively. Furthermore, as expected, the body fat rate decreased by 44% in the CDT_L group, while the body fat rate in the CDT_H group decreased by 38% (Figure 1C). More notably, the difference in body weight and body fat rate was not ascribed to reduced food intake and water consumption, since no significant difference was found in food intake and water consumption between all groups (Figures 1D, E). As shown in Figure 1F, after drinking low- and high-concentrations of CDT, the fasting blood glucose levels of the CDT_L and CDT_H groups were reduced to varying degrees ($P < 0.05$ and $P < 0.01$, respectively). Similar trends were observed in the results of the OGTT among the groups; the OGTT was significantly reduced in both the CDT_L and CDT_H groups (Figure 1G, $P < 0.01$). Moreover, HFD treatment caused notable increases in the mice's insulin, resistin, HOMA-IR, and leptin values, which were restored in the CDT_L and CDT_H groups (Figures 1H–K). Compared with the Con group, drinking low- and high-concentrations of CDT significantly increased the content of GLP-1 (Figure 1L, $P < 0.05$). By measuring serum lipid markers, the serum levels of TG, TC, HDL-C, and LDL-C were higher in HFD-fed mice than in the CDT_L and CDT_H groups (Figures 1M–P).

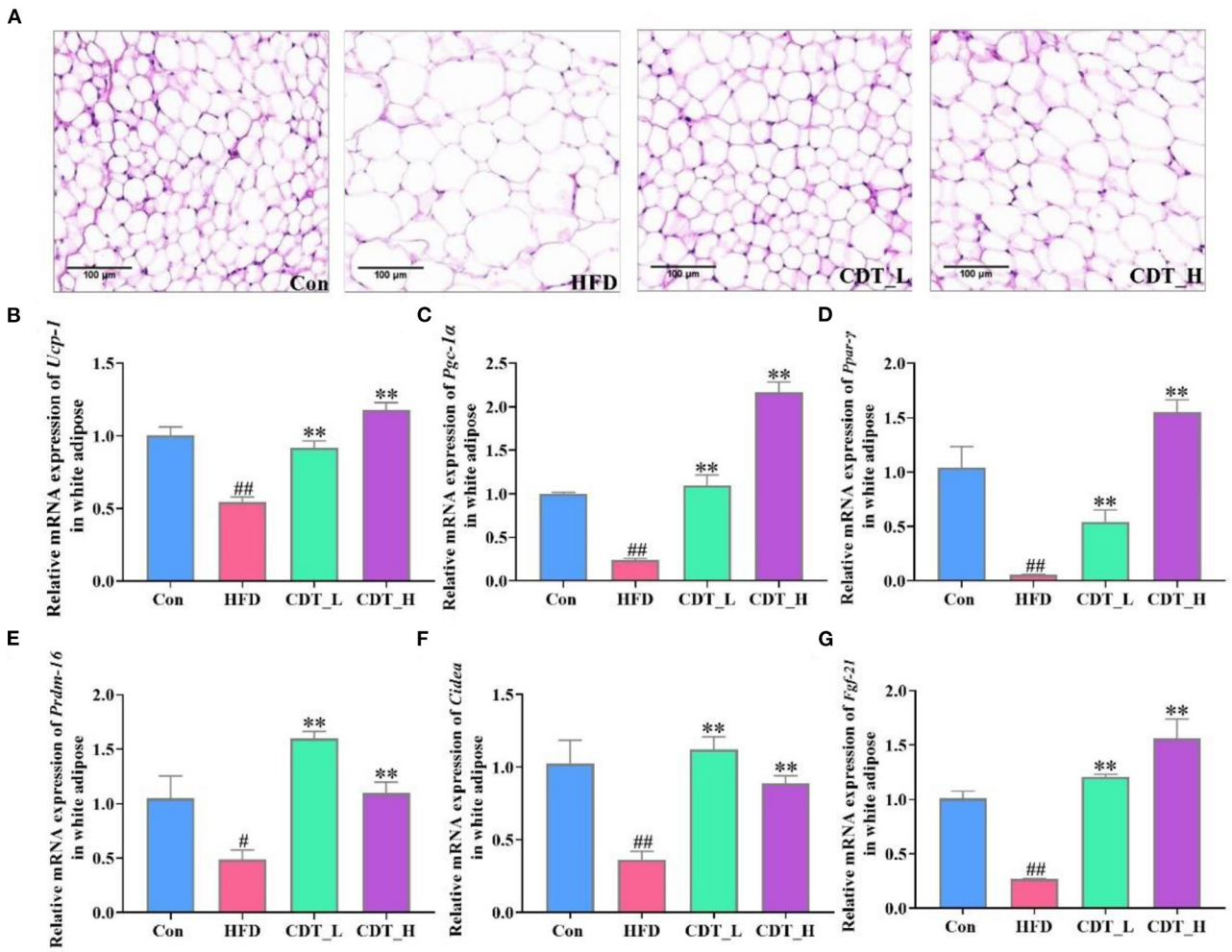

FIGURE 2
CDT improve fat cell morphology and lipid metabolism disorders of white adipose tissue in HFD-fed mice. **(A)** H&E staining of subcutaneous adipose tissue. **(B–G)** mRNA expression of *Ucp-1*, *Pgc-1α*, *Ppar-γ*, *Prdm-16*, *Cidea*, and *Fgf-21* in the white adipose tissue. $N = 5$ in A and $n = 3$ in **(B–G)**. All data are shown as mean ± SEM. $^{**}P < 0.01$ compared with that of the HFD group; $^{\#}P < 0.05$, $^{\#\#}P < 0.01$ compared with that of the Con group by Kruskal–Wallis rank-sum test.

3.2. Effects of CDT on fat cell morphology and lipid metabolism in HFD-fed mice

When comparing obesity-related traits, we demonstrated that representative histological slices of subcutaneous adipose tissue, as presented in Figure 2A, suggested that CDT significantly lowered the mean adipocyte size in HFD-fed mice. Interestingly, the CDT_L group had a better effect on reducing the size of adipocytes than the CDT_H group. In addition, CDT was able to reduce the size of brown adipose cells on the HFD, as shown in Figure 3A, and the effect of the CDT_H group was better than that of the CDT_L group. Previous studies have reported that the body upregulates the expression of the brown adipose tissue-specific gene, uncoupling protein 1 (Ucp-1), enhances energy expenditure, and promotes browning of subcutaneous adipose tissue, preventing weight gain (35). Therefore, to determine whether the increased energy expenditure in the CDT_L and CDT_H groups was associated with adaptive thermogenesis, we assessed the effects of CDT administration on brown adipose tissue. Immunohistochemical analysis of Ucp-1 revealed that CDT administration promoted thermogenesis of brown adipose tissue compared to that in the HFD group (Figures 3B, C, $P < 0.05$). To further understand the effects of CDT intervention on lipid metabolism, we analyzed the expression of relevant genes in the white and brown adipose tissues. We observed lower mRNA expression of thermoregulatory markers and lipid metabolism-related genes, including *Ucp-1*, peroxisome proliferation-activated receptor-gamma coactivator 1 alpha (*Pgc-1α*), peroxisome proliferator-activated receptor gamma (*Ppar-γ*), PR domain containing 16 (*Prdm-16*), cell death-inducing DNA fragmentation factor alpha-like effector A (*Cidea*), and fibroblast growth factor 21 (*Fgf-21*), in the white adipose tissue of the HFD group than in the Con group. However, the CDT_L and CDT_H groups expressed higher mRNA levels of these thermoregulatory markers and lipid metabolism-related genes than the HFD group (Figures 2B–G, $P < 0.01$). Furthermore, to examine the changes in mRNA expression of thermoregulatory markers and lipid metabolism-related genes in brown adipose tissue by HFD, the mRNA expression of thermoregulatory markers and

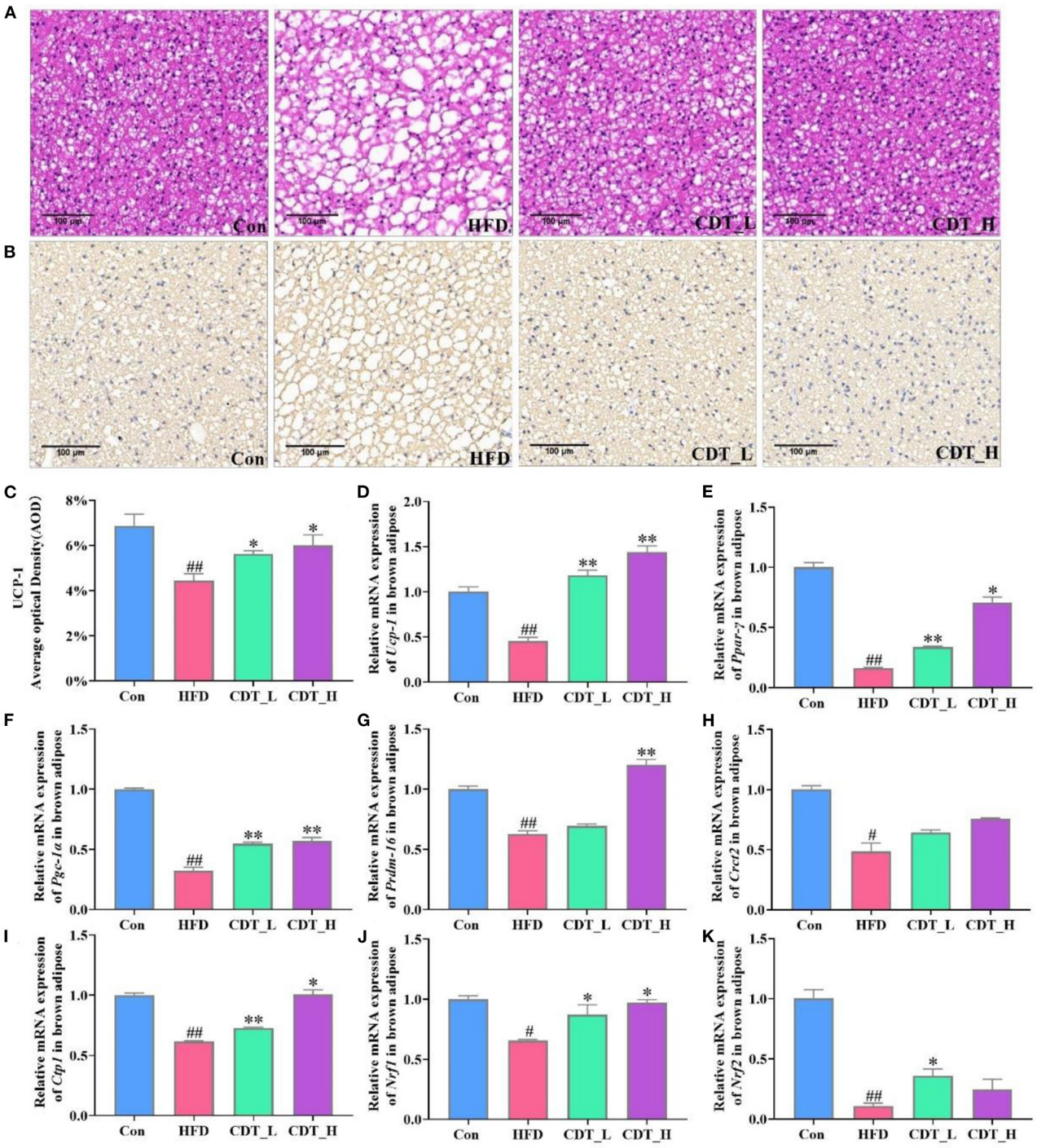

FIGURE 3
CDT improve fat cell morphology and lipid metabolism disorders of brown adipose tissue in HFD-fed mice. **(A)** H&E staining of brown adipose tissue. **(B)** Immunohistochemical analysis of Ucp-1 in the brown adipose tissue. **(C)** Average optical density of Ucp-1. D-K: mRNA expression of *Ucp-1*, *Ppar-γ*, *Pgc-1α*, *Prdm-16*, *Crct2*, *Ctp1*, *Nrf1*, and *Nrf2* in the brown adipose tissue. $N = 5$ in **(A–C)** and $n = 3$ in **(D–K)**. All data are shown as mean ± SEM. $^{*}P < 0.05$, $^{**}P < 0.01$ compared with that of the HFD group; $^{\#}P < 0.05$, $^{\#\#}P < 0.01$ compared with that of the Con group by Kruskal–Wallis rank-sum test.

lipid metabolism-related genes was determined (Figures 3D–K). The expression of *Ucp-1*, *Ppar-γ*, *Pgc-1α*, *Prdm-16*, CREB-regulated transcription coactivator 2 (*Crct2*), carnitine palmitoyltransferase 1 (*Ctp1*), nuclear respiratory factor 1 (*Nrf1*), and *Nrf2* was lower in HFD-fed mice than in the Con group. However, the CDT_L group exhibited a significantly upregulated mRNA expression of *Ucp-1*, *Ppar-γ*, *Pgc-1α*, and *Ctp1* ($P < 0.01$) and upregulated mRNA expression of *Nrf1* and *Nrf2* compared with the HFD group ($P < 0.05$). The CDT_H group exhibited a significantly upregulated mRNA expression of *Ucp-1*, *Pgc-1α*, and *Prdm-16* ($P < 0.01$) and

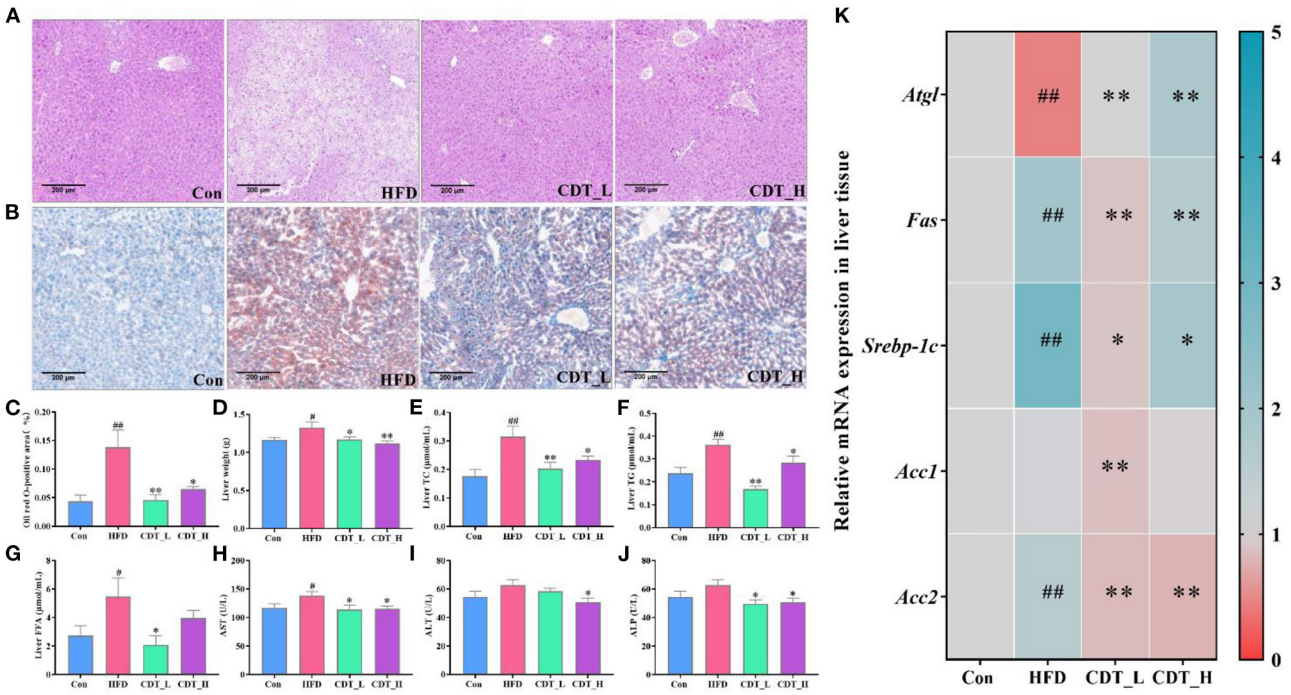

FIGURE 4
CDT improves liver function and lipid metabolism in HFD-fed mice. **(A)** H&E staining of liver tissues; **(B)** oil red O staining of liver tissues; **(C)** oil red O-positive area; **(D)** liver weight; **(E)** liver TC; **(F)** liver TG; **(G)** liver FFA; **(H)** AST activity; **(I)** ALT activity; **(J)** ALP activity; **(K)** mRNA expression of *Atgl*, *Fas*, *Srebp-1c*, *Acc1*, and *Acc2* in the liver. $n = 5$ in **(A–C)**, $n = 7$ in **(D–J)**, and $n = 3$ in **(K)**. All data are shown as mean ± SEM. $^{*}P < 0.05$, $^{**}P < 0.01$ by one-way ANOVA $^{*}P < 0.05$, $^{**}P < 0.01$ compared with that of the HFD group. $^{\#}P < 0.05$, $^{\#\#}P < 0.01$ compared with that of the Con group by one-way ANOVA ($n = 7$) and Kruskal–Wallis rank-sum test ($n \leq 5$).

upregulated mRNA expression of *Ppar-γ*, *Ctp1*, and *Nrf1* compared with the HFD group ($P < 0.05$).

3.3. Effects of CDT on liver function and lipid metabolism in HFD-fed mice

As shown in Figure 4A, H&E staining of liver sections revealed that HFD-induced indistinct cell boundaries, denaturation, irregular damaged cells with cytoplasmic vacuolation and that the CDT_L and CDT_H interventions improved this outcome. Oil red O staining revealed that CDT_L and CDT_H alleviated HFD-induced hepatic steatosis, and the effect of CDT_L was greater than that of CDT_H (Figures 4B, C). Liver weight was significantly increased in HFD-fed mice compared to that in the Con group, whereas CDT_L and CDT_H intervention remarkably lowered liver weight in mice on HFD (Figure 4D, $P < 0.05$ and $P < 0.01$, respectively). CDT_L and CDT_H also markedly reduced the levels of hepatic TC and TG in HFD-fed mice (Figures 4E, F; $P < 0.01$ and $P < 0.05$, respectively). Furthermore, CDT_L significantly reduced liver FFA levels in HFD-fed mice (Figure 4G, $P < 0.05$). The elevated levels of ALT in the HFD group were significantly ameliorated by CDT_H treatment (Figure 4I). In addition, Figures 4H, J demonstrates that CDT_L and CDT_H enhanced the increase AST and ALP levels in the HFD group, indicating that CDT_L and CDT_H exert protective effects on hepatotoxicity. Furthermore, to examine the changes in hepatic lipid metabolism regulated by HFD, the expression of lipid metabolism-related genes was determined (Figure 4K). The expression of genes, including adipose triglyceride lipase (*Atgl*), was lower in the HFD-fed mice than in the Con group. However, CDT_L and CDT_H significantly upregulated the mRNA expression of *Atgl* compared to that in the HFD group ($P < 0.01$). At the same time, the expression of sterol regulatory element-binding protein 1c (*Srebp-1c*), *Fas*, and acetyl-CoA carboxylase 2 (*Acc2*), which are related to lipid synthesis in the liver, was upregulated under HFD conditions. However, CDT_L and CDT_H significantly reduced the mRNA expression of *Srebp-1c*, *Fas*, and *Acc2* compared with the HFD group. In addition, the expression of Acc1 is significantly reduced in the CDT_L group compared to that in the HFD group ($P < 0.01$).

3.4. Effects of CDT on the gut microbiota in mice

The effects of HFD and CDT on the gut microbiota of mice were analyzed in the current study. After removing the unqualified sequence, as shown in Figure 5A, the Con group displayed 531 operational taxonomic units (OTUs), whereas the HFD, CDT_L, and CDT_H groups displayed 534, 558, and 578 OTUs, respectively. As shown in Figure 5B, the Shannon index at the OTU level was not significantly different among the four groups, but there was an upward trend in the CDT_L group compared with the other three groups. The Sobs index of OTU level results demonstrated a significant increase in the CDT_H group compared with the HFD group ($P < 0.05$).

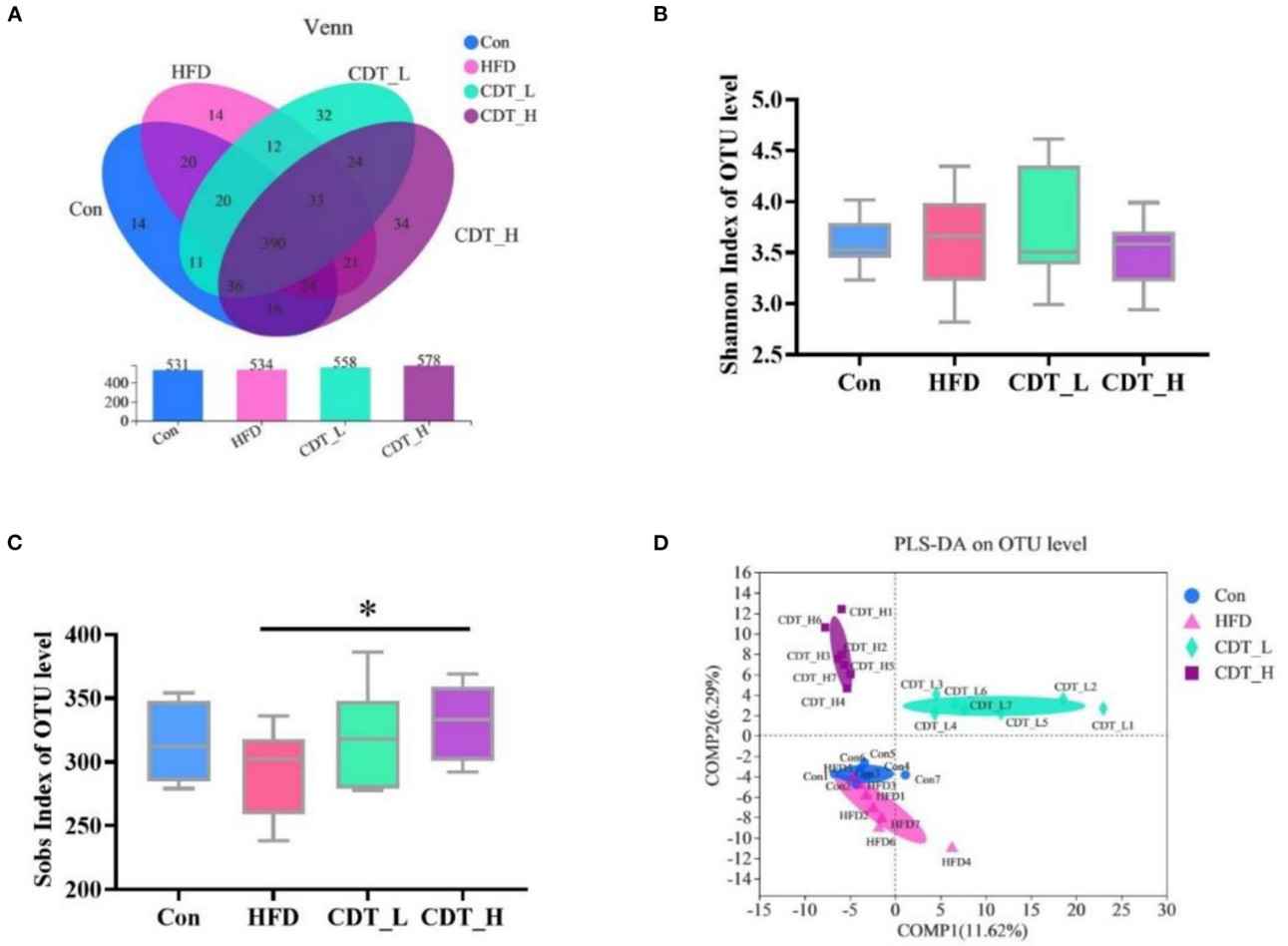

FIGURE 5
CDT alters the gut microbiota composition in HFD-fed mice. **(A)** Venn diagrams showing the unique and shared OTUs in the gut microbiota among groups. **(B)** Shannon index of OTU level. **(C)** Sobs index of OTU level. **(D)** PLS-DA on OTU level. $N = 7$. $^*P < 0.05$ compared with that of the HFD group by one-way ANOVA.

In addition, it was observed that there was a tendency to reduce the Sob index of the HFD group compared with the Con and CDT_L groups (Figure 5C). Moreover, PLS-DA analysis revealed differences between the HFD, CDT_L, and CDT_H groups (Figure 5D).

3.5. CDT regulates the composition of gut microbiota in mice

To explore differences in gut microbial composition, the relative abundance of bacterial communities at the phylum and genus levels was analyzed. At the phylum level, the gut flora of the four groups was dominated by *Firmicutes*, *Bacteroidota*, *Desulfobacterota,* and *Actinobacteria* (Figure 6A). As shown in Figure 6B, at the phylum level, *Desulfobacterota* accounted for 12.25% of the intestinal flora in the Con group, and this type of bacteria constituted 5.64% of the microbial profile in the CDT_L group. Actinobacteria accounted for 8.95% of the intestinal flora in the CDT_H group and 3.17% of the microbial profile in the CDT_L group (Figure 6C). At the order level, an increased abundance of *Clostridiales* was observed in the CDT_L group (Figure 6D). In addition, high dietary fiber intake significantly increased the relative abundance of *Rhizobiales* in HFD-fed mice (Figure 6E). High concentrations of CDT significantly increased the relative abundance of *Clostridia_vadinBB60_group*, compared with those in both the HFD and CDT_L groups (Figure 6F). Compared with the HFD group, the relative abundance of *Burkholderiales* in the CDT_H group decreased ($P < 0.05$) (Figure 6G). At the genus level, the Con group possessed significantly higher levels of *Desulfovibrio* than did the CDT_L group (Figure 6H). Meanwhile, high concentrations of CDT led to an increase in the relative abundance of *Bifidobacterium* compared to the CDT_L group (Figure 6I). In addition, the low concentration of CDT markedly increased the relative abundances of multiple genera, including *norank_f__Eubacterium_coprostanoligenes* and *Ruminococcus*, when compared to the HFD group (Figures 6J, K). The CDT_H group possessed significantly higher levels of *Lactococcus* but lower levels of *Parasutterella* than those in the HFD group (Figures 6L, M).

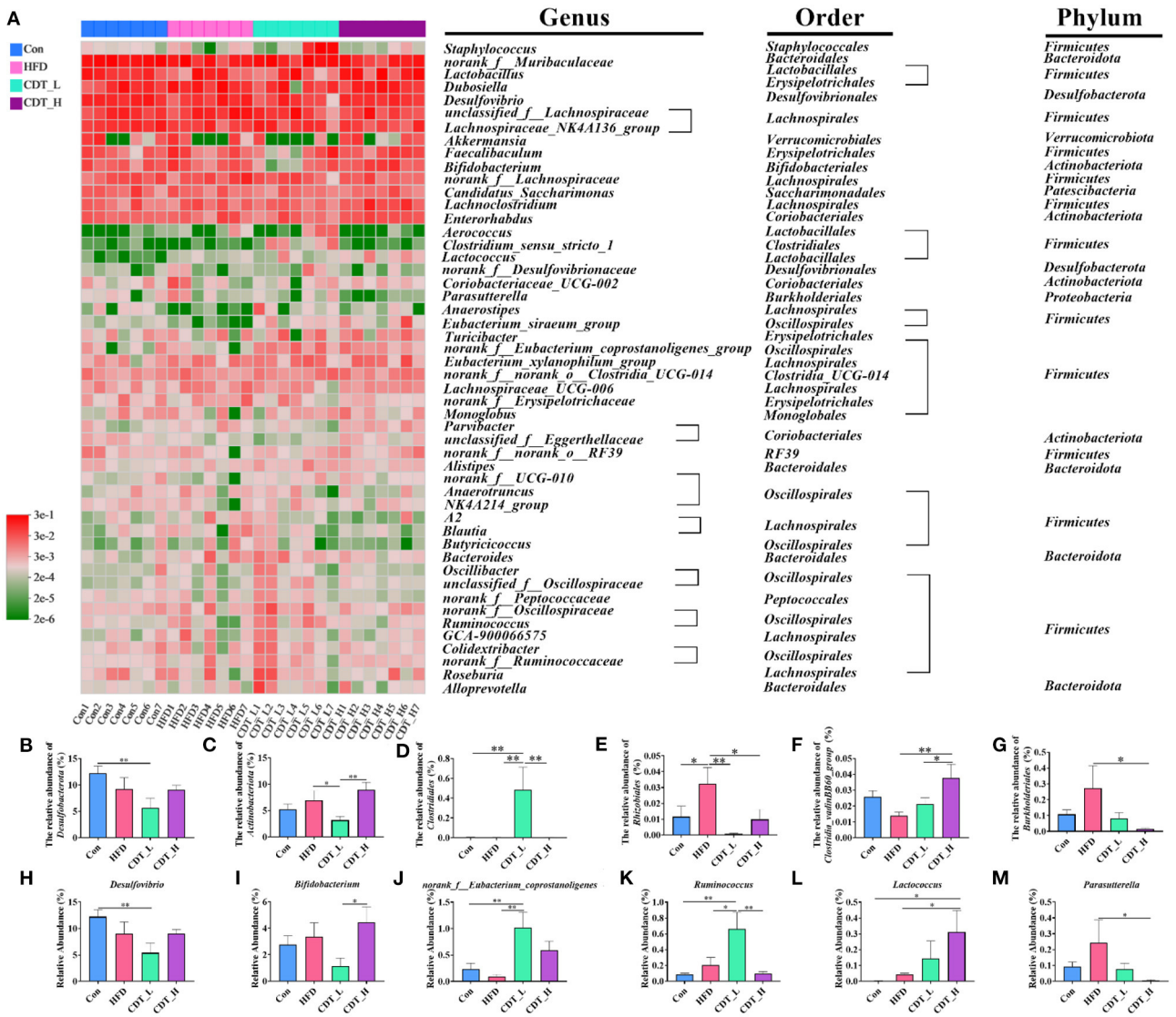

FIGURE 6
CDT regulates the gut microbiota composition in mice. **(A)** Heatmap of bacterial taxonomic profiling at the genus, order, and phylum. **(B, C)** Relative abundance of cecal *Desulfobacterota* and *Actinobacteriota* at the phylum level in each group. **(D–G)** Relative abundance of *Clostridiales*, *Rhizobiales*, *Clostridia_vadinBB60_group*, and *Burkholderiales* at the order level in each group. **(H–M)** relative abundance of six representative genera. $N = 7$. $^{*}P < 0.05$, $^{**}P < 0.01$ by one-way ANOVA.

3.6. Correlation analysis of intestinal microbiota with phenotype in mice

Spearman's correlation analysis was performed to understand the association between differentially enriched microbes and obesity-related traits (Figure 7). Nineteen and 12 OTUs were negatively and positively correlated with obesity-related traits, respectively. *Bifidobacterium* (OUT 91) was positively correlated with ALP. Low-concentration CDT significantly increased the relative abundance of *Bifidobacterium* compared to that in the CDT_H group (Figure 6I). *norank_f__Eubacterium_coprostanoligenes* (OUT 587) was observed to be negatively correlated with the weight gain, ALP, and AUC of the OGTT. Meanwhile, low concentrations of CDT led to an increase in the relative abundance of *norank_f__Eubacterium_coprostanoligenes* compared to the Con and HFD groups (Figure 6J). The gut flora of the two groups were dominated by *norank_f__Muribaculaceae* and *Lachnospiraceae_NK4A136_group* at the genus level. The *norank_f__Muribaculaceae* was negatively correlated with body weight, fat percentage, weight gain, AUC of OGTT, liver TC, HDL-C, LDL-C, HOMA-IR, insulin, resistin, and leptin, including OUTs 591, 499, and 593, OTU 654, and OUTs 448, 16, 483, 33, 319, 458, and 480. Similarly, the *Lachnospiraceae_NK4A136_group* was negatively correlated with body weight, fat percentage, weight gain, AUC of OGTT, liver TC, HDL-C, LDL-C, AST, ALP, HOMA-IR, blood glucose, insulin, resistin, and leptin, including OUTs 56, 102, 336, 42, and 581. Taken together, these results suggest that the low-concentration CDT intervention modulates HFD-induced gut microbiota dysbiosis in mice.

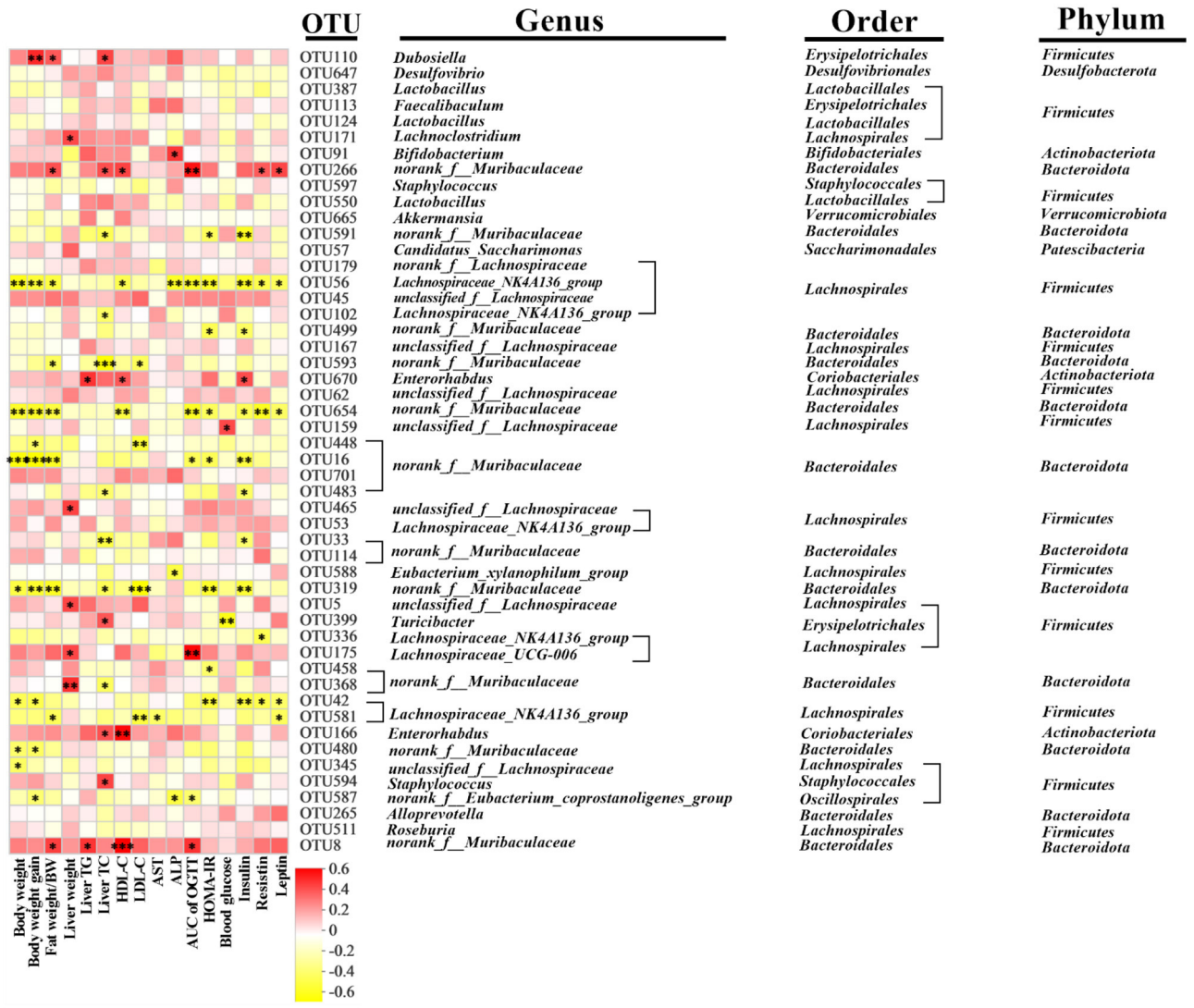

FIGURE 7
Predictive analysis of intestinal microbiota phenotype in mice. Heatmap of Spearman's correlation between OTUs and indexes related to obesity-related indexes in mice altered by HFD or CDT intervention. A total 33 OTUs were significantly correlated at least with one of the parameters including body weight, fat percentage, weight gain, AUC of OGTT, liver weight, liver TC, liver TG, HDL-C, LDL-C, AST, ALP, HOMA-IR, blood glucose, insulin, resistin, and leptin. $N = 7$. $^{*}P < 0.05$, $^{**}P < 0.01$ by one-way ANOVA.

4. Discussion

It is well-known that dark tea contains polysaccharides, polyphenols, and alkaloids, which have various effects on the body, including anti-inflammatory, antioxidant, lipid-lowering, and antiobesity effects (36). In our experiments, CDT was based on Fu brick tea, to which green tea, *Ilex latifolia Thunb* (kuding tea), and *Momordica grosvenori* (Luo Han Guo) were added to improve the taste and antiobesity effects of CDT. Consistent with previous studies, mice fed a HFD for 18 weeks demonstrated that CDT had lipid-lowering and antiobesity effects (37). It is noteworthy that, in this study, low-concentration CDT prevented abdominal obesity in mice better than high-concentration CDT, setting the stage for future decisions on the concentration of CDT consumption. Yang and Hong (38) also demonstrated that drinking tea was a good resistance to abdominal obesity, based on the lack of a significant difference in feed intake.

Obesity usually leads to an increase in the level of blood glucose and insulin resistance, which are regarded as early symptoms of diabetes (39). Meanwhile, blood glucose levels are key indicators of diabetes (40). CDT was demonstrated to positively regulate blood glucose levels in HFD-fed mice by measuring fasting blood glucose levels and performing the OGTT. The results of diabetes-related indicators demonstrate that, although HFD can increase the content of insulin, the significant increase in the resistin and insulin resistance index indicated that HFD led to a significant decrease in the sensitivity of mice to insulin and that long-term drinking of CDT can reduce the resistin and insulin resistance index and improve insulin sensitivity. In a study of sweet tea, it was also demonstrated that sweet tea leaf extract reduced the resistin and leptin levels (41). Leptin is a product of obesity, plays an important role in regulating food intake, body weight, and lipolysis (42), and is positively correlated with leptin content (43). In our study, leptin levels in HFD-fed mice increased significantly, and drinking the two concentrations of CDT led to a

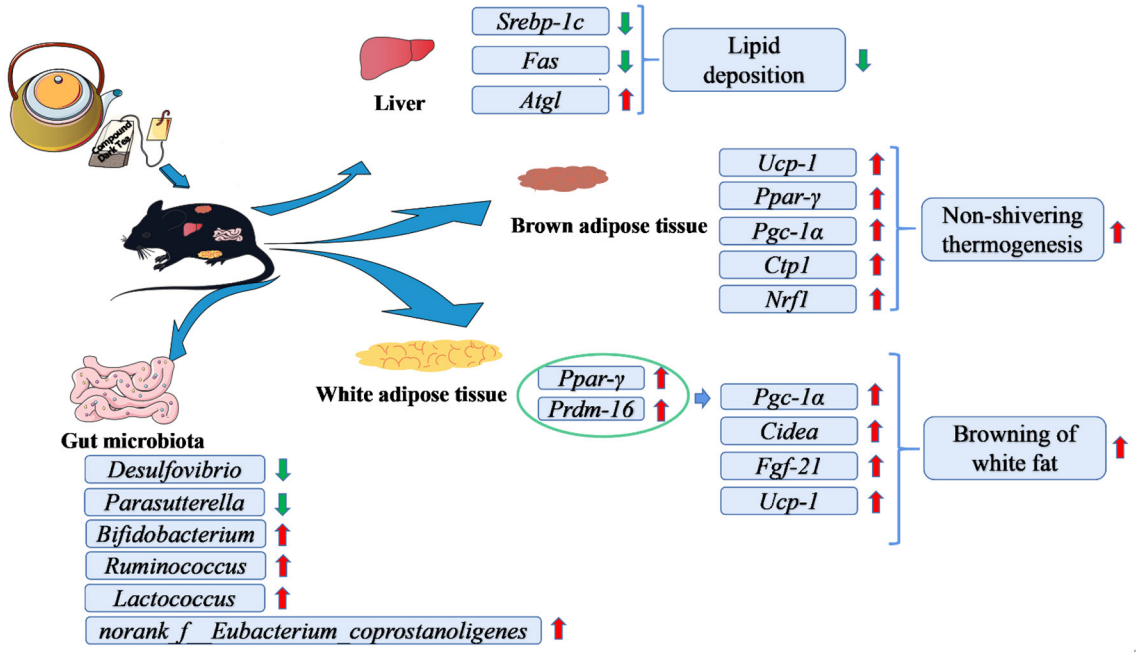

FIGURE 8
Schematic diagram of the effects of CDT in alleviating high-diet-induced obesity and hepatic steatosis and modulating the gut microbiota.

significant decrease in leptin levels. GLP-1 is secreted after eating, reducing blood glucose concentration by increasing insulin secretion and inhibiting glucagon release (44). Drinking CDT can significantly increase the GLP-1 content, which is similar to the results for resistin and leptin, demonstrating that CDT can increase insulin sensitivity and decrease blood glucose. In addition, consistent with previous studies, serum levels of TC, TG, LDL-C, and HDL-C were reduced in the CDT group (45). These results demonstrate that CDT has lipid-lowering and antiobesity effects in mice; however, the underlying mechanism requires further study.

The primary locations for lipid metabolism are adipose tissue and the liver, where energy metabolism, lipogenesis, and obesity are regulated (46). Obesity is caused by excessive accumulation of fat and is often accompanied by disorders of glucose and lipid metabolism (47). In our study, CDT decreased the area of subcutaneous fat and brown fat cells induced by the HFD. Immunohistochemical analysis revealed that CDT increased brown fat Ucp-1. Similar to our results, it was demonstrated that administering white tea to rats with removed ovaries activated mRNA expression of brown adipose tissue Ucp-1 in a trial of white tea (48). Brown fat is a special adipose tissue rich in mitochondria, and its activity is inversely correlated with obesity, blood glucose concentration, and insulin sensitivity (49). Ucp-1 plays a vital role in thermogenesis and energy regulation in brown fat (50). Brown fat, a good fat, is usually obtained by browning white fat through different pathways. *Ppar-γ* is the primary transcriptional regulator of fat differentiation and activates *Pgc-1α* with *Prdm-16* to induce brown fat gene expression (51–53). Additionally, fat browning is driven by *Fgf-21* (54). As a result, white fat is converted to beige fat, which eventually becomes brown fat. Beige fat has higher levels of *Ucp-1* and *Cidea* than white fat (55, 56). In the present study, CDT upregulated the expression of key transcription factors (*Ucp-1*, *Pgc-1α*, *Ppar-γ*, *Prdm-16*, *Cidea*, and *Fgf-21*), thereby promoting the browning of white fat. In addition, the activation of *Nrf2* increases energy consumption and facilitates the browning of white fat to prevent obesity (57). *Nrf1*, a key gene for maintaining brown fat, is the basic regulator of brown adipose tissue that increases metabolism in cold or obese conditions through proteasome function (58). *Nrf1* and *Nrf2* were significantly up-regulated in the CDT_L group. In addition, a significant upregulation of *Ctp1* can increase energy consumption (59), and *Ctp1* is significantly upregulated following the CDT intervention. These results demonstrate that CDT can accelerate energy consumption and the browning of white fat to reduce fat and ameriolate obesity. The liver is the central organ for fatty acid metabolism, and under normal circumstances, it only has a small amount of fat. Excess nutrition or obesity leads to liver function damage, lipid metabolism disorders, and accumulation of triglycerides in the liver cells (60). AST, ALT, and ALP levels in the HFD group increased in this trial, indicating that the HFD caused liver function impairment (61). To further verify whether impairment of liver function causes lipid deposition, we examined the levels of liver TC, TG, and FFA. The results demonstrated that the TC, TG, and FFA levels were significantly increased, indicating that HFD led to a large amount of lipid deposition in the liver, which is consistent with the results of previous studies (62). The two concentrations of CDT improved lipid deposition and liver function, and the effect of low-concentration CDT was better than that of high-concentration CDT. Tea and its extracts have also been demonstrated to exert protective effects on liver function and lipid metabolism (63). The inhibition of hepatic steatosis is associated with many mechanisms, including reduced fat production, increased fatty acid β-oxidation, increased insulin sensitivity, the inhibition of oxidative stress, and the inhibition of activation of the inflammatory pathway (64). To explore this mechanism, the molecular mechanisms underlying liver lipid metabolism were investigated. Activation of

AMP-activated protein kinase (AMPK) plays a significant role in regulating lipid formation and fatty acid oxidation in adipose tissue (65), and lipogenesis in the liver is mainly regulated by *Srebp-1c*, which further regulates the expression of *Acc1*, the main regulator of lipid biosynthesis by inhibiting *Srebp-1c* in the nucleus (66). Both high- and low-concentration CDT inhibited the expression of *Srebp-1c* compared with the HFD, but only low-concentration CDT significantly inhibited the expression of *Acc1*. Fat synthesis also relies on the activation of *Acc2* (67), and both high- and low-concentration CDT can significantly reduce the mRNA expression of *Acc2*. In addition, *Fas* and *Srebp-1c* have the same effect on fat synthesis (68), and low concentrations of CDT can significantly reduce the relative expression of *Fas*, indicating that low concentrations of CDT significantly reduce hepatic lipogenesis. In addition to the discovery of the inhibitory effect of CDT on hepatic lipogenesis, we also demonstrated that high and low doses of CDT could activate the expression of *Atgl* genes (69), which are related to lipolysis, accelerating the metabolism of liver fat. Combining the above results, it can be concluded that CDT can increase liver fat metabolism and inhibit liver fat synthesis, thereby improving liver lipid deposition and lipid metabolism disorders induced by HFD.

An increasing amount of research demonstrates that the intestinal flora plays an important role in human health (70). In general, experimental studies on obesity and intestinal flora include an HFD model group, and the intestinal flora of the HFD model group will change (15). In our experiment, we demonstrated that HFD decreased the species richness of the gut microbiota compared with CDT_H (71). In addition, PLS-DA analysis revealed that the HFD group and the two concentrations of CDT had different intestinal flora. Interestingly, mice in the Con and HFD groups had the most similar intestinal profiles. We suspect that the PLS-DA analysis results may be because most of the microbiota in the Con and HFD groups did not differ significantly at the phylum and genus levels and that most of the differences were generated between the drinking compound dark tea and the drinking water group. By analyzing the differences in the flora at the genus level in our study, it was demonstrated that a low concentration of CDT was able to reduce the level of *Desulfovibrio*, which has been demonstrated to be harmful in previous studies, and the endotoxin of *Desulfovibrio* was associated with inflammation; therefore, *Desulfovibrio* was positively associated with inflammation and obesity (72). Few studies have examined the function of the *norank_f__Eubacterium_coprostanoligenes genus*, but it has been observed that adding perilla fruit leaves to dairy cow feed can increase the abundance of *Eubacterium coprostanoligenes*, and the abundance of this bacterium is inversely correlated with dairy cow fat (73), which is similar to the results of the CDT_L group in our study. In addition, the abundance of the genus *Ruminococcus* in the CDT_L group was higher than that in the other three groups, and multiple studies have demonstrated that the abundance of *Ruminococcus* is inversely correlated with obesity (74, 75). As a beneficial bacterium, *Bifidobacterium* can alleviate obesity, regulate glucose homeostasis, and produce short-chain fatty acids (SCFAs) (76, 77). In addition, a previous study has demonstrated that the growth of *Bifidobacterium* can be promoted by diet (78). In our study, the high concentration of CDT increased the abundance of *Bifidobacterium*. In addition, the abundance of *Lactococcus* in the CDT_H group was higher than that in the Con and HFD groups, which was consistent with a previous study demonstrating that the abundance of *Lactococcus* is inversely correlated with obesity (79). In addition, the abundance of *Parasutterella*, which is associated with chronic intestinal inflammation, was decreased in the CDT_H group (80).

5. Conclusion

The schematic diagram of CDT is concluded in Figure 8. In this study, we found that CDT upregulated the expression of thermogenic genes in brown fat and browning-related genes in white fat tissues. CDT also significantly upregulated the expression of lipolysis-related genes and downregulated that of lipid synthesis-related genes in the liver. As a result, the CDT reduced fat deposition and alleviated hepatic steatosis in HFD-fed mice. Additionally, CDT increased the abundance of beneficial bacteria and reduced the abundance of harmful bacteria in the intestine. This study suggests that CDT can significantly ameliorate lipid metabolism in mice and opens new avenues for the development of functional compound tea drinks.

Data availability statement

The datasets presented in this study can be found in online repositories. The names of the repository/repositories and accession number(s) can be found in the article/ Supplementary material.

Ethics statement

The animal study was reviewed and approved by the Ethics Committee of Hunan Agricultural University.

Author contributions

JQ and MY designed the experiment. CW is the first inventor of the compound dark tea patent. JQ wrote original draft. MY, JQ, and CW prepared the experiment and made all H&E and oil red staining sections. JQ, XL, LZ, and ML analyzed the data and prepared for graph. JW and LW wrote original draft and reviewed manuscript. JW reviewed manuscript and checked the grammar. LW and ZL reviewed manuscript and provided funding acquisition. All authors have read and agreed to the published version of the manuscript.

Funding

This research was funded by Special Funds for Construction of Innovative Provinces in Hunan Province (2020NK2032).

Acknowledgments

The authors would like to thank the Hunan Chu Ming Tea Industry Co., Ltd.

Conflict of interest

CW was employed by Hunan Chu Ming Tea Industry Co., Ltd. JW was employed by Changsha Lvye Biotechnology Co., Ltd.

The remaining authors declare that the research was conducted in the absence of any commercial or financial relationships that could be construed as a potential conflict of interest.

Publisher's note

All claims expressed in this article are solely those of the authors and do not necessarily represent those of their affiliated organizations, or those of the publisher, the editors and the reviewers. Any product that may be evaluated in this article, or claim that may be made by its manufacturer, is not guaranteed or endorsed by the publisher.

Supplementary material

The Supplementary Material for this article can be found online at: https://www.frontiersin.org/articles/10.3389/fnut.2023.1082250/full#supplementary-material

References

1. Prasun P. Mitochondrial dysfunction in metabolic syndrome. *Biochim Biophys Acta Mol Basis Dis.* (2020) 1866:165838. doi: 10.1016/j.bbadis.2020.165838

2. Hoffman DJ, Powell TL, Barrett ES, Hardy DB. Developmental origins of metabolic diseases. *Physiol Rev.* (2021) 101:739–95. doi: 10.1152/physrev.00002.2020

3. Maurice J, Manousou P. Non-alcoholic fatty liver disease. *Clin Med (Lond).* (2018) 18:245–50. doi: 10.7861/clinmedicine.18-3-245

4. Shaunak M, Byrne CD, Davis N, Afolabi P, Faust SN, Davies JH, et al. Non-alcoholic fatty liver disease and childhood obesity. *Arch Dis Child.* (2021) 106:3–8. doi: 10.1136/archdischild-2019-318063

5. Safari Z, Gerard P. The links between the gut microbiome and non-alcoholic fatty liver disease (NAFLD). *Cell Mol Life Sci.* (2019) 76:1541–58. doi: 10.1007/s00018-019-03011-w

6. Gomes AC, Hoffmann C, Mota JF. The human gut microbiota: Metabolism and perspective in obesity. *Gut Microbes.* (2018) 9:308–25. doi: 10.1080/19490976.2018.1465157

7. Sergeev IN, Aljutaily T, Walton G, Huarte E. Effects of synbiotic supplement on human gut microbiota, body composition and weight loss in obesity. *Nutrients.* (2020) 12:222. doi: 10.3390/nu12010222

8. Wang P, Li D, Ke W, Liang D, Hu X, Chen F, et al. Resveratrol-induced gut microbiota reduces obesity in high-fat diet-fed mice. *Int J Obes (Lond).* (2020) 44:213–25. doi: 10.1038/s41366-019-0332-1

9. Cao H. Polysaccharides from Chinese tea: recent advance on bioactivity and function. *Int J Biol Macromol.* (2013) 62:76–9. doi: 10.1016/j.ijbiomac.2013.08.033

10. Hayat K, Iqbal H, Malik U, Bilal U, Mushtaq S. Tea and its consumption: benefits and risks. *Crit Rev Food Sci Nutr.* (2015) 55:939–54. doi: 10.1080/10408398.2012.678949

11. Tang GY, Meng X, Gan RY, Zhao CN, Liu Q, Feng YB, et al. Health functions and related molecular mechanisms of tea components: an update review. *Int J Mol Sci.* (2019) 20:6196. doi: 10.3390/ijms20246196

12. Lee LS, Choi JH, Sung MJ, Hur JY, Hur HJ, Park JD, et al. Green tea changes serum and liver metabolomic profiles in mice with high-fat diet-induced obesity. *Mol Nutr Food Res.* (2015) 59:784–94. doi: 10.1002/mnfr.201400470

13. Turkozu D, Tek NA, A. minireview of effects of green tea on energy expenditure. *Crit Rev Food Sci Nutr.* (2017) 57:254–8. doi: 10.1080/10408398.2014.986672

14. Wupper S, Luersen K, Rimbach G. Chemical composition, bioactivity and safety aspects of kuding tea-from beverage to herbal extract. *Nutrients.* (2020) 12:2796. doi: 10.3390/nu12092796

15. Ye J, Zhao Y, Chen X, Zhou H, Yang Y, Zhang X, et al. Pu-erh tea ameliorates obesity and modulates gut microbiota in high fat diet fed mice. *Food Res Int.* (2021) 144:110360. doi: 10.1016/j.foodres.2021.110360

16. Wu Y, Sun H, Yi R, Tan F, Zhao X. Anti-obesity effect of Liupao tea extract by modulating lipid metabolism and oxidative stress in high-fat-diet-induced obese mice. *J Food Sci.* (2021) 86:215–27. doi: 10.1111/1750-3841.15551

17. Kang D, Su M, Duan Y, Huang Y. Eurotium cristatum, a potential probiotic fungus from Fuzhuan brick tea, alleviated obesity in mice by modulating gut microbiota. *Food Funct.* (2019) 10:5032–45. doi: 10.1039/C9FO00604D

18. Zhu MZ Li N, Zhou F, Ouyang J, Lu DM, Xu W, et al. Microbial bioconversion of the chemical components in dark tea. *Food Chem.* (2020) 312:126043. doi: 10.1016/j.foodchem.2019.126043

19. Luo ZM, Du HX Li LX, An MQ, Zhang ZZ, Wan XC, et al. Fuzhuanins A and B: the B-ring fission lactones of flavan-3-ols from Fuzhuan brick-tea. *J Agric Food Chem.* (2013) 61:6982–90. doi: 10.1021/jf401724w

20. Zhu YF, Chen JJ Ji XM, Hu X, Ling TJ, Zhang ZZ, et al. Changes of major tea polyphenols and production of four new B-ring fission metabolites of catechins from post-fermented Jing-Wei Fu brick tea. *Food Chem.* (2015) 170:110–7. doi: 10.1016/j.foodchem.2014.08.075

21. Xu J, Hu FL, Wang W, Wan XC, Bao GH. Investigation on biochemical compositional changes during the microbial fermentation process of Fu brick tea by LC-MS based metabolomics. *Food Chem.* (2015) 186:176–84. doi: 10.1016/j.foodchem.2014.12.045

22. Zhou F, Li YL, Zhang X, Wang KB, Huang JA, Liu ZH, et al. Polyphenols from fu brick tea reduce obesity via modulation of gut microbiota and gut microbiota-related intestinal oxidative stress and barrier function. *J Agric Food Chem.* (2021) 69:14530–43. doi: 10.1021/acs.jafc.1c04553

23. Gao X, Xie Q, Kong P, Liu L, Sun S, Xiong B, et al. Polyphenol- and Caffeine-Rich Postfermented Pu-erh Tea Improves Diet-Induced Metabolic Syndrome by Remodeling Intestinal Homeostasis in Mice. *Infect Immun.* (2018) 86:e00601–17. doi: 10.1128/IAI.00601-17

24. Khan N, Mukhtar H. Tea polyphenols in promotion of human health. *Nutrients.* (2018) 11:39. doi: 10.3390/nu11010039

25. Balentine DA, Wiseman SA, Bouwens LC. The chemistry of tea flavonoids. *Crit Rev Food Sci Nutr.* (1997) 37:693–704. doi: 10.1080/10408399709527797

26. Sang S, Lambert JD, Ho CT, Yang CS. The chemistry and biotransformation of tea constituents. *Pharmacol Res.* (2011) 64:87–99. doi: 10.1016/j.phrs.2011.02.007

27. Wu H, Chen YL Yu Y, Zang J, Wu Y, He Z, et al. Ilex latifolia Thunb protects mice from HFD-induced body weight gain. *Sci Rep.* (2017) 7:14660. doi: 10.1038/s41598-017-15292-x

28. Ong JS, Hwang LD, Zhong VW, An J, Gharahkhani P, Breslin PAS, et al. Understanding the role of bitter taste perception in coffee, tea and alcohol consumption through Mendelian randomization. *Sci Rep.* (2018) 8:16414. doi: 10.1038/s41598-018-34713-z

29. Song F, Chen W, Jia W, Yao P, Nussler AK, Sun X, et al. A natural sweetener, Momordica grosvenori, attenuates the imbalance of cellular immune functions in alloxan-induced diabetic mice. *Phytother Res.* (2006) 20:552–60. doi: 10.1002/ptr.1903

30. Di R, Huang MT, Ho CT. Anti-inflammatory activities of mogrosides from Momordica grosvenori in murine macrophages and a murine ear edema model. *J Agric Food Chem.* (2011) 59:7474–81. doi: 10.1021/jf201207m

31. Wen JJ, Gao H, Hu JL, Nie QX, Chen HH, Xiong T, et al. Polysaccharides from fermented Momordica charantia ameliorate obesity in high-fat induced obese rats. *Food Funct.* (2019) 10:448–57. doi: 10.1039/C8FO01609G

32. Safar FH, Mojiminiyi OA, Al-Rumaih HM, Diejomaoh MF. Computational methods are significant determinants of the associations and definitions of insulin resistance using the homeostasis model assessment in women of reproductive age. *Clin Chem.* (2011) 57:279–85. doi: 10.1373/clinchem.2010.152025

33. Zheng J, Xiao KL, Chen L, Wu C, Hu X, Zeng T, et al. Insulin sensitizers improve the GLP-1 secretion and the amount of intestinal L cells on high-fat-diet-induced catch-up growth. *Nutrition.* (2017) 39:82–91. doi: 10.1016/j.nut.2017.01.002

34. Hou Y, Wei W, Guan X, Liu Y, Bian G, He D, et al. A diet-microbial metabolism feedforward loop modulates intestinal stem cell renewal in the stressed gut. *Nat Commun.* (2021) 12:271. doi: 10.1038/s41467-020-20673-4

35. Yoo A, Jung Kim M, Ahn J, Hwa Jung C, Deok Seo H, Yung Ly S, et al. Fuzhuan brick tea extract prevents diet-induced obesity via stimulation of fat browning in mice. *Food Chem.* (2022) 377:132006. doi: 10.1016/j.foodchem.2021.132006

36. Ling W, Li S, Zhang X, Xu Y, Gao Y, Du Q, et al. Evaluation of anti-obesity activity, acute toxicity, and subacute toxicity of probiotic dark tea. *Biomolecules.* (2018) 8:99. doi: 10.3390/biom8040099

37. Ma W, Shi Y, Yang G, Shi J, Ji J, Zhang Y, et al. Hypolipidaemic and antioxidant effects of various Chinese dark tea extracts obtained from the same raw material and their main chemical components. *Food Chem.* (2022) 375:131877. doi: 10.1016/j.foodchem.2021.131877

38. Yang CS, Hong J. Prevention of chronic diseases by tea: possible mechanisms and human relevance. *Annu Rev Nutr.* (2013) 33:161–81. doi: 10.1146/annurev-nutr-071811-150717

39. Benchoula K, Arya A, Parhar IS, Hwa WE. FoxO1 signaling as a therapeutic target for type 2 diabetes and obesity. *Eur J Pharmacol.* (2021) 891:173758. doi: 10.1016/j.ejphar.2020.173758

40. Kuzuya T. Early diagnosis, early treatment and the new diagnostic criteria of diabetes mellitus. *Br J Nutr.* (2000) 84:S177–181. doi: 10.1079/096582197388644

41. Zhou CJ, Huang S, Liu JQ, Qiu SQ, Xie FY, Song HP, et al. Sweet tea leaves extract improves leptin resistance in diet-induced obese rats. *J Ethnopharmacol.* (2013) 145:386–92. doi: 10.1016/j.jep.2012.09.057

42. Obradovic M, Sudar-Milovanovic E, Soskic S, Essack M, Arya S, Stewart AJ, et al. Leptin and Obesity: Role and Clinical Implication. *Front Endocrinol (Lausanne).* (2021) 12:585887. doi: 10.3389/fendo.2021.585887

43. Paz-Filho G, Mastronardi CA, Licinio J. Leptin treatment: facts and expectations. *Metabolism.* (2015) 64:146–56. doi: 10.1016/j.metabol.2014.07.014

44. Meier JJ. GLP-1 receptor agonists for individualized treatment of type 2 diabetes mellitus. *Nat Rev Endocrinol.* (2012) 8:728–42. doi: 10.1038/nrendo.2012.140

45. Chen G, Xie M, Dai Z, Wan P, Ye H, Zeng X, et al. Kudingcha and fuzhuan brick tea prevent obesity and modulate gut microbiota in high-fat diet fed mice. *Mol Nutr Food Res.* (2018) 62:e1700485. doi: 10.1002/mnfr.201700485

46. Wallace M, Metallo CM. Tracing insights into de novo lipogenesis in liver and adipose tissues. *Semin Cell Dev Biol.* (2020) 108:65–71. doi: 10.1016/j.semcdb.2020.02.012

47. Greenway F. Obesity medications and the treatment of type 2 diabetes. *Diabetes Technol Ther.* (1999) 1:277–87. doi: 10.1089/152091599317198

48. Saral S, Saydam F, Dokumacioglu E, Atak M, Tumkaya L, Uydu HA, et al. Effect of white tea consumption on serum leptin, TNF-alpha and UCP1 gene expression in ovariectomized rats. *Eur Cytokine Netw.* (2021) 32:31–8. doi: 10.1684/ecn.2021.0467

49. Okla M, Kim J, Koehler K, Chung S. Dietary factors promoting brown and beige fat development and thermogenesis. *Adv Nutr.* (2017) 8:473–83. doi: 10.3945/an.116.014332

50. Wang G, Meyer JG, Cai W, Softic S, Li ME, Verdin E, et al. Regulation of UCP1 and mitochondrial metabolism in brown adipose tissue by reversible succinylation. *Mol Cell.* (2019) 74:844–857.e847. doi: 10.1016/j.molcel.2019.03.021

51. Petrovic N, Walden TB, Shabalina IG, Timmons JA, Cannon B, Nedergaard J, et al. Chronic peroxisome proliferator-activated receptor gamma (PPARgamma) activation of epididymally derived white adipocyte cultures reveals a population of thermogenically competent, UCP1-containing adipocytes molecularly distinct from classic brown adipocytes. *J Biol Chem.* (2010) 285:7153–64. doi: 10.1074/jbc.M109.053942

52. Bostrom P, Wu J, Jedrychowski MP, Korde A, Ye L, Lo JC, et al. A PGC1-alpha-dependent myokine that drives brown-fat-like development of white fat and thermogenesis. *Nature.* (2012) 481:463–8. doi: 10.1038/nature10777

53. Harms M, Seale P. Brown and beige fat: development, function and therapeutic potential. *Nat Med.* (2013) 19:1252–63. doi: 10.1038/nm.3361

54. Fisher FM, Kleiner S, Douris N, Fox EC, Mepani RJ, Verdeguer F, et al. FGF21 regulates PGC-1alpha and browning of white adipose tissues in adaptive thermogenesis. *Genes Dev.* (2012) 26:271–81. doi: 10.1101/gad.177857.111

55. Seale P, Bjork B, Yang W, Kajimura S, Chin S, Kuang S, et al. PRDM16 controls a brown fat/skeletal muscle switch. *Nature.* (2008) 454:961–7. doi: 10.1038/nature07182

56. Kajimura S, Seale P, Kubota K, Lunsford E, Frangioni JV, Gygi SP, et al. Initiation of myoblast to brown fat switch by a PRDM16-C/EBP-beta transcriptional complex. *Nature.* (2009) 460:1154–8. doi: 10.1038/nature08262

57. Xu L, Nagata N, Ota T. Glucoraphanin: a broccoli sprout extract that ameliorates obesity-induced inflammation and insulin resistance. *Adipocyte.* (2018) 7:218–25. doi: 10.1080/21623945.2018.1474669

58. Bartelt A, Widenmaier SB, Schlein C, Johann K, Goncalves RLS, Eguchi K, et al. Brown adipose tissue thermogenic adaptation requires Nrf1-mediated proteasomal activity. *Nat Med.* (2018) 24:292–303. doi: 10.1038/nm.4481

59. Ghanem N, Zayed M, Mohamed I, Mohammady M, Shehata MF. Co-expression of candidate genes regulating growth performance and carcass traits of Barki lambs in Egypt. *Trop Anim Health Prod.* (2022) 54:260. doi: 10.1007/s11250-022-03263-y

60. Alves-Bezerra M, Cohen DE. Triglyceride metabolism in the liver. *Compr Physiol.* (2017) 8:1–8. doi: 10.1002/cphy.c170012

61. Lozano-Paniagua D, Parron T, Alarcon R, Requena M, Lopez-Guarnido O, Lacasana M, et al. Evaluation of conventional and non-conventional biomarkers of liver toxicity in greenhouse workers occupationally exposed to pesticides. *Food Chem Toxicol.* (2021) 151:112127. doi: 10.1016/j.fct.2021.112127

62. Gong L, Guo S, Zou Z. Resveratrol ameliorates metabolic disorders and insulin resistance in high-fat diet-fed mice. *Life Sci.* (2020) 242:117212. doi: 10.1016/j.lfs.2019.117212

63. Zhou J, Yu Y, Ding L, Xu P, Wang Y. Matcha green tea alleviates non-alcoholic fatty liver disease in high-fat diet-induced obese mice by regulating lipid metabolism and inflammatory responses. *Nutrients.* (2021) 13:1950. doi: 10.3390/nu13061950

64. Li S, Xu Y, Guo W, Chen F, Zhang C, Tan HY, et al. The Impacts of Herbal Medicines and Natural Products on Regulating the Hepatic Lipid Metabolism. *Front Pharmacol.* (2020) 11:351. doi: 10.3389/fphar.2020.00351

65. Hsu WH, Chen TH, Lee BH, Hsu YW, Pan TM. Monascin and ankaflavin act as natural AMPK activators with PPARalpha agonist activity to down-regulate nonalcoholic steatohepatitis in high-fat diet-fed C57BL/6 mice. *Food Chem Toxicol.* (2014) 64:94–103. doi: 10.1016/j.fct.2013.11.015

66. Meng Q, Duan XP, Wang CY, Liu ZH, Sun PY, Huo XK, et al. Alisol B 23-acetate protects against non-alcoholic steatohepatitis in mice via farnesoid X receptor activation. *Acta Pharmacol Sin.* (2017) 38:69–79. doi: 10.1038/aps.2016.119

67. Fullerton MD, Galic S, Marcinko K, Sikkema S, Pulinilkunnil T, Chen ZP, et al. Single phosphorylation sites in Acc1 and Acc2 regulate lipid homeostasis and the insulin-sensitizing effects of metformin. *Nat Med.* (2013) 19:1649–54. doi: 10.1038/nm.3372

68. Fang K, Wu F, Chen G, Dong H, Li J, Zhao Y, et al. Diosgenin ameliorates palmitic acid-induced lipid accumulation via AMPK/ACC/CPT-1A and SREBP-1c/FAS signaling pathways in LO2 cells. *BMC Complement Altern Med.* (2019) 19:255. doi: 10.1186/s12906-019-2671-9

69. Lei P, Tian S, Teng C, Huang L, Liu X, Wang J, et al. Sulforaphane improves lipid metabolism by enhancing mitochondrial function and biogenesis in vivo and in vitro. *Mol Nutr Food Res.* (2019) 63:e1800795. doi: 10.1002/mnfr.201800795

70. Heintz-Buschart A, Wilmes P. Human gut microbiome: function matters. *Trends Microbiol.* (2018) 26:563–74. doi: 10.1016/j.tim.2017.11.002

71. Wang P, Gao J, Ke W, Wang J, Li D, Liu R, et al. Resveratrol reduces obesity in high-fat diet-fed mice via modulating the composition and metabolic function of the gut microbiota. *Free Radic Biol Med.* (2020) 156:83–98. doi: 10.1016/j.freeradbiomed.2020.04.013

72. Xu P, Hong F, Wang J, Cong Y, Dai S, Wang S, et al. Microbiome remodeling via the montmorillonite adsorption-excretion axis prevents obesity-related metabolic disorders. *EBioMedicine.* (2017) 16:251–61. doi: 10.1016/j.ebiom.2017.01.019

73. Sun Z, Yu Z, Wang B. Perilla frutescens leaf alters the rumen microbial community of lactating dairy cows. *Microorganisms.* (2019) 7:562. doi: 10.3390/microorganisms7110562

74. Bai J, Hu Y, Bruner DW. Composition of gut microbiota and its association with body mass index and lifestyle factors in a cohort of 7-18 years old children from the American Gut Project. *Pediatr Obes.* (2019) 14:e12480. doi: 10.1111/ijpo.12480

75. Chen X, Sun H, Jiang F, Shen Y, Li X, Hu X, et al. Alteration of the gut microbiota associated with childhood obesity by 16S rRNA gene sequencing. *PeerJ.* (2020) 8:e8317. doi: 10.7717/peerj.8317

76. Xie M, Chen G, Wan P, Dai Z, Zeng X, Sun Y, et al. Effects of dicaffeoylquinic acids from ilex kudingcha on lipid metabolism and intestinal microbiota in high-fat-diet-fed mice. *J Agric Food Chem.* (2019) 67:171–83. doi: 10.1021/acs.jafc.8b05444

77. Si X, Shang W, Zhou Z, Strappe P, Wang B, Bird A, et al. Gut Microbiome-Induced Shift of Acetate to Butyrate Positively Manages Dysbiosis in High Fat Diet. *Mol Nutr Food Res.* (2018) 62:1700670. doi: 10.1002/mnfr.201700670

78. Zhou XL, Yan BB, Xiao Y, Zhou YM, Liu TY. Tartary buckwheat protein prevented dyslipidemia in high-fat diet-fed mice associated with gut microbiota changes. *Food Chem Toxicol.* (2018) 119:296–301. doi: 10.1016/j.fct.2018.02.052

79. Kong C, Gao R, Yan X, Huang L, Qin H. Probiotics improve gut microbiota dysbiosis in obese mice fed a high-fat or high-sucrose diet. *Nutrition.* (2019) 60:175–84. doi: 10.1016/j.nut.2018.10.002

80. Chen YJ, Wu H, Wu SD, Lu N, Wang YT, Liu HN, et al. Parasutterella, in association with irritable bowel syndrome and intestinal chronic inflammation. *J Gastroenterol Hepatol.* (2018) 33:1844–52. doi: 10.1111/jgh.14281

frontiers | Frontiers in Nutrition

TYPE Original Research
PUBLISHED 17 May 2023
DOI 10.3389/fnut.2023.1105254

OPEN ACCESS

EDITED BY
Gianni Biolo,
University of Trieste, Italy

REVIEWED BY
Zhijie Michael Yu,
University Health Network (UHN), Canada
Stephanie Shiau,
Rutgers,
The State University of New Jersey,
United States

*CORRESPONDENCE
Evangelista Malindisa
✉ maryvianey12@gmail.com

RECEIVED 22 November 2022
ACCEPTED 13 April 2023
PUBLISHED 17 May 2023

CITATION
Malindisa E, Dika H, Rehman AM, Olsen MF, Francis F, Friis H, Faurholt-Jepsen D, Filteau S and PrayGod G (2023) Dietary patterns and diabetes mellitus among people living with and without HIV: a cross-sectional study in Tanzania.
Front. Nutr. 10:1105254.
doi: 10.3389/fnut.2023.1105254

Dietary patterns and diabetes mellitus among people living with and without HIV: a cross-sectional study in Tanzania

Evangelista Malindisa[1,2]*, Haruna Dika[1], Andrea M. Rehman[3], Mette Frahm Olsen[4], Filbert Francis[5], Henrik Friis[6], Daniel Faurholt-Jepsen[4], Suzanne Filteau[3] and George PrayGod[2]

[1]Department of Physiology, The Catholic University of Health and Allied Sciences Bugando, Mwanza, Tanzania, [2]Mwanza Research Centre, National Institute for Medical Research, Mwanza, Tanzania, [3]Faculty of Epidemiology and Population Health, London School of Hygiene & Tropical Medicine, London, United Kingdom, [4]Department of Infectious Diseases, Rigshospitalet, Copenhagen, Denmark, [5]Tanga Research Centre, National Institute for Medical Research, Tanga, Tanzania, [6]Department of Nutrition, Exercise, and Sports, University of Copenhagen, Copenhagen, Denmark

Background: Due to the complexity of human diets, it is difficult to relate single foods to health outcomes. We aimed to identify the dietary patterns and associated factors and to assess the association of dietary patterns with prediabetes/diabetes among adults living with and without HIV in Tanzania.

Methods: Diet data were collected by a food frequency questionnaire (FFQ) and dietary patterns were derived by principal component analysis (PCA) and reduced rank regression (RRR). The associations between dietary patterns and associated factors as well as with prediabetes/diabetes were assessed using multinomial logistic regression and presented by marginal plots.

Results: Of 572 recruited, 63% were people living with HIV. The mean (±SD) age was 42.6 (±11.7) years and 60% were females. The PCA identified two major dietary patterns, i.e., vegetable-rich pattern (VRP) and vegetable-poor pattern (VPP) whereas RRR identified one dietary pattern, i.e., carbohydrate-dense pattern (CDP). In comparison to females, males had higher adherence to VPP and CDP, but less to VRP. Higher socioeconomic status was associated with higher adherence to VRP and VPP but low adherence to CDP. Compared to HIV-negative participants, people living with HIV had higher adherence to VRP but less adherence to CDP. Compared to younger people, older people had lower adherence to VPP. High adherence to CDP or VRP was positively associated with prediabetes. Higher adherence to VRP was associated with a borderline decrease in diabetes. No association was observed between VPP with either prediabetes or diabetes.

Conclusion: Our findings suggest that dietary patterns may impact the risk of prediabetes and diabetes differently. Awareness of the health benefits of VRP should be encouraged in the community, especially for men who seem to consume fewer vegetables. Longitudinal studies are needed to explore the contribution of dietary patterns to prediabetes/diabetes development in sub-Saharan Africa.

KEYWORDS

dietary patterns, associated factors, prediabetes, diabetes, HIV

Background

Many studies have found that the intake of individual macronutrients and micronutrients may influence health (1, 2). However, due to the complexity of the human diet, it is difficult to conclude if a single food, ingredient, or nutrient is associated with health outcomes (3). Therefore the focus has shifted to investigating the role of the entire diet on health outcomes (3).

Several factors such as food availability, commercial interests, and socioeconomic status (SES) may influence food choices and eating behaviors (4). Studies in high-income countries have suggested higher SES is associated with having a healthier dietary pattern (5). However, similar studies in sub-Saharan Africa (SSA) are few and inconsistent. For example in Ghana, school children from high SES households had an unhealthy eating pattern (6), while in Seychelles wealthy families had a high intake of fruits and vegetables (4). Infectious diseases such as HIV and tuberculosis could influence the choice of dietary patterns (7). In South Africa, it was found that dietary patterns differed by HIV status, but this has not been widely replicated in other parts of Africa (8). A recent study in El Salvador found that children living with HIV had unhealthy dietary patterns, and suggested that dietary patterns in people living with HIV might contribute to malnutrition-related diseases in this population (9). However, such data are limited for both people living with HIV and people with no HIV in SSA. This hinders the development of strategies to improve the intake of healthier diets to reduce the risk of non-communicable diseases (NCDs) like diabetes.

The interplay of traditional risk factors such as obesity, energy-dense diets, and physical inactivity is implicated in reduced insulin secretion, increased insulin resistance, and the development of diabetes mellitus (10). However, diabetes in SSA may have a different etiology, as suggested by data showing a high prevalence of diabetes in non-overweight people and low insulin secretion as well as insulin resistance (11, 12). We aimed to determine dietary patterns and factors associated with and explore the association between dietary patterns with prediabetes and diabetes among adults in Mwanza, Tanzania.

Methods

Study design and area

This analysis was part of the role of environmental enteropathy on HIV-associated diabetes (REEHAD) study, a cross-sectional study investigating the links between environmental enteric dysfunction and diabetes in Mwanza (clinicaltrials.gov NCT03713502). REEHAD is nested within the Chronic Infections, Co-morbidities, and Diabetes in Africa (CICADA) study, a prospective cohort study investigating the burden of, and risk factors for diabetes and other NCDs among Tanzanian adults with and without HIV (13). The REEHAD study enrolled participants between May 2019 and March 2021.

Sample size estimation and recruitment

The sample size was calculated using Open Source Epidemiologic Statistics for Public Health (OpenEpi) sample size calculator for cross-sectional studies 2013 (14, 15). Based on prior data from the CICADA study, we assumed that the proportion of diabetes measured by oral glucose tolerance test (OGTT) in people adhering to healthy patterns and unhealthy patterns are 3 and 10%, respectively (13). To demonstrate these differences between the highest and lowest terciles with 80% power at a 5% significance level, we required a minimum sample size of 555, divided into terciles of adherence to dietary patterns. Participants were consecutively recruited during their clinic visits until this sample size was reached.

Data collection

Socio-demographic characteristics and NCDs behavioral risk factors

Data on socio-demographic characteristics including age, sex, employment status, marital status, and education level were collected using pre-tested structured questionnaires. In addition, data on possession of assets (residential house, electric or gas cooker, bicycle, motorcycle, car, sewing machine, radio, television, air-conditioner, mobile phone, animals (goats/cows), chickens, boat, and any rented property), source of water for domestic use and type of toilet used were collected and used to compute SES score using principal component analysis (PCA) (16) from which the first component was grouped in terciles (i.e., lower, middle and upper) for analysis. The World Health Organization (WHO) Global Physical Activity Questionnaire (GPAQ) was used to collect reported data on the level of physical activity (17). Total physical activity was computed to metabolic equivalents of tasks (MET) in minutes per week and categorized as an adequate level of physical activity if MET was ≥600 as recommended by WHO (18). Smoking status was elicited and grouped as never smoked, past smoker (quit smoking for >1 year), and current smoker (smoking within the past 1 year). Alcohol consumption was grouped as never consumed, past consumption (quit intake for >1 year), and current consumption (consuming within the past 1 year). HIV tests were done during CICADA recruitment as published (13). Antiretroviral therapy (ART) history was collected from participants' ART cards and verified with ART clinic records.

Anthropometric measurements

Body weight was determined to the nearest 0.1 kg using a digital scale (Seca, Germany) while participants were barefoot and with minimal clothing. Height was measured to the nearest 0.1 cm using a stadiometer fixed to the clinic wall (Seca, Germany). BMI was categorized as underweight (BMI < 18.5 kg/m^2), normal weight (BMI 18.5–24.9 kg/m^2), or overweight/obese (BMI ≥ 25 kg/m^2). Waist circumference was measured by a non–stretchable measuring tape to the nearest 0.1 cm taken at the midpoint between the lower costal margin and the iliac crest, with the subject standing erect in a relaxed position and feet placed 25–30 cm apart. Values >94 cm for males

Abbreviations: FFQ, Food frequency questionnaire; BMI, Body mass index; WHO, World Health Organization; GPAQ, Global physical activity questionnaire; HIV, Human immunodeficiency virus; SSA, Sub Saharan Africa; NCD, Non-communicable diseases; PCA, principal component analysis; RRR, reduced rank regression; MET, The metabolic equivalent of tasks; REEHAD, Role of environmental enteropathy on HIV associated diabetes; CICADA, Chronic infections, co-morbidities, and diabetes in Africa cohort.; VRP, Vegetable-rich pattern; VPP, Vegetable-poor dietary pattern; CDP, Carbohydrate-dense dietary pattern; ARRR, adjusted relative risk ratio.

and > 80 cm for females were regarded as abdominal obesity according to WHO (19).

Diabetes assessment

Diabetes was defined by 2 h OGTT. Participants were contacted 1 day before the clinic visit and instructed to fast overnight for at least 8 h and come to the clinic early in the morning (between 8 am to 10 am). Blood for glucose measurement (Hemocue 201 RT, Hemocue AB, Angelholm, Sweden) was drawn from fasted participants. They were then given 82.5 g of dextrose monohydrate (equivalent to 75 g of anhydrous glucose) diluted in 250 ml of drinking water to drink within 5 min for OGTT. We used WHO criteria to classify participants with normal blood glucose (<7.8 mmol/L), prediabetes (7.8–11.0 mmol/L), or diabetes (≥11.1 mmol/L). In addition, we looked at HbA1c as a supplementary test, because it is recommended by WHO in diabetes diagnosis (20, 21), however it underestimates diabetes in hemoglobinopathy and 20% of people in the study population have sickle cell trait (22, 23). Participants were classified as normal (≤ 5.6%), prediabetes (5.7–6.4%), and diabetes (≥6.5%).

Dietary assessment

A food frequency questionnaire (FFQ) was used to assess dietary habits. The FFQ was adapted from the validated Africa/Harvard School of Public Health Partnership for Cohort Research &Training (PaCT) questionnaire (24) which was modified to fit the Tanzanian context. The modified FFQ had over 350 food items that are found in the Tanzania food composition tables (25). Participants were asked to recall the usual intake of food items in terms of frequency and quantity for the past 12 months, and these were then aggregated into 30 food groups based on their nutrient profile and culinary use (26). The groups included refined grains, unrefined grains, mixed dish grains, natural fruits and juices, artificially sweetened beverages, legumes, red meat (beef, goat, and lamb), chicken-based dishes, fish-based dishes, milk, eggs, pork, banana dishes, potato dishes, chips and crisps, yams, pumpkins, cassava dishes, green vegetables, cruciferous vegetables, dark-yellow-orange vegetables, tomatoes, alcohol, sweets and desserts, edible insects, honey and sugar, coffee, mixed-dish tubers, tea without sugar and seeds and nuts.

Generation of dietary patterns

Based on the reported frequencies of intake of each food group, participants were assigned to the eating frequency of each food group into "never" if they never ate, "rarely" if they ate 1–3 times a month, "moderate" if they ate once a week, "regular" if they ate 2–6 per week and "very regular" if they ate on daily basis. Dietary patterns were derived using PCA and reduced rank regression (RRR) as described by Hoffman et al. (27). The two methods are conceptually different, but complementary in understanding the role of dietary patterns on health outcomes (28). PCA derives dietary patterns through data reduction; however, literature has shown that PCA-derived patterns might not be associated with health outcomes of interest (27). On the other hand, RRR analysis derives dietary patterns using intermediate variables or response variables that are known to be associated with the outcome of interest (27, 29). RRR requires a minimum of 2 response variables and in the current analysis, the two response variables were selected based on their strength of association with diabetes and based on previous studies, BMI and waist circumference (30, 31) were selected; both variables were left-skewed and were log-transformed before analysis. For PCA analysis, we checked sample adequacy using Kaiser-Meyer-Olken (KMO) test (32). We also rotated component loadings of the retained factors to create less correlation between the components and facilitate interpretability (32). A Scree plot was used to retain the components for subsequent analysis (Supplementary Figure 1); factors above the elbow of the scree plot were retained (32).

Data management and analysis

Data were entered into CSPro and analyzed in STATA 15. Background characteristics of the study participants (i.e., age categories, sex, marital status, SES, employment status, alcohol drinking, physical activity, smoking, body fat, BMI, HIV status, and education level) were presented as counts (percentages) or means (SD) as appropriate. In addition, we investigated the differences in continuous and categorical variables between REEHAD participants included in this analysis and those not included using student *t*-test and chi-squared test, respectively. For the analysis of factors associated with dietary patterns, dietary pattern scores (defined by PCA or RRR and divided into terciles, upper tercile representing high adherence to the pattern and the lower tercile representing low consumption) were the primary outcomes while background factors (age, sex, HIV status, SES, employment status, education level, and physical activity) were the main predictor factors. For analyses exploring associations of dietary patterns and diabetes, dietary patterns were the exposure while the above background factors were adjusted for potential confounders. Multinomial logistic regression was used to assess associations between outcome variables and independent variables. In addition, the associations between dietary patterns with prediabetes and diabetes were presented by marginal effects plots. p value <0.05 was considered statistically significant.

Results

Of 1,174 participants recruited in the REEHAD study, 572 (49%) with diet data were included in the current analysis. There were no differences between REEHAD participants included and those not included in the analysis except that those included had more self-employed participants (overall $p = 0.01$; Table 1). The mean (±SD) age of the study participants was 43 (±12) years and 59% were females. Over half (57%) of participants were married/cohabiting and most (79%) were self-employed. About 6% were current smokers, 24% were current alcohol drinkers and 63% were people living with HIV and on ART. Prediabetes and diabetes were present in 25 and 4%, respectively (Table 1). The intake frequency of all food groups has been presented in Figure 1.

Dietary patterns

In the PCA of 30 food groups, the first two components, with eigenvalues of 4.3 and 1.7, explained 20% of the total variation and were retained for further analysis (32) (Supplementary Table 1). Kaiser-Meyer-Olkin's measure was 0.8, indicating sampling adequacy (32). Food groups with factor loadings ≥|0.25| were used to name the patterns in each component (26), and high negative loadings were

TABLE 1 Characteristics of the role of environmental enteropathy on HIV-associated diabetes (REEHAD) participants included in the analysis (*N*=572) versus those not analyzed (*N*=600).

Characteristic	Categories	Participants analyzed[1]	Participants not analyzed[1]	Overall *p*-value
Age, mean (SD)[2]	-	42.6 ± 11.7	39.8 ± 11.6	0.91
Sex	Female sex	338 (59)	355 (59.2)	0.95
Education	Never attended school	107 (19)	97 (16.2)	0.08
	Primary school	387 (67.7)	394 (65.7)	
	Secondary School and Higher	78 (13.6)	109 (18.2)	
Marital status	Married/cohabiting	324 (56.7)	336 (56.0)	0.3
	Widowed	86 (15.0)	77 (12.8)	
	Separated/divorced	139 (24.3)	149 (24.8)	
	Single/never married	23 (4.0)	38 (6.3)	
Employment	Salaried employee	60 (10.5)	89 (14.8)	**0.01**
	Self employed	451 (78.8)	425 (70.8)	
	Unemployed/House wife	61 (10.7)	86 (14.4)	
SES terciles	Lower	210 (36.8)	200 (33.3)	0.2
	Middle	198 (34.7)	200 (33.3)	
	Upper	163 (28.6)	200 (33.3)	
Smoking status	Never	433 (75.7)	456 (76.0)	0.9
	Past-smoker	104 (18.2)	105 (17.5)	
	Current smoker	35 (6.1)	39 (6.5)	
Alcohol drinking	Never	174 (30.4)	185 (30.8)	0.9
	Past-drinker	260 (45.5)	266 (44.4)	
	Current-drinker	138 (24.1)	149 (24.8)	
Physical activity	Active (≥600 MET minutes/ week)	547 (95.5)	556 (92.7)	0.05
Waist circumference	Abnormal	255 (44.50)	280 (46.67)	0.46
BMI (kg/m^2), mean (SD)[2]	-	22.5 (4.4)	23.4 (4.9)	0.97
HIV status	HIV positive	362 (63.3)	365 (60.8)	0.38

[1]Values are *n* (%) unless otherwise specified.
[2]Standard deviations.
[1]BMI calculated as weight (kg)/height (m); [2]MET, Metabolic equivalent of tasks; [3]Diabetes was defined by WHO guidelines using oral glucose test results (33).
The bold values show the statistical significant values.

rarely seen (Supplementary Table 2). Component 1 had high positive loadings for natural fruits and juices, bananas, potatoes, green vegetables, cruciferous vegetables, dark orange vegetables, and tomatoes; therefore this component was named vegetable-rich pattern (VRP). Component 2 had high positive loadings for artificially sweetened beverages, red meat, milk, chips and crisps, and alcohol, and a high negative loading for tomatoes, this was named the vegetable-poor pattern (VPP). RRR analysis yielded two factors, of which the first factor explained much more (98%) of the total variance in the intermediate response variables than the second; the first factor was therefore retained for the subsequent analysis. The total variation of the response variables explained by RRR factors was 17.1%, while the variation of predictors, i.e., the food groups, explained by RRR factors was 8.2%. Supplementary Table 3 shows the factor loadings for the RRR retained factors. Refined grains had a factor loading of |0.72| while the rest of the food groups had factor loadings less than |0.25|, this pattern has therefore been named carbohydrate-dense pattern (CDP).

Factors associated with dietary patterns

In fully adjusted models (Table 2), males had lower adherence to VRP than women (OR 0.4, 95% CI 0.3, 0.7). In comparison to participants in the lower socio-economic class, those in the upper socio-economic class had higher adherence to VRP (OR 2.3, 95% CI 1.3, 4.1). Compared with those who never attended school; primary school and secondary school (or above) attendees had higher adherence to VRP (OR 1.8, 95% CI 1.0, 3.3 and OR 6.8, 95% CI 2.6, 17.6 respectively). Participants with HIV had higher adherence to VRP than those without HIV (OR 2.0, 95% CI 1.3, 3.2). Age, physical activity, and employment status had no significant association with VRP (Table 2).

Compared to women, males had higher adherence to VPP (OR 3.9, 95% CI 2.3, 6.3). In comparison to younger age groups; older age groups had lower adherence to VPP (OR 0.3, 95% CI 0.2, 0.7). Participants in the middle and upper SES class had higher adherence

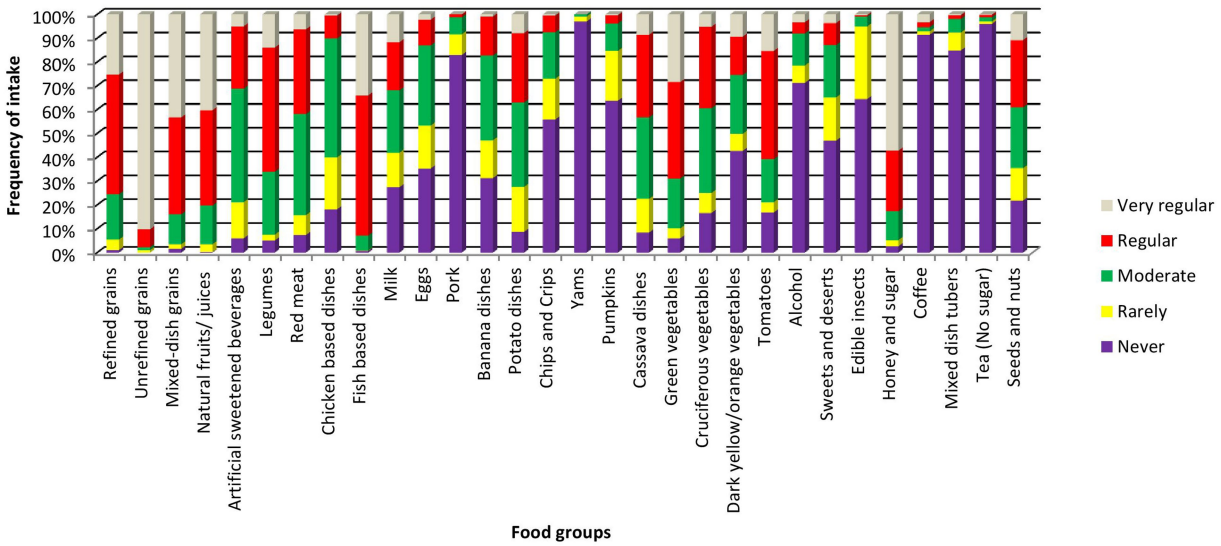

FIGURE 1
Frequencies of intake of the food groups. Very regular; if eaten on daily basis, regular; if eaten 2-6 per week, moderate; if eaten once a week, rarely; if eaten1-3 times a month, never; if was never eaten.

to VPP than participants in the lower class (OR 2.3, 95% CI 1.4, 4.0 and OR 5.4, 95% CI 2.9, 10.2 respectively). Selfand salary-employed participants had higher adherence to VPP than the unemployed and housewives (OR 2.7, 95% CI 1.1, 6.3 and OR 4.5, 95% CI 1.5, 13.8 respectively). Physical activity, education level, and HIV status had no significant association with VPP scores (Table 3).

In comparison to women, males had higher adherence to CDP (OR 1.7, 95% CI 1.1, 2.8). Participants in the upper socioeconomic class had lower adherence to CDP compared to those in the low socioeconomic class (OR 0.3, 95% CI 0.2, 0.6). Participants living with HIV had lower adherence to CDP than participants living without HIV (OR 0.5, 95% CI 0.31, 0.8). Age, physical activity, education level, and employment status were not associated with CDP (Table 4).

Association of dietary patterns with prediabetes and diabetes

Using 2 h OGTT data, in a fully adjusted models, compared to the lower tercile, high VRP consumption was associated with a greater risk of prediabetes (ARRR = 2.12, 95% CI: 1.24, 3.66) but inversely associated with diabetes (ARRR = 0.26, 95% CI: 0.07, 0.95). High adherence to CDP was positively associated with prediabetes (ARRR = 1.92, 95% CI 1.12, 3.29), but there was no association with frank diabetes. VPP consumption was not significantly associated with either prediabetes or diabetes. Figure 2 shows the marginal plots for the probabilities of prediabetes and diabetes across the terciles of dietary patterns after fully adjusted multinomial logistic regression models. In VRP, the probability of having prediabetes increases in the upper tercile, while there is no change in the probability of having diabetes. There are no observed changes in the probability of having prediabetes or diabetes in the upper tercile of VPP. In CDP, there is an increased probability of having prediabetes, and a slight increase in the probability of diabetes in the upper tercile.

Using HbA1c data, in fully adjusted models, we observed no significant associations between prediabetes and diabetes with terciles of all 3 dietary patterns (Supplementary Figure 2).

Discussion

Among adult Tanzanians, we found that higher adherence to VRP was positively associated with the female sex, higher SES, high level of education, and living with HIV. Higher adherence to VPP was positively associated with male sex, higher SES, younger age, and having employment. Higher adherence to CDP was positively associated with the male sex, lower SES, and living without HIV. Higher adherence to VRP was associated with a lower probability of having diabetes, but surprisingly it was associated with a higher probability of pre-diabetes. Higher adherence to CDP was associated with increased probabilities of prediabetes as well as diabetes. VPP was not associated with either prediabetes or diabetes.

Studies on the association between SES and dietary patterns in high-income countries have observed people from higher socioeconomic classes eat healthier foods, including vegetables and fruits, than those in the low socioeconomic class (4, 5, 34, 35). Data on SES and dietary patterns in low-and middle-income countries (LMIC) are few with different directions of associations (5). A multinational study conducted among children in 11 LMICs including Kenya (the ISCOLE study) observed that higher SES was associated with a healthy diet (35). On the other hand, a review of cross-sectional studies of LMIC found a positive association between higher SES and unhealthy diets in some studies (5). The finding that SES is associated with higher scores of both healthy (VRP) and unhealthy (VPP) diets suggests that relatively wealthy people in Tanzania consume both healthy and unhealthy foods. Unlike the situation in high-resource settings where healthy foods including vegetables and fruits are expensive, in Tanzania vegetables are less expensive compared to fast foods (36). Thus, the intake of unhealthy foods among those from

10.3389/fnut.2023.1105254

TABLE 2 Socio-demographic characteristics associated with terciles of vegetable-rich pattern scores.

		Univariable model				Multivariable model			
		Middle tercile		Upper tercile		Middle tercile		Upper tercile	
		Relative risk ratio (95% CI)	Overall *P*	Relative risk ratio, 95% CI	Overall *P*	Adjusted relative risk ratio, 95% CI	Overall *P*	Adjusted relative risk ratio, 95% CI	Overall *P*
Sex	Female	Reference	0.09	Reference	**0.01**	Reference	**0.01**	Reference	**<0.001**
	Male	0.7 (0.5, 1.1)		0.6 (0.4, 0.9)		0.5 (0.3, 0.8)		0.4 (0.3, 0.7)	
Age (years)	18–30	Reference	0.4	Reference	0.2	Reference	0.5	Reference	0.8
	31–40	1(0.5, 1.9)		0.8 (0.4, 1.5)		1.3 (0.7, 2.5)		1.1 (0.6, 2.1)	
	41–50	0.7 (0.4, 1.3)		0.6 (0.3, 1.1)		0.9 (0.5, 1.8)		0.8 (0.4, 1.6)	
	50+	0.8 (0.4, 1.5)		0.5 (0.3, 1)		1.3 (0.6, 2.6)		0.96 (0.5, 1.97)	
SES[1]	Lower	Reference	**0.003**	Reference	**<0.001**	Reference	**0.02**	Reference	**0.02**
	Middle	1.7 (1.1, 2.8)		1.5 (0.9, 2.5)		1.8 (1.1, 2.9)		1.5 (0.9, 2.5)	
	Upper	2.5(1.5, 4.2)		2.8 (1.6, 4.6)		2.1 (1.2, 3.8)		2.3(1.3, 4.1)	
PA[2]	Not active	Reference	0.9	Reference	0.8	Reference	0.95	Reference	0.98
	Active	1 (0.4, 2.6)		1.1 (0.4, 2.98)		1.03 (0.4, 2.9)		0.98 (0.3, 2.8)	
Edu. level[3]	Never attended	Reference	**0.002**	Reference	**<0.001**	Reference	**0.01**	Reference	**<0.001**
	Primary	1.2 (0.7, 1.96)		1.8 (1, 3)		1.1 (0.7, 1.96)		1.8 (1.03, 3.3)	
	Secondary and above	4.2 (1.8, 9.7)		6.6(2.8, 15.6)		4.0 (1.6, 10.1)		6.8 (2.6, 17.6)	
Employment	Unemployed/ house wife	Reference	0.09	Reference	0.6	Reference	0.07	Reference	0.6
	Self-employment/ other	1.4(0.7, 2.7)		1 (0.5, 1.9)		1.6 (0.8, 3.4)		1.2 (0.6, 2.4)	
	Salary employed	2.7 (1.1, 6.6)		1.5 (0.6, 3.7)		3.2 (1.2, 8.7)		1.7 (0.6, 4.5)	
HIV status	Negative	Reference	0.09	Reference	**0.04**	Reference	**0.01**	Reference	**0.003**
	Positive	1.4 (0.95, 2.2)		1.6 (1, 2.4)		1.8 (1.1, 2.8)		2(1.3, 3.2)	

[1]Socioeconomic status.
[2]Physical activity.
[3]Education level.
Variables (i.e., sex, age, HIV, socioeconomic status, physical activity, education level and employment) adjusted for each other. Lower tercile is the reference for the middle and upper terciles.
The bold values show the statistical significant values.

high socioeconomic classes may be due to inappropriate perceptions, cultural beliefs, and lack of education on the role of vegetables and fruits in healthy living, although we found the association was independent of the level of education. On the other hand, low adherence to VRP among those with low SES may reflect the inability to afford healthy foods due to extreme poverty.

Similar to many other studies, gender differences have an impact on adherence to dietary patterns; this is due to differences in roles, behavior, and attitudes that exist between different genders. Compared to women, men had higher scores of VPP and CDP. Women had higher scores of VRP but relatively lower scores of VPP and CDP. This result is in agreement with many other studies (37, 38), and the possible explanation is that women may avoid foods that may increase their weight, although there is no evidence for this in Tanzania where cultural perspectives of weight gain have been different (37). Another explanation would be that men go more frequently to fast food restaurants; studies in the USA have reported that men eat more restaurant meals and fast foods than women (39, 40). This is likely to be the same in Tanzania, although published data are limited, where it is rare to find vegetables and fruits incorporated in the food menu of the local restaurants, possibly explaining why men do not take as much of VRP. The majority of those who drink alcohol are men, and most bars sell beers together with red meat (Swahili "nyamachoma") and fried potatoes with eggs (Swahili "chips mayai") (41).

The positive association between HIV infection and higher scores of VRP observed in this study may be explained by the fact that national guidelines on support for people with HIV emphasize that people with HIV should be encouraged to meet their vitamin and mineral needs from their diet by eating a variety of fruits and vegetables (42).

In the current study, increasing age (>40 years) was negatively associated with higher scores of VPP. Similar findings have been reported in Taiwan (43), the Republic of Seychelles (4), and Serbia where older people ate healthier diets than the young populations

TABLE 3 Socio-demographic characteristics associated with terciles of vegetable-poor pattern scores.

		Univariable model				Multivariable model			
		Middle tercile		Upper tercile		Middle tercile		Upper tercile	
		Relative risk ratio, (95% CI)	Overall *P*	Relative risk ratio, 95% CI	Overall *P*	Adjusted Relative risk ratio, 95% CI	Overall *P*	Adjusted Relative risk ratio, 95% CI	Overall *P*
Sex	Female	Reference	**0.02**	Reference	**<0.001**	Reference	**0.01**	Reference	**<0.001**
	Male	1.7 (1.1, 2.6)		3.9 (2.5, 5.9)		1.8 (1.1, 3)		3.9 (2.3, 6.3)	
Age (years)	18–30	Reference	0.2	Reference	0.06	Reference	0.1	Reference	**0.01**
	31–40	0.7 (0.4, 1.3)		0.7 (0.4, 1.3)		0.7 (0.3, 1.3)		0.6 (0.3, 1.2)	
	41–50	0.5 (0.3, 0.9)		0.5 (0.2, 0.9)		0.5 (0.2, 0.9)		0.3 (0.2, 0.7)	
	50+	0.8 (0.4, 1.5)		0.5 (0.3, 0.98)		0.7 (0.3, 1.4)		0.3 (0.2, 0.7)	
SES[1]	Lower	Reference	**0.01**	Reference	**<0.001**	Reference	**0.01**	Reference	**<0.001**
	Middle	1.2 (0.8, 1.9)		2.2 (1.4, 3.7)		1.3 (0.8, 2)		2.3 (1.4, 4)	
	Upper	2.4 (1.4, 4.2)		6.2 (3.6, 10.9)		2.4 (1.3, 4.4)		5.4 (2.9, 10.2)	
PA[2]	Not active	Reference	0.99	Reference	0.07	Reference	0.8	Reference	0.4
	Active	0.99 (0.3, 3.1)		0.4 (0.2, 1.1)		1.2 (0.4, 4)		0.6 (0.2, 1.9)	
Edu. level[3]	Never attended	Reference	**0.02**	Reference	**<0.001**	Reference	0.2	Reference	0.30
	Primary	1.9 (1.2, 3.2)		2.4 (1.4, 4.2)		1.6 (0.9, 2.7)		1.5 (0.8, 2.7)	
	Secondary and above	2.6 (1.1, 5.8)		7.4 (3.4, 16.2)		1.4 (0.6, 3.4)		2 (0.8, 4.9)	
Employment	Unemployed/ house wife	Reference	0.9	Reference	**<0.001**	Reference	0.9	Reference	**0.03**
	Self-employment/ other	1.1 (0.6, 1.9)		2.8 (1.3, 6.2)		1.1 (0.6, 2)		2.7 (1.1, 6.3)	
	Salary employed	1.3 (0.5, 3.4)		9.8 (3.6, 27)		0.9 (0.3, 2.5)		4.5 (1.5, 13.8)	
HIV status	Negative	Reference	0.8	Reference	0.8	Reference	0.2	Reference	0.1
	Positive	1.1 (0.7, 1.6)		0.9 (0.6, 1.4)		1.4 (0.9, 2.2)		1.5 (0.9, 2.4)	

[1]Socioeconomic status.
[2]Physical activity.
[3]Education level.
Variables (i.e., sex, age, HIV, socioeconomic status, physical activity, education level and employment) adjusted for each other. Lower tercile is the reference for the middle and upper terciles.
The bold values show the statistical significant values.

(44). This may suggest that people over 40 years of age may be aware of their increased risk of NCDs like diabetes, therefore they may be avoiding unhealthy diets. It is also possible that the dietary transition from traditional healthy diets to junk foods has less affected older people who have preserved their preference more for VRP and less for VPP than the younger ones.

We expected to observe a negative association between VRP with prediabetes and diabetes (45), unexpectedly; the VRP was associated with an increased risk of prediabetes. We also expected positive associations between VPP and CDP with prediabetes and diabetes (46). We found that the CDP was associated with a higher risk of prediabetes but, VPP showed no association with either prediabetes or diabetes. Similar to our study, a recent study in Tanzania reported a lack of association between unhealthy dietary pattern with adiposity in adolescents (47). Another study in Tanzania has found a lack of association between being overweight and prediabetes/diabetes (13), indicating that prediabetes/diabetes in SSA may not be linked to being overweight and hence not driven by the traditional risk factors known from studies in high-income countries.

Our findings could be explained by the fact people with high SES take both VRP and VPP. The intake of unhealthy diets may overwhelm the beneficial effects of VRP leading to a higher risk of prediabetes. Although we adjusted for SES, based on an asset index, this may not have completely removed the effect of SES which includes other aspects in addition to asset ownership. Unlike associations of prediabetes with presumably healthy diets, we found that VRP lowered diabetes risk. This may reflect the beneficial effects of vegetables and fruits intake since it is known that vegetable and fruits contain antioxidants that may reduce insulin resistance and β-cells apoptosis thus reducing the risk of diabetes (48). While recall bias is a known problem with diet assessment by FFQ, this was likely to be similar across diabetes groups since we did not specifically inform study participants that FFQ were meant to collect data to

TABLE 4 Socio-demographic characteristics associated with terciles of carbohydrate-dense pattern scores.

		Univariable model				Multivariable model			
		Middle tercile		Upper tercile		Middle tercile		Upper tercile	
		Relative risk ratio, (95% CI)	Overall *P*	Relative risk ratio, 95% CI	Overall *P*	Adjusted Relative risk ratio, 95% CI	Overall *P*	Adjusted Relative risk ratio, 95% CI	Overall *P*
Sex	Female	Reference	**0. 003**	Reference	**<0.001**	Reference	**<0.001**	Reference	**0.03**
	Male	0.5 (0.4, 0.8)		0.4 (0.2, 0.6)		3.8 (2.3, 6.3)		1.7 (1.1, 2.8)	
Age (years)	18–30	Reference	0.2	Reference	0.05	Reference	0.5	Reference	0.5
	31–40	1.4 (0.8, 2.8)		0.8 (0.4, 1.5)		0.9 (0.5, 1.9)		1.6(0.9, 3)	
	41–50	0.8 (0.4, 1.6)		0.5 (0.3, 0.9)		1.5 (0.7, 2.9)		1.6 (0.8, 3)	
	50+	0.9 (0.5, 1.8)		0.6 (0.3, 1.1)		0.98 (0.5, 2.1)		1.2 (0.6, 2.5)	
SES[1]	Lower	Reference	**<0.001**	Reference	**<0.001**	Reference	**<0.001**	Reference	**0.001**
	Middle	0.5 (0.3, 0.8)		0.6 (0.4, 1.1)		0.5 (0.3, 0.8)		0.6 (0.3, 1)	
	Upper	0.1 (0.06, 0.2)		0.4 (0.2, 0.6)		0.1 (0.04, 0.2)		0.3 (0.2, 0.6)	
PA[2]	Not active	Reference	0.5	Reference	0.3	Reference	0.5	Reference	0.9
	Active	1.4 (0.6, 3.6)		1.6 (0.6, 4.2)		0.7 (0.2, 2)		1.1 (0.4, 3.2)	
Edu. level[3]	Never attended	Reference	0.4	Reference	**0.01**	Reference	0.2	Reference	0.5
	Primary	1.3 (0.8, 2.2)		1.7 (1, 3)		0.6 (0.3, 1.1)		0.8 (0.5, 1.5)	
	Secondary and above	1.6 (0.8, 3.5)		3.5 (1.6, 7.3)		0.5 (0.2, 1.2)		0.6 (0.3, 1.4)	
Employment	Unemployed/ house wife	Reference	0.9	Reference	0.2	Reference	0.6	Reference	0.7
	Self-employment/ other	1.04 (0.5, 2.1)		0.7 (0.4, 1.4)		1.1 (0.5, 2.3)		1.1 (0.6, 2.3)	
	Salary employed	1.2 (0.5, 3.02)		1.3 (0.5, 3.1)		0.7 (0.2, 2)		0.8 (0.3, 2.2)	
HIV status	Negative	Reference	0.2	Reference	0.4	Reference	**0.02**	Reference	**0.003**
	Positive	0.8 (0.5, 1.2)		1.2 (0.8, 1.9)		0.5 (0.3,0.9)		0.5 (0.31, 0.8)	

[1]Socioeconomic status.
[2]Physical activity.
[3]Education level.
Variables (i.e., sex, age, HIV,SES, physical activity, education level and employment) adjusted for each other.
Lower tercile is the reference for the middle and upper terciles. The bold values show the statistical significant values.

assess their risk for diabetes, and data collectors were unaware of diabetes status of participants.

This study had several strengths and limitations. First, we included both people living with HIV and people with no HIV, which increases the generalizability of findings. Secondly, we have used two different methods to derive dietary patterns; while PCA-derived patterns reflect general dietary behavior in the population, RRR-derived pattern reflects a dietary pattern that associates with the response variables (BMI and waist circumference) which are the markers of the diseases of interest (prediabetes and diabetes in the current study) (29). The use of the two methods has led to different patterns that have fostered the understanding of the behavioral dietary patterns but also the patterns that associate with the markers of diabetes (49). This study also had several limitations: it was cross-sectional thus causality cannot be confirmed and involved participants from previous cohorts so survival bias may have been introduced. Another limitation is, these participants were from a cohort, it is possible that some of them were previously diagnosed with prediabetes or diabetes and could have changed their diet recently. Also, we have used 2 h OGTT results to define prediabetes and diabetes in the current study; this may underestimate the diabetes burden in this population. Although we also used HbA1c, this is less reliable in this population, it under-diagnoses diabetes in hemoglobinopathies (20), and about 20% of this population has sickle cell trait (22, 23). Fasting blood glucose levels have been high in this population (13), questioning the influence of other factors as reported elsewhere (13, 50).

Conclusion

Our findings suggest that dietary patterns may impact the risk of prediabetes and diabetes differently. Education for adherence to VRP

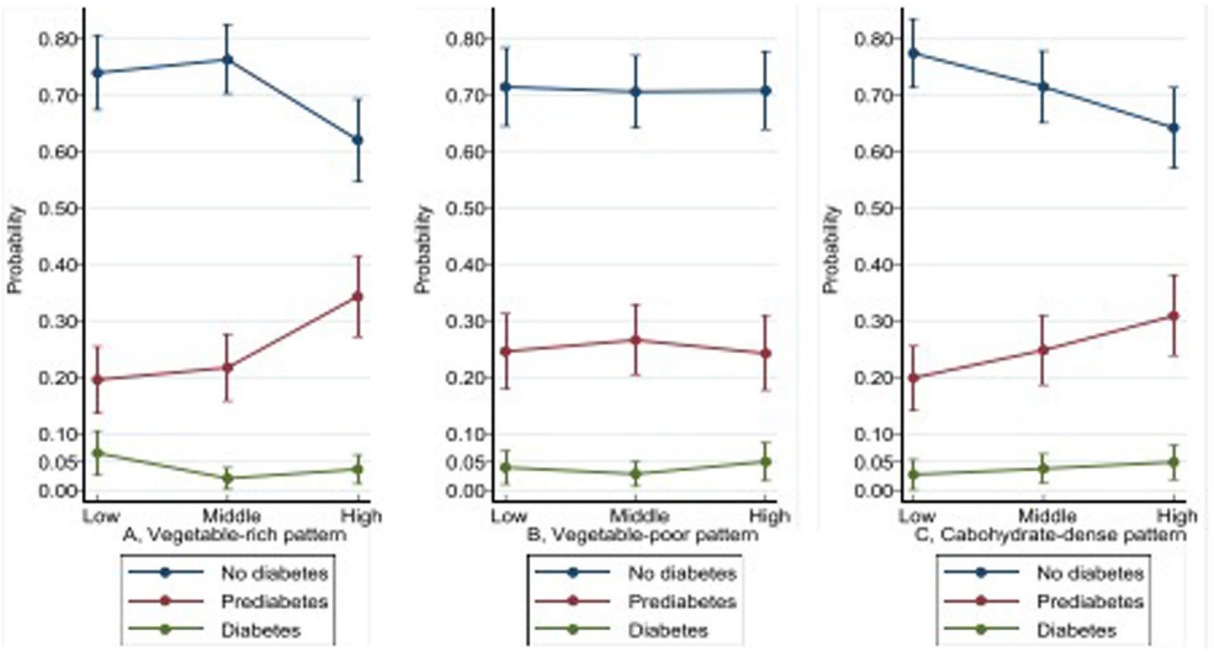

FIGURE 2
Distribution of the probabilities of prediabetes and diabetes across terciles of dietary patterns Vegetable-rich pattern: (vegetables, banana based dishes, potato based dishes, natural fruits and juices). Vegetable–poor: (artificial sweetened beverages, milk, red meat, alcohol, chips and crisps). Carbohydrate-dense pattern: (unrefined grains (rice, millet, wheat, maize)). Multivariable analyses have been adjusted for the age, sex, socio-economic status, education level, physical activity, HIV status and for other pattern in PCA-derived patterns. Diabetes status was based on blood glucose at 120min in an oral glucose tolerance test: no-diabetes <7.8mmol/L (reference); prediabetes: 7.8–11.0mmol/L; diabetes ≥11.1mmol/L.

should be encouraged in the community, especially for men who seem to consume fewer vegetables. Longitudinal studies should be conducted to explore the contribution of dietary patterns on prediabetes and diabetes mellitus in sub-Saharan Africa.

Data availability statement

The datasets presented in this article are not readily available because include de-identified data that cannot be shared publicly, and according to Tanzanian ethics guidelines, it is not possible to share any data including de-identified data without approval of the Medical Research Coordinating Committee (MRCC). Data are available from the National Institute for Medical Research (NIMR) and can be shared with researchers who meet the criteria for access to confidential data only after completing a data transfer agreement and approval by the MRCC. Requests to access the datasets should be directed to ethics@nimr.or.tz.

Ethics statement

This study received ethical approval from the Medical Research Coordinating Committee of the National Institute for Medical Research and the joint Catholic University of Health and Allied Sciences/Bugando Medical Center Research Ethics and Review Committee. In addition, the CICADA study was approved by the Research Ethics Committee of the London School of Hygiene and Tropical Medicine, and consultative approval was provided by the National Committee on Health Research Ethics in Denmark. All methods were under the Declaration of Helsinki. Participants were enrolled after written informed consent and those with diabetes and other illnesses were referred to Sekou-Toure referral hospital for care.

Author contributions

EM, DF-J, AR, HF, SF, and GP conceived the study. EM, HD, and GP collected data. EM analyzed data with help from FF and AR and wrote the first draft. All authors contributed to the article and approved the submitted version.

Funding

This project is part of the EDCTP2 program supported by the European Union (grant agreement number: TMA2017GSF-1965-REEHAD). It received additional support from the Ministry of Foreign Affairs of Denmark through DANIDA Fellowship Centre (grant: 16-P01-TAN). The funding agencies had no role in the study design, data collection and analysis, and decision to publish results. The information contained in this publication is not the responsibility of the funding agencies, and any use of it is not their responsibility either.

Acknowledgments

The authors thank all participants of this study. Sincere appreciations go to the Clinical Research department staff at NIMR and Physiology department staff at CUHAS for their support.

Conflict of interest

The authors declare that the research was conducted in the absence of any commercial or financial relationships that could be construed as a potential conflict of interest.

Publisher's note

Supplementary material

The Supplementary material for this article can be found online at: https://www.frontiersin.org/articles/10.3389/fnut.2023.1105254/full#supplementary-material

SUPPLEMENTARY FIGURE 1
Sree plot of Eigenvalues after PCA.

SUPPLEMENTARY FIGURE 2
Distribution of the probabilities of prediabetes and diabetes across terciles of dietary patterns Vegetable-rich pattern: (vegetables, banana based dishes, potato based dishes, natural fruits and juices).Vegetable–poor: (artificial sweetened beverages, milk, red meat, alcohol, chips and crisps). Carbohydrate-dense pattern: (unrefined grains (rice, millet, wheat, maize)). Multivariable analyses have been adjusted for the age, sex, socio-economic status, education level, physical activity, HIV status and for other pattern in PCA-derived patterns. Diabetes status was based on HbA1c: no-diabetes ≤ 5.6% (reference); prediabetes: 5.7-6.4% diabetes ≥ 6.5%.

References

1. Jansen J, Karges W, Rink L. Zinc and diabetes — clinical links and molecular mechanisms. *J Nutr Biochem*. (2009) 20:399–417. doi: 10.1016/j.jnutbio.2009.01.009

2. Anhe FF, Roy D, Pilon G, Dudonne S, Matamoros S, Varin TV, et al. A polyphenol-rich cranberry extract protects from diet-induced obesity, insulin resistance and intestinal inflammation in association with increased Akkermansia spp. population in the gut microbiota of mice. *Gut*. (2015) 64:872–83. doi: 10.1136/gutjnl-2014-307142

3. Slattery ML. Analysis of dietary patterns in epidemiological research. *Appl Physiol Nutr Metab*. (2010) 35:207–10. doi: 10.1139/H10-006

4. Mayen AL, Bovet P, Marti-Soler H, Viswanathan B, Gedeon J, Paccaud F, et al. Socioeconomic differences in dietary patterns in an east African country: evidence from the Republic of Seychelles. *PLoS One*. (2016) 11:e0155617. doi: 10.1371/journal.pone.0155617

5. Hinnig PF, Monteiro JS, de Assis MAA, Levy RB, Peres MA, Perazi FM, et al. Dietary patterns of children and adolescents from high, medium and low human development countries and associated socioeconomic factors: a systematic review. *Nutrients*. (2018) 10:436. doi: 10.3390/nu10040436

6. Abizari AR, Ali Z. Dietary patterns and associated factors of schooling Ghanaian adolescents. *J Health Popul Nutr*. (2019) 38:5. doi: 10.1186/s41043-019-0162-8

7. Baum MK, Tamargo JA, Wanke C. Nutrition in HIV and tuberculosis In: DL Humphries, ME Scott and SH Vermund, editors. *Nutrition and infectious diseases: Shifting the clinical paradigm*. Cham: Springer International Publishing (2021). 243–81.

8. Annan RAJA, Margetts BM, Vorster H. Dietary patterns and nutrient intakes of a south African. *Afr J Food Agric Nutr Dev*. (2015) 15:9838–54.

9. Martin-Canavate R, Sonego M, Sagrado MJ, Escobar G, Rivas E, Ayala S, et al. Dietary patterns and nutritional status of HIV-infected children and adolescents in El Salvador: a cross-sectional study. *PLoS One*. (2018) 13:e0196380. doi: 10.1371/journal.pone.0196380

10. Bailey RR, Singleton JR, Majersik JJ. Association of obesity and diabetes with physical activity and fruit and vegetable consumption in stroke survivors. *Fam Pract*. (2021) 38:56–61. doi: 10.1093/fampra/cmaa101

11. Kibirige D, Sekitoleko I, Lumu W, Jones AG, Hattersley AT, Smeeth L, et al. Understanding the pathogenesis of lean non-autoimmune diabetes in an African population with newly diagnosed diabetes. *Diabetologia*. (2022) 65:675–83. doi: 10.1007/s00125-021-05644-8

12. Filteau S, PrayGod G, Rehman AM, Peck R, Jeremiah K, Krogh-Madsen R, et al. Prior undernutrition and insulin production several years later in Tanzanian adults. *Am J Clin Nutr*. (2021) 113:1600–8. doi: 10.1093/ajcn/nqaa438

13. Jeremiah K, Filteau S, Faurholt-Jepsen D, Kitilya B, Kavishe BB, Krogh-Madsen R, et al. Diabetes prevalence by HbA1c and oral glucose tolerance test among HIV-infected and uninfected Tanzanian adults. *PLoS One*. (2020) 15:e0230723. doi: 10.1371/journal.pone.0230723

14. Dean AG, Sullivan KM, MM S. Open source epidemiologic statistics for public health (2013) (cited 2022 26/8). Available from: https://www.openepi.com/SampleSize/SSCohort.htm.

15. Charan J, Biswas T. How to calculate sample size for different study designs in medical research? *Indian J Psychol Med*. (2013) 35:121–6. doi: 10.4103/0253-7176.116232

16. Filmer D, Pritchett LH. Estimating wealth effects without expenditure data—or tears: an application to educational enrollments in states of India. *Demography*. (2001) 38:115–32. doi: 10.2307/3088292

17. Cleland CL, Hunter RF, Kee F, Cupples ME, Sallis JF, Tully AMA. Validity of the global physical activity questionnaire (GPAQ) in assessing levels and change in moderate-vigorous physical activity and sedentary behaviour. *BMC Public Health*. (2014) 14. doi: 10.1186/1471-2458-14-1255

18. Chu AH, Ng SH, Koh D, Muller-Riemenschneider F. Reliability and validity of the self-and interviewer-administered versions of the global physical activity questionnaire (GPAQ). *PLoS One*. (2015) 10:e0136944. doi: 10.1371/journal.pone.0136944

19. Organization WH. *Waist Circumference and Waist–Hip Ratio: Report of a WHO Expert Consultation*, Geneva: WHO (2011), 8–11.

20. WHO. *Diagnosis and Management of Type 2 Diabetes (HEARTS-D)*. Geneva: (2020).

21. American Diabetes Association Professional Practice C. 2. Classification and diagnosis of diabetes: standards of medical Care in Diabetes-2022. *Diabetes Care*. (2022) 45:S17–38. doi: 10.2337/dc22-S002

22. Ambrose EE, Makani J, Chami N, Masoza T, Kabyemera R, Peck RN, et al. High birth prevalence of sickle cell disease in northwestern Tanzania. *Pediatr Blood Cancer*. (2018) 65:e26735. doi: 10.1002/pbc.26735

23. Kweka B, Lyimo E, Jeremiah K, Filteau S, Rehman AM, Friis H, et al. Influence of hemoglobinopathies and glucose-6-phosphate dehydrogenase deficiency on diagnosis of diabetes by HbA1c among Tanzanian adults with and without HIV: a cross-sectional study. *PLoS One*. (2020) 15:e0244782. doi: 10.1371/journal.pone.0244782

24. Dalal S, Holmes MD, Laurence C, Bajunirwe F, Guwatudde D, Njelekela M, et al. Feasibility of a large cohort study in sub-Saharan Africa assessed through a four-country study. *Glob Health Action*. (2015) 8:27422. doi: 10.3402/gha.v8.27422

25. Lukmanji ZHE, Mlingi N, Assey V. Tanzania food composition tables. Dar-es-salaam, editor. Tanzania: MUHAS,TFNC, HSPH (2008):259.

26. Galbete C, Nicolaou M, Meeks K, Klipstein-Grobusch K, De-Graft Aikins A, Addo J, et al. Dietary patterns and type 2 diabetes among Ghanaian migrants in Europe and their compatriots in Ghana: the RODAM study. *Nutr Diabetes*. (2018):8. doi: 10.1038/s41387-018-0029

27. Hoffmann K, Schulze MB, Schienkiewitz A, Nothlings U, Boeing H. Application of a new statistical method to derive dietary patterns in nutritional epidemiology. *Am J Epidemiol*. (2004) 159:935–44. doi: 10.1093/aje/kwh134

28. Batis C, Mendez MA, Gordon-Larsen P, Sotres-Alvarez D, Adair L, Popkin B. Using both principal component analysis and reduced rank regression to study dietary patterns and diabetes in Chinese adults. *Public Health Nutr*. (2016) 19:195–203. doi: 10.1017/S1368980014003103

29. Weikert C, Schulze MB. Evaluating dietary patterns: the role of reduced rank regression. *Curr Opin Clin Nutr Metab Care*. (2016) 19:341–6. doi: 10.1097/MCO.0000000000000308

30. Böckerman P, Gupta S, Bansal S. Does a rise in BMI cause an increased risk of diabetes?: evidence from India. *PLoS One*. (2020) 15:e0229716. doi: 10.1371/journal.pone.0229716

31. Zhang FL, Ren JX, Zhang P, Jin H, Qu Y, Yu Y, et al. Strong Association of Waist Circumference (WC), body mass index (BMI), waist-to-height ratio (WHtR), and waist-to-hip ratio (WHR) with diabetes: a population-based cross-sectional study in Jilin Province. *China J Diabetes Res*. (2021) 2021:1–9. doi: 10.1155/2021/8812431

32. Stata.com. PCA postestimation commands. Available from: https://www.stata.com/manuals/mvpcapostestimation.pdf ed:Stata.com. (2021):9.

33. Organization WH. Definition and diagnosis of diabetes mellitus and intermediate hyperglycemia: Report of a WHO/IDF consultation. Geneva; (2006). Report No.: 978 92 4 159493 6.

34. Czarnocinska J, Wadolowska L, Lonnie M, Kowalkowska J, Jezewska-Zychowicz M, Babicz-Zielinska E. Regional and socioeconomic variations in dietary patterns in a representative sample of young polish females: a cross-sectional study (GEBaHealth project). *Nutr J*. (2020) 19:26. doi: 10.1186/s12937-020-00546-8

35. Manyanga T, Tremblay MS, Chaput JP, Katzmarzyk PT, Fogelholm M, Hu G, et al. Socioeconomic status and dietary patterns in children from around the world: different associations by levels of country human development? *BMC Public Health*. (2017) 17:457. doi: 10.1186/s12889-017-4383-8

36. Makorere R, Mariki J, Mrisha S. The effect of Price on fresh vegetable choices in selected Markets of Morogoro Region, Tanzania. *Int J Sust Develop Res*. (2019) 5:79–90. doi: 10.11648/j.ijsdr.20190503.13

37. Wah CS. Gender differences in eating behaviour. International journal of Accounting & Business. *Management*. (2016) 4

38. Natalie L, Caine-Bish BS. Gender differences in food preferences of school-aged children and adolescents. *J Sch Health*. (2009) 79:532–40. doi: 10.1111/j.1746-1561.2009.00445.x

39. Paeratakul S, Ferdinand DP, Champagne CM, Ryan DH, Bray GA. Fast-food consumption among US adults and children: dietary and nutrient intake profile. *J Am Diet Assoc*. (2003) 103:1332–8. doi: 10.1016/S0002-8223(03)01086-1

40. Driskell JA, Meckna BR, Scales NE. Differences exist in the eating habits of university men and women at fast-food restaurants. *Nutr Res*. (2006) 26:524–30. doi: 10.1016/j.nutres.2006.09.003

41. Allan E. *Empowerment power: NGOs feminisms in Dar Es Salaam*. Vancouver: The University of British Columbia (2017).

42. Tanzania TURo. National Guidelines for the management of HIV and AIDS. (2019) 132–3.

43. Lin YH, Hsu HC, Bai CH, Wu WC. Dietary patterns among older people and the associations with social environment and individual factors in Taiwan: a multilevel analysis. *Int J Environ Res Public Health*. (2022) 19

44. Stosovic D, Vasiljevic N, Jovanovic V, Cirkovic A, Paunovic K, Davidovic D. Dietary habits of older adults in Serbia: findings from the National Health Survey. *Front Public Health*. (2021) 9:610873. doi: 10.3389/fpubh.2021.610873

45. Shen XM, Huang YQ, Zhang XY, Tong XQ, Zheng PF, Shu L. Association between dietary patterns and prediabetes risk in a middle-aged Chinese population. *Nutr J*. (2020) 19:77. doi: 10.1186/s12937-020-00593-1

46. Gao M, Jebb SA, Aveyard P, Ambrosini GL, Perez-Cornago A, Papier K, et al. Associations between dietary patterns and incident type 2 diabetes: prospective cohort study of 120,343 UK biobank participants. *Diabetes Care*. (2022) 45:1315–25. doi: 10.2337/dc21-2258

47. Mosha MV, Paulo HA, Msuya SE, Grosskurth H, Filteau S. Lack of an association between dietary patterns and adiposity among primary school children in Kilimanjaro Tanzania. *BMC Nutr*. (2022) 8:35. doi: 10.1186/s40795-022-00529-4

48. Chen GC, Koh WP, Yuan JM, Qin LQ, van Dam RM. Green leafy and cruciferous vegetable consumption and risk of type 2 diabetes: results from the Singapore Chinese health study and meta-analysis. *Br J Nutr*. (2018) 119:1057–67. doi: 10.1017/S0007114518000119

49. Sauvageot N, Leite S, Alkerwi A, Sisanni L, Zannad F, Saverio S, et al. Association of empirically derived dietary patterns with cardiovascular risk factors: a comparison of PCA and RRR methods. *PLoS One*. (2016) 11:e0161298. doi: 10.1371/journal.pone.0161298

50. Bonora E, Tuomilehto J. The pros and cons of diagnosing diabetes with A1C. *Diabetes Care*. (2011) 34:S184–90. doi: 10.2337/dc11-s216

frontiers | Frontiers in Nutrition

TYPE Original Research
PUBLISHED 19 September 2023
DOI 10.3389/fnut.2023.1104859

OPEN ACCESS

EDITED BY
Ellen E. Blaak,
Maastricht University, Netherlands

REVIEWED BY
Norbert Stefan,
University of Tübingen, Germany
Haseeb Sattar,
Huazhong University of Science and Technology, China

*CORRESPONDENCE
Lei Liu
✉ liulei19890403@163.com
Changfa Wang
✉ wongdove@163.com

†These authors have contributed equally to this work

RECEIVED 22 November 2022
ACCEPTED 07 September 2023
PUBLISHED 19 September 2023

CITATION
Wang Y, Yuan T, Deng S, Zhu X, Deng Y, Liu X, Liu L and Wang C (2023) Metabolic health phenotype better predicts subclinical atherosclerosis than body mass index-based obesity phenotype in the non-alcoholic fatty liver disease population.
Front. Nutr. 10:1104859.
doi: 10.3389/fnut.2023.1104859

Metabolic health phenotype better predicts subclinical atherosclerosis than body mass index-based obesity phenotype in the non-alcoholic fatty liver disease population

Yaqin Wang[1], Ting Yuan[1], Shuwen Deng[1], Xiaoling Zhu[1], Yuling Deng[1], Xuelian Liu[1], Lei Liu[1*†] and Changfa Wang[2*†]

[1]Health Management Center, The Third Xiangya Hospital, Central South University, Changsha, China, [2]Department of General Surgery, The Third Xiangya Hospital, Central South University, Changsha, China

Background: Non-alcoholic fatty liver disease (NAFLD), especially lean NAFLD is associated with an increased risk of atherosclerotic cardiovascular disease (CVD). It is not currently known which clinical phenotypes of NAFLD contribute most to individual subclinical atherosclerosis risk. We examined the relationship between body mass index (BMI), the metabolically healthy status, and subclinical atherosclerosis in the NAFLD population.

Methods: Data from asymptomatic NAFLD subjects who participated in a routine health check-up examination were collected. Participants were stratified by BMI (cutoff values: 24.0–27.9 kg/m^2 for overweight and ≥28.0 kg/m^2 for obesity) and metabolic status, which was defined by Adult Treatment Panel III criteria. Subclinical atherosclerosis was evaluated by brachial-ankle pulse wave velocity (baPWV) in 27,738 participants and by carotid plaque in 14,323 participants.

Results: Within each BMI strata, metabolically unhealthy subjects had a significantly higher prevalence of subclinical atherosclerosis than metabolically healthy subjects, whereas fewer differences were observed across subjects within the same metabolic category. When BMI and metabolic status were assessed together, a metabolically unhealthy status was the main contributor to the association of clinical phenotypes with the subclinical atherosclerosis burden (all $p < 0.001$). When BMI and metabolic abnormalities were assessed separately, the incidence of subclinical disease did not increase across BMI categories; however, it increased with an increase in the number of metabolic abnormalities (0, 1, 2 and ≥3).

Conclusion: A metabolically healthy status in NAFLD patients was closely correlated with subclinical atherosclerosis, beyond that of the BMI-based obesity phenotype. The application of metabolic phenotyping strategies could enable more precise classification in evaluating cardiovascular risk in NAFLD.

KEYWORDS

cross-sectional study, metabolic status, obesity phenotype, subclinical atherosclerosis, non-alcoholic fatty liver disease

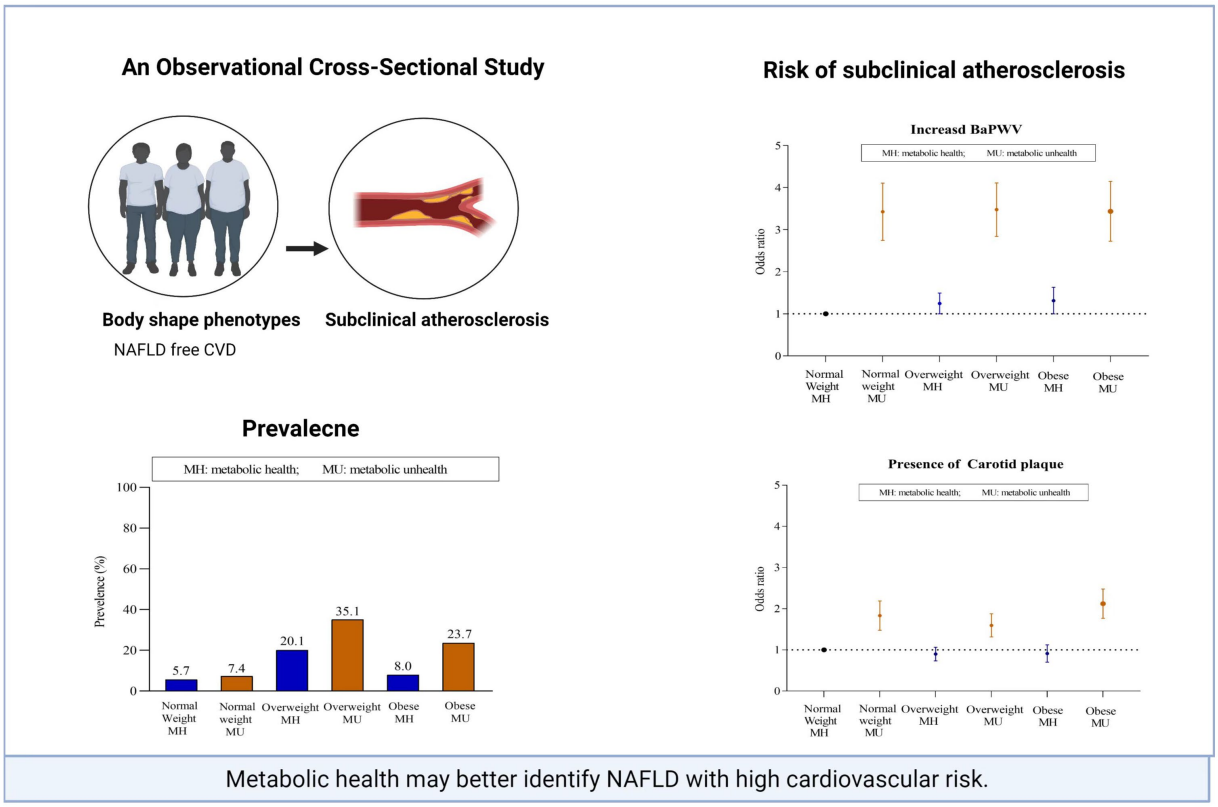

GRAPHICAL ABSTRACT

Introduction

Non-alcoholic fatty liver disease (NAFLD) is currently the most common hepatic disease and a highly heterogeneous metabolic disorder (1, 2). The prognosis of NAFLD is not as benign as thought and confers substantial increases in morbidity and mortality in those individuals who are affected. Evolving data from meta-analyses and cohort studies support the notion that the most common cause of death in the NAFLD population is cardiovascular disease (CVD), followed by extrahepatic malignancies and liver-related complications (3–5).

Although NAFLD is particularly common among subjects with obesity, it is increasingly being identified in lean individuals. The prevalence of lean NAFLD in the NAFLD population ranges from 10% to 20%, with the highest prevalence seen in Asian people (4). In addition, NAFLD interacts with the regulation of multiple metabolic pathways and is bidirectionally linked with components of metabolic syndrome (MetS). In 2020, a panel of international experts proposed that the nomenclature be changed from NAFLD to metabolic dysfunction-associated fatty liver disease (MAFLD) (6). However, the relationship between BMI and metabolic abnormalities is not generally uniform in the NAFLD population (1). There is a subgroup of individuals with obesity who are resistant to metabolic abnormalities, while there is another subset of subjects with normal weight who are prone to metabolic disturbances.

Beyond the association of NAFLD with CVD events, substantial epidemiological evidence links it to subclinical atherosclerosis, including carotid artery intima-media thickness (CIMT), carotid plaque, brachial-ankle pulse wave velocity (baPWV), coronary artery calcification (CAC) and brachial arterial flow-mediated dilation (FMD) (7, 8). However, no studies have investigated the impact of body size and shape combined with metabolic status on cardiovascular risk in the NAFLD population. The underlying relationship between obesity, poor metabolic health and subclinical atherosclerosis remains poorly understood. Awareness of the association is important for clinical practice and could provide proper risk stratification for early lifestyle intervention, which includes a healthy dietary composition in fruits and vegetables, legumes, whole grains, a minimal intake of trans-fats, ultra-processed food, red meat, sugar-sweetened beverages and regular physical activity, and so on improve long-term clinical outcomes (9).

In view of the aforementioned gaps, we examined the associations among the BMI-based obesity phenotype, metabolic health phenotype and subclinical CVD burden, including increased arterial wall stiffness and the presence of carotid plaque, in a large sample of asymptomatic NAFLD subjects without known cardiovascular disease.

Methods

Study design and population

We identified 96,963 adults aged 18–90 years who underwent routine health examinations at the Third Xiangya Hospital of Central South University in Changsha between August 2017 and

July 2021. The population consisted of a mix of urban and rural residents. After excluding participants with incomplete information, prior cardiovascular disease, and malignancy and those not meeting the definition of NAFLD, 27,738 NAFLD subjects remained for the cross-sectional study 1 analyses of the risk associated with arterial stiffness. We further excluded participants with no carotid vascular ultrasonography, leaving a final sample of 14,323 NAFLD participants for the cross-sectional study 2 analyses of the risk associated with carotid plaque (Figure 1). Informed consent and the protocol of the overall physical examination were reviewed and approved by the institutional review board at the Third Xiangya Hospital (No. 2018-S393).

Clinical characteristics

All participants completed a computerized National Physical Examination Questionnaire (10, 11). Personal details (demographic characteristics, health-related habits, family history, current medication information from pill bottles, previous medical diagnoses, etc.) were recorded according to standard protocols. The assessment and definitions of lifestyle factors, hypertension and diabetes are detailed in the Online Appendix.

Physical examination and laboratory measurements

The detailed methods used for physical examinations and laboratory evaluations have been previously described (11). Briefly, body weight, height, waist circumference (WC), heart rate and blood pressure were measured. BMI was calculated as weight in kilograms divided by height in meters squared (kg/m^2).

After the participants fasted overnight for at least 8 h, blood samples were collected and immediately processed and analyzed for alanine aminotransferase (ALT), aspartate aminotransferase (AST), albumin, total bilirubin, uric acid, creatinine, glucose, lipids and platelet count at the clinical laboratory of the Third Xiangya Hospital. The sample analysis was performed in accordance with the manufacturer's specifications. FIB-4 was used as a noninvasive and accurate marker of fibrosis based on the following formula: FIB-4 index = age × AST(U/L)/platelet count ($\times 10^9$/L) $\sqrt{ALT(U/L)}$ (12). The estimated glomerular filtration rate (eGFR) was used as an index

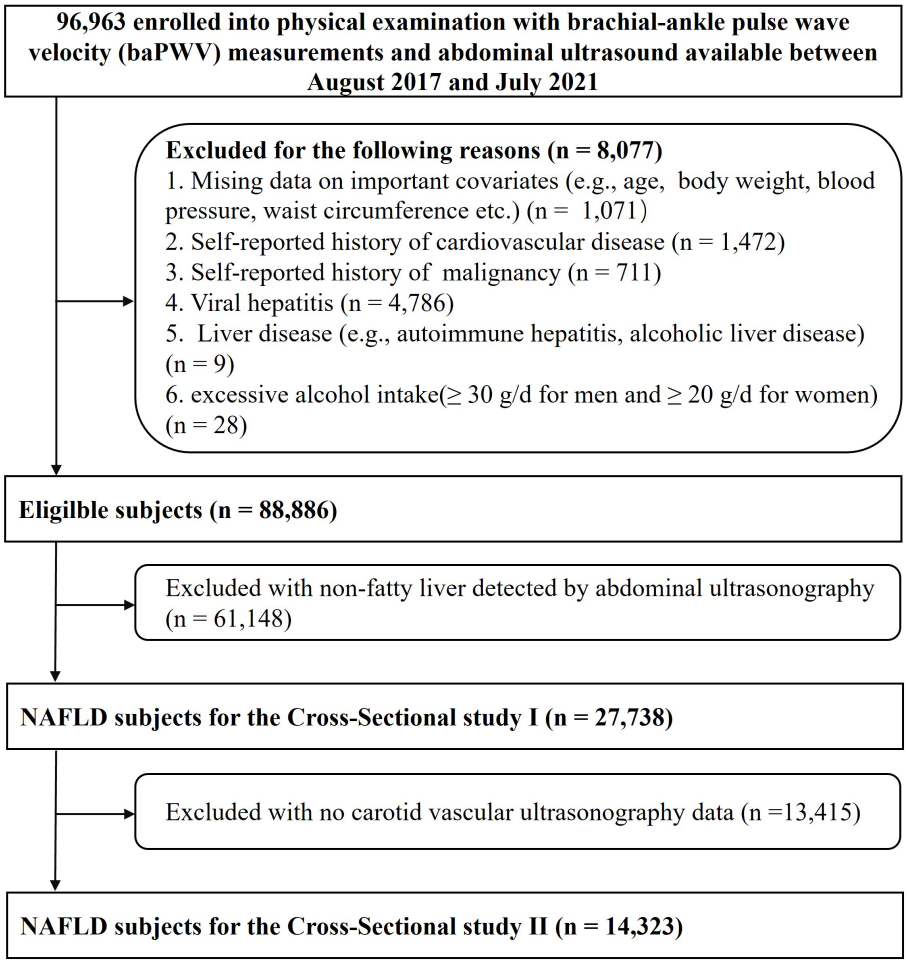

FIGURE 1
Flow chart of participant selection.

of renal disease based on the modification of diet in renal disease formula for Chinese subjects: $eGFR = 175 \times Scr^{-1.234} \times age^{-0.179}$ [if female, ×0.79] (13).

Determination of NAFLD and clinical phenotypes

NAFLD was defined as the presence of hepatic steatosis without excessive alcohol consumption (≥30 g/d in men and ≥20 g/d in women) or concomitant liver disease (14). The method used for detecting hepatic steatosis was hepatic ultrasound (Logiq 9, GE Medical System, Milwaukee, WI, United States). Positive abdominal ultrasound findings included the following 5 criteria: (1) parenchymal brightness, (2) liver-to-kidney contrast, (3) deep beam attenuation, (4) bright vessel walls and (5) gallbladder wall definition (15). Subjects with at least two abnormal findings were diagnosed with hepatic steatosis (16).

In accordance with the Working Group on Obesity in China (17), BMIs of 18.5–23.9 kg/m^2 were defined as normal weight; BMIs of 24.0–27.9 kg/m^2 were defined as overweight and ≥28.0 kg/m^2 were defined as obesity. The MetS definition in the National Cholesterol Education Program-Adult Treatment Panel III International Diabetes Federation (IDF) criteria (18) included elevated triglyceride (TG) levels (≥1.69 mmol/L) or the use of lipid-lowering drugs, low high-density lipoprotein (HDL) cholesterol levels (<1.03 mmol/L in men and <1.29 mmol/L in women), elevated systolic blood pressure (≥130 mmHg) or diastolic blood pressure (≥85 mmHg) or the use of antihypertensive drugs, and elevated blood glucose levels (≥5.6 mmol/L) or the use of any medications for diabetes (insulin or oral glucose-lowering medications). WC was not included because of collinearity with BMI. Individuals with one or fewer of these components were deemed metabolically healthy (MH), with two or more being deemed metabolically unhealthy (MU) according to the Framingham Heart Study (19).

Based on the combination of BMI categories and metabolic health status, the clinical phenotypes of NAFLD were then categorized into 6 groups: normal weight-MH, normal weight-MU, overweight-MH, overweight-MU, obese-MH and obese-MU.

Assessment of baPWV and carotid plague

As previously reported (11), baPWV was measured with an automatic waveform analyzer (BP-203 RPE III, Omron Health Medical, Dalian, China). After a minimum rest of 5 min in the supine position, 4 cuffs were wrapped around the extremities (upper arms and ankles) and then connected to the plethysmography sensor (volume pulse form) and an oscillometric pressure sensor. Pressure waveforms were recorded at both the brachial and tibial arteries to assess the transmission time between the initial increases in these waves. The measurements were performed twice, and the mean of the left- and right-side baPWV values were calculated. Moreover, substantial side differences in the baPWV of more than 10 m/s indicated problems with measurement, and the measurement should be repeated. The highest baPWV quartile (>1,590 cm/s) was classified as increased baPWV (arterial stiffness) (20).

As previously reported (21), carotid plaque was assessed using carotid artery sonography (Siemens AcusonSequoiaTM512 Ultrasound System, Mountain View, CA, United States) with a 9 MHz linear array transducer. Experienced sonographers performed carotid examinations, including bilateral visualization of the common, internal, and external carotid arteries. Carotid plaque was defined as a focal wall thickening of at least 0.5 mm or 50% of the surrounding CIMT that encroached into the arterial lumen or a focal region with CIMT greater than 1.5 mm that protruded into any carotid segment (22).

Statistical analyses

Descriptive characteristics are presented as the mean ± SD or median (interquartile range) for continuous variables and as the number (percentage) for categorical variables. The covariates between different groups were compared using a t test or the Mann–Whitney *U* test for continuous variables and the chi-square test for categorical variables. Multivariate logistic regression models were performed to assess the association of baPWV (the highest quartile versus other quartiles) and carotid plaques (presence versus absence) with (1) the 6 clinical phenotypes above; (2) the 3 BMI categories (normal weight, overweight and obese); (3) the 4 different categories of metabolic abnormalities (0, 1, 2 and ≥3 indices); and (4) individual metabolic abnormality risk factors (elevated blood pressure, triglyceridemia, hyperglycemia levels and low HDL-cholesterol). In addition, multiple linear regression analysis was used to evaluate the associations between baPWV (defined as a continuous variable) and the 6 clinical phenotypes. Potential covariates were adjusted for age, sex, demographic characteristics, lifestyles, WC, heart rate, albumin, total bilirubin, FIB-4, uric acid and eGFR.

Additional sensitivity analysis was performed to replicate our main findings with stricter definitions of metabolically healthy status, including the WC criterion (cutoff points of ≥90 cm for men and ≥85 cm for women) for the definition and defining metabolically healthy participants as having none of the five possible metabolic abnormality risk factors.

A p-value <0.05 was considered statistically significant. Statistical analyses were performed using SAS version 9.4 (SAS Institute, Cary, NC), and graphs were drawn by GraphPad Prism version 6.00 (GraphPad Software, La Jolla California, United States).

Results

Study population

The cross-sectional analysis included 27,738 overall participants (mean age: 49.8 years; 80.3% were male) with complete baPWV information in cross-sectional study sample I. A total of 14,323 individuals (mean age: 60 years; 76.7% were male) with complete carotid plaque information were included in cross-sectional study sample II.

Prevalence and characteristics of body size phenotypes

Of the 27,738 NAFLD participants, 13.2%, 55.1% and 31.7% fell into the normal weight, overweight and obese categories, respectively (Figure 2A). In the normal weight group, the MH

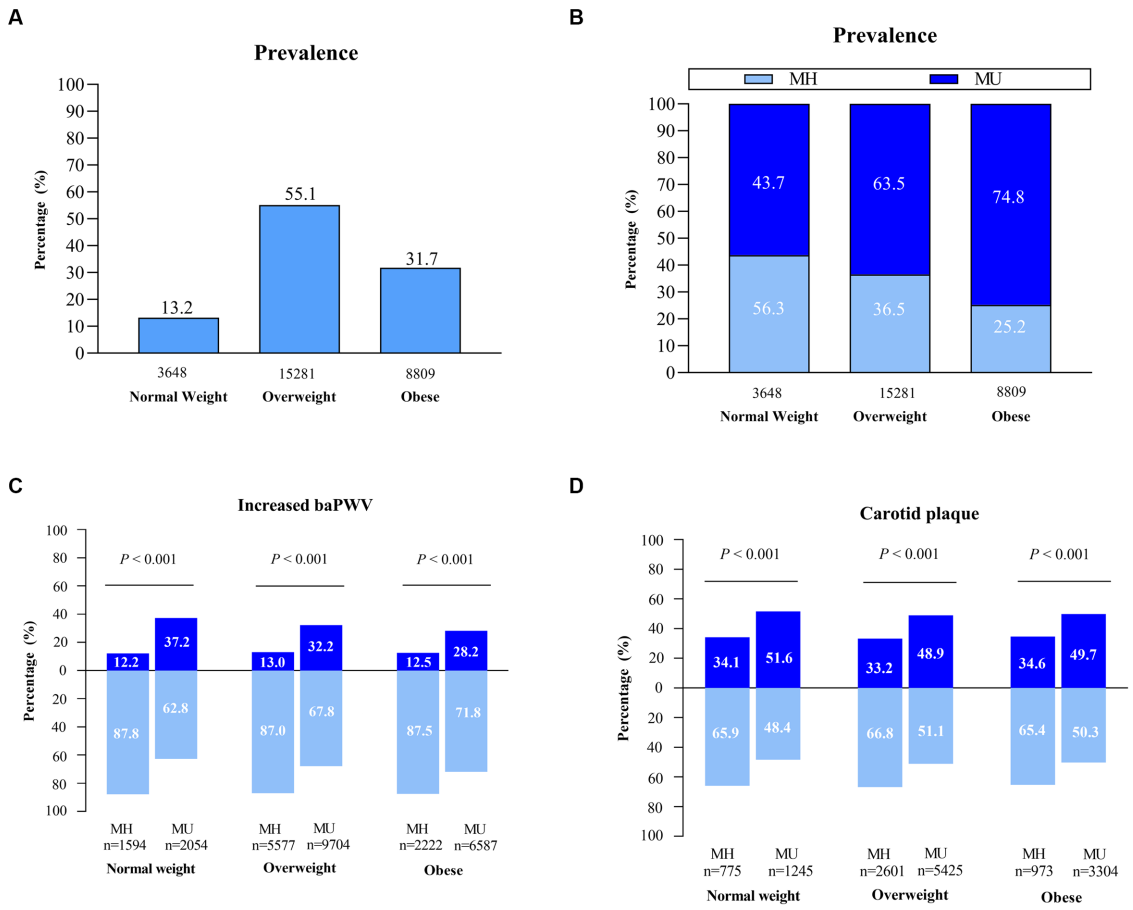

FIGURE 2
The prevalence of clinical phenotypes and distribution of subclinical atherosclerosis in the NAFLD population. **(A–C)** Assessment in NAFLD cross-sectional sample I (n = 27,738). **(D)** Assessment in NAFLD cross-sectional sample II (n = 14,323). MH, metabolically healthy; MU, metabolically unhealthy.

subjects accounted for a higher percentage than did the MU subjects (56.3% vs. 43.7%), whereas MU status was predominant in the overweight and obese groups (63.5% vs. 36.5%; 74.8% vs. 25.2%) (Figure 2B).

Within each BMI strata, MU individuals were older, had a higher proportion of poor diet scores, had a higher prevalence of diabetes and hypertension, and had higher WC, heart rate, blood pressure, and levels of fasting glucose, triglycerides, liver enzymes and uric acid than MH individuals. In contrast, a greater proportion of MH participants had a university degree, a worker occupation and a short sleep duration, and they had significantly greater levels of HDL-C and total bilirubin than participants with MU (Table 1).

Subclinical atherosclerosis profile

The MU individuals had an obviously higher prevalence of increased baPWV and carotid plaque than the MH individuals across all BMI categories. The extent of subclinical atherosclerosis was similar among MH individuals across BMI categories. For MU individuals, the extension was relatively higher for normal-weight individuals than for overweight and obese individuals (37.2% vs. 32.2% vs. 28.2%; 51.6% vs. 48.9% vs. 49.7%) (Figures 2C,D). A possible reason is that lean NAFLD subjects tend to be older than non-lean NAFLD subjects (52.2 vs. 49.5 years).

Association between subclinical atherosclerosis and clinical phenotypes

Increased baPWV and the presence of carotid plaque were available for the analysis in cross-sectional study sample I and sample II, respectively.

First, we evaluated the association between subclinical atherosclerosis and clinical phenotypes (6 subgroups) after adjusting for potential confounding factors (Table 2). The associations, which were defined according to the highest baPWV quartiles and carotid plaque, were evaluated using multiple logistic regression analysis. With the normal weight-MH subgroup as a reference, among MU subjects, normal weight, overweight and obesity were all significantly associated with a higher risk for increased baPWV and carotid plaque, and the adjusted odds ratio of risk was similar across BMI categories; however, among MH individuals, overweight and obesity showed a much lower but marginally significant risk of increased baPWV but were not associated with carotid plaque. Additionally, we conducted linear regression analysis for baPWV, which was defined as a continuous

TABLE 1 Study population clinical characteristics stratified by clinical phenotypes in cross-sectional sample I.

	Overall	Normal weight		Overweight		Obese	
		MH	MU	MH	MU	MH	MU
Prevalence, *n* (%)	27,738 (100%)	1,594 (5.7%)	2054 (7.4%)	5,577 (20.1%)	9,704 (35.1%)	2,222 (8.0%)	6,587 (23.7%)
Demographic factors							
Age, years	49.8 ± 10.7	50.3 ± 10.2	53.6 ± 10.3	48.8 ± 10.6	51.3 ± 10.3	46.9 ± 11.1	48.1 ± 10.7
Male sex, *n* (%)	22,274 (80.3%)	1,141 (71.6)	1,302 (63.4)	4,597 (82.4)	7,801 (80.4)	1864 (83.9)	5,569 (84.5)^{ns}
University degree, *n* (%)	11,797 (42.5)	837 (52.5)	805 (39.2)	2,760 (49.5)	4,056 (41.8)	928 (41.8)	2,411 (36.6)
Being married, *n* (%)	23,872 (86.1)	1,412 (88.6)	1782 (86.8)	4,896 (87.8)	8,411 (86.7)	1843 (82.9)	5,528 (83.9)^{ns}
Workers (occupation), *n* (%)	15,997 (57.7)	1,103 (69.2)	1,198 (58.3)	3,575 (64.1)	5,500 (56.7)	1,296 (58.3)	3,325 (50.5)
Lifestyle status							
Current smoker, *n* (%)	9,412 (33.9)	511 (32.1)	592 (28.8)	1835 (32.9)	3,272 (33.7)^{ns}	795 (35.8)	2,407 (36.5)^{ns}
Current drinker, *n* (%)	12,132 (43.7)	588 (36.9)	743 (36.2)^{ns}	2,424 (43.5)	4,302 (44.3)^{ns}	988 (44.5)	3,087 (46.9)^{ns}
Physical activity, n (%)							
Inactive	12,004 (43.3)	631 (39.6)	868 (42.3)^{ns}	2,193 (39.3)	4,064 (41.9)	1,024 (46.1)	3,224 (48.9)^{ns}
Moderately active	4,351 (15.7)	238 (14.9)	292 (14.2)^{ns}	832 (14.9)	1,550 (16.0)	368 (16.6)	1,071 (16.3)^{ns}
Active	11,383 (41.0)	725 (45.5)	894 (43.5)^{ns}	2,552 (45.8)	4,090 (42.1)	830 (37.4)	2,292 (34.8)^{ns}
Healthy diet							
Poor	11,126 (40.1)	500 (31.4)	724 (35.2)	1968 (35.3)	3,960 (40.8)	941 (42.3)	3,033 (46.0)
Intermediate	15,874 (57.2)	1,022 (64.1)	1,266 (61.6)	3,421 (61.3)	5,494 (56.6)	1,228 (55.3)	3,443 (52.3)
Ideal	738 (2.7)	72 (4.5)	64 (3.1)	188 (3.4)	250 (2.6)	53 (2.4)	111 (1.7)
Short sleep duration, *n* (%)	9,004 (32.5)	738 (46.3)	758 (36.9)	2065 (37.0)	3,014 (31.1)	690 (31.1)	1739 (26.4)
Classic vascular risk factors							
Body-mass index, kg/m^2	26.9 ± 2.8	22.8 ± 0.97	22.9 ± 0.93 ^{ns}	26.0 ± 1.1	26.1 ± 1.1	29.8 ± 1.7	30.3 ± 2.1
Waist circumference, cm	91.2 ± 7.7	81.6 ± 4.9	82.4 ± 4.9	88.8 ± 5.1	89.7 ± 5.2	97.1 ± 6.3	98.5 ± 6.6
Heart rate, beats/min	73.5 ± 11.0	71.0 ± 10.2	75.3 ± 11.3	70.6 ± 10.0	74.2 ± 11.1	71.7 ± 10.3	75.7 ± 11.2
Systolic blood pressure, mm Hg	130.9 ± 16.3	120.8 ± 13.6	132.6 ± 16.5	123.1 ± 14.1	134.1 ± 15.8	125.4 ± 14.0	136.3 ± 16.0
Diastolic blood pressure, mm Hg	81.9 ± 11.3	75.2 ± 9.3	81.1 ± 10.7	77.1 ± 9.6	84.0 ± 10.9	78.6 ± 10.1	86.2 ± 11.4
Hypertension, *n* (%)	7,021 (25.3)	142 (8.9)	532 (25.9)	708 (12.7)	2,917 (30.1)	367 (16.5)	2,355 (35.8)
Anti-hypertensive medication, *n* (%)	1,544 (5.6)	12 (0.8)	89 (4.3)	78 (1.4)	663 (6.8)	68 (3.1)	634 (9.6)
Fasting glucose, mmol/L	5.6 (5.1, 6.2)	5.2 (4.9, 5.4)	5.8 (5.3, 6.6)	5.2 (4.9, 5.5)	5.9 (5.4, 6.6)	5.2 (4.9, 5.5)	5.9 (5.4, 6.7)
Diabetes mellitus, *n* (%)	3,937 (14.2)	74 (4.6)	425 (20.7)	201 (3.6)	188 (19.4)	75 (3.4)	1,276 (19.4)
Anti-diabetes medication, *n* (%)	553 (2.0)	12 (0.8)	63 (3.1)	22 (0.4)	276 (2.8)	11 (0.5)	169 (2.6)
Triglycerides, mmol/L	2.1 (1.5, 3.1)	1.4 (1.1, 1.8)	2.3 (1.8, 3.3)	1.5 (1.1, 2.0)	2.5 (1.8, 3.6)	1.5 (1.2, 2.1)	2.6 (1.9, 3.8)
HDL-C cholesterol, mmol/L	1.22 ± 0.27	1.4 ± 0.30	1.2 ± 0.29	1.32 ± 0.25	1.18 ± 0.25	1.27 ± 0.23	1.13 ± 0.23
LDL-C cholesterol, mmol/L	2.86 ± 0.91	3.05 ± 0.81	3.07 ± 0.96^{ns}	3.03 ± 0.79	3.04 ± 0.94^{ns}	3.06 ± 0.77	3.06 ± 0.94^{ns}
Anti-dyslipidemia medication, *n* (%)	274 (1.0)	2 (0.1)	16 (0.8)	5 (0.1)	139 (1.4)	7 (0.3)	105 (1.6)

(Continued)

TABLE 1 (Continued)

	Overall	Normal weight		Overweight		Obese	
		MH	MU	MH	MU	MH	MU
Emerging risk factors and others							
ALT, U/L	31.0 (22.0, 44.0)	24.0 (18.0, 33.0)	26.0 (20.0, 37.0)	28.0 (21.0, 39.0)	31.0 (22.0, 44.0)	32.0 (23.0, 47.3)	37.0 (25.0, 54.0)
AST, U/L	21.0 (25.0, 27.0)	24.0 (20.0, 27.0)	25.0 (20.0, 27.0)	25.0 (20.0, 27.0)	25.0 (21.0, 27.0)	25.0 (21.0, 28.0)	25.0 (22.0, 30.0)
Albumin, g/L	45.3 ± 10.6	45.9 ± 7.0	45.5 ± 9.9[ns]	45.8 ± 8.3	45.3 ± 10.8[ns]	45.3 ± 10.0	44.7 ± 12.8[ns]
Total bilirubin, μmol/L	14.8 ± 5.8	16.0 ± 5.9	14.9 ± 6.2	15.6 ± 5.8	14.6 ± 5.8	14.8 ± 5.9	13.9 ± 5.3
FIB-4	0.36 (0.24, 0.52)	0.43 (0.29, 0.62)	0.43 (0.30, 0.61)[ns]	0.37 (0.26, 0.54)	0.37 (0.25, 0.54)[ns]	0.32 (0.21, 0.47)	0.31 (0.21, 0.46)[ns]
Uric acid, mmol/L	387 ± 88	346 ± 82	363 ± 88	375 ± 83	388 ± 86	393 ± 88	409 ± 89
eGFR, mL/min/1.73m^2	102 (89, 117)	105 (91, 120)	106 (92, 122)[ns]	101 (89, 116)	101 (88, 116)[ns]	100 (89, 114)	101 (88, 117)

Data are presented as the mean ± standard deviation, median (interquartile range), or count (percentage).
Uric acid was available for 27,712 participants, FIB-4 was available for 27,710 participants, and ALB and total bilirubin was available for 27,708 participants. The remaining baseline characteristics were available for all subjects.
MH, metabolically healthy; MU, metabolically unhealthy; BMI, body mass index; BP, blood pressure; LDL-C, low-density lipoprotein cholesterol; HDL-C, high-density lipoprotein cholesterol; ALT, alanine aminotransferase; AST: aspartate aminotransferase; FIB-4, eGFR, estimated glomerular filtration rate.
[ns]Nonsignificant for the comparison between MH (metabolic healthy) and MU (metabolic unhealthy) within each BMI strata. The remaining comparisons were statistically significant.

variable. Similar patterns were found regarding the relationship of subclinical atherosclerosis and MAFLD clinical phenotypes.

Second, to further explore whether the increased risk was mediated by metabolic abnormalities but not by increased BMI, we performed separate analyses to further assess the association between subclinical atherosclerosis and body size phenotypes after adjustment for confounding variables (Figures 3A,B,D,E). Whereas increased baPWV and carotid plaque increased with the increase in the number of metabolic abnormalities, there was no increase in the incidence of subclinical disease across BMI categories.

Finally, the adjusted risk for subclinical disease was also calculated according to individual and joint metabolic risk factors. Both the presence of elevated blood pressure and elevated glucose levels were revealed to be obviously significant covariates in predicting subclinical disease. Elevated triglyceride levels and decreased HDL levels were borderline or not significantly associated with subclinical disease (Figures 3C,F).

Sensitivity analyses

Using a strict definition of metabolic health led to a slight reinforcement of the magnitude of the associations. However, this did not generally affect the trend of these associations (Supplementary Table S1 and Supplementary Figure S1).

Discussion

Main findings

We report here, for the first time, evidence of an association between clinical phenotypes and subclinical atherosclerosis in light of two different indices. We found a wide spectrum of clinical phenotypes in the NAFLD population. The poor metabolic profile was noticeable in overweight and obese individuals. Compared with metabolically healthy subjects, metabolically unhealthy subjects had a higher burden of subclinical atherosclerosis regardless of their BMI phenotypes. Unhealthy metabolic status, but not BMI-based body size, was the main contributor to the associations of clinical phenotypes with subclinical atherosclerosis. An increasing number of comorbid MetS traits were linked with a higher risk in this cohort. Among the MetS components, elevated blood pressure and blood glucose levels were stronger risk factors associated with the prevalence of subclinical diseases. Our results held true not only when we used a clinical definition of metabolic healthy status (presence of one or fewer of the 4 metabolic risk factors) but also when we used a more stringent definition (presence of none of the 5 cardiometabolic risk factors).

Comparison with previous studies

The presence of carotid plaque was validated as an excellent marker of atherosclerotic lesions and structural abnormalities, reflecting generalized atherosclerosis. Increased baPWV is a reliable index of early vascular functional stiffness. A growing body of studies has reported that NAFLD is associated with the two markers of preclinical atherosclerosis, notably independent of established CVD risk factors (8, 23). However, these previous studies have several limitations. First, the most frequently included populations were hospital-based or outpatient cohorts, and some patients were diagnosed with liver biopsy, which resulted in a relatively small sample and led to selection bias. Hence, the results might lead to an overestimation of the effect (24–28). Second, the subjects among whom this link was observed were simply NAFLD vs. non-NAFLD. Thus, the findings can be interpreted that the NAFLD population could be recognized as having a high risk of atherosclerotic CVD. However, it is important to determine how risk discrimination can be performed within the NAFLD population. In our study, the metabolic profile was the greatest contributor to the relationship of subclinical atherosclerosis with different clinical phenotypes. This was illustrated by the effect of risk in subclinical atherosclerosis being concentrated among subjects in the metabolic abnormality subgroups, suggesting a major role for metabolic health in comparison with BMI ranges. Our findings highlight the message that precise metabolic

TABLE 2 The associations of clinical phenotypes with increased arterial stiffness in cross-sectional study sample I and carotid plaque in cross-sectional study sample II.

Cross-sectional sample 1 (n = 27,738)	Model 1		Model 2		Model 3	
	OR (95% CI)	p-value	OR (95% CI)	p-value	OR (95% CI)	p-value
baPWV—binary variable[a]						
NAFLD normal weight-MH	Reference		Reference		Reference	
NAFLD normal weight-MU	4.09 (3.38–4.96)	<0.001	4.03 (3.32–4.89)	<0.001	3.38 (2.77–4.13)	<0.001
NAFLD overweight-MH	1.25 (1.04–1.50)	0.020	1.23 (1.02–1.48)	0.028	1.23 (1.01–1.50)	0.038
NAFLD overweight-MU	4.06 (3.42–4.82)	<0.001	3.93 (3.31–4.67)	<0.001	3.44 (2.86–4.13)	<0.001
NAFLD obese-MH	1.44 (1.16–1.78)	0.001	1.37 (1.10–1.70)	0.005	1.29 (1.01–1.64)	0.041
NAFLD obese-MU	4.51 (3.79–5.38)	<0.001	4.25 (3.56–5.07)	<0.001	3.39 (2.75–4.17)	<0.001

Cross-sectional sample 1 (n = 27,738)	Model 1		Model 2		Model 3	
	β (95% CI)	p-value	β (95% CI)	p-value	β (95% CI)	p-value
baPWV—continuous variable[b]						
NAFLD normal weight-MH	Reference		Reference		Reference	
NAFLD normal weight-MU	159.9 (145.0–174.9)	<0.001	157.2 (142.2–172.1)	<0.001	128.9 (114.6–143.3)	<0.001
NAFLD overweight-MH	26.1 (13.4–38.8)	<0.001	24.4 (11.7–37.1)	<0.001	24.7 (12.1–37.3)	<0.001
NAFLD overweight-MU	148.7 (136.6–160.8)	<0.001	144.7 (132.6–156.8)	<0.001	122.5 (110.3–134.7)	<0.001
NAFLD obese-MH	36.3 (21.6–51.0)	<0.001	31.1 (16.3–45.8)	<0.001	22.6 (6.69–38.5)	0.005
NAFLD obese-MU	154.9 (142.4–167.4)	<0.001	147.8 (135.2–160.4)	<0.001	114.1 (99.7–128.6)	<0.001

Cross-sectional sample 2 (n = 14,323)	Model 1		Model 2		Model 3	
	OR (95% CI)	p-value	OR (95% CI)	p-value	OR (95% CI)	p-value
carotid plaque—binary variable						
NAFLD normal weight-MH	Reference		Reference		Reference	
NAFLD normal weight-MU	2.06 (1.70–2.49)	<0.001	1.95 (1.61–2.36)	<0.001	1.81 (1.49–2.20)	<0.001
NAFLD overweight-MH	0.96 (0.81–1.14)	0.660	0.93 (0.78–1.11)	0.429	0.89 (0.74–1.07)	0.204
NAFLD overweight-MU	1.87 (1.59–2.19)	<0.001	1.74 (1.48–2.05)	<0.001	1.57 (1.33–1.87)	<0.001
NAFLD obese-MH	1.08 (0.88–1.32)	0.466	0.99 (0.81–1.22)	0.950	0.90 (0.71–1.13)	0.346
NAFLD obese-MU	2.10 (1.78–2.49)	<0.001	1.91 (1.61–2.26)	<0.001	2.10 (1.78–2.49)	<0.001

Model 1 was adjusted for sex and age.
Model 2 was further adjusted for education level, marital status, occupation, current smoking, current drinking, physical activity, sleeping duration, and diet status plus model 1.
Model 3 was further adjusted for waist circumference (WC), heart rate, albumin, total bilirubin, FIB-4, uric acid and eGFR plus model 2.
OR, odds ratio; MH, metabolically healthy; MU, metabolically unhealthy.
[a]baPWV as binary outcome for highest quartile versus the other quartiles performed by logistic regression.
[b]baPWV as a continuous outcome for independent variables performed by linear regression.

phenotyping assessment beyond BMI could enable proper classification of NAFLD patients.

Several previous studies have reported an association between clinical phenotypes and the prognosis of NAFLD. In *Gut*, Younes et al. (29) reported a multicenter study comparing the long-term prognosis, including the onset of diabetes and long-term CVD events, between lean and non-lean NAFLD populations. They found that hepatic and non-hepatic clinical complications of the two subgroups did not differ significantly over a decade of follow-up. In addition, they found that 77.5% of the lean NAFLD patients stayed at a normal weight at the end follow-up, which implied that the longitudinal progression to obesity did not contribute to the disease outcomes in such lean subjects. Another study (30) investigated the effect of metabolic abnormalities on the risk of hepatic prognosis among patients with NAFLD over a 9 years period. Among lean NAFLD patients with one or zero metabolic risk factors, the future risk is very low. Therefore, these studies challenged that a BMI-driven strategy for screening NAFLD subjects for cardiovascular or liver damage outcomes can be misleading and should be reevaluated as metabolic derangements.

Potential mechanisms

Although BMI is an acceptable marker for overall adiposity, it cannot distinguish between muscle and fat and does not capture assessments of body-fat distribution, such as visceral and subcutaneous adipose tissue (31). Lean NAFLD is a common phenotype among Asian people, especially as they seem to have higher amounts of central fat deposition than White people and

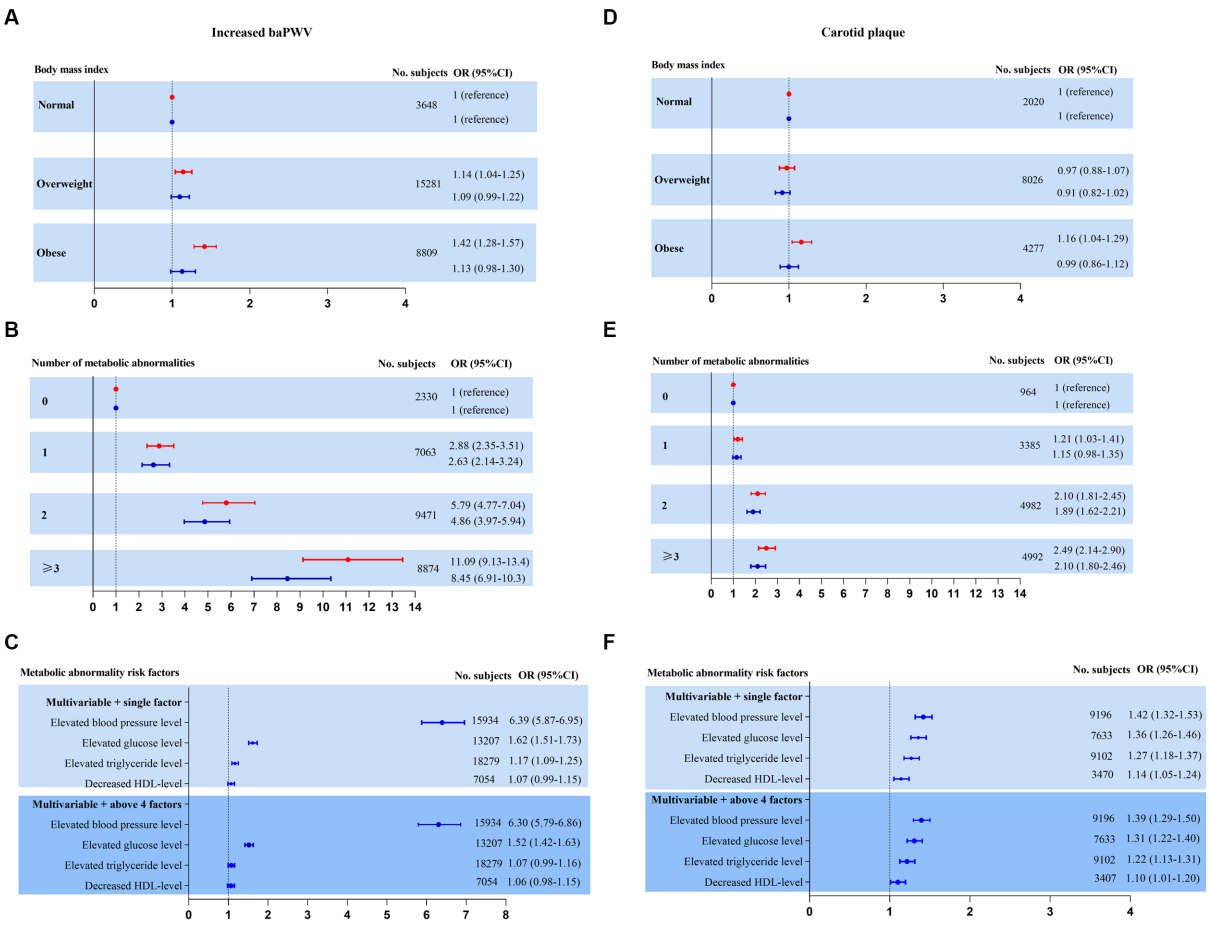

FIGURE 3
Risk for subclinical atherosclerosis stratified by body mass index, number of metabolic abnormalities and individual metabolic risk factor categories. Adjusted model 1 (red estimates) and fully adjusted model 2 (blue estimates) are both reported. Multivariate model 1 was adjusted for age and sex. Multivariate model 2 was further adjusted for education level, marital status, occupation, current smoking, current drinking, physical activity, sleeping duration, diet status, waist circumference, heart rate, ALB, total bilirubin, FIB-4, uric acid and eGFR plus model 1. **(A–C)** Increased baPWV was performed as a binary outcome for the highest quartile versus the other quartiles by logistic regression in NAFLD cross-sectional sample 1 (*n* = 27,738). **(D–F)** Carotid plaque as a binary outcome for presence versus absence by logistic regression in NAFLD cross-sectional sample 2 (*n* = 14,323).

develop NAFLD and metabolic complications within a low BMI range (32, 33). Findings from body composition studies showed that increased BMI was a poor surrogate for increased visceral adipose tissue and intrahepatic fat, both of which are strongly associated with NAFLD and cardiometabolic risk factors (34–37). In contrast, several studies revealed that WC was a reliable anthropometric index of visceral adiposity. Additionally, it was recommended that health professionals should be trained to properly perform this simple measurement and consider it an important "vital sign" in clinical practice. Therefore, importantly, BMI might be a suboptimal parameter for evaluating the association between obesity and subclinical atherosclerosis in the NAFLD population. Further studies that include precise quantification of different fat distributions could help to resolve this issue.

In this study, MetS itself or components of metabolic syndrome were consistent correlates of subclinical atherosclerosis. A complicated and dynamic interaction between a multitude of factors, including genetic, epigenetic, nutrition and dietary factors, lifestyle factors, and gut microbiota, is likely to shape individual metabolic profiles (1). In addition, NAFLD and MetS share a bidirectional association as a cause and a consequence (38). NAFLD is accompanied by impaired insulin-mediated suppression of hepatic glucose production, leading to liver steatosis, hyperglycemia and dyslipidemia. In turn, selective hepatic insulin resistance is thought to result in the development of both hepatic and peripheral metabolic dysfunction. Several types of pathophysiological crosstalk between NAFLD and MetS, including insulin resistance, abnormal lipoprotein metabolism, chronic low-grade inflammation, lipotoxicity and excessive oxidative stress, exert a proatherogenic effect on blood vessels (7). Similarly, Lee et al. (39) and Wang et al. (40) present evidence from large cohort studies from Korea and China, respectively, on the utility of the MAFLD definition for incident CVD and the risk of all-cause deaths. As expected from the positive definition (with a set of accompanying metabolic abnormalities), it is appealing to cover more patients with CVD and death under the umbrella term MAFLD compared with NAFLD. However, a dissociation between NAFLD and insulin resistance/dyslipidemia/CVD is present. NAFLD patients with a specific "liver-genetic" background have a

lower risk of CVD, which may partially explain why a subgroup of patients with NAFLD are metabolically healthy (41). In addition, NAFLD impacts metabolism and CVD risk through hepatokines, such as fetuin-A, ANGPTL3 (angiopoietin-related protein 3), FGF21 (fibroblast growth factor 21), SHBG (sex hormone-binding globulin), selenoprotein P, fetuin-B and follistatin (42).

We also tried to disentangle the effects of individual metabolic traits and found no correlation or only a weak effect of low HDL levels and hypertriglyceridemia on the risk of NAFLD atherosclerosis. Among the indices of lipid metabolism, only HDL cholesterol and triglyceride levels are used to define MetS. Nevertheless, total cholesterol and LDL cholesterol are risk factors for atherosclerotic lesions and structural abnormalities, which are not included in the definition.

Implications

This study adds an important facet to the NAFLD cardiometabolic risk factor research spectrum in which, within the heterogeneity of body shape phenotype, metabolic health is more closely related to subclinical atherosclerosis, above and beyond adiposity defined by BMI. Our findings add to evidence that metabolic health conferred important clues to cardiometabolic risk that BMI may not explain.

In regard to the risk stratification implications, the strategy is solely stratified by BMI, and lean subjects with NAFLD may be misclassified as low risk and "metabolically healthy." Obese NAFLD subjects who are "metabolically healthy" will be misclassified as being at higher risk. Accordingly, screening at-risk CVD populations instead of considering obesity or lean NAFLD as particular subgroups and performing a comprehensive assessment of specific metabolic profiles should be recommended. In other words, a novel definition of MH may be better suited to stratify subjects based on cardiometabolic risk parameters. In regard to the intervention management implications, lifestyle interventions remain the cornerstone of treatment. Weight loss has been shown substantial benefits not only for intrahepatic fat loss but also for improvement in metabolic parameters of glucose control and insulin sensitivity, whether NAFLD with overweight or normal weight (43). Several diet regimens were recommended, such as Mediterranean diet, low-carbohydrate diet, a low-fat diet and intermittent fasting over a regular diet (9, 44, 45). High adherence to the Mediterranean diet is associated with better profile of MetS features in NAFLD subjects owing to its close association with CVD (46). Nonetheless, further research is needed for its contribution on the development of subclinical atherosclerosis. In addition, some evidence showed that drinking three or more cups of coffee daily, dietary intake of vitamins E and C and phenolic acids had a protective association with NAFLD and its metabolic factors (47–49).

Strengths and limitations

The strengths of our study include many NAFLD participants; data on both structural and functional markers of subclinical disease; rich covariable adjustments encompassing sociodemographic factors and related CVD risk factors; and additional sensitivity analysis with strict MetS criteria, which added robustness to our findings.

Moreover, our results need to be interpreted with certain limitations. First, our cross-sectional design fails to determine causal relationships between clinical phenotypes and the development of subclinical atherosclerosis. Second, this study population consisted mostly of men, which potentially limits the generalizability of the results. Third, although we used two different versions of the MetS definition, impaired glucose tolerance and the inflammatory index, which are important components of new metabolic dysfunction criteria, were not included in this study (50). Fourth, recent data suggest that clinical phenotypes might be transient for a large proportion of individuals (19). Thus, the presence of phenotypes during one clinical examination could not capture the natural course of the variability within individuals, which remains controversial regarding the findings. Fifth, we chose only two markers of subclinical atherosclerosis, and other surrogate markers, such as coronary artery calcification (CAC) and brachial arterial flow-mediated dilation (FMD), were not included in our analysis. Sixth, we did not include information on emerging "nontraditional" CVD risk factors, such as decreased vitamin D and adiponectin levels, which may influence the relationship (51, 52). Lastly, carotid plaque indexes (such as carotid plaque burden and maximum carotid plaque thickness) are better predictors of cardiovascular disease risk than CIMT, and we did not obtain quantitative indicators of CIMT in our study (53).

Conclusion

In this health checkup-based study, different clinical phenotypes were associated with a greater subclinical CVD burden evaluated in subjects with NAFLD. However, this association remained significant only for the metabolic traits above and beyond the contribution of BMI-based body size. Our findings highlight the importance of metabolic status in screening fatty liver subjects at higher CVD risk. Although several treatments for NAFLD are currently in the pipeline, it would be preferable to establish treatment strategies with known benefits for improving both fat distribution and metabolic abnormalities in to achieve a better cardiovascular prognosis in the future.

Data availability statement

The raw data supporting the conclusions of this article will be made available by the authors, without undue reservation.

Ethics statement

The studies involving human participants were reviewed and approved by institutional review board at the Third Xiangya Hospital (No. 2018-S393). The patients/participants provided their written informed consent to participate in this study. Written informed consent was obtained from the individual(s) for the publication of any potentially identifiable images or data included in this article.

Author contributions

YW: study design, acquisition of clinical data, statistical analysis, and writing the manuscript. TY, SD, XZ, YD, and XL: acquisition of clinical data. LL and CW: acquisition of clinical data and modification of the manuscript. All authors contributed to the article and approved the submitted version.

Funding

This study was funded by the Changsha Natural Science Foundation (kq2208351), the National Natural Science Foundation of China (82001338), Hunan Provincial Natural Science Foundation (2020JJ4854, 2021JJ40934, and 2021JJ30989) and the Special Funding for the Construction of Innovative Provinces in Hunan (2020SK2055).

Acknowledgments

The authors would like to thank all of the participants for their support.

Conflict of interest

The authors declare that the research was conducted in the absence of any commercial or financial relationships that could be construed as a potential conflict of interest.

Publisher's note

Supplementary material

The Supplementary material for this article can be found online at: https://www.frontiersin.org/articles/10.3389/fnut.2023.1104859/full#supplementary-material

References

1. Eslam M, Fan JG, Mendez-Sanchez N. Non-alcoholic fatty liver disease in non-obese individuals: the impact of metabolic health. *Lancet Gastroenterol Hepatol.* (2020) 5:713–5. doi: 10.1016/S2468-1253(20)30090-X

2. Diehl AM, Day C. Cause pathogenesis, and treatment of nonalcoholic steatohepatitis. *N Engl J Med*. (2017) 377:2063–72. doi: 10.1056/NEJMra1503519

3. Zou B, Yeo YH, Nguyen VH, Cheung R, Ingelsson E, Nguyen MH. Prevalence, characteristics and mortality outcomes of obese, nonobese and lean NAFLD in the United States, 1999–2016. *J Intern Med.* (2020) 288:139–51. doi: 10.1111/joim.13069

4. Ye Q, Zou B, Yeo YH, Li J, Huang DQ, Wu Y, et al. Global prevalence, incidence, and outcomes of non-obese or lean non-alcoholic fatty liver disease: a systematic review and meta-analysis. *Lancet Gastroenterol Hepatol.* (2020) 5:739–52. doi: 10.1016/s2468-1253(20)30077-7

5. Lu FB, Zheng KI, Rios RS, Targher G, Byrne CD, Zheng MH. Global epidemiology of lean non-alcoholic fatty liver disease: a systematic review and meta-analysis. *J Gastroenterol Hepatol.* (2020) 35:2041–50. doi: 10.1111/jgh.15156

6. Eslam M, Newsome PN, Sarin SK, Anstee QM, Targher G, Romero-Gomez M, et al. A new definition for metabolic dysfunction-associated fatty liver disease: an international expert consensus statement. *J Hepatol.* (2020) 73:202–9. doi: 10.1016/j.jhep.2020.03.039

7. Adams LA, Anstee QM, Tilg H, Targher G. Non-alcoholic fatty liver disease and its relationship with cardiovascular disease and other extrahepatic diseases. *Gut.* (2017) 66:1138–53. doi: 10.1136/gutjnl-2017-313884

8. Zhou YY, Zhou XD, Wu SJ, Fan DH, van Poucke S, Chen YP, et al. Nonalcoholic fatty liver disease contributes to subclinical atherosclerosis: a systematic review and meta-analysis. *Hepatol Commun.* (2018) 2:376–92. doi: 10.1002/hep4.1155

9. Younossi ZM, Zelber-Sagi S, Henry L, Gerber LH. Lifestyle interventions in nonalcoholic fatty liver disease. *Nat Rev Gastroenterol Hepatol.* (2023). doi: 10.1038/s41575-023-00800-4 [Epub ahead of print].

10. Wang Y, Li L, Li Y, Liu M, Gan G, Zhou Y, et al. The impact of dietary diversity, lifestyle, and blood lipids on carotid atherosclerosis: a cross-sectional study. *Nutrients.* (2022) 14:815. doi: 10.3390/nu14040815

11. Lu Y, Pechlaner R, Cai J, Yuan H, Huang Z, Yang G, et al. Trajectories of age-related arterial stiffness in Chinese men and women. *J Am Coll Cardiol.* (2020) 75:870–80. doi: 10.1016/j.jacc.2019.12.039

12. Zhou F, Zhou J, Wang W, Zhang XJ, Ji YX, Zhang P, et al. Unexpected rapid increase in the burden of NAFLD in China from 2008 to 2018: a systematic review and meta-analysis. *Hepatology.* (2019) 70:1119–33. doi: 10.1002/hep.30702

13. Teo BW, Zhang L, Guh JY, Tang SCW, Jha V, Kang DH, et al. Glomerular filtration rates in Asians. *Adv Chronic Kidney Dis.* (2018) 25:41–8. doi: 10.1053/j.ackd.2017.10.005

14. European Association for the Study of the Liver (EASL), European Association for the Study of Diabetes (EASD) and European Association for the Study of Obesity (EASO). EASL-EASD-EASO Clinical Practice Guidelines for the management of non-alcoholic fatty liver disease. *J Hepatol.* (2016) 64:1388–402. doi: 10.1016/j.jhep.2015.11.004

15. National Health and Nutrition Examination Survey (NHANES) III. (2010). *Hepatic steatosis ultrasound images assessment procedures manual*. National Health and Nutrition Examination Survey (NHANES) III.

16. Farrell GC, Chitturi S, Lau GK, Sollano JDAsia-Pacific Working Party on NAFLD1. Guidelines for the assessment and management of non-alcoholic fatty liver disease in the Asia-Pacific region: executive summary. *J Gastroenterol Hepatol.* (2007) 22:775–7. doi: 10.1111/j.1440-1746.2007.05002.x

17. Pan XF, Wang L, Pan A. Epidemiology and determinants of obesity in China. *Lancet Diabetes Endocrinol.* (2021) 9:373–92. doi: 10.1016/S2213-8587(21)00045-0

18. Expert Panel on Detection, Evaluation, and Treatment of High Blood Cholesterol in Adults. Treatment of high blood cholesterol in executive summary of the third report of the National Cholesterol Education Program (NCEP) expert panel on detection, evaluation, and treatment of high blood cholesterol in adults (adult treatment panel III). *JAMA*. (2001) 285:2486–97. doi: 10.1001/jama.285.19.2486

19. Echouffo-Tcheugui JB, Short MI, Xanthakis V, Field P, Sponholtz TR, Larson MG, et al. Natural history of obesity subphenotypes: dynamic changes over two decades and prognosis in the Framingham Heart Study. *J Clin Endocrinol Metab*. (2019) 104:738–52. doi: 10.1210/jc.2018-01321

20. Lee YH, Shin MH, Choi JS, Rhee JA, Nam HS, Jeong SK, et al. HbA1c is significantly associated with arterial stiffness but not with carotid atherosclerosis in a community-based population without type 2 diabetes: the Dong-gu study. *Atherosclerosis*. (2016) 247:1–6. doi: 10.1016/j.atherosclerosis.2016.01.032

21. Zhu X, Chen Z, Yang P, Liu L, Wu L, Wang Y. The association of subclinical atherosclerosis with prediabetes is stronger in people with dyslipidaemia than in those with normoglycaemia: a cross-sectional study in Chinese adults. *Prim Care Diabetes*. (2020) 14:760–7. doi: 10.1016/j.pcd.2020.07.007

22. Mancia G, Fagard R, Narkiewicz K, Redon J, Zanchetti A, Böhm M, et al. 2013 ESH/ESC guidelines for the management of arterial hypertension: the task force for the Management of Arterial Hypertension of the European Society of Hypertension (ESH) and of the European Society of Cardiology (ESC). *Eur Heart J.* (2013) 34:2159–219. doi: 10.1093/eurheartj/eht151

23. Kapuria D, Takyar VK, Etzion O, Surana P, O'Keefe JH, Koh C. Association of hepatic steatosis with subclinical atherosclerosis: systematic review and meta-analysis. *Hepatol Commun.* (2018) 2:873–83. doi: 10.1002/hep4.1199

24. Kang JH, Cho KI, Kim SM, Lee JY, Kim JJ, Goo JJ, et al. Relationship between nonalcoholic fatty liver disease and carotid artery atherosclerosis beyond metabolic disorders in non-diabetic patients. *J Cardiovasc Ultrasound*. (2012) 20:126–33. doi: 10.4250/jcu.2012.20.3.126

25. Brea A, Mosquera D, Martin E, Martín E, Arizti A, Cordero JL, et al. Nonalcoholic fatty liver disease is associated with carotid atherosclerosis: a case-control study.

Arterioscler Thromb Vasc Biol. (2005) 25:1045–50. doi: 10.1161/01.ATV.0000160613.57985.18

26. Chung GE, Choi SY, Kim D, Kwak MS, Park HE, Kim MK, et al. Nonalcoholic fatty liver disease as a risk factor of arterial stiffness measured by the cardioankle vascular index. *Medicine*. (2015) 94:e654. doi: 10.1097/MD.0000000000000654

27. Kim BJ, Kim NH, Kim BS, Kang JH. The association between nonalcoholic fatty liver disease, metabolic syndrome and arterial stiffness in nondiabetic, nonhypertensive individuals. *Cardiology*. (2012) 123:54–61. doi: 10.1159/000341248

28. Taharboucht S, Guermaz R, Brouri M, Chibane A. Subclinical atherosclerosis and arterial stiffness in nonalcoholic fatty liver disease: a case-control study in Algerian population. *J Med Vasc*. (2021) 46:129–38. doi: 10.1016/j.jdmv.2021.03.008

29. Younes R, Govaere O, Petta S, Miele L, Tiniakos D, Burt A, et al. Caucasian lean subjects with non-alcoholic fatty liver disease share long-term prognosis of non-lean: time for reappraisal of BMI-driven approach? *Gut*. (2021) 71:382–90. doi: 10.1136/gutjnl-2020-322564

30. Kanwal F, Kramer JR, Li L, Dai J, Natarajan Y, Yu X, et al. Effect of metabolic traits on the risk of cirrhosis and hepatocellular cancer in nonalcoholic fatty liver disease. *Hepatology*. (2020) 71:808–19. doi: 10.1002/hep.31014

31. Neeland IJ, Ross R, Després JP, Matsuzawa Y, Yamashita S, Shai I, et al. Visceral and ectopic fat, atherosclerosis, and cardiometabolic disease: a position statement. *Lancet Diabetes Endocrinol*. (2019) 7:715–25. doi: 10.1016/S2213-8587(19)30084-1

32. Fan JG, Kim SU, Wong VW. New trends on obesity and NAFLD in Asia. *J Hepatol*. (2017) 67:862–73. doi: 10.1016/j.jhep.2017.06.003

33. Lear SA, Lesser IA. A review of obesity and body fat distribution and its relationship to cardio-metabolic risk in men and women of Chinese origin. *Cardiovasc Hematol Disord Drug Targets*. (2012) 12:113–8. doi: 10.2174/1871529x11202020113

34. Lee JJ, Pedley A, Hoffmann U, Massaro JM, Levy D, Long MT. Visceral and intrahepatic fat are associated with cardiometabolic risk factors above other ectopic fat depots: the Framingham Heart Study. *Am J Med*. (2018) 131:684–692.e12. doi: 10.1016/j.amjmed.2018.02.002

35. Stefan N. Causes, consequences, and treatment of metabolically unhealthy fat distribution. *Lancet Diabetes Endocrinol*. (2020) 8:616–27. doi: 10.1016/S2213-8587(20)30110-8

36. Bril F, Barb D, Portillo-Sanchez P, Biernacki D, Lomonaco R, Suman A, et al. Metabolic and histological implications of intrahepatic triglyceride content in nonalcoholic fatty liver disease. *Hepatology*. (2017) 65:1132–44. doi: 10.1002/hep.28985

37. Stefan N, Haring HU, Cusi K. Non-alcoholic fatty liver disease: causes, diagnosis, cardiometabolic consequences, and treatment strategies. *Lancet Diabetes Endocrinol*. (2019) 7:313–24. doi: 10.1016/S2213-8587(18)30154-2

38. Cariou B, Byrne CD, Loomba R, Sanyal AJ. Nonalcoholic fatty liver disease as a metabolic disease in humans: a literature review. *Diabetes Obes Metab*. (2021) 23:1069–83. doi: 10.1111/dom.14322

39. Lee H, Lee YH, Kim SU, Kim HC. Metabolic dysfunction-associated fatty liver disease and incident cardiovascular disease risk: a nationwide cohort study. *Clin Gastroenterol Hepatol*. (2021) 19:2138–2147.e10. doi: 10.1016/j.cgh.2020.12.022

40. Wang X, Wu S, Yuan X, Chen S, Fu Q, Sun Y, et al. Metabolic dysfunction-associated fatty liver disease and mortality among Chinese adults: a prospective cohort study. *J Clin Endocrinol Metab*. (2022) 107:e745–55. doi: 10.1210/clinem/dgab644

41. Stefan N, Cusi K. A global view of the interplay between non-alcoholic fatty liver disease and diabetes. *Lancet Diabetes Endocrinol*. (2022) 10:284–96. doi: 10.1016/S2213-8587(22)00003-1

42. Stefan N, Schick F, Birkenfeld AL, Häring HU, White MF. The role of hepatokines in NAFLD. *Cell Metab*. (2023) 35:236–52. doi: 10.1016/j.cmet.2023.01.006

43. Younossi ZM, Corey KE, Lim JK. AGA clinical practice update on lifestyle modification using diet and exercise to achieve weight loss in the management of nonalcoholic fatty liver disease: expert review. *Gastroenterology*. (2021) 160:912–8. doi: 10.1053/j.gastro.2020.11.051

44. Houttu V, Csader S, Nieuwdorp M, Holleboom AG, Schwab U. Dietary interventions in patients with non-alcoholic fatty liver disease: a systematic review and meta-analysis. *Front Nutr*. (2021) 8:716783. doi: 10.3389/fnut.2021.716783

45. Yin C, Li Z, Xiang Y, Peng H, Yang P, Yuan S, et al. Effect of intermittent fasting on non-alcoholic fatty liver disease: systematic review and meta-analysis. *Front Nutr*. (2021) 8:709683. doi: 10.3389/fnut.2021.709683

46. Montemayor S, Mascaró CM, Ugarriza L, Casares M, Llompart I, Abete I, et al. Adherence to Mediterranean diet and NAFLD in patients with metabolic syndrome: the FLIPAN study. *Nutrients*. (2022) 14:3186. doi: 10.3390/nu14153186

47. Chen YP, Lu FB, Hu YB, Xu LM, Zheng MH, Hu ED. A systematic review and a dose-response meta-analysis of coffee dose and nonalcoholic fatty liver disease. *Clin Nutr*. (2019) 38:2552–7. doi: 10.1016/j.clnu.2018.11.030

48. Sanyal AJ, Chalasani N, Kowdley KV, McCullough A, Diehl AM, Bass NM, et al. Pioglitazone, vitamin E, or placebo for nonalcoholic steatohepatitis. *N Engl J Med*. (2010) 362:1675–85. doi: 10.1056/NEJMoa0907929

49. Xie ZQ, Li HX, Tan WL, Yang L, Ma XW, Li WX, et al. Association of serum vitamin C with NAFLD and MAFLD among adults in the United States. *Front Nutr*. (2022) 8:795391. doi: 10.3389/fnut.2021.795391

50. Stefan N, Häring HU, Hu FB, Schulze MB. Metabolically healthy obesity: epidemiology, mechanisms, and clinical implications. *Lancet Diabetes Endocrinol*. (2013) 1:152–62. doi: 10.1016/S2213-8587(13)70062-7

51. Bugianesi E, Pagotto U, Manini R, Vanni E, Gastaldelli A, de Iasio R, et al. Plasma adiponectin in nonalcoholic fatty liver is related to hepatic insulin resistance and hepatic fat content, not to liver disease severity. *J Clin Endocrinol Metab*. (2005) 90:3498–504. doi: 10.1210/jc.2004-2240

52. Kwok RM, Torres DM, Harrison SA. Vitamin D and nonalcoholic fatty liver disease (NAFLD): is it more than just an association? *Hepatology*. (2013) 58:1166–74. doi: 10.1002/hep.26390

53. Sillesen H, Sartori S, Sandholt B, Baber U, Mehran R, Fuster V. Carotid plaque thickness and carotid plaque burden predict future cardiovascular events in asymptomatic adult Americans. *Eur Heart J Cardiovasc Imaging*. (2018) 19:1042–50. doi: 10.1093/ehjci/jex239

Frontiers in Nutrition

Explores what and how we eat in the context of health, sustainability and 21st century food science

A multidisciplinary journal that integrates research on dietary behavior, agronomy and 21st century food science with a focus on human health.

Discover the latest Research Topics

See more →

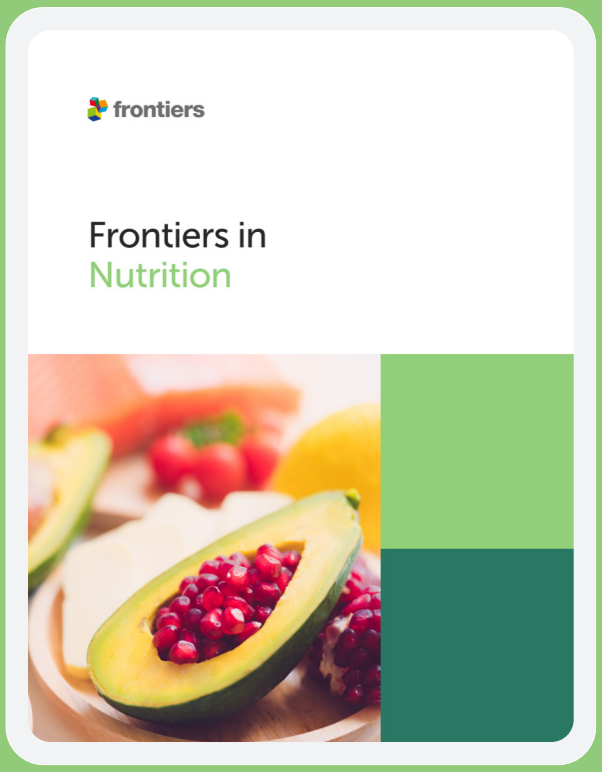

Frontiers

Avenue du Tribunal-Fédéral 34
1005 Lausanne, Switzerland
frontiersin.org

Contact us

+41 (0)21 510 17 00
frontiersin.org/about/contact